THE DEVELOPMENT OF A SYNTHETIC STRATEGY TOWARD OXAZINE-CONTAINING NATURAL PRODUCTS ENABLED BY NOVEL COPPER CATALYSIS

Thesis by
Nicholas Glenn William Cowper

In Partial Fulfillment of the Requirements
for the Degree of

Doctor of Philosophy

CALIFORNIA INSTITUTE OF TECHNOLOGY

Pasadena, California

2018

(Defended July 6th, 2018)

© 2018

Nicholas Glenn William Cowper

All Rights Reserved

For Grandad,

ACKNOWLEDGEMENTS

Foremost, I wish to thank my research advisor, Professor Sarah Reisman, for allowing me the privilege of conducting my graduate studies under her guidance and support. Her insight, creativity, passion, and patience make her exceptional in a truly great community at Caltech. She is a great scientist and teacher who has always had my best interests at heart.

I am also grateful to my thesis committee members Professors Dennis Doughtery, Brian Stoltz, and chairman, Professor Gregory Fu. Their perspective and experience have been critical in approaching both my research and career aspirations. Their incisive questions and feedback in our annual meeting have greatly informed my development as a scientist. Furthermore, the collaborative atmosphere fostered by them and the rest of the faculty has made research as a graduate student inspiring experience.

The staff scientists at Caltech are incredible. Not only do they maintain a state-of-the-art research facility but also provide a wealth of knowledge and make themselves available to assist students in specialized experiments. In particular, I would like to thank David van der Velde who not only taught me a great deal about NMR but also gave me experience in instrument troubleshooting as a GLA.

I would also like to thank Scott Virgil for whom the depth of my gratitude is difficult to express. As a scientist, he has a been always a positive force. He has provided innumerable thoughtful comments on my synthetic approach as well as technical insight on laboratory procedures and instrumentation. He has been a constant source of encouragement in an often-challenging project. He and Silva have also been great friends, always generous with their time and their care.

It is imperative that I thank the members of the Reisman lab, past and present. The members of the lab have made it a fun, engaging and intellectually stimulating place work. In particular I would like to thank Dr. Lauren Chapman, Dr. Kangway Chaung, Dr. Elliot Farney, Denise Grunenfelder, Dr. Matthew Hesse, Dr. Victor Mak, Dr. Haoxuan Wang.

There are many more people to thank, friends and family, who have supported me in this journey. I could not have accomplished any small fraction of this without you.

ABSTRACT

1,2-oxazine natural products are a small closely related family of highly oxidized compounds. Herein, the development of a synthetic strategy toward gliovirin and the trichodermamides is described which enabled the synthesis of the western fragments of gliovirin and trichodermamide B. To that end, we developed two novel copper-catalyzed transformations: the asymmetric propargylation of an oxime and the diasteroeselective oxidative cyclization of hydroxamic acid with a diene.

The challenge of working with tetrahydro-1,2-oxazines is their sensitivity to a variety of reaction conditions and purification methods. Extensive optimization of each transformation was accomplished, bringing to bear the state-of-the-art in oxidative modifications, including a palladium-catalyzed direct desaturation of an epoxy ketone. As well as this work led to the rare observation of a vinylogous Payne rearrangement.

The successful synthesis of the fully functionalized western and eastern fragments of gliovirin are described toward a late-stage diketopiperazine formation and thiolation. Interrogation of our late-stage strategy with these fragments demonstrates that the coupling of the fully functionalized western and eastern fragments is not an effective strategy toward gliovirin proof-of-concept experiments suggest this chemistry could be used toward the synthesis of the trichodermamides.

TABLE OF CONTENTS

LIST OF ABBREVIATIONS

$[\alpha]_D$	angle of optical rotation of plane-polarized light
Å	angstrom(s)
Ac	acetyl
acac	acetylacetonate
AIBN	azobisisobutyronitrile
aq	aqueous
Ar	aryl group
atm	atmosphere(s)
BINOL	1,1'-bi-2,2'-naphthol
Bn	benzyl
Boc	*tert*-butoxycarbonyl
bp	boiling point
br	broad
Bu	butyl
n-Bu	butyl or *norm*-butyl
t-Bu	*tert*-butyl
BQ	1,4-benzoquinone
Bz	benzoyl

c	concentration of sample for measurement of optical rotation
^{13}C	carbon-13 isotope
/C	supported on activated carbon charcoal
°C	degrees Celcius
calc'd	calculated
cat.	catalyst
Cbz	benzyloxycarbonyl
cf.	consult or compare to (Latin: *confer*)
cis	on the same side
cm^{-1}	wavenumber(s)
conc.	concentrated
conv.	conversion
Cy	cyclohexyl
Δ	heat or difference
δ	chemical shift in ppm
d	doublet
d	deutero or dextrorotatory
D	deuterium
DCE	1,2-dichloroethane
de novo	starting from the beginning; anew
DIPEA	*N*,*N*-diisopropylethylamine
DIBAL	diisobutylaluminum hydride
DKP	diketopiperazine

DMAP	4-(dimethylamino)pyridine
DMF	*N*,*N*-dimethylformamide
DMSO	dimethylsulfoxide
dr	diastereomeric ratio
ee	enantiomeric excess
E^+	electrophile
E	*trans* (entgegen) olefin geometry
EDCI	*N*-(3-dimethylaminopropyl)-*N*'-ethylcarbodiimide hydrochloride
e.g.	for example (Latin: *exempli gratia*)
EI	electron impact
ent	enantiomer of
epi	epimeric
equiv	equivalent(s)
ESI	electrospray ionization
Et	ethyl
ETP	epipolythiodiketopiperazine
et al.	and others (Latin: *et alii*)
FTIR	fourier transform infrared spectroscopy
g	gram(s)
h	hour(s)
^1H	proton
[H]	reduction
HFIP	hexafluoroisopropanol

HG-II	Hoveyda–Grubbs' catalyst™ 2nd generation
HMBC	heteronuclear multiple-bond correlation spectroscopy
HMDS	hexamethyldisilazide
$h\nu$	irradiation with light
HPLC	high performance liquid chromatography
HRMS	high resolution mass spectrometry
Hz	hertz
i.e.	that is (Latin: *id est*)
iso	isomeric
J	coupling constant in Hz
k	rate constant
kcal	kilocalorie(s)
kg	kilogram(s)
L	liter or neutral ligand
l	levorotatory
LA	Lewis acid
LC/MS	liquid chromatography–mass spectrometry
m	multiplet or meter(s)
M	molar or molecular ion
m	*meta*
μ	micro
m-CPBA	*meta*-chloroperbenzoic acid
Me	methyl

Mes-HG-II	Hoveya-Grubbs' catalyst™ 2nd generation
mg	milligram(s)
MHz	megahertz
min	minute(s)
mL	milliliter(s)
MM	multi-mode
mol	mole(s)
MOM	methoxymethyl
Ms	methanesulfonyl (mesyl)
MS	molecular sieves
m/*z*	mass-to-charge ratio
NBS	*N*-bromosuccinimide
ND	not determined
nm	nanometer(s)
NMO	*N*-methylmorpholine *N*-oxide
NMR	nuclear magnetic resonance
NOE	nuclear Overhauser effect
NOESY	nuclear Overhauser enhancement spectroscopy
NPh	naphthyl
Nu^-	nucleophile
o	*ortho*
[O]	oxidation
P	peak

p	*para*
PCC	pyridinium chlorochromate
PDC	pyridinium dichromate
Ph	phenyl
pH	hydrogen ion concentration in aqueous solution
PHAL	1,4-phthalazinediyl diether
PIDA	[bis(acetoxy)iodo]benzene
Pin	pinacol
PivOH	pivalic acid
pK_a	acid dissociation constant
pm	picometer(s)
PMP	*para*-methoxyphenyl
ppm	parts per million
i-Pr	isopropyl
q	quartet
quant.	quantitative
R	generic (alkyl) group
R_L	large group
R	rectus
recry.	recrystallization
ref	reference
R_f	retention factor
rgt.	reagent

rt	ambient temperature
s	singlet or seconds
S	sinister
sat.	saturated
t	triplet
TBAF	tetra-*n*-butylammonium fluoride
TBME	*tert*-butyl methyl ether
TBS	*tert*-butyldimethylsilyl
temp	temperature
Tf	trifluoromethanesulfonyl
TFA	trifluoroacetic acid
THF	tetrahydrofuran
TLC	thin layer chromatography
TMS	trimethylsilyl
TOF	time-of-flight
tol	tolyl
trans	on the opposite side
Ts	*para*-toluenesulfonyl (tosyl)
UV	ultraviolet
vide infra	see below
w/v	weight per volume
X	anionic ligand or halide
xs	excess

Z	*cis* (zusammen) olefin geometry

Chapter 1

An Introduction to Total Synthesis, Polythiodiketopiperazines, and Related Natural Products

1.1 INTRODUCTION TO TOTAL SYNTHESIS

Natural product synthesis is the use of chemical methods to generate complex molecules structurally identical to materials isolated from natural sources. The study of natural product synthesis has served, and continues to serve, the development of fundamental synthetic organic chemistry. Initially, it was used as a tool to provide the strongest form of evidence toward the elucidation of complex chemical structures. With the advent of advanced analytical techniques, the principle role of natural product total synthesis has shifted. In more recent years, it has demonstrated value as a platform to expose gaps in current chemical knowledge, motivating the development of new chemical transformations to form these challenging structures.

Natural product total synthesis as a discipline is characterized by two intellectual pursuits: strategy and tactics. Strategy focuses on retrosynthetic analysis, a conceptual framework

developed in the mid 20th century with contributions from many prominent chemists but championed most notably by Prof. E.J. Corey.[1] This method of analysis identifies bond disconnections which simplify complex structures by recognizing embedded structural motifs. By recognizing these underlying motifs, one can redefine the problem of natural product synthesis to simpler target molecules to inform a forward route. Through iterative application of this approach, one can methodically unravel a complex natural product to readily available feedstock materials.

In contrast to the aim of pattern recognition and structural simplification in retrosynthetic analysis; synthetic tactics are defined as the methods one uses to realize the forward synthesis. While there are no fundamental constraints on the disconnections made in a retrosynthesis, tactics are limited to transformations either previously known or novel methods based on a fundamental understanding of chemical reactivity. The efficiency of these transformations is of the utmost importance; to that end chemoselective methods are engaged to minimize side products with an emphasis on functional group tolerance to minimize substrate decomposition. Despite the development of high-yielding chemical transformations, reactive conditions often generate by-products or minor impurities. These impurities in the crude material can interfere with later chemical manipulations and, therefore, are typically purged from the crude reaction mixture. There are four main approaches to accomplish this goal, exploiting the physical properties of different components in the mixture: distillation (boiling point), crystallization (solubility and physical morphology), solvent partitioning (hydrophobicity), or elution through polar solid media (polarity).[2] When considering the value of a method therefore, it is not only important to consider the ability of the method to generate the desired species but also the ease with which it can be isolated from the crude mixture effectively.

Through the use of strategic thinking, a viable retrosynthesis selects bond disconnections that take advantage of efficient chemical transformations that will generate the target molecule in fewest number of steps. A common strategy to improve the efficiency of a synthesis is the incorporation of a convergent step. By independently functionalizing two fragments and combining them at a later stage one can maximize the number of independent chemical transformations while minimizing the number of steps in the longest linear sequence (LLS) from commercially available materials. Overman's synthesis[3] of (–)-actinophyllic acid (**7**, Scheme 1.1) is an excellent example of a convergent synthesis. However, the implementation of novel chemical methods can facilitate the rapid generation of intermediates of similar complexity. For example, the functionalized indole **5** is generated in 6 steps LLS while indole **10** generated in Kwon's synthesis[4] of **7** is accessed in 2 steps. However it is important, not to hold step count as the sole metric to measure a total synthesis. Chen's synthesis[5] of **7** has the lowest LLS of the syntheses

Scheme 1.1. *Syntheses of (–)-actinophyllic acid contrasting different bond disconnections*

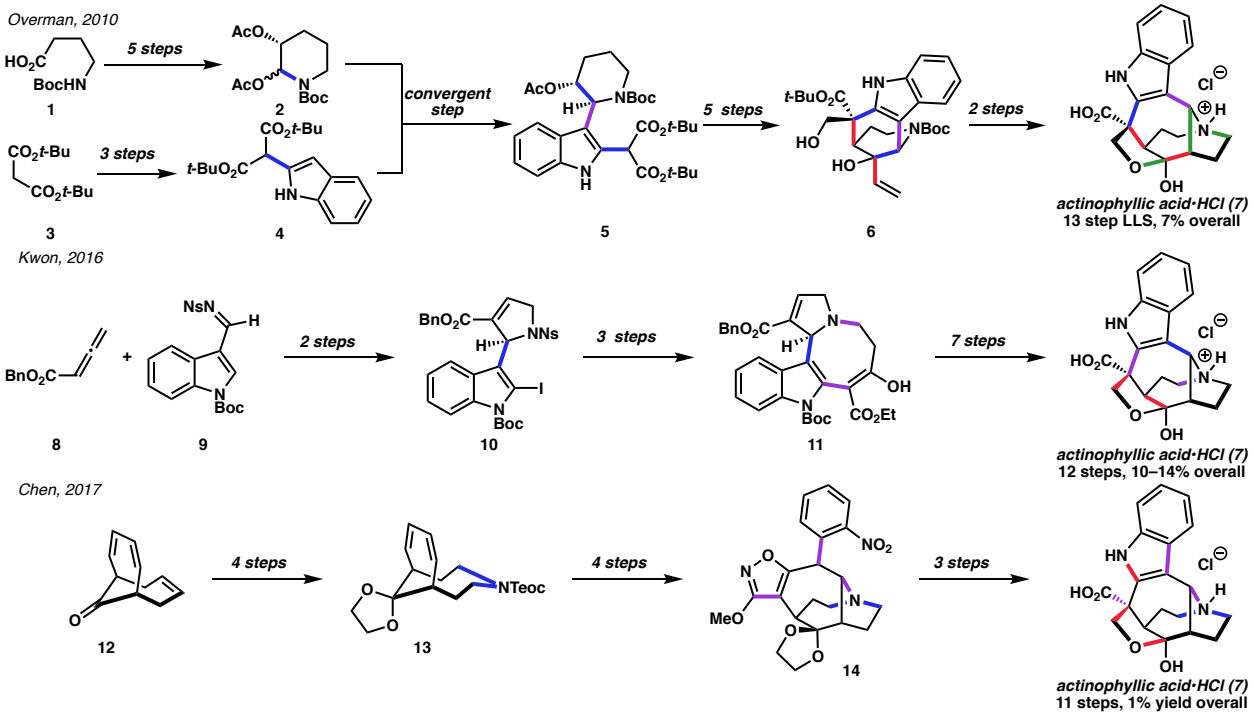

shown, yet it has the lowest overall yield. This is due to several low-yielding steps which resulted either from a lack of chemoselectivity or instability of the intermediates. Each of these syntheses stage the formation of key bond connections differently (Scheme 1.1 *as highlighted*), this defines the tactics and limits possible conditions based upon the stability of the intermediates and their functionality. Thus, the best retrosynthetic analysis identifies key intermediates that can be married with efficient tactics to form the desired functionality.

An optimal synthesis provides the product with the minimum number of chemical manipulations, high purity, and excellent yield. As scale requirements increase engineering problems such as safety, replicability, and cost are also taken into account. These ancillary practical principles are a key concern for larger scale syntheses undertaken in industrial process chemistry. At its heart, the total synthesis of natural products is the confluence of creative thinking, pattern recognition, and methodology development.

1.2 POLYTHIODIKETOPIPERAZINES

Polythiodiketopiperazines (PTPs) are a diverse class of natural products characterized by a cyclized dipeptide bearing a sulfur bridging moiety. This sulfur bridge usually spans a diketopiperazine (DKP) core as a disulfide; this class of PTPs are commonly referred to as 3,6-epipolythiodiketopiperazines(3,6-ETPs). While these isolated compounds are initially generated from a limited number of canonical amino acids, their structural is the result of extensive enzyme-mediated oxidative modifications of the amino acid side chains. The first 3,6-ETP isolated was gliotoxin (**16,** Figure 1.1) in 1936;[6] however, extensive studies[7–18] were required before the native structure was proposed in 1958[19] with final confirmation of the structure by X-ray crystallography studies in 1967.[20] It gained interest not only for its compact and highly functionalized structure but

also for it intriguing biological activity. Since 1936, a variety of compounds have been isolated with this 3,6-ETP core motif from fungi and plants, and have been the subject of several reviews of their structures and properties.[21,22]

3,6-ETPs can be categorized by the mother amino acids, elucidated through feeding studies with isotopically labelled amino acids.[21] While 3,6-ETPs can be either symmetrical or unsymmetrical all known 3,6-ETPs incorporate an amino acid with an aromatic moiety: either phenylalanine, tyrosine and tryptophan, and demonstrate high structural diversity.

Figure 1.1. *3,6-ETP natural products derived from phenyalanine*

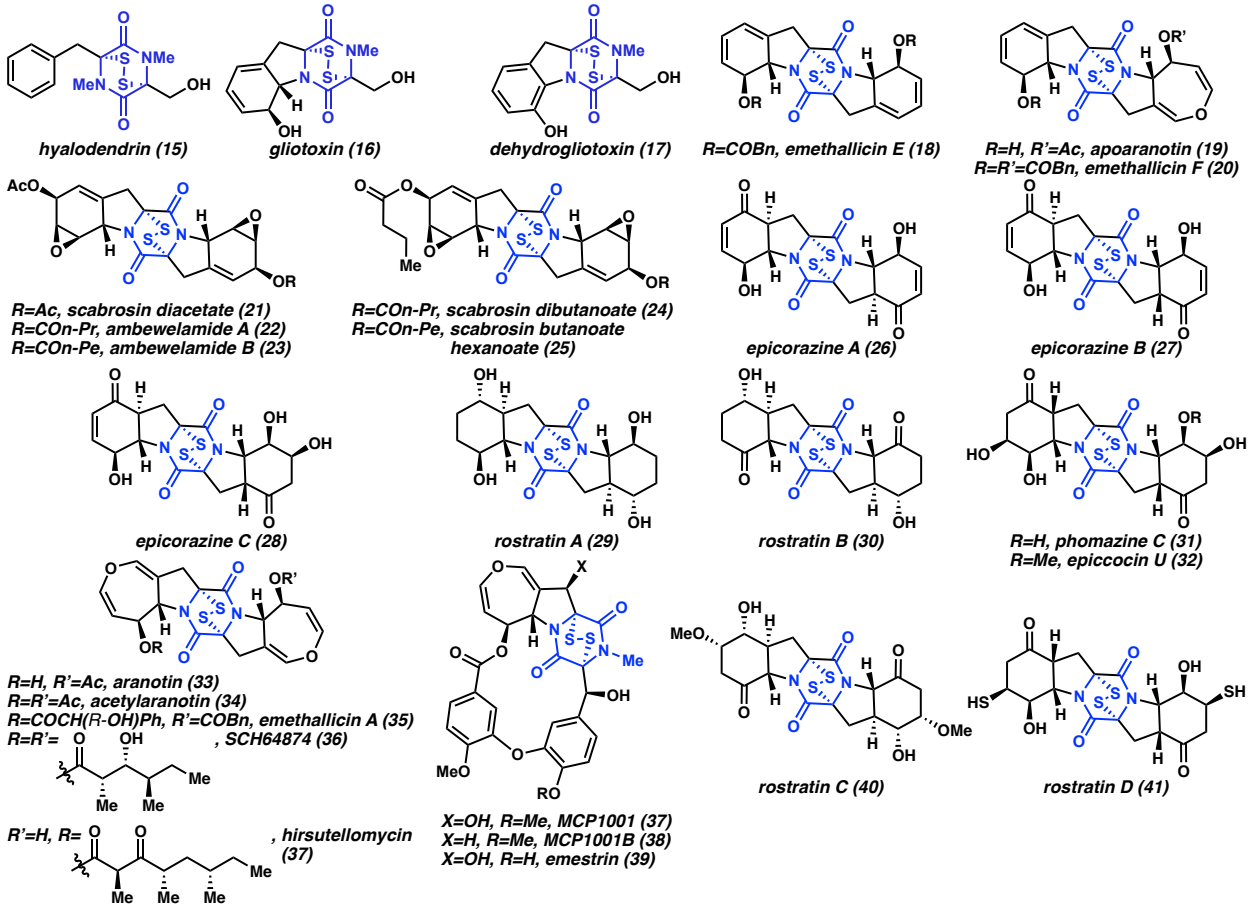

Phenyalanine–derived 3,6-ETPs are the largest family of 3,6-ETPs, with a wide variety of oxidative patterns. Hyalodendrin (**15**), one of the simplest 3,6-ETPs isolated,[23] is an unsymmetrical 3,6-ETP resulting from the dimerization of phenylalanine and serine. The 5-6 dihydroindoline

motif featured in **16** can also be observed in other 3,6-ETPs such as emethallicin E&F (**18** & **20**) and apoaranotin (**19**).[24,25] Further oxidized 5-6 systems can be differentiated by their oxidative patterns shown in the epoxy allylic alcohol motifs of the scabrosins[26] (**21**, **24**, **25**) and ambewelamides[27] (**22**, **23**); are contrasted by the γ- hydroxy enone motif of the epicorazines[28–30] (**26-28**). Other ETP natural products featuring the 5-6 ring system include: rostratins[31] (**29-30, 40-41)**, phomazine C[32] (**31**), and epicoccin U[33] (**32)** which show a striking analogy to the epicorazine core. Exemplified by aranotin (**33**), the incorporation of a dihydrooxepine heterocycle as fused a 5-7 bicycle is an anomalous motif, observed in many phenylalanine-derived ETPs is.[34–39]

Figure 1.2. *3,6-ETP natural products derived from tyrosine*

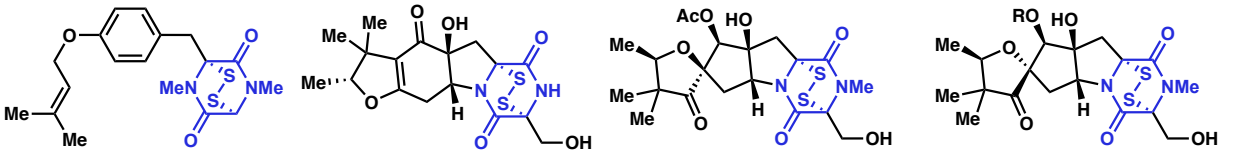

Tyrosine–derived ETPs are the smallest family of ETPs. Prenylation of the tyrosinyl phenol on substrate derived from cyclization with glycine yields dithiosilvatin[40] (**36**, Figure 1.2). The other ETPs of this family incorporate serine in analogy to **16** and demonstrate similar oxidative dearomatization as demonstrated by phomalirazine[41] (**37**) with its fused 5-6-5 tricyclic sidechain and the epimeric spirocyclic structures of the sirodesmins[42,43] (**38-40**).

Unlike the ETPs derived from phenylalanine, tryptophan-derived ETPs do not present the same variety of oxidative patterns. Instead they all contain a pyrroloindoline motif with substitution at the benzylic position. Structural variation in this family instead results from arene functionalization, as seen in the sporidesmins[44,45] (**41-43**, Figure 1.3), and manifold substitution at C3 of the mother indole, including dimerization of the pyrroloindoline exemplified by chaetocin A[46] (**45**). Furthermore, this family incorporates the widest variety of aliphatic amino acids,

products distinguished exclusively by C3 substitution on the ETP core: symmetryical dimeric ETPs[47–50] (**49–53**), unsymmetrical dimeric ETPs[51–53] (**48**, **54–58**) and indolinated substituted ETPs[54–59] (**46-47**, **59–63**).

Figure 1.3. *3,6-ETP natural products derived from tryptophan*

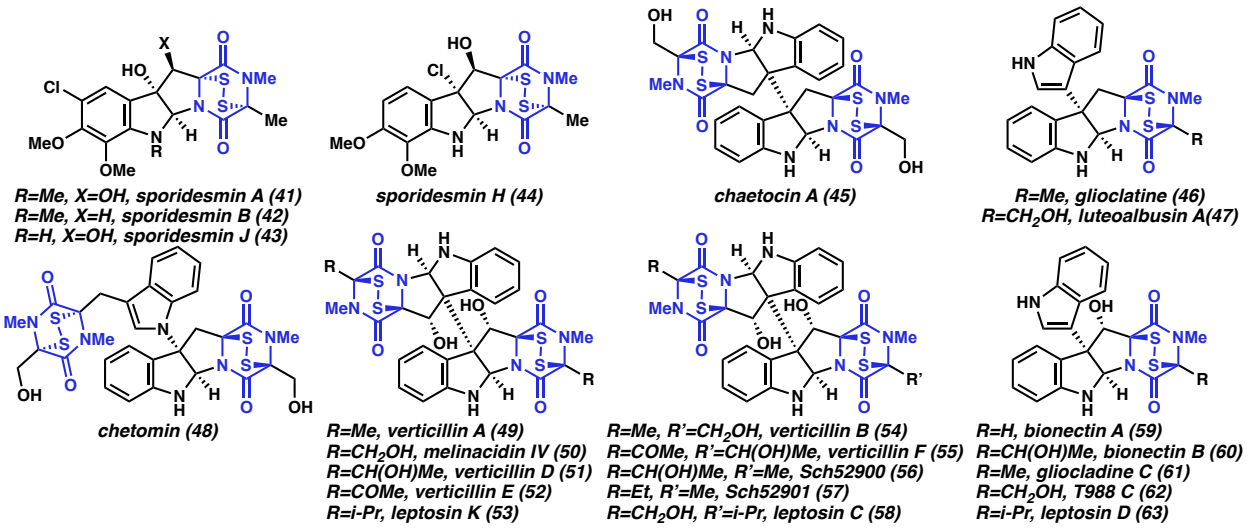

3,6-ETPs, with their noted [2.2.2]-disulfide core, are the most plentiful group of PTP natural products; however, other sulfur-containing DKP motifs have also been isolated. Many of the 3,6-ETPs shown above have sulfur bridge analogs, typically the trisulfide (**64**, Figure 1.4) and tetrasulfide (**65**).[60] Furthermore, 3,6-dithiomethylated analogs, including gliovictin[61,62] (**66**) as an analog of **15**, are also prevalent and have also been the subject of total synthesis efforts.[63–71] The least common motifs observed are mono-thiolated, unsaturated DKPs,[72] including emethacin A (**67**), and DKP natural products dimerized through two disulfides exclusively observed in the vertihemiptellides (**68–69**).[73]

The polythio linkage in some PTPs can also extend out from the α-carbon of DKP to the sidechain. As a result, the geometry of these disulfides diverge from 3,6-ETPs affecting both redox potential and overall stability of the disulfide.[74] Currently the mechanism by which these unusual linkages are formed biosynthetically is unclear. The epiccocins (**70-78**, Figure 1.4) demonstrate a

Figure 1.4: *PTP natural products which feature unusual sulfur connectivity*

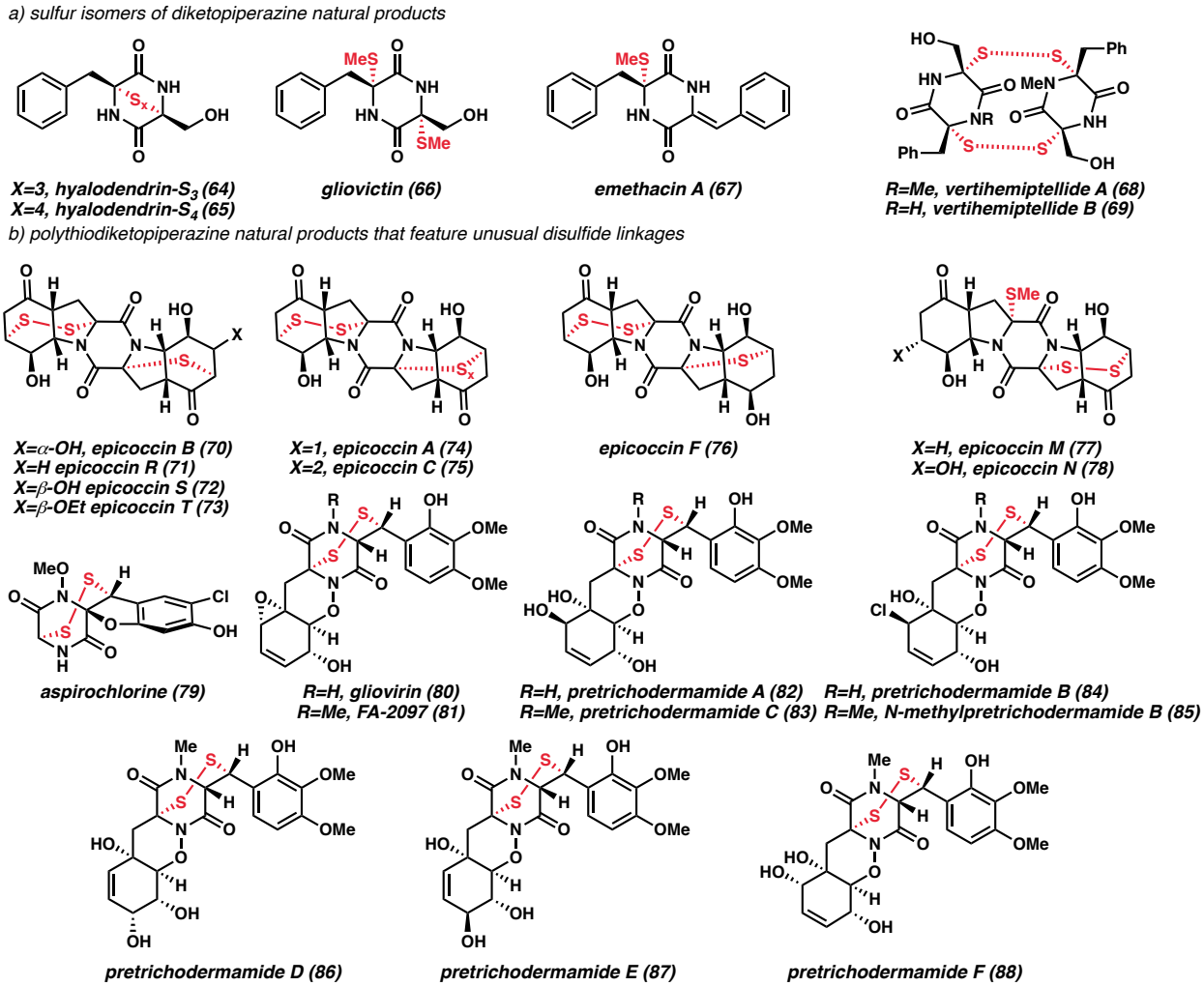

high degree of structural analogy with **26-28** (Figure 1.1) and also result from the functionalization of a Phe-Phe DKP; suggestively, however, the disulfide forms either at C7 or C8 where unsaturation observed in the epicorazines. Structural variation within the epicoccin family occurs in the variation of oxidation alpha to the side chain sulfur. Whether these products form through downstream enzymatic pathways from epicorazine biosynthesis or are generated through a disparate pathway that has not been identified through biochemical studies.

Finally, [2.2.3]-ETPs have been isolated exhibiting disulfide bridges with thiolation at an electron-rich benzylic position alpha to the DKP. Unique amongst PTPs, all known [2.2.3]-ETPs

have *N*-oxidation at an amide nitrogen, with many taking the form of an atypical heterocycle: a 1,2-tetrahydrooxazine. Aspirochlorine (**79**, Figure 1.4) was the first of this class of natural product to be isolated, initially termed A30641, in 1976.[75] As a result of its unusual connectivity the structure of **79** was not elucidated until semisynthetic studies were carried out by Sakata and Clardy in 1987.[76] Gliovirin[77] (**80**) and its *N*-methylated analog, FA-2097[78] (**81**), were isolated independently in 1982. While the structure of **80** was disclosed in the initial report, the structure of FA-2097 was not fully elucidated until 1984.[79] For 24 years, these three natural products remained the sole known [2.2.3]-ETPs, until the pretichodermamides A-F(**82-88**) were isolated from related fungi.[80–82] These newly isolated compounds had a high level of structural fidelity with **80** with only small variations occurring in the oxidation pattern of the western fragment and *N*-methylation of the amide nitrogen.

1.2.2 KNOWN MODES OF 3,6-ETP BIOACTIVITY

Due to their low availability from natural sources, the study of ETPs in biological systems has been, by no means, exhaustive; however, initial studies have established that their diverse structures demonstrate wide–ranging activity as antifungal agents, cytotoxins, antibiotics, antimicrobials, and antitumor agents.[83]

The bioactivity of ETPs is chiefly ascribed to the redox-active disulfide bond; the other functionality modifying the specificity of the protein–small molecule interactions. This disulfide moiety can interfere with biological processes through four distinct modes. ETPs can modulate the activity of proteins through interaction with cysteine residues by either directly forming protein-ETP conjugates[84] (Figure 1.5A) or modifying the confirmation of the protein through formation of disulfide bonds not present within native protein[85] (Figure 1.5B). ETPs can also

Figure 1.5. *Known modes of 3,6-ETP toxicity.*

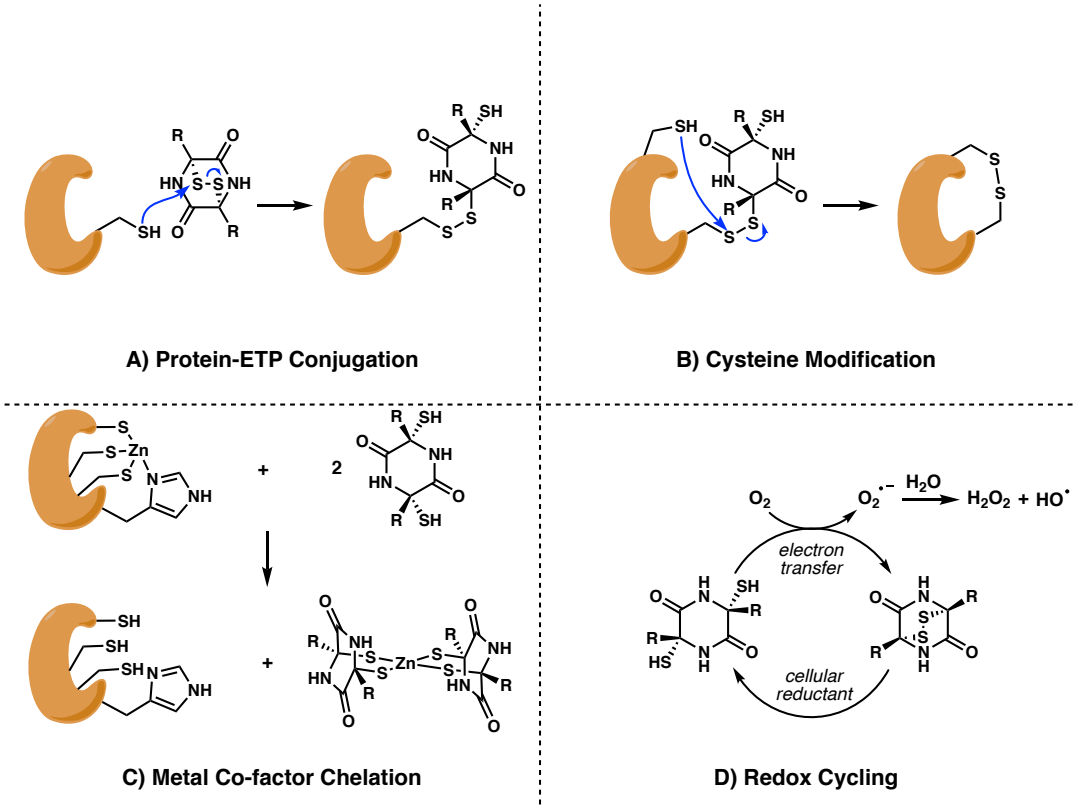

chelate metal co-factors to deactivate proteins.[86] Furthermore, these molecules can undergo a redox cycle to produce reactive oxygen species (ROS), such as superoxide radical anion or hydroxide radical, when in the presence of an appropriate reductant in the cellular environment (Figure 1.5C).[87,88] An ETP natural product can have multiple modes of toxicity operative to provide a given phenotype; therfore considerable biological studies are required to fully characterize the origins of their bioactivity.

1.2.3 BIOSYNTHESIS OF 3,6-ETPs

3,6-ETP biosynthesis has been the subject of much study with the greater portion directed toward the enzyme-mediated formation of gliotoxin, **16**. In the cell, gliotoxin synthesis begins with the cyclization of serine-phenylalanine dipeptide to form a diketopiperazine (DKP) carried out by

a non-ribosomal peptide synthetase (NRPS).[89,90] Thiolation of the resulting DKP is proceeds in two steps beginning with concombinant bishydrodroxylation at C3 and C6 of the DKP by a p450 monooxygenase (GliC). This hemiaminal **89** can then undergo subsequent thiolation with glutathione facilitated by a S-transferase (GliG).[91] An enzymatic cascade generates the dithiol (**98**, Scheme 1.3) from **90** through iterative degradation of the glutathione sidechains.[92] First, the naked cysteine residue is unveiled through action of a γ-cyclotransferase (GliK) and a dipetidase[93] (GliJ). Then a pyridoxal 5'-phosphate (PLP, **96**) dependent lyase (GliI) reveals the dithiol through the transient generation of a Schiff base **95**, before expelling pyruvate (**97**) and regenerating PLP.[94] Oxidation of **98** to the disulfide **99** is then facilitated by a dedicated dithiol oxidase (GliT). With the core ETP **99** formed in Scharf's studies. It has not been clearly established whether the biosynthetic pathway of **16** proceeds through dithiol or disulfide intermediates. However, given that as the disulfide moiety undergoes reversible reduction, and both **98** and the reduced form of **16** are substrates for GliT, the oxidase may act as oxidative regulator during the final oxidative manipulations en route to **16**. For simplicity, the pathway will be shown proceeding through **99**.

Scheme 1.2. *Enzymatic glutathione incorporation and degradation to a 3,6-dicysteinyl DKP*

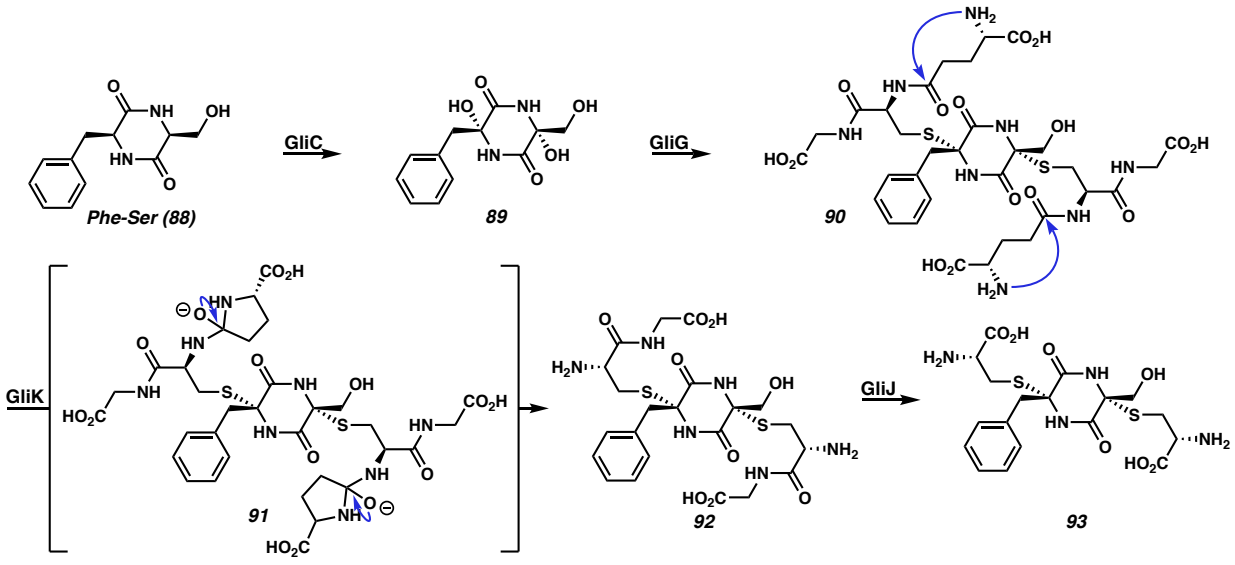

Scheme 1.3. *Conversion of a 3,6-dicysteinyl DKP to 3,6-ETP core and oxidation to gliotoxin*

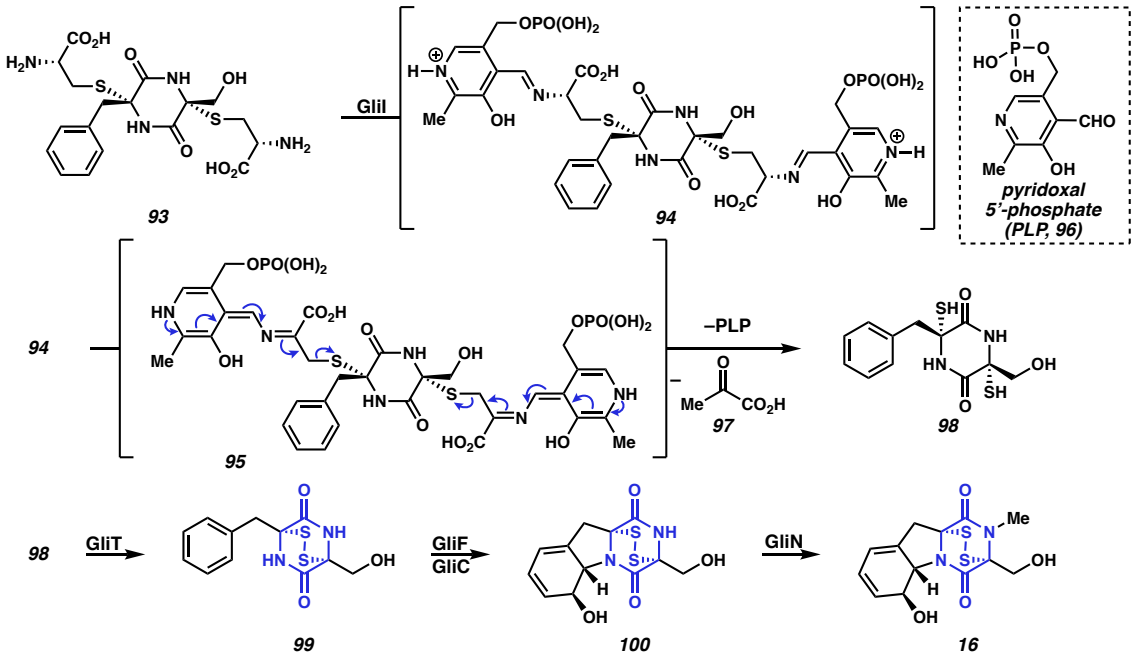

To complete the biosynthesis of **16**, the phenylalanine sidechain is proposed to be oxidatively dearomatized to the epoxy diene through the action of a p450 monooxygenase (GliF or GliC), which undergoes spontaneous ring closure via nucleophilic attack of the amide nitrogen to yield **100**. Finally, *N*-methylation of the amide proceeds through a methyl transferase (GliN) to yield **16**.

The biosyntheses of the other members are proposed to proceed in an analogy to **16** through a three-phase sequence: NRPS-mediated formation of the DKP from canonical amino acids; formation of ETP core via an enzymatic cascade; and oxidative modifications the ETP sidechains. ETPs are diverse family of natural products; however, their structures result from a small subset of canonical amino acids: Phe, Ser, Tyr, Trp, Ala, Val, Gly, Thr. Therefore, most of the variation in the biosynthetic pathway should reside in the enzyme-mediated modifications to the sidechains, after forming the core ETP as a common intermediate.

Aside from **15**, all phenylalanine derived ETPs feature cyclization of the amide. While rigorous biochemical studies have not been undertaken for the formation of the epicorazines or scabrosins, it is proposed that these derivatives are formed through further modification of a gliotoxin subunit (**102**) formed by analogous p450 monooxygenase-mediated cyclization of the amide.[27] To access the epicorazine motif (**105**) it is thought that the enone is formed through initial epoxidation of the more substituted alkene followed by a Meinwald rearrangement.[95] This electrophilic enone can then undergo a Michael addition or conjugate addition to generate a rostratin unit (**106**). Conversely, the scabrosin motif is thought to diverge from the gliotoxin pathway, instead proceeding through an S_N2'-type pathway to form dienol **108** facililated by some GliC or GliF mutant. The resulting intermediate (**108**) can then undergo epoxidation under the influence of a monooxygenase.

Originally, the dihydrooxepine moeity observed in both symmetrical and unsymmetrical ETPs, exemplified by **33** and **37** (Figure 1.1), were proposed to form through a sigmatropic ring expansion of **107** to form **110**, before undergoing a further oxidation and subsequent amide

Scheme 1.4. *Sidechain modification in the biosynthesis of phenylalanine-derived 3,6-ETPs*

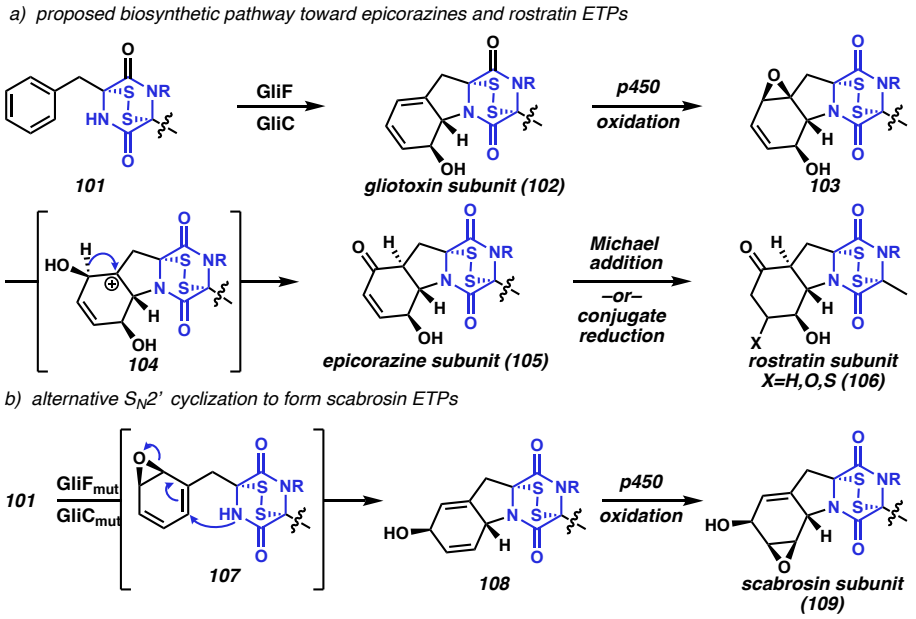

cyclization (Scheme 1.5a).[96] However, through genome-based deletion analysis, it has recently been shown that these 3,6-ETPs proceed through an analogous cyclization to other phenylalanine-derived ETPs, proceeding through **114** as a key intermediate before undergoing a direct oxidative ring expansion to form **34** (Scheme 1.5b).[97]

Scheme 1.5. *Sidechain modification in the biosynthesis of dihydrooxepine–containing 3,6-ETPs*

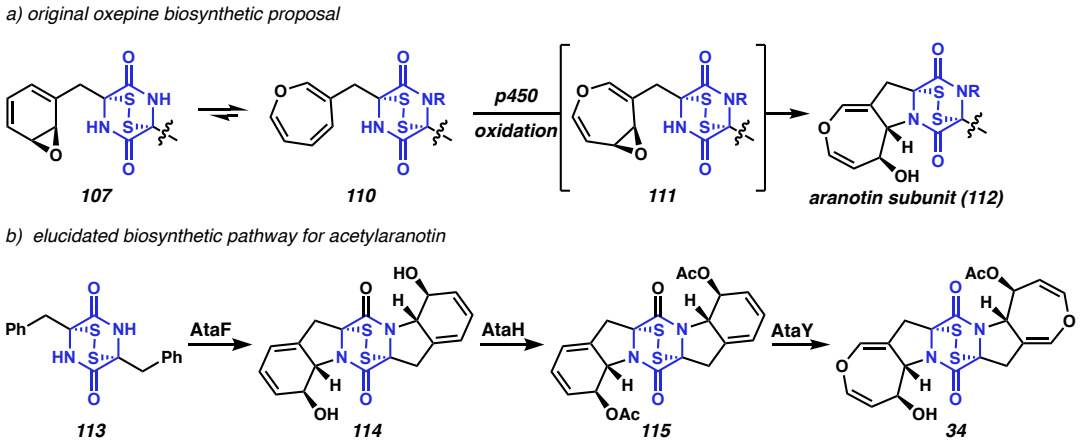

The gene cluster responsible for the biosynthesis of tyrosine-derived ETPs has been the subject of biochemical study; however, unlike **34** and **16** the distinct roles and order of each coded gene have not been fully elucidated.[98] A putative biosynthetic route has instead been proposed through labelling experiments and isolation of intermediates. In constrast to phenyalanine-derived ETPs, a prenyl transferase caps the phenolic oxygen prior to sulfenylation, either as the amino acid or after DKP formation.[99] The prenylated DKP **116** undergoes sulfenylation in analogy to other 3,6-ETPs to yield **117**. Bis *N*-methylation of **117** would yield **36** (Figure 1.2); however, **117** can also undergo a Claisen rearrangement and subsequent cyclization to form **119**.[100] The dihydrobenzofuran **119** can then undergo a p450 monooxygenase-mediated amide cyclization to form **120**, which can be further oxidation leading to the formation of phomalirazine (**37**). The sirodesmins can be generated from **37** through an oxidative rearrangement. Tetrasubstituted epoxide **121**, is prone to oxygen-assisted fragmentation. The resulting oxonium **122** can then be

Scheme 1.6. *Proposed biosynthesis of sirodesmin family of ETPs*

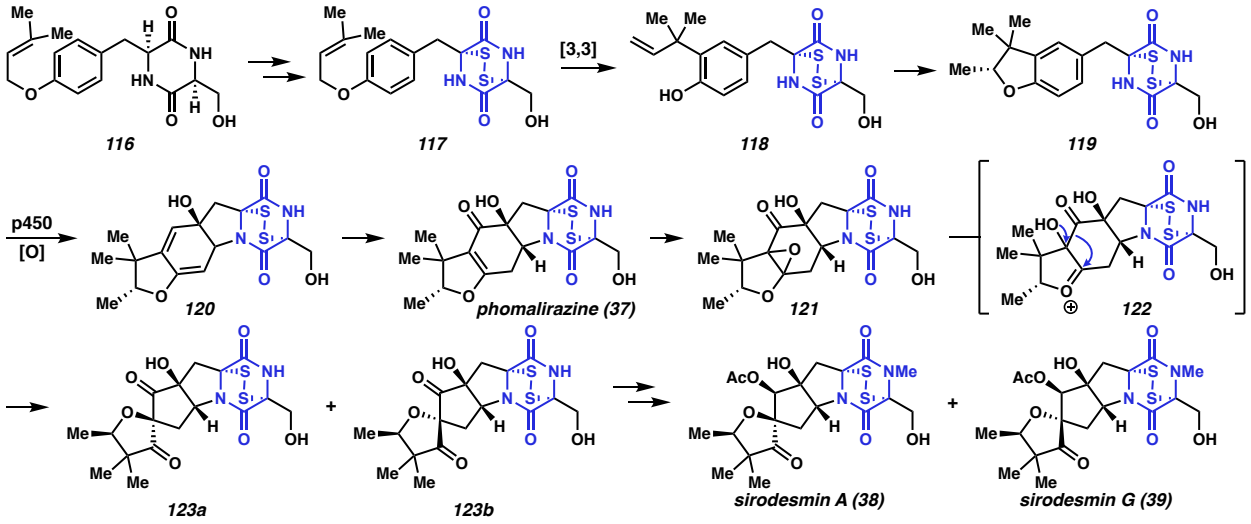

quenched through 1,2-carbonyl migration.[101,102] Based on the diasteroselectivity of the ring contraction epimeric spirocycles **123a** and **123b** are generated. Elaboration of these siprocyclic substrates via 1,2-reduction of the carbonyl, *O*-acylation, and *N*-methylation delivers sirodesmins **38** and **39**.

The gene cluster responsible for **45** biosynthesis has been sequenced and compared with those of **16** and **38**. As previously proposed, the sequences coding for 3,6-ETP core synthesis demonstrated homology with previously identified sequences in other biochemical studies.[103] The DKP **124** is formed through the action of a NRPS. Conversion of **124** to the 3,6-ETP core **125** occurs through *bis*-hydroxylation with p450 monooxygenase, chaC, followed by an analogous glutathione thiolation and degradation. Formation of the pyrroloindoline motif **126** is characteristic

Scheme 1.7*. Proposed biosynthesis of pyrolloindoline 3,6-ETPs via oxidative cyclization*

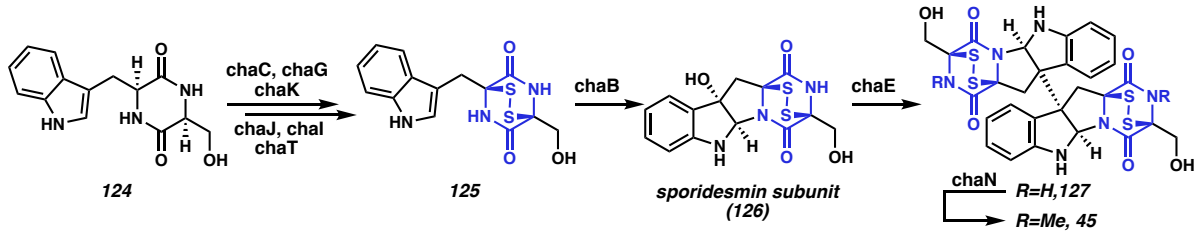

of tryptophan–derived 3,6-ETPs and proceeds via oxidative cyclization of the amide which is initiated a cyctochrome p450, chaB. Dimerization of the 3,6-ETP to form desmethyl-chaetocin A **127** is then facilitated by another cytochrome p450, claE. Finally, in analogy to **16** *N*-methylation of the remaining free amides would deliver the fully elaborated **45**.

1.2.3 BIOSYNTHESIS OF [2.2.3]-ETPs AND RELATED NATURAL PRODUCTS

The gene clusters responsible biosynthesis of [2.2.3]-ETPs **79** and **80** have been sequenced and compared with known enzymes.[104,105] Despite the structural dissimilarities of **79** and **80** both natural products are synthesized Phe-Phe DKPs. While the sequences responsible for [2.2.3]-ETP core synthesis were identified, their specific substrates and intermediates have not been fully elucidated. Hence, whether the origin of [2.2.3]-ETP specificity occurs due to rearrangement of 3,6-ETP (**130**) or through direct benzylic functionalization (**132**) remains a mystery. Despite this,

Scheme 1.8. *Proposed biosynthetic pathways for the formation of [2.2.3]-ETPs*

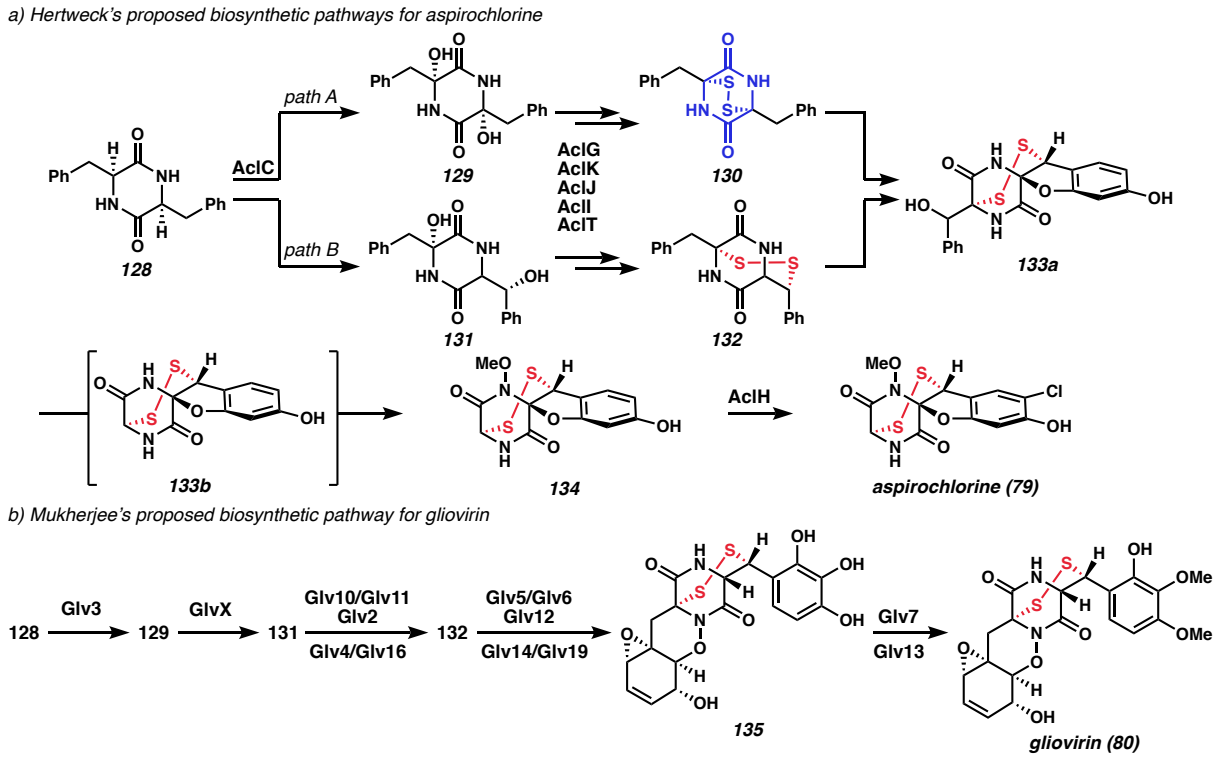

several key observations have been established. In the synthesis of **79**, the first on-pathway intermediate in the biosynthesis of **79** is **133**, with [2.2.3]-ETP core and extensive sidechain oxidation already incorporated. It is only after oxidative cleavage of the benzylic sidechain that *N*-methoxylation occurs. This observation runs in contrasts to previous results in the gliotoxin biosynthetic pathway where *N*-oxidized DKPs were observed in glutathione transferase deletion mutants.[106] Interestingly, to the characteristic aryl chloride of **79** is incorporated in the last step. In the biosynthesis of **80** Mukherjee proposes conversion from **129** to **131** prior to thiolation to install the [2.2.3]-ETP, however none of those intermediates were characterized in though their deletion studies. However, based upon Hertweck's study of **79** it is likely that [2.2.3]-ETP core synthesis and oxidation to the triphenol precedes both *N*-oxidation and the oxidative dearomatization to form the 1,2-tetrahydroxazine.

[2.2.3]-ETPs are densely functionalized natural products with reactive functionality,

Figure 1.6. *Natural products with structural homology to known [2.2.3]-ETPs*

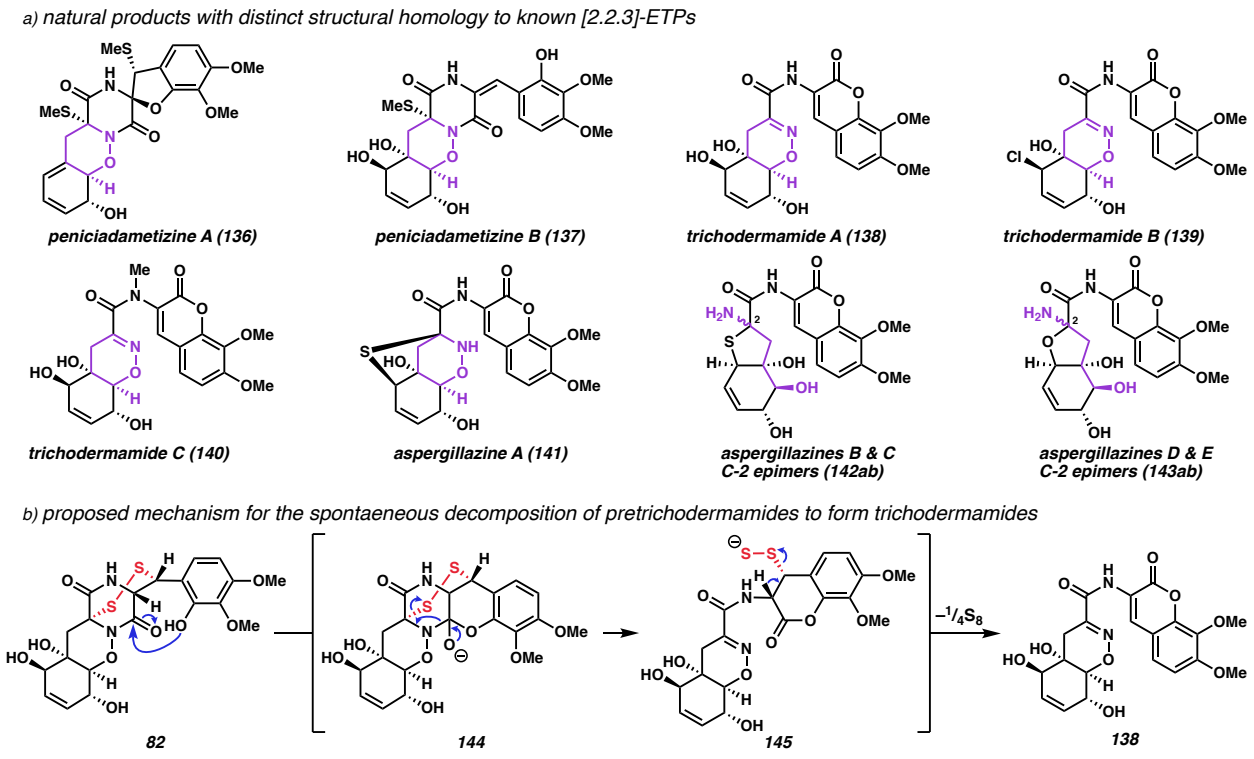

therefore, it is unsurprising that related natural products resulting from shunt pathways or through core rearrangement occurring in the cell media. Thiomethylated derivatives, **136** and **137** (Figure 1.6), were recently isolated in analogy to sulfur isomers **66** and **67** (Figure 1.4).[107] Furthermore, the trichodermamides (**138–140**) which were originally isolated independently from endophytic fungi[108,109] but are now proposed to be generated through spontaeneous decomposition of **83–85** as **138** was formed from **83** under mild protic conditions expelling the disulfide as elemental sulfur.[80] Other natural products appears to precipitate from N-O bond scission, as observed in the aspergillazines B-E (**142ab**, **143ab**).[110,111]

1.3 SYNTHETIC EFFORTS TOWARD EPIPOLYTHIODIKETOPIPERAZINES

The total synthesis of 3,6-ETPs has a rich history in organic chemistry motivated by their powerful bioactivity, their low availability from biological sources, and their diverse and highly functionalized structures. One the key area of study to enable this work is the development of methods toward the synthesis of the 3,6-ETP core.

Most methods for 3,6-ETP core synthesis proceed through an α-functionalized DKP substrate, reminiscent of the biological sulfenylation pathway. The 3,6-ETP core was first accessed by Trown through nucleophilic displacement of dibromide **146** (Scheme 1.9) with thioacetate followed by saponification to generate a dithiol, which is subsequently oxidized to the requisite disulfide **147**.[103] Method development accelerated in the 1970s through the sulfenylation of DKP substrates with varying α-functionalization. Schmidt demonstrated that dibromide **147** could be sulfenylated with a polydithiolate, subsequent reduction of the polythio bridge and re-oxidation generates the desired core.[113] Kishi showed that under Lewis–acidic conditions unsaturated DKP **148** could be thiolated by an aryltrithiolane, to form a thioacetal which can be unmasked generate

Scheme 1.9. *Selected methods for 3,6-ETP core synthesis from the α-functionalized substrates*

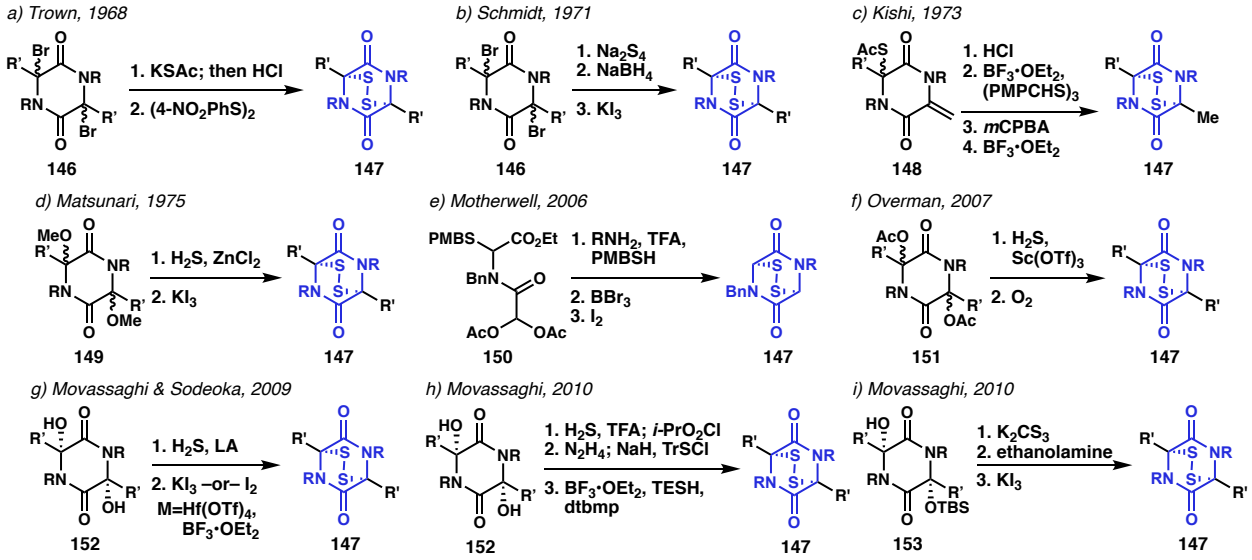

147 in two steps.[114] As a major advance direct formation of the dithiol was attained by Matsunari, using hydrogen sulfide as a nucleophile in conjugation with zinc chloride to activate bismethoxylated **149**, through the generation of an iminium intermediate.[115] These methods remained the state of the art for almost 30 years until a tandem cyclization–sulfenylation presented itself as an orthogonal approach. While this method was concise, it was not adopted widely toward the synthesis of 3,6-ETPs.[116] Instead synthetic groups revisited Matsunari's approach using hydrogen sulfide through the optimization of Lewis acids and the α-oxidized DKP substrates.[117–119] These modified conditions were efficacious in a variety of applications; however, some substrates were unreactive. To generate the desired motif in these less reactive substrates, the Movassaghi lab found that integration of a polysulfide chain at a singular position on a DKP substrate could undergo subsequent Lewis acid-mediated cyclization to generate the 3,6-ETP core,[120] as well other sulfur nucleophiles could be used.[118]

While the lion's share of 3,6-ETP core synthesis resulted from the thiolation of α-functionalized DKPs, direct thiolation has been observed. Treatment of elemental sulfur with

Scheme 1.10. *Selected methods for 3,6-ETP core synthesis through direct sulfenylation of DKPs*

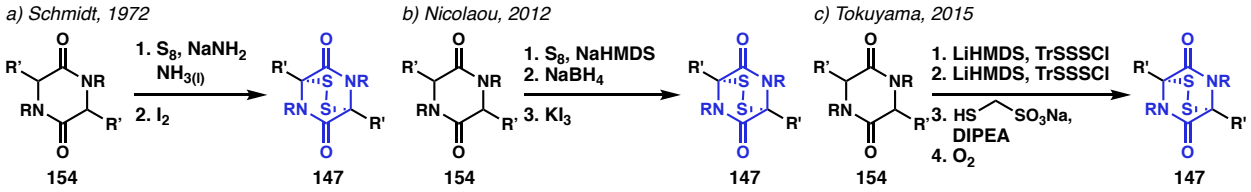

sodium amide in ammonia, results in generation of a dithiol which could then be oxidized to form the disulfide (**147**, Scheme 1.10a**)**.[121] These conditions were not amenable to more sensitive substrates; yet the substitution of bulky strong bases, the hexamethyldisilazides, in place of sodium amide gave improved results for the direct thiolation of DKPs, both with elemental sulfur[122] and a protected sulfur chloride.[123] Unlike Schmidt's original conditions, these novel conditions yield polythiolated intermediates which are reduced to the dithiol prior to the final oxidation to yield the disulfide bridge.

Methods for 3,6-ETP core synthesis have been optimized under both Lewis acidic and strongly basic conditions, ensuring that the synthetic chemist has flexibility in the substrates that can be targeted as intermediates in the total synthesis of 3,6-ETP natural products.

1.3.2 TOTAL SYNTHESES OF EPIPOLYTHIODIKETOPIPERAZINES

The earliest syntheses of 3,6-ETPs were accomplished in studies by Kishi and coworkers. Their first synthetic efforts were toward to sporidesmin A&B (**41-42**, Figure 1.3).[114,124] Strategically, Kishi targeted a protected 3,6-ETP core as a key intermediate (**157**) before incorporating the sidechain functionality. An unsaturated monothiolated DKP (**156**, Scheme 1.11) was generated in two steps, which was subsequently converted to the thioacetal **157** after deprotection of the thioacetate. Stoichiometric deprotonation of **157** occurs selectively alpha to the MOM protecting group, which efficiently coupled with a functionalized acid chloride **158**, an

Scheme 1.11. *Kishi's syntheses of sporidesmin A&B*

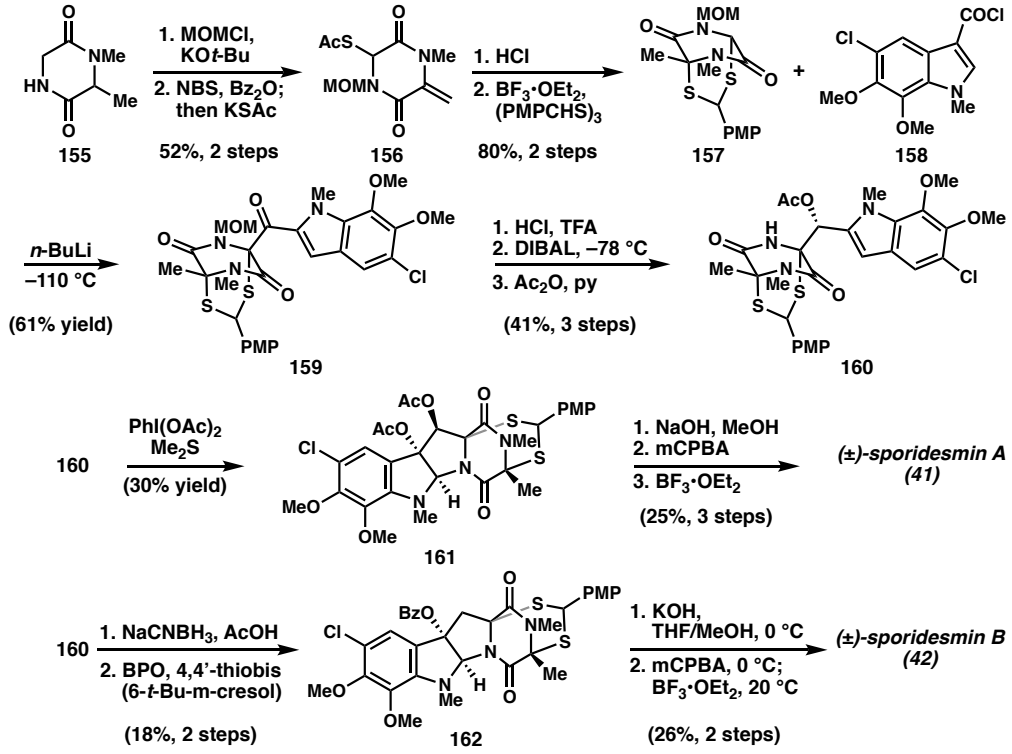

indole substrate accessed from commercially available starting materials in 4 steps and 51% cumulative yield. Coupled product **159** was converted to **160** in three steps, with installation of the hydroxyl group through diastereoselective reduction. Acetate **160** acts as a key intermediate for the divergent synthesis of **41** and **42**. Direct oxidative cyclization **160** gave **161**, which could be converted to **41** in three steps. To synthesize **42** the acetate was reduced to the methylene before being subjected modified oxidative cyclization conditions to generate **162** which could be advanced to **42** in two steps analogous to the final sequence of to access **41**. Despite their reliance on some low yielding transformations, these syntheses were ground breaking. Furthermore, the use of an oxidative cyclization to install the key pyrroloindoline motif would be later revisited and extensively refined by other synthetic groups in the pursuit of other tryptophan-derived 3,6-ETP natural products.

With Kishi's success in the synthesis of **41** and **42**, it was consider whether this strategy of

Scheme 1.12. *Kishi's racemic synthesis of gliotoxin*

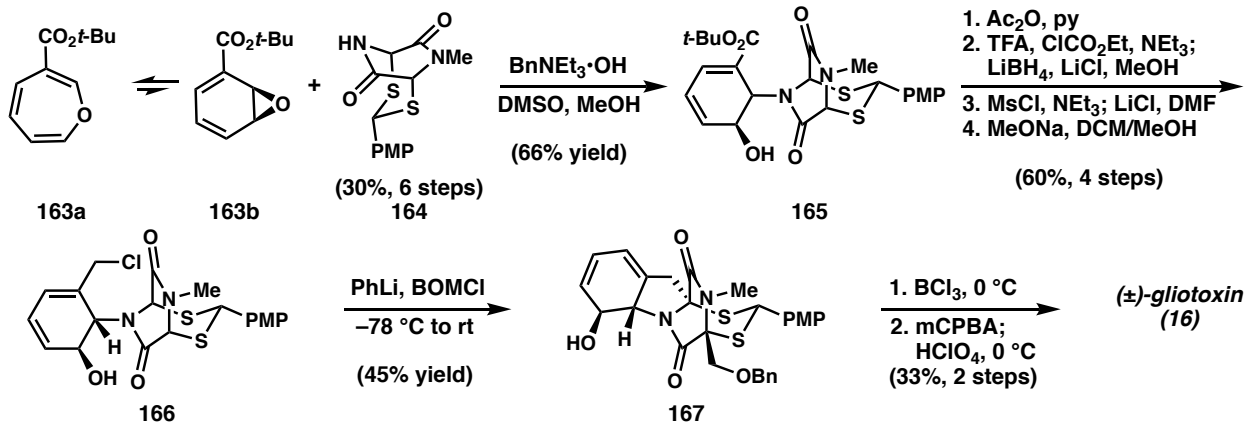

3,6-ETP core generation followed by elaboration of the side-chains could be generally applied to the synthesis of other 3,6-ETPs. With that in mind, they turned their efforts toward the synthesis of **16**[125] (Scheme 1.12) and its aromatized analog **17** (Scheme 1.13).[126] The protected 3,6-ETP **164** is synthesized in six steps, using the Trown conditions to generate the dithiol (Scheme 1.9a), with the 3,6-ETP core in hand, base–mediated attack of epoxy diene **163b**, in equilibrium with oxepin **163a**,[127] generates **165** as the major diastereomer. A four-step sequence converts the ester to benzyl chloride **166**. Upon exposure to excess strong base not only promotes cyclization to generate the desired pyrollidine, additional deprotonation at the bridgehead site on the opposite side can be quenched with a chloromethyl ether to install the serine side chain to generate **167**; a further two steps unveil **16**.

As **17** had less sensitive functionality than **16**, Kishi took an alternative approach integrating the aryl moiety prior to formation of the protected 3,6-ETP core.[126] While Kishi showed that copper–catalyzed *N*-arylation of DKP **169** generates their sulfenylation substrate **171**, later work by Wood[128] showed that direct DKP formation from the aniline **168b** was a more scalable alternative. The rest of the synthesis proceed in analogy to **16**, through tandem cyclization of a benzyl chloride **173** with concomitant alkylation with a chloromethyl ether. This is followed by

Scheme 1.13. *Kishi's total synthesis and Wood's formal synthesis of dehydrogliotoxin*

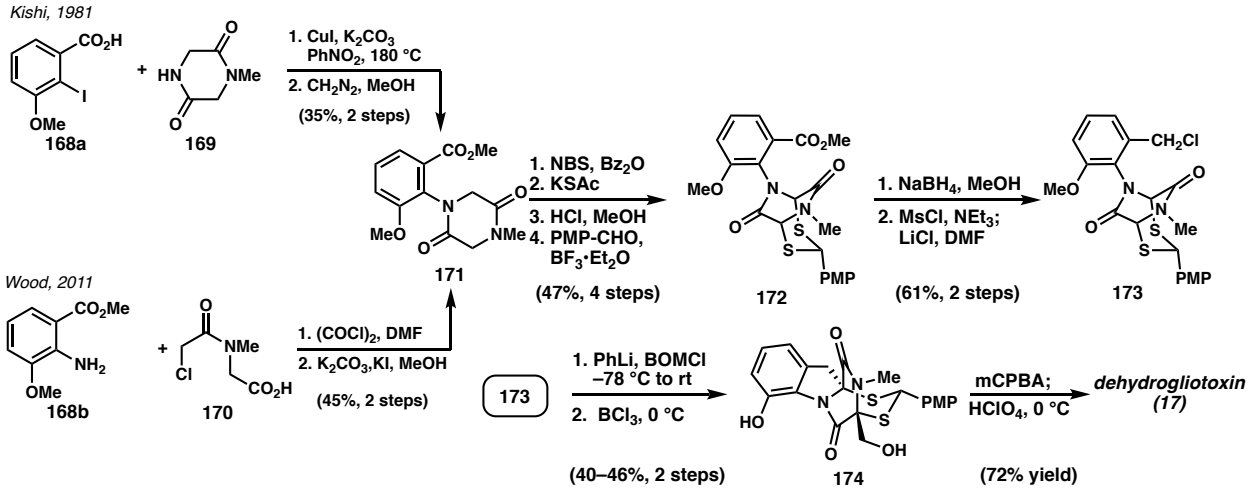

global deprotection and formation of the disulfide to yield the target **17**.

The first synthesis of **15** by other chemists followed the an identical strategy to Kishi (Scheme 1.14a); through iterative alkylation of a symmetrical protected 3,6-ETP **175** to generate **176**, followed by similar deprotection and disulfide formation.[129] The synthesis of **16** was revisited by Williams, in 1980, with a novel strategy focused on side chain substitution prior to sulfenylation to form the 3,6-ETP core.[130] The hydoxymethylene is incorporated through

Scheme 1.14. *Early syntheses of hyalodendrin*

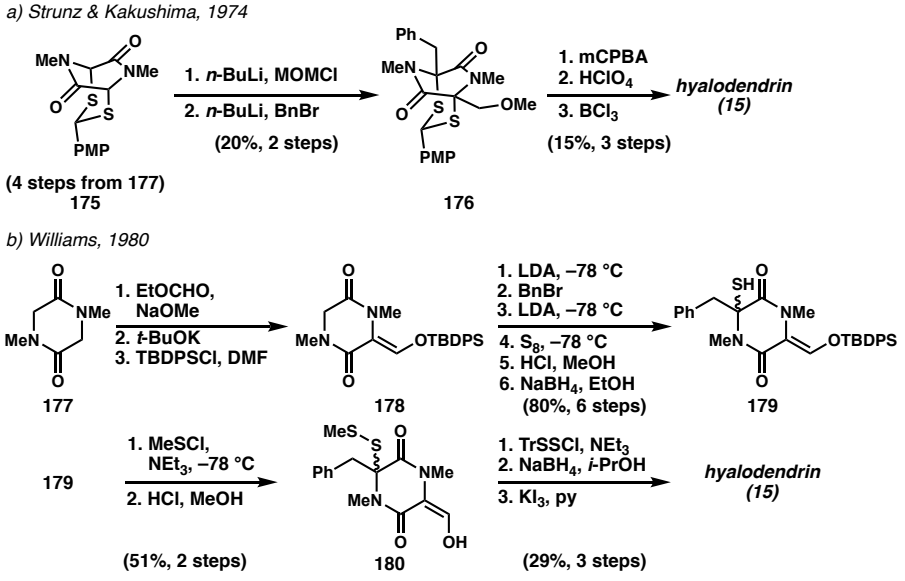

Scheme 1.15. *Fukuyama's novel synthesis to of hyalodendrin*

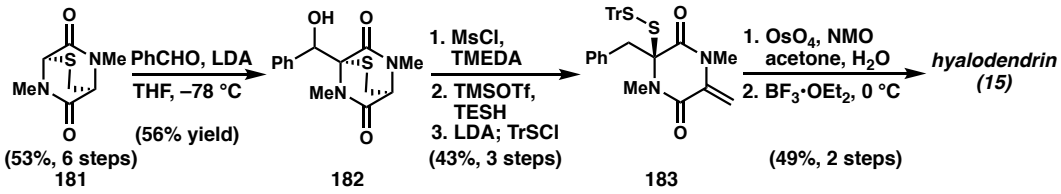

an aldol reaction, which subsequently protected as the silyl enol ether **178**. Benzylation occurs through enolate alkylation, which is followed by monothiolation through a Schmidt reaction (Scheme 1.9b) to provide **179**. The monothiol is capped as a disulfide before the thiolation of the enol proceeds with a sulfur chloride electrophile. The resulting *bis*-disulfide is then reduced to the dithiol before being re-oxidized to the disulfide **15**. While, Williams synthesis has higher step count from DKP **177** when compared to the Strunz & Kakushima synthesis (14 steps versus nine steps) the overall yield is significantly improved.

Finally, Fukuyama demonstrated an orthogonal strategy to synthesizing **15** as a proof-of-concept from a novel bicyclic intermediate **181**, accessible in 6 steps from commercial materials.[131] The benzyl moiety is integrated through an aldol reaction. The benzylic alcohol activated with mesyl chloride prior to reduction. The reduced product is then exposed to strong base in the presence of a sulfur chloride which cleaves the bridging thioether to yield and unsaturated disulfide **183**. The synthesis is then completed through dihydroxylation of exocyclic olefin followed by activation of C6 under Lewis acidic conditions reminiscent of a Movassaghi sulfenylation strategies (Scheme 1.9h). While Fukuyama's synthetic strategy has merit for its novel approach, it does not represent a significant increase in synthetic efficiency toward **15**.

Synthetic studies towards oxidatively modified phenylalanine-derived 3,6-ETPs were initiated by the Diver group toward the scabrosins (**21-25**, Figure 1.1). In contrast to Kishi and Williams, their strategy proposed accessing the scabrosins through the synthesis of the constituent

non-canonical amino acids prior to DKP formation and sulfenylation. Tactically, synthesis of an enantioenriched propargyl glycine **185** proceeds smoothly through enantioselective alkylation followed by enyne metathesis to form a cyclohexadienyl amino acid. Unfortunately, the Backvall chloroacetoxylation was low yielding and featured no diastereoselectivity; however, the desired diastereomer could be isolated cleanly to provide **186**. *N*-deprotection was followed by a base–mediated cyclization to form the desired 6-5 bicyclic motif **187**. This key intermediate **187** was advanced to the DKP **190** through the coupling *N*-boc amino acid **188** with amino ester **189** followed by cyclization. While this strategy was able to form the pentacyclic core, **190** could not be further elabolated through further oxidation or sulfenylation toward the synthesis of **21**.

The synthesis of scabrosins was revisited by Carriera[132], strategically in line with Williams

Scheme 1.16. *Unsuccessful synthetic approaches to the scabrosin pentacyclic framework*

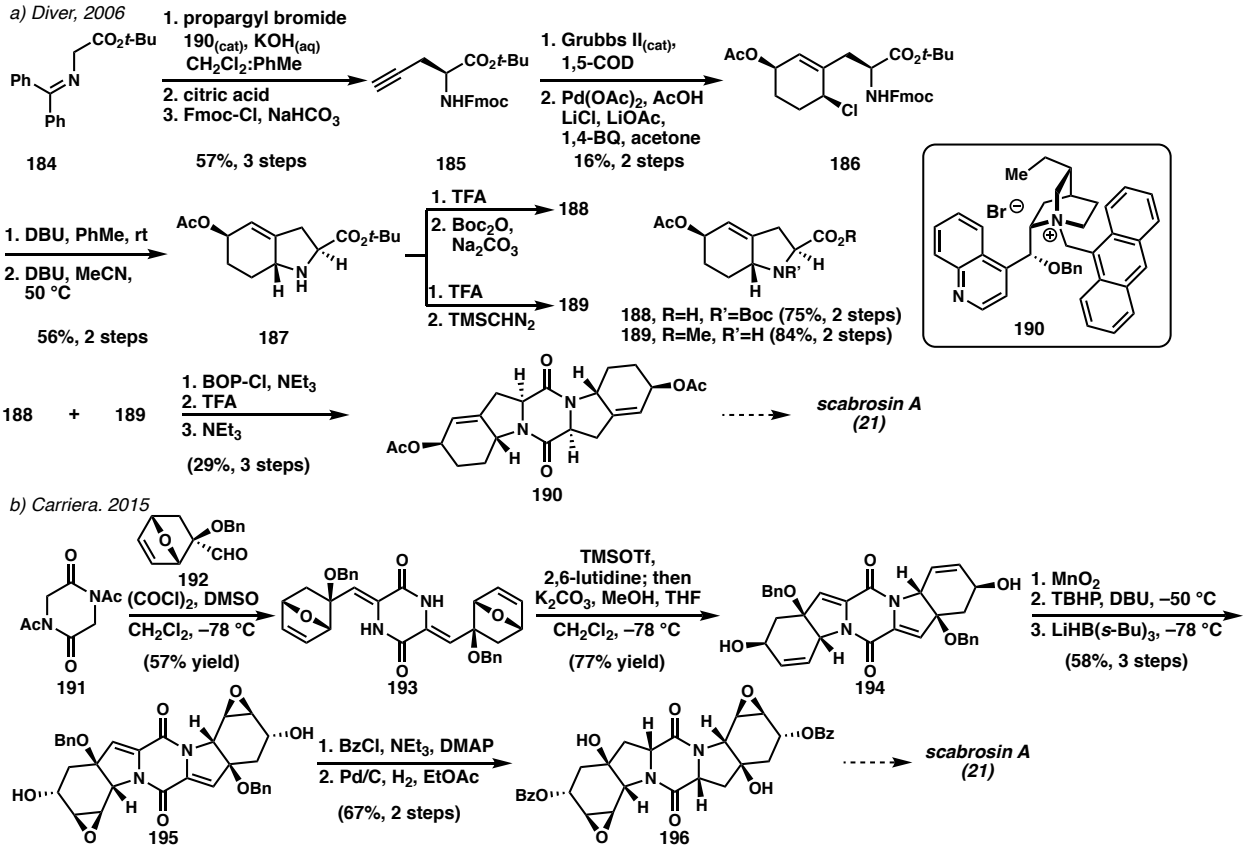

elaborating a DKP substrate before late-stage sulfenylation. Enabled by studies by Loughlin[133] a *bis*-*N*-acylated DKP was directly converted to the unsaturated **193**, formation of the requisite 6-5 bicyclic sidechains proceeds efficiently through Lewis acidic activation of the bicylic ether. Directed epoxidation of *bis*-allylic alcohol led exclusively decomposition. To circumvent this deleterious reactivity, the allylic alcohol was oxidized to the enone which readily undergoes epoxidation under modified Weitz-Sheffer conditions. Unfortunately, 1,2-reduction generates the opposite diastereomer and further oxidative elaboration to the allylic epoxy alcohol was unsuccessful.

While efforts toward the scabrosins were unsuccessful, efforts toward tryptophan-derived 3,6-ETPs were more fruitful. A concise synthesis of (+)-11,11'-dideoxyverticillin A (**200**, Scheme 1.17) was accomplished by Movassaghi.[118] Unlike the early syntheses of 3,6-ETPs their strategy focused upon late-stage dimerization and sulfenylation. Similar to Kishi's oxidative cyclization in the syntheses of the sporidesmins, the DKP **197** can undergo a bromocyclization yielding an intermediate with a functional handle for a radical cobalt-mediated dimerization. Following dimerization, both DKPs were activated for sulfenylation through tetraoxidation prior to exposure to thiocarbonate as a nucleophilic sulfur source. The disulfide **200** was unveiled through two-step sequence.

This bromocyclization strategy was effectively used by Movassaghi in the synthesis of another dimeric 3,6-ETP chaetocin[120] (**45**, Scheme 1.18) as well the indolinated 3,6-ETP

Scheme 1.17. *Movassaghi's Synthesis of (+)-11,11'-dideoxyverticillin A*

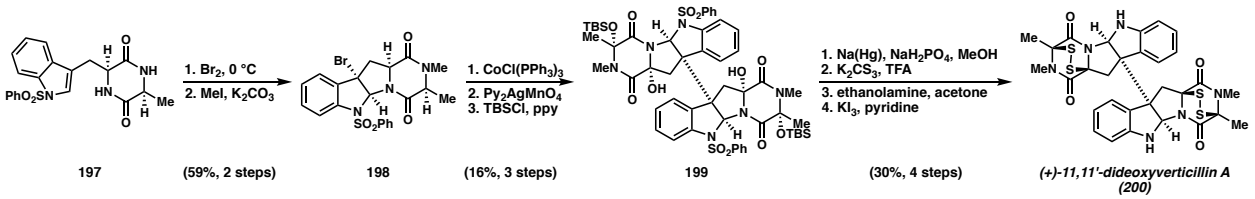

Scheme 1.18. *Movassaghi's syntheses of chaetocin and luteoalbusin*

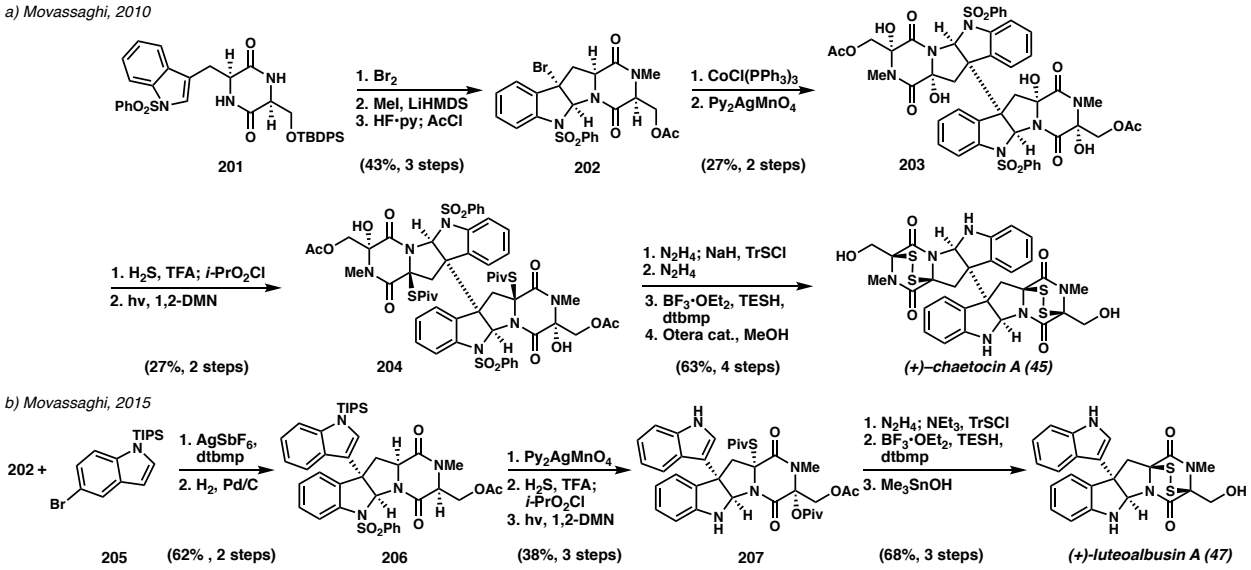

luteoalbusin A[134] (**47**). To synthesize **45**, an analogous dimeric tetrahydroxylated DKP **203** was readily accessed; however, in contrast to their synthesis of **200** the intial sulfenylation of the activated **203** led only to monothiolation of each DKP subunit. However formation of an acyclic disulfide was successful, with the disulfide incorporated, further activation of the DKP under Lewis acidic conditions resulted in an intramolecular cyclization to yield the disulfide moiety of the natural product **45**. This same sulfenylation tactic was successful in the later synthesis of **47** which diverged from **45** only in the early incorporation of the indole through a silver-mediated coupling with key intermediate **202.**

Movassagahi was also successful in the synthesis of bionectin A (**59**, Figure 1.3) an indolinated 3,6-ETP with an additional oxidation on the bicycle. Strategically, this synthesis focused on the initial synthesis of a DKP derived from non-canonical amino acids followed by incorporation of the indole and late stage sulfenylation.[68] The additional oxidation was incorporated early through an aldol reaction with **208** and **209** with high diastereoselectivity informed by a chiral auxiliary (Scheme 1.19). Amide coupling with sarcosine followed by

Scheme 1.19. *Movassaghi's Synthesis of (+)–bionectin A*

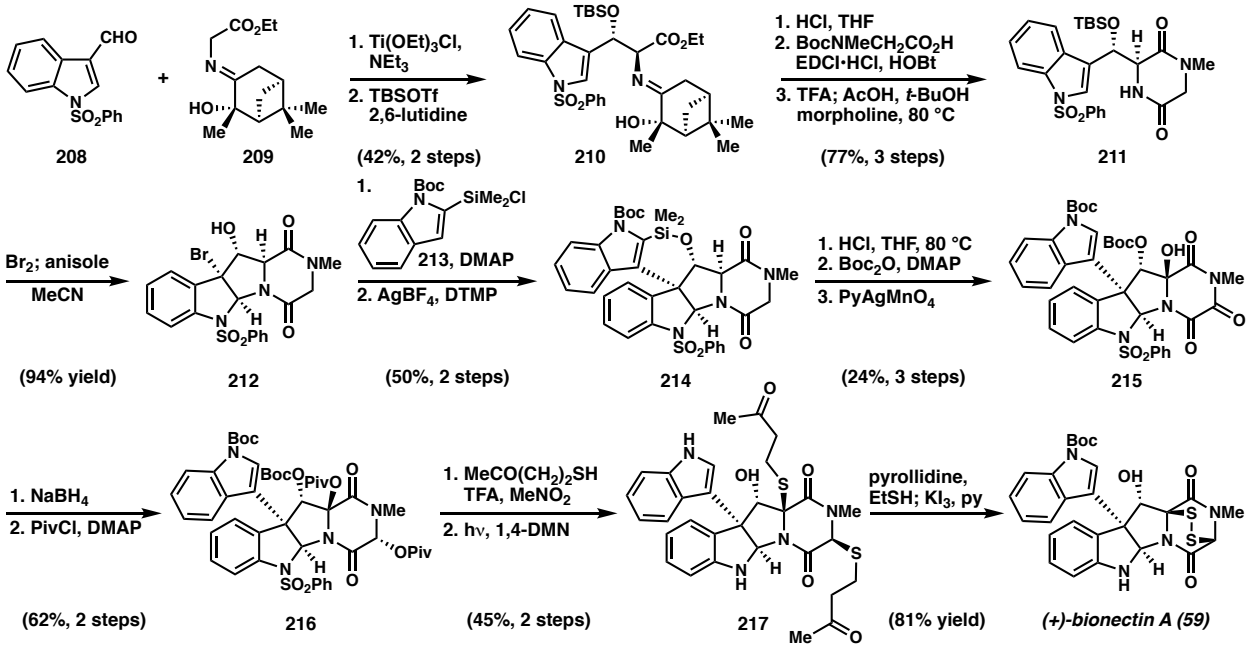

intramolecular cyclization provided the DKP substrate **211** primed for bromocylization. To incorporate the indole moiety in this synthesis they chose to bring it in with a silyl tether prior to the C-C bonding step. Protecting group exchange was important prior to *bis*-hydroxylation of the DKP which again activated the substrate for sulfenylation with a nucleophilic sulfur source, which could be converted to the dusilfude **59** in a one-pot procedure.

Concurrent with Movassaghi's program, Overman developed a unified strategy toward C10-indolinated 3,6-ETPs. Favoring synthesis of the indolated sidechain through asymmetric carboxylation of C2-indolinated oxindole **219** (Scheme 1.20) prior to incorporating into an unsaturated DKP **223** through condensation. In contrast to Movassaghi's work resulting unsaturated **244** could cyclize under Lewis-acid activation of a hemiaminal to form **225** as a key intermediate. Exposure to Grignard or a strong reductant led to mono-hydroxylated DKPs **226-228**. The unsaturaturation was then used as a handle to incorporate necessary oxidation diastereoselectively but also to activate the DKP for Lewis acid-mediated sulfenylation which

Scheme 1.20. *Overman's Unified Strategy to Access C10-indole pyrroloindoline 3,6-ETPs*

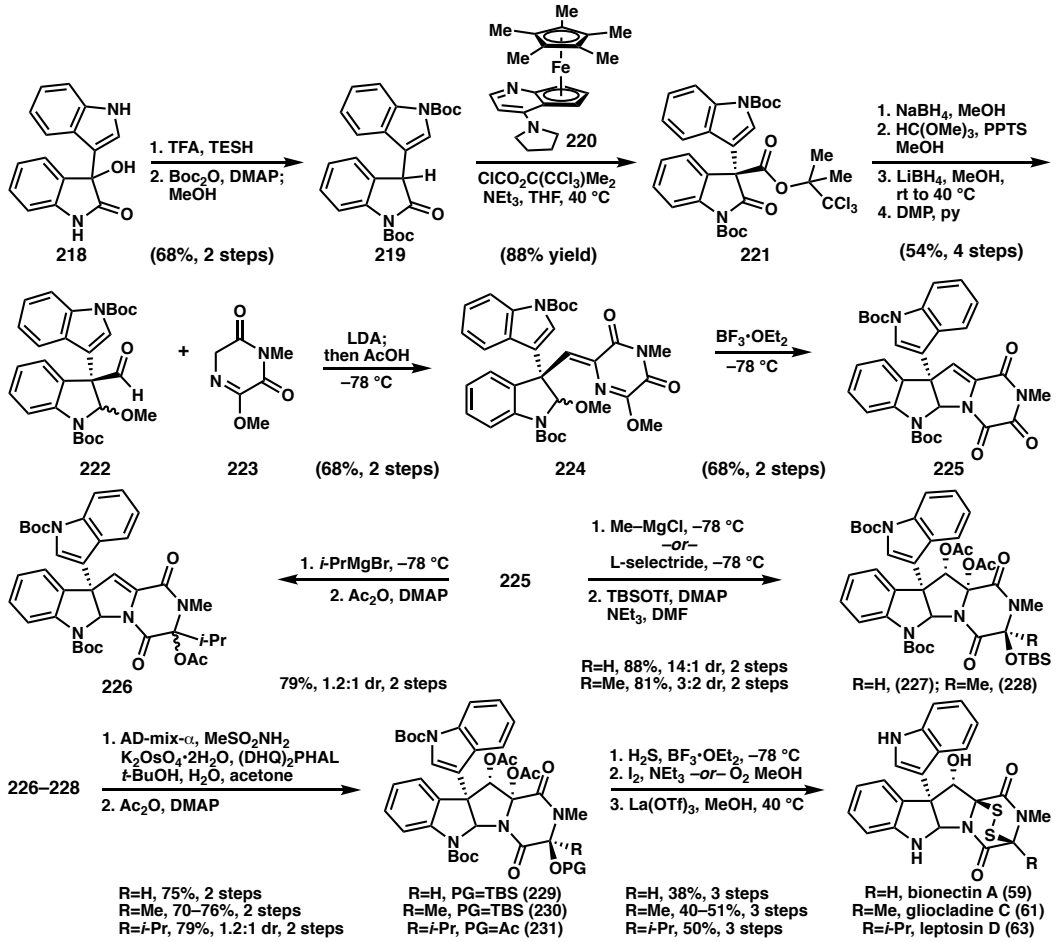

could be expediently converted into three C10-indolinated 3,6-ETPs **59**, **61**, and **63**.

Martin was later able to generate racemic formal syntheses of C10-indolinated 3,6-ETPs in a similar fashion to Overman's approach while refining some of the tactics.[135] Generating a *bis*–enamide *in situ* prior to exposure to the highly electrophile isatin to generate **234**. Unlike Overman, Martin then incorporates the requisite indole through Lewis acidic activation of the allylic alcohol. Cyclization was then accomplished under reducing Lewis acidic conditions to yield unsaturated DKP **236**. This key intermediate could either be brought through Overman's sequence to access **62** in seven steps or radical hydroxylation and protecting group manipulations could generate **237** which could be advanced **61** in a further 4 steps.

Scheme 1.21. *Martin's formal syntheses of (+/–)-gliocladine C and (+/–)-T988C*

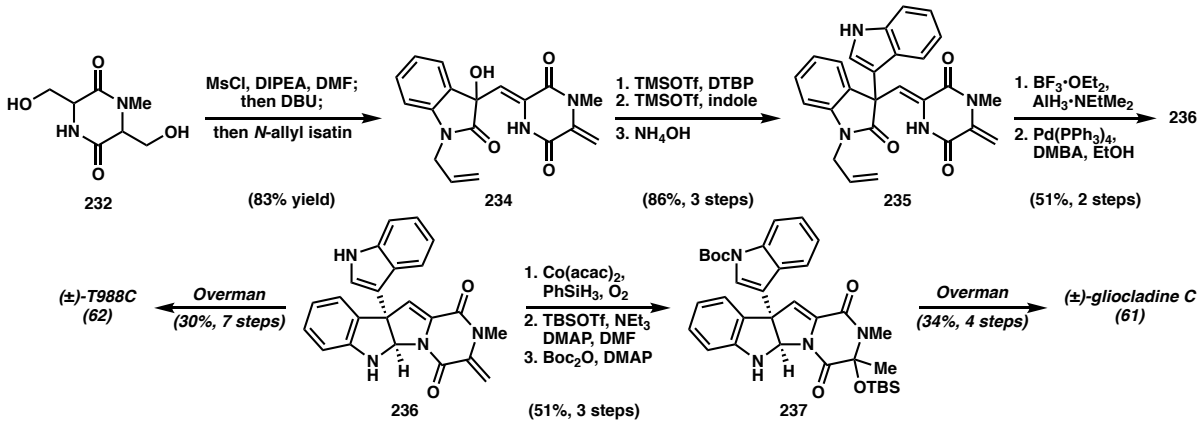

The synthesis dimeric trypophan-derived 3,6-ETPs was also revisited by Sodeoka taking Movassaghi's synthetic strategy and refining the tactics, resulting in a more efficient synthesis of **45** (Scheme 1.22). Paramount to this effort was the recognition that an efficient *bis*-hydroxylation could be carried out prior to cobalt-mediated dimerization. Furthermore, engaging the resulting tetrahydroxylated dimer with the sulfenylation conditions that had been refined by Overman in his synthesis of C-10 indolinated 3,6-ETPs directly formed the tetrathiol which could be directly oxidized to **45**.

Since, Kishi's landmark synthesis of **16** the further synthetic studies were not undertaken until Nicolaou. In contrast to Kishi's building-out strategy, Nicolaou took a similar approach as other modern 3,6-ETP synthetic strategies, through the synthesis of fully functionalized non-canonical amino acids and late stage sulfenylation.[65] **240**, derived from tyrosine, could be

Scheme 1.22. *Sodeoka's Concise Synthesis of (+)–chaetocin A*

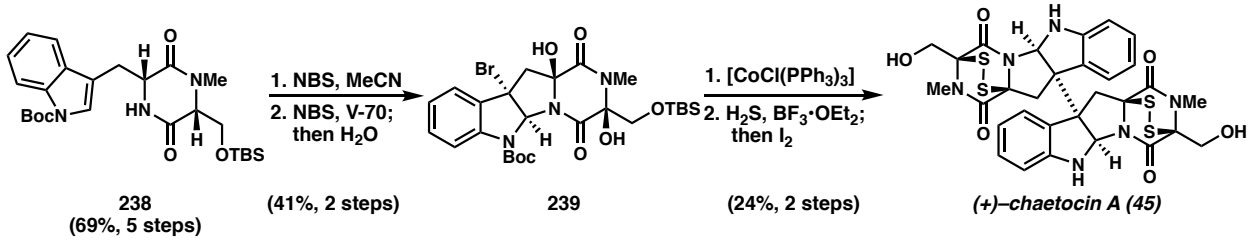

converted to dienyl **241** in three steps through palladium mediated elimination of an allylic acetate. A successful [4+2] with singlet oxygen formed an endo peroxide which could reduced to the triol **242**. The gliotoxin amino acid was finally generated through Corey-Winter olefination, forming **243.**

This unnatural *N*-boc amino ester **243** was a versatile intermediate, coupling with a protected serine derivative to generate **16** or could be further elaborated to the symmetrical 3,6-ETP **18**. Direct sulfenylation was a novel procedure as a refinement of Schmidt's early work. Furthermore, Nicolaou through the synthesis of an epimeric rostratin derivative (**255**) that early formation of the 6-5-6-5-6 pentacylic framework could set up the substrate for expedient oxidation

Scheme 1.23. *Nicolaou's synthesis of 3,6-ETPs containing the gliovirin subunit*

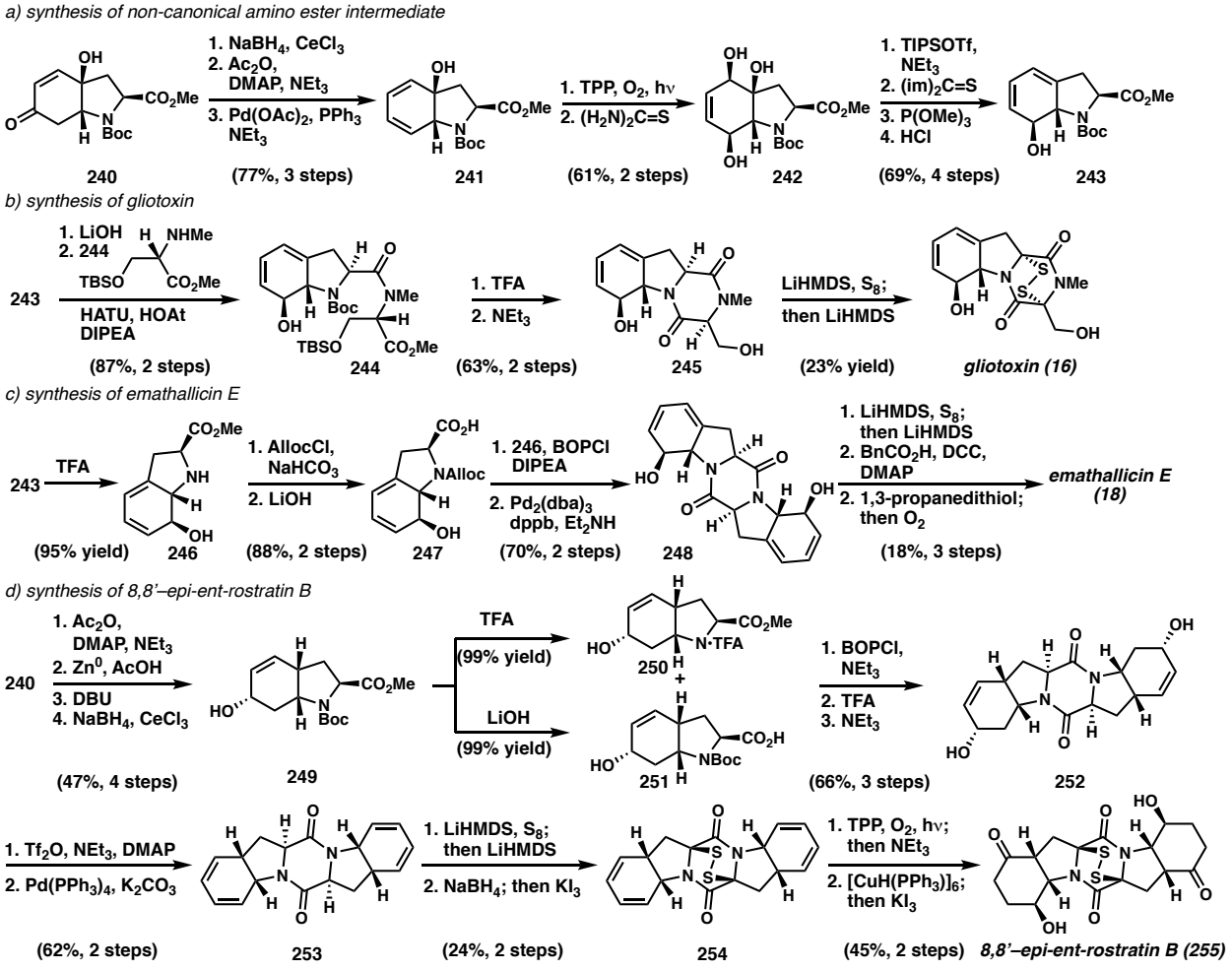

of the side chains after disulfide formation. Unsaturated 3,6-ETP **254** was rapidly functionalized through a singlet oxygen [4+2] in analogy to **242**; however, a Kornblum–DeLaMare rearrangement generated the keto-alcohol instead of the diol. Subsequent conjugate addition followed by oxidative work-up provides the highly functionalized 3,6-ETP **255**.

The first successful synthesis of dihydrooxipene ETP was accomplished by Reisman in 2012, through the synthesis of a non-canonical amino acids and late-stage sulfenylation .[136] In contrast to other 3,6-ETP syntheses the stereochemistry of the pyrollidine was set first through a dipolar cycloaddition of an azomethine ylide. Pyrollidine **257** could be elaborated to propargylated alcohol **260** in a further eight steps which underwent rhodium-mediated cyclization to generation

Scheme 1.24. *Reisman's Syntheses of oxepine-containing 3,6-ETPs*

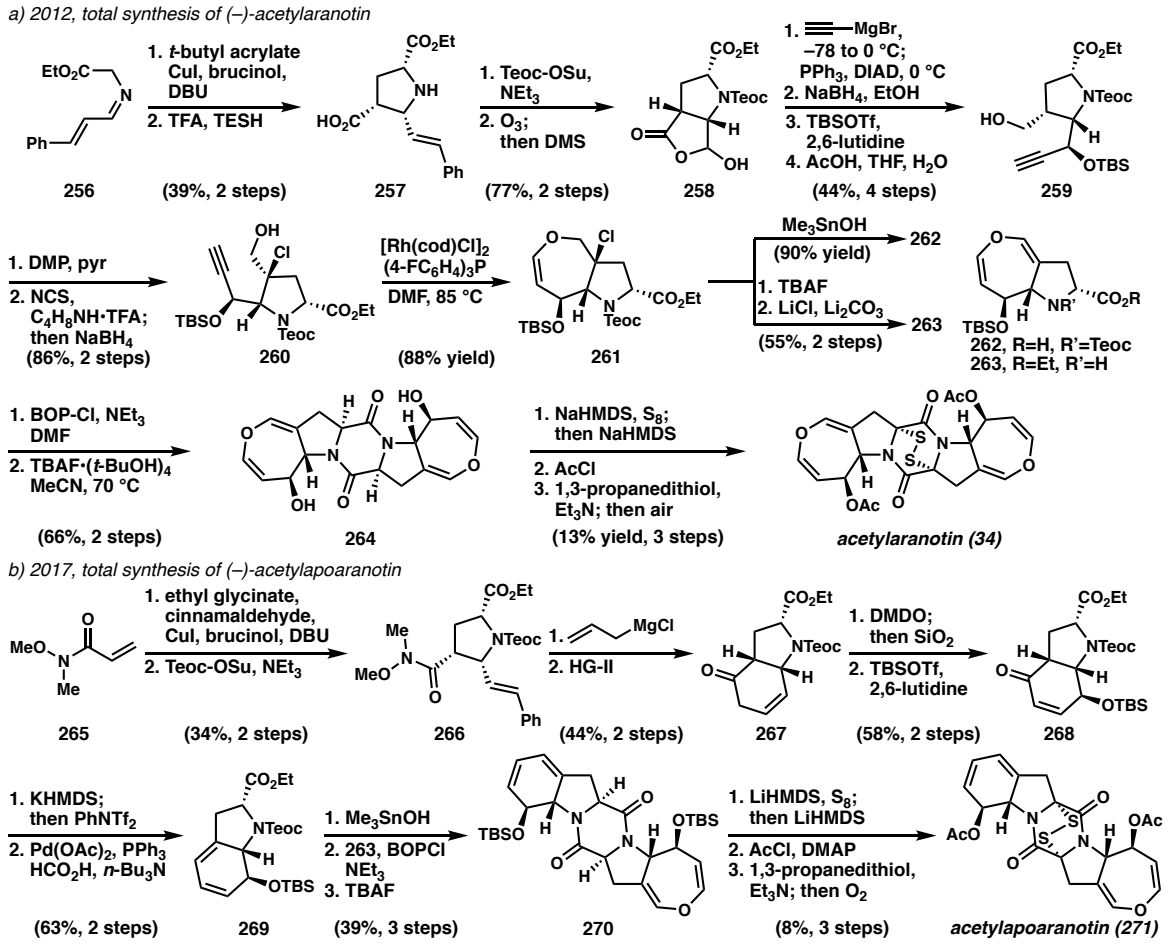

the desired seven-membered ring. Orthogonal protecting groups are removed to form **262** and **263** which can undergo amide coupling and cyclization to generate a fully functionalized DKP **264**. The natural product could be formed through the Nicolaou's direct sulfenylation protocol.

The pyrollindine-first strategy was further applied to the synthesis of the gliotoxin monomer **269** en route to the unsymmetrical aceylapoaranotin (**271**). Chiral pyrollidine could be allylated prior to undergoing ring closing metathesis. Elimination of a epoxide provides unsaturated **268**. Which can then be converted the desired dienyl alcohol **269** through the reduction of a vinyl triflate. While plagued with competitive aromatization pathways the DKP formation and direct sulfenylation were accomplished to form **271** in analogy to **34.**

Tokuyama was also successful in the synthesis of **34**[137] engaging a similar synthetic strategy, targeting fully functionalized non-canonical amino acid monomers prior to DKP formation and direct sulfenylation. Their approach toward the synthesis of the dihydrooxepine subunit was more in line with Nicolaou's strategy in the synthesis of the gliotoxin intermediate **243**. As opposed to a cyclization strategy, the seven-membered ring was formed through a Baeyer-Villiger oxidation of the enone **274** followed by reduction of the corresponding vinyl triflate. Following a similar two step amide coupling-cyclization to form the DKP the alcohols were easily inverted in a two-step sequence to form **264**. A similar direct sulfenylation as seen in the Reisman synthesis provided their target natural product **34**.

Taking lessons from their synthesis of **34** they were also able to accomplish the synthesis of the macrocyclic 3,6-ETP **38**. Coupling of the dihydroxepine **277** with sarcosine formed the DKP core of the natural product **279**. The macrocycle was formed through esterification of the diaryl ether **281** followed by an aldol reaction under highly optimized conditions follow by oxidation to generate the macrocyclic ketone **282**. A novel direct sulfenylation was then accomplished through

Scheme 1.25. *Tokuyama's Syntheses of oxepine-containing 3,6-ETPs*

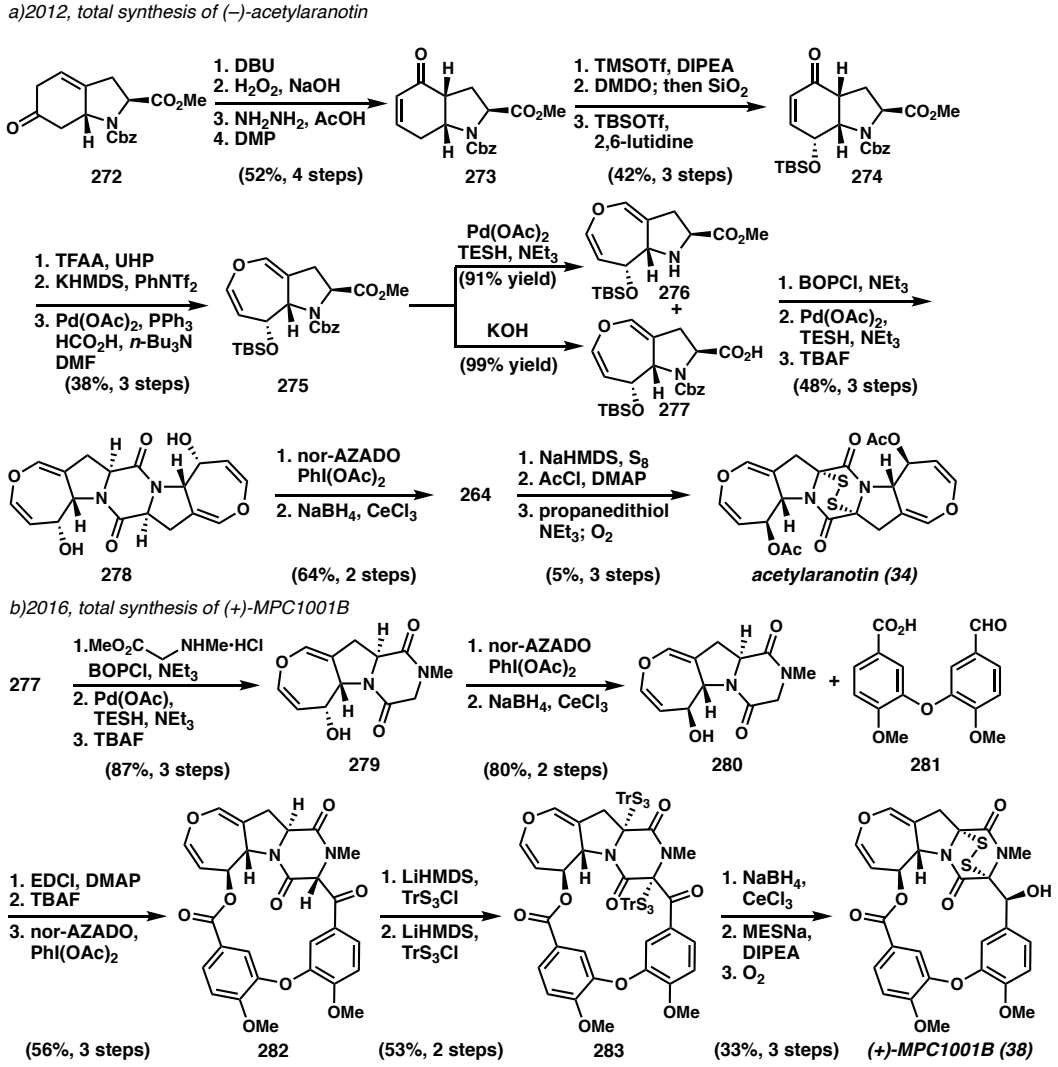

the iterative incorporation of trisulfides from protected sulfur chlorides. This *bis*-trisulfide was then reduced to the dithiol followed by oxidation to the disulfide to deliver **34**.

A wide variety of strategies have been used to access 3,6-ETP natural products. While early work pioneered by Kishi focused on the early formation of a masked 3,6-ETP core followed by decoration of the side chains, later work on more structurally complex 3,6-ETPs has taken a radically different approach through synthesis of fully functionalized monomers which can undergo later stage DKP formation and sulfenylation.

1.3.2 APPROACHES TO ASPIROCHLORINE

In constrast to the substantial amount of work found the synthesis of 3,6-ETPs, natural products incorporating the [2.2.3]-ETP core have arguably not been explored synthetically to any great extent. The only successful total synthesis of a [2.2.3]-ETP was William's synthesis of **79**. Strategically, this work focused upon a bromocyclization to generate the spirocyclic motif and provide benzylic functionalization which could be leveraged for later sulfenylation.[138]

The benzofuran **285** could be synthesized in three steps from bisphenol **284**. Conversion the acid chloride facilitates coupling with a glycine equivalent, followed by incorporation methoxylamine to generate **286**. Exposure to NBS leads to bromocyclization in good yield. In an additional 4 steps the *bis*-methoxylated **289** is primed for thiolation with thioacetate similar to Trown's approach but with a substrate in analogy that pioneered by Matsuri (Scheme1.9ad) to yield **79**.

While Williams' work remains the exclusive total synthesis of [2.2.3]-ETP, Danishefsky proposed an alternative three step protocol to simultaneously generate a benzofuran-derived spirocyle and unusual disulfide linkage.[139] This approach uses the Kishi strategy, stoichiometric

Scheme 1.26. *Williams' Synthesis of (+)–aspirochlorine*

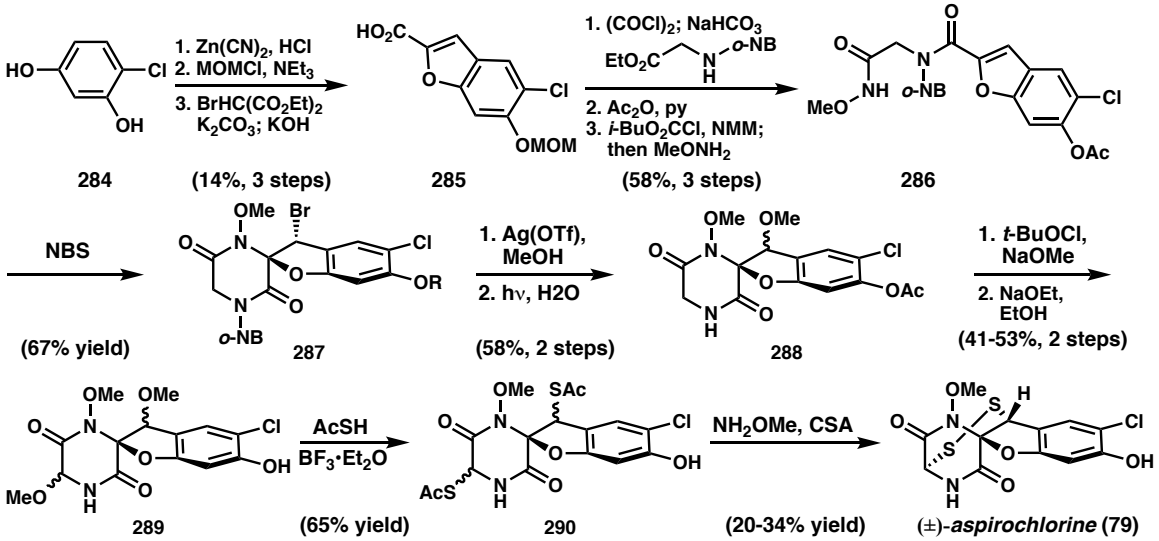

Scheme 1.27. *Danishefsky's Approach to the spirocyclic aspirochlorine core*

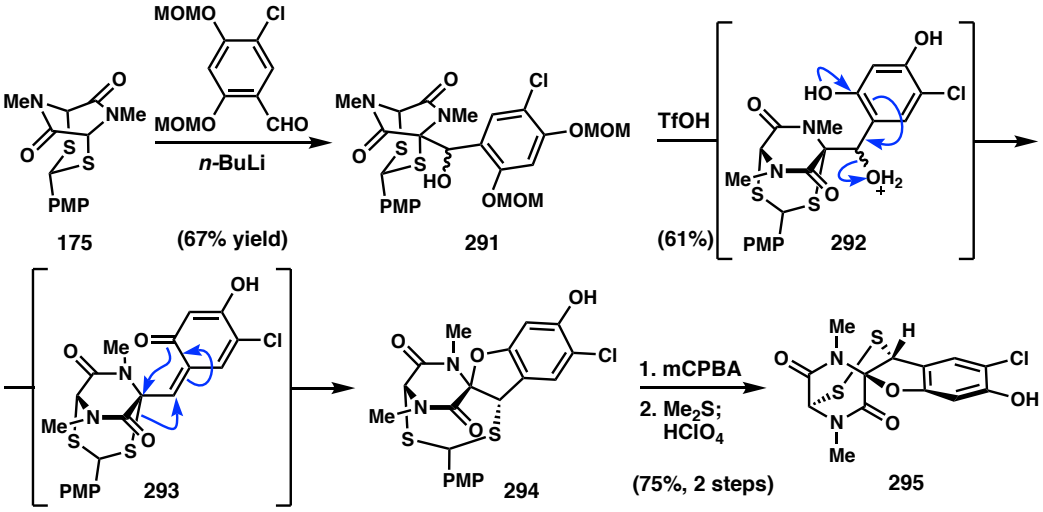

deprotonation of the masked ETP **175** is able to undergo 1,2-addition with an electron-rich benzaldehyde to generate **291**. Exposure of this intermediate to strongly acidic conditions presumably leads to ionization of the benzylic alcohol to form *ortho*-quinone methide **293**, a strong electrophile. This species can undergo subsequent 1,2-sulfur migration with concurrent cyclization to quench the developing positive charge on the DKP. While remarkable, whether this rearrangement is biologically relevant is remains unknown.

1.4 SYNTHESES OF THE TRICHODERMAMIDES

In contrast to their disulfide-containing cousins, the presumed decomposition products of [2.2.3]-ETPs, the trichodermamides, have been the subject of several synthetic efforts. The first successful synthesis was disclosed by Zakarian[140] utilizing an 1,2-oxo-aza Cope rearrangement which they pioneered to generated the key bicyclic oxazine fragment.[141] Unfortunately, the substrate for this rearrangement required extensive synthetic efforts. The bicyclic framework was initially generated through a Diels-Alder reaction followed by an retro aldol-aldol sequence to set

Scheme 1.28. *Zakarian's synthesis of trichodermamides B*

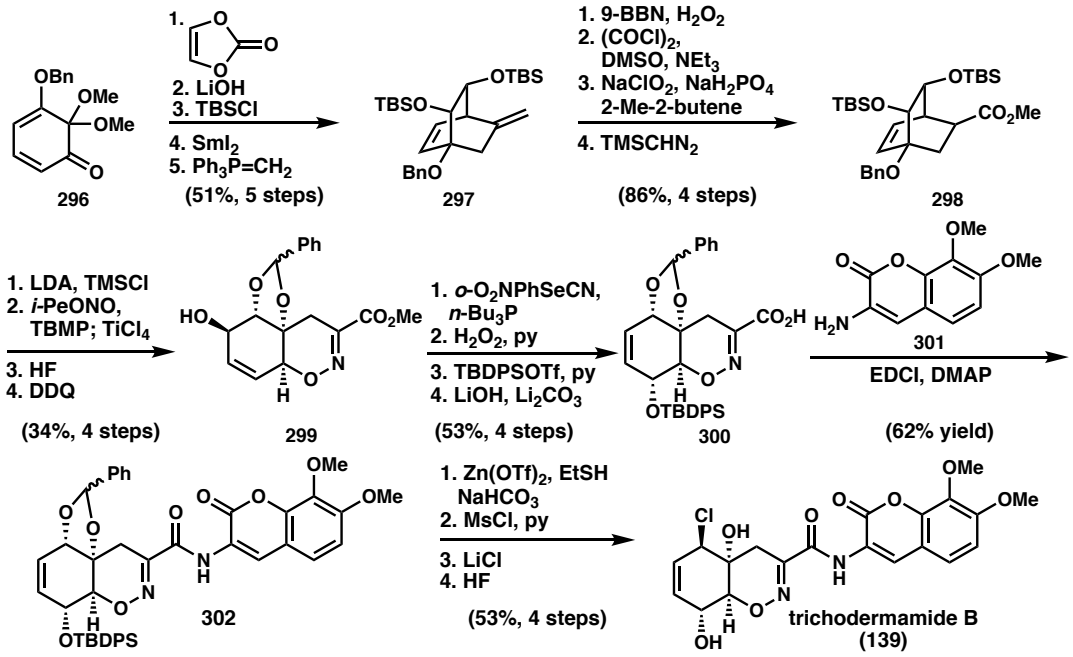

the requisite bridgehead trans-diol along with some redox manipulations to generate **298** in 9 steps from **296**. The rearrangement proceeded smoothly and protecting group manipulations generated **299**, the appropriate oxidation pattern was generated through Grieco transposition and subsequent saponification provided **300** which could be coupled with aminocoumarin **301** to generate **302**. Chlorination occur through invertive displacement of an allylic mesylate to generate the target **139.**

Joullie successfully completed the enantiospecific syntheses of **138** and **139**.[142] Epoxy ketone **303** could be synthesized in 18 steps from the chiral pool. One-pot oxime formation and acid mediated cyclization generated the bicyclic oxazine fragment. Oxidative elaboration of **304** was challenging for the authors, especially the low-yielding allylic oxidation to generate enone **306**. Furthermore 1,2-reduction of that moiety, while high yielding, was completely unselective provide inseparable products; however, conversion to **307a** and **307b** provided to a separable mixture. Taking advantage of both diastereomers, **307b** could be advanced to **138** in three steps

Scheme 1.29. *Jouillie's syntheses of trichodermamides A&B*

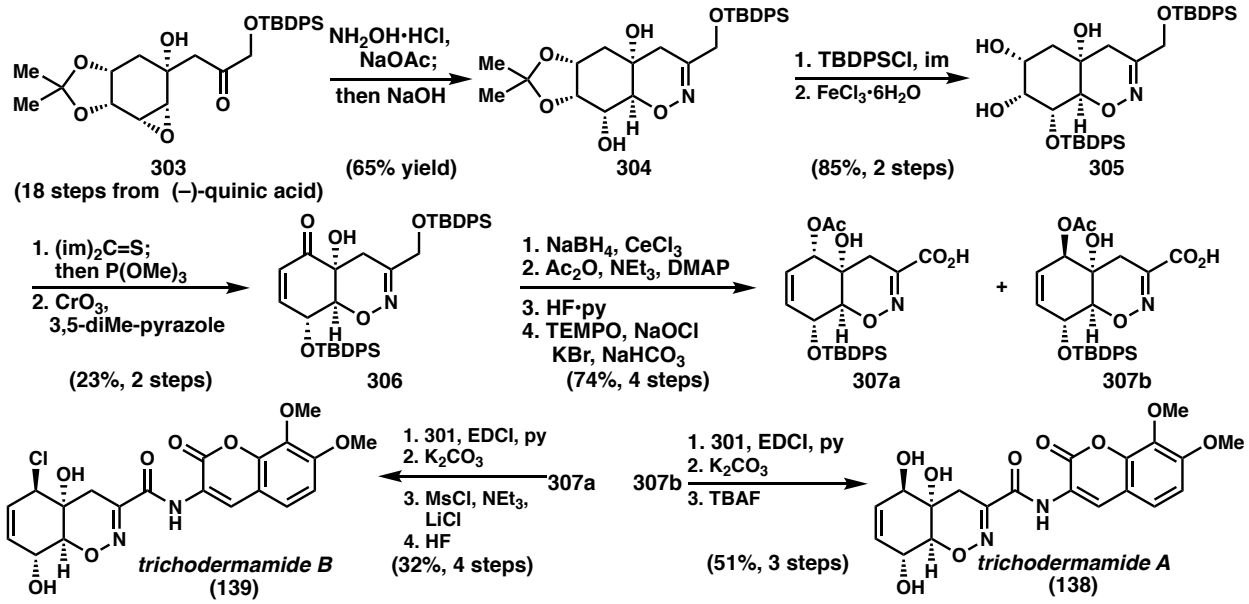

while **307a** could converted to **139** in four steps, with a chlorination analogous to that used by Zakarian.

Recently, Larionov disclosed concise racemic syntheses of the trichodermamides A-C through the rapid synthesis of the bicylic oxazine core.[143] This was accomplished in a one-pot procedure. Stoichiometric deprotonation of **308** formed a hard nucleophile which performed a 1,2-addition on 1,4-benzoquinone (BQ) following unveiling of the oxime oxygen under acidic conditions an oxy-Michael generates **309**. A three-step sequence featuring a palladium catalyzed elimination of a carbonate analogous to that observed in Nicolaou's route to the gliotoxin subunit(**241**, Scheme 1.23) generates their key intermediate **310**.

A manganese-catalyzed epoxidation of the dienyl alcohol is selective for the distal olefin. To provide the desired trans diol, epoxide opening proceeds with phenylselenol to provide **312.** This allylic selenide is then saponified under mild conditions prior to amide coupling with **301**. The resulting allylic selenide **313** readily undergoes a [2,3]-rearrangement under mildly oxidizing conditions to yield **138**. The direct formation of the core, lack of protecting groups manipulations,

Scheme 1.30. *Larionov's synthesis of trichodermamide A*

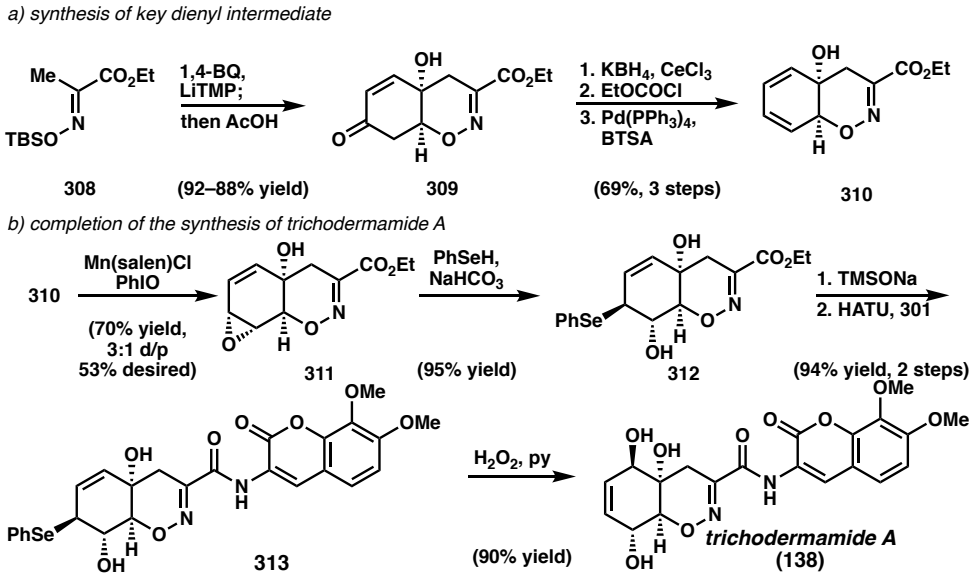

and rapid incorporation of the oxidation results in a swift, scalable synthesis.

Larionov was able to further leverage **310** in the synthesis of **139** and **140** (Scheme 1.31). Direct coupling of the dienyl substrate with **301** yields **314**. This is followed by a highly efficient allylic epoxidation to yield **315**. A double displacement at the allylic position provides an appropriately disposed allylic selenide for the [2,3]-rearrangement so effectively utilized toward **138**. Tosylation of the newly formed secondary alcohol prior to [2,3]-rearrangement prevents undesired decomposition pathways. Under mildly oxidizing conditions **316** undergoes allylic transposition followed by chlorination of the newly activated allylic tosylate to generate **139**.

Finally, to synthesize **140**, methylation of **314** provided a substrate for analogous epoxidation as that seen in **138**, while expedient from a step-count standpoint the efficiency of the epoxidation was reduced. However, with the coupled allylic epoxide **317** in hand the two step selenation-transposition sequence proceeded in high yield to generate the natural product **140**. Synthetic efforts towards the trichodermamides have demonstrated that rapid formation of the key bicyclic oxazine is critical for an expedient synthesis. Furthermore, the oxidative manipulation and

Scheme 1.31. *The Completion of Larinov's syntheses of trichodermamides B&C*

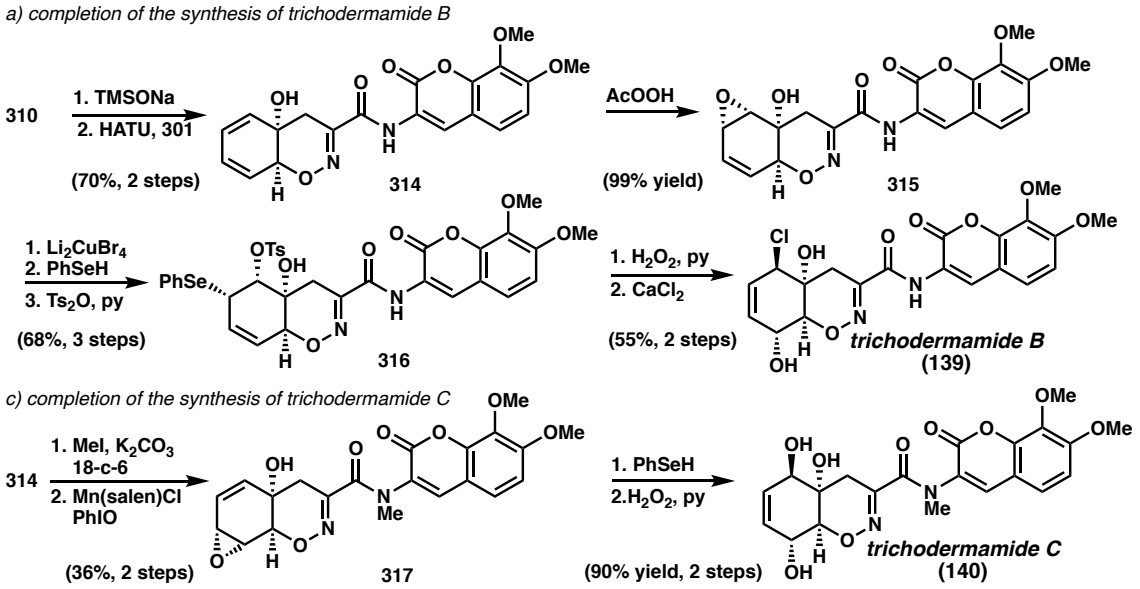

diastereoselectivity of chemical transformations with these substrates can be non-trivial. While concise syntheses have now been realized an enantioselective synthesis of the trichodermamides has yet to been accomplished.

1.5 REFERENCES

(1) Corey, E. J.; Cheng, X.-M. *The Logic of Chemical Synthesis*; Wiley-Interscience: New York, 1995.

(2) Caron, S. *Practical Synthetic Organic Chemistry: Reactions, Principles, and Techniques*; Hoboken, N.J., 2011.

(3) Martin, C. L.; Overman, L. E.; Rohde, J. M. Total Synthesis of (±)- and (−)-Actinophyllic Acid. *J. Am. Chem. Soc.* **2010**, *132* (13), 4894–4906.

(4) Cai, L.; Zhang, K.; Kwon, O. Catalytic Asymmetric Total Synthesis of (−)-Actinophyllic Acid. *J. Am. Chem. Soc.* **2016**, *138* (10), 3298–3301.

(5) Yoshii Yu; Tokuyama Hidetoshi; Chen David Y.-K. Total Synthesis of Actinophyllic Acid. *Angew. Chem. Int. Ed.* **2017**, *56* (40), 12277–12281.

(6) Weindling, R.; Emerson, O. H. The Isolation of a Toxic Substance from the Culture Filtrate of Trichoderma. *Phytopathology* **1936**, *26* (11), 1068–1070.

(7) Johnson, J. R.; McCrone, W. C.; Bruce, W. F. GLIOTOXIN, THE ANTIBIOTIC PRINCIPLE OF GLIOCLADIUM FIMBRIATUM1. *J. Am. Chem. Soc.* **1944**, *66* (3), 501–501.

(8) Bruce, W. F.; Dutcher, J. D.; Johnson, J. R.; Miller, L. L. Gliotoxin, the Antibiotic Principle of Gliocladium Fimbriatum. II. General Chemical Behavior and Crystalline Derivatives1. *J. Am. Chem. Soc.* **1944**, *66* (4), 614–616.
(9) Dutcher, J. D.; Johnson, J. R.; Bruce, W. F. Gliotoxin, The Antibiotic Principle of Gliocladium Fimbriatum. III. The Structure of Gliotoxin: Degradation by Hydriodic Acid1. *J. Am. Chem. Soc.* **1944**, *66* (4), 617–619.
(10) Dutcher, J. D.; Johnson, J. R.; Bruce, W. F. Gliotoxin, the Antibiotic Principle of Gliocladium Fimbriatum. IV. The Structure of Gliotoxin: The Action of Selenium. *J. Am. Chem. Soc.* **1944**, *66* (4), 619–621.
(11) Johnson, J. R.; Hasbrouck, R. B.; Dutcher, J. D.; Bruce, W. F. Gliotoxin. V. The Structure of Certain Indole Derivatives Related to Gliotoxin1,2. *J. Am. Chem. Soc.* **1945**, *67* (3), 423–430.
(12) Dutcher, J. D.; Johnson, J. R.; Bruce, W. F. Gliotoxin. VI. The Nature of the Sulfur Linkages. Conversion to Desthiogliotoxin1,2. *J. Am. Chem. Soc.* **1945**, *67* (10), 1736–1745.
(13) Johnson, J. R.; Larsen, A. A.; Holley, A. D.; Gerzon, K. Gliotoxin. VII. Synthesis of Pyrazinoindolones and Pyridindolones1. *J. Am. Chem. Soc.* **1947**, *69* (10), 2364–2370.
(14) Johnson, J. R.; Andreen, J. H. Gliotoxin. VIII. Derivatives of 3-Hydroxyindoline-2-Carboxylic Acid1. *J. Am. Chem. Soc.* **1950**, *72* (7), 2862–2864.
(15) Johnson, J. R.; Buchanan, J. B. Gliotoxin. IX. Synthesis of the C11H8N2OS Degradation Product1. *J. Am. Chem. Soc.* **1951**, *73* (8), 3749–3751.
(16) Dutcher, J. D.; Kjaer, A. Studies on the C11H8N2OS Degradation Product of Gliotoxin1. *J. Am. Chem. Soc.* **1951**, *73* (9), 4139–4141.
(17) Johnson, J. R.; Buchanan, J. B. Gliotoxin. X. Dethiogliotoxin and Related Compounds1. *J. Am. Chem. Soc.* **1953**, *75* (9), 2103–2109.
(18) Johnson, J. R.; Kidwai, A. R.; Warner, J. S. Gliotoxin. XI. A Related Antibiotic from Penicillium Terlikowski: Gliotoxin Monoacetate1. *J. Am. Chem. Soc.* **1953**, *75* (9), 2110–2112.
(19) Bell, M. R.; Johnson, J. R.; Wildi, B. S.; Woodward, R. B. THE STRUCTURE OF GLIOTOXIN. *J. Am. Chem. Soc.* **1958**, *80* (4), 1001–1001.
(20) Fridrichsons, J.; McL Mathieson, A. The Crystal Structure of Gliotoxin. *Acta Crystallogr.* **1967**, *23* (3), 439–448.
(21) Gardiner, D. M.; Waring, P.; Howlett, B. J. The Epipolythiodioxopiperazine (ETP) Class of Fungal Toxins: Distribution, Mode of Action, Functions and Biosynthesis. *Microbiology* **2005**, *151* (4), 1021–1032.
(22) Iwasa, E.; Hamashima, Y.; Sodeoka, M. Epipolythiodiketopiperazine Alkaloids: Total Syntheses and Biological Activities. *Isr. J. Chem.* **2011**, *51* (3–4), 420–433.
(23) Stillwell, M. A.; Magasi, L. P.; Strunz, G. M. Production, Isolation, and Antimicrobial Activity of Hyalodendrin, a New Antibiotic Produced by a Species of Hyalodendron. *Can. J. Microbiol.* **1974**, *20* (5), 759–764.
(24) Kawai, K.; Kawahara, N.; Nozawa, K.; Yamazaki, M.; Nakajima, S. Novel Epidithiodioxopiperazines, Emethallicins E and F, from Emericella Heterothallica. *HETEROCYCLES* **1990**, *30* (1), 507.
(25) Choi E.J.; Park J.-S.; Kim Y.-J.; Jung J.-H.; Lee J.K.; Kwon H.C.; Yang H.O. Apoptosis-inducing Effect of Diketopiperazine Disulfides Produced by Aspergillus Sp. KMD 901

Isolated from Marine Sediment on HCT116 Colon Cancer Cell Lines. *J. Appl. Microbiol.* **2010**, *110* (1), 304–313.
(26) Begg, W. R.; Elix, J. A.; Jones, A. J. Nonacyclic Amides from Lichens of the Genus Xanthoparmelia. *Tetrahedron Lett.* **1978**, *19* (12), 1047–1050.
(27) Williams, D. E.; Bombuwala, K.; Lobkovsky, E.; de Silva, E. D.; Karunatne, V.; Allen, T. M.; Clardy, J.; Andersen, R. J. Ambewelamides A and B, Antineoplastic Epidithiapiperazinediones Isolated from the Lichen Usnea Sp. *Tetrahedron Lett.* **1998**, *39* (52), 9579–9582.
(28) Deffieux, G.; Baute, M.-A.; Baute, R.; Filleau, M.-J. NEW ANTIBIOTICS FROM THE FUNGUS EPICOCCUM NIGRUM. *J. Antibiot. (Tokyo)* **1978**, *31* (11), 1102–1105.
(29) Deffieux, G.; Filleau, M.-J.; Baute, R. NEW ANTIBIOTICS FROM THE FUNGUS EPICOCCUM NIGRUM. *J. Antibiot. (Tokyo)* **1978**, *31* (11), 1106–1109.
(30) Kleinwächter, P.; Dahse, H.-M.; Luhmann, U.; Schlegel, B.; Dornberger, K. Epicorazine C, an Antimicrobial Metabolite from Stereum Hirsutum HKI 0195. *J. Antibiot. (Tokyo)* **2001**, *54* (6), 521–525.
(31) Tan, R. X.; Jensen, P. R.; Williams, P. G.; Fenical, W. Isolation and Structure Assignments of Rostratins A−D, Cytotoxic Disulfides Produced by the Marine-Derived Fungus Exserohilum Rostratum. *J. Nat. Prod.* **2004**, *67* (8), 1374–1382.
(32) Kong, F.; Wang, Y.; Liu, P.; Dong, T.; Zhu, W. Thiodiketopiperazines from the Marine-Derived Fungus Phoma Sp. OUCMDZ-1847. *J. Nat. Prod.* **2014**, *77* (1), 132–137.
(33) Chunyu, W.-X.; Ding, Z.-G.; Zhao, J.-Y.; Wang, Y.-X.; Han, X.-L.; Li, M.-G.; Wen, M.-L. Two New Diketopiperazines from the Tin Mine Tailings-Derived Fungus Schizophyllum Commune YIM DT 10058. *Nat. Prod. Res.* **2017**, *31* (13), 1566–1572.
(34) Nagarajan, R.; Huckstep, L. L.; Lively, D. H.; DeLong, D. C.; Marsh, M. M.; Neuss, N. Aranotin and Related Metabolites from Arachniotus Aureus. I. Determination of Structure. *J. Am. Chem. Soc.* **1968**, *90* (11), 2980–2982.
(35) Kawahara, N.; Nakajima, S.; Yamazaki, M.; Kawai, K. Structure of a Novel Epidithiodioxopiperazine, Emethallicin A, a Potent Inhibitor of Histamine Release, from Emericella Heterothallica. *Chem. Pharm. Bull. (Tokyo)* **1989**, *37* (10), 2592–2595.
(36) Hegde, V. R.; Dai, P.; Patel, M.; Das, P. R.; Puar, M. S. Novel Thiodiketopiperazine Fungal Metabolites as Epidermal Growth Factor Receptor Antagonists. *Tetrahedron Lett.* **1997**, *38* (6), 911–914.
(37) Onodera, H.; Hasegawa, A.; Tsumagari, N.; Nakai, R.; Ogawa, T.; Kanda, Y. MPC1001 and Its Analogues: New Antitumor Agents from the Fungus Cladorrhinum Species. *Org. Lett.* **2004**, *6* (22), 4101–4104.
(38) Isaka, M.; Kittakoop, P.; Kirtikara, K.; Hywel-Jones, N. L.; Thebtaranonth, Y. Bioactive Substances from Insect Pathogenic Fungi. *Acc. Chem. Res.* **2005**, *38* (10), 813–823.
(39) Tokuyama, H.; Yamada, K.; Fujiwara, H.; Sakata, J.; Okano, K.; Sappan, M.; Isaka, M. Structural Determination of (−)-SCH 64874 and Hirsutellomycin by Semisynthesis. *J. Org. Chem.* **2017**, *82* (1), 353–371.
(40) Kawahara, N.; Nozawa, K.; Nakajima, S.; Kawai, K. Studies on Fungal Products. Part 13. Isolation and Structures of Dithiosilvatin and Silvathione, Novel Dioxopiperazine Derivatives from Aspergillus Silvaticus. *J. Chem. Soc. [Perkin 1]* **1987**, *0* (0), 2099–2101.
(41) Pedras, M. S. C.; Abrams, S. R.; Seguin-Swartz, G.; Quail, J. W.; Jia, Z. Phomalirazine, a Novel Toxin from the Phytopathogenic Fungus Phoma Lingam. *J. Am. Chem. Soc.* **1989**, *111* (5), 1904–1905.

(42) Rouxel, T.; Chupeau, Y.; Fritz, R.; Kollmann, A.; Bousquet, J.-F. Biological Effects of Sirodesmin PL, a Phytotoxin Produced by Leptosphaeria Maculans. *Plant Sci.* **1988**, *57* (1), 45–53.
(43) Marjanović-Jeromela Ana M.; Grahovac Nada L.; Milošević Drago M.; Marisavljević Dragana P.; Sakač Zvonimir O.; Mitrović Petar M.; Orčić Dejan Z. Characterization of Sirodesmins Isolated from the Phytopathogenic Fungus Leptosphaeria Maculans. *J. Serbian Chem. Soc.* **2012**, *77* (10), 1363–1379.
(44) Ronaldson, J. W.; Taylor, A.; White, E. P.; Abraham, R. J. 592. Sporidesmins. Part I. Isolation and Characterisation of Sporidesmin and Sporidesmin-B. *J. Chem. Soc. Resumed* **1963**, *0* (0), 3172–3180.
(45) Rahman, R.; Safe, S.; Taylor, A. Sporidesmins. Part 17. Isolation of Sporidesmin H and Sporidesmin J. *J. Chem. Soc. [Perkin 1]* **1978**, *0* (12), 1476–1479.
(46) Hauser D.; Weber H. P.; Sigg H. P. Isolierung Und Strukturaufklärung von Chaetocin. *Helv. Chim. Acta* **2004**, *53* (5), 1061–1073.
(47) Minato, H.; Matsumoto, M.; Katayama, T. Studies on the Metabolites of Verticillium Sp. Structures of Verticillins A, B, and C. *J. Chem. Soc. [Perkin 1]* **1973**, *0* (0), 1819–1825.
(48) Joshi, B. K.; Gloer, J. B.; Wicklow, D. T. New Verticillin and Glisoprenin Analogues from Gliocladium Catenulatum, a Mycoparasite of Aspergillus Flavus Sclerotia. *J. Nat. Prod.* **1999**, *62* (5), 730–733.
(49) Ebead, G. A.; Overy, D. P.; Berrué, F.; Kerr, R. G. Westerdykella Reniformis Sp. Nov., Producing the Antibiotic Metabolites Melinacidin Iv and Chetracin B. *IMA Fungus* **2012**, *3* (2), 189–201.
(50) Takahashi, C.; Minoura, K.; Yamada, T.; Numata, A.; Kushida, K.; Shingu, T.; Hagishita, S.; Nakai, H.; Sato, T.; Harada, H. Potent Cytotoxic Metabolites from a Leptosphaeria Species. Structure Determination and Conformational Analysis. *Tetrahedron* **1995**, *51* (12), 3483–3498.
(51) Waksman, S. A.; Bugie, E. Chaetomin, a New Antibiotic Substance Produced by Chaetomium Cochliodes I. Formation and Properties. *J. Bacteriol.* **1944**, *48* (5), 527–530.
(52) Yanagihara Miyako; Sasaki-Takahashi Noriko; Sugahara Tetsuo; Yamamoto Seiko; Shinomi Masahito; Yamashita Izumi; Hayashida Masashi; Yamanoha Banri; Numata Atsushi; Yamori Takao; et al. Leptosins Isolated from Marine Fungus Leptoshaeria Species Inhibit DNA Topoisomerases I and/or II and Induce Apoptosis by Inactivation of Akt/Protein Kinase B. *Cancer Sci.* **2005**, *96* (11), 816–824.
(53) Chu, M.; Truumees, I.; Rothofsky, M. L.; Patel, M. G.; Gentile, F.; Das, P. R.; Puar, M. S.; Lin, S. L. Nhibition of C-Fos Proto-Oncogene Induction by Sch 52900 and Sch 52901, Novel Diketopiperazines Produced by Gliocladium Sp. *J. Antibiot. (Tokyo)* **1995**, *48* (12), 1440–1445.
(54) Takahashi, C.; Numata, A.; Ito, Y.; Matsumura, E.; Araki, H.; Iwaki, H.; Kushida, K. Leptosins, Antitumour Metabolites of a Fungus Isolated from a Marine Alga. *J. Chem. Soc. [Perkin 1]* **1994**, *0* (13), 1859–1864.
(55) Feng, Y.; Blunt, J. W.; Cole, A. L. J.; Munro, M. H. G. Novel Cytotoxic Thiodiketopiperazine Derivatives from a Tilachlidium Sp. *J. Nat. Prod.* **2004**, *67* (12), 2090–2092.
(56) Dong, J.-Y.; He, H.-P.; Shen, Y.-M.; Zhang, K.-Q. Nematicidal Epipolysulfanyldioxopiperazines from Gliocladium Roseum. *J. Nat. Prod.* **2005**, *68* (10), 1510–1513.

(57) Zheng, C.-J.; Kim, C.-J.; Bae, K. S.; Kim, Y.-H.; Kim, W.-G. Bionectins A−C, Epidithiodioxopiperazines with Anti-MRSA Activity, from Bionectra Byssicola F120. *J. Nat. Prod.* **2006**, *69* (12), 1816–1819.
(58) Dong, J. Y.; Zhou, W.; Li, L.; Li, G. H.; Liu, Y. J.; Zhang, K. Q. A New Epidithiodioxopiperazine Metabolite Isolated from Gliocladium Roseum YMF1.00133. *Chin. Chem. Lett.* **2006**, *17* (7), 922–924.
(59) Wang, F.-Z.; Huang, Z.; Shi, X.-F.; Chen, Y.-C.; Zhang, W.-M.; Tian, X.-P.; Li, J.; Zhang, S. Cytotoxic Indole Diketopiperazines from the Deep Sea-Derived Fungus Acrostalagmus Luteoalbus SCSIO F457. *Bioorg. Med. Chem. Lett.* **2012**, *22* (23), 7265–7267.
(60) Devault, R. L.; Rosenbrook, W. A NOVEL CLASS OF DIKETOPIPERAZINES. *J. Antibiot. (Tokyo)* **1973**, *26* (9), 532–534.
(61) Strunz, G. M.; Heissner, C. J.; Kakushima, M.; Stillwell, M. A. Metabolites of Hyalodendron Sp.: Bisdethiodi(Methylthio)Hyalodendrin. *Can. J. Chem.* **1974**, *52* (2), 325–326.
(62) Shin, J.; Fenical, W. Isolation of Gliovictin from the Marine Deuteromycete Asteromyces Cruciatus. *Phytochemistry* **1987**, *26* (12), 3347.
(63) Shin, C.; Yonezawa, Y.; Shimizu, K.; Uchiyama, M.; Kagawa, N. Total Syntheses of Naturally Occurring Bis(Methylthio)Silvatin and Its Three Stereoisomers. *HETEROCYCLES* **1997**, *45* (6), 1151.
(64) Nicolaou, K. C.; Totokotsopoulos, S.; Giguère, D.; Sun, Y.-P.; Sarlah, D. Total Synthesis of Epicoccin G. *J. Am. Chem. Soc.* **2011**, *133* (21), 8150–8153.
(65) Nicolaou, K. C.; Lu, M.; Totokotsopoulos, S.; Heretsch, P.; Giguère, D.; Sun, Y.-P.; Sarlah, D.; Nguyen, T. H.; Wolf, I. C.; Smee, D. F.; et al. Synthesis and Biological Evaluation of Epidithio-, Epitetrathio-, and Bis-(Methylthio)Diketopiperazines: Synthetic Methodology, Enantioselective Total Synthesis of Epicoccin G, 8,8′-Epi-Ent-Rostratin B, Gliotoxin, Gliotoxin G, Emethallicin E, and Haematocin and Discovery of New Antiviral and Antimalarial Agents. *J. Am. Chem. Soc.* **2012**, *134* (41), 17320–17332.
(66) Boyer, N.; Movassaghi, M. Concise Total Synthesis of (+)-Gliocladins B and C. *Chem. Sci.* **2012**, *3* (6), 1798–1803.
(67) Boyer, N.; Morrison, K. C.; Kim, J.; Hergenrother, P. J.; Movassaghi, M. Synthesis and Anticancer Activity of Epipolythiodiketopiperazine Alkaloids. *Chem. Sci.* **2013**, *4* (4), 1646–1657.
(68) Coste, A.; Kim, J.; Adams, T. C.; Movassaghi, M. Concise Total Synthesis of (+)-Bionectins A and C. *Chem. Sci.* **2013**, *4* (8), 3191–3197.
(69) DeLorbe, J. E.; Horne, D.; Jove, R.; Mennen, S. M.; Nam, S.; Zhang, F.-L.; Overman, L. E. General Approach for Preparing Epidithiodioxopiperazines from Trioxopiperazine Precursors: Enantioselective Total Syntheses of (+)- and (−)-Gliocladine C, (+)-Leptosin D, (+)-T988C, (+)-Bionectin A, and (+)-Gliocladin A. *J. Am. Chem. Soc.* **2013**, *135* (10), 4117–4128.
(70) Jabri, S. Y.; Overman, L. E. Enantioselective Total Synthesis of Plectosphaeroic Acid B. *J. Am. Chem. Soc.* **2013**, *135* (11), 4231–4234.
(71) Jabri, S. Y.; Overman, L. E. Enantioselective Total Syntheses of Plectosphaeroic Acids B and C. *J. Org. Chem.* **2013**, *78* (17), 8766–8788.
(72) Kawai, K.; Kawahara, N.; Nozawa, K.; Nakajima, S.; Yamazaki, M. Sulfur-Containing Dioxopiperazine Derivatives from Emericella Heterothallica. *HETEROCYCLES* **1989**, *29* (2), 397.

(73) Isaka, M.; Palasarn, S.; Rachtawee, P.; Vimuttipong, S.; Kongsaeree, P. Unique Diketopiperazine Dimers from the Insect Pathogenic Fungus Verticillium Hemipterigenum BCC 1449. *Org. Lett.* **2005**, *7* (11), 2257–2260.
(74) Katz, B. A.; Kossiakoff, A. The Crystallographically Determined Structures of Atypical Strained Disulfides Engineered into Subtilisin. *J. Biol. Chem.* **1986**, *261* (33), 15480–15485.
(75) Berg, D. H.; Massing, R. P.; Hoehn, M. M.; Boeck, L. D.; Hamill, R. L. A30641, A NEW EPIDITHIODIKETOPIPERAZINE WITH ANTIFUNGAL ACTIVITY. *J. Antibiot. (Tokyo)* **1976**, *29* (4), 394–397.
(76) Sakata, K.; Maruyama, M.; Uzawa, J.; Sakurai, A.; Lu, H. S. M.; Clardy, J. Structural Revision of Aspirochlorine (=antibiotic A30641), a Novel Epidithiopiperazine-2, 5-Dione Produced Byaspergillus SPP. *Tetrahedron Lett.* **1987**, *28* (46), 5607–5610.
(77) Stipanovic, R. D.; Howell, C. R. THE STRUCTURE OF GLIOVIRIN, A NEW ANTIBIOTIC FROM GLIOCLADIUM VIRENS. *J. Antibiot. (Tokyo)* **1982**, *35* (10), 1326–1330.
(78) Miyamoto, C.; Yokose, K.; Furumai, T.; Maruyama, H. B. A NEW EPIDITHIODIKETOPIPERAZINE GROUP ANTIBIOTIC, FA-2097. *J. Antibiot. (Tokyo)* **1982**, *35* (3), 374–377.
(79) Okose, K.; Nakayama, N.; Miyamoto, C.; Furumai, T.; Maruyama, H. B.; Stipanovic, R. D.; Howell, C. R. STRUCTURE OF FA-2097, A NEW MEMBER OF THE DIOXOPIPERAZINE ANTIBIOTICS. *J. Antibiot. (Tokyo)* **1984**, *37* (6), 667–669.
(80) Seephonkai, P.; Kongsaeree, P.; Prabpai, S.; Isaka, M.; Thebtaranonth, Y. Transformation of an Irregularly Bridged Epidithiodiketopiperazine to Trichodermamide A. *Org. Lett.* **2006**, *8* (14), 3073–3075.
(81) Orfali, R. S.; Aly, A. H.; Ebrahim, W.; Abdel-Aziz, M. S.; Müller, W. E. G.; Lin, W.; Daletos, G.; Proksch, P. Pretrichodermamide C and N-Methylpretrichodermamide B, Two New Cytotoxic Epidithiodiketopiperazines from Hyper Saline Lake Derived Penicillium Sp. *Phytochem. Lett.* **2015**, *11*, 168–172.
(82) Yurchenko, A. N.; Smetanina, O. F.; Ivanets, E. V.; Kalinovsky, A. I.; Khudyakova, Y. V.; Kirichuk, N. N.; Popov, R. S.; Bokemeyer, C.; von Amsberg, G.; Chingizova, E. A.; et al. Pretrichodermamides D–F from a Marine Algicolous Fungus Penicillium Sp. KMM 4672. *Mar. Drugs* **2016**, *14* (7), 122.
(83) Bräse, S.; Encinas, A.; Keck, J.; Nising, C. F. Chemistry and Biology of Mycotoxins and Related Fungal Metabolites. *Chem. Rev.* **2009**, *109* (9), 3903–3990.
(84) Waring, P.; Sjaarda, A.; Lin, Q. H. Gliotoxin Inactivates Alcohol Dehydrogenase by Either Covalent Modification or Free Radical Damage Mediated by Redox Cycling. *Biochem. Pharmacol.* **1995**, *49* (9), 1195–1201.
(85) Hurne, A. M.; Chai, C. L. L.; Waring, P. Inactivation of Rabbit Muscle Creatine Kinase by Reversible Formation of an Internal Disulfide Bond Induced by the Fungal Toxin Gliotoxin. *J. Biol. Chem.* **2000**, *275* (33), 25202–25206.
(86) Cook, K. M.; Hilton, S. T.; Mecinović, J.; Motherwell, W. B.; Figg, W. D.; Schofield, C. J. Epidithiodiketopiperazines Block the Interaction between Hypoxia-Inducible Factor-1α (HIF-1α) and P300 by a Zinc Ejection Mechanism. *J. Biol. Chem.* **2009**, *284* (39), 26831–26838.
(87) Munday R. Studies on the Mechanism of Toxicity of the Mycotoxin, Sporidesmin. V. Generation of Hydroxyl Radical by Sporidesmin. *J. Appl. Toxicol.* **2006**, *7* (1), 17–22.

(88) Munday R. Studies on the Mechanism of Toxicity of the Mycotoxin Sporidesmin 3—inhibition by Metals of the Generation of Superoxide Radical by Sporidesmin. *J. Appl. Toxicol.* **2006**, *4* (4), 182–186.
(89) Kirby, G. W.; Patrick, G. L.; Robins, D. J. Cyclo-(L-Phenylalanyl-L-Seryl) as an Intermediate in the Biosynthesis of Gliotoxin. *J. Chem. Soc. [Perkin 1]* **1978**, *0* (11), 1336–1338.
(90) Cramer, R. A.; Gamcsik, M. P.; Brooking, R. M.; Najvar, L. K.; Kirkpatrick, W. R.; Patterson, T. F.; Balibar, C. J.; Graybill, J. R.; Perfect, J. R.; Abraham, S. N.; et al. Disruption of a Nonribosomal Peptide Synthetase in Aspergillus Fumigatus Eliminates Gliotoxin Production. *Eukaryot. Cell* **2006**, *5* (6), 972–980.
(91) Scharf, D. H.; Remme, N.; Habel, A.; Chankhamjon, P.; Scherlach, K.; Heinekamp, T.; Hortschansky, P.; Brakhage, A. A.; Hertweck, C. A Dedicated Glutathione S-Transferase Mediates Carbon–Sulfur Bond Formation in Gliotoxin Biosynthesis. *J. Am. Chem. Soc.* **2011**, *133* (32), 12322–12325.
(92) Scharf Daniel H.; Chankhamjon Pranatchareeya; Scherlach Kirstin; Heinekamp Thorsten; Willing Karsten; Brakhage Axel A.; Hertweck Christian. Epidithiodiketopiperazine Biosynthesis: A Four-Enzyme Cascade Converts Glutathione Conjugates into Transannular Disulfide Bridges. *Angew. Chem. Int. Ed.* **2013**, *52* (42), 11092–11095.
(93) Marion, A.; Groll, M.; Scharf, D. H.; Scherlach, K.; Glaser, M.; Sievers, H.; Schuster, M.; Hertweck, C.; Brakhage, A. A.; Antes, I.; et al. Gliotoxin Biosynthesis: Structure, Mechanism, and Metal Promiscuity of Carboxypeptidase GliJ. *ACS Chem. Biol.* **2017**, *12* (7), 1874–1882.
(94) Scharf Daniel H.; Chankhamjon Pranatchareeya; Scherlach Kirstin; Heinekamp Thorsten; Roth Martin; Brakhage Axel A.; Hertweck Christian. Epidithiol Formation by an Unprecedented Twin Carbon–Sulfur Lyase in the Gliotoxin Pathway. *Angew. Chem. Int. Ed.* **2012**, *51* (40), 10064–10068.
(95) Erden, I.; Basada, J.; Poli, D.; Cabrera, G.; Xu, F.; Gronert, S. Unusual Hydroxyl Effect on Fulvene Endoperoxide Decompositions. *Tetrahedron Lett.* **2016**, *57* (20), 2190–2193.
(96) Neuss, N.; Nagarajan, R.; Molloy, B. B.; Huckstep, L. L. Aranotin and Related Metabolites. II. Isolation, Characterization, and Structures of Two New Metabolites. *Tetrahedron Lett.* **1968**, *9* (42), 4467–4471.
(97) Guo, C.-J.; Yeh, H.-H.; Chiang, Y.-M.; Sanchez, J. F.; Chang, S.-L.; Bruno, K. S.; Wang, C. C. C. Biosynthetic Pathway for the Epipolythiodioxopiperazine Acetylaranotin in Aspergillus Terreus Revealed by Genome-Based Deletion Analysis. *J. Am. Chem. Soc.* **2013**, *135* (19), 7205–7213.
(98) Gardiner, D. M.; Cozijnsen, A. J.; Wilson, L. M.; Pedras, M. S. C.; Howlett, B. J. The Sirodesmin Biosynthetic Gene Cluster of the Plant Pathogenic Fungus Leptosphaeria Maculans. *Mol. Microbiol.* **2004**, *53* (5), 1307–1318.
(99) Ferezou, J.-P.; Quesneau-Thierry, A.; Servy, C.; Zissmann, E.; Barbier, M. Sirodesmin PL Biosynthesis in Phoma Lingam Tode. *J. Chem. Soc. [Perkin 1]* **1980**, *0* (0), 1739–1746.
(100) Bulock, J. D.; Clough, L. E. Sirodesmin Biosynthesis. *Aust. J. Chem.* **1992**, *45* (1), 39–45.
(101) Bach, R. D.; Klix, R. C. Concerted 1,2-Carbonyl Migrations in Organic Synthesis. A Practical Synthesis of Spiro Cyclic 1,3-Diketones. *J. Org. Chem.* **1985**, *50* (25), 5438–5440.
(102) Klix, R. C.; Bach, R. D. 1,2-Carbonyl Migrations in Organic Synthesis. An Approach to the Perhydroindanones. *J. Org. Chem.* **1987**, *52* (4), 580–586.

(103) Gerken Thomas; Walsh Christopher T. Cloning and Sequencing of the Chaetocin Biosynthetic Gene Cluster. *ChemBioChem* **2013**, *14* (17), 2256–2258.
(104) Chankhamjon, P.; Boettger-Schmidt, D.; Scherlach, K.; Urbansky, B.; Lackner, G.; Kalb, D.; Dahse, H.-M.; Hoffmeister, D.; Hertweck, C. Biosynthesis of the Halogenated Mycotoxin Aspirochlorine in Koji Mold Involves a Cryptic Amino Acid Conversion. *Angew. Chem. Int. Ed.* **2014**, *53* (49), 13409–13413.
(105) Sherkhane, P. D.; Bansal, R.; Banerjee, K.; Chatterjee, S.; Oulkar, D.; Jain, P.; Rosenfelder, L.; Elgavish, S.; Horwitz, B. A.; Mukherjee, P. K. Genomics-Driven Discovery of the Gliovirin Biosynthesis Gene Cluster in the Plant Beneficial Fungus Trichoderma Virens. *ChemistrySelect* **2017**, *2* (11), 3347–3352.
(106) Davis, C.; Carberry, S.; Schrettl, M.; Singh, I.; Stephens, J. C.; Barry, S. M.; Kavanagh, K.; Challis, G. L.; Brougham, D.; Doyle, S. The Role of Glutathione S-Transferase GliG in Gliotoxin Biosynthesis in Aspergillus Fumigatus. *Chem. Biol.* **2011**, *18* (4), 542–552.
(107) Liu, Y.; Mándi, A.; Li, X.-M.; Meng, L.-H.; Kurtán, T.; Wang, B.-G. Peniciadametizine A, a Dithiodiketopiperazine with a Unique Spiro[Furan-2,7'-Pyrazino[1,2-b][1,2]Oxazine] Skeleton, and a Related Analogue, Peniciadametizine B, from the Marine Sponge-Derived Fungus Penicillium Adametzioides. *Mar. Drugs* **2015**, *13* (6), 3640–3652.
(108) Garo, E.; Starks, C. M.; Jensen, P. R.; Fenical, W.; Lobkovsky, E.; Clardy, J. Trichodermamides A and B, Cytotoxic Modified Dipeptides from the Marine-Derived Fungus Trichoderma Virens. *J. Nat. Prod.* **2003**, *66* (3), 423–426.
(109) Davis, R. A.; Longden, J.; Avery, V. M.; Healy, P. C. The Isolation, Structure Determination and Cytotoxicity of the New Fungal Metabolite, Trichodermamide C. *Bioorg. Med. Chem. Lett.* **2008**, *18* (9), 2836–2839.
(110) Capon, R. J.; Ratnayake, R.; Stewart, M.; Lacey, E.; Tennant, S.; Gill, J. H. Aspergillazines A–E: Novel Heterocyclic Dipeptides from an Australian Strain of Aspergillus Unilateralis. *Org. Biomol. Chem.* **2005**, *3* (1), 123–129.
(111) Zheng, X. F.; Wang, X. L.; Chang, J. B.; Zhao, K. Novel Rearrangement of 1H-2,3-Benzoxazines to Cyclic N-Acyl Hemiaminals: Application to the Synthesis of 1-Arylnaphthalene Skeletal Congeners. *Tetrahedron* **2008**, *64* (1), 39–44.
(112) Trown, P. W. Antiviral Activity of N,N′-Dimethyl-Epidithiapiperazinedione, a Synthetic Compound Related to the Gliotoxins, LL-S88α and β, Chetomin and the Sporidesmins. *Biochem. Biophys. Res. Commun.* **1968**, *33* (3), 402–407.
(113) Poisel Hans; Schmidt Ulrich. Synthesis of 2,5-Piperazinediones Having Sulfur-Containing Bridges between C$^{\alpha}$3 and C$^{\alpha}$6. *Angew. Chem. Int. Ed. Engl.* **1971**, *10* (2), 130–131.
(114) Kishi, Y.; Nakatsuka, S.; Fukuyama, T.; Havel, M. Total Synthesis of Sporidesmin A. *J. Am. Chem. Soc.* **1973**, *95* (19), 6493–6495.
(115) Yoshimura, J.; Nakamura, H.; Matsunari, K. A New Synthesis of 3,6-Dialkyl-1,4-Dimethyl-3,6-Epithio-and -3,6-Epidithio-2,5-Piperazinediones. *Bull. Chem. Soc. Jpn.* **1975**, *48* (2), 605–609.
(116) Aliev, A. E.; Hilton, S. T.; Motherwell, W. B.; Selwood, D. L. A Concise Approach to the Epidithiodiketopiperazine (ETP) Core. *Tetrahedron Lett.* **2006**, *47* (14), 2387–2390.
(117) Overman, L. E.; Sato, T. Construction of Epidithiodioxopiperazines by Directed Oxidation of Hydroxyproline-Derived Dioxopiperazines. *Org. Lett.* **2007**, *9* (25), 5267–5270.
(118) Kim, J.; Ashenhurst, J. A.; Movassaghi, M. Total Synthesis of (+)-11,11'-Dideoxyverticillin A. *Science* **2009**, *324* (5924), 238–241.

(119) Iwasa, E.; Hamashima, Y.; Fujishiro, S.; Higuchi, E.; Ito, A.; Yoshida, M.; Sodeoka, M. Total Synthesis of (+)-Chaetocin and Its Analogues: Their Histone Methyltransferase G9a Inhibitory Activity. *J. Am. Chem. Soc.* **2010**, *132* (12), 4078–4079.
(120) Kim, J.; Movassaghi, M. General Approach to Epipolythiodiketopiperazine Alkaloids: Total Synthesis of (+)-Chaetocins A and C and (+)-12,12′-Dideoxychetracin A. *J. Am. Chem. Soc.* **2010**, *132* (41), 14376–14378.
(121) Öhler, Elisabeth; Poisel, Hans; Tataruch, Frieda; Schmidt, Ulrich. Syntheseversuche in Der Reihe Der 3.6-Epidithio-2.5-dioxo-piperazin-Antibiotika Gliotoxin, Sporidesmin, Aranotin Und Chaetocin, IV. Synthese Des Epidithio-L-prolyl-L-prolinanhydrids. *Chem. Ber.* **1972**, *105* (2), 635–641.
(122) Nicolaou, K. C.; Giguère, D.; Totokotsopoulos, S.; Sun, Y.-P. A Practical Sulfenylation of 2,5-Diketopiperazines. *Angew. Chem. Int. Ed.* **2012**, *51* (3), 728–732.
(123) Kurogi, T.; Okaya, S.; Fujiwara, H.; Okano, K.; Tokuyama, H. Total Synthesis of (+)-MPC1001B. *Angew. Chem. Int. Ed.* **2016**, *55* (1), 283–287.
(124) Nakatsuka, S.; Fukuyama, T.; Kishi, Y. A Total Synthesis of d,l-Sporidesmin B. *Tetrahedron Lett.* **1974**, *15* (16), 1549–1552.
(125) Fukuyama, T.; Kishi, Y. A Total Synthesis of Gliotoxin. *J. Am. Chem. Soc.* **1976**, *98* (21), 6723–6724.
(126) Fukuyama, T.; Nakatsuka, S.-I.; Kishi, Y. Total Synthesis of Gliotoxin, Dehydrogliotoxin and Hyalodendrin. *Tetrahedron* **1981**, *37* (11), 2045–2078.
(127) Vogel E.; Günther H. Benzene Oxide-Oxepin Valence Tautomerism. *Angew. Chem. Int. Ed. Engl.* **1967**, *6* (5), 385–401.
(128) McMahon, T. C.; Stanley, S.; Kazyanskaya, E.; Hung, D.; Wood, J. L. A Scaleable Formal Total Synthesis of Dehydrogliotoxin. *Tetrahedron Lett.* **2011**, *52* (17), 2262–2264.
(129) Strunz, G. M.; Kakushima, M. Total Synthesis of (±) Hyalodendrin. *Experientia* **1974**, *30* (7), 719–720.
(130) Williams, R. M.; Rastetter William H. Syntheses of the Fungal Metabolites (.+-.)-Gliovictin and (.+-.)-Hyalodendrin. *J. Org. Chem.* **1980**, *45* (13), 2625–2631.
(131) Takeuchi, R.; Shimokawa, J.; Fukuyama, T. Development of a Route to Chiral Epidithiodioxopiperazine Moieties and Application to the Asymmetric Synthesis of (+)-Hyalodendrin. *Chem. Sci.* **2014**, *5* (5), 2003–2006.
(132) Zipfel, H. F.; Carreira, E. M. A Unified Strategy to 6–5–6–5–6-Membered Epipolythiodiketopiperazines: Studies towards the Total Synthesis of Scabrosin Diacetate and Haematocin. *Chem. – Eur. J.* **2015**, *21* (35), 12475–12480.
(133) Loughlin, W. A.; Marshall, R. L.; Carreiro, A.; Elson, K. E. Solution-Phase Combinatorial Synthesis and Evaluation of Piperazine-2,5-Dione Derivatives. *Bioorg. Med. Chem. Lett.* **2000**, *10* (2), 91–94.
(134) Adams, T. C.; Payette, J. N.; Cheah, J. H.; Movassaghi, M. Concise Total Synthesis of (+)-Luteoalbusins A and B. *Org. Lett.* **2015**, *17* (17), 4268–4271.
(135) Hodges, T. R.; Benjamin, N. M.; Martin, S. F. Syntheses of Gliocladin C and Related Alkaloids. *Org. Lett.* **2017**, *19* (9), 2254–2257.
(136) Codelli, J. A.; Puchlopek, A. L. A.; Reisman, S. E. Enantioselective Total Synthesis of (−)-Acetylaranotin, a Dihydrooxepine Epidithiodiketopiperazine. *J. Am. Chem. Soc.* **2012**, *134* (4), 1930–1933.
(137) Fujiwara Hideto; Kurogi Taichi; Okaya Shun; Okano Kentaro; Tokuyama Hidetoshi. Total Synthesis of (−)-Acetylaranotin. *Angew. Chem. Int. Ed.* **2012**, *51* (52), 13062–13065.

(138) Miknis, G. F.; Williams, R. M. Total Synthesis of (.+-.)-Aspirochlorine. *J. Am. Chem. Soc.* **1993**, *115* (2), 536–547.
(139) Wu, Z.; Williams, L. J.; Danishefsky, S. J. A Three-Step Entry to the Aspirochlorine Family of Antifungal Agents. *Angew. Chem. Int. Ed.* **2000**, *39* (21), 3866–3868.
(140) Lu, C.-D.; Zakarian, A. Total Synthesis of (±)-Trichodermamide B and of a Putative Biosynthetic Precursor to Aspergillazine A Using an Oxaza-Cope Rearrangement. *Angew. Chem. Int. Ed.* **2008**, *47* (36), 6829–6831.
(141) Zakarian, A.; Lu, C.-D. Development of the 1,2-Oxaza-Cope Rearrangement. *J. Am. Chem. Soc.* **2006**, *128* (16), 5356–5357.
(142) Wan, X.; Joullié, M. M. Enantioselective Total Syntheses of Trichodermamides A and B. *J. Am. Chem. Soc.* **2008**, *130* (51), 17236–17237.
(143) Mfuh, A. M.; Zhang, Y.; Stephens, D. E.; Vo, A. X. T.; Arman, H. D.; Larionov, O. V. Concise Total Synthesis of Trichodermamides A, B, and C Enabled by an Efficient Construction of the 1,2-Oxazadecaline Core. *J. Am. Chem. Soc.* **2015**, *137* (25), 8050–8053.

Chapter 2

A Synthetic Strategy Toward the Oxazinyl Natural Products Gliovirin, the Pretrichodermamides and the Trichodermamides

2.1 INTRODUCTION

Tetrahydro-1,2-oxazines and Dihydro-1,2-oxazines are a motif rarely found in natural products. Yet, oxazine-containing natural products display a highly-conserved oxidation pattern and structure, suggestive of a common intermediate.[1] These can be categorized into three main classes: non-classical ETPs such as gliovirin (**80**),[2,3] rearrangement products including the peniciadametizines,[4] and elimination products exemplified by the trichodermamides (Figure 2.1).[5,6]

We were drawn to **80** as a synthetic target as it was isolated in an undisclosed yield, suggesting low availability from biological sources, and its unusual structure imparts intriguing bioactivity. Along with the tetrahydro-1,2-oxazine contained within its densely-functionalize

***Figure 2.1**. Examples of oxazine–containing natural products*

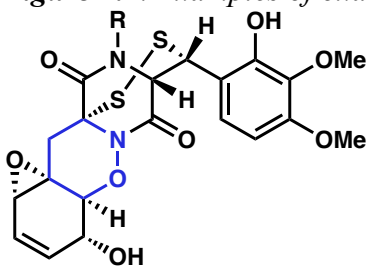

R=H, gliovirin (80)
R=Me, FA-2097(81)

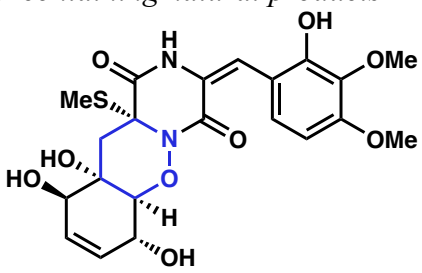

peniciadametizine B (137)

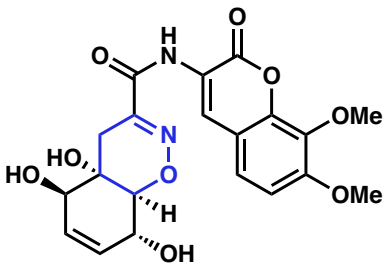

trichodermamide A (138)

structure it also features an anomalous [2.2.3]-ETP core, seven stereocenters and is replete with oxidation. Due to its restricted availability and structural complexity a full understanding of its biological activity has been limited. Despite these challenges, gliovirin has shown antimicrobial activity against prominent phytopathogens including *Phytopthora sp.* and *Pythium ultimum*.[7] More recently, **80** has also demonstrated activity as an inhibitor of inducible TNF-α expression in human T-cells and macrophages.[8]

The proposed synthetic strategy to access **80** is to generate the DKP at a late stage and install the disulfide linker as the final step. This approach, therefore, relies upon the synthesis of two fully functionalized non-canonical amino acids: the eastern fragment, an oxidized phenylalanine derivative (**315,** Scheme 2.1), and the western fragment, a highly oxidized bicyclic tetrahydroxazine (**314**, Scheme 2.1**)**.

Based upon Williams' and Danishefsky's work (see Section 1.3.2, Chapter 1) on the aspirochlorine core there was good precedent for benzylic sulfenylation either through direct benzylic functionalization or a 1,2-sulfur migration.[9,10] Furthermore, the opposing strategy, pre-integration of the benzylic sulfur, provided additional challenges beyond the scope of the desired area of research. Synthetic tactics to install the benzylic sulfur earlier in the route, including sulfa–Michael additions or an aziridine ring–openings, often present poor selectivities and depressed

Scheme 2.1. *Retrosynthetic analysis of gliovirin*

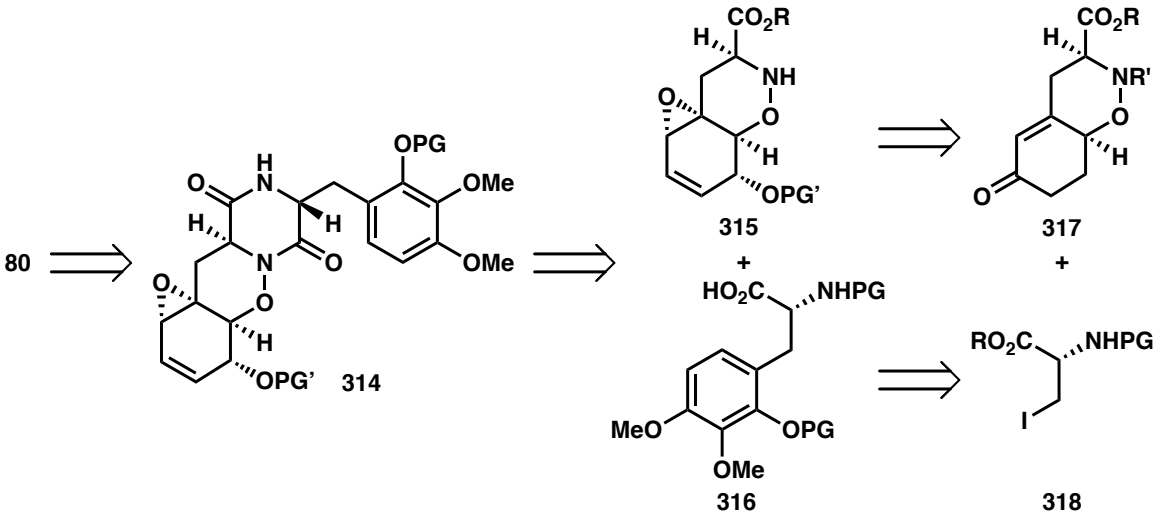

yields for the necessary electron-rich substrates. As shown in Scheme 2.1 synthesis of the eastern fragment would be enabled through the palladium-catalyzed Negishi cross-coupling of a iodoserine derivative **318** with an aryl iodide.[11]

The western fragment, a highly oxidized bicyclic tetrahydroxazine, provides an enormous synthetic challenge. In our strategy, this highly functionalized intermediate **315** could be generated through oxidative manipulations of an enantioenriched biyclic oxazine **317**. This critical intermediate **317** would be generated either through radical cyclization of a hydroxamate or through a hetero Diels–Alder reaction.

In approaching the synthesis of **315** there are several considerations that place limitations on the synthetic tactics one is able to engage. An important consideration is the oxazine N-O bond which is prone to reduction under a variety of conditions to form 1,4-aminoalcohols (Scheme 2.2a).[12–18] This reactivity has exploited in a variety of syntheses (Scheme 2.2b).[19–30] Furthermore, the acidic α-proton of the tetrahydro-1,2-oxazine can enolize readily which facilitates subsequent N-O bond cleavage and tetrahydrofuran formation (Scheme 2.2a). The reactivity could be implicated in formation of 2-aminotetrahydrofuran natural products, such as **143ab** (Scheme

2.2c).[31] The oxidized ring of the western fragment **315** is likely unstable to oxidation as it could readily form an aromatic system or undergo an electrocyclic rearrangement (Scheme 2.2d).[32]

Scheme 2.2. *Transformations associated with tetrahydro-1,2-oxazines and the western fragment*

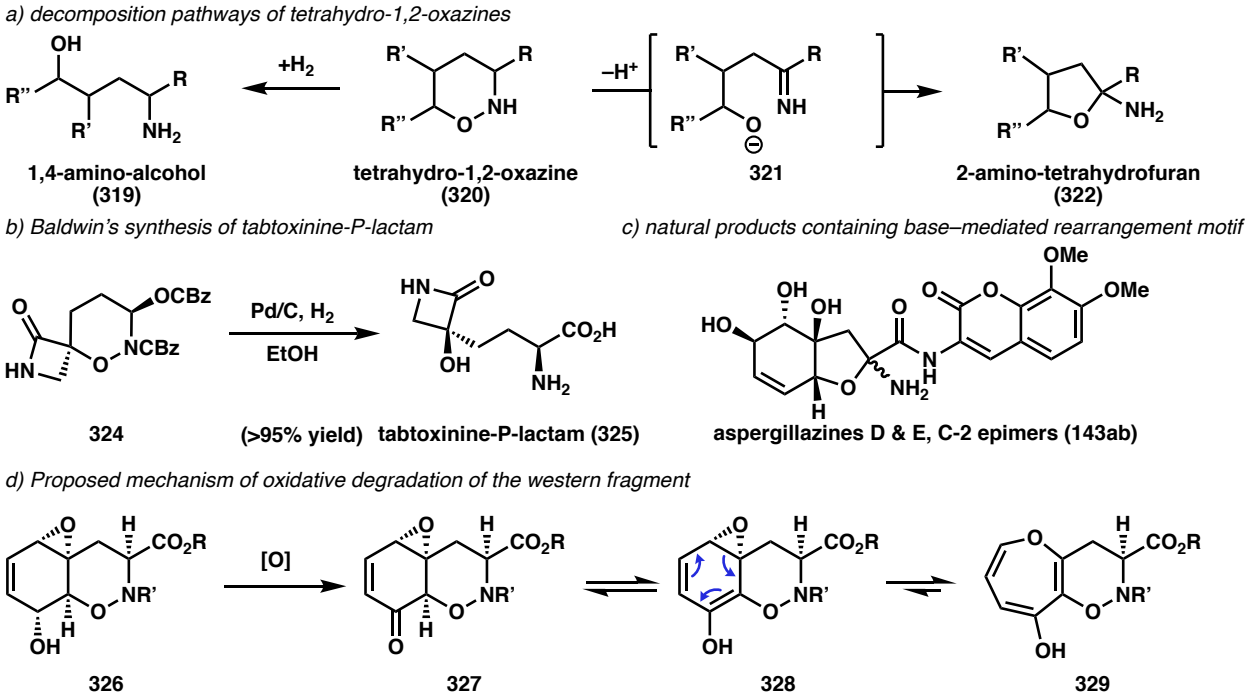

2.2 HETERO DIELS-ALDER DERIVATIVES

The use of a hetero Diels–Alder cyclization to form the bicylic oxazine was attractive to us as a direct way to form the desired bicyclic motif. A reactive nitroso-alkene is known to be generated *in situ* from oxime **326**, which can react with electron-rich olefins including silyl enol ethers and dienes.[33] To further evaluate the strategy, the reaction was carried out with 1,3-cyclohexadiene to generate the bicyclic dihydro-1,2-oxazine **327** in excellent diastereoselectivity and tractable yield on scale (Scheme 2.3). It would be advantageous if one could directly integrate oxidation at C4 using the appropriate silyl enol ether; however, previous studies show a high selectivity for integration at C9. Therefore, elaboration **327** was attempted to access the desired western fragment through redox manipulations. 1,2-Reduction of cyclic oxime proceeded with

modest diastereoselectivity for the desired *syn–syn* product **328**. Optimization of the 1,2–reduction to improve the diastereoselectivity was untenable due to cross reactivity with the reduction-prone N-O bond. Further oxidative elaboration of the all-carbon ring was also met with challenges. While the C7-C8 olefin of **327** could be epoxidized diasteroselectively to form **329**, the desired base–mediated elimination to yield the allylic alcohol motif present in **80** did not proceed.[34] Instead, only minor epimerization of the starting material was observed at the ring fusion.

Therefore, while the [4+2] approach generated the bicyclic framework rapidly, it did not lend itself easily to oxidative elaboration. Furthermore, the preparation of enantioenriched cycloadducts would require substantial method development.[35] The racemic intermediate **321** generated by this study was later used to evaluate amide coupling of the eastern and western fragments in model studies.

Scheme 2.3. *Elaboration of hetero Diels–Alder product*

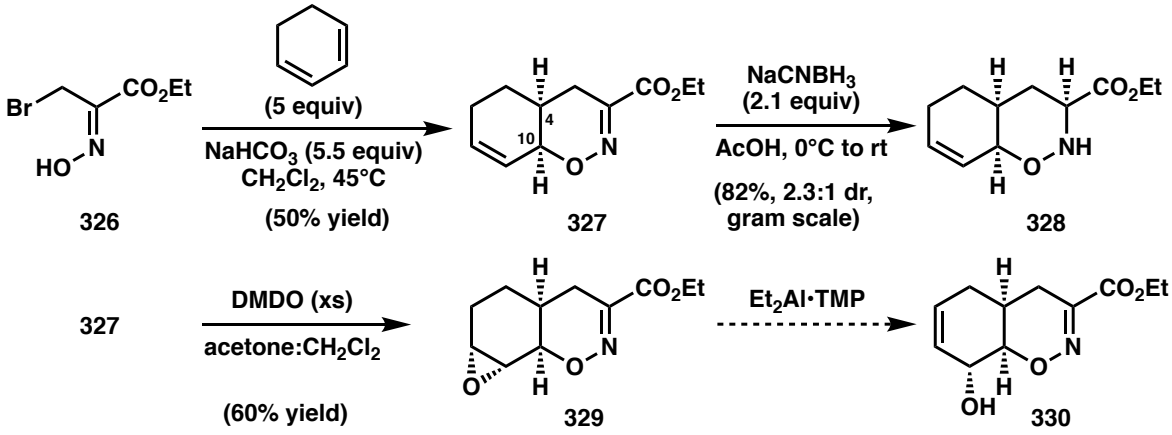

2.3 SYNTHESIS OF OXIDATIVE CYCLIZATION SUBSTRATES

The biosynthetically inspired cyclization of a modified *N*-oxy-phenylalanine derivative was identified as a valuable strategy. Using an *N*-oxy amino ester as a cyclization substrate one could integrate a stereocenter early in the synthesis to later leverage in diastereoselective reactions.

The cyclization intermediates targeted for evaluation were *N*-hydroxy-3,4-dihydrophenylalanines, such as **333**, as the product would retain two conjugated synthetic handles on the all-carbon ring. To access the desired enantioenriched diene motif several approaches were attempted. *N*-oxidation of the known amino acids resulted in no desired product formation (Scheme 2.4a).[36] A Second approach employs protected hydroxylamines to engage with activated enals electrophiles to undergo asymmetric conjugate addition to form *bis*-protected *N*-hydroxy amino ester **337** (Scheme 2.4b).[37,38] Yet, when **337** was subjected to modified Seyferth–Gilbert[39] conditions using the Ohira–Bestmann reagent **338**[40] to homologate to the desired alkyne **339**, unproductive decomposition was observed. Control experiments showed that the substrate was not stable to the mildly basic conditions used in the transformation.

Scheme 2.4. *Failed approaches to an oxidative cyclization substrate*

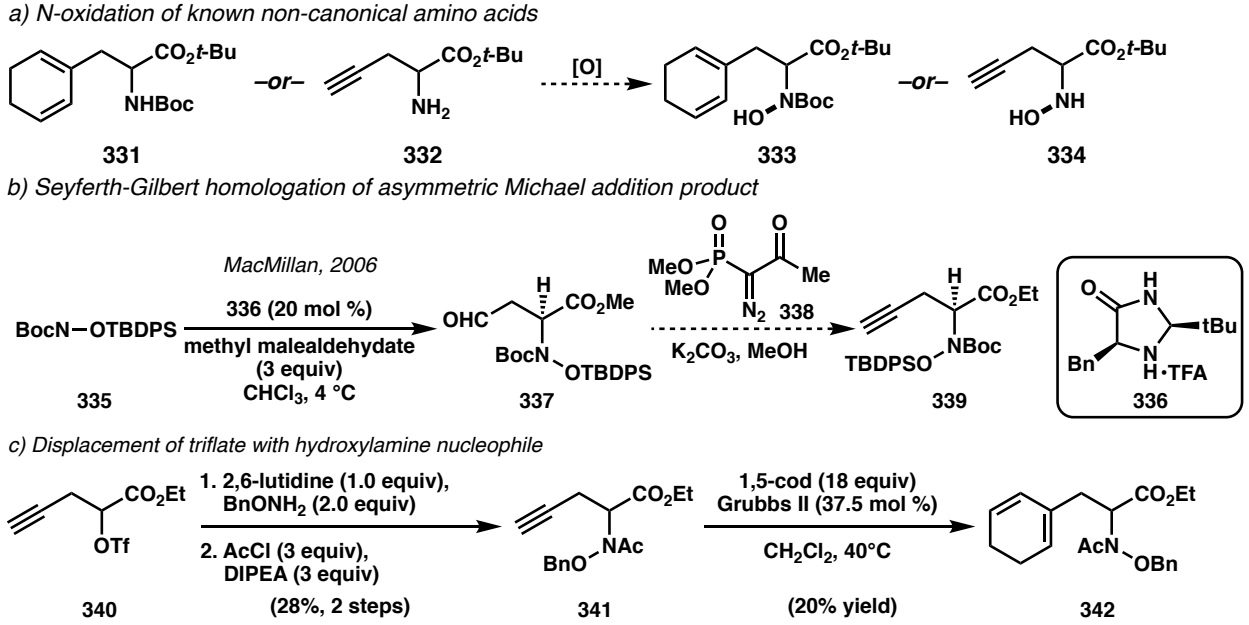

In subsequent series of attempts the desired **342**, a known α-hydroxy ester was activated as the triflate, **340** (Scheme 2.4c).[41] Displacement with a hydroxylamine nucleophile and subsequent *N*-acylation generates a stable protected hydroxylamino ester **341** in a low yield.[42]

Gratifyingly, the alkyne **341** could undergo an inefficient enyne metathesis reaction to generate the *N*-hydroxy-3,4-dihydrophenylalanine **342**. Attempts to debenzylate **342** under Lewis acidic conditions led to unproductive decomposition of the starting material.[43] Due to the presence of an electron-rich diene, debenzylation under reductive conditions could not be attempted without competitive alkene reduction. Substitution of an orthogonal protecting group, trimethylsilyl (TMS), in place of the benzyl group on the hydroxylamine nucleophile was unsuccessful. HPLC-MS analysis of the reaction media suggested that displacement **330** with *O*-trimethylsilyl hydroxylamine had occurred; however, no desired product was ever recovered from the crude reaction. As a result of the low yielding transformations of the displacement strategy and a lack of flexibility in its protecting group strategy a more direct route was explored.

Scheme 2.5. *Racemic and asymmetric syntheses of N-siloxy propargyl glycine*

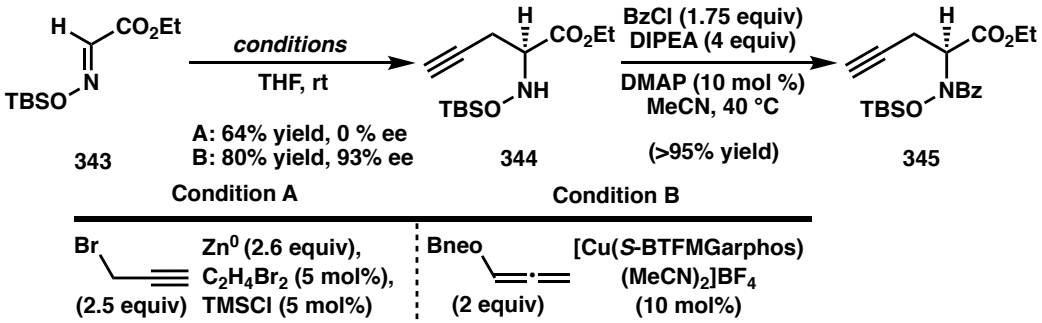

Finally, it was hypothesized that a direct homopropargylation of the oxime ester **332** could efficiently access *N*-siloxy propargyl glycine **333**. While **332** was initially resistant to functionalization, two methods were discovered to provide the desired product. The addition of allenyl zinc bromide, generated *in situ*, provided the racemic alkyne as the major product with a minor allenyl impurity (Conditions A, Scheme 2.5).[44] Furthermore, copper–catalyzed asymmetric alkylation developed in the Reisman group (See Chapter 3) was also implemented to provide the enantioenriched product, formed in good yield and high enantiomeric excess with no allenyl

impurity observed (Conditions B, Scheme 2.2d). To the best of our knowledge this is the first example of a catalytic asymmetric alkylation of an oxime. The *N*-siloxyamino ester **344**, was benzoylated efficiently but **345** was unstable to standard silica purification; a plug of Florisil®,[45] however, provided clean product in excellent yield.

Our Early attempts to perform a methylene-free enyne metathesis based on the initial disclosure by Diver led to high conversions but low yields (entry 1, Table 2.1).[46,47] Darkening of the solution was suggestive of catalyst decomposition.[48] Regardless, the yields remained intractable whether using a higher catalyst loadings or portion-wise catalyst addition. Similarly, different catalysts and common additives had negligible effect on yield.

Table 2.1. *Enyne metathesis optimization studies*

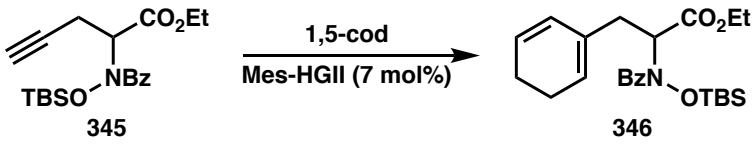

345 346

entry	1,5-cod (equiv)	addition (h)	solvent (conc, mM)	temp (°C)	conversion (%)	yield (%)
1	10	6	CH_2Cl_2 (10–5)	0–>20	70	9
2	2	0.5	PhMe (1.6–0.8)	0–>20	79	--
3	20	0.5	PhMe (56–28)	0–>20	68	24
4	10	1.5	PhMe (15–7.5)	20	90	1
5	10	7.4	PhMe (10–5)	20	74	43
6	10	6	EtOAc (10–5)	20	43	8
7	9	6	Hexane (10–5)	20	52	11
8	9	6	PhH (10–5)	20	56	28
9	10	12	PhH (19–5)	20	100	96

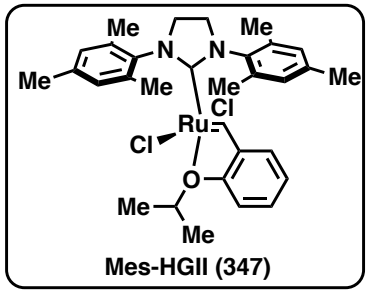

Mes-HGII (347)

The stability of a Hoveyda-Grubbs' catalyst is dependent upon solvent. A screen of a series of solvents for this reaction demonstrated that the efficiency of the reaction improved in argon-degassed benzene (entry 8, Table 2.1). Slow addition of a solution of **345** and careful control of the concentration of catalyst in the reaction mixture was essential for productive reactivity. To further improve the yield of the transformation kinetic studies of other intermolecular enyne

metathesis reactions were used as a guide. These studies demonstrate that the productive enyne pathway is first order in cyclooctadiene and catalyst, but zero order in the substrate.[49] Therefore, decreasing the concentration of the substrate in the reaction medium, raising the catalyst concentration (19–5 mM), and extending the addition time of **345** results in an excellent yield of the desired diene **346** (entry 9, Table 2.1).

2.4 OXIDATIVE CYCLIZATION OF AN *N*-HYDROXY AMINO ESTER

To accomplish the proposed oxidative cyclization, we were motivated to build upon previous studies on radical cyclizations of hydroxamic acids with olefinic substrates. This class of reactivity was first observed by Perkins when aromatic **336** spontaneously cyclized in air to generate a hydroperoxide **337** (Scheme 2.3a). Alexanian later systematically explored this reaction on a variety of substrates converting the intermediate cyclized hydroperoxides to alcohols or ketones, we particularly by the encouraged by their ability to generate 6-6 bicyles (Scheme 2.3b) and highly diastereoenriched products (Scheme 2.3c) in good yields.[50,51] Our investigations focused on analogous reactivity in novel substrates; unlike Alexanian's work we identified a copper catalyst as an efficient catalyst to facilitate cyclization. Since our optimization studies, several disclosures of intermolecular radical additions in simplified systems were published utilizing copper sources as catalysts (Scheme 2.3d–f).[52–54]

In contrast to previous work, where stereocenters were formed in close proximity to one another (Scheme 2.3ab), the goal of the present study was to form disparate stereocenters on **350** at C7 and C10, with diastereocontrol relative to the C3 α-carbon. Prior to undertaking these studies, it was hoped that a reductive work-up of the intermediate allylic hydroperoxide would

provide an α–disposed alcohol at the newly formed C7 allylic site which could be subsequently leveraged as a directing group to ensure facile installation of the desired tri-substituted epoxide

Scheme 2.6. *Oxidative radical additions of N-oxides to olefins*

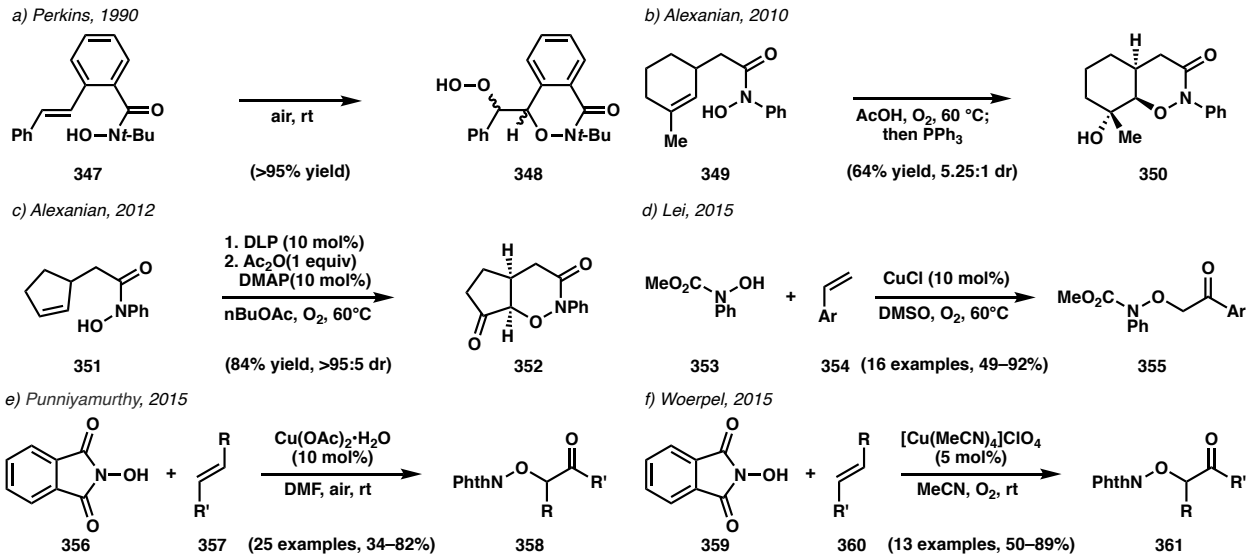

present in the **80**. Despite these aspirations, upon silyl deprotection and subsequent oxidative cyclization a complex mixture of allylic alcohols was observed in low yields with the major product being the *syn-anti*-β-OH **350** (Scheme 2.4). Along with the mixture of allylic alcohols, enone products were also formed despite the reductive work-up exhibiting with the desired C3-C10 *syn*-diastereomer **351** as the major product.

The selectivity at C7 for the undesired diastereomer can be rationalized through conformational analysis informed by previous computational studies by Houk in which it was shown that triplet oxygen and cyclic allylic combine through an antiperiplanar trajectory in the transition state.[55] A qualitative comparision of the transition state conformers for axial (**353**$_{\mathbf{axial}}$, Scheme 2.5) and equatorial (**353**$_{\mathbf{equatorial}}$) oxygen capture, suggest that they are close in energy; however, it appears that axial capture would generate less torsional strain during the formation of

the intermediate hydroperoxide **354**$_{\mathbf{axial}}$ which upon reduction forms the observed major diastereomer (**350**).

Scheme 2.7. *Initial studies and conformational analysis of an oxidative cycylization*

a) oxidative cyclization of an N*-hydroxy amino ester with a reductive workup*

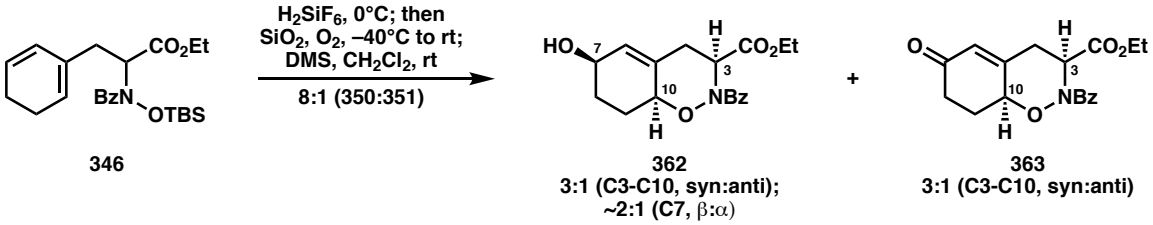

b) conformational analysis to rationalize diastereoselectivity in C7–oxygenation

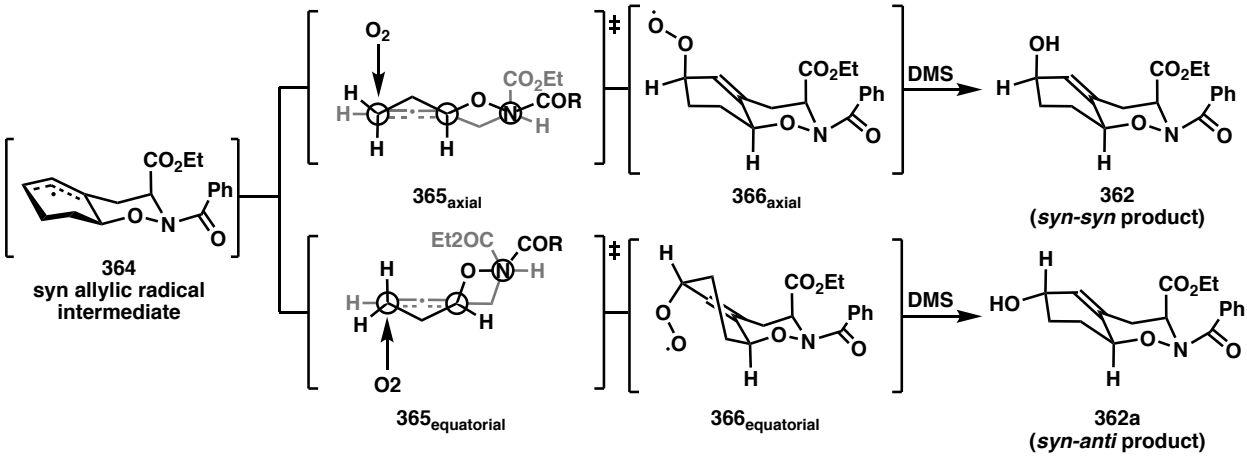

Guided by this analysis, it suggested that this diastereoselectivity would not be easily improved and therefore optimization toward the selective generation of the *syn*-enone **351** was undertaken. To that end, a Kornblum-DeLaMare[56] work-up was employed in a similar fashion to that used previously by Alexanian (Scheme 2.3c). A solvent screen identified acetonitrile as a superior solvent for the transformation and while a fluoride-mediated deprotection was efficacious, an acidic deprotection using methanesulfonic acid could be substituted and simplified the work-up. The addition of a copper salt appeared to facilitate the reaction at a lower temperature. A screen of copper-diamine complexes inspired by the work of Stack in Cu-monooxygenase models[57,58]

identified tetramethylethylenediamine (TMEDA) as the optimal additive (entry 3, Table 2.2). Use of a non-coordinating counterion provides a small but consistent improvement to the yield (entry 5, Table 2.2). The reaction required dilute conditions for good reactivity, as concentrations above 0.1M provided only trace product (entry 6, Table 2.2). Finally, a base screen of the Kornblum-DeLaMare work-up showed that the weak base pyridine out-performed other nitrogenous bases in a separate screen and had improved scalability.

Table 2.2. *Optimization of the oxidative cyclization of* N-*siloxy-dihydrophenyalanine*

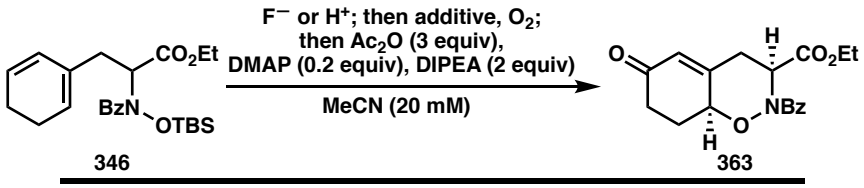

346 363

entry	deprotection	temp (°C)	additive	yield(%)[dr]
1	H_2SiF_6	rt; 0 to rt	SiO_2	57 [3.7:1]
2	$MeSO_3H$ (1 equiv)	rt; –40 to rt	$Cu(TEPDA)Cl_2$	34 [4.7:1]
3	$MeSO_3H$ (1 equiv)	rt; –40 to rt	$Cu(TMEDA)_2Cl_2$	41 [4.9:1]
4	$MeSO_3H$ (2 equiv)	rt; 0 to rt	$Cu(TMEDA)_2(BF_4)_2$	53 [4.9:1]
5	$MeSO_3H$ (2 equiv)	rt; –40 to rt	$Cu(TMEDA)_2(BF_4)_2$	63 [5.3:1]
6	$MeSO_3H$ (2 equiv)	rt; –40 to rt	$Cu(TMEDA)_2(BF_4)_2$	5 [5:1][a]
7	$MeSO_3H$ (0.5 equiv)	rt; –40 to rt	$Cu(TMEDA)_2(BF_4)_2$	64 [5.3:1][b]

[a]reaction run at 0.1 M [b]pyridine used in place DMAP/DIPEA

Upon completion of this optimization we wished to vary the substrate **335** to improve the diastereoselectivity and yield of the reaction further. Interestingly, substitution of a bulkier ester had no effect on the diastereoselectivity of the cyclization (entry 2, Table 2.3). Acyl substitution at the acyl substituent was varied, however, a significant increase in the preference for the *syn*-product was observed (entry 3, Table 2.3).. The overall yield of the transformation was not perturbed by this *N*–substitution, suggesting a negligible effect on the competitive decomposition pathways; yet, the shift in diastereoselectivity was a strongly indicative that the acyl substitutent had a key role in differentiation of the *syn* and *anti* reaction pathways.

Previous studies have shown that cyclic amides have a preference for an equatorial disposition and will develop $A^{1,3}$–type strain with α-substituents.[59] Integrating these observations into conformational analysis of the initial cyclization step, one can rationalize the inherent *syn*-preference of the cyclization. To generate the observed major diastereomer, the reaction would proceed through a low-energy chair-like conformation with the C3 ester in an axial disposition (**356$_{chair}$**, Scheme 2.6) to alleviate developing $A^{1,3}$–type strain in the transition state. This conformational preference would be substantiated by crystal structure (See Table 2.6). Alternatively, the reaction could proceed through a transition state with a higher energy boat-like conformation (**356$_{boat}$**) with $A^{1,3}$ minimization or through another chair-like conformation (**356$_{chair*}$**) with strain developing between the hydroxamate and the α-substitutent. Both of these higher energy conformations would lead to the minor diastereomer, though to discern their relative contributions to the reaction will require a more thorough computational analysis.

Table 2.3. *Structural effects on the oxidative cyclization of* N-*siloxy-dihydrophenyalanine*

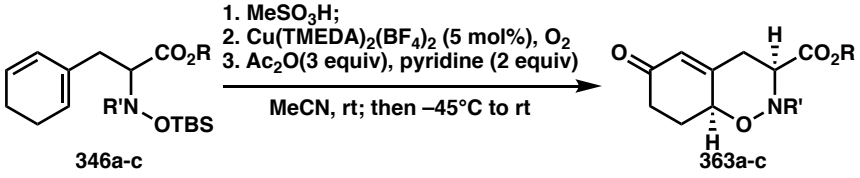

entry	R	R'	yield (%)	dr (*syn*:*anti*)
1	Et	Bz	68[a]	5.2:1
2	iPr	Bz	56[b]	5.2:1
3	Et	Ac	62	13:1

[a]2g scale [b]DMAP/DIPEA used in place of pyridine

This novel copper-catalyzed cyclization inspired by Stack and Alexanian is a scalable method in hand to produce the key intermediate ***syn*-351** as the major product. Furthermore, this transformation occurs under mild conditions, low catalyst loading, and can proceed at cryogenic

temperature. With the bicylic framework of the western fragment established the oxidative elaboration of the enone to the desired epoxy allylic alcohol was undertaken.

Scheme 2.8. *Conformational analysis to rationalize syn–diastereoselectivity in C10–cyclization*

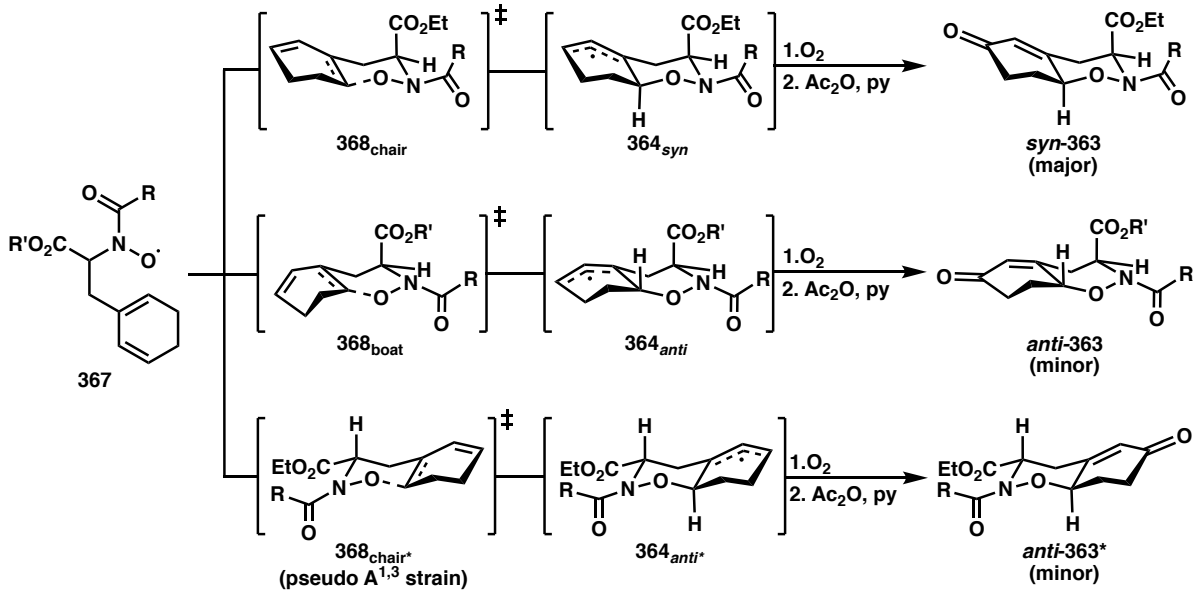

2.5 EPOXIDATION STUDIES

The copper–catalyzed cyclization provides an enone product with unsaturation at C5-C6 which corresponds to the epoxide in gliovirin. Therefore, direct installation of the requisite oxidation was pursued using either the allylic alcohol or enone precursor.

Initial studies were focused on the directed epoxidation of an α-disposed allylic alcohol (**α-350**, Scheme 2.7) as diastereoselectivity was a concern. Attempts to achieve a directed epoxidation of **α-350** were mired by messy reaction profiles and, most prominently, competitive oxidation of the allylic alcohol to form the enone. Competitive C–H oxidation is a known side reaction of directed epoxidations and appeared unavoidable on this substrate. While a high-yielding epoxidation of the allylic alcohol was unable to be achieved, the ratio of desired **357** to ***syn*-251** would shift based on the conditions used: vanadyl acetylacetonate–mediated oxidation

favored enone formation, while mCPBA favored epoxide formation. This reactivity is likely due to conformational effects. An equatorially–disposed alcohol accelerates the rate of epoxidation by mCPBA while vanadyl acetylacetonate prefers an axially-disposed alcohol in the transition state.[60] While the application of these reactions proved fruitless toward the synthesis of oxazine-containing natural products it was appealing to see pronounced differential activity in these unusual substrates.

Scheme 2.9. *Directed epoxidation studies on the allylic alcohol*

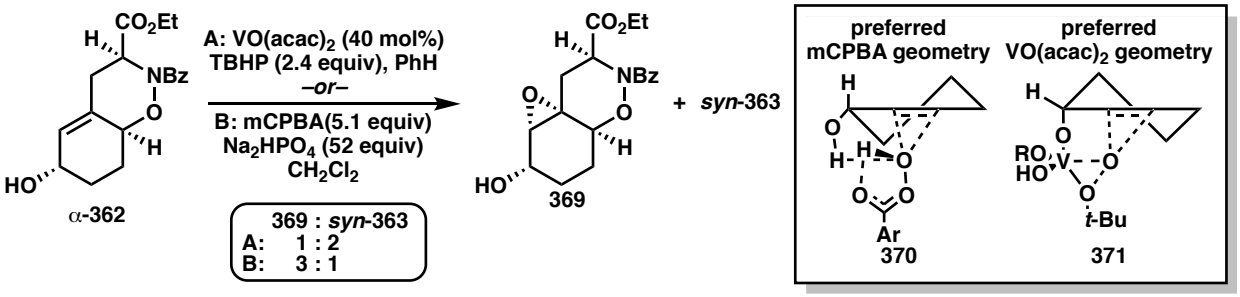

Attention turned to epoxidation of **351**. Standard Weitz-Scheffer conditions led to complete decomposition, with a small amount of desired product isolated only when a catalytic amount of base was used (entry 1, Table 2.4).[61] To avoid strongly basic conditions, attempts to use enamine catalysis specifically designed for the epoxidation of cyclic enones gave no reaction.[62] Similarly, other oxidants which epoxidize more electron-rich and less polarized olefins, such as DMDO, led to no reaction.

After an extensive survey of the literature, we were inspired by Magnus' synthesis of (+)–pancrastistatin.[63] To avoid decomposition of their especially base–sensitive substrate the authors found that a mixture of H_2O_2 and $NaHCO_3$ could generate a high yield of epoxide. To our delight, the first attempt of these conditions provided a 46% yield of the desired epoxide as a single diastereomer after 48h at 0 °C; however, these results were challenging to replicate, providing **360**

in variable yield (entry 2, Table 2.4). Encouraged by these promising results, however, reaction optimization studies began in earnest.

Table 2.4. *Selected entries from enone epoxidation optimization studies*

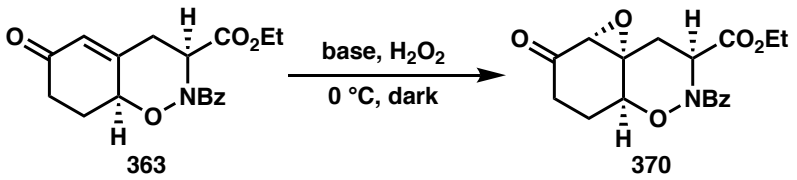

363 370

entry	oxidant	base	solvent	yield (%)
1	H_2O_2 (15.5 equiv)	LiOH(0.7 mol%)	EtOH	22
2	H_2O_2 (5 equiv)	$NaHCO_3$(4 equiv)	MeOH:THF:H_2O	16–61
3	H_2O_2 (5 equiv)	$NaHCO_3$(4 equiv)	tBuOH:THF:H_2O	65
4	H_2O_2 (5 equiv)	$NaHCO_3$(4 equiv)	tBuOH:THF:H_2O	70[a]
5	NaOCl (10 equiv)	$NaHCO_3$(1 equiv)	tBuOH:THF:H_2O	71[a]

[a] $CrCl_3$·3THF (4 mol%) added

Epoxidations of isolated olefins mediated by H_2O_2/$NaHCO_3$ were studied methodically by Burgess, noting that a low concentration of $NaHCO_3$ was key to generating high yields of product.[64,65] Lowering the concentration of $NaHCO_3$ to 2.0M did not increase the yield of the reaction significantly (~50%) but the reaction time shortened and, importantly, scale-up of these conditions were replicable in contrast to Magnus' conditions. Substitution of *t*-butanol for methanol led to an increase in yield (entry 3, Table 2.4). Finally, a screen of Lewis acid additives showed that catalytic $CrCl_3$ consistently improved the yield of the epoxide to 70% isolated. Further experimentation showed that slow addition of a mixture of $NaHCO_3$ and $CrCl_3$ in *t*-BuOH and water to a cold solution of substrate and H_2O_2 in THF gave excellent yields on large scale. Despite this highly-involved optimization and mild conditions of the transformation when the epoxidation was attempted with a new bottle of H_2O_2 complete decomposition occurred. This was discouraging; however, it was found that sodium hypochlorite could be used in the place of H_2O_2 with little decomposition observed and comparable yields on scale (entry 5, Table 2.4).

2.6 GENERATION OF EPOXY-ENE OXIDATION SUBSTRATE

Several strategies for the oxidative elaboration of **363** to the desired epoxy allylic alcohol motif were explored. The first of which was a focus on the conversion of the carbonyl to the alkene followed by an allylic oxidation at C9. The dehydration substrate **371**, while accessible through the inefficient epoxidation **α-362** (Scheme 2.9) was more expeditiously generated through a 1,2-reduction of **370** using Luche conditions (Scheme 2.10). Typical dehydration conditions through activation of **371** as a sulfonate ester either returned the starting material or led to complete decomposition upon heating. Desired product **372** was formed when the Martin's sulfurane was employed, yet again significant C-H oxidation was observed with competitive formation of **370**.[66]

Scheme 2.10. *Inefficient elimination of epoxy alcohol through dehydration*

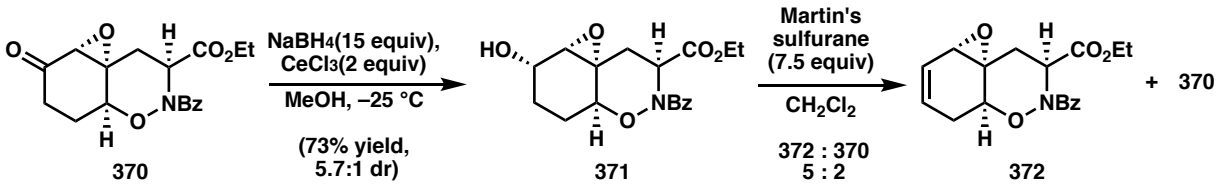

We wished to interrogate a palladium–mediated reduction of an epoxy vinyl triflate; however attempts to form the vinyl triflate did not produce an isolable intermediate. Further studies into this tactic were abandoned as α-epoxy vinyl triflates are prone to a myriad of decomposition and rearrangement pathways when subjected to palladium-catalyzed reductive conditions.[67]

Finally, a three–step procedure was successful in generating the desired epoxy alkene **365**. First, a modified Wharton protocol (for Method Development, see Section 2.10) generated a tertiary allylic alcohol **362** in high yield (Scheme 2.9).[68] This intermediate could then be submitted to a light–mediated allylic bromination with *N*-bromosuccimide (NBS) to generate a diastereomeric and isomeric mixture of allylic bromides.[69] The crude mixture of allylic bromides

was not fully characterized but carried on crude through a silver–mediated halide elimination to form the desired epoxy alkene in excellent yield, two steps from **373**.[70]

Scheme 2.9. *Efficient synthesis of the epoxy alkene from the epoxy ketone*

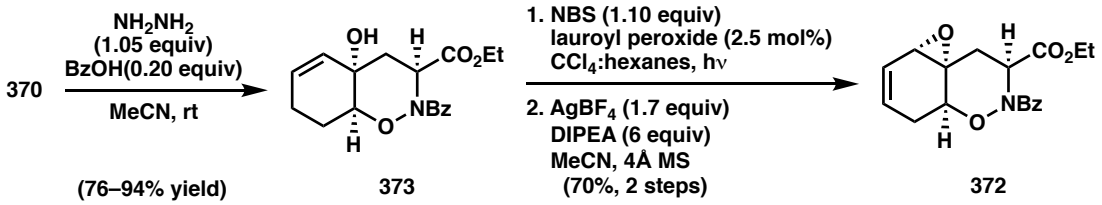

2.7 STUDIES ON C9-ALLYLIC FUNCTIONALIZATION

With **372** in hand the efficient introduction of oxidation at the C9 allylic methylene would complete the synthesis of the fully elaborated western fragment **315** (Scheme 2.1). Allylic oxidation has been the subject of much study in organic chemistry and applied to a number of total syntheses.[71] These methods were brought to bear in the attempted oxidation of **361**. The use of selenium dioxide as an oxidizing reagent under a variety of solvent mixtures and additives provided no desired reactivity.[72] Use of a phosphate buffer or pyridine co-solvent prevented epoxide opening; however, no oxidation was observed. Increasing the reaction temperature to 40 °C unfortunately led to complete decomposition of the materials.

Scheme 2.10. *Desired oxidative functionalization of epoxy alkene*

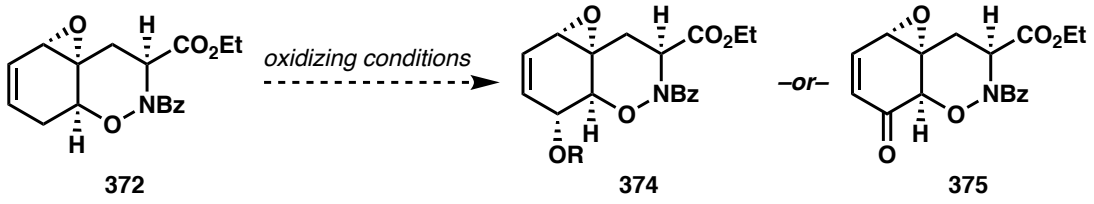

The oxidation substrate, **372**, was also unreactive to Kharasch-Sosnovsky oxidations[73] while metal-free oxidations, including NHPI–mediated oxidations,[74,75] led to complete decomposition. When manganese triacetate was used together with THBP, as a stoichiometric

oxidant, a mixture of an mixture of products was generated, yet evidence of desired product formation was observed by mass spectrometry. Unfortunately, repeated attempts to optimize, scale-up and isolated these potential oxidation products were unfruitful.[76]

With these negative results in mind, one's attention inevitably returns to previously successful tactics: allylic bromination. Yet, the epoxy alkene **372** did not react when subjected to the previously optimized conditions for **373**. Several trace bromide–containing products were detected, however no selectivity observed. Hoping to once again funnel the crude mixture to a single product, the crude was treated with silver(I) tetrafluoroborate and triethylsilanol resulting in the trace formation of an intractable mixture of silyl ether products.[70] The low efficiency and selectivity this bromination–displacement approach led to its rejection.

While the outlook of the oxidation of the C9-deoxy substrate is poor, it would be of value to evaluate the ability of P450 mutants to facilitate this especially difficult C9 oxidation due to their ability to reverse the selectivity of known chemical methods and proceed at room temperature.[77]

2.7 DESATURATION STUDIES

As the C9 allylic oxidation currently provides an inordinate challenge; therefore, alternative strategies were explored. A stereoretentive allylic transposition of a C7 oxidative handle to C9 was hoped to be thermodynamically favored. To interrogate this hypothesis, an allylic alcohol (**377a**, Table 2.6) must be accessed through the successful 1,2–reduction of a desaturated epoxy enone substrate (**376**, Table 2.5).

Conversion of the **370** to **376** like many of these transformations in this series was challenging. Typically, a ketone is converted to the corresponding silyl enol ether which can then

be subjected to a variety of conditions to form the desaturated product.[78–80] There are two general approaches to silyl enol ether formation: kinetic deprotonation with a strong base and quenching with a silyl halide or milder thermodynamic conditions using an amine base in conjunction with sodium iodide and a silyl triflate. Unfortunately, under kinetic conditions the epoxy ketone decomposed while thermodynamic conditions returned starting material. Attempts to form the allyl enol carbonate also led to decomposition.

Scheme 2.11. *Revised retrosynthetic plan for a fully elaborated western fragment*

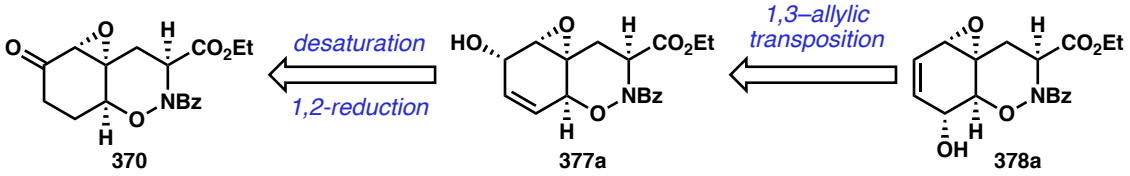

Recently, several direct methods for ketone desaturation have been disclosed. Encouraged by these discoveries, a direct desaturation was explored. Use of hypervalent iodine reagent lead to either recovery of the starting material or decomposition (entry 1, Table 2.5).[81] Alpha–selenation under thermal conditions gave a very messy reaction profile but appeared to have a small amount of a new enone–containing product (entry 3, Table 2.5). Isolation confirmed the formation of the desired **364** and while encouraged that the desired transformation could occur in one pot, the competitive decomposition observed suggested alternative approaches should be explored.

Palladium catalysis has a rich history in ketone desaturation exemplified by the Saegusa–Ito and Tsuji oxidations.[78,82] New advances in the literature have avoided the stoichiometric generation of a functionalized enol, employing more Lewis acidic palladium sources, perhaps to encourage enolization and α-palladation.[83] Submitting the epoxy ketone to these conditions (entry 2, Table 2.5) provided trace amounts of the **364**. Subjecting **360** to conditions derived from the White lab's tandem Wacker-Desaturation cascade, in the absence of water, provided the highest

observed yield of **364** (entry 4, Table 2.5).[84] Furthermore, the clean reaction profile and low reaction temperature made these conditions attractive for further optimization.

Table 2.5. *Selected entries in the optimization of the direct ketone desaturation*

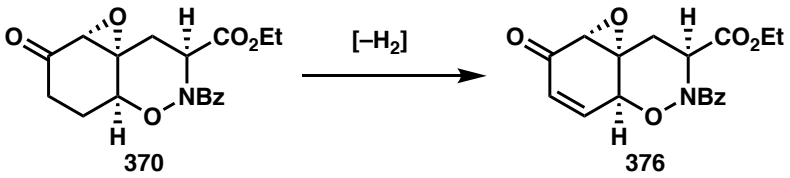

370 376

entry	reagents	solvent	temp (°C)	yield(%)
1	IBX(3.1 equiv), MPO·xH_2O(3.1 equiv)	DMSO	50	0
2	$Pd(tfa)_2(DMSO)_2$ (5mol%), O_2	Dioxane	125	trace
3	$(PhSeO)_2O$ (1.05 equiv)	PhCl	95	15
4	$Pd(MeCN)_4(BF_4)_2$ (15mol%), PIDA(25 mol%), 1,4-BQ(1 equiv)	DMSO	35	30
5	$Pd(MeCN)_4(BF_4)_2$ (15mol%), PIDA(25 mol%), 1,4-BQ(1.25 equiv)	DMSO	50	67

A solvent screen indicated that DMSO was anomalous in its ability to foster productive reactivity, with acetonitrile being the only other solvent that provided a trace of product. By raising the temperature from 35 °C to 50 °C the yield increased from 30% yield (75% brsm) to 50% yield (60% brsm) with a minimal decrease in the overall efficiency of the transformation. Improving conversion was critical as the product and starting material were difficult to separate chromatographically. This provided a challenge in reaction monitoring as **360** and **364** had identical retentions on reverse–phase HPLC and TLC. The reaction could, however, be monitored by NMR (Figure 2.2) suggesting that the majority of productive chemistry occurred in the first 50 hours before non–productive decomposition became competitive. Raising the palladium catalyst loading, maintaining a slight excess of BQ provided improved and scalable yields of the epoxy enone **364** (entry 5, Table 2.5).

Figure 2.2 *^{1}H NMR Monitoring of the palladium-catalyzed desaturation in deuterated DMSO*

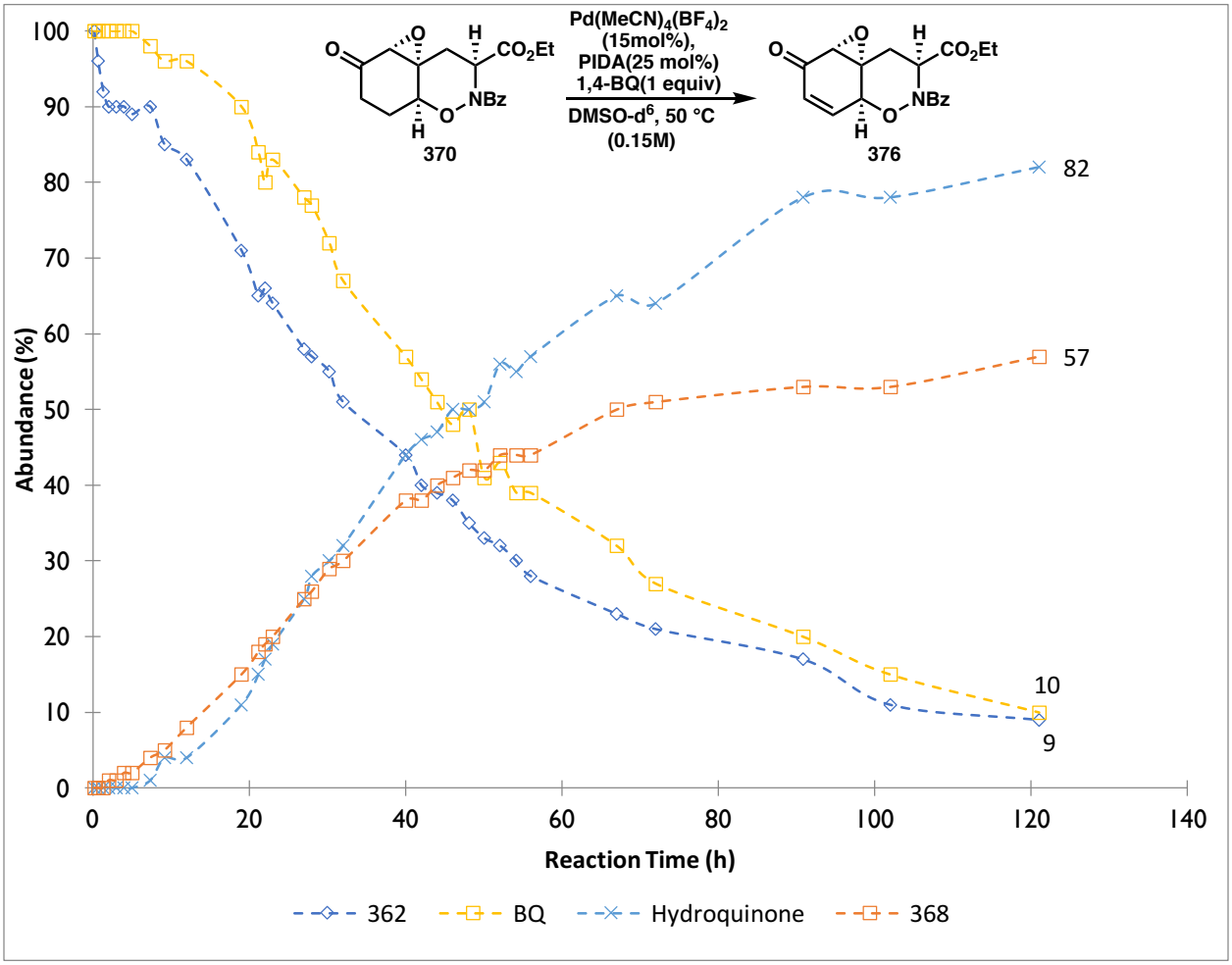

2.9 ALLYLIC TRANSPOSITION

To generate the desired allylic transposition substrate (**365a**, Table 2.6) the enone **364** was readily reduced under Luche conditions to give a separable mixture of allylic alcohols (entry 1, Table 2.6).[85] Attempts to form the desired α-disposed **365a** selectively were unsuccessful; as bulkier reductants provided lower yields and preferentially formed **365b** (entries 2&3, Table 2.6).[86] Though NMR signals were inconclusive in the structural determination of these new products, an X-ray quality single crystal of **369b** was recovered. Notable in the crystal structure of **369b** is the

chair-like conformation of the tetrahydro-1,2-oxazine ring and the axial disposition of the ester consistent with our previous conformational hypotheses.

Table 2.6. *1,2-reduction to generate substrates for allylic transposition studies*

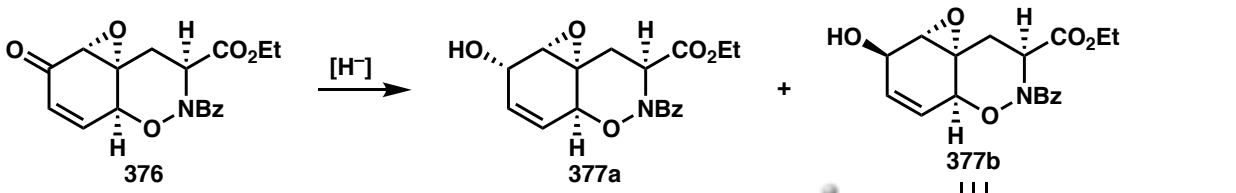

entry	reductant	temp (°C)	yield(%)	α :β
1	$NaBH_4/CeCl_3$	–20	90	2:1
2	$K(OiPr)_3BH$	–78 to 23	44	1:>20
3	L-selectride	–78	36	1:>20

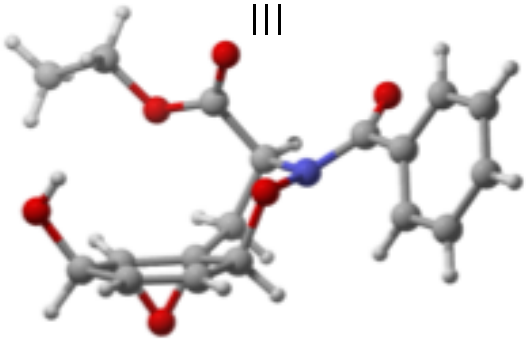

With clean samples of both diastereomers of the allylic alcohol in hand, their reactivity could be evaluated in rhenium-mediated conditions for allylic transposition. Initial test reactions with common rhenium additives, including methyl trioxorhenium (VII) (MTO), showed that both **377a** & **377b** were quite unstable.[87,88] It was only through the use of freshly prepared Osborn catalyst ($Ph_3SiOReO_3$), known for its high activity and attenuated Lewis acidity, that trace new products were observed as minor constituents of the reaction mixture. While the yields of isomerized material were similar for both diastereomers; discouragingly, **377a** had a greater degree of decomposition. THF and CH_2Cl_2 modulated the poor reactivity of the transformation; yet further screens did not appear generate a more tractable yield. Although the greater stability of **377b** to the reaction conditions were initially attractive inversion of the hindered C9 secondary alcohol appeared challenging. Efficient rhenium-mediated allylic transpositions often have a strong thermodynamic bias for the desired isomer or some method of trapping the desired alcohol.[89] While it was hypothesized that the epoxy-allylic alcohol motif found in **80** and **378a**

would be lower in energy than **377a** due to hyperconjugative effects this is not reflected in our experimental observations.

Table 2.7. *Allylic transposition studies on the both allylic alcohol diastereomers*

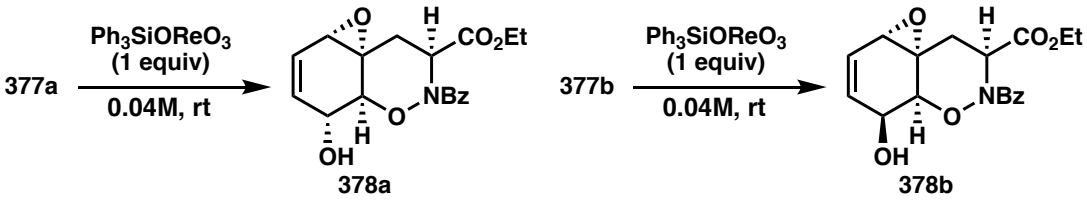

entry	solvent	conv (%)	yield (%)
1	Et_2O	65	20
2	THF	26	11
3	CH_2Cl_2	25	14
4	PhH	43	18
5	PhMe	53	20
6	MeCN	56	15

entry	solvent	conv (%)	yield (%)
1	Et_2O	15	8
2	THF	22	22
3	CH_2Cl_2	36	30
4	PhH	17	17
5	PhMe	27	22
6	MeCN	31	29

2.10 OXIDATIVE FUNCTIONALIZATION OF THE EPOXY ENONE

The intransigence of the C9 oxidation of **372** and the poor reactivity observed in the allylic transposition of **377a** led to a re-evaulation of the approach toward oxidative manipulation of the bicyclic oxazine **364**. To circumvent these challenges, the strategic installation of a functional handle at C9 prior to formation of the inert epoxy alkene motif would provide facile access to the desired fully functionalized western fragment.

To that end, oxidation of the epoxy enone **376** was attempted. Gratifyingly, both dihydroxylation and epoxidation proceeded diaseteroselectively with high crude yields. Importantly, these compounds while isolated with minimal impurities through aqueous work-ups but were completely unstable to further purification via column chromatography regardless of the choice of chromatographic phase.

Scheme 2.12. *Efficient oxidative modifications of the epoxy enone*

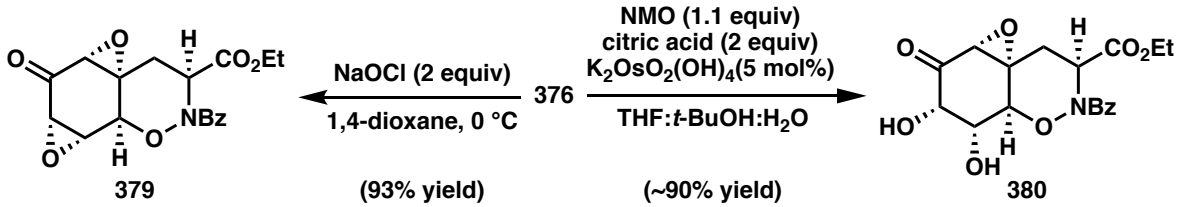

2.11 DEOXYGENATIVE REARRANGEMENTS OF C9-OXIDIZED SUBSTRATES

A Wharton rearrangement of these C9–oxidized substrates would generate an olefin–containing product at the desired oxidation level. The *bis*-epoxy ketone was the substrate upon which the lion's share of optimization was undertaken as it provided direct access to the epoxy allylic alcohol motif.

The Wharton rearrangement is an interesting reaction which is proposed to proceed through disparate mechanisms differentiated by either a basic or acidic additive employed to facilitate the reaction. The base–mediated reaction is proposed to proceed through a polar mechanism culminating in the protonation of a vinyl anion while acidic conditions are proposed to proceed through a radical mechanism with the expulsion of nitrogen and recombination of a hydrogen atom with a vinyl radical.[90]

There are four variants of the Wharton rearrangement known in the literature. The original conditions used by Wharton and Bohlen were excess hydrazine hydrate and catalytic acetic acid in methanol.[68] Later application of conditions analogous to the Wolff-Kishner reduction showed that heating the substrate with a hydroxide base instead of acetic acid gave higher yields when applied to steroidal substrates.[91] For many years, little systematic development of the Wharton rearrangement was undertaken until Luche, of the eponymous reduction, turned his attention to the transformation.[92] A combination of hydrazine hydrochloride and triethylamine in anhydrous

acetonitrile afforded significant improvements to the transposition of more sensitive substrates and was later applied to several effective syntheses. Finally, conditions were developed by Wiemer using a mixture of hydrazine hydrate and trimethyl silyl chloride in DMF. These conditions were found to also improve the reaction in comparison to Wharton's original conditions in some substrates.[93]

There are three examples of a Wharton rearrangement on *bis*–epoxy ketone substrate. The first two examples are found in Ichihara's synthetic studies of (±)–senepoxyde and (±)–crotepoxide.[94] In these studies, the authors used neutral hydrazine in a mixed solvent system. Discouragingly, they do not disclose a yield for either transformation despite reporting yields on the other reactions in the paper. The final example was demonstrated in the Hoye's studies of (+)–scyphostatin, using canonical Wharton conditions.[95] The authors note that the reaction is highly dependent on the hydrazine stoichiometry and reaction time affording the desired products in variable yield (30–40%).

As a result of the base sensitivity of the 1,2–tetrohydroazines, conditions involving strong base were not pursued during reaction development on the *bis*-epoxy ketone **379**. Instead, the initial focus was held on conditions that were proposed to proceed through the radical mechanism. Canonical Wharton conditions lead to decomposition, a trace amount of product–like substance was observed in the crude mixture but lacked an epoxide moiety (entry 1, Table, 2.8). Applying the conditions developed by Wiemer and Luche the desired product was observed, without epoxide opening or reduction, albeit in low yield as a mixture of constitutional isomers (entries 3&4, Table, 2.8). Stoichiometry studies indicated that excess hydrazine had a deleterious effect on the yield of the desired product.

Integrating some of the lessons from Luche's studies with the original conditions developed by Wharton, we conducted a solvent and additive screen and identified benzoic acid as a superior catalyst to acetic acid and dried ethyl acetate as an optimal solvent. Unfortunately, these conditions gave the two isomeric products in a 2:1 ratio, favoring the tertiary alcohol, in a cumulative 34% yield. This yield, while low, is consistent with the other *bis*-epoxy ketone substrates known in the literature. Further attempts to optimize this yield were unsuccessful and complicated by difficulties in replicability.

Table 2.8. *Selected entries in the optimization of Wharton rearrangement of the bis-epoxy ketone*

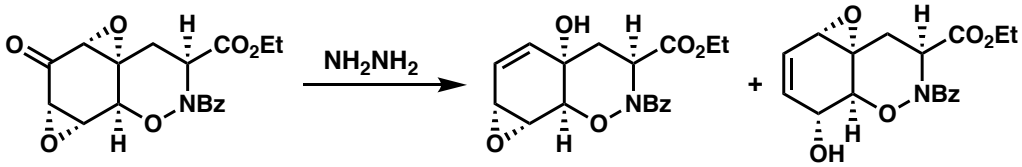

379 **381** **382**

entry	hydrazine	additive	solvent	381 (%)	382 (%)
1	$NH_2H_2 \cdot H_2O$(2 equiv)	AcOH(2 equiv)	MeOH	–	–
2	NH_2NH_2(1 equiv)	BzOH(1 equiv)	MeOH	14	6
3	NH_2NH_2(5 equiv)	TMSCl (2 equiv)	DMF	22	6
4	$NH_2NH_2 \cdot HCl$(1 equiv)	NEt_3 (3 equiv)	DMF	11	1
5	NH_2NH_2(1 equiv)	–	MeCN	22	7
6	NH_2NH_2(1 equiv)	BzOH (20 mol%)	EtOAc	21	13

The undesired tertiary allylic alcohol isomer **381**, is favored in the reaction but upon purification on triethylamine–neutralized fluorosil the isomeric ratio shifted toward 1:1 with negligible deviations between NMR yield and isolated yield. This shift in the isomeric ratio was suggestive that a background vinylogous Payne rearrangement is operative, analogous to that studied by Hoye and exploited by Myers.[95,96]

Possible complications of the reaction could be the competitive formation of inert azines via hydrazone exchange or pyrazole formation from cyclization of the intermediate hydrazone

followed by dehydrative aromatization.[97–99] Azine formation can be accelerated by under acidic conditions; however, if the acid catalyst is removed from the reaction of **367** the yield is unperturbed while the reaction time for full conversion of the starting material is elongated. In an alternative approach to alleviate possible deleterious side reactivity, The use of protected hydrazones were evaluated. Clean conversion to the desired silylated and carbamate capped hydrazones was observed by TLC and LCMS; however, when the hydrazone was unmasked no productive reactivity was observed. These results were confusing but given the sensitivity of the initial reaction it is possible that the added deprotection reagents causes critical interference with the productive reaction pathway.

Scheme 2.12. *Wharton transposition on dihydroxylated substrate*

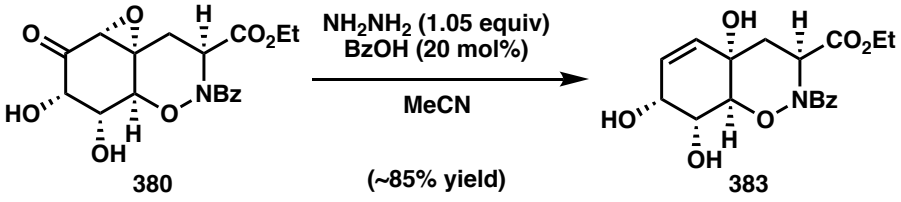

In contrast to the *bis*–epoxy ketone applying partially optimized conditions to the epoxy ketone diol **380** provided the desired allylic triol **383** in ~85% by quantitative ^{1}H NMR. This could be indicative that the product of the *bis*-epoxide Wharton rearrangement is decomposing during the reaction. The resultant allylic epoxide is an excellent soft electrophile and hydrazine and hydrazones have soft nucleophilic character as a result of the alpha effect, similar to hydroxylamines.[100]

Several alternatives to the Wharton rearrangement were interrogated. Initial reduction of **379** formed the *bis*-epoxy alcohol **384** which was then exposed to modified Mitsonobu conditions with a sulfonyl hydrazide developed by Myers and Movassaghi, however **384** was unreactive to these conditions.[101] Radical deoxygenation of *bis*-epoxy alcohols has found effective application

in the synthesis of tripolide analogues and hindered polycylic substrates through the formation of an intermediate xanthate.[102] While this strategy would increase the step count it could circumvent the sensitivity of the **382**.[103] In contrast to thioimidazolides and thiocarbonates in the literature, the intermediates generated from the **384** for radical decomposition were unstable to mild heating, work-up conditions, or direct column chromatography. However, if generated using DMAP to facilitate thioacylation the crude material could be cleanly converted to the desired activated substrates *in situ* (**385** & **386**, Scheme 2.13).

***Scheme 2.13**. Studies on a photoredox catalyzed radical deoxygenation*

a) failed light–mediated reduction of bis-*epoxythiocarbonate generated* in situ

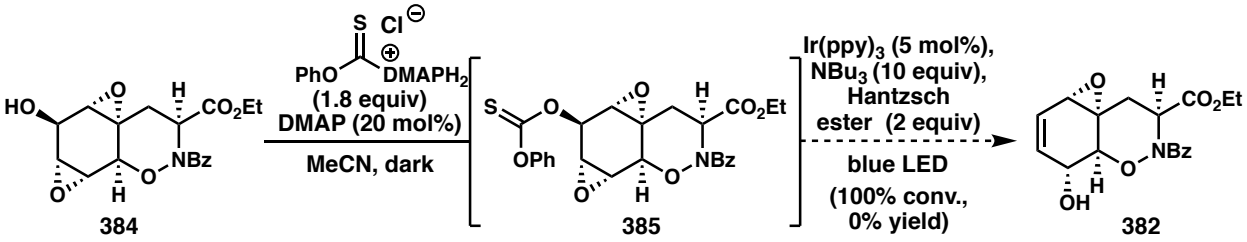

b) selected entries in the optimization studies on the light–mediated reduction of bis-*epoxythioimidazolide generated* in situ

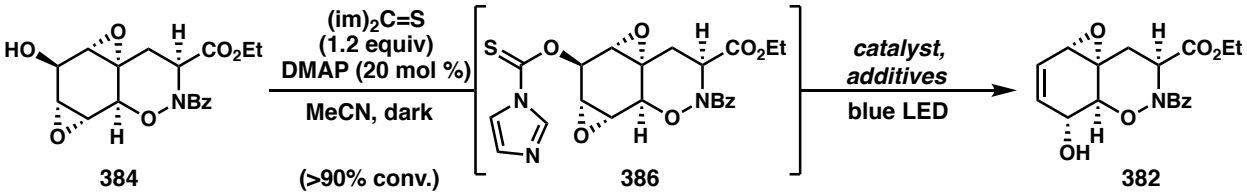

entry	catalyst	base	reductant	conv (%)	yield (%)
1	$Ir(ppy)_3$ (5 mol%)	iPr_2NEt (5 equiv)	—	95	11
2	$Ir(ppy)_3$ (5 mol%)	NBu_3 (10 equiv)	HCO_2H (10 equiv)	95	10
3	$Ir(ppy)_3$ (5 mol%)	NBu_3 (2 equiv)	Hantzsch ester (2 equiv)	83	10
4	$Ir(ppy)_3$ (5 mol%)	NBu_3 (10 equiv)	Hantzsch ester (2 equiv)	100	trace
5	$Ir(dF\text{-}ppy)_3$ (5 mol%)	NBu_3 (10 equiv)	Hantzsch ester (2 equiv)	100	8
6	$Ir(dtbbpy)(ppy)_2$ (5 mol%)	NBu_3 (10 equiv)	Hantzsch ester (2 equiv)	100	2
7	$Ru(phen)_3$ (5 mol%)	NBu_3 (10 equiv)	Hantzsch ester (2 equiv)	93	7

In the literature, these activated thiocarbonyl compounds are typically reacted under heating in the presence of the AIBN and Bu_3SnH; however, the thermal instability of the *in situ* generated substrate prohibited the effective use of these conditions. To circumvent this challenge,

classical O_2/BEt_3 radical initiation conditions were initially engaged instead. Disappointingly, no product was observed in the crude reaction.[104] A photoredox–catalyzed reduction of thiocarbonyl derivatives had been disclosed, appreciating the ability of these conditions to facilitate reactivity in challenging substrates this tactic was applied to the reduction of **385** and **386**.[105] The thiocarbonate **385** merely decomposed unproductively (Scheme 2.12a) but the corresponding thioimidazolide **386** provided a low yield of the epoxy allylic alcohol exclusively as the desired isomer **382** (Scheme 2.12b). Despite this encouraging selectivity, variation in photocatalyst, hydrogen donor, and amine additive did not raise the yield of the reaction. To further probe the nature of the activating group on the reduction, a fluorinated electron-poor benzoate was generated however no desired product was observed.[106]

2.12 REALIZATION OF THE SYNTHESIS OF THE WESTERN FRAGMENT

Inspired by apparent background vinylogous Payne rearrangements exchanging **381** and **382** during purification of the bis-epoxy ketone Wharton transposition, the mixture of the isomeric epoxy allylic alcohols was exposed to $TBSOTf/NEt_3$.[96] To our delight, the secondary silyl ether **387** as the exclusive product. Initially, the yield was quite low. Decreasing the temperature of the reaction and quenching excess silyl triflate with cold *iso*-propanol improved the reaction on a small scale. These results were challenging to maintain on scale, providing yields between 30–40%. When **381** is isolated and exposed to the reaction conditions, the yield does not improve suggesting an overall instability to the reaction conditions. Substitution of THF as a solvent generates **387** while retaining **381** in the reaction mixture. Upon purification on neutralized fluorosil, recovered starting material is returned as a 1:1 mixture of **381** and **382** further substantiating the presence of the rarely observed vinylogous Payne rearrangement.

Scheme 2.14. *Final oxidative modifications to form the epoxy allylic alcohol*

a) Silylation of a mixture of epoxy allylic alcohol isomers

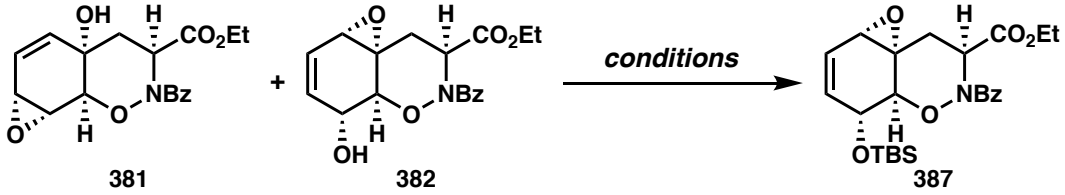

entry	TBSOTf	base	solvent	yield
1	3 equiv	NEt_3 (15 equiv)	CH_2Cl_2, 10 °C	37%
2	7.5 equiv	DIPEA (30 equiv)	CH_2Cl_2, 0 °C	36%[a]
3	7.5 equiv	DIPEA (15 equiv)	THF, 0 °C	31% (39% brsm)

[a]382 reacted as a singular substrate

b) Unsuccessful functionalization of the triol

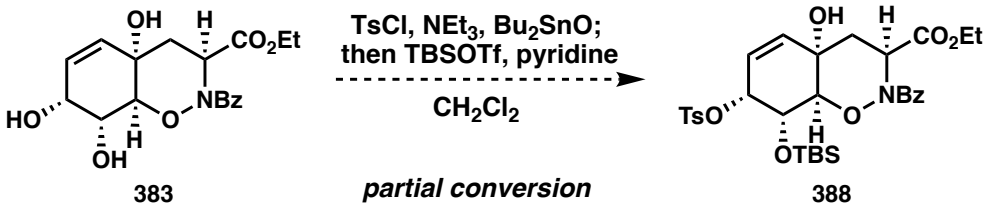

As a result of the low yields observed in the conversion of **379** to **387** an alternative route proceeding through triol **383** was envisaged improve efficiency by functionalizing the C8 allylic alcohol as a leaving group and performing an S_N2' displacement to generate **382**. Initial studies to selectively mesylate the C8 allylic alcohol were met with decomposition; however, dibutyl tin oxide was able to facilitate selective formation the allylic tosylate. Treating this intermediate with TBSOTf resulted in partial conversion to the silyl ether. Yet, despite the Lewis acidic conditions no epoxide formation was observed. Currently, the triol intermediate has not been successfully advanced to the desired motif.

With **376** now successfully synthesized, a variety of deprotection conditions were attempted to cleave the *N*-benzoyl group. The transformation was intractable until use of Schwartz's reagent was able to generate the free tetrahydro-1,2-oxazine **388** in a low yield (entry

1, Scheme 2.15).[107] Careful control of the stoichiometry of the reagent and study of the work-up conditions substantially improved the yield (entry 2, Scheme 2.15). With **388** in hand, the peptide coupling was now ready to be studied. Thermal instability and base sensitivity of the substrate were retained in this new substrate; any attempt to saponify the ester was met with decomposition.[108,109] As a result, we were limited to coupling an eastern fragment amino acid with the oxazine nitrogen followed by cyclization to form the DKP.

Scheme 2.15. *N-deprotection of the fully elaborated western fragment*

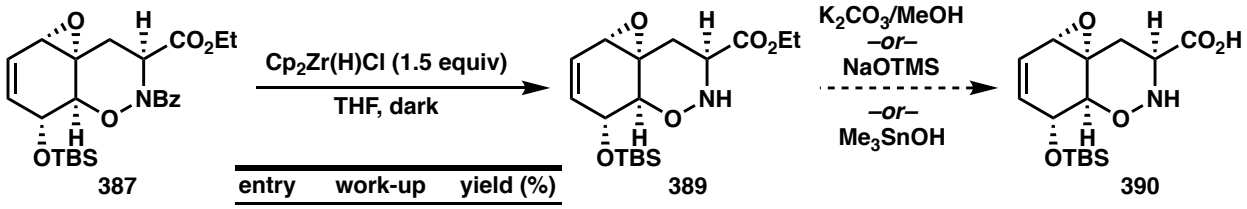

entry	work-up	yield (%)
1	$NaHCO_{3(aq)}$	42
2	pH=7 buffer	79

2.13 SYNTHESIS OF THE EASTERN FRAGMENT

With the fully elaborated Western fragment in hand, the eastern fragment needed to be synthesized. To that end a palladium catalyzed Negishi coupling between a protected iodoserine derivative **380** and an electron rich aryl iodide **381** provided the non-canonical Boc-protected amino ester **382**.[11] It is notable that the use of a coordinating protecting group (MOM) in place of a methyl *ortho* to the iodide dramatically improved the yield of the coupling. Saponification of the methyl ester proceeds unremarkably and affords good yield to provide a substrate for amide coupling. Foreseeing that the orthogonal and facile cleavage of the phenol and amine protecting groups may be necessary, Boc-protected **394b** was expediently converted to Fmoc–protected derivative **396** in a three–step sequence now with a silyl protecting that could be unveiled in a final deprotection step after thiolation.

Scheme 2.16. *Synthesis of unnatural phenylalanine derivatives*

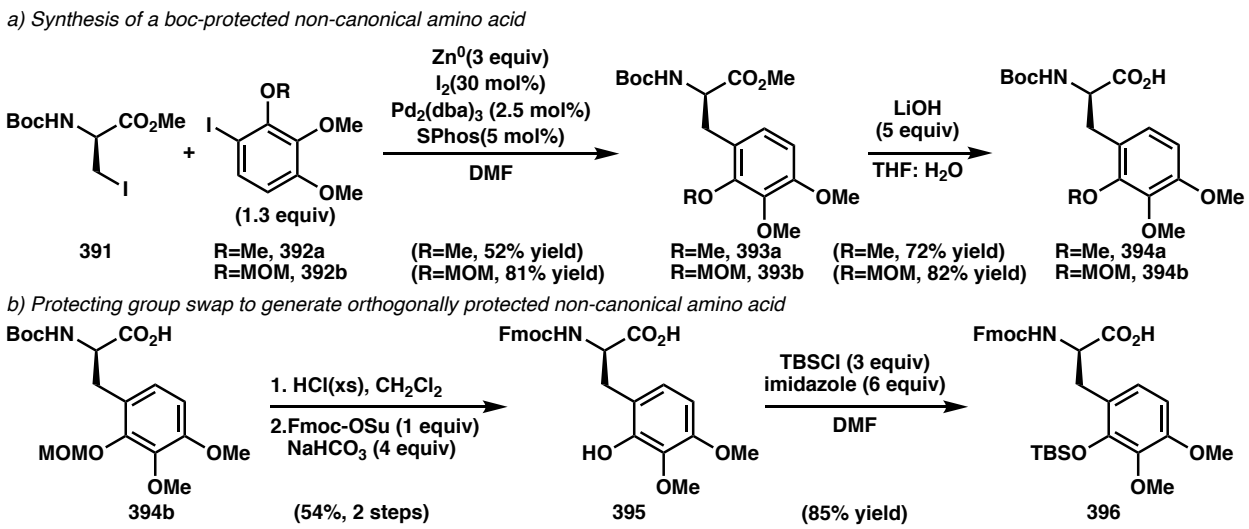

2.14 ATTEMPTED COUPLING OF EASTERN AND WESTERN FRAGMENTS

While the peptide coupling substituted of isoxazolidine substrates is known using standard coupling reagents; the newly deprotected compound **389** was completely unreactive to any peptide coupling conditions. An exhaustive screen of reagents specifically designed for hindered or non-nucleophilic amines (eg. BEP, HATU, TFFH) generated no desired product.[110] To further evaluate the reactivity of tetrahydro-1,2-oxazines in coupling reaction model compounds **328** and **397** were also screened under a variety of peptide coupling conditions yet again a similar lack of reactivity was observed (Scheme 2.17).

Exposing the deprotected material to pivaloyl chloride resulted in clean formation of an acylated acylated. Encouraged by this result, further study showed that Fmoc-Phe-Cl was also able to form a coupled product **399** (Scheme 2.18).[111] Unfortunately, attempts couple the acid chloride

Scheme 2.17. *Unsuccessful bicylic tetrahydro-1,2-oxazine substrates in amide coupling*

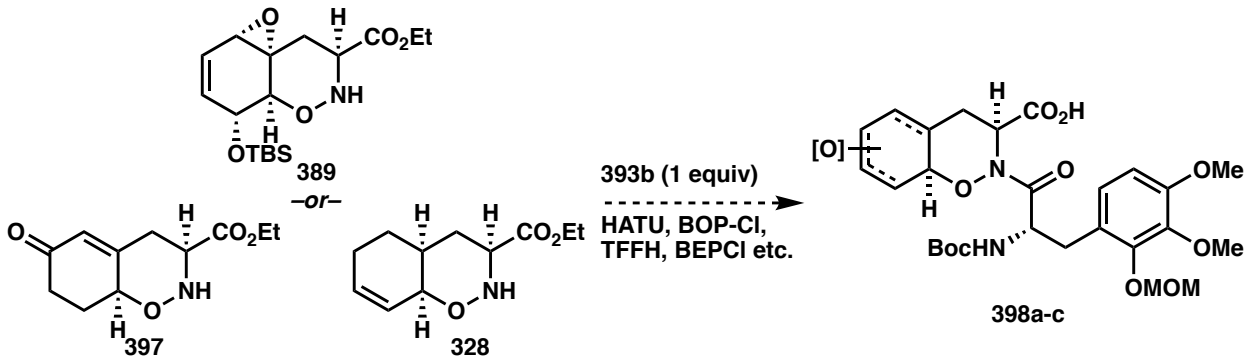

derived from the polyoxygenated eastern fragment **396** failed possibly due instability of the intermediate acid chloride under the conditions or a lowered reaction rate due to increased bulk. While further work may have resolved these incompatibilities, studies on the phenylalanine coupled **399** show that, despite facile Fmoc-deprotection, the resulting amine **400** would not undergo intramolecular cyclize to form the DKP **401**. Attempts to drive the reaction thermally or the addition of stronger bases lead to decomposition.

Scheme 2.18. *Amide coupling of a model amino acid chloride with the Western fragment*

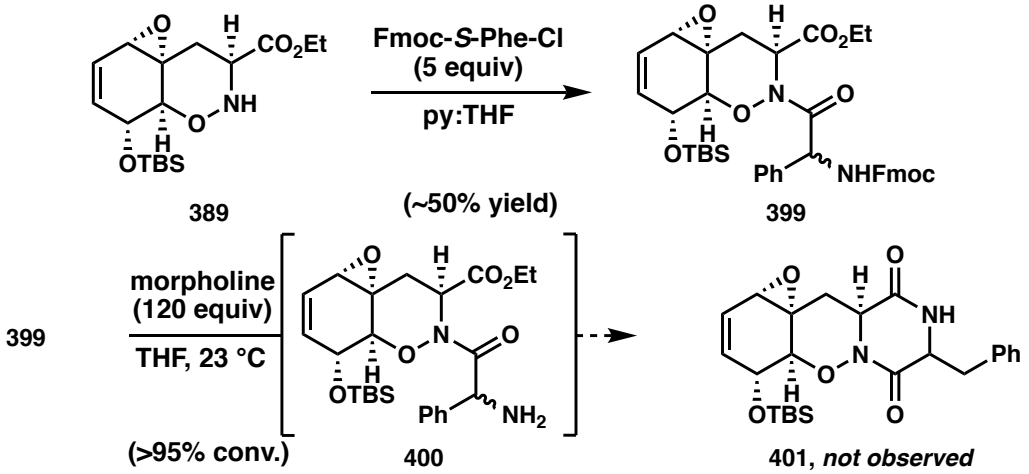

2.15 CONCLUSION OF STUDIES TOWARD GLIOVIRIN

Cyclization to form DKPs can occur under mild conditions through ester saponification and the use of a peptide coupling reagent (See Chapter 1), direct DKP formation typically requires strong base or heating.[112] As the saponification of the ethyl ester on the oxazine fragment is

untenable and the intermediate **400** demonstrates instability to base and mild heating it appears clear that this late stage DKP formation–sulfenylation strategy is not appropriate for the synthesis of gliovirin (**80**). To successfully generate this natural product, it behooves the synthetic chemist to reassess the synthetic route. Early stage amide coupling could generate a more robust substrate for DKP formation, however the transformations that have been successfully implemented in the *N*–benzoyl system in this work would require substantial re-optimization and the protecting group strategy would be non-trivial. Furthermore, early installation of the DKP would planarize the C3 substituent upon cyclization which would destroy the key conformational element which imposes diastereocontrol during the oxidative modifications required to establish the epoxy allylic alcohol motif. Replacement of the ethyl group at the ester with an orthogonally cleavable subsitutent would be optimal however this would require further development as classic examples, including allyl and TMS-ethyl, would undergo undesirable cross reactivity in the current route.

2.16 STUDIES TOWARD THE TRICHODERMAMIDES

With the deprotected oxazine **389** in hand, one could imagine a simple conversion to the trichodermamide family; indeed, upon exposure to lead tetraacetate the 1,2-dihydrooxazine **402** is formed cleanly (Scheme 2.18). With this compound in hand, epoxide opening provided the allylic chlorohydrin **403** to generate the western fragement of trichodermamide B. Attempts to generate trans-diol **394** only generated in trace yield.[113] Disappointingly, attempts to saponify **392** were unsuccessful, prohibiting interrogation of the penultimate amide coupling to synthesize trichodermamide B. With these promising results in hand perhaps this synthetic route can lead to an enantioselective synthesis of the trichodermamides. However, the difficulty in handling these

intermediates and the inefficient Wharton–silylation sequence provide challenges toward the successful realization of that end.

Scheme 2.18. *Synthetic studies toward the trichodermamides*

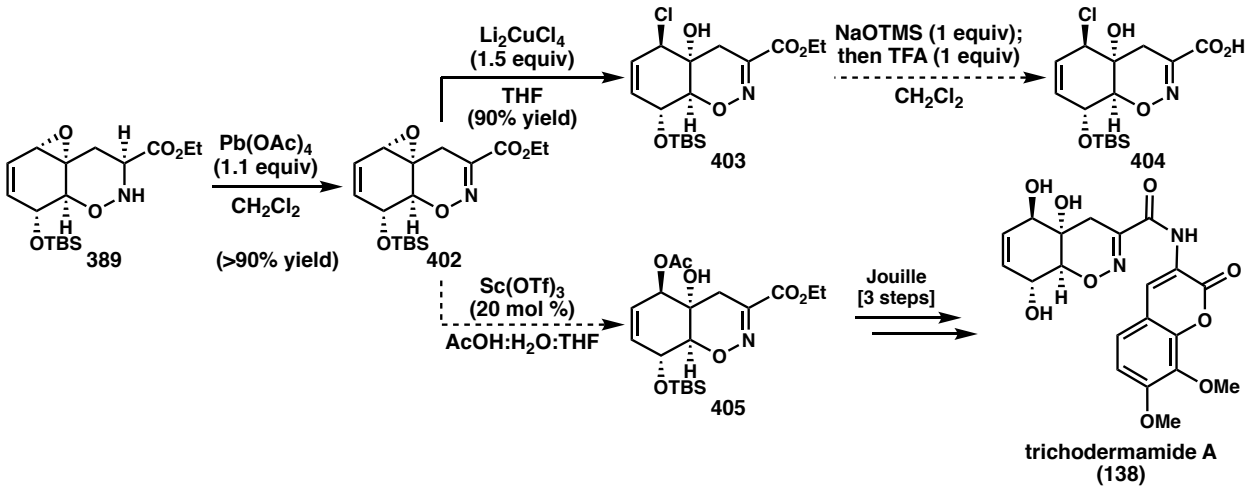

2.17 EXPERIMENTAL SECTION

2.17.1 MATERIALS AND METHODS

Unless otherwise stated, reactions were performed under a nitrogen atmosphere using

freshly dried solvents. Tetrahydrofuran (THF), methylene chloride CH_2Cl_2), acetonitrile (MeCN), dimethylformamide (DMF), benzene (PhH), diethyl ether (Et_2O) and toluene (PhMe) were dried by passing through activated alumina columns. Unless otherwise stated, chemicals and reagents were used as received. Triethylamine (Et_3N) was distilled over calcium hydride prior to use. All reactions were monitored by thin-layer chromatography using EMD/Merck silica gel 60 F254 pre-coated plates (0.25 mm) and were visualized by UV, *p*-anisaldehyde, vanillian, CAM or $KMnO_4$ staining. Flash column chromatography was performed either as described by Still et al.[31] using silica gel (partical size 0.032-0.063) purchased from Silicycle. Optical rotations were measured on a Jasco P-2000 polarimeter using a 100 mm path-length cell at 589 nm. ^1H and ^{13}C NMR spectra were recorded on a Varian 400 MR (at 400 MHz and 101 MHz, respectively), or a Varian Inova 500 (at 500 MHz and 126 MHz, respectively), and are reported relative to internal $CHCl_3$ (^1H, δ = 7.26), or DMSO (^1H, δ = 2.50), and $CDCl_3$ (^{13}C, δ = 77.0), or DMSO (^{13}C, δ =40.0). Data for ^1H NMR spectra are reported as follows: chemical shift (δ ppm) (multiplicity, coupling constant (Hz), integration). Multiplicity and qualifier abbreviations are as follows: s =singlet, d = doublet, t = triplet, q = quartet, m = multiplet, br = broad, app = apparent. IR spectra were recorded on a Thermo Fisher Nicolet iS5 FTIR spectrometer and are reported in frequency of absorption ($cm.^{-1}$). HRMS were acquired using an Agilent 6200 Series TOF with an Agilent G1978A Multimode source in electrospray ionization (ESI), atmospheric pressure chemical ionization (APCI), or mixed (MM) ionization mode. Analytical chiral HPLC was performed with an Agilent 1100 Series HPLC utilizing Chiralpak AD or Chiralcel OD-H columns (4.6 mm x 25 S7 cm) obtained from Daicel Chemical Industries, Ltd with visualization at 254 nm. Low-temperature X-ray diffraction data (φ-and ω-scans) were collected on a Bruker AXS D8 VENTURE KAPPA diffractometer coupled to a PHOTON 100 CMOS detector with Cu-Kα radiation (λ = 1.54178 Å) from an IμS

micro-source.

2.17.3 PREPERATIVE PROCEDURES AND SPECTROSCOPIC DATA

Cycloaddition of *in situ*–generated nitroso alkene and 1,3–cyclohexadiene

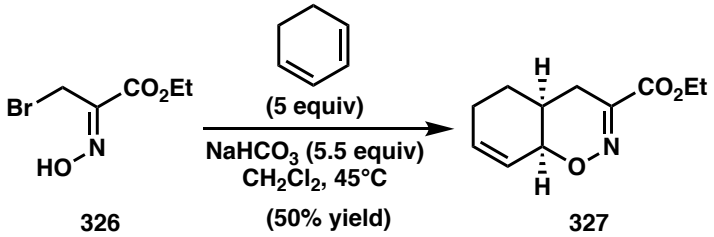

Stir 1,3-cyclohexadiene (4.2g, 5.0 mL, 52.5 mmol, 5 equiv) and anhydrous $NaHCO_3$ (6.121g, 57.8 mmol, 5.5 equiv) in CH_2Cl_2 (40 mL) at 45 °C. Add a solution of ethyl bromopyruvate 2-oxime (2.204 g, 10.5 mmol, 1 equiv) in CH_2Cl_2 (40 mL) at a rate of 2 mL•h^{-1}; after addition is complete stir overnight at 45 °C. Upon completion of the reaction, filter off salts and wash salts with CH_2Cl_2. Dry over Na_2SO_4, filter and concentrate *in vacuo* to yield crude product. Purify the by flash chromatography (silica, 4% EtOAc/$CHCl_3$) to give dihydro-1,2-oxazine **XX** as a yellow oil (1.10g, 5.26 mmol, 50% yield)

^{1}H NMR (400 MHz, $CDCl_3$) δ 6.02 (dt, *J* = 9.7, 3.7 Hz, 1H), 5.85 (ddt, *J* = 9.9, 4.5, 2.3 Hz, 1H), 4.37 – 4.28 (m, 2H), 4.25 (d, *J* = 3.8 Hz, 1H), 2.61 (dd, *J* = 19.6, 7.8 Hz, 1H), 2.29 (dd, *J* = 19.6, 3.2 Hz, 1H), 2.25 – 2.06 (m, 3H), 1.62 (td, *J* = 7.8, 7.4, 5.3 Hz, 2H), 1.38 – 1.31 (m, 3H).

^{13}C NMR (101 MHz, $CDCl_3$) δ 163.79, 149.09, 134.16, 123.97, 71.02, 61.84, 26.97, 25.07, 24.53, 23.57, 14.13.

FTIR (AT-IR) 2924.94, 2359.12, 2340.2, 1713.03, 1597.78, 1422.35, 1373.19, 1345.19, 1292.61, 1261.43, 1225.74, 1172.33, 1152.55, 1109.52, 1078.81, 1037.42, 1004.62, 950.38, 913.42, 885.09, 853.47, 826.41, 748.95, 699.46, 667.98, 631.01 cm^{-1}

HRMS (TOF, ES+) calc'd for $C_{11}H_{15}NO_3$ $[M+H]^+$ 210.1125, found 210.1123 (ppm=0.81)

Diastereoselective 1,2-reduction of bicyclic dihydro-1,2-oxazine

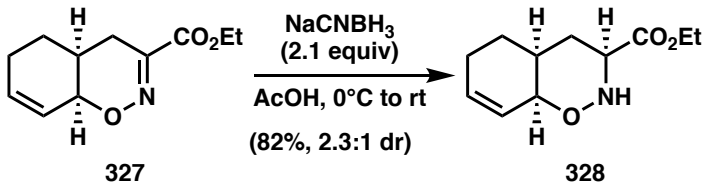

327 328

To a frozen solution of dihydro-1,2-oxazine (1.09 g, 5.21 mmol, 1.0 equiv) in AcOH (40 mL) in an ice bath add $NaCNBH_3$ (687 mg, 10.94 mmol, 2.1 equiv) as a single portion. Stir to ambient temperature for 18h. Neutralize crude mixture 6M $NaOH_{(aq)}$ and adjust with pH=7 phosphate buffer. Extract reaction twice with EtOAc. Dry organic layer over Na_2SO_4, filter and concentrate *in vacuo* to yield crude product. Purification by flash chromatography (silica deactivated with NEt_3, 5%EtOAc/50%$CHCl_3$/Hexanes) provided a 2.3:1 diastereomeric mixture of tetrahydro-1,2-oxazine (900 mg, 4.26 mmol, 82% yield) as a pale oil. A second separation of the mixture by flash chromatography (silica, 5%NEt_3/5%EtOAc/50%$CHCl_3$/Hexanes) provided a sample pure syn-product (109 mg, 0.516 mmol) along with mixed fractions.

^{1}H NMR (500 MHz, $CDCl_3$) δ 6.01 (dddt, J = 9.8, 4.8, 2.4, 0.9 Hz, 1H), 5.74 (dddd, J = 9.4, 4.4, 2.5, 1.7 Hz, 1H), 5.65 (s, 1H), 4.19 (qd, J = 7.2, 1.3 Hz, 2H), 4.12 (s, 1H), 3.93 (dd, J = 10.9, 3.5 Hz, 1H), 2.22 – 2.12 (m, 1H), 2.10 – 2.01 (m, 2H), 1.97 (dt, J = 13.5, 3.2 Hz, 1H), 1.90 (dt, J = 10.1, 6.0 Hz, 2H), 1.53 – 1.44 (m, 1H), 1.28 (t, J = 7.1 Hz, 3H).

^{13}C NMR (126 MHz, $CDCl_3$) δ 171.29, 134.18, 124.55, 74.14, 61.26, 56.37, 31.70, 31.55, 25.44, 22.62, 14.29.

FTIR (AT-IR) 3295.02, 3028.05, 2923.56, 2358.40, 1732.28, 1431.63, 1368.92, 1306.19, 1261.56, 1203.94, 1179.62, 1134.70, 1098.47, 1066.71, 1022.02, 1005.65, 920.47, 879.26, 846.60, 731.82, 685.99, 667.68, 623.57 cm^{-1}

HRMS (TOF, ES+) calc'd for $C_{11}H_{17}NO_3$ $[M+H]^+$ 212.1281, found 212.1291 (ppm=–4.62).

Epoxidation of bicyclic dihydro-1,2-oxazine

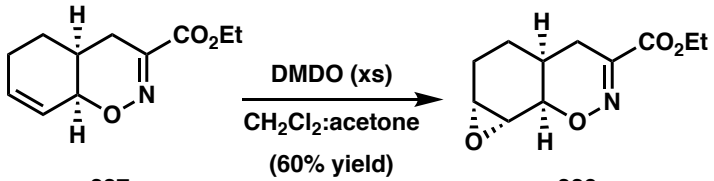

327 329

To a solution of dihydro-1,2-oxazine (10.9 mg 0.0521 mmol) in CH_2Cl_2 (0.2 mL) add a solution of freshly prepared DMDO[114] (10 mL) stir at ambient temperature in air for 2h. Concentrate reaction mixture *in vacuo* to yield crude product. Purify the by flash chromatography (silica, 15% EtOAc/$CHCl_3$) to give dihydro-1,2-oxazine as a clear oil (7.0 mg, 0.0311 mmol, 60% yield)

^{1}H NMR (600 MHz, $CDCl_3$) δ 4.33 (qd, *J* = 7.1, 3.1 Hz, 2H), 4.28 (s, 1H), 3.41 (t, *J* = 3.0 Hz, 1H), 3.26 (t, *J* = 4.3 Hz, 0H), 2.52 (dd, *J* = 19.5, 7.6 Hz, 0H), 2.27 (dd, *J* = 19.7, 2.1 Hz, 1H), 2.17 – 2.10 (m, 1H), 2.08 – 2.02 (m, 2H), 2.00 – 1.89 (m, 1H), 1.37 (t, *J* = 7.1 Hz, 3H).

^{13}C NMR (101 MHz, $CDCl_3$) δ 163.58, 149.69, 72.49, 62.21, 52.46, 52.00, 25.97, 23.66, 22.23, 21.15, 14.27.

FTIR (AT-IR) 2984.93, 2935.69, 1714.23, 1599.17, 1442.07, 1425.20, 1375.31, 1345.17, 1291.72, 1264.12, 1229.17, 1172.76, 1120.80, 1105.88, 1070.87, 1037.02, 1006.52, 965.14, 930.32, 861.13, 832.18, 810.22, 780.45, 746.53, 632.12 cm^{-1}

HRMS (TOF, ES+) calc'd for $C_{11}H_{15}NO_4$ $[M+H]^+$ 226.1074, found 226.1074 (ppm=–0.07).

Formation of propargylic triflate

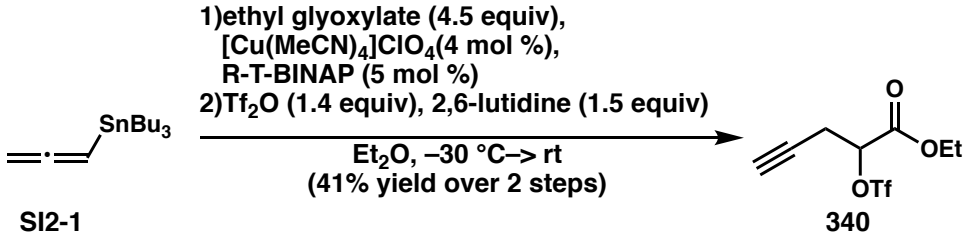

Stir $Cu(MeCN)_4ClO_4$ (205 mg, 0.626 mmol, 4 mol %) and *R*-T-BINAP (513 mg, 0.756 mmol, 5 mol %) at ambient temperature for 30 minutes in Et_2O (62.5 mL) and then chill to –30 °C. Add allenyl stannane (4.00 mL, 5.00g, 15.19 mmol, 1.0 equiv) and freshly distilled ethyl glyoxylate in toluene (13.51 mL, 68.18 mmol, 4.5 equiv). Stir reaction for 48h, then add 10% $KF_{(aq)}$ (60 mL) separate organic phase. The aqueous phase was washed with diethyl ether. Dry the combined organics over Na_2SO_4 and concentrate partially before flushing through a silica plug (50% Et_2O/ pentanes). Concentrate the resulting solution partially to yield a solution of the crude intermediate alcohol. Stir the solution at 0 °C, add 2,6-lutidine (2.64 mL, 22.73 mmol, 1.5 equiv) and triflic anhydride (3.57mL, 21.21 mmol, 1.4 equiv). Allow reaction to warm to ambient temperature and continue stirring for 10h. Filter the crude reaction mixture through celite and wash with DI H_2O (100 mL). Dry the organic over Na_2SO_4, filter and concentrate to yield a red oil. Purify by flash chromatography (silica, 15%EtOAc/Hexanes) to provide **340** (1.684 g, 6.14 mmol, 41% yield) as a clear oil.

^{1}H NMR (400 MHz, $CDCl_3$) δ 5.19 (dd, J = 6.8, 5.0 Hz, 1H), 4.43 – 4.24 (m, 2H), 3.03 – 2.84 (m, 2H), 2.16 (t, J = 2.7 Hz, 1H), 1.33 (td, J = 7.2, 1.0 Hz, 3H).

^{13}C NMR (101 MHz, $CDCl_3$) δ 165.61, 118.55 (q, J = 319.5 Hz), 80.68, 75.66, 72.87, 63.36, 22.97, 14.06.

FTIR (AT-IR) 3302.74, 2988.13, 2359.29, 1751.07, 1417.39, 1375.39, 1349.38, 1282.85, 1202.33, 1139.73, 1024.07, 998.37, 960.68, 920.94, 855.24, 793.29, 752.6, 735.62, 610.26 cm^{-1}

HRMS (TOF, ES+) calc'd for $C_8H_9F_3O_5S$ $[M+NH_4]^+$ 292.0461, found 292.0459 (ppm=0.70)

Nucleophilic displacement of triflate with *O*-benzyl hydroxylamine

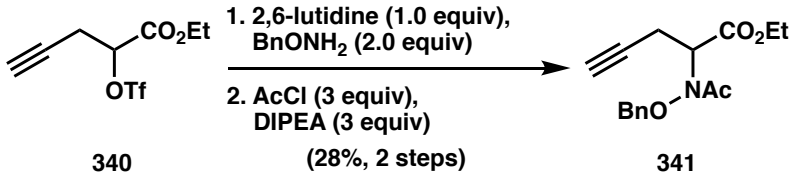

To a solution of triflate **331** (300 mg, 1.09mmol) in CH_2Cl_2 (24 mL) was added 2,6-lutidine (126.8 μL, 1.09 mmol). Cool solution was to 0 °C and add benzyloxylamine (256 μL, 2.18 mmol). Stir solution overnight to ambient temperature. Cool once again to 0 °C and add both Hunig's base (572 μL, 3.27mmol) and acetyl chloride (234 μL, 3.27 mmol). Stir an additional 12h then quench with dilute citric acid and extract with CH_2Cl_2. Dry organic phase over Na_2SO_4, filter, and concentrate. Purify by flash chromatography (silica, 3%NEt_3/15%EtOAc/Hexanes) to provide **341** as a clear oil (89.0 mg, 0.308 mmol, 28% yield)

^{1}H NMR (400 MHz, $CDCl_3$) δ 5.19 (dd, J = 6.8, 5.0 Hz, 1H), 4.43 – 4.24 (m, 2H), 3.03 – 2.84 (m, 2H), 2.16 (t, J = 2.7 Hz, 1H), 1.33 (td, J = 7.2, 1.0 Hz, 3H).\

^{13}C NMR (126 MHz, $CDCl_3$) δ) δ 175.50, 168.70, 134.59, 129.28, 129.03, 128.79, 80.39, 78.45, 71.08, 62.01, 60.67, 29.80, 20.89, 19.15, 14.21.

FTIR (AT-IR) 3287.62, 2931.45, 2359.45, 2340.27, 1738.45, 1679.1, 1454.99, 1370.69, 1262.61, 1228.39, 1190.09, 1081.39, 1019.76, 912.28, 845.00, 795.48, 755.58, 698.22, 667.93 cm^{-1}

HRMS (TOF, MM) calc'd for $C_{16}H_{19}NO_4$ $[M+H]^+$ 290.1387, found 290.1390 (ppm=0.69)

Formation of protected *rac*-N-hydroxydihydrophenylalanine

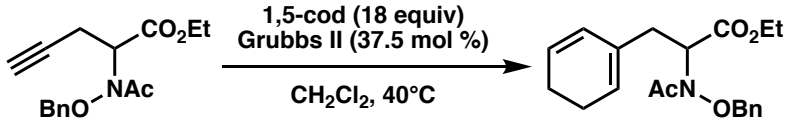

341 (20% yield) **342**

To a solution of 1,5-cyclooctadiene (74 μL, 0.603 mmol) in CH_2Cl_2 (1.1 mL) was added Grubbs II (4.2mg, 0.005 mmol). Stir two minutes. Attach reflux condenser and bring solution to 40 °C. Slow addition of alkyne (19.4 mg, 0.0671 mmol) over 1.5h. Stir addition 16h. Incomplete conversion observed. Added additional Grubbs II (4.2 mg, 0.005 mmol). Stir 14h. Added additional Grubbs II (12.6 mg, 0.015 mmol) and 1,5-cyclooctadiene (74 μL, 0.603 mmol). Stir 16h at 40 °C. Allow to cool to room temperature. Concentrate and titurate three times with ice-cold methanol. Filter methanol solution through celite. Purification by flash chromatography (silica, 20%EtOAc/Hexanes) provided **342** as a clear oil (4.6 mg, 0.0134mmol, 20% yield)

^{1}H NMR (400 MHz, $CDCl_3$) δ 7.37 (s, 5H), 5.91 – 5.79 (m, 2H), 5.68 – 5.55 (m, 1H), 4.97 (d, *J* = 10.4 Hz, 2H), 4.86 (d, *J* = 10.5 Hz, 1H), 4.20 (qd, *J* = 7.1, 2.1 Hz, 2H), 2.75 (dd, *J* = 7.6, 1.4 Hz, 2H), 2.15 – 2.04 (m, 7H), 1.27 (t, *J* = 7.1 Hz, 3H).

^{13}C NMR (101 MHz, $CDCl_3$) δ 174.55, 170.27, 134.78, 131.52, 128.95, 128.76, 128.63, 127.43, 126.51, 123.62, 77.89, 61.52, 60.70, 34.17, 22.40, 22.15, 20.80, 14.17.

FTIR (AT-IR) 3031.57, 2929.89, 2871.95, 2822.06, 2361.24, 2340.37, 1738.15, 1677.73, 1497.43, 1454.30, 1425.97, 1368.64, 1293.30, 1265.01, 1213.72, 1184.55, 1087.66, 1028.46, 971.50, 911.10, 845.33, 807.08, 735.32, 697.43, 667.87 cm^{-1}

HRMS (TOF, MM) calc'd for $C_{20}H_{25}NO_4$ $[M+H]^+$ 344.1856, found 344.1866 (ppm=2.91)

Formation of ethyl ester oxime

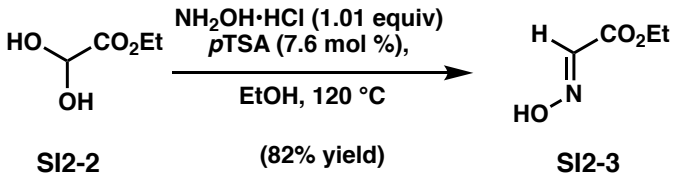

SI2-2 SI2-3

Charge a round bottom flask with glyoxylic acid monohydrate (20.0 g, 217 mmol 1.00 equiv), hydroxylamine hydrochloride (15.3 g, 220 mmol, 1.01 equiv), *p*TSA•H_2O (3.12 g, 16 mmol, 7.6 mol%) and ethanol (260 mL). Fit with a Socklett extractor charged with activated 4Å molecular sieves and a reflux condenser. Heat the mixture at 120°C for 9 hours. Cool reaction to room temperature. Concentrate in vacuo then dilute oil in Et_2O (400 mL) and $NaHCO_{3(sat)}$ (240 mL). Separate organic layer and wash organics with $NH_4Cl_{(sat)}$ (100mL) followed by pH=7 buffer (100 mL). Test aqueous layer for product and re-extract with Et_2O(150 mL), if necessary. Wash combined organics with brine(100 mL). Dry over Na_2SO_4, filter, and concentrate *in vacuo* to give clean **SI2-3** (20.9 g, 174 mmol, 82% yield) as a pale yellow oil. Physical and spectral properties were consistent with literature values.[115]

Silylation of ethyl ester oxime

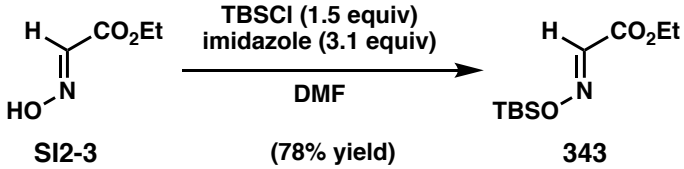

SI2-3 343

Combine **S2** (31.18g, 266 mmol), imidazole(55.76g, 819 mmol) and TBSCl (61.80g, 410 mmol) in DMF (). Stir at ambient temperature for 72h. Pour mixture into 6:1 DI:brine (2.1 L). Extract with Et_2O (1.5L). Wash organic layer with brine(300 mL). Dry over Na_2SO_4 , filter and concentrate in vacuo to yield crude product. Purify by flash chromatography (silica, 3.5-4.5% Et_2O/Hexanes) to provide **343** (47.8 g, 207 mmol, 78% yield) as a clear oil.

^{1}H NMR (400 MHz, $CDCl_3$) δ 7.59 (d, *J* = 1.5 Hz, 1H), 4.27 (qd, *J* = 7.1, 1.4 Hz, 2H), 1.31 (td, *J* = 7.1, 1.5 Hz, 3H), 0.92 (d, *J* = 1.9 Hz, 9H), 0.21 (d, *J* = 1.7 Hz, 6H).

^{13}C NMR (101 MHz, $CDCl_3$) δ 162.41, 146.20, 61.42, 25.91, 18.18, 14.22, -5.23.

FTIR (AT-IR) 2931.13, 2858.75, 1748.31, 1724.71, 1596.54, 1472.39, 1370.02, 1315.12, 1258.21, 1189.18, 1034.56, 967.56, 835.8, 785.55, 690.19, 667.95 cm^{-1}

HRMS (TOF, ES+) calc'd for $C_{20}H_{21}NO_3Si$ $[M+H]^+$ 232.1363, found 232.1365 (ppm=-0.66)

Formation of *iso*–propyl ester siloxime

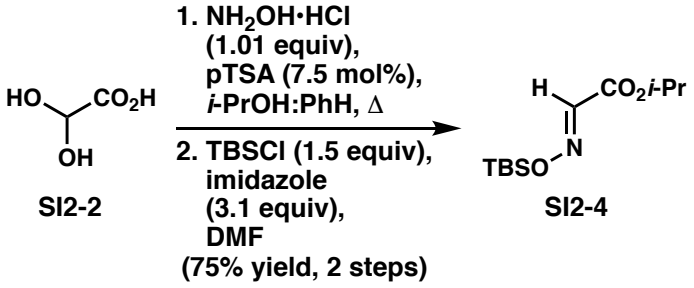

Charge a round bottom flask with glyoxylic acid monohydrate (10.00 g, 109 mmol 1.00 equiv), hydroxylamine hydrochloride (7.65 g, 110 mmol, 1.01 equiv), *p*TSA•H_2O (1.56 g, 8.2 mmol, 7.5 mol %), *iso*-propanol (108 mL), and benzene (12 mL). Fit with a Dean-Stark trap. Stir the mixture at 80°C until mixture is homogeneous. Raise reaction temperature to 115 °C and stir at reflux 19h. Cool reaction to room temperature. Concentrate in vacuo then dilute oil in Et_2O (200 mL) and $NaHCO_{3(sat)}$ (120 mL). Separate organic layer and wash organics with $NH_4Cl_{(sat)}$ (50mL) followed by pH=7 buffer (50 mL) and brine (50 mL). Dry over Na_2SO_4, filter, and concentrate *in vacuo* to give clean **oxime** (12.1 g, 92.2 mmol) as a white solid. Dissolve oxime in DMF (140 mL), cool to 0 °C. Add TBSCl (20.9g, 138.5 mmol, 1.5 equiv) and imidazole (19.5g, 286.1 mmol, 3.1 equiv). Allow reaction to stir at ambient temperature for 24h. Dilute with 6:1 DI H_2O:brine (740 mL). Extract crude mixture with Et_2O (525 mL) and wash organic layer with brine (100 mL). Dry over

Na_2SO_4, filter and concentrate to yield crude product. Purification by flash chromatography (silica, 5→7%EtOAc/Hexanes) provided **SI2-4** as a clear oil (20.1g, 81.9 mmol, 75% yield over 2 steps).

^{1}H NMR (400 MHz, $CDCl_3$) δ 7.54 (d, *J* = 1.4 Hz, 1H), 5.09 (pd, *J* = 6.3, 1.2 Hz, 1H), 1.24 (dd, *J* = 6.3, 1.4 Hz, 6H), 0.97 – 0.82 (m, 9H), 0.17 (t, *J* = 1.5 Hz, 6H).

^{13}C NMR (101 MHz, $CDCl_3$) δ 161.75, 146.38, 69.02, 25.85, 21.72, 18.07, -5.32.

FTIR (AT-IR) 2931.17, 2858.84, 1744.61, 1719.90, 1596.43, 1472.16, 1362.77, 1311.40, 1252.73, 1193.62, 1145.34, 1107.77, 1003.84, 967.44, 836.79, 785.92, 686.88 cm^{-1}

HRMS (TOF, ES+) calc'd for $C_{21}H_{23}NO_3Si$ $[M+H]^+$ 246.1520, found 246.1523 (ppm=-1.23)

Organozinc 1,2-addition into glyoxalate-derived oxime

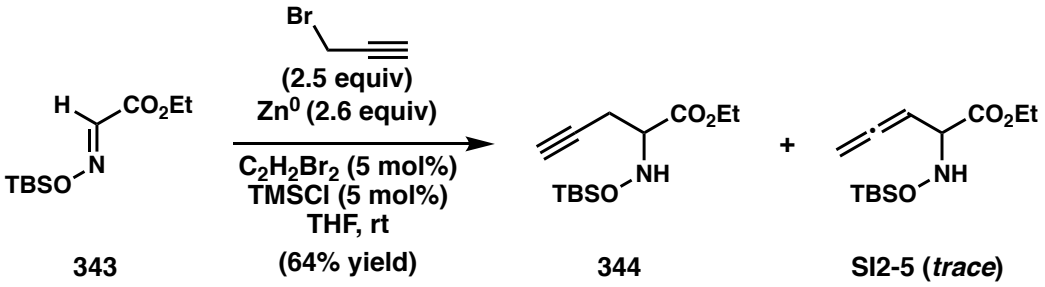

Suspend dry Zn^0 (14.13 g, 224.74 mmol, 2.6 equiv) in THF (400 mL). Add 1,2-dibromoethane (0.37 mL, 812 mg, 4.32 mmol, 5 mol %) and TMSCl (0.55 mL, 469 mg, 4.32 mmol, 5 mol %), stir at room temperature for 45 min. Add a solution of propargyl bromide, 80%wt in PhMe, (0.20 mL, 1.80 mmol, 2 mol %). Heat gently until initiation is observed. Add the remainder of propargyl bromide, 80 wt% in PhMe, (23.9 mL, 214.57 mmol, 2.58 equiv) dropwise. With addition complete, stir 30 min at ambient temperature vigorously, until zinc is no longer consumed. Cannulate fresh organozinc into a solution of ethyl 2-(((*t*-butyldimethylsilyl)oxy)imino)acetate (20.00 g, 86.44 mmol, 1.0 equiv) in THF (400 mL) chilled to 0 °C, over a three hour period. Upon disappearance of starting material quench with $NaHCO_{3(sat)}$ (200 mL). Filter off salts through a sand pad. Wash

salts Et_2O(3×200 mL). Wash combined organics with 1:1 DI H_2O:brine then brine. Dry over Na_2SO_4, filter and concentrate in vacuo to yield crude product. Purification by flash chromatography (silica 500g, 5% EtOAc/Hexanes) yields XX (15.1g, 55.6 mmol, 64% yield) as a pale yellow oil. Trace allene **S1** was also isolated for characterization.

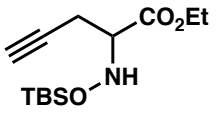

344

^{1}H NMR (400 MHz, $CDCl_3$) δ 5.60 (d, *J* = 9.5 Hz, 1H), 4.24 (q, *J* = 7.1 Hz, 2H), 3.79 – 3.46 (m, 1H), 2.57 (dt, *J* = 6.4, 2.8 Hz, 2H), 2.02 (t, *J* = 2.7 Hz, 1H), 1.29 (t, *J* = 7.1 Hz, 3H), 0.89 (s, 9H), 0.11 (d, *J* = 1.2 Hz, 6H).

^{13}C NMR (101 MHz, $CDCl_3$) δ 171.77, 79.37, 70.86, 63.89, 61.25, 26.21, 19.37, 18.01, 14.34, -5.43, -5.49.

FTIR (AT-IR) 3313.49, 2929.08, 2856.83, 2361.12, 2340.34, 1738.61, 1472.12, 1370.05, 1342.99, 1248.41, 1215.41, 1186.14, 1054.34, 904.00, 834.61, 780.54, 667.96 cm^{-1}

HRMS (TOF, ES+) calc'd for $C_{13}H_{26}NO_3$ $[M+H]^+$ 272.1676, found 272.1673(ppm=-1.28)

$[\alpha]_D^{23}$ –18.0° (*c* = 1.0, $CHCl_3$).

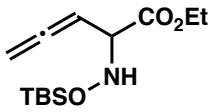

SI2-5 (*trace*)

^{1}H NMR (400 MHz, $CDCl_3$) δ 5.48 (d, *J* = 10.6 Hz, 1H), 5.12 (q, *J* = 6.8 Hz, 1H), 4.80 (dd, *J* = 6.7, 2.5 Hz, 2H), 4.18 (qd, *J* = 7.1, 0.9 Hz, 2H), 3.98 (ddt, *J* = 9.8, 7.0, 2.3 Hz, 1H), 1.23 (t, *J* = 7.1 Hz, 3H), 0.84 (d, *J* = 1.1 Hz, 9H), 0.05 (d, *J* = 1.0 Hz, 6H).

^{13}C NMR (101 MHz, $CDCl_3$) δ 209.30, 171.64, 85.51, 77.47, 64.67, 64.64, 61.08, 26.19, 26.15, 26.13, 17.96, 14.34, 14.30, -5.49, -5.53, -5.57.

FTIR (AT-IR) 2929.12, 2856.96, 1957.66, 1741.62, 1472.28, 1390.00, 1368.67, 1301.88, 1247.48, 1183.61, 1043.73, 832.33, 779.68, 666.29 cm^{-1}

HRMS (TOF, ES+) calc'd for $C_{11}H_{25}NO_3Si$ $[M+H]^+$ 272.1676, found 272.1686 (ppm=3.67)

Organozinc 1,2-addition into glyoxalate-derived oxime

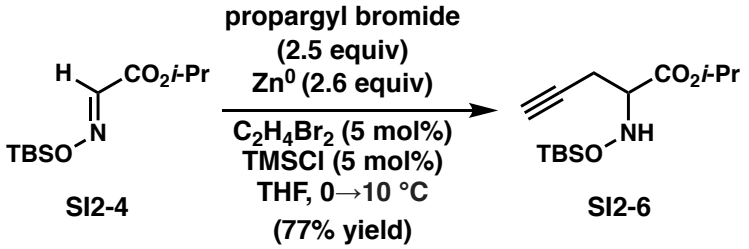

Suspend Zn^0 (3.47 g, 52.99 mmol, 2.6 equiv) in THF (100 mL). Add TMSCl (0.13 mL, 111 mg, 1.02 mmol, 5 mol %) followed by 1,2-dibromoethane (0.9 mL, 192 mg, 1.02 mmol, 5 mol %) and stir at ambient temperature for 10 minutes. Add propargyl bromide, 80 wt% in PhMe, (0.2 mL, 1.80 mmol, 9 mol %) and heat mixture slightly to initiate organozinc formation. Add the remainder of propargyl bromide, 80 wt% in PhMe, (5.47 mL, 49.11 mmol, 2.41 equiv) dropwise. After addition is complete stir an additional 25 minutes. Chill a solution of siloxime (5.00g, 20.38 mmol, 1.0 equiv) in THF (100 mL) to 0 °C. Cannulate the previously prepared organozinc solution dropwise over one hour. Quench reaction with $NaHCO_{3(aq)}$ (47 mL). Filter off precipitate through sand. Rinse retained salts with Et_2O (3×50 mL). Wash combined organic layer with $NaHCO_{3(aq)}$ (3×150 mL) then brine (50 mL). Dry organic phase over Na_2SO_4, filter and concentrate. Purify by flash chromatography (silica, 5 →20% Et_2O/Hexanes) to yield **SI2-6** (4.49g, 15.7 mmol, 77% yield) as a clear oil.

^{1}H NMR (400 MHz, $CDCl_3$) δ 5.60 (s, 1H), 5.12 (p, *J* = 6.3 Hz, 1H), 3.59 (d, *J* = 6.4 Hz, 1H), 2.72 – 2.38 (m, 2H), 2.01 (t, *J* = 2.7 Hz, 1H), 1.27 (dd, *J* = 6.3, 2.7 Hz, 6H), 0.88 (s, 9H), 0.11 (d, *J* = 0.6 Hz, 6H).

^{13}C NMR (101 MHz, $CDCl_3$) δ 171.39, 79.44, 70.76, 68.86, 64.01, 26.20, 21.90, 19.32, 17.98, -5.42, -5.51.

FTIR (AT-IR) 3314.32, 2956.64, 2929.43, 2885.87, 2857.05, 1732.83, 1472.12, 1387.98, 1374.66, 1361.80, 1325.04, 1248.31, 1221.75, 1190.63, 1145.40, 1106.94, 1054.85, 1006.08, 968.73, 890.80, 833.48, 780.20, 665.95, 642.72 cm^{-1}

HRMS (TOF, ES+) calc'd for $C_{14}H_{27}NO_3Si$ $[M+H]^+$ 286.1833, found 286.1830 (ppm=1.04)

Benzoylation of *N*-siloxyamino ethyl ester

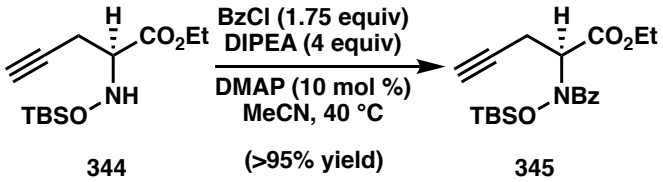

344 345

To a solution of substrate (3.99 g, 14.70 mmol, 1.0 equiv) in MeCN (14.7 mL) add DIPEA (5.13 mL, 3.80 g, 29.40 mmol, 2.0 equiv) and benzoyl chloride (2.99 mL, 3.62 g, 25.73 mmol, 1.75 equiv) at ambient temperature and stir 30 minutes. Heat mixture to 40 °C stirring vigorously for 7 hours. Dilute in Et_2O (140 mL) and wash organics with with pH=7 phosphate buffer (30 mL), then brine (30 mL). Dry organic layer with Na_2SO_4, filter through celite, and concentrate. Purify by flash chromatography (florisil, 20% Et_2O/Hexanes) to yield **345** (5.5g, 14.65 mmol, >95% yield) as pale white crystals.

SFC analysis (IC, 5% *i*-PrOH in CO_2) peak 1(major): 6.748 min; peak 2(minor): 8.324 min; 94% ee

^{1}H NMR (400 MHz, $CDCl_3$) δ 7.76 – 7.65 (m, 2H), 7.53 – 7.35 (m, 3H), 4.65 (dd, *J* = 10.5, 4.5 Hz, 1H), 4.21 (qdd, *J* = 10.7, 7.0, 3.6 Hz, 2H), 2.97 (ddd, *J* = 17.4, 10.6, 2.7 Hz, 1H), 2.89 – 2.70 (m, 1H), 2.14 (t, *J* = 2.7 Hz, 1H), 1.30 (t, *J* = 7.1 Hz, 3H), 0.95 (s, 9H), 0.30 (s, 3H), 0.21 (s, 3H).

^{13}C NMR (101 MHz, $CDCl_3$) δ 173.13, 168.28, 134.61, 131.05, 128.59, 128.48, 80.35, 71.70, 63.97, 62.11, 26.18, 18.58, 14.31, -4.31, -4.51.

FTIR (AT-IR) 3310.03, 2929.56, 2857.22, 2359.18, 1744.02, 1694.62, 1472.02, 1446.93, 1390.26, 1362.25, 1289.85, 1250.00, 1226.16, 1186.10, 1072.43, 1017.66, 964.62, 920.36, 831.69, 809.32, 783.13, 748.13, 703.47, 674.24, 654.39 cm^{-1}

HRMS (TOF, ES+) calc'd for $C_{20}H_{30}NO_4Si$ $[M+H]^+$ 376.1939, found 376.1934

$[\alpha]_D^{23}$ –89.9° (*c*=1.0, $CHCl_3$)

Benzoylation of *N*-siloxyamino *iso*-propyl ester

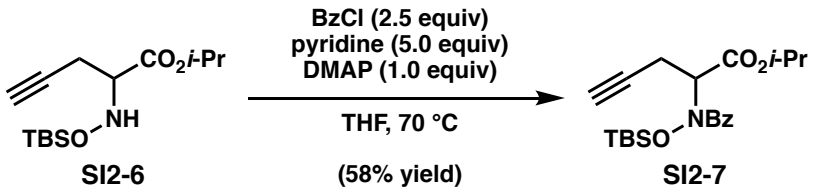

Dissolve **SI2-6** (4.49g, 15.71 mmol, 1.0 equiv) in THF (60 mL). Add pyridine (6.40 mL, 6.21 g, 78.55 mmol, 5 equiv) followed by benzoyl chloride (4.60 mL, 5.52 g, 39.28 mmol, 2.5 equiv) and DMAP (1.92 g, 15.71 mmol, 1.0 equiv). Wash the sides of flask with THF (90 mL). Heat mixture to reflux and stir 27h. Cool reaction to ambient temperature and dilute in Et_2O (200 mL). Wash crude mixture with dilute citric acid (150 mL), pH=7 phosphate buffer (150 mL), and brine (150 mL). Dry organic layer with Na_2SO_4, filter, and concentrate to yield crude product. A two stage purification by flash chromatography (silica, 5→12% EtOAc/Hexanes; then, fluorosil, 5→100% Et_2O/Hexanes) yields **SI2-7** (3.55g, 9.11 mmol, 58% yield) as a white solid.

^{1}H NMR (500 MHz, $CDCl_3$) δ 5.60 (d, *J* = 9.6 Hz, 1H), 5.12 (p, *J* = 6.2 Hz, 1H), 3.59 (dt, *J* = 9.6, 6.4 Hz, 1H), 2.65 – 2.46 (m, 2H), 2.01 (t, *J* = 2.7 Hz, 1H), 1.27 (dd, *J* = 6.3, 3.5 Hz, 6H), 0.88 (s, 9H), 0.10 (d, *J* = 0.9 Hz, 6H).

^{13}C NMR (101 MHz, $CDCl_3$) δ 173.54, 167.71, 134.70, 130.99, 128.52, 128.43, 80.57, 71.61, 70.05, 64.08, 26.15, 21.89, 21.83, 18.77, 18.53, -4.45, -4.46.

FTIR (AT-IR) 2930.02, 2857.32, 1739.8, 1698.57, 1471.80, 1447.34, 1375.01, 1361.30, 1288.72, 1250.34, 1226.66, 1188.79, 1144.53, 1105.46, 963.93, 920.96, 834.33, 782.72, 749.05, 703.61, 674.83 cm^{-1}

HRMS (TOF, ES+) calc'd for $C_{21}H_{31}NO_4Si$ $[M+H]^+$ 390.2095, found 390.2090 (ppm=1.31)

Acylation of *N*-siloxyamino ethyl ester

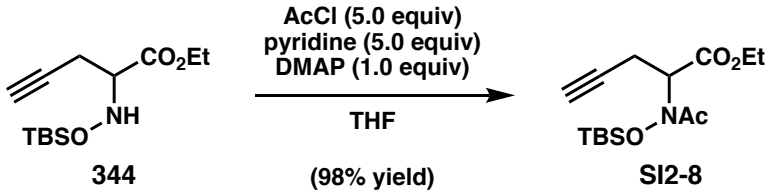

Add pyridine (1.48 mL, 1.46 g, 18.42 mmol, 5.0 equiv) and DMAP (450 mg, 3.83 mmol, 0.96 equiv) to solution of **344** (1.04 g, 3.83 mmol, 1.0 equiv) in THF (60 mL). Add acetyl chloride (1.31 mL, 1.45 g, 18.42 mmol, 5.0 equiv) and stir vigorously at ambient temperature for 18h. Dilute in Et_2O (50 mL) and wash with pH=7 phosphate buffer (50mL) then brine (50 mL). Dry organic phase over Na_2SO_4, filter and concentrate gave **SI2-8** (1.18 g, 3.76 mmol, 98% yield) as a pale-yellow oil with no further purification necessary.

^{1}H NMR (400 MHz, $CDCl_3$) δ 4.56 (t, *J* = 7.5 Hz, 1H), 4.21 (q, *J* = 7.1 Hz, 2H), 3.01 – 2.83 (m, 2H), 2.16 (s, 3H), 2.02 (t, *J* = 2.7 Hz, 1H), 1.27 (t, *J* = 7.1 Hz, 3H), 0.96 (s, 9H), 0.29 (s, 3H), 0.24 (s, 3H).

^{13}C NMR (126 MHz, $CDCl_3$) δ 176.42, 168.14, 80.35, 70.42, 63.61, 61.72, 25.80, 21.52, 18.68, 17.93, 14.08, -4.51, -4.76.

FTIR (AT-IR) 3282.17, 2930.95, 2858.52, 2361.30, 1742.64, 1674.63, 1472.78, 1463.68, 1367.92, 1253.56, 1185.00, 1080.68, 1018.10, 983.77, 965.14, 938.25, 833.87, 784.10, 667.99 cm^{-1}

HRMS (TOF, ES+) calc'd for $C_{15}H_{27}NO_4Si$ $[M+H]^+$ 314.1782, found 314.1780 (ppm=0.67)

Chloroacylation of *N*-siloxyamino ethyl ester

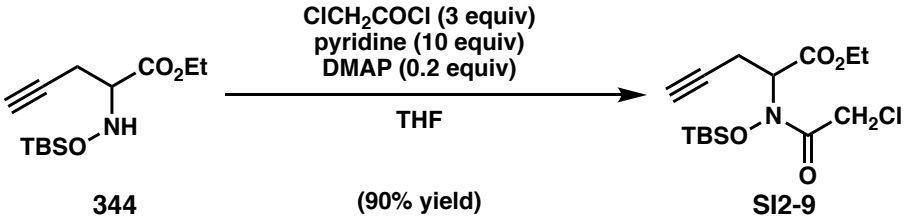

344 (90% yield) **SI2-9**

Add pyridine (0.45mL, 439 mg, 5.55 mmol, 5.0 equiv) and DMAP (27.1mg, 0.22 mmol, 0.20 equiv) to solution substrate (300mg, 1.11mmol, 1.0 equiv) in THF (15mL). Add chloroacetyl chloride (0.13 mL, 188.6 mg, 1.67 mmol, 1.5 equiv) and stir vigorously at ambient temperature for 5h. Dilute in Et_2O (50 mL) and wash with pH=7 phosphate buffer (50mL) then brine (50 mL). Dry organic phase over Na_2SO_4, filter and concentrate. Purification by flash chromatography (florisil, 20% EtOAc/Hexanes) provided **SI2-9** as a pale oil (347 mg, 0.0XXmmol, 90% yield).

^{1}H NMR (400 MHz, $CDCl_3$) δ 4.56 – 4.42 (m, 1H), 4.36 – 4.24 (m, 2H), 4.21 (q, *J* = 7.1 Hz, 2H), 3.13 – 2.79 (m, 2H), 2.03 (t, *J* = 2.6 Hz, 1H), 1.26 (td, *J* = 7.1, 0.9 Hz, 3H), 0.95 (s, 9H), 0.30 (s, 3H), 0.26 (s, 3H).

^{13}C NMR (101 MHz, $CDCl_3$) δ 170.71, 166.64, 79.03, 70.06, 63.97, 61.21, 41.63, 24.81, 18.02, 17.08, 13.17, -5.42, -5.75.

FTIR (AT-IR) 3303.84, 2931.44, 2859.45, 2361.24, 1742.56, 1683.23, 1472.71, 1367.63, 1318.42, 1254.23, 1187.67, 1016.74, 959.4, 938.47, 835.12, 784.06, 667.94 cm^{-1}

HRMS (TOF, ES+) calc'd for $C_XH_xNO_xSi$ $[M+H]^+$ 348.1392, found 348.1396 (ppm=-1.04)

Enyne metathesis of benzoylated siloxyamino ethyl ester

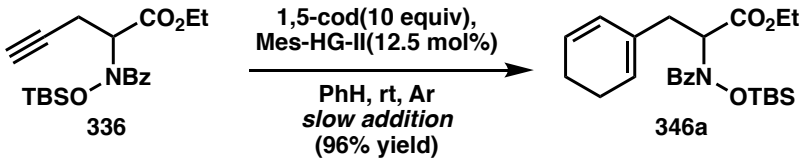

Solvate Mes-HG-II (692 mg, 1.103 mmol, 7.5 mol%) stored in the glovebox in benzene (55 mL). Maintain an Ar atmosphere. Add distilled and degassed 1,5-cyclooctadiene (18.0 mL, 15.90 g, 147.0 mmol, 10 equiv), stir five minutes. Concurrently, both a solution of **336** (5.50 g, 14.70 mmol, 1.0 equiv) in benzene (360 mL) and a solution of Mes-HG-II (461 mg, 0.735 mmol, 5 mol%) in benzene (10.6 mL) were added by syringe pumps over 12h. Stir at room temperature for 2h. Concentrate the crude reaction onto celite (50 g) overnight. Purify by flash chromatography (silica 150 g, 10→20% Et_2O/Hexanes). Concentrate to an oil and dilute in cold MeCN (50 mL). Filter off precipitate with celite and wash the celite pad twice with cold MeCN (50 mL). Concentrate to yield **346a** (6.09 g, 14.2 mmol, 96% yield) a beige oil.

^{1}H NMR (400 MHz, $CDCl_3$) δ 7.56 (dt, *J* = 6.8, 1.5 Hz, 2H), 7.45 – 7.37 (m, 1H), 7.37 (s, 2H), 5.79 (dd, *J* = 9.5, 4.3 Hz, 1H), 5.70 – 5.54 (m, 2H), 4.45 (dd, *J* = 10.1, 4.4 Hz, 1H), 4.32 – 4.13 (m, 3H), 2.85 (dd, *J* = 14.2, 10.1 Hz, 1H), 2.60 (d, *J* = 14.1 Hz, 1H), 2.15 – 2.09 (m, 4H), 1.33 (t, *J* = 7.1 Hz, 4H), 0.92 (s, 10H), 0.29 (s, 3H), 0.13 (s, 3H).

^{13}C NMR (101 MHz, $CDCl_3$) δ 170.80, 169.47, 134.72, 131.16, 130.60, 129.83, 128.26, 127.25, 126.70, 124.77, 64.74, 61.74, 33.61, 26.19, 22.55, 22.19, 18.87, 14.29, -3.86, -4.52.

FTIR (AT-IR) 2929.77, 2857.11, 2359.5, 2340.28, 1742.71, 1653.06, 1471.97, 1447.06, 1249.13, 1183.09, 1019.33, 969.71, 919.13, 826.95, 783.52, 735.42, 700.25, 667.9 cm^{-1}

HRMS (TOF, ES+) calc'd for $C_{24}H_{35}NO_4Si$ $[M+H]^+$ 430.2408, found 430.2395 (ppm=3.05)

Enyne metathesis of benzoylated siloxyamino *iso*-propyl ester

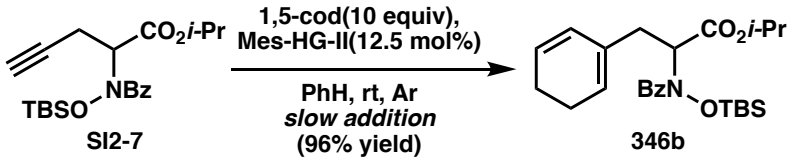

Solvate Mes-HG-II (60.2 mg, 0.096 mmol, 7.5 mol%) stored in the glovebox in benzene(5 mL). Maintain an Ar atmosphere. Add distilled and degassed 1,5-cyclooctadiene (1.57 mL, 1.38 g, 12.80 mmol, 10 equiv). Concurrently, both a solution of **SI2-7** (500 mg, 1.28 mmol, 1 equiv) in benzene (25 mL) and a solution of Mes-HG-II (45 mg, 0.072 mmol, 5 mol%) in benzene (2 mL) were added by syringe pumps over 7h50m. Stir at room temperature for 2h. Concentrate the crude reaction onto celite overnight. Purify by flash chromatography (silica, 5→27.5% Et_2O/Hexanes) concentrate to product with trace impurities. Filter off precipitate with celite pad, wash with CH_2Cl_2 and concentrate to yield pure **346b** (546.8 mg, 1.23 mmol, 96% yield) as a pale oil.

^{1}H NMR (500 MHz, $CDCl_3$) δ 7.60 – 7.49 (m, 2H), 7.43 – 7.37 (m, 1H), 7.36 – 7.30 (m, 2H), 5.80 (dd, J = 9.4, 4.4 Hz, 1H), 5.68 (s, 1H), 5.62 (h, J = 1.7 Hz, 1H), 5.05 (p, J = 6.3 Hz, 1H), 4.36 (dd, J = 9.9, 4.6 Hz, 1H), 2.81 (dd, J = 14.2, 9.9 Hz, 1H), 2.62 (dd, J = 14.4, 4.5 Hz, 1H), 2.12 (dtd, J = 5.4, 3.8, 1.6 Hz, 4H), 1.29 (d, J = 6.2 Hz, 3H), 1.27 (d, J = 6.3 Hz, 3H), 0.97 – 0.86 (m, 9H), 0.21 (d, J = 61.6 Hz, 6H).

^{13}C NMR (126 MHz, $CDCl_3$) δ 171.19, 168.82, 134.81, 131.41, 130.56, 128.23, 127.24, 126.82, 124.54, 69.52, 64.97, 33.70, 26.24, 22.54, 22.24, 21.96, 21.94, 18.89, -3.94, -4.24.

FTIR (AT-IR) 2929.39, 2856.62, 2359.77, 2340.47, 1739.64, 1661.23, 1579.37, 1471.53, 1447.32, 1386.82, 1374.19, 1360.95, 1248.97, 1179.95, 1144.34, 1106.04, 990.36, 960.89, 918.86, 827.13, 783.07, 733.48, 700.54, 667.71 cm^{-1}

HRMS (TOF, ES+) calc'd for $C_{25}H_{37}NO_4Si$ $[M+H]^+$ 444.2565, found 444.2565 (ppm=0.00)

Enyne metathesis of acylated siloxyamino ethyl ester

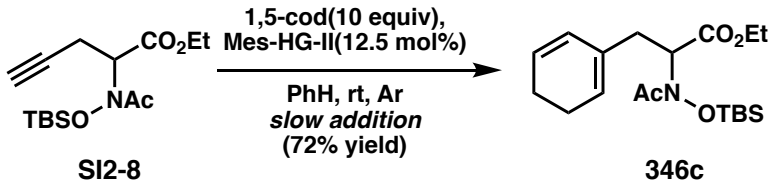

SI2-8 **346c**

Solvate Mes-HG-II (176.7 mg, 0.282 mmol, 7.5 mol%) stored in the glovebox in benzene(14 mL). Maintain an Ar atmosphere. Add distilled and degassed 1,5-cyclooctadiene (4.62 mL, 4.07g, 37.64 mmol, 10 equiv), stirring vigorously (700 rpm). Concurrently, both a solution of **SI2-8** (1.18g, 3.76mmol, 1 equiv) in benzene (90 mL) and a solution of Mes-HG-II (117.8 mg, 0.188 mmol, 5 mol%) in benzene (3.5 mL) were added by syringe pumps over 10h. Stir at room temperature for 3h. Concentrate the crude reaction onto celite overnight. Purify by flash chromatography (silica, 7.5→10% EtOAc/Hexanes). Add $P(CH_2CH_2OH)_3$ (1.16g, 20 equiv) to product-contained fractions along with silica and was sonicate until the combined solution is clear. Filter the solution was then and concentrate to yield **346c** (991mg, 2.70 mmol, 72% yield) a clear oil.

^{1}H NMR (500 MHz, $CDCl_3$) δ 5.81 (d, J = 1.3 Hz, 2H), 5.58 (d, J = 4.5 Hz, 1H), 4.47 (s, 1H), 4.26 – 4.08 (m, 2H), 2.78 (ddd, J = 14.2, 10.3, 0.9 Hz, 1H), 2.65 (dd, J = 14.4, 4.8 Hz, 1H), 2.10 – 2.04 (m, 7H), 1.27 (t, J = 7.1 Hz, 3H), 0.94 (s, 9H), 0.26 (s, 3H), 0.18 (s, 3H).

^{13}C NMR (101 MHz, $CDCl_3$) δ 175.10, 169.64, 131.84, 127.11, 126.84, 123.88, 64.01, 61.53, 33.64, 25.97, 22.52, 22.24, 21.62, 18.07, 14.22, -4.53.

FTIR (AT-IR) 2930.65, 2857.62, 2359.56, 2340.27, 1742.48, 1667.8, 1367.59, 1252.92, 1031.68, 832.83, 783.93, 667.92 cm^{-1}

HRMS (TOF, ES+) calc'd for $C_{19}H_{33}NO_4Si$ $[M+H]^+$ 368.2252, found 368.2253 (ppm=–0.38)

Enyne metathesis of chloroacylated siloxyamino ethyl ester

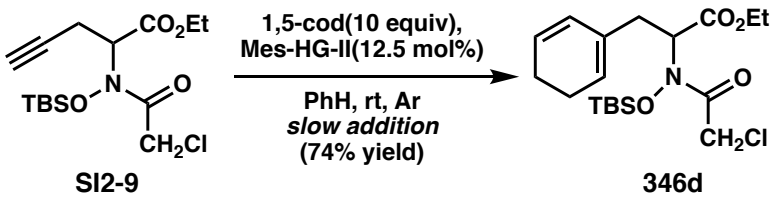

SI2-9 **346d**

Solvate Mes-HG-II(47.0 mg, 0.075 mmol, 0.075 equiv) stored in the glovebox in argon–degassed benzene (3.5 mL). Maintain an Ar atmosphere. Add distilled and degassed 1,5-cyclooctadiene (1.22 mL, 1.08g, 9.98 mmol, 10 equiv), stirring vigorously (700 rpm). Concurrently, both a solution of alkyne (347.1 mg, 0.998mmol, 1 equiv) in benzene (24 mL) and a solution of Mes-HG-II (31.3 mg, 0.050 mmol, 0.05 equiv) in benzene (1.0mL) were added by syringe pumps over 10h. Stir at room temperature for 3h. Concentrate the crude reaction onto celite overnight. Purify by flash chromatography (silica, 7.5→10% EtOAc/Hexanes). Yields **SI2-9** (296 mg, 74% yield) as a pale oil.

^{1}H NMR (500 MHz, $CDCl_3$) δ 5.86 – 5.76 (m, 2H), 5.58 (d, J = 4.5 Hz, 1H), 4.39 (dd, J = 10.6, 4.7 Hz, 1H), 4.30 – 4.11 (m, 4H), 2.85 (dd, J = 14.2, 10.6 Hz, 1H), 2.72 – 2.60 (m, 1H), 2.13 – 2.01 (m, 4H), 1.26 (t, J = 7.1 Hz, 3H), 0.92 (s, 9H), 0.25 (s, 3H), 0.19 (s, 3H).

^{13}C NMR (126 MHz, $CDCl_3$) δ 170.52, 169.01, 131.54, 127.46, 126.63, 124.35, 65.63, 61.83, 42.77, 33.83, 25.82, 22.47, 22.21, 17.97, 14.20, -4.68.

FTIR (AT-IR) 2931.1, 2859.38, 2361.15, 2340.18, 1742.03, 1673.54, 1472.41, 1463.48, 1391.13, 1364.3, 1318.5, 1251.92, 1213.32, 1184.41, 1083.27, 1017.52, 912.03, 836.04, 783.58, 731.43, 668.09, 646.92 cm^{-1}

HRMS (TOF, ES+) calc'd for $C_{19}H_{32}ClNO_4Si$ $[M+H]^+$ 402.1862, found 402.1862 (ppm=-0.03)

Copper–catalyzed oxidative cyclization of benzoylated diene ethyl ester

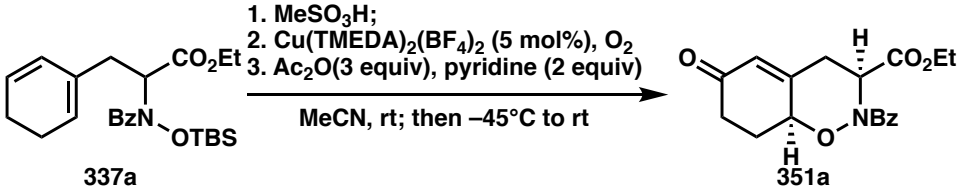

Add $MeSO_3H$ (0.23mL, 325mg, 3.49 mmol, 0.5 equiv) to substrate () under argon in wet MeCN (350 mL) and begin cool to –35 °C. Sparge reaction with O_2 and add $Cu(TMEDA)_2(BF4)_2$ (0.0349 mmol, 0.05 equiv) as a solution in MeCN (1 mL). Note: $Cu(TMEDA)_2(BF4)_2$ made by dissolving $Cu(BF_4)_2 \cdot xH_2O$ (20 wt% Cu) (111 mg, 0.349 mmol, 0.05 equiv) and TMEDA (0.10 mL, 81 mg, 0.10 equiv) in MeCN(1 mL). Continue cooling to –45 °C. Stop O_2 sparge after 10 minutes at –45 °C. Slowly allow reaction return to room temperature. Add acetic anhydride (3.84 mL, 4.16 g, 40.48 mmol, 6.0 equiv), stir 1 minute then add pyridine (0.54 mL, 534 mg, 6.75 mmol, 1 equiv) allow to stir under air overnight. Dilute with EtOAc (350 mL) wash with an aqueous solution (357 mL) composed of EDTA pH=9 buffer (7 mL), DI H_2O (175mL) and brine (175mL). Wash organic with additional brine (50 mL). Extract combined aqueous layer with EtOAc (2x100mL). Dry combined organic layers over Na_2SO_4, filter and concentrate. Separate crude material on silica (215 g) with 40% EtOAc in Hexanes. 1.512g total product isolated (4.59 mmol, 69% yield)

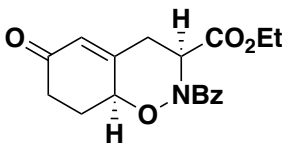

351a-*syn*: ^{1}H NMR (400 MHz, $CDCl_3$) δ 7.78 (d, *J* = 7.6 Hz, 2H), 7.57 – 7.49 (m, 1H), 7.45 (ddt, *J* = 8.3, 6.6, 1.3 Hz, 2H), 6.02 (d, *J* = 2.3 Hz, 1H), 5.54 (s, 1H), 4.62 (s, 1H), 4.26 (q, *J* = 7.2 Hz, 2H), 3.16 (d, *J* = 15.7 Hz, 1H), 2.96 (dd, *J* = 15.8, 7.0 Hz, 1H), 2.51 (d, *J* = 16.7 Hz, 1H), 2.30 (td, *J* = 16.5, 15.9, 5.0 Hz, 1H), 2.13 (d, *J* = 23.1 Hz, 1H), 1.97 – 1.80 (m, 1H), 1.29 (t, *J* = 7.2 Hz, 4H).

^{13}C NMR (101 MHz, $CDCl_3$) δ 196.87, 170.20, 168.39, 153.52, 132.54, 131.83, 128.94, 128.27, 127.95, 78.86, 77.52, 62.33, 35.05, 31.33, 29.87, 26.33, 14.33.

FTIR (AT-IR) 2979.74, 2359.59, 1738.00, 1667.46, 1600.60, 1578.10, 1447.41, 1387.71, 1364.39, 1316.29, 1254.3, 1197.39, 1139.88, 1077.16, 1027.25, 975.89, 899.81, 871.89, 789.33, 758.51, 706.03, 617.25 cm^{-1}

HRMS (TOF, ES+) calc'd for $C_{18}H_{19}NO_5$ $[M+H]^+$ 330.1336, found 330.1337 (ppm=-0.31)

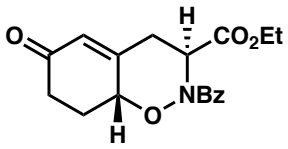

351a-*anti*:

^{1}H NMR (400 MHz, CDCl3) δ 7.80 (dt, *J* = 8.5, 1.6 Hz, 2H), 7.53 – 7.46 (m, 1H), 7.46 – 7.38 (m, 2H), 6.02 – 5.93 (m, 1H), 4.99 (dd, *J* = 9.6, 7.6 Hz, 1H), 4.76 (t, *J* = 8.3 Hz, 1H), 4.36 – 4.22 (m, 2H), 3.14 – 2.96 (m, 2H), 2.53 – 2.44 (m, 1H), 2.33 – 2.14 (m, 1H), 1.89 (ddd, *J* = 9.7, 8.0, 5.0 Hz, 2H), 1.35 – 1.29 (m, 3H).

^{1}H NMR (500 MHz, $CDCl_3$) δ 7.82 – 7.77 (m, 2H), 7.52 – 7.46 (m, 1H), 7.45 – 7.39 (m, 2H), 6.01 – 5.96 (m, 1H), 4.98 (dd, *J* = 9.6, 7.5 Hz, 1H), 4.81 – 4.68 (m, 1H), 4.28 (q, *J* = 7.1 Hz, 2H), 3.10 – 2.95 (m, 2H), 2.49 (dddd, *J* = 17.2, 4.4, 2.9, 1.2 Hz, 1H), 2.31 – 2.19 (m, 1H), 1.97 – 1.80 (m, 2H), 1.31 (t, *J* = 7.1 Hz, 3H).

^{13}C NMR (101 MHz, $CDCl_3$) δ 196.64, 170.15, 168.93, 157.09, 132.65, 131.60, 129.22, 128.10, 127.77, 80.96, 62.26, 58.14, 35.41, 30.86, 27.55, 14.28.

FTIR (AT-IR) 2359.53, 2340.23, 1729.8, 1637.97, 1577.29, 1448.88, 1394.9, 1300.99, 1245.96, 1199.42, 1098.44, 1008.47, 981.15, 962.42, 904.15, 844.43, 790.7, 736.73, 707.82, 667.97, 635.45 cm^{-1}

HRMS (TOF, ES+) calc'd for $C_{18}H_{19}NO_5$ $[M+H]^+$ 330.1336, found 330.1334 (ppm=0.60)

Copper–catalyzed oxidative cyclization of benzoylated diene *iso*-propyl ester

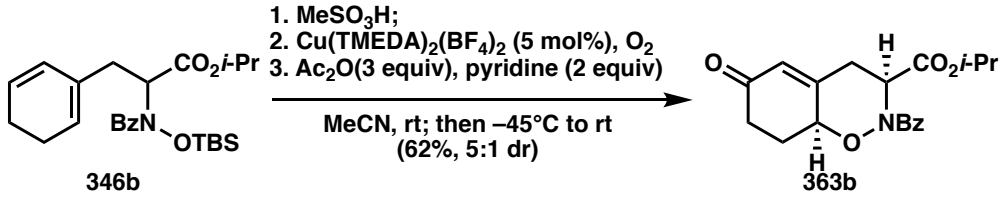

Add $MeSO_3H$ (24 μL, 35.6 mg, 3.49 mmol, 0.5 equiv) to **346b** (329 mg, 0.741 mmol) under argon in wet MeCN (35 mL) and begin cool to –35 °C. Sparge reaction with O_2 and add $Cu(TMEDA)_2(BF4)_2$ (0.0349 mmol, 0.05 equiv) as a solution in MeCN (1 mL). Note: $Cu(TMEDA)_2(BF4)_2$ made by dissolving $Cu(BF_4)_2 \bullet xH_2O$ (20 wt% Cu) (12 mg, 0.0.0371 mmol, 0.05 equiv) and TMEDA (11 μL, 8.6 mg, 0.0742 mmol, 0.10 equiv) in MeCN (2 mL). Continue cooling to –45 °C. Stop O_2 sparge after 10 minutes but continue stirring at –45 °C for 2h. Slowly allow reaction return to room temperature. Add acetic anhydride (0.21 mL, 229 mg, 40.48 mmol, 3.0 equiv), stir 1 minute then add pyridine (60 μL, 58.6 mg, 6.75 mmol, 2 equiv) allow to stir under air overnight. Dilute with EtOAc (35 mL) wash with an aqueous solution (35 mL) composed of EDTA pH=9 buffer (0.7 mL), DI H_2O (17.5mL) and brine (17.5mL). Wash organic with additional brine (5 mL). Extract combined aqueous layer with EtOAc (2x100mL). Dry combined organic layers over Na_2SO_4, filter and concentrate. Separate crude material on silica with 40% EtOAc in Hexanes. 156.7 mg total product isolated (0.456 mmol, 62% yield, 5:1 dr)

^{1}H NMR (500 MHz, $CDCl_3$) δ 7.75 (d, J = 7.7 Hz, 2H), 7.53 – 7.47 (m, 1H), 7.46 – 7.39 (m, 2H), 5.99 (dt, J = 2.2, 1.2 Hz, 1H), 5.51 (d, J = 20.8 Hz, 1H), 5.07 (p, J = 6.3 Hz, 1H), 4.60 (s, 1H), 3.12 (d, J = 15.7 Hz, 1H), 3.00 – 2.81 (m, 1H), 2.55 – 2.40 (m, 1H), 2.28 (td, J = 16.4, 15.9, 4.9 Hz, 1H), 2.21 – 2.04 (m, 1H), 1.86 (t, J = 13.9 Hz, 1H), 1.24 (d, J = 6.1 Hz, 6H).

^{13}C NMR (126 MHz, $CDCl_3$) δ 196.87, 170.15, 167.72, 153.70, 132.56, 131.68, 128.81, 128.16, 127.75, 78.69, 70.11, 54.66, 34.95, 31.35, 26.27, 21.84, 21.82.

FTIR (AT-IR) 2980.74, 2250.35, 1733.31, 1668.08, 1600.87, 1578.34, 1447.99, 1386.42, 1374.01, 1312.85, 1253.98, 1200.97, 1143.54, 1103.75, 1018.30, 976.54, 899.45, 823.75, 788.51, 728.2, 706.22, 646.73 cm^{-1}

HRMS (TOF, ES+) calc'd for $C_{19}H_{21}NO_5$ $[M+H]^+$ 344.1492, found 344.1494 (ppm=-0.44)

Copper–catalyzed oxidative cyclization of acylated diene ethyl ester

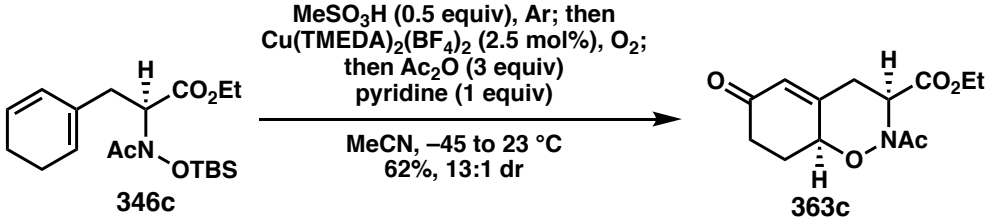

Add $MeSO_3H$ (18 µL, 26.1 mg, 0.272 mmol, 0.5 equiv) in MeCN (0.5 mL) to **346c** (200 mg, 0.544 mmol, 1.0 equiv) under argon in wet MeCN (26 mL) and begin cool to –35 °C. Sparge reaction with O_2 and add $Cu(TMEDA)_2(BF4)_2$ (0.00.136 mmol, 0.05 equiv) as a solution in MeCN (0.5 mL). Note: $Cu(TMEDA)_2(BF4)_2$ made by dissolving $Cu(BF_4)_2 \bullet xH_2O$ (20 wt% Cu) (4.3 mg, 0.0.0136 mmol, 0.05 equiv) and TMEDA (4 µL, 3.2 mg, 0.0272 mmol, 0.10 equiv) in MeCN (0.5 mL). Continue cooling to –45 °C. Stop O_2 sparge after 10 minutes but continue stirring at –45 °C for 2h. Slowly allow reaction return to room temperature. Add acetic anhydride (0.16 mL, 168 mg, 1.632 mmol, 3.0 equiv), stir 1 minute then add pyridine (44 µL, 43 mg, 0.544 mmol, 1 equiv) allow to stir under air overnight. Dilute with EtOAc (20 mL) wash with an aqueous solution (35 mL) composed of EDTA pH=9 buffer (10 mL), DI H_2O (5mL) and brine (5 mL). Extract combined aqueous with EOAc (10 mL) Wash combined organics with additional brine (20 mL). Dry combined organic layers over Na_2SO_4, filter and concentrate. Purify crude material by flash chromatography on silica with 100% Et_2O then 75% to 100%EtOAc/Hexanes. 90 mg total product isolated (0.337 mmol, 62% yield, 13:1 dr)

^{1}H NMR (600 MHz, $CDCl_3$) δ 6.01 (q, *J* = 1.5 Hz, 1H), 5.41 (dd, *J* = 7.2, 1.4 Hz, 1H), 4.68 (dd, *J* = 10.7, 5.1 Hz, 1H), 4.27 – 4.15 (m, 2H), 3.11 (ddt, *J* = 15.7, 1.5, 0.7 Hz, 1H), 2.84 (dddd, *J* = 15.7, 7.2, 2.5, 1.6 Hz, 1H), 2.63 – 2.55 (m, 1H), 2.41 – 2.33 (m, 2H), 2.25 (s, 3H), 1.98 (dddd, *J* = 16.2, 14.1, 9.0, 3.3 Hz, 1H), 1.26 (td, *J* = 7.1, 1.0 Hz, 4H).

^{13}C NMR (126 MHz, $CDCl_3$) δ 196.79, 171.44, 168.28, 153.41, 127.93, 78.79, 62.19, 53.60, 35.02, 31.50, 26.38, 20.30, 14.26.

FTIR (AT-IR) 2931.38, 2360.54, 1737.83, 1668.55, 1402.03, 1368.95, 1314.81, 1256.65, 1198.38, 1026.43, 975.46, 945.41, 900.55, 725.65 cm^{-1}

HRMS (TOF, ES+) calc'd for $C_{13}H_{17}NO_5$ $[M+H]^+$ 268.1179, found 268.1180 (ppm=-0.19)

Copper–catalyzed oxidative cyclization of chloroacylated diene ethyl ester

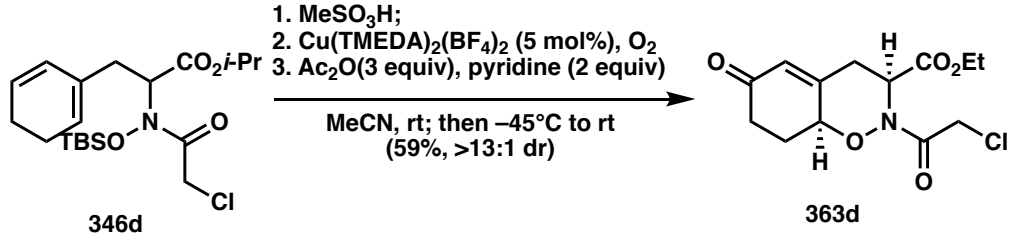

Add $MeSO_3H$ (0.99 mL, 1.47 g, 15.25 mmol, 0.75 equiv) in MeCN (5 mL) to **346c** (8.11 g, 20.17 mmol, 1.0 equiv) under argon in wet MeCN (1.0 L) and begin cool to –35 °C. Sparge reaction with O_2 and add $Cu(TMEDA)_2(BF4)_2$ (1.01 mmol, 0.05 equiv) as a solution in MeCN (5 mL). Note: $Cu(TMEDA)_2(BF4)_2$ made by dissolving $Cu(BF_4)_2 \bullet xH_2O$ (20 wt% Cu) (320.9 mg, 0.101 mmol, 0.05 equiv) and TMEDA (0.30 mL, 235 mg, 2.02 mmol, 0.10 equiv) in MeCN (5 mL). Continue cooling to –45 °C. Stop O_2 sparge after 10 minutes but continue stirring at –45 °C for 2h. Slowly allow reaction return to room temperature overnight. Add acetic anhydride (5.75 mL, 6.23 g, 60.51 mmol, 3.0 equiv), stir 1 minute then add pyridine (2.97 mL, 2.91 g, 36.87 mmol, 1.8 equiv) allow to stir under air overnight. Dilute with EtOAc (700 mL) wash twice with EDTA pH=9 buffer (100

mL), then brine (500 mL). Dry combined organic layers over Na_2SO_4, filter and concentrate. Purify crude material by flash chromatography on silica with 75% to 100%EtOAc/Hexanes. Syn-diastereomer recover exclusively (3.6 g, 11.9 mmol, 59% yield, >13:1 dr)

^{1}H NMR (500 MHz, $CDCl_3$) δ 6.00 (q, J = 1.4 Hz, 1H), 5.33 (dd, J = 7.3, 1.4 Hz, 1H), 4.83 – 4.78 (m, 1H), 4.42 (d, J = 13.3 Hz, 1H), 4.21 (tt, J = 7.1, 3.7 Hz, 2H), 4.17 (d, J = 13.3 Hz, 1H), 3.13 (ddt, J = 15.7, 1.5, 0.8 Hz, 1H), 2.88 (dddd, J = 15.7, 7.2, 2.5, 1.6 Hz, 1H), 2.61 – 2.52 (m, 1H), 2.43 – 2.33 (m, 2H), 2.02 – 1.89 (m, 1H), 1.24 (t, J = 7.1 Hz, 3H).

^{13}C NMR (126 MHz, $CDCl_3$) δ 196.61, 167.61, 167.13, 152.49, 128.11, 79.24, 62.44, 54.24, 40.77, 34.93, 31.25, 26.14, 14.22.

FTIR (AT-IR) 2960.80, 2358.75, 1738.21, 1669.87, 1414.36, 1367.74, 1329.02, 1239.72, 1189.30, 1094.68, 1024.45, 976.25, 955.89, 902.07, 858.34, 790.90, 767.92, 727.65, 667.80, 646.77 cm^{-1}

HRMS (TOF, ES+) calc'd for $C_{13}H_{16}ClNO_5$ $[M+H]^+$ 302.0790, found 302.0789 (ppm=0.25)

Deprotection of chloroacylated bicyclic tetrahydro-1,2-oxazine

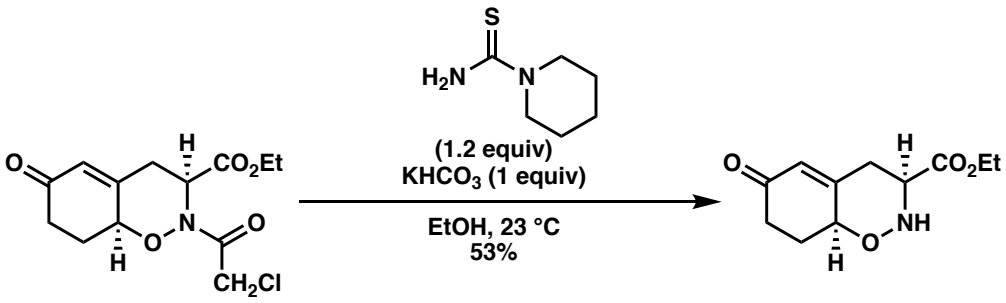

Add $KHCO_3$ (49.8mg, 0.497 mmol, 1.0 equiv) and XX (150 mg, 0.497 mmol, 1 equiv) to dried EtOH (5mL). Add N-piperidyl thiocarboxamide (86 mg, 0.597 mmol, 1.0 equiv) to) and sparge reaction with argon for five minutes. Stir at ambient temperature for 14 hours. Quench with pH=7

phosphate buffer:brine (1:1), Extract with EtOAc then four times with 10% *i*-PrOH CH_2Cl_2. Dry organic layer over Na_2SO_4, filter, and concentrate *in vacuo* to yield crude product. Purification by filtering through a florisil plug (75% EtOAc/Hexanes) followed by flash chromatography (silica, 2%NEt_3/5%EtOAc/50%CH_2Cl_2/Hexanes) provided **397** as a pale brown oil with an intractable impurity (31 mg, 0.138mmol, ~53% yield).

^{1}H NMR (400 MHz, $CDCl_3$) δ 6.70 – 6.07 (m, 1H), 5.88 (dd, *J* = 2.7, 1.4 Hz, 1H), 5.83 (s, 1H), 4.59 (dt, *J* = 10.8, 3.4 Hz, 1H), 4.21 (dddd, *J* = 17.9, 10.7, 7.2, 3.6 Hz, 2H), 3.81 (dd, *J* = 6.2, 1.9 Hz, 1H), 3.74 (s, 2H), 3.03 – 2.86 (m, 2H), 2.47 (dddd, *J* = 16.7, 4.3, 2.8, 1.2 Hz, 1H), 2.31 (ddd, *J* = 16.7, 14.8, 5.0 Hz, 1H), 2.20 (dtt, *J* = 12.9, 5.1, 2.5 Hz, 1H), 1.77 (dddd, *J* = 15.4, 12.6, 10.8, 4.6 Hz, 1H), 1.25 (td, *J* = 7.0, 2.3 Hz, 3H).

^{13}C NMR (101 MHz, CDCl3) δ 197.81, 171.20, 156.80, 126.16, 76.32, 61.73, 59.30, 35.42, 31.42, 26.80, 14.21.

FTIR (AT-IR) 3291.5, 2978.95, 2360.16, 1704.04, 1667.76, 1564.22, 1417.99, 1367.73, 1327.17, 1289.66, 1254.9, 1193.24, 1094.39, 1057.29, 1021.77, 981.68, 942.38, 888.76, 842.06, 772.03 cm^{-1}

HRMS (TOF, ES+) calc'd for $C_{11}H_{15}NO_4$ $[M+H]^+$ 226.1074, found 226.1073 (ppm=0.37)

Luche reduction of benzoylated bicyclic tetrahydro-1,2-oxazine

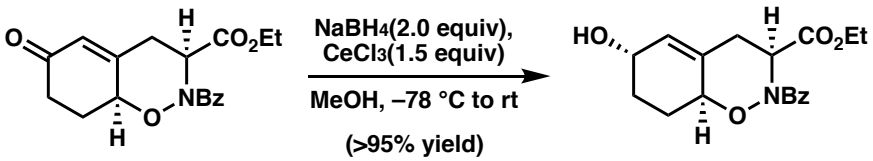

Cool solution of XX (50 mg, 0.152 mmol, 1.00 equiv) and $CeCl_3$•$7H_2O$ (84.8 mg, 0.228 mmol, 1.50 equiv) in MeOH (5.0 mL) to –78 °C. Add a solution of $NaBH_4$ (11.5 mg, 0.304 mg, 2.00 equiv) in MeOH (2.5 mL) dropwise. After addition allow reaction to warm to ambient temperature and quench with pH=7 buffer (5.0 mL). Extract crude mixture with three times EtOAc. Dry organic

phase over Na_2SO_4, filter, and concentrate *in vacuo* to yield XX (51 mg, 0.152 mmol, >95% yield) as a white solid.

^{1}H NMR (400 MHz, $CDCl_3$) δ 7.76 (d, *J* = 7.5 Hz, 2H), 7.54 – 7.45 (m, 1H), 7.45 – 7.35 (m, 2H), 5.74 (t, *J* = 1.8 Hz, 1H), 5.52 (s, 1H), 4.36 – 4.20 (m, 3H), 2.94 (d, *J* = 14.5 Hz, 1H), 2.75 (s, 1H), 2.06 (dd, *J* = 11.0, 5.0 Hz, 1H), 1.90 (s, 1H), 1.54 (d, *J* = 6.2 Hz, 1H), 1.41 – 1.31 (m, 1H), 1.28 (t, *J* = 7.1 Hz, 3H).

^{13}C NMR (101 MHz, $CDCl_3$) 169.75, 168.75, 132.91, 132.12, 131.20, 130.52, 128.84, 127.84, 79.78, 66.61, 64.17, 61.74, 55.12, 31.28, 30.14, 24.79, 14.20

FTIR (AT-IR): 3420.19, 2948.51, 2359.38, 2340.25, 1739.06, 1652.65, 1600.91, 1576.59, 1447.96, 1405.11, 1367.49, 1331.48, 1267.29, 1193.98, 1147.61, 1029.11, 917.95, 866.62, 788.7, 706.33, 667.96, 617.29 cm^{-1}

HRMS (TOF, ES+) calc'd for $C_{18}H_{21}NO_5$ $[M+H]^+$ 332.1492, found 332.1493 (ppm=-0.15)

Diastereoselective epoxidation of benzoylated bicyclic tetrahydro-1,2-oxazine

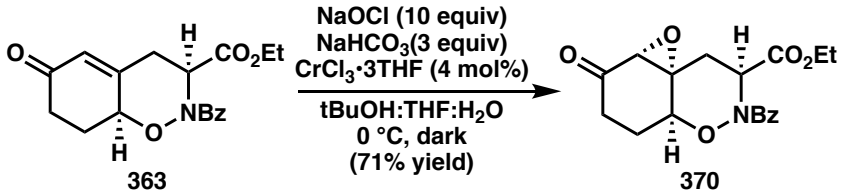

Substrate **363** (726.8mg, 2.207 mmol, 1 equiv) was dissolved in THF (37 mL) and pH=7 phosphate buffer (11 mL), reaction is kept dark, cooled to 0 °C. Cannulate suspension of $CrCl_3$•3THF (33mg, 0.088 mmol, 0.04 equiv) and $NaHCO_3$ (556 mg, 6.620 mmol, 3.0 equiv) in THF (74 mL) and H_2O (33 mL) dropwise. After 75 minutes, reaction is complete. Add 0.20M sodium thiosulfate and pH=7 phosphate buffer, Extract with CH_2Cl_2 3x (note: an emulsion forms, allow to settle). Wash organic layer with brine. Dry organics over Na_2SO_4 filter and concentrate. Separate crude material

on florisil (35g) with a gradient 20–50% EtOAc in Hexanes to provide **370** (540.7 mg, 1.56 mmol, 71% yield) as a white solid

^{1}H NMR (500 MHz, $CDCl_3$) δ 7.74 (d, *J* = 7.6 Hz, 2H), 7.55 – 7.49 (m, 1H), 7.48 – 7.40 (m, 2H), 5.68 (s, 1H), 4.36 (s, 1H), 3.30 (s, 1H), 2.62 (dd, *J* = 13.5, 6.1 Hz, 1H), 2.36 (dt, *J* = 17.3, 5.2 Hz, 1H), 2.22 (dd, *J* = 20.4, 15.0 Hz, 2H), 2.11 (d, *J* = 15.4 Hz, 1H), 1.79 (s, 1H), 1.28 (t, *J* = 7.2 Hz, 3H).

^{13}C NMR (126 MHz, $CDCl_3$) δ 202.53, 170.07, 168.33, 131.70, 128.81, 128.17, 78.81, 62.40, 60.80, 60.30, 55.39, 31.71, 30.86, 22.01, 14.29.

FTIR(AT-IR) 2979.80, 2359.60, 1716.02, 1656.84, 1578.52, 1447.13, 1389.33, 1366.88, 1309.09, 1257.56, 1178.77, 1092.65, 1026.42, 974.69, 920.18, 870.32, 788.06, 748.64, 707.41 cm^{-1}

HRMS (TOF, ES+) calc'd for $C_{18}H_{19}NO_6$ $[M+H]^+$ 346.1285, found 346.1291 (ppm=–1.69)

Ref NC-VI-225

Diastereoselective 1,2-reduction of tetrahydro-1,2-oxazine epoxy ketone

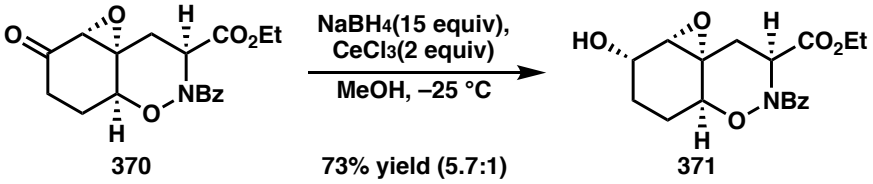

To a solution of **370** (4.1 mg, 0.0119 mmol, 1.0 equiv) and $CeCl_3$•$7H_2O$ (10.5 mg, 0.028 mmol, 2.0 equiv) in MeOH (0.8 mL) was brought to –25 °C, stir 5 minutes. Add $NaBH_4$ (6.9 mg, 0.182 mmol, 15.0 equiv) in MeOH (0.4 mL) and allow mixture to slowly warm. Reaction complete at –20 °C, quench with DI H_2O (0.8 mL). Extract three times with Et_2O (3×2.0 mL). Wash combined organics with brine and dry over Na_2SO_4, filter, and concentrate to yield crude product . Purify by

flash chromatography (silica, 50%EtOAc/Hexanes) to yield **371** (3.0 mg, 0.0086 mmol, 73% yield) as a white solid.

^{1}H NMR (400 MHz, $CDCl_3$) δ 7.75 (d, *J* = 7.6 Hz, 2H), 7.55 – 7.46 (m, 1H), 7.46 – 7.38 (m, 2H), 5.54 (s, 1H), 4.38 – 4.23 (m, 2H), 4.14 – 4.05 (m, 1H), 3.94 (dt, *J* = 8.7, 5.7 Hz, 1H), 3.20 (s, 1H), 2.51 (dd, *J* = 13.5, 6.2 Hz, 1H), 2.12 (dd, *J* = 13.5, 2.3 Hz, 1H), 1.86 (d, *J* = 6.3 Hz, 1H), 1.72 – 1.63 (m, 1H), 1.49 (s, 1H), 1.46 – 1.36 (m, 1H), 1.33 (t, *J* = 7.1 Hz, 3H).

^{13}C NMR (101 MHz, $CDCl_3$) δ 169.86, 169.01, 132.70, 131.52, 128.90, 128.09, 78.98, 65.86, 65.00, 62.27, 56.12, 55.46, 31.01, 25.09, 20.81, 14.36.

FTIR (AT-IR) 3433.47, 2932.85, 1736.83, 1644.41, 1577.8, 1447.82, 1391.49, 1367.35, 1310.52, 1234.61, 1193.83, 1082.95, 1018.30, 918.35, 893.00, 871.28, 788.07, 707.48 cm^{-1}

HRMS (TOF, ES+) calc'd for $C_{18}H_{21}NO_6$ $[M+H]^+$ 348.1442, found 348.1438 (ppm=1.05)

Wharton rearrangement of tetrahydro-1,2-oxazine epoxy ketone

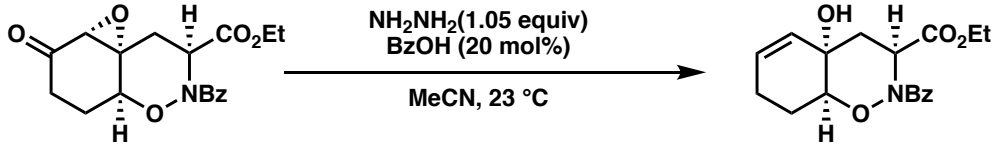

370 **(91% yield)** **373**

To a solution **370** (20 mg, 0.0579 mmol, 1 equiv) and benzoic acid (1.4 mg, 0.116 mmol, 0.20 equiv) in MeCN(0.75 mL) add a solution of NH_2NH_2 (2.0 mg, 0.0608 mmol, 1.05 equiv) in MeCN(0.35 mL) stir at ambient temperature for 3h. Dilute in eluent solution (5% NEt_3/45%EtOAc/50% Hexanes). Purification by elution through a NEt_3-neutralized florisil plug to yield the **373** (17.5 mg, 0.0528 mmol, 91% yield)

^{1}H NMR (500 MHz, $CDCl_3$) δ 7.73 (s, 2H), 7.50 – 7.44 (m, 1H), 7.43 – 7.37 (m, 2H), 5.91 (ddd, J = 9.9, 5.0, 2.2 Hz, 1H), 5.54 (ddt, J = 10.0, 3.4, 1.6 Hz, 1H), 5.42 (s, 1H), 4.24 – 4.12 (m, 2H),

3.93 (s, 1H), 2.62 (d, J = 13.5 Hz, 1H), 2.19 (dd, J = 13.2, 6.5 Hz, 1H), 2.08 (d, J = 18.9 Hz, 1H), 1.94 (d, J = 3.0 Hz, 1H), 1.89 (d, J = 14.7 Hz, 2H), 1.71 (s, 1H), 1.26 (t, J = 7.1 Hz, 3H).

^{13}C NMR (126 MHz, $CDCl_3$) δ 169.89, 168.76, 133.17, 132.90, 131.18, 128.86, 128.40, 127.91, 82.54, 64.29, 61.68, 53.74, 36.88, 21.64, 20.46, 14.26.

FTIR (AT-IR) 3408.37, 2932.03, 1732.70, 1633.99, 1577.31, 1447.64, 1402.33, 1367.67, 1316.25, 1228.24, 1188.30, 1082.79, 1030.05, 995.14, 921.35, 871.17, 780.89, 732.50, 707.45, 667.99 cm^{-1}

HRMS (TOF, ES+) calc'd for $C_{18}H_{21}NO_5$ $[M+H]^+$ 332.1492, found 332.1487 (ppm=1.65)

Allylic bromination and halide displacement of tertiary allylic alcohol

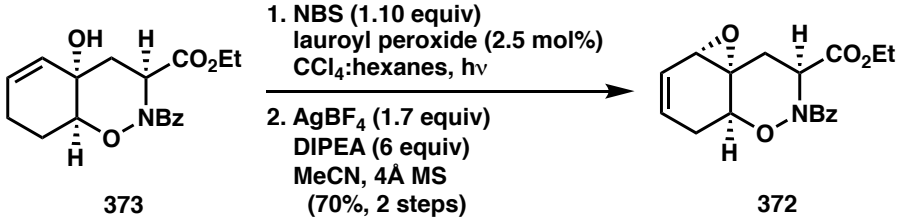

373 **372**

Suspend **373** (127.1 mg, 0.383 mmol, 1.0 equiv), NBS (75.1 mg, 0.422 mmol, 1.10 equiv), and lauroyl peroxide (3.0 mg, 0.0077 mmol, 0.02 equiv) in CCl_4 (9.6 mL). Wash down sides of flask with hexanes (3 mL). Stir under mercury floodlamp illumination with fan cooling for one hour. Dilute mixture with 10% EtOAc/Hexanes (20 mL) and filter through celite. Vacuum transfer solvent mixture then azeotrope the resulting crude mixture from toluene to yield a mixture of allylic bromination products and trace starting material as a pale yellow foam. Suspend the crude mixture in MeCN (15 mL). Add DIPEA (0.27 mL, 198 mg, 1.53 mmol, 4.0 equiv) then $AgBF_4$ (112 mg, 0.421 equiv, 1.10 equiv) as a solution in MeCN (0.7 mL). Add 4 beads of activated 4Å MS. Stir in the dark at ambient temperature for 9 hours. Add additional $AgBF_4$ (14.9 mg, 0.077 mmol, 0.20 equiv) in MeCN (0.1 mL) and DIPEA (0.14mL, 99 mg, 0.76 mmol, 2.0 equiv) and

continue stirring 9h30m. Dilute in 20% EtOAc/Hexanes (20 mL) and filter through celite. Add NEt_3 (1 mL) and concentrate crude on celite. Purify by flash chromatography (fluorosil, 0→60% EtOAc/Hexanes) to yield **372** (88.1 mg, 0.268 mmol, 70% yield) as a white solid.

^{1}H NMR (400 MHz, $CDCl_3$) δ 7.72 (d, *J* = 7.6 Hz, 2H), 7.49 (ddt, *J* = 8.4, 6.6, 1.4 Hz, 1H), 7.45 – 7.37 (m, 2H), 5.93 (dt, *J* = 9.9, 3.7 Hz, 1H), 5.78 – 5.59 (m, 2H), 4.33 – 4.28 (m, 1H), 4.25 (q, *J* = 7.1 Hz, 2H), 3.36 – 3.27 (m, 1H), 2.61 (dd, *J* = 13.3, 6.2 Hz, 1H), 2.43 – 2.30 (m, 1H), 2.26 (d, *J* = 13.3 Hz, 1H), 2.17 – 2.01 (m, 1H), 1.28 (t, *J* = 7.1 Hz, 3H).

^{13}C NMR (126 MHz, $CDCl_3$) δ 170.03, 168.86, 132.72, 131.43, 129.10, 128.85, 127.98, 122.17, 79.33, 62.12, 57.05, 55.25, 54.63, 31.66, 27.13, 14.32.

FTIR (AT-IR) 2981.11, 2361.34, 1736.53, 1655.94, 1578.36, 1447.47, 1388.17, 1317.21, 1274.26, 1227.59, 1185.7, 1030.03, 926.32, 882.31, 787.32, 742.03, 708.43, 667.92 cm^{-1}

HRMS (TOF, ES+) calc'd for $C_{18}H_{19}NO_5$ $[M+H]^+$ 330.1336, found 330.1339 (ppm=–0.91)

Desaturation of tetrahydro-1,2-oxazine epoxy ketone

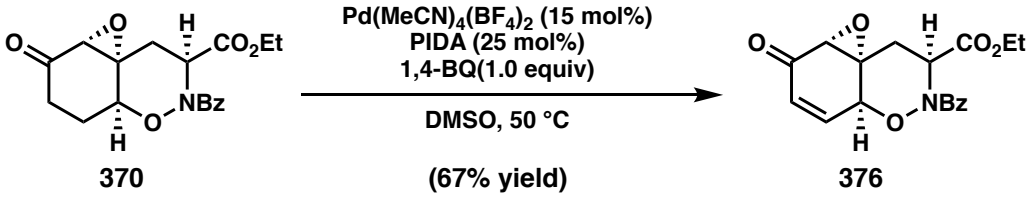

To a solution of substrate **370** (1.688 g, 4.89 mmol, 1.0 equiv) in DMSO(0.15M, 32.5 mL) add 1,4-benzoquinone (660 mg, 6.11 mmol, 1.25 equiv), $Pd(MeCN)_4(BF)_4$ (325.7 mg, 0.733 mmol, 0.15 equiv), and PIDA(394 mg, 1.22 mmol, 0.25 equiv). Heat to 50 °C, stir 96h. Cool to ambient temperature. Add 75 mL $NaHCO_3$(aq), extract 4x175 mL EtOAc. Wash organic layer with 40 mL brine. Dry organic layer with Na_2SO_4, filter, and concentrate. Purify by flash chromatography (silica 175 g, 15%EtOAc/40%CH_2Cl_2/Hexanes) to yield **376** (1.12g, 3.26 mmol, 67% yield).

^{1}H NMR (400 MHz, $CDCl_3$) δ 7.79 – 7.69 (m, 2H), 7.58 – 7.50 (m, 1H), 7.49 – 7.41 (m, 2H), 6.30 (s, 1H), 6.08 (dt, *J* = 10.6, 1.4 Hz, 1H), 5.65 (s, 1H), 4.72 (s, 1H), 4.34 – 4.12 (m, 3H), 3.53 (t, *J* = 1.6 Hz, 1H), 2.70 (dd, *J* = 13.9, 6.2 Hz, 1H), 2.28 (d, *J* = 14.0 Hz, 1H), 1.27 (t, *J* = 7.1 Hz, 4H).

^{13}C NMR (101 MHz, $CDCl_3$) δ 192.45, 170.22, 168.04, 136.07, 132.22, 131.90, 130.64, 128.71, 128.27, 76.11, 62.50, 60.42, 59.24, 55.60, 29.61, 14.19.

FTIR (AT-IR) 2982.21, 1737.29, 1690.76, 1661.42, 1600.80, 1579.13, 1447.34, 1390.80, 1365.58, 1334.93, 1306.37, 1266.83, 1226.57, 1187.35, 1026.36, 947.14, 910.44, 859.39, 826.78, 780.45, 729.61, 708.37, 647.95 cm^{-1}

HRMS (TOF, ES+) calc'd for $C_{18}H_{17}NO_6$ $[M+H]^+$ 344.1129, found 344.1127 (ppm=0.48)

Ref NC-V-003, NC-V-211

Unselective Luche reduction of tetrahydro-1,2-oxazine epoxy enone

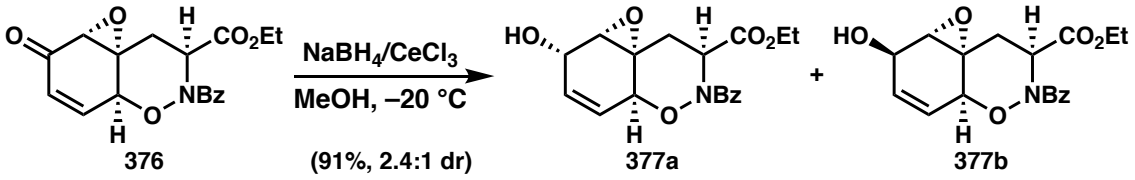

Cool **368** (140 mg, 0.408mg, 1.0 equiv) and $CeCl_3$•$7H_2O$ (304mg, 0.816 mmol, 2.0 equiv) in MeOH (6.7 mL) to –20 °C. Add a solution of $NaBH_4$ (30.9 mg, 0.816 mmol, 2.0 equiv) and stir for 30 minutes before raising the temperature to 0 °C. Add $NaHCO_{3(aq)}$ (9 mL). Extract with EtOAc four times. Wash combined organics with brine. Dry over Na_2SO_4, filter, and concentrate. Purification by flash chromatography (fine silica, 20% PhMe/40% Acetone/Hexanes) provided **369a** (63.3 mg, 0.183 mmol, 45% yield) and some mixed fractions which were subsequently purified on normal phase prep-HPLC (45% EtOAc/Hexanes) to provide additional **369a** (27.0mg, 0.078 mmol, 19% yield) and **369b** (38.4 mg, 0.111 mmol, 27% yield).

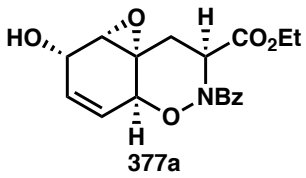

377a

369a(f2): ^{1}H NMR (500 MHz, $CDCl_3$) δ 7.74 (d, *J* = 7.6 Hz, 2H), 7.54 – 7.48 (m, 1H), 7.46 – 7.39 (m, 2H), 5.79 (d, *J* = 10.3 Hz, 1H), 5.66 (s, 1H), 5.38 (s, 1H), 4.47 (s, 1H), 4.40 (s, 1H), 4.32 – 4.18 (m, 2H), 3.59 (t, *J* = 2.0 Hz, 1H), 2.66 – 2.53 (m, 1H), 2.24 (d, *J* = 13.7 Hz, 1H), 2.08 (s, 1H), 1.64 (s, 1H), 1.29 (t, *J* = 7.1 Hz, 3H).

^{13}C NMR (126 MHz, $CDCl_3$) δ 170.09, 168.74, 133.50, 131.72, 128.88, 128.16, 119.84, 76.90, 65.00, 62.29, 62.01, 56.89, 55.35, 30.65, 14.31.

FTIR (AT-IR) 3515.22, 2359.36, 2340.32, 1713.29, 1651.27, 1448.14, 1400.82, 1371.84, 1300.75, 1271.34, 1237.79, 1198.4, 1086.26, 1044.77, 1015.91, 974.42, 917.96, 850.56, 808.77, 791.48, 707.66, 668.00, 627.70 cm^{-1}

HRMS (TOF, ES+) calc'd for $C_{18}H_{19}NO_6$ $[M+H]^+$ 346.1285, found 346.1281 (ppm=1.20)

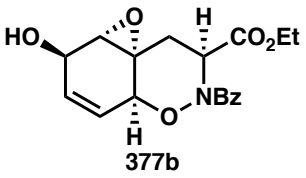

377b

369b(f1): ^{1}H NMR (500 MHz, $CDCl_3$) δ 7.74 (d, *J* = 7.6 Hz, 2H), 7.55 – 7.47 (m, 1H), 7.46 – 7.40 (m, 2H), 5.96 (ddd, *J* = 9.6, 4.6, 2.0 Hz, 1H), 5.55 (d, *J* = 74.0 Hz, 2H), 4.50 (s, 1H), 4.41 (s, 1H), 4.34 – 4.19 (m, 2H), 3.37 (q, *J* = 1.6 Hz, 1H), 2.60 (dd, *J* = 13.6, 6.1 Hz, 1H), 2.16 (dd, *J* = 13.7, 1.9 Hz, 1H), 1.93 (s, 1H), 1.31 (td, *J* = 7.1, 0.9 Hz, 3H).

^{13}C NMR (126 MHz, $CDCl_3$) δ 170.24, 168.80, 131.97, 131.75, 128.90, 128.18, 120.92, 76.79, 63.26, 62.39, 60.50, 55.64, 53.93, 30.96, 14.32.

FTIR (AT-IR) 3506.46, 2925.60, 2359.53, 2340.3, 1733.94, 1653.54, 1578.26, 1447.05, 1367.84, 1298.39, 1233.21, 1189.33, 1025.82, 905.79, 867.34, 831.29, 790.72, 768.16, 730.21, 706.66, 667.91 cm^{-1}

HRMS (TOF, ES+) calc'd for $C_{18}H_{19}NO_6$ $[M+H]^+$ 346.1285, found 346.1275 (ppm=1.20)

Diastereoselective epoxidation of tetrahydro-1,2-oxazine epoxy enone

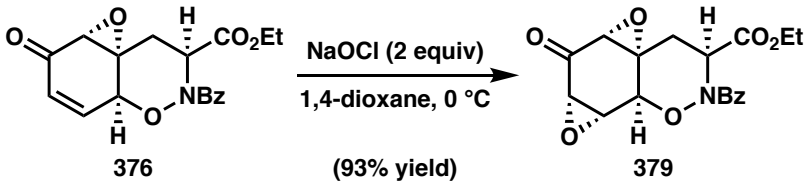

376 (93% yield) 379

To chill a solution of substrate (1.1207g, 3.26 mmol, 1 equiv) in wet dioxane (13 mL dioxane, 0.1mL DI H_2O) to 0 °C. Add NaOCl (12.5 wt% in H_2O) (3.62mL, 4.37g (243 mg NaOCl), 2.25 equiv) Stir 5h at 0 °C. Dilute in 1:1 brine/DI H_2O (65 mL). Extract with EtOAc 3x75mL. Dry organics over Na_2SO_4. Filter and concentrate. Take up crude in benzene, concentrate; take up again in hexanes and re-concentrate. Yields **371** (1.09g, 93% yield) as a white foam. **Note**: **371** was not amenable to chromatographic purification due to instability and was used with no further purification.

^{1}H NMR (400 MHz, $CDCl_3$) δ 7.78 – 7.69 (m, 2H), 7.56 – 7.49 (m, 1H), 7.49 – 7.40 (m, 2H), 5.53 (s, 0H), 4.74 (s, 1H), 3.43 (d, J = 1.8 Hz, 1H), 3.40 (s, 1H), 3.39 – 3.33 (m, 1H), 2.63 (dd, J = 14.0, 6.1 Hz, 1H), 2.11 (dd, J = 14.1, 1.8 Hz, 1H), 1.28 (t, J = 7.1 Hz, 4H).

^{13}C NMR (101 MHz, $CDCl_3$) δ 197.03, 170.44, 167.70, 132.10, 131.96, 128.50, 128.32, 75.09, 63.75, 62.60, 61.63, 56.77, 55.37, 54.25, 31.10, 14.14.

FTIR (AT-IR) 1736.36, 1707.34, 1666.01, 1447.25, 1368.08, 1303.87, 1226.04, 1185.33, 1022.17, 947.87, 912.99, 868.45, 788.53, 708.45 cm^{-1}

HRMS (TOF, ES+) calc'd for $C_{18}H_{17}NO_7$ $[M+H]^+$ 360.1078, found 360.1078 (ppm=–0.06)

Diastereoselective dihydroxylation of tetrahydro-1,2-oxazine epoxy enone

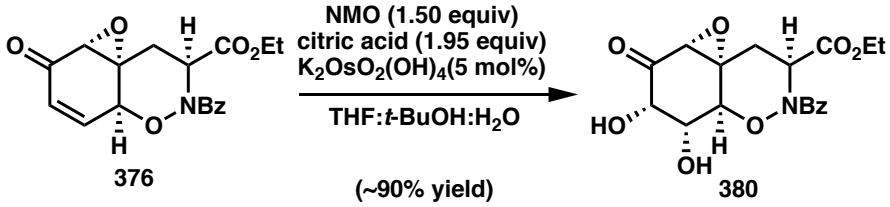

Dissolve $K_2OsO_2(OH)_4$ (1.5 mg, 0.00407 mmol, 0.05 equiv), NMO (14.1 mg, 0.120 mmol, 1.5 equiv), and citric acid monohydrate (33.0 mg, 0.157 mmol, 1.95 equiv) in DI H_2O (1.5 mL). Add *t*-BuOH (1.5 mL) to the aqueous solution to generate a pale a pale yellow solution. Add the osmium solution to **368** (27.6 mg, 0.0804 mmol, 1.0 equiv) in THF (0.9 mL). Sparge reaction mixture for 10 minutes and continue stirring under argon at ambient temperature for 2h20m. Add pH=7 phosphate buffer (1 mL) and brine (2 mL) and extract six times with EtOAc (6×3 mL). Dry combined organics over Na_2SO_4, filter, and concentrate to yield crude product. Take up crude material in MeCN (3 mL) and wash twice with pentanes (2×4 mL). Concentrate to yield **372** with trace impurities (27.6 mg, 0.0731 mmol, ~90% yield) as a pale yellow oil. **Note**: **372** was not amenable to chromatographic purification due to instability and was used with no further purification.

^{1}H NMR (400 MHz, $CDCl_3$) δ 7.77 – 7.66 (m, 2H), 7.59 – 7.50 (m, 1H), 7.49 – 7.43 (m, 2H), 5.93 – 5.30 (m, 1H), 4.51 (s, 1H), 4.29 – 4.19 (m, 2H), 4.12 (d, J = 3.7 Hz, 1H), 4.04 (s, 1H), 3.51 (d, J = 1.2 Hz, 1H), 2.63 (dd, J = 13.6, 6.0 Hz, 1H), 2.19 (dd, J = 13.7, 2.0 Hz, 1H), 1.28 (t, J = 7.1 Hz, 3H).

^{13}C NMR (101 MHz, $CDCl_3$) δ 170.29, 168.41, 132.16, 132.00, 128.78, 128.42, 79.78, 74.77, 69.03, 69.01, 62.57, 58.35, 32.02, 30.19, 29.16, 22.83, 22.02, 14.35, 14.31, 14.27.

FTIR (AT-IR) 3447.39, 2981.48, 2361.33, 2341.29, 1734.63, 1653.82, 1600.95, 1578.07, 1447.91, 1390.57, 1368.42, 1308.69, 1227.00, 1191.68, 1121.21, 1060.54, 1025.05, 954.00, 910.67, 881.89, 861.12, 787.53, 728.04, 709.00, 667.94, 647.54 cm^{-1}

HRMS (TOF, ES+) calc'd for $C_{18}H_{19}NO_8$ $[M+H]^+$ 378.1183, found 377.1174 (ppm=2.49)

Wharton rearrangement of tetrahydro-1,2-oxazine *bis*-epoxy ketone

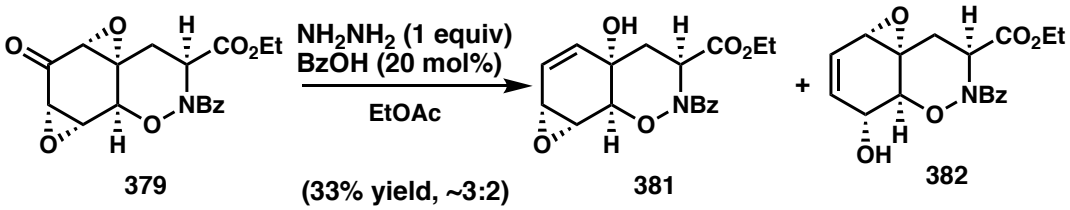

Cool to solution of benzoic acid (6.8 mg, 0.057 mmol, 0.20 equiv) in EtOAc (2mL) to 10 °C. Concurrently, add solutions of NH_2NH_2 (8.9 mg, 8.7µL, 0.278 mmol) in EtOAc (5 mL) and **379** (100 mg, 0.278 mmol) in EtOAc (5 mL) dropwise via syringes to the cooled reaction flask over 30 minutes. Rinse substrate syringe with EtOAc (1 mL). Bring reaction to ambient temperature and stir five minutes before adding triethylamine (1 mL). Filter through a neutralized florisil plug and rinse plug with (5% NEt_3/EtOAc). Purification of that crude mixture by flash chromatography (florisil 5.0g, 5% NEt_3/50%EtOAc/Hexanes) to yield a 3:2 mixture of **381** and **382** (31.4mg, 0.091mmol, 33% yield) which were carried forward as a mixture. **382** could be isolated cleanly for characterization by flash chromatography (40%EtOAc/Hexanes).

382: ^{1}H NMR (400 MHz, $CDCl_3$) δ 7.72 (d, J = 7.7 Hz, 2H), 7.56 – 7.47 (m, 1H), 7.46 – 7.36 (m, 2H), 6.19 (dd, J = 9.8, 4.0 Hz, 1H), 6.13 – 6.02 (m, 1H), 5.66 (s, 1H), 4.30 (s, 1H), 4.24 (q, J = 7.1 Hz, 2H), 3.92 (s, 1H), 3.41 (dt, J = 4.1, 1.3 Hz, 1H), 2.69 (dd, J = 13.3, 6.2 Hz, 1H), 2.39 – 2.22 (m, 1H), 1.73 – 1.62 (m, 1H), 1.27 (t, J = 7.1 Hz, 3H).

^{13}C NMR (101 MHz, $CDCl_3$) δ 170.16, 168.79, 136.71, 133.28, 131.70, 128.76, 128.19, 126.98, 81.68, 64.57, 62.28, 59.83, 55.26, 54.45, 31.04, 14.34.

FTIR (AT-IR) 3457.65, 2981.45, 2359.53, 2340.24, 1739.24, 1652.54, 1576.29, 1447.92, 1394.23, 1317.61, 1274.82, 1267.49, 1230.14, 1189.56, 1028.04, 954.06, 867.43, 809.44, 788.73, 763.78, 749.59, 708.28, 667.92 cm^{-1}

HRMS (TOF, ES+) alc'd for $C_{18}H_{19}NO_6$ $[M+H]^+$ 346.1285, found 346.1282 (ppm=0.91)

Wharton rearrangement of tetrahydro-1,2-oxazine epoxy keto-diol

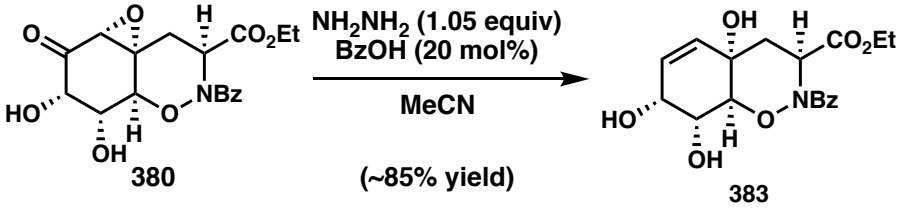

Add **380** (39 mg, 0.103 mmol, 1.0 equiv) and BzOH (2.5 mg, 0.021 mmol, 0.20 equiv) in MeCN (4.2 mL). NH_2NH_2 (3.5 mg, 3.4 μL, 0.109 mmol, 1.05 equiv) in MeCN (1.0 mL). Stir 20 minutes at ambient temperature and then add pH=7 phosphate buffer. Extract three with EtOAc. Wash organic phase with brine. Dry over Na_2SO_4, filter, and concentrate to yield product (33 mg, 0.090 mmol, ~85% yield).

^{1}H NMR (400 MHz, $CDCl_3$) δ 7.68 (s, 2H), 7.54 – 7.46 (m, 1H), 7.42 (ddt, J = 8.4, 6.8, 1.2 Hz, 2H), 5.64 (s, 2H), 5.33 (d, J = 23.4 Hz, 1H), 4.27 (s, 1H), 4.19 (qd, J = 7.1, 4.2 Hz, 2H), 4.02 (s, 1H), 3.56 (s, 1H), 3.24 (d, J = 83.5 Hz, 1H), 2.59 (s, 1H), 2.24 (dd, J = 13.6, 6.7 Hz, 1H), 1.27 (t, J = 7.1 Hz, 3H).

^{13}C NMR (101 MHz, $CDCl_3$) δ 170.32, 168.57, 132.88, 131.56, 131.38, 129.24, 128.51, 128.26, 82.87, 77.36, 68.54, 65.47, 61.96, 35.60, 14.29.

FTIR (AT-IR) 3387.29, 2930.19, 1735.10, 1636.40, 1576.98, 1448.32, 1400.27, 1368.76, 1323.20, 1226.31, 1193.94, 1129.64, 1066.18, 1022.40, 917.90, 833.76, 787.43, 707.14, 678.99, 645.09 cm^{-1}

HRMS (TOF, ES+) calc'd for $C_{18}H_{21}NO_7$ $[M+H]^+$ 364.1391, found 364.1390 (ppm=0.22)

Convergent silylation of Wharton rearrangement products

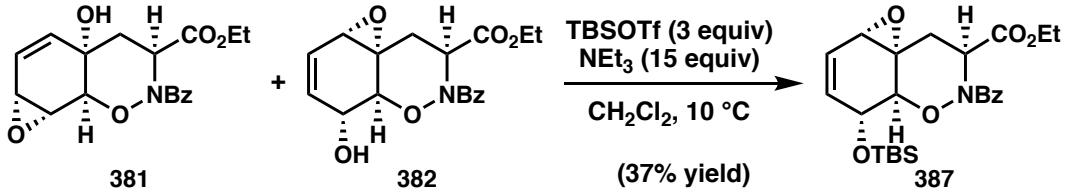

Cool solution of **373** and **374** (31.6 mg, 0.0915 mmol) to –5 °C. Add triethylamine (93mg, 128 μL, 0.915 mmol, 10 equiv) followed by TBSOTf (48.4 mg, 42 μL, 0.183 mmol, 2.0 equiv). Warm to 10 °C and stir 25 minutes. Add additional triethylamine (44 mg, 60 μL, 0.430 mmol, 4.7 equiv) followed by TBSOTf (23 mg, 20 μL, 0.087 mmol, 0.95 equiv). Quench excess TBSOTf with *i*-PrOH (25 μL) and stir at ambient temperature for 5 minutes. Concentrate crude reaction and purify by flash chromatography (florisil 3.6g, 2% NEt_3/5→15%EtOAc/Hexanes) provides XX (9.6mg, 38% yield)

^{1}H NMR (400 MHz, $CDCl_3$) δ 7.78 – 7.68 (m, 2H), 7.48 (d, *J* = 1.6 Hz, 1H), 7.44 – 7.38 (m, 2H), 6.04 (ddd, *J* = 10.0, 3.6, 1.3 Hz, 1H), 5.77 (ddd, *J* = 10.0, 4.1, 1.1 Hz, 1H), 5.46 (s, 1H), 4.23 (d, *J* = 5.7 Hz, 2H), 4.16 (s, 1H), 4.08 (d, *J* = 3.8 Hz, 1H), 3.24 (dt, *J* = 3.6, 1.0 Hz, 1H), 2.45 (dd, *J* = 13.8, 5.1 Hz, 2H), 1.29 (t, *J* = 7.1 Hz, 3H), 0.78 (s, 9H), -0.10 (d, *J* = 34.0 Hz, 6H).

^{13}C NMR (101 MHz, $CDCl_3$) δ 169.81, 169.07, 134.70, 132.72, 131.30, 128.61, 128.04, 124.94, 84.87, 66.65, 61.89, 58.77, 52.47, 30.67, 29.69, 25.75, 18.04, 14.19, -4.88, -4.92.

FTIR (AT-IR) 2954.10, 2928.42, 2856.26, 2361.06, 2340.36, 1739.52, 1652.91, 1471.97, 1447.94, 1389.33, 1315.95, 1253.02, 1226.52, 1188.91, 1094.5, 1027.62, 915.93, 878.84, 837.35, 814.81, 778.37, 746.41, 706.37, 668.03, 654.57, 648.90, 632.41, 617.5, 608.61 cm^{-1}

HRMS (TOF, ES+) calc'd for $C_{24}H_{33}NO_6Si$ $[M+H]^+$ 460.2150, found 460.2146 (ppm=0.85)

1,2-reduction of tetrahydro-1,2-oxazine *bis*-epoxy ketone

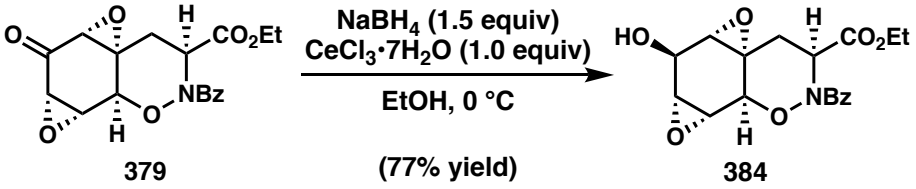

Chill a solution of XX (74 mg, 0.206 mmol, 1.0 equiv) in EtOH (0.3M, 6.9 ml) to 0 °C. Add $CeCl_3$•$7H_2O$ (76.7 mg, 0.206 mmol, 1.0 equiv), stir two minutes. Add $NaBH_4$ (11.7 mg,) as a single portion stir at 0 °C for 30 minutes. Add EtOAc (5 mL) and brine (5mL), stir five minutes. Extract the crude mixture with EtOAc (3×5 mL). Dry over Na_2SO_4 and concentrate. Reconcentrate crude residue with benzene. Purify on by flash chromatography (florisil, 20–100% EtOAc/Hexanes) provides **377** as a white solid (57.5mg, 0.159 mmol, 77% yield).

^{1}H NMR (400 MHz, $CDCl_3$) δ 7.75 (dt, *J* = 7.0, 1.4 Hz, 2H), 7.58 – 7.50 (m, 1H), 7.49 – 7.42 (m, 2H), 5.52 (s, 1H), 4.55 (d, *J* = 10.1 Hz, 2H), 4.28 (qq, *J* = 7.3, 3.6 Hz, 2H), 3.22 (q, *J* = 1.6, 1.0 Hz, 1H), 3.21 – 3.15 (m, 1H), 2.98 (s, 1H), 2.54 (dd, *J* = 13.8, 6.0 Hz, 1H), 2.41 (d, *J* = 9.3 Hz, 1H), 1.99 (dd, *J* = 13.8, 1.9 Hz, 1H), 1.33 (t, *J* = 7.1 Hz, 3H).

^{13}C NMR (101 MHz, $CDCl_3$) δ 170.51, 168.84, 132.27, 131.96, 128.69, 128.31, 75.25, 62.54, 61.54, 60.48, 55.63(br), 53.24, 52.37, 49.41, 31.36, 14.21.

FTIR (AT-IR) 3446.83, 2984.12, 2359.39, 2340.30, 1738.02, 1652.45, 1578.62, 1447.75, 1367.96, 1232.41, 1191.59, 1048.24, 1019.26, 953.47, 864.87, 825.47, 788.76, 709.54, 667.93

cm^{-1}

HRMS (TOF, ES+) calc'd for $C_{18}H_{17}NO_7$ $[M+H]^+$ 360.0078, found 360.0077 (ppm=0.22)

Recovery of *bis*-epoxy ketone through Stahl oxidation

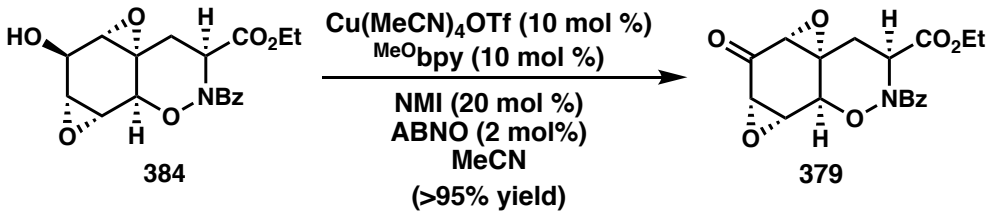

Dissolve substrate (41.6 mg, 0.115 mmol, 1.0 equiv) in wet MeCN (1.15 mL). Add $Cu(MeCN)_4OTf$ (4.4 mg, 0.0115 mmol, 0.10 equiv), 4,4'-methoxybipyridine (2.5 mg, 0.0115 mmol 0.10 equiv), ABNO (0.3mg, 0.0022 mmol 0.020 equiv) and NMI (1.9mg, 1.9 μL, 0.0229 mmol, 0.20 equiv). Stir in air 40 minutes. Dilute in pH=7 buffer, and extract crude mixture three times with EtOAc. Dry organic phase over Na_2SO_4, filter, and concentrate. Take up residue in PhMe and filter through celite to remove insoluble material. Concentrate to yield **379** (41.3 mg, 0.114 mmol, >95% yield) as a pale yellow tacky oil.

Schwartz reduction of *N*-benzoylated western fragment tetrahydro-1,2-oxazine

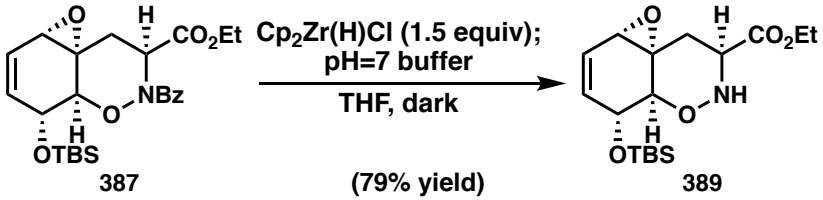

To a stirred suspension of $Cp_2Zr(H)Cl$ (12.4 mg, 0.0320 mmol, 1.5 equiv) in THF(0.15 mL) add substrate **380** (14.7 mg, 0.0320 mmol, 1.0 equiv) in a steady stream as a solution in THF (1.75 mL). Rinse substrate syringe with THF (3×0.15mL) Stir at ambient temperature for 10 minutes. Quench reaction with the rapid addition of a pH=7 phosphate buffer (0.50 mL). Extract aqueous

four times with EtOAc. Dry organics over Na_2SO_4. Filter and concentrate, purify crude product by flash chromatography (florisil 1.50 g, 10–60% EtOAc/Hexanes, +10% EtOAc/10 mL eluent). Concentrate and re–concentrate from dry toluene to yield **382** as a white solid (9.0 mg, 0.0253 mmol, 79% yield).

^{1}H NMR (400 MHz, $CDCl_3$) δ 6.41 (s, 1H), 6.06 (d, J = 3.8 Hz, 1H), 5.82 (dddd, J = 10.0, 5.0, 1.3, 0.7 Hz, 1H), 4.34 – 4.16 (m, 2H), 4.15 (dt, J = 1.7, 0.8 Hz, 1H), 4.13 (ddd, J = 5.0, 1.9, 0.8 Hz, 1H), 3.90 (ddd, J = 6.0, 2.8, 1.0 Hz, 1H), 3.21 (dt, J = 4.0, 1.2 Hz, 1H), 2.57 (dd, J = 13.4, 5.9 Hz, 1H), 2.12 (dt, J = 13.4, 2.3 Hz, 1H), 1.29 (t, J = 7.1 Hz, 3H), 0.89 (s, 9H), 0.09 (d, J = 8.4 Hz, 6H).

^{13}C NMR (126 MHz, $CDCl_3$) δ 171.70, 133.48, 125.45, 81.96, 67.70, 61.78, 59.88, 59.68, 53.79, 31.59, 26.08, 18.43, 14.41, -4.34.

FTIR (AT-IR) 2928.00, 2855.59, 2361.23, 2339.00, 1734.81, 1472.07, 1462.93, 1388.10, 1251.36, 1225.94, 1180.11, 1082.99, 1026.99, 1005.17, 931.05, 859.36, 836.96, 776.80, 739.28, 667.95 cm^{-1}

HRMS (TOF, ES+) calc'd for $C_{17}H_{29}NO_5Si$ $[M+H]^+$ 356.1888, found 356.1891 (ppm=-0.91)

***Ortho*-iodonation of MOM-protected phenol**

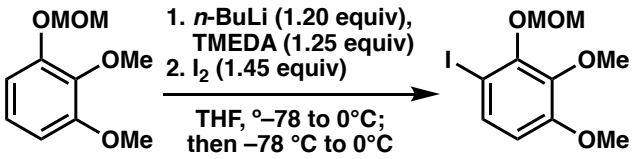

S2-10 **(64% yield)** **392b**

Cool a solution of **S2-10**[116] (2.51g, 12.64 mmol, 1.00 equiv) and TMEDA (1.84 g, 2.36 mL, 15.80 mmol, 1.25 equiv) in THF (45 mL) to –78 °C. Add freshly titrated n-BuLi (2.24 M in Hexanes, 6.77 mL, 15.17 mmol, 1.20 equiv). Stir at –78 °C for 10 minutes then warm to 0 °C and stir 2h.

Cool once more to –78 °C and cannulate I_2 (4.65g, 18.33 mmol, 1.45 equiv) as a solution in THF (65 mL) dropwise into the reaction mixture. After addition is complete, continue stirring at –78 °C for 2h. Raise temperature to 0 °C and stir 30 minutes. Quench mixture with $NaHCO_{3(aq)}$ (13 mL), stirring vigorously. Dilute with EtOAc (80 mL) wash organic layer with DI H_2O (50 mL) and twice with $Na_2S_2O_{3(sat)}$ (2×50 mL) then brine (40 mL). Dry organics over Na_2SO_4. Filter and concentrate, purify crude product by flash chromatography (silica, 125 g, 15% EtOAc/Hexanes) to yield pure **385b** (2.63g, 8.11 mmol, 64% yield) as a pale-yellow oil.

^{1}H NMR (500 MHz, $CDCl_3$) δ 7.41 (d, J = 8.8 Hz, 1H), 6.47 (d, J = 8.8 Hz, 1H), 5.17 (s, 2H), 3.82 (s, 3H), 3.80 (s, 3H), 3.64 (s, 3H).

^{13}C NMR (126 MHz, $CDCl_3$) δ 154.47, 150.39, 142.32, 133.11, 109.91, 99.29, 81.39, 60.87, 58.37, 56.16.

FTIR (AT-IR) 2935.62, 2833.84, 2361.14, 1571.01, 1474.8, 1447.25, 1434.1, 1421.14, 1389.3, 1288.37, 1218.22, 1156.21, 1083.61, 1063.49, 1002.39, 966.15, 905.55, 833.64, 792.64, 768.38, 694.05 cm^{-1}

HRMS (TOF, ES+) calc'd for $C_{10}H_{13}IO_4$ $[M+H]^+$ 324.9931, found 324.9924 (ppm=2.24)

Negishi cross-coupling of 384 with 2,3,4-trimethoxyiodobenzene

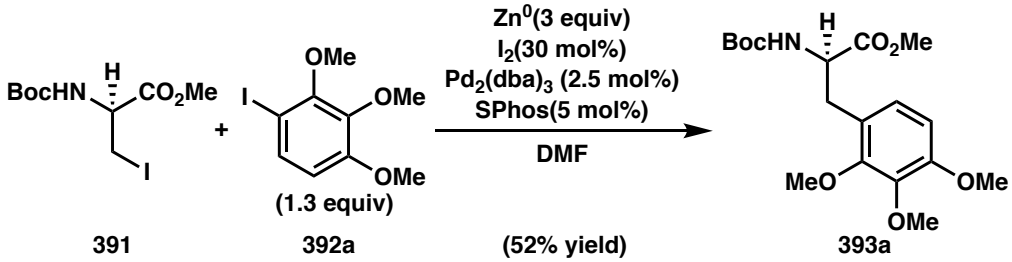

Suspend Zn^0 (596 mg, 9.12 mmol, 3.0 equiv) in DMF (3.0 mL) and add I_2 (116 mg, 0.46 mmol, 0.015 equiv) as a single portion. Stir at ambient temperature until solution is colorless. Add **384**

(1.00 g, 3.04 mmol, 1.0 equiv) followed by an additional portion of I_2 (116 mg, 0.46 mmol, 0.015 equiv). An exotherm is observed, stir 15 minutes or until cooled. Add $Pd_2(dba)_3$ (69.6 mg, 0.076 mmol, 0.025 equiv) and SPhos (62.4 mg, 0.15 mmol, 0.05 equiv) followed by **385a** (1.16g. 3.95 mmol, 1.3 equiv). Seal and stir at ambient temperature 48h. Purify by flash chromatography (silica, 5→50% EtOAc/PhMe) by directly applying the crude mixture to column to provide **386a** (589.5 mg, 1.60 mmol, 52% yield) as an orange viscous oil.

^{1}H NMR (400 MHz, $CDCl_3$) δ 6.77 (d, J = 8.5 Hz, 1H), 6.58 (d, J = 8.5 Hz, 1H), 5.25 (d, J = 7.9 Hz, 1H), 4.41 (td, J = 7.8, 5.6 Hz, 1H), 3.87 (s, 3H), 3.83 (s, 3H), 3.82 (s, 3H), 3.69 (s, 3H), 2.96 (qd, J = 13.7, 6.7 Hz, 2H), 1.36 (s, 9H).

^{13}C NMR (101 MHz, $CDCl_3$) δ 172.85, 155.33, 153.04, 152.23, 142.10, 125.04, 122.13, 107.26, 79.62, 60.89, 60.75, 56.02, 54.60, 52.20, 32.52, 28.35.

FTIR (AT-IR) 3365.29, 2936.72, 1744.06, 1712.45, 1602.02, 1494.22, 1467.17, 1435.51, 1417.74, 1391.30, 1365.18, 1276.05, 1199.34, 1162.53, 1096.71, 1045.69, 1014.85, 906.91, 855.78, 795.36, 730.34 cm^{-1}

HRMS (TOF, ES+) calc'd for $C_{10}H_{13}IO_4$ $[M+H]^+$ 370.1860, found 370.1862 (ppm=-0.46)

$[\alpha]_D^{23}$ +21.5° (*c* = 1.0, $CHCl_3$).

Negishi cross-coupling of 384 with 3,4-dimethoxy-2-(methoxymethoxy)iodobenzene

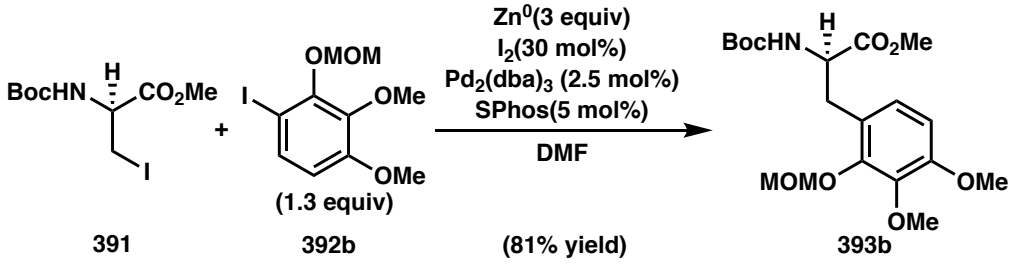

391 392b (81% yield) 393b

Suspend Zn^0 (1.396 mg, 21.36 mmol, 3.0 equiv) in DMF (5.9 mL) and add I_2 (271 mg, 1.07 mmol, 0.015 equiv) as a single portion. Stir at ambient temperature until solution is colorless. Add **384** (2.34 g, 7.12 mmol, 1.0 equiv) followed by an additional portion of I_2 (271 mg, 1.07 mmol, 0.015 equiv). An exotherm is observed, stir 15 minutes or until cooled. Add $Pd_2(dba)_3$ (163 mg, 0.178 mmol, 0.025 equiv) and SPhos (146 mg, 0.356 mmol, 0.05 equiv) followed by **385b** (3.00 g. 9.26 mmol, 1.3 equiv). Seal and stir at ambient temperature 24h. Purify by flash chromatography (silica, 10→15%EtOAc/20%CH_2Cl_2/Hexanes) by directly applying the crude mixture to column to provide impure product. Second purification with silica plug. Flush plug with 0→5%EtOAc/ CH_2Cl_2 to remove color impurities before flushing off the product with EtOAc. Provides 386b (2.44g (6 wt% biaryl), 5.74 mmol, 81% yield) as a thick oil with trace biaryl Wurtz coupling impurity (6 wt%).

^{1}H NMR (400 MHz, $CDCl_3$) δ 6.79 (d, J = 8.5 Hz, 1H), 6.58 (d, J = 8.6 Hz, 1H), 5.48 (d, J = 8.1 Hz, 1H), 5.10 (d, J = 1.0 Hz, 2H), 4.44 (td, J = 8.0, 5.9 Hz, 1H), 3.78 (s, 3H), 3.76 (s, 3H), 3.67 (s, 3H), 3.53 (s, 3H), 3.08 – 2.81 (m, 2H), 1.31 (s, 9H).

^{13}C NMR (101 MHz, $CDCl_3$) δ 172.94, 155.44, 152.90, 150.02, 141.58, 125.48, 125.04, 122.62, 107.81, 99.72, 79.51, 60.67, 57.53, 56.03, 54.60, 52.22, 32.29, 28.35.

FTIR (AT-IR) 3365.74, 2935.22, 2838.00, 1744.76, 1714.13, 1602.67, 1496.11, 1459.01, 1437.74, 1392.02, 1365.56, 1278.40, 1212.16, 1161.19, 1100.05, 1067.79, 983.03, 924.74, 795.66 cm^{-1}

HRMS (TOF, ES+) calc'd for $C_{10}H_{13}IO_4$ $[M+H]^+$ 400.1966, found 400.1972 (ppm=-1.52)

$[\alpha]_D^{23}$ +25.1° (*c* = 1.0, $CHCl_3$).

Saponification of 2,3,4-trimethoxyphenylalanine 386a

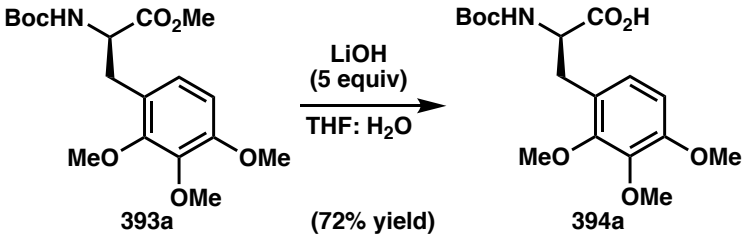

Chill **386a** (200 mg, 0.541 mmol, 1.0 equiv) in THF (3 mL) and H_2O (1.5 mL) to 0 °C. Add LiOH•H_2O (113.3mg, 2.70 mmol. 5 equiv) stir for 4h50m allowing the reaction to warm to ambient temperature. Add NaH_2PO_4 (373 mg) dissolved in DI H_2O (3 mL). Extract crude mixture twice with $CHCl_3$. Acidify aqueous layer to pH=5 with 1M $HCl_{(aq)}$ extract with $CHCl_3$ once. Further acidify the aqueous solution to pH=3 and extract twice with 10% *i*-PrOH/$CHCl_3$. Dry organics over Na_2SO_4, filter and concentrate to yield pure **387a** (137.7mg, 0.387 mmol, 72% yield) as a clear oil.

^{1}H NMR (400 MHz, $CDCl_3$) δ 6.85 (d, J = 8.5 Hz, 1H), 6.62 (d, J = 8.5 Hz, 1H), 5.44 (d, J = 7.1 Hz, 1H), 4.38 (d, J = 6.8 Hz, 1H), 3.90 (s, 3H), 3.86 (s, 3H), 3.84 (s, 3H), 3.23 – 2.79 (m, 2H), 1.38 (s, 9H).

^{13}C NMR (101 MHz, $CDCl_3$) δ 176.32, 156.23, 153.21, 152.15, 142.13, 125.25, 122.06, 107.48, 80.36, 61.04, 60.88, 56.12, 55.04, 31.90, 28.42.

FTIR (AT-IR) 3342.19, 2976.23, 2932.13, 2361.42, 2340.28, 1716.10, 1602.88, 1495.73, 1468.39, 1435.89, 1418.07, 1393.78, 1367.62, 1276.94, 1260.45, 1234.79, 1165.23, 1098.96, 1049.02, 1017.44, 903.85, 851.00, 797.75, 764.67, 750.62, 684.65, 667.91, 643.91 cm^{-1}

HRMS (TOF, ES+) calc'd for $C_{18}H_{29}NO_8$ $[M+H]^+$ 400.1966, found 400.1960 (ppm=1.48)

$[\alpha]_D^{23}$ +8.2° (c = 0.5, $CHCl_3$).

Saponification 3,4-dimethoxy-2-(methoxymethoxy)phenylalanine 386b

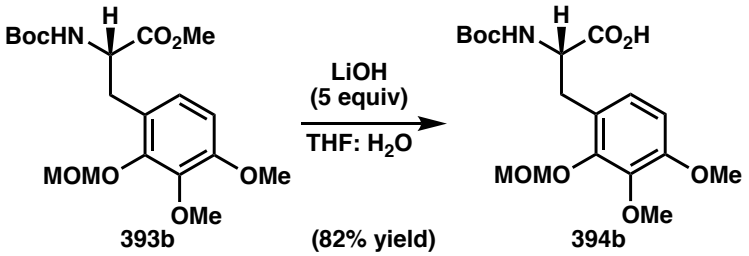

Cool **386b** (132.7 mg, 0.332 mmol, 1.0 equiv) to 0°C stirring in THF (11 mL). Add solution of LiOH•H_2O (70.0 mg, 1.661 mmol, 5.0 equiv) as a solution in DI H_2O (2.0 mL). Allow reaction to warm to ambient temperature and stir 20h. Add DI H_2O (5.0 mL) and extract mixture with 2:1 Hexanes: CH_2Cl_2 (15 mL) and set aside. Lower of aqueous layer to pH=4 and extract twice with 10% *i*-PrOH/$CHCl_3$ (~30 mL). Concentrate crude and azeotrope with PhMe. Dissolve in minimal Et_2O and crash out with Hexanes, remove solvent. Purify by flash chromatography (silica, 4.0 g, 0.75%AcOH/19.25%Hexanes in EtOAc) **387b** (105mg, 82% yield) was recovered as a tacky oil.

^{1}H NMR (400 MHz, $CDCl_3$) δ 6.90 (d, *J* = 8.5 Hz, 1H), 6.66 (d, *J* = 8.6 Hz, 1H), 5.76 (s, 1H), 5.19 (s, 2H), 4.42 (d, *J* = 7.2 Hz, 1H), 3.85 (s, 3H), 3.82 (s, 3H), 3.58 (s, 3H), 3.12 (d, *J* = 7.1 Hz, 2H), 1.38 (s, 9H).

^{13}C NMR (101 MHz, $CDCl_3$) δ 176.72, 156.17, 153.01, 150.04, 141.57, 125.15, 122.54, 108.00, 99.79, 80.11, 60.75, 57.63, 56.11, 54.94, 31.66, 28.40.

FTIR (AT-IR) 3330.56, 2975.53, 2935.51, 2837.19, 1713.56, 1603.46, 1496.44, 1458.64, 1426.45, 1394.22, 1367.28, 1278.34, 1211.14, 1160.04, 1100.99, 1067.90, 983.76, 925.03. 902.54, 852, 799.42, 667.97, 623.011, 613.00, 605.77, 602.38 cm^{-1}

HRMS (TOF, ES+) calc'd for $C_{18}H_{27}NO_8$ $[M+H]^+$ 386.1809, found 386.1806 (ppm=0.89)

$[\alpha]_D^{23}$ +23.5° (c = 1.0, $CHCl_3$).

Conversion to Fmoc-protected amino acid

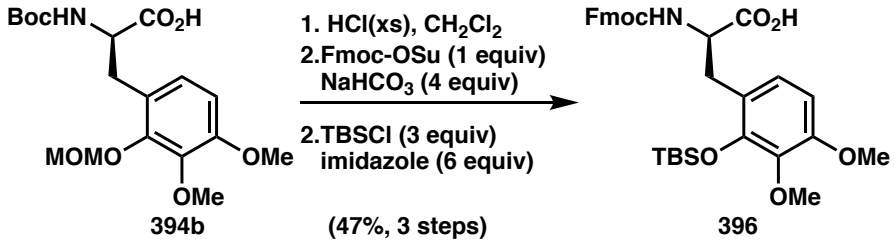

Bubble dried $HCl_{(g)}$, generated from $NaCl_{(s)}$ and $H_2SO_{4(conc)}$, through a solution of **387b** (166 mg, 0.431 mmol, 1.0 equiv) in CH_2Cl_2 (17.3 mL) stirring vigorously at ambient temperature for 55 minutes, reactions became cloudy. Concentrate mixture to a white powder *in vacuo* before diluting the crude intermediate in water (1.7 mL) and 1,4-dioxane (1.7 mL). Add $NaHCO_3$ (145mg, 1.723 mmol, 4.0 equiv) followed by Fmoc-OSu (145.4 mg, 0.431 mmol, 1.0 equiv). Stir at ambient temperature for 17h. Acidify with 1M $HCl_{(aq)}$ and extract the crude aqueous mixture three times $CHCl_3$. Dry organic layer over Na_2SO_4. Filter and concentrate. Flushing crude intermediate through a silica plug (50% EtOAc/1% AcOH/Hexanes) provided as a white solid (154 mg, 0.333 mmol). The intermediate was split, dissolve (76 mg, 0.164 mmol, 1.0 equiv) in DMF (0.5 mL). Add imidazole (67mg, 0.984 mmol, 6.0 equiv) and TBSCl (74 mg, 0.492 mmol, 3.0 equiv); wash down solids with additional DMF (0.6 mL) and stir at ambient temperature. Dilute with DI H_2O (4.0 mL) extract with three times CH_2Cl_2 (3×10 mL). Wash combined organics with DI H_2O and brine. Dry organic layer over Na_2SO_4. Filter, concentrate, azeotrope from PhMe then purify crude product by flash chromatography (silica, 1% AcOH/50% EtOAc/Hexanes) to yield impure **389**. Take up in $CHCl_3$ wash with DI H_2O:brine (2:1) as a white solid. Dry organic layer over Na_2SO_4, filter, concentrate to yield a pure **389** (58 mg, 0.100 mmol, 47% yield, 3 steps)

^{1}H NMR (400 MHz, $CDCl_3$) δ 7.73 (d, *J* = 7.5 Hz, 2H), 7.56 – 7.47 (m, 2H), 7.36 (tdd, *J* = 7.5, 2.2, 1.1 Hz, 2H), 7.26 – 7.20 (m, 2H), 6.85 (d, *J* = 8.5 Hz, 1H), 6.49 (d, *J* = 8.5 Hz, 1H), 6.03 (d, *J* = 6.6 Hz, 1H), 4.45 – 4.36 (m, 1H), 4.36 – 4.22 (m, 2H), 4.12 (t, *J* = 7.0 Hz, 1H), 3.78 (s, 3H), 3.70 (s, 3H), 3.10 (qd, *J* = 14.0, 7.2 Hz, 2H), 1.01 (s, 9H), 0.26 (s, 3H), 0.21 (s, 3H).

^{13}C NMR (101 MHz, $CDCl_3$) δ 176.72, 156.61, 152.96, 147.72, 143.97, 143.90, 141.35, 141.33, 140.13, 127.74, 127.09, 125.19, 125.14, 121.15, 120.03, 105.79, 67.09, 60.49, 56.37, 55.90, 47.21, 31.91, 26.28, 18.84, -3.82, -4.02.

FTIR (AT-IR) 2929.71, 2857.1, 1716.2, 1604.17, 1518.77, 1493.02, 1462.32, 1425.95, 1251.58, 1101.83, 1042.85, 983.26, 908.33, 833.54, 782.87, 757.89, 731.04, 646.98, 634.01, 621.45, 610.72 cm^{-1}

HRMS (TOF, ES+) calc'd for $C_{32}H_{39}NO_7Si$ $[M+H]^+$ 578.2569, found 578.2560 (ppm=-1.56)

$[\alpha]_D^{23}$ –9.7° (c = 1.0, $CHCl_3$).

C-H oxidation of western fragment to form a dihydro-1,2-oxazine

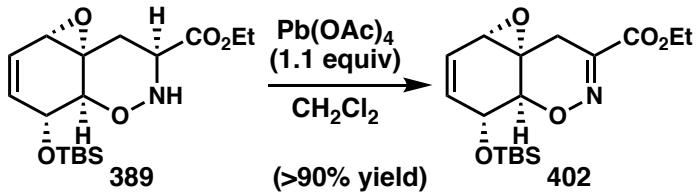

Add $Pb(OAc)_4$ (1.4 mg, 0.00309 mmol, 1.10 equiv) to solution of **382** (1.0mg, 0.0028 mmol, 1.0 equiv) cooled in an ice bath. Remove ice bath and stir at ambient temperature for 5 minutes. Add ethylene glycol (10 μL) and stir 1 minute. Dilute with DI H_2O (1 mL) and extract with CH_2Cl_2 twice. Dry over Na_2SO_4, filter, and concentrate. Azeotrope from toluene to yield 395 (1.0mg, 0.0028 mmol, >90% yield)

^{1}H NMR (400 MHz, $CDCl_3$) δ 6.08 (dd, *J* = 10.2, 3.6 Hz, 1H), 5.92 (dd, *J* = 9.9, 4.5 Hz, 1H), 4.46 (t, *J* = 3.7 Hz, 1H), 4.36 (q, *J* = 7.1 Hz, 2H), 4.04 (d, *J* = 3.0 Hz, 1H), 3.29 (d, *J* = 3.7 Hz, 1H), 2.99 (d, *J* = 18.7 Hz, 1H), 2.59 (d, *J* = 18.7 Hz, 1H), 1.38 (t, *J* = 7.1 Hz, 3H), 0.90 (s, 9H), 0.13 (d, *J* = 16.6 Hz, 6H).

^{13}C NMR (101 MHz, $CDCl_3$) δ 162.46, 152.79, 134.39, 124.80, 78.55, 67.03, 62.63, 58.50, 53.39, 29.85, 28.78, 25.99, 14.26, -4.42, -4.46.

FTIR (AT-IR) 2927.27, 2855.36, 1722.27, 1598.14, 1463.24, 1375.48, 1285.23, 1250.16, 1177.33, 1100.85, 1005.97, 980.91, 915.69, 837.45, 777.06, 750.28, 695.41, 667.18 cm^{-1}

HRMS (TOF, ES+) calc'd for $C_{17}H_{27}NO_5Si$ $[M+H]^+$ 354.1731, found 354.1733 (ppm=-0.49)

Selective copper-mediated formation of chlorohydrin

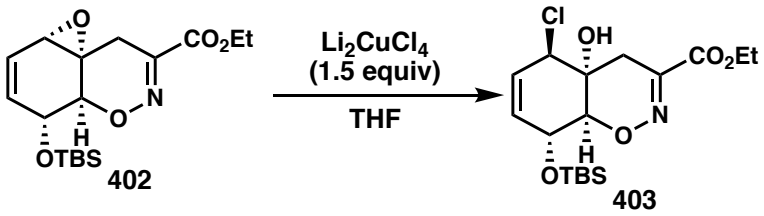

To a solution of substrate (1.0 mg, 0.00282 mmol, 1 equiv) in THF(0.2 mL) add solution Li_2CuCl_4 [composed of LiCl (0.36mg, 0.00846 mmol, 3.0 equiv) and $CuCl_2$ (0.57mg, 0.00423 mmol, 1.5 equiv)] in THF (0.1mL). Stir mixture at ambient temperature for 70 minutes. Add pH=7 phosphate buffer (0.5 mL). Extract three times with EtOAc. Dry organic layer over Na_2SO_4, filter and concentrate *in vacuo* to yield **396** (1.0 mg, 0.00256 mmol, 91%) as a white solid.

^{1}H NMR (600 MHz, $CDCl_3$) δ 5.71 (ddd, J = 10.3, 2.5, 1.8 Hz, 1H), 5.59 (dt, J = 10.4, 2.5 Hz, 1H), 4.80 (q, J = 2.4 Hz, 1H), 4.37 (qd, J = 7.1, 4.0 Hz, 2H), 4.19 (dq, J = 6.9, 2.5 Hz, 1H), 4.15 (dd, J = 6.7, 2.2 Hz, 1H), 2.76 – 2.71 (m, 2H), 2.51 (d, J = 19.5 Hz, 1H), 1.38 (t, J = 7.1 Hz, 3H), 0.90 (s, 9H), 0.15 (s, 3H), 0.08 (s, 3H).

^{13}C NMR (101 MHz, $CDCl_3$) δ 160.28, 129.35, 127.32, 82.82, 68.01, 67.17, 63.02, 62.54, 29.85, 28.64, 25.82, 14.30, -4.58, -5.00.

FTIR (AT-IR) 3428.5, 2948.98, 2881.42, 2361.23 ,2339.97, 1720.97, 1472.4, 1386.18, 1282.69, 1250.2, 1114.29, 1071.89, 1015.57, 905.99, 876.79, 838.12, 801.94, 779.67, 667.89, 654.80, 623.98, 617.77, 609.26 cm^{-1}

HRMS (TOF, ES+) calc'd for $C_{17}H_{28}ClNO_5Si$ $[M+H]^+$ 390.1498, found 390.1509 (ppm=-2.81)

2.17.4 CRYSTALLOGRAPHIC DATA OF 369b (a16027_a)

X-ray quality crystals of **396b** obtained layer diffusion between 1:1 $CHCl_3$/Hexanes and Hexanes.

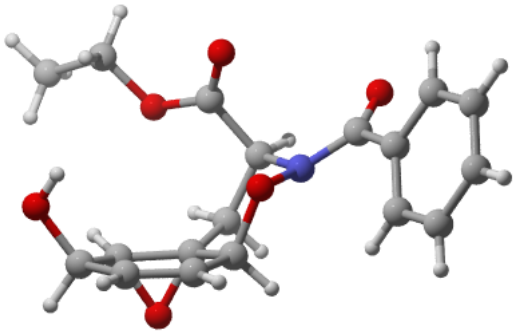

Table 1. Crystal data and structure refinement for a16027_a.cif.

Identification code	a16027_a	
Empirical formula	C18 H19 N O6	
Formula weight	345.34	
Temperature	99.99 K	
Wavelength	0.71073 Å	
Crystal system	Triclinic	
Space group	P-1	
Unit cell dimensions	a = 9.4539(6) Å	α= 114.437(3)°.
	b = 9.8703(7) Å	β= 105.326(3)°.
	c = 10.6887(7) Å	γ = 102.469(3)°.
Volume	813.45(10) $Å^3$	
Z	2	
Density (calculated)	1.410 Mg/m^3	
Absorption coefficient	0.107 mm^{-1}	
F(000)	364	
Crystal size	0.8 x 0.45 x 0.35 mm3	
Theta range for data collection	2.281 to 37.744°.	
Index ranges	-15<=h<=16, -16<=k<=16, -18<=l<=18	
Reflections collected	65383	
Independent reflections	8412 [R(int) = 0.0252]	
Completeness to theta = 26.000°	99.9 %	
Absorption correction	Semi-empirical from equivalents	
Max. and min. transmissio n	0.7474 and 0.7156	

Refinement method	Full-matrix least-squares on F2
Data / restraints / parameters	8412 / 0 / 228
Goodness-of-fit on F2	1.043
Final R indices [I>2sigma(I)]	R1 = 0.0343, wR2 = 0.1005
R indices (all data)	R1 = 0.0395, wR2 = 0.1046
Extinction coefficient	n/a
Largest diff. peak and hole	0.555 and -0.205 e.Å^{-3}

Table 2. Atomic coordinates (x 10^4) and equivalent isotropic displacement parameters (Å^{2}x 10^3) for a16027_a. $U_{(eq)}$ is defined as one third of the trace of the orthogonalized U_{ij} tensor.

	x	y	z	U(eq)
O(1)	6873(1)	5237(1)	993(1)	23(1)
O(2)	4078(1)	7342(1)	4849(1)	21(1)
O(3)	1513(1)	4450(1)	837(1)	21(1)
O(4)	6198(1)	8195(1)	2623(1)	12(1)
O(5)	10068(1)	8470(1)	3357(1)	20(1)
O(6)	5780(1)	4128(1)	2137(1)	17(1)
N(1)	7672(1)	8243(1)	3435(1)	13(1)
C(1)	6678(1)	5329(1)	2092(1)	14(1)
C(2)	7469(1)	6856(1)	3630(1)	14(1)
C(3)	6542(1)	6982(1)	4627(1)	17(1)
C(4)	5059(1)	7241(1)	4009(1)	14(1)
C(5)	3483(1)	6000(1)	3339(1)	17(1)
C(6)	2082(1)	5930(1)	2205(1)	18(1)
C(7)	2411(1)	7354(1)	1984(1)	18(1)
C(8)	3827(1)	8515(1)	2614(1)	17(1)
C(9)	5306(1)	8516(1)	3564(1)	14(1)
C(10)	8946(1)	8903(1)	3200(1)	14(1)
C(11)	8956(1)	10245(1)	2885(1)	15(1)
C(12)	9779(1)	10449(1)	2025(1)	20(1)
C(13)	9905(1)	11734(1)	1767(1)	26(1)
C(14)	9229(1)	12823(1)	2380(1)	27(1)
C(15)	8441(1)	12645(1)	3270(1)	23(1)
C(16)	8295(1)	11352(1)	3517(1)	17(1)
C(17)	4949(1)	2613(1)	725(1)	22(1)
C(18)	4116(1)	1415(1)	1064(1)	27(1)

Table 3. Bond lengths [Å] and angles [°] for a16027_a

O(1)-C(1)	1.2069(7)
O(2)-C(4)	1.4424(7)
O(2)-C(5)	1.4510(7)
O(3)-H(3)	0.8400
O(3)-C(6)	1.4277(8)
O(4)-N(1)	1.4127(6)
O(4)-C(9)	1.4561(6)
O(5)-C(10)	1.2234(7)
O(6)-C(1)	1.3270(7)
O(6)-C(17)	1.4591(7)
N(1)-C(2)	1.4480(7)
N(1)-C(10)	1.3767(7)
C(1)-C(2)	1.5316(7)
C(2)-H(2)	1.0000

C(2)-C(3)	1.5339(8)
C(3)-H(3A)	0.9900
C(3)-H(3B)	0.9900
C(3)-C(4)	1.5075(8)
C(4)-C(5)	1.4682(8)
C(4)-C(9)	1.5140(8)
C(5)-H(5)	1.0000
C(5)-C(6)	1.5068(9)
C(6)-H(6)	1.0000
C(6)-C(7)	1.5011(8)
C(7)-H(7)	0.9500
C(7)-C(8)	1.3347(8)
C(8)-H(8)	0.9500
C(8)-C(9)	1.4944(8)
C(9)-H(9)	1.0000
C(10)-C(11)	1.4945(8)
C(11)-C(12)	1.3977(8)
C(11)-C(16)	1.3956(8)
C(12)-H(12)	0.9500
C(12)-C(13)	1.3932(10)
C(13)-H(13)	0.9500
C(13)-C(14)	1.3882(12)
C(14)-H(14)	0.9500
C(14)-C(15)	1.3950(10)
C(15)-H(15)	0.9500
C(15)-C(16)	1.3928(8)
C(16)-H(16)	0.9500
C(17)-H(17A)	0.9900
C(17)-H(17B)	0.9900
C(17)-C(18)	1.5017(10)
C(18)-H(18A)	0.9800
C(18)-H(18B)	0.9800
C(18)-H(18C)	0.9800

C(4)-O(2)-C(5)	60.99(3)
C(6)-O(3)-H(3)	109.5
N(1)-O(4)-C(9)	109.45(4)
C(1)-O(6)-C(17)	116.14(5)
O(4)-N(1)-C(2)	110.53(4)
C(10)-N(1)-O(4)	116.60(4)
C(10)-N(1)-C(2)	122.41(4)
O(1)-C(1)-O(6)	124.83(5)
O(1)-C(1)-C(2)	123.79(5)
O(6)-C(1)-C(2)	111.38(4)
N(1)-C(2)-C(1)	109.45(4)
N(1)-C(2)-H(2)	108.5
N(1)-C(2)-C(3)	107.27(4)
C(1)-C(2)-H(2)	108.5
C(1)-C(2)-C(3)	114.37(4)
C(3)-C(2)-H(2)	108.5
C(2)-C(3)-H(3A)	109.6
C(2)-C(3)-H(3B)	109.6
H(3A)-C(3)-H(3B)	108.1
C(4)-C(3)-C(2)	110.42(4)
C(4)-C(3)-H(3A)	109.6
C(4)-C(3)-H(3B)	109.6

O(2)-C(4)-C(3)	114.92(4)
O(2)-C(4)-C(5)	59.80(4)
O(2)-C(4)-C(9)	114.11(5)
C(3)-C(4)-C(9)	114.18(4)
C(5)-C(4)-C(3)	122.07(5)
C(5)-C(4)-C(9)	119.51(5)
O(2)-C(5)-C(4)	59.22(3)
O(2)-C(5)-H(5)	115.7
O(2)-C(5)-C(6)	115.76(5)
C(4)-C(5)-H(5)	115.7
C(4)-C(5)-C(6)	122.52(5)
C(6)-C(5)-H(5)	115.7
O(3)-C(6)-C(5)	109.05(5)
O(3)-C(6)-H(6)	107.2
O(3)-C(6)-C(7)	112.48(5)
C(5)-C(6)-H(6)	107.2
C(7)-C(6)-C(5)	113.46(5)
C(7)-C(6)-H(6)	107.2
C(6)-C(7)-H(7)	117.8
C(8)-C(7)-C(6)	124.41(5)
C(8)-C(7)-H(7)	117.8
C(7)-C(8)-H(8)	117.9
C(7)-C(8)-C(9)	124.22(5)
C(9)-C(8)-H(8)	117.9
O(4)-C(9)-C(4)	108.30(4)
O(4)-C(9)-C(8)	104.16(4)
O(4)-C(9)-H(9)	109.8
C(4)-C(9)-H(9)	109.8
C(8)-C(9)-C(4)	114.81(4)
C(8)-C(9)-H(9)	109.8
O(5)-C(10)-N(1)	120.20(5)
O(5)-C(10)-C(11)	122.11(5)
N(1)-C(10)-C(11)	117.49(4)
C(12)-C(11)-C(10)	117.52(5)
C(16)-C(11)-C(10)	122.35(5)
C(16)-C(11)-C(12)	119.92(5)
C(11)-C(12)-H(12)	120.0
C(13)-C(12)-C(11)	120.05(6)
C(13)-C(12)-H(12)	120.0
C(12)-C(13)-H(13)	120.0
C(14)-C(13)-C(12)	119.93(6)
C(14)-C(13)-H(13)	120.0
C(13)-C(14)-H(14)	119.9
C(13)-C(14)-C(15)	120.18(6)
C(15)-C(14)-H(14)	119.9
C(14)-C(15)-H(15)	119.9
C(16)-C(15)-C(14)	120.11(6)
C(16)-C(15)-H(15)	119.9
C(11)-C(16)-H(16)	120.1
C(15)-C(16)-C(11)	119.79(5)
C(15)-C(16)-H(16)	120.1
O(6)-C(17)-H(17A)	110.4
O(6)-C(17)-H(17B)	110.4
O(6)-C(17)-C(18)	106.77(5)
H(17A)-C(17)-H(17B)	108.6
C(18)-C(17)-H(17A)	110.4

C(18)-C(17)-H(17B)	110.4
C(17)-C(18)-H(18A)	109.5
C(17)-C(18)-H(18B)	109.5
C(17)-C(18)-H(18C)	109.5
H(18A)-C(18)-H(18B)	109.5
H(18A)-C(18)-H(18C)	109.5
H(18B)-C(18)-H(18C)	109.5

Symmetry transformations used to generate equivalent atoms:

Table 4. Anisotropic displacement parameters ($Å^2 x\ 10^3$) for a16027_a. The anisotropic displacement factor exponent takes the form: -2p2[h2 a*2U11 + ... + 2 h k a* b* U12]

	U^{11}	U^{22}	U^{33}	U^{23}	U^{13}	U^{12}
O(1)	34(1)	20(1)	18(1)	9(1)	16(1)	9(1)
O(2)	23(1)	22(1)	17(1)	6(1)	14(1)	4(1)
O(3)	19(1)	17(1)	21(1)	8(1)	7(1)	0(1)
O(4)	9(1)	14(1)	14(1)	6(1)	6(1)	5(1)
O(5)	15(1)	29(1)	24(1)	15(1)	10(1)	13(1)
O(6)	23(1)	12(1)	15(1)	7(1)	6(1)	5(1)
N(1)	10(1)	14(1)	16(1)	8(1)	5(1)	4(1)
C(1)	18(1)	13(1)	15(1)	8(1)	7(1)	8(1)
C(2)	14(1)	15(1)	13(1)	7(1)	5(1)	5(1)
C(3)	18(1)	19(1)	11(1)	7(1)	5(1)	5(1)
C(4)	16(1)	14(1)	12(1)	5(1)	8(1)	4(1)
C(5)	18(1)	15(1)	16(1)	8(1)	10(1)	3(1)
C(6)	14(1)	16(1)	22(1)	9(1)	10(1)	3(1)
C(7)	13(1)	18(1)	27(1)	12(1)	11(1)	7(1)
C(8)	14(1)	14(1)	26(1)	11(1)	11(1)	7(1)
C(9)	13(1)	12(1)	16(1)	5(1)	9(1)	4(1)
C(10)	11(1)	17(1)	13(1)	7(1)	6(1)	5(1)
C(11)	10(1)	18(1)	15(1)	9(1)	5(1)	3(1)
C(12)	14(1)	28(1)	20(1)	13(1)	8(1)	4(1)
C(13)	17(1)	34(1)	27(1)	21(1)	8(1)	2(1)
C(14)	19(1)	27(1)	34(1)	23(1)	6(1)	1(1)
C(15)	17(1)	19(1)	31(1)	16(1)	7(1)	4(1)
C(16)	13(1)	17(1)	21(1)	10(1)	7(1)	4(1)
C(17)	30(1)	13(1)	17(1)	5(1)	6(1)	6(1)
C(18)	23(1)	18(1)	28(1)	11(1)	3(1)	0(1)

Table 5. Hydrogen coordinates ($x\ 10^4$) and isotropic displacement parameters ($Å^2 x\ 10^3$) for a16027_a.

	x	y	z	U(eq)
H(3)	2000	4558	310	31
H(2)	8535	6899	4164	17
H(3A)	6262	5987	4680	20
H(3B)	7208	7887	5655	20
H(5)	3460	4949	3261	20
H(6)	1229	5920	2593	21
H(7)	1553	7434	1352	22

H(8)	3900	9397	2448	20
H(9)	5908	9597	4480	17
H(12)	10252	9711	1616	24
H(13)	10453	11866	1172	31
H(14)	9304	13692	2194	32
H(15)	8003	13407	3708	27
H(16)	7748	11224	4113	20
H(17A)	5707	2261	308	27
H(17B)	4178	2734	-14	27
H(18A)	3545	373	142	40
H(18B)	3366	1775	1470	40
H(18C)	4892	1313	1801	40

Table 6. Torsion angles [°] for a16027_a.

O(1)-C(1)-C(2)-N(1)	32.43(7)
O(1)-C(1)-C(2)-C(3)	152.80(6)
O(2)-C(4)-C(5)-C(6)	102.72(6)
O(2)-C(4)-C(9)-O(4)	-175.31(4)
O(2)-C(4)-C(9)-C(8)	-59.41(6)
O(2)-C(5)-C(6)-O(3)	-172.59(4)
O(2)-C(5)-C(6)-C(7)	61.20(6)
O(3)-C(6)-C(7)-C(8)	-118.76(6)
O(4)-N(1)-C(2)-C(1)	59.09(5)
O(4)-N(1)-C(2)-C(3)	-65.52(5)
O(4)-N(1)-C(10)-O(5)	-151.78(5)
O(4)-N(1)-C(10)-C(11)	33.40(6)
O(5)-C(10)-C(11)-C(12)	33.04(8)
O(5)-C(10)-C(11)-C(16)	-141.58(6)
O(6)-C(1)-C(2)-N(1)	-148.56(4)
O(6)-C(1)-C(2)-C(3)	-28.19(6)
N(1)-O(4)-C(9)-C(4)	-60.15(5)
N(1)-O(4)-C(9)-C(8)	177.21(4)
N(1)-C(2)-C(3)-C(4)	52.05(5)
N(1)-C(10)-C(11)-C(12)	-152.25(5)
N(1)-C(10)-C(11)-C(16)	33.14(7)
C(1)-O(6)-C(17)-C(18)	175.96(5)
C(1)-C(2)-C(3)-C(4)	-69.52(6)
C(2)-N(1)-C(10)-O(5)	-10.28(8)
C(2)-N(1)-C(10)-C(11)	174.90(4)
C(2)-C(3)-C(4)-O(2)	178.71(4)
C(2)-C(3)-C(4)-C(5)	110.02(5)
C(2)-C(3)-C(4)-C(9)	-46.69(6)
C(3)-C(4)-C(5)-O(2)	102.16(5)
C(3)-C(4)-C(5)-C(6)	-155.13(5)
C(3)-C(4)-C(9)-O(4)	49.71(6)
C(3)-C(4)-C(9)-C(8)	165.61(4)
C(4)-O(2)-C(5)-C(6)	-114.03(5)
C(4)-C(5)-C(6)-O(3)	118.90(5)
C(4)-C(5)-C(6)-C(7)	-7.31(8)
C(5)-O(2)-C(4)-C(3)	-114.02(5)
C(5)-O(2)-C(4)-C(9)	111.34(5)
C(5)-C(4)-C(9)-O(4)	-107.64(5)
C(5)-C(4)-C(9)-C(8)	8.26(7)
C(5)-C(6)-C(7)-C(8)	5.62(8)

C(6)-C(7)-C(8)-C(9)	3.49(9)
C(7)-C(8)-C(9)-O(4)	107.72(6)
C(7)-C(8)-C(9)-C(4)	-10.54(8)
C(9)-O(4)-N(1)-C(2)	71.68(5)
C(9)-O(4)-N(1)-C(10)	-142.45(4)
C(9)-C(4)-C(5)-O(2)	-102.33(5)
C(9)-C(4)-C(5)-C(6)	0.39(8)
C(10)-N(1)-C(2)-C(1)	-84.44(6)
C(10)-N(1)-C(2)-C(3)	150.94(5)
C(10)-C(11)-C(12)-C(13)	-176.34(5)
C(10)-C(11)-C(16)-C(15)	175.33(5)
C(11)-C(12)-C(13)-C(14)	0.77(9)
C(12)-C(11)-C(16)-C(15)	0.83(8)
C(12)-C(13)-C(14)-C(15)	0.80(10)
C(13)-C(14)-C(15)-C(16)	-1.55(10)
C(14)-C(15)-C(16)-C(11)	0.73(9)
C(16)-C(11)-C(12)-C(13)	-1.59(8)
C(17)-O(6)-C(1)-O(1)	-1.75(8)
C(17)-O(6)-C(1)-C(2)	179.25(5)

Symmetry transformations used to generate equivalent atoms:

2.18 REFERENCES

(1) Seephonkai, P.; Kongsaeree, P.; Prabpai, S.; Isaka, M.; Thebtaranonth, Y. Transformation of an Irregularly Bridged Epidithiodiketopiperazine to Trichodermamide A. *Org. Lett.* **2006**, *8* (14), 3073–3075.

(2) Stipanovic, R. D.; Howell, C. R. THE STRUCTURE OF GLIOVIRIN, A NEW ANTIBIOTIC FROM GLIOCLADIUM VIRENS. *J. Antibiot. (Tokyo)* **1982**, *35* (10), 1326–1330.

(3) Okose, K.; Nakayama, N.; Miyamoto, C.; Furumai, T.; Maruyama, H. B.; Stipanovic, R. D.; Howell, C. R. STRUCTURE OF FA-2097, A NEW MEMBER OF THE DIOXOPIPERAZINE ANTIBIOTICS. *J. Antibiot. (Tokyo)* **1984**, *37* (6), 667–669.

(4) Liu, Y.; Mándi, A.; Li, X.-M.; Meng, L.-H.; Kurtán, T.; Wang, B.-G. Peniciadametizine A, a Dithiodiketopiperazine with a Unique Spiro[Furan-2,7'-Pyrazino[1,2-b][1,2]Oxazine] Skeleton, and a Related Analogue, Peniciadametizine B, from the Marine Sponge-Derived Fungus Penicillium Adametzioides. *Mar. Drugs* **2015**, *13* (6), 3640–3652.

(5) Garo, E.; Starks, C. M.; Jensen, P. R.; Fenical, W.; Lobkovsky, E.; Clardy, J. Trichodermamides A and B, Cytotoxic Modified Dipeptides from the Marine-Derived Fungus Trichoderma Virens. *J. Nat. Prod.* **2003**, *66* (3), 423–426.

(6) Davis, R. A.; Longden, J.; Avery, V. M.; Healy, P. C. The Isolation, Structure Determination and Cytotoxicity of the New Fungal Metabolite, Trichodermamide C. *Bioorg. Med. Chem. Lett.* **2008**, *18* (9), 2836–2839.

(7) Howell, C. R.; Stipanovic, R. D. Gliovirin, a New Antibiotic from Gliocladium Virens, and Its Role in the Biological Control of Pythium Ultimum. *Can. J. Microbiol.* **1983**, *29* (3), 321–324.

(8) Rether, J.; Serwe, A.; Anke, T.; Erkel, G. Inhibition of Inducible Tumor Necrosis Factor-α Expression by the Fungal Epipolythiodiketopiperazine Gliovirin. *Biol. Chem.* **2007**, *388* (6), 627–637.
(9) Miknis, G. F.; Williams, R. M. Total Synthesis of (.+-.)-Aspirochlorine. *J. Am. Chem. Soc.* **1993**, *115* (2), 536–547.
(10) Wu, Z.; Williams, L. J.; Danishefsky, S. J. A Three-Step Entry to the Aspirochlorine Family of Antifungal Agents. *Angew. Chem. Int. Ed.* **2000**, *39* (21), 3866–3868.
(11) Ross, A. J.; Lang, H. L.; Jackson, R. F. W. Much Improved Conditions for the Negishi Cross-Coupling of Iodoalanine Derived Zinc Reagents with Aryl Halides https://pubs.acs.org/doi/abs/10.1021/jo902238n (accessed Apr 11, 2018).
(12) Rayburn, C. H.; Harlan, W. R.; Hanmer, H. R. Rearrangement of Nicotine Oxide. *J. Am. Chem. Soc.* **1950**, *72* (4), 1721–1723.
(13) Belleau, B.; Au-Young, Y.-K. Stereospecific Total Synthesis of Two 5-Amino-5,6-Dideoxy-DL-Hexonic Acids, a Novel Class of Aminosugar Related Compounds. *J. Am. Chem. Soc.* **1963**, *85* (1), 64–71.
(14) Keck, G. E.; Fleming, S.; Nickell, D.; Weider, P. Mild and Efficient Methods for the Reductive Cleavage of Nitrogen-Oxygen Bonds. *Synth. Commun.* **1979**, *9* (4), 281–286.
(15) Chan, T.-M.; Friary, R.; Pramanik, B.; Puar, M. S.; Seidl, V.; Mc Phail, A. T. Synthesis, Structure, and Reductive Rearrangement of a Novel Tricyclic Isoxazolidine. *Tetrahedron* **1986**, *42* (17), 4661–4670.
(16) Defoin, A.; Fritz, H.; Geffroy, G.; Streith, J. Total Syntheses of (±) Aminoallose Derivatives. *Tetrahedron Lett.* **1986**, *27* (39), 4727–4730.
(17) Ritter, A. R.; Miller, M. J. Amino Acid-Derived Chiral Acyl Nitroso Compounds: Diastereoselectivity in Intermolecular Hetero Diels-Alder Reactions. *J. Org. Chem.* **1994**, *59* (16), 4602–4611.
(18) Keck, G. E.; McHardy, S. F.; Wager, T. T. Reductive Cleavage of N–O Bonds in Hydroxylamine and Hydroxamic Acid Derivatives Using SmI2/THF. *Tetrahedron Lett.* **1995**, *36* (41), 7419–7422.
(19) Aoyagi, S.; Tanaka, R.; Naruse, M.; Kibayashi, C. Asymmetric Total Synthesis of (−)-Epibatidine. *Tetrahedron Lett.* **1998**, *39* (25), 4513–4516.
(20) Iida, H.; Watanabe, Y.; Kibayashi, C. Stereospecific Total Synthesis of (.+-.)-Gephyrotoxin 223AB. *J. Am. Chem. Soc.* **1985**, *107* (19), 5534–5535.
(21) Baldwin, J. E.; Otsuka, M.; Wallace, P. M. Synthesis of a Naturally Occurring Inhibitor of Glutamine Synthetase, Tabtoxinene-β-Lactam. *J. Chem. Soc. Chem. Commun.* **1985**, *0* (22), 1549–1550.
(22) Iida, H.; Watanabe, Y.; Kibayashi, C. A Stereoselective Synthesis of the Ant Trail Pheromone (±)-Monomorine I. *Tetrahedron Lett.* **1986**, *27* (45), 5513–5514.
(23) Watanabe, Y.; Iida, H.; Kibayashi, C. Total Synthesis of (.+-.)-Dihydropinidine, (.+-.)-Monomorine I, and (.+-.)-Indolizidine 223AB (Gephyrotoxin 223AB) by Intramolecular Nitroso Diels-Alder Reaction. *J. Org. Chem.* **1989**, *54* (17), 4088–4097.
(24) Aoyagi, S.; Shishido, Y.; Kibayashi, C. Total Synthesis of (−)-Nupharamine and (+)-3-Epinupharamine via Asymmetric Nitroso Diels-Alder Reaction. *Tetrahedron Lett.* **1991**, *32* (34), 4325–4328.
(25) Vanhessche, K.; Bello, C. G.; Vandewalle, M. Total Synthesis of (-)-Neplanocin A from L-Ribulose. *Synlett* **1991**, *1991* (12), 921–922.

(26) Hudlicky, T.; Olivo, H. F. A Short Synthesis of (+)-Lycoricidine. *J. Am. Chem. Soc.* **1992**, *114* (24), 9694–9696.
(27) Naruse, M.; Aoyagi, S.; Kibayashi, C. Stereoselective Total Synthesis of (–)-Pumiliotoxin C by an Aqueous Intramolecular Acylnitroso Diels–Alder Approach. *J. Chem. Soc. [Perkin 1]* **1996**, *0* (11), 1113–1124.
(28) Abe, H.; Aoyagi, S.; Kibayashi, C. First Total Synthesis of the Marine Alkaloids (±)-Fasicularin and (±)-Lepadiformine Based on Stereocontrolled Intramolecular Acylnitroso-Diels−Alder Reaction. *J. Am. Chem. Soc.* **2000**, *122* (19), 4583–4592.
(29) Kumar, J. C.; Armido, S. Total Synthesis of (+)-trans-Dihydronarciclasine by a Catalytic Enantioselective Regiodivergent Nitroso Diels–Alder Reaction. *Chem. – Eur. J.* **2008**, *14* (21), 6326–6328.
(30) Camilla, P.; Francesca, C.; Leonardo, G.; Hans-Ulrich, R.; Andrea, G. Stereocomplementary Routes to Hydroxylated Nitrogen Heterocycles: Total Syntheses of Casuarine, Australine, and 7-epi-Australine. *Chem. – Eur. J.* **2013**, *19* (32), 10595–10604.
(31) Desai, M. C.; Doty, J. L.; Stephens, L. M.; Brighty, K. E. Novel Fragmentation of 3-Lithio-3,6-Dihydro-1,2-Oxazines: Synthesis of 2,5-Dihydro-2-Furanylamines. *Tetrahedron Lett.* **1993**, *34* (6), 961–962.
(32) Fukuyama, T.; Nakatsuka, S.-I.; Kishi, Y. Total Synthesis of Gliotoxin, Dehydrogliotoxin and Hyalodendrin. *Tetrahedron* **1981**, *37* (11), 2045–2078.
(33) Gilchrist, T. L.; Roberts, T. G. Addition and Cycloaddition Reactions of the Electrophilic Vinyl Nitroso Compounds 3-Nitrosobut-3-En-2-One, 2-Nitrosopropenal, and Ethyl 2-Nitrosopropenoate. *J. Chem. Soc. [Perkin 1]* **1983**, *0* (0), 1283–1292.
(34) Yasuda, A.; Tanaka, S.; Oshima, K.; Yamamoto, H.; Nozaki, H. Organoaluminum Reagents of Type R1R2NAlEt2 Which Allow Regiospecific Isomerization of Epoxides to Allylic Alcohols. *J. Am. Chem. Soc.* **2002**, *96* (20), 6513–6514.
(35) Zhang Yu; Stephens David; Hernandez Graciela; Mendoza Rosalinda; Larionov Oleg V. Catalytic Diastereo- and Enantioselective Annulations between Transient Nitrosoalkenes and Indoles. *Chem. – Eur. J.* **2012**, *18* (52), 16612–16615.
(36) Fukuzumi, T.; Bode, J. W. A Reagent for the Convenient, Solid-Phase Synthesis of N-Terminal Peptide Hydroxylamines for Chemoselective Ligations. *J. Am. Chem. Soc.* **2009**, *131* (11), 3864–3865.
(37) Chen, Y. K.; Yoshida, M.; MacMillan, D. W. C. Enantioselective Organocatalytic Amine Conjugate Addition. *J. Am. Chem. Soc.* **2006**, *128* (29), 9328–9329.
(38) Vesely, J.; Ibrahem, I.; Rios, R.; Zhao, G.-L.; Xu, Y.; Córdova, A. Enantioselective Organocatalytic Conjugate Addition of Amines to α,β-Unsaturated Aldehydes: One-Pot Asymmetric Synthesis of β-Amino Acids and 1,3-Diamines. *Tetrahedron Lett.* **2007**, *48* (12), 2193–2198.
(39) Gilbert, J. C.; Weerasooriya, U. Diazoethenes: Their Attempted Synthesis from Aldehydes and Aromatic Ketones by Way of the Horner-Emmons Modification of the Wittig Reaction. A Facile Synthesis of Alkynes. *J. Org. Chem.* **1982**, *47* (10), 1837–1845.
(40) Müller, S.; Liepold, B.; Roth, G. J.; Bestmann, H. J. An Improved One-Pot Procedure for the Synthesis of Alkynes from Aldehydes. *Synlett* **1996**, *1996* (06), 521–522.
(41) Chen, L.; Dovalsantos, E.; Yu, J.; O'Neill-Slawecki, S.; Mitchell, M.; Sakata, S.; Borer, B. A Simple Preparation of a (Pyridonyl-1)Propargylacetic Acid Derivative. *Org. Process Res. Dev.* **2006**, *10* (4), 838–840.

(42) Feenstra, R. W.; Stokkingreef, E. H. M.; Nivard, R. J. F.; Ottenheijm, H. C. J. Interconversion of (R) and (S)-α-Hydroxy Esters: Precursors of (S) and (R)-o-Benzyl-α-Hydroxylamino Acid Esters of High Optical Purity. *Tetrahedron* **1988**, *44* (17), 5583–5595.
(43) Congreve, M. S.; Davison, E. C.; Fuhry, M. A. M.; Holmes, A. B.; Payne, A. N.; Robinson, R. A.; Ward, S. E. Selective Cleavage of Benzyl Ethers. *Synlett* **1993**, *1993* (9), 663–664.
(44) Courtois, G.; Miginiac, L. Etude de La Régiosélectivité de l'action Des Organozinciques Sur Les α-Iminoesters: Synthèse d'α-Aminoesters C-Substitués Par Un Groupe α-Insaturé Ou α-Fonctionnel. *J. Organomet. Chem.* **1989**, *376* (2), 235–243.
(45) Snyder, L. R. Linear Elution Adsorption Chromatography: VI. Deactivated Florisil as Adsorbent. *J. Chromatogr. A* **1963**, *12*, 488–509.
(46) Kulkarni, A. A.; Diver, S. T. Ring Synthesis by Stereoselective, Methylene-Free Enyne Cross Metathesis. *J. Am. Chem. Soc.* **2004**, *126* (26), 8110–8111.
(47) Peppers, B. P.; Kulkarni, A. A.; Diver, S. T. Functional Group Scope in the Methylene-Free, Tandem Enyne Metathesis. *Org. Lett.* **2006**, *8* (12), 2539–2542.
(48) Hong, S. H.; Wenzel, A. G.; Salguero, T. T.; Day, M. W.; Grubbs, R. H. Decomposition of Ruthenium Olefin Metathesis Catalysts. *J. Am. Chem. Soc.* **2007**, *129* (25), 7961–7968.
(49) Galan, B. R.; Giessert, A. J.; Keister, J. B.; Diver, S. T. Studies on the Mechanism of Intermolecular Enyne Metathesis: Kinetic Method and Alkyne Substituent Effects. *J. Am. Chem. Soc.* **2005**, *127* (16), 5762–5763.
(50) Schmidt, V. A.; Alexanian, E. J. Metal-Free, Aerobic Dioxygenation of Alkenes Using Hydroxamic Acids. *Angew. Chem. Int. Ed.* **2010**, *49* (26), 4491–4494.
(51) Schmidt, V. A.; Alexanian, E. J. Metal-Free, Aerobic Ketooxygenation of Alkenes Using Hydroxamic Acids. *Chem. Sci.* **2012**, *3* (5), 1672–1674.
(52) Lu, Q.; Liu, Z.; Luo, Y.; Zhang, G.; Huang, Z.; Wang, H.; Liu, C.; Miller, J. T.; Lei, A. Copper-/Cobalt-Catalyzed Highly Selective Radical Dioxygenation of Alkenes. *Org. Lett.* **2015**, *17* (14), 3402–3405.
(53) Bag, R.; Sar, D.; Punniyamurthy, T. Copper(II)-Catalyzed Direct Dioxygenation of Alkenes with Air and N-Hydroxyphthalimide: Synthesis of β-Keto-N-Alkoxyphthalimides. *Org. Lett.* **2015**, *17* (8), 2010–2013.
(54) Andia, A. A.; Miner, M. R.; Woerpel, K. A. Copper(I)-Catalyzed Oxidation of Alkenes Using Molecular Oxygen and Hydroxylamines: Synthesis and Reactivity of α-Oxygenated Ketones. *Org. Lett.* **2015**, *17* (11), 2704–2707.
(55) Paddon-Row, M. N.; Rondan, N. G.; Houk, K. N. Staggered Models for Asymmetric Induction: Attack Trajectories and Conformations of Allylic Bonds from Ab Initio Transition Structures of Addition Reactions. *J. Am. Chem. Soc.* **1982**, *104* (25), 7162–7166.
(56) Kornblum, N.; DeLaMare, H. E. THE BASE CATALYZED DECOMPOSITION OF A DIALKYL PEROXIDE. *J. Am. Chem. Soc.* **1951**, *73* (2), 880–881.
(57) Cole, A. P.; Mahadevan, V.; Mirica, L. M.; Ottenwaelder, X.; Stack, T. D. P. Bis(μ-Oxo)Dicopper(III) Complexes of a Homologous Series of Simple Peralkylated 1,2-Diamines: Steric Modulation of Structure, Stability, and Reactivity. *Inorg. Chem.* **2005**, *44* (21), 7345–7364.
(58) Kang, P.; Bobyr, E.; Dustman, J.; Hodgson, K. O.; Hedman, B.; Solomon, E. I.; Stack, T. D. P. Bis(μ-Oxo) Dicopper(III) Species of the Simplest Peralkylated Diamine: Enhanced Reactivity toward Exogenous Substrates. *Inorg. Chem.* **2010**, *49* (23), 11030–11038.
(59) Chow, Y. L.; Colón, C. J.; Tam, J. N. S. A(1,3) Interaction and Conformational Energy of Axial–Axial 1,3-Dimethyl Interaction. *Can. J. Chem.* **1968**, *46* (17), 2821–2825.

(60) Hoveyda, A. H.; Evans, D. A.; Fu, G. C. Substrate-Directable Chemical Reactions. *Chem. Rev.* **1993**, *93* (4), 1307–1370.
(61) Ernst, W.; Alfred, S. Über Die Einwirkung von Alkalischem Wasserstoffsuperoxyd Auf Ungesättigte Verbindungen. *Chem. Ber.* **1921**, *54* (9), 2327–2344.
(62) Wang, X.; Reisinger, C. M.; List, B. Catalytic Asymmetric Epoxidation of Cyclic Enones. *J. Am. Chem. Soc.* **2008**, *130* (19), 6070–6071.
(63) Magnus, P.; Sebhat, I. K. Synthesis of the Antitumor Alkaloid (+)-Pancratistatin Using the β-Azidonation Reaction via a Prochiral 4-Arylcyclohexanone Derivative. *J. Am. Chem. Soc.* **1998**, *120* (21), 5341–5342.
(64) Lane, B. S.; Burgess, K. A Cheap, Catalytic, Scalable, and Environmentally Benign Method for Alkene Epoxidations. *J. Am. Chem. Soc.* **2001**, *123* (12), 2933–2934.
(65) Lane, B. S.; Vogt, M.; DeRose, V. J.; Burgess, K. Manganese-Catalyzed Epoxidations of Alkenes in Bicarbonate Solutions. *J. Am. Chem. Soc.* **2002**, *124* (40), 11946–11954.
(66) Martin, J. C.; Arhart, R. J. Sulfuranes. III. Reagent for the Dehydration of Alcohols. *J. Am. Chem. Soc.* **1971**, *93* (17), 4327–4329.
(67) Yamamoto, K.; Heathcock, C. H. α,β-Epoxy Vinyl Triflates in Pd-Catalyzed Reactions. *Org. Lett.* **2000**, *2* (12), 1709–1712.
(68) Wharton, P.; Bohlen, D. Communications- Hydrazine Reduction of α, β-Epoxy Ketones to Allylic Alcohols. *J. Org. Chem.* **1961**, *26* (9), 3615–3616.
(69) Cookson, R. C.; Crumbie, R. L. Conversion of Ketones into Vinyl-Oxiranes. *Tetrahedron Lett.* **1985**, *26* (28), 3377–3380.
(70) Wilde, N. C.; Isomura, M.; Mendoza, A.; Baran, P. S. Two-Phase Synthesis of (−)-Taxuyunnanine D. *J. Am. Chem. Soc.* **2014**, *136* (13), 4909–4912.
(71) Nakamura, A.; Nakada, M. Allylic Oxidations in Natural Product Synthesis. *Synthesis* **2013**, *45* (11), 1421–1451.
(72) Młochowski, J.; Wójtowicz-Młochowska, H. Developments in Synthetic Application of Selenium(IV) Oxide and Organoselenium Compounds as Oxygen Donors and Oxygen-Transfer Agents. *Molecules* **2015**, *20* (6), 10205–10243.
(73) Tan, Q.; Hayashi, M. Asymmetric Desymmetrization of 4,5-Epoxycyclohex-1-Ene by Enantioselective Allylic Oxidation. *Org. Lett.* **2009**, *11* (15), 3314–3317.
(74) Recupero, F.; Punta, C. Free Radical Functionalization of Organic Compounds Catalyzed by N-Hydroxyphthalimide. *Chem. Rev.* **2007**, *107* (9), 3800–3842.
(75) Horn, E. J.; Rosen, B. R.; Chen, Y.; Tang, J.; Chen, K.; Eastgate, M. D.; Baran, P. S. Scalable and Sustainable Electrochemical Allylic C–H Oxidation. *Nature* **2016**, *533* (7601), 77–81.
(76) Shing, T. K. M.; Yeung; Su, P. L. Mild Manganese(III) Acetate Catalyzed Allylic Oxidation: Application to Simple and Complex Alkenes. *Org. Lett.* **2006**, *8* (14), 3149–3151.
(77) Loskot, S. A.; Romney, D. K.; Arnold, F. H.; Stoltz, B. M. Enantioselective Total Synthesis of Nigelladine A via Late-Stage C–H Oxidation Enabled by an Engineered P450 Enzyme. *J. Am. Chem. Soc.* **2017**, *139* (30), 10196–10199.
(78) Ito, Y.; Hirao, T.; Saegusa, T. Synthesis of .Alpha.,.Beta.-Unsaturated Carbonyl Compounds by Palladium(II)-Catalyzed Dehydrosilylation of Silyl Enol Ethers. *J. Org. Chem.* **1978**, *43* (5), 1011–1013.
(79) Paquette, L. A.; Belmont, D. T.; Asu, Y. L. Regiospecific and Stereoselective Alkylation of the Octahydronaphthal-8(9)-En-3-One Nucleus. *J. Org. Chem.* **1985**, *50* (24), 4667–4672.

(80) Mincione, E.; Bovicelli, P.; Cerrini, S.; Lamba, D. Heterosteroids via Organoiron Complexes: Enantioselectine Synthesis of the 9-(4-Keto-1-Methylcyclohex-2-Enyl)-8-Keto-Des-AB-Ergosta-14,15-22,23-Diene; An Easy Rearrangement of the Title Compound into a 6-Oxo-B-nor-Heterosteroid Structure. *HETEROCYCLES* **1988**, *27* (3), 605.
(81) Nicolaou, K. C.; Montagnon, T.; Baran, P. S. Modulation of the Reactivity Profile of IBX by Ligand Complexation: Ambient Temperature Dehydrogenation of Aldehydes and Ketones to α,β-Unsaturated Carbonyl Compounds. *Angew. Chem. Int. Ed.* **2002**, *41* (6), 993–996.
(82) Tsuji, J.; Minami, I.; Shimizu, I. A Novel Palladium-Catalyzed Preparative Method of α,β-Unsaturated Ketones and Aldehydes from Saturated Ketones and Aldehydes via Their Silyl Enol Ethers. *Tetrahedron Lett.* **1983**, *24* (50), 5635–5638.
(83) Diao, T.; Stahl, S. S. Synthesis of Cyclic Enones via Direct Palladium-Catalyzed Aerobic Dehydrogenation of Ketones. *J. Am. Chem. Soc.* **2011**, *133* (37), 14566–14569.
(84) Bigi, M. A.; White, M. C. Terminal Olefins to Linear α,β-Unsaturated Ketones: Pd(II)/Hypervalent Iodine Co-Catalyzed Wacker Oxidation–Dehydrogenation. *J. Am. Chem. Soc.* **2013**, *135* (21), 7831–7834.
(85) Luche, J. L. Lanthanides in Organic Chemistry. 1. Selective 1,2 Reductions of Conjugated Ketones. *J. Am. Chem. Soc.* **1978**, *100* (7), 2226–2227.
(86) Brown, H. C.; Cha, J. S.; Nazer, B.; Kim, S. C.; Krishnamurthy, S.; Brown, C. A. Selective Reductions. 33. Potassium Triisopropoxyborohydride as a Selective Reducing Agent in Organic Synthesis. Reaction with Selected Organic Compounds Containing Representative Functional Groups. *J. Org. Chem.* **1984**, *49* (5), 885–892.
(87) Jacob, J.; Espenson, J. H.; Jensen, J. H.; Gordon, M. S. 1,3-Transposition of Allylic Alcohols Catalyzed by Methyltrioxorhenium. *Organometallics* **1998**, *17* (9), 1835–1840.
(88) Bellemin-Laponnaz, S.; Le Ny, J.-P. Metal Oxo Complexes as Catalysts for the Isomerisation of Allylic Alcohols. *Comptes Rendus Chim.* **2002**, *5* (4), 217–224.
(89) Volchkov, I.; Lee, D. Recent Developments of Direct Rhenium-Catalyzed [1,3]-Transpositions of Allylic Alcohols and Their Silyl Ethers. *Chem. Soc. Rev.* **2014**, *43* (13), 4381–4394.
(90) Stork, G.; Williard, P. G. Five- and Six-Membered-Ring Formation from Olefinic .Alpha.,.Beta.-Epoxy Ketones and Hydrazine. *J. Am. Chem. Soc.* **1977**, *99* (21), 7067–7068.
(91) Kessar, S. V.; Rampal, A. L. Synthetic Studies in Steroidal Sapogenins and Alkaloids—III: The Synthesis and Stereochemistry of Isomeric 16-Hydroxy- and 16-Oxo-5,17(20)-Pregnadien-3β-Ols. *Tetrahedron* **1968**, *24* (2), 887–892.
(92) Dupuy, C.; Luche, J. L. New Developments of the Wharton Transposition. *Tetrahedron* **1989**, *45* (11), 3437–3444.
(93) Maas, D. D.; Blagg, M.; Wiemer, D. F. Synthesis and Reactions of (-)- and (+)-Carenones. *J. Org. Chem.* **1984**, *49* (5), 853–856.
(94) Ichihara, A.; Oda, K.; Kobayashi, M.; Sakamura, S. Stereoselective Synthesis of (±)-Senepoxyde and (±)-Crotepoxide1. *Tetrahedron* **1980**, *36* (2), 183–188.
(95) Hoye, T. R.; Jeffrey, C. S.; Nelson, D. P. Dynamic Kinetic Resolution During a Vinylogous Payne Rearrangement: A Concise Synthesis of the Polar Pharmacophoric Subunit of (+)-Scyphostatin. *Org. Lett.* **2010**, *12* (1), 52–55.
(96) Myers, A. G.; Siegel, D. R.; Buzard, D. J.; Charest, M. G. Synthesis of a Broad Array of Highly Functionalized, Enantiomerically Pure Cyclohexanecarboxylic Acid Derivatives by

Microbial Dihydroxylation of Benzoic Acid and Subsequent Oxidative and Rearrangement Reactions. *Org. Lett.* **2001**, *3* (18), 2923–2926.
(97) Curtius, T.; Thun, K. Einwirkung von Hydrazinhydrat Auf Monoketone Und Orthodiketone. *J. Für Prakt. Chem.* **1891**, *44* (1), 161–186.
(98) Benn, W. R.; Dodson, R. M. The Synthesis and Stereochemistry of Isomeric 16-Hydroxy-17(20)-Pregnenes. *J. Org. Chem.* **1964**, *29* (5), 1142–1148.
(99) Coffen, D. L.; Korzan, D. G. Synthetic Quinine Analogs. III. Frangomeric and Anchimeric Processes in the Preparation and Reactions of .Alpha.,.Beta.-Epoxy Ketones. *J. Org. Chem.* **1971**, *36* (3), 390–395.
(100) Jencks, W. P.; Carriuolo, J. Reactivity of Nucleophilic Reagents toward Esters. *J. Am. Chem. Soc.* **1960**, *82* (7), 1778–1786.
(101) Myers, A. G.; Movassaghi, M.; Zheng, B. Single-Step Process for the Reductive Deoxygenation of Unhindered Alcohols. *J. Am. Chem. Soc.* **1997**, *119* (36), 8572–8573.
(102) Aoyagi, Y.; Hitotsuyanagi, Y.; Hasuda, T.; Fukaya, H.; Takeya, K.; Aiyama, R.; Matsuzaki, T.; Hashimoto, S. Semisynthesis of C-Ring Modified Triptolide Analogues and Their Cytotoxic Activities. *Bioorg. Med. Chem. Lett.* **2006**, *16* (7), 1947–1949.
(103) Thomas, A. F.; Giorgio, R. D.; Guntern, O. Apparent Failure of the Wharton Rearrangement in a Tricyclo[7.1.1.02,7]Undecane. *Helv. Chim. Acta* **1989**, *72* (4), 767–773.
(104) Jasperse, C. P.; Curran, D. P.; Fevig, T. L. Radical Reactions in Natural Product Synthesis. *Chem. Rev.* **1991**, *91* (6), 1237–1286.
(105) Chenneberg, L.; Baralle, A.; Daniel, M.; Fensterbank, L.; Goddard, J.-P.; Ollivier, C. Visible Light Photocatalytic Reduction of O-Thiocarbamates: Development of a Tin-Free Barton–McCombie Deoxygenation Reaction. *Adv. Synth. Catal.* **2014**, *356* (13), 2756–2762.
(106) Rackl, D.; Kais, V.; Kreitmeier, P.; Reiser, O. Visible Light Photoredox-Catalyzed Deoxygenation of Alcohols. *Beilstein J. Org. Chem.* **2014**, *10* (1), 2157–2165.
(107) Spletstoser, J. T.; White, J. M.; Tunoori, A. R.; Georg, G. I. Mild and Selective Hydrozirconation of Amides to Aldehydes Using Cp2Zr(H)Cl: Scope and Mechanistic Insight. *J. Am. Chem. Soc.* **2007**, *129* (11), 3408–3419.
(108) Nicolaou, K. C.; Estrada, A. A.; Zak, M.; Lee, S. H.; Safina, B. S. A Mild and Selective Method for the Hydrolysis of Esters with Trimethyltin Hydroxide. *Angew. Chem. Int. Ed.* **2005**, *44* (9), 1378–1382.
(109) Lovrić, M.; Cepanec, I.; Litvić, M.; Bartolinčić, A.; Vinković, V. Scope and Limitations of Sodium and Potassium Trimethylsilanolate as Reagents for Conversion of Esters to Carboxylic Acids. *Croat. Chem. Acta* **2007**, *80* (1), 109–115.
(110) Guo, H.; Kato, D.; Kirschberg, T.; Liu, H.; Link, J.; Mitchell, M.; Parrish, J.; Squires, N.; Sun, J.; Taylor, J.; et al. Antiviral Compounds. WO2010132601 (A1), November 18, 2010.
(111) Ding, P.; Miller, M. J.; Chen, Y.; Helquist, P.; Oliver, A. J.; Wiest, O. Syntheses of Conformationally Constricted Molecules as Potential NAALADase/PSMA Inhibitors. *Org. Lett.* **2004**, *6* (11), 1805–1808.
(112) Tullberg, M.; Grøtli, M.; Luthman, K. Efficient Synthesis of 2,5-Diketopiperazines Using Microwave Assisted Heating. *Tetrahedron* **2006**, *62* (31), 7484–7491.
(113) Guo, Z.-X.; Haines, A. H.; Taylor, R. J. K. The Reaction of Dilithium Tetrachlorocuprate and Dilithium Tetrabromonickelate with Unsaturated Epoxides: The Preparation of Novel Analogues of the Antiviral Agent, Bromoconduritol. *Synlett* **1993**, *1993* (08), 607–608.

(114) Adam, W.; Chan, Y. Y.; Cremer, D.; Gauss, J.; Scheutzow, D.; Schindler, M. Spectral and Chemical Properties of Dimethyldioxirane as Determined by Experiment and Ab Initio Calculations. *J. Org. Chem.* **1987**, *52* (13), 2800–2803.
(115) Mower, M. P.; Blackmond, D. G. Mechanistic Rationalization of Unusual Sigmoidal Kinetic Profiles in the Machetti–De Sarlo Cycloaddition Reaction. *J. Am. Chem. Soc.* **2015**, *137* (6), 2386–2391.
(116) McElroy, W. T.; DeShong, P. Synthesis of the CD-Ring of the Anticancer Agent Streptonigrin: Studies of Aryl–Aryl Coupling Methodologies. *Tetrahedron* **2006**, *62* (29), 6945–6954.

Appendix 1

Spectra Relevant to Chapter 2:

A Synthetic Strategy Toward the Oxazinyl Natural Products Gliovirin and the Trichodermamides

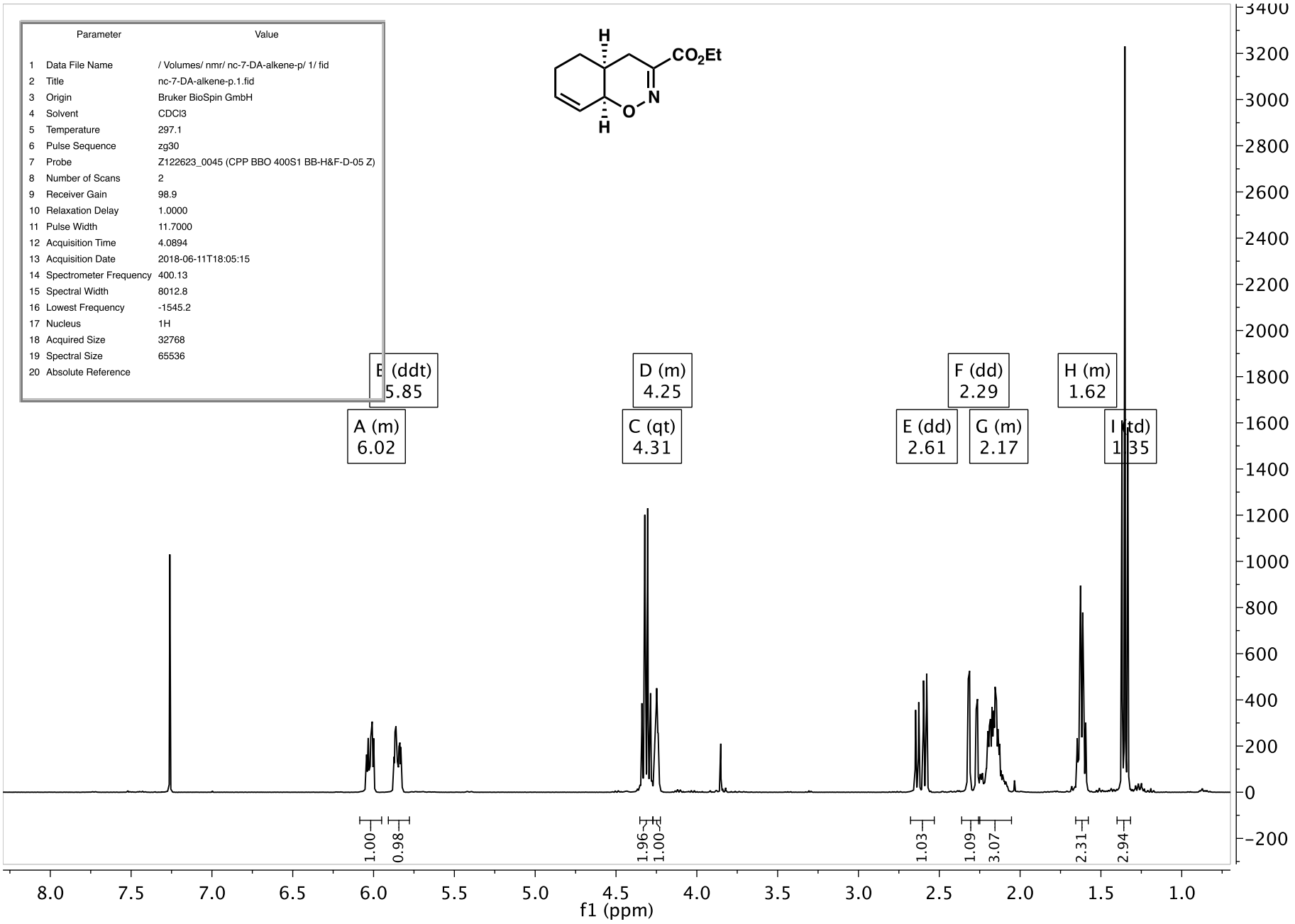
Parameter Value
1 Data File Name / Volumes/ nmr/ nc-7-DA-alkene-p/ 1/ fid
2 Title nc-7-DA-alkene-p.1.fid
3 Origin Bruker BioSpin GmbH
4 Solvent CDCl3
5 Temperature 297.1
6 Pulse Sequence zg30
7 Probe Z122623_0045 (CPP BBO 400S1 BB-H&F-D-05 Z)
8 Number of Scans 2
9 Receiver Gain 98.9
10 Relaxation Delay 1.0000
11 Pulse Width 11.7000
12 Acquisition Time 4.0894
13 Acquisition Date 2018-06-11T18:05:15
14 Spectrometer Frequency 400.13
15 Spectral Width 8012.8
16 Lowest Frequency -1545.2
17 Nucleus 1H
18 Acquired Size 32768
19 Spectral Size 65536
20 Absolute Reference
H
CO2Et
N
O
H
B (ddt) 5.85
A (m) 6.02
D (m) 4.25
C (qt) 4.31
F (dd) 2.29
E (dd) 2.61
G (m) 2.17
H (m) 1.62
I (td) 1.35
1.00
0.98
1.96
1.00
1.03
1.09
3.07
2.31
2.94
8.0
7.5
7.0
6.5
6.0
5.5
5.0
4.5
4.0
3.5
3.0
2.5
2.0
1.5
1.0
f1 (ppm)
3400
3200
3000
2800
2600
2400
2200
2000
1800
1600
1400
1200
1000
800
600
400
200
0
-200

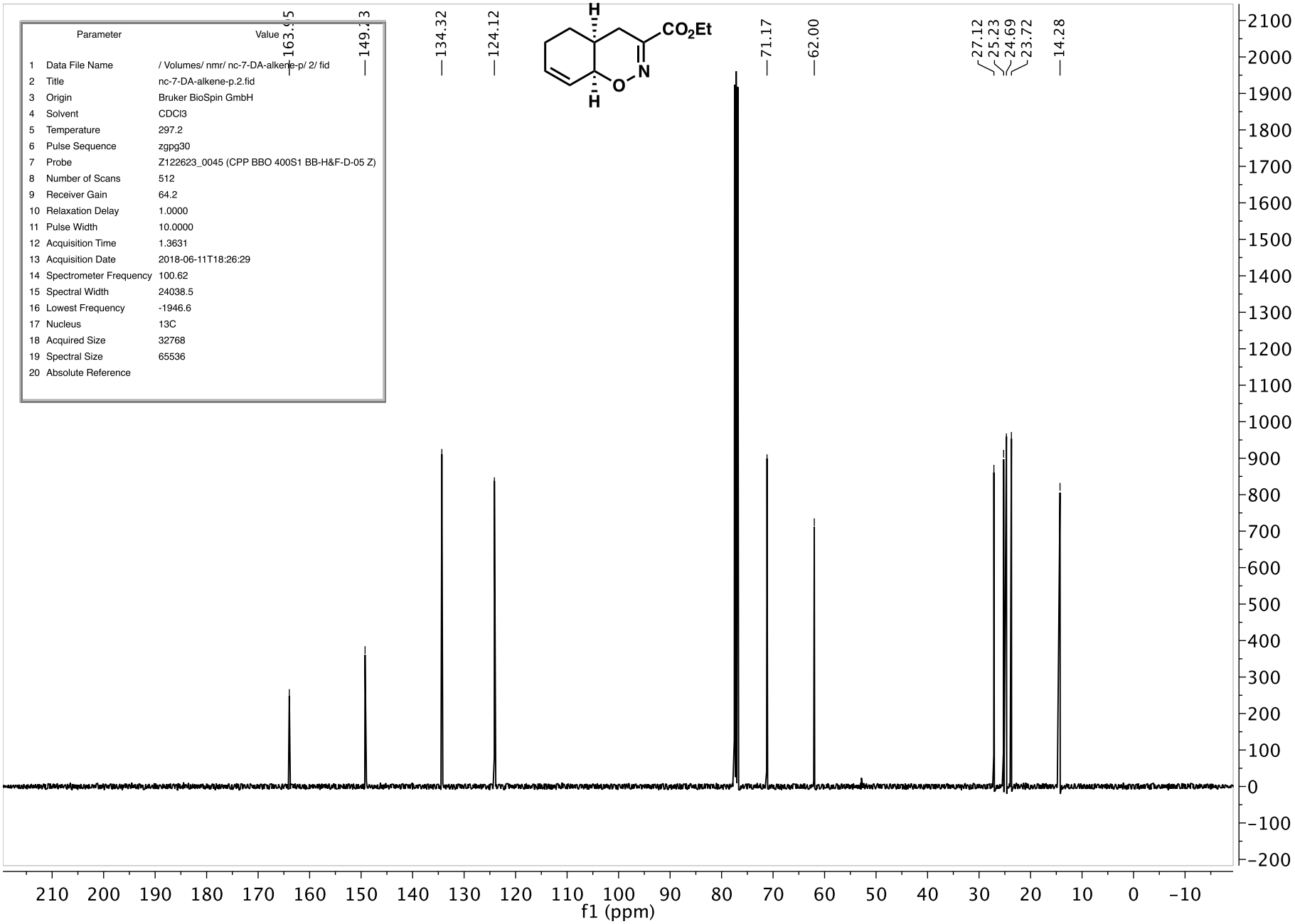
Parameter Value
1 Data File Name / Volumes/ nmr/ nc-7-DA-alkene-p/ 2/ fid
2 Title nc-7-DA-alkene-p.2.fid
3 Origin Bruker BioSpin GmbH
4 Solvent CDCl3
5 Temperature 297.2
6 Pulse Sequence zgpg30
7 Probe Z122623_0045 (CPP BBO 400S1 BB-H&F-D-05 Z)
8 Number of Scans 512
9 Receiver Gain 64.2
10 Relaxation Delay 1.0000
11 Pulse Width 10.0000
12 Acquisition Time 1.3631
13 Acquisition Date 2018-06-11T18:26:29
14 Spectrometer Frequency 100.62
15 Spectral Width 24038.5
16 Lowest Frequency -1946.6
17 Nucleus 13C
18 Acquired Size 32768
19 Spectral Size 65536
20 Absolute Reference
163.95
149.23
134.32
124.12
71.17
62.00
27.12
25.23
24.69
23.72
14.28
H
CO2Et
N
O
H
f1 (ppm)

	Parameter	Value
1	Data File Name	/ Volumes/ data-1/ nc-7-DA-red-majPdt/ PROTON01.fid/ fid
2	Title	PROTON01
3	Origin	Varian
4	Spectrometer	inova
5	Solvent	cdcl3
6	Temperature	25.0
7	Pulse Sequence	s2pul
8	Experiment	1D
9	Probe	autox7991
10	Number of Scans	4
11	Receiver Gain	52
12	Relaxation Delay	1.0000
13	Pulse Width	5.8000
14	Acquisition Date	2018-06-21T16:40:55
15	Spectrometer Frequency	499.64
16	Spectral Width	8000.0
17	Lowest Frequency	-1015.2
18	Nucleus	1H
19	Acquired Size	80000
20	Spectral Size	262144

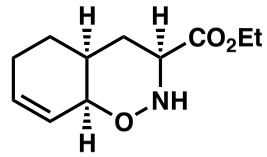

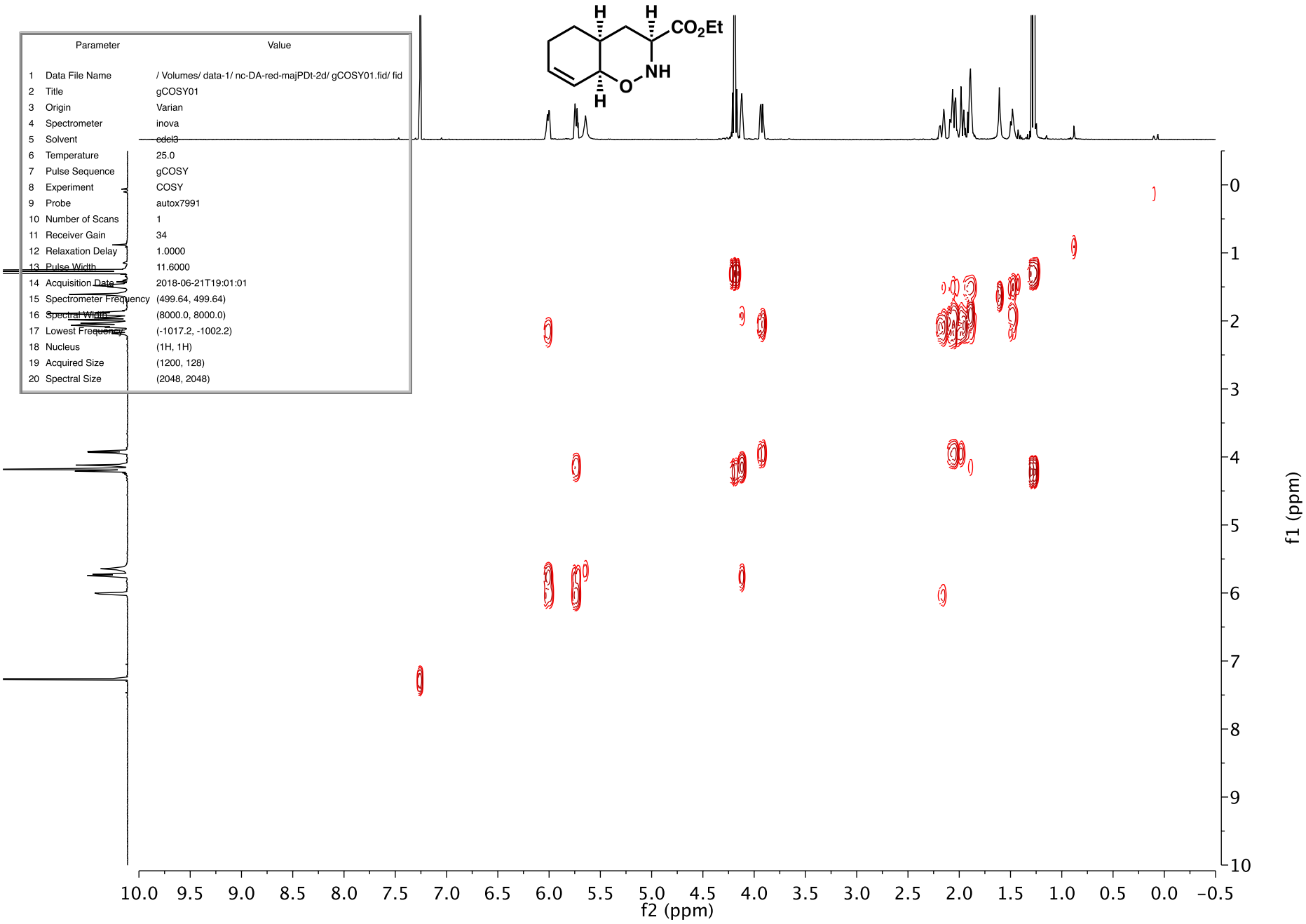
H
H
CO2Et
NH
O
H
Parameter
Value
1 Data File Name / Volumes/ data-1/ nc-DA-red-majPDt-2d/ gCOSY01.fid/ fid
2 Title gCOSY01
3 Origin Varian
4 Spectrometer inova
5 Solvent cdcl3
6 Temperature 25.0
7 Pulse Sequence gCOSY
8 Experiment COSY
9 Probe autox7991
10 Number of Scans 1
11 Receiver Gain 34
12 Relaxation Delay 1.0000
13 Pulse Width 11.6000
14 Acquisition Date 2018-06-21T19:01:01
15 Spectrometer Frequency (499.64, 499.64)
16 Spectral Width (8000.0, 8000.0)
17 Lowest Frequency (-1017.2, -1002.2)
18 Nucleus (1H, 1H)
19 Acquired Size (1200, 128)
20 Spectral Size (2048, 2048)
10.0 9.5 9.0 8.5 8.0 7.5 7.0 6.5 6.0 5.5 5.0 4.5 4.0 3.5 3.0 2.5 2.0 1.5 1.0 0.5 0.0 -0.5
f2 (ppm)
0 1 2 3 4 5 6 7 8 9 10
f1 (ppm)

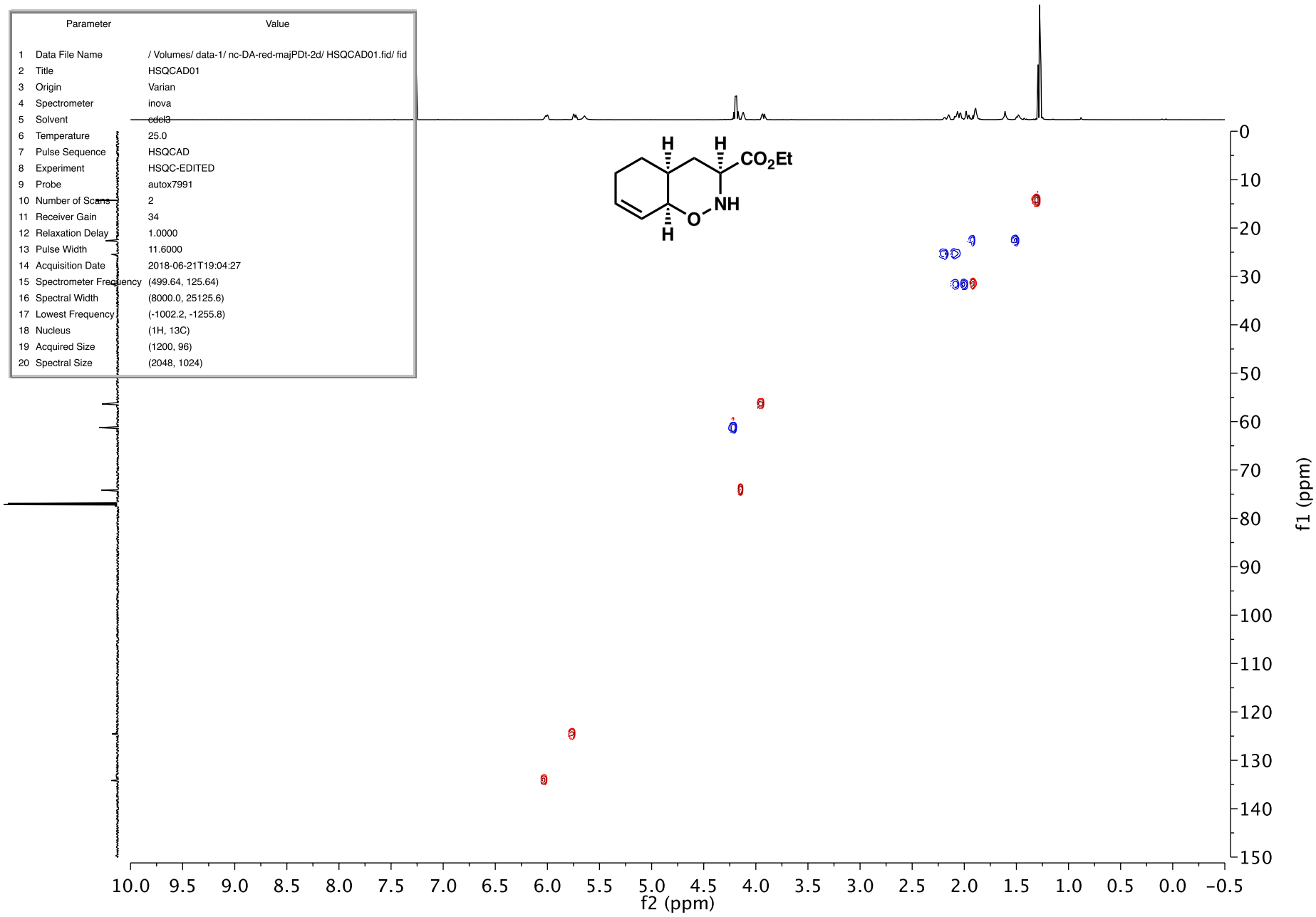
Parameter Value
1 Data File Name / Volumes/ data-1/ nc-DA-red-majPDt-2d/ HSQCAD01.fid/ fid
2 Title HSQCAD01
3 Origin Varian
4 Spectrometer inova
5 Solvent cdcl3
6 Temperature 25.0
7 Pulse Sequence HSQCAD
8 Experiment HSQC-EDITED
9 Probe autox7991
10 Number of Scans 2
11 Receiver Gain 34
12 Relaxation Delay 1.0000
13 Pulse Width 11.6000
14 Acquisition Date 2018-06-21T19:04:27
15 Spectrometer Frequency (499.64, 125.64)
16 Spectral Width (8000.0, 25125.6)
17 Lowest Frequency (-1002.2, -1255.8)
18 Nucleus (1H, 13C)
19 Acquired Size (1200, 96)
20 Spectral Size (2048, 1024)
H
H
CO2Et
NH
O
H
f2 (ppm)
f1 (ppm)

	Parameter	Value
1	Data File Name	/ Volumes/ data-1/ nc-7-DA-red-majPdt/ CARBON01.fid/ fid
2	Title	CARBON01
3	Origin	Varian
4	Spectrometer	inova
5	Solvent	cdcl3
6	Temperature	25.0
7	Pulse Sequence	s2pul
8	Experiment	1D
9	Probe	autox7991
10	Number of Scans	1000
11	Receiver Gain	30
12	Relaxation Delay	1.0000
13	Pulse Width	4.6125
14	Acquisition Date	2018-06-21T16:41:55
15	Spectrometer Frequency	125.65
16	Spectral Width	31446.5
17	Lowest Frequency	-1887.4
18	Nucleus	13C
19	Acquired Size	32768
20	Spectral Size	65536

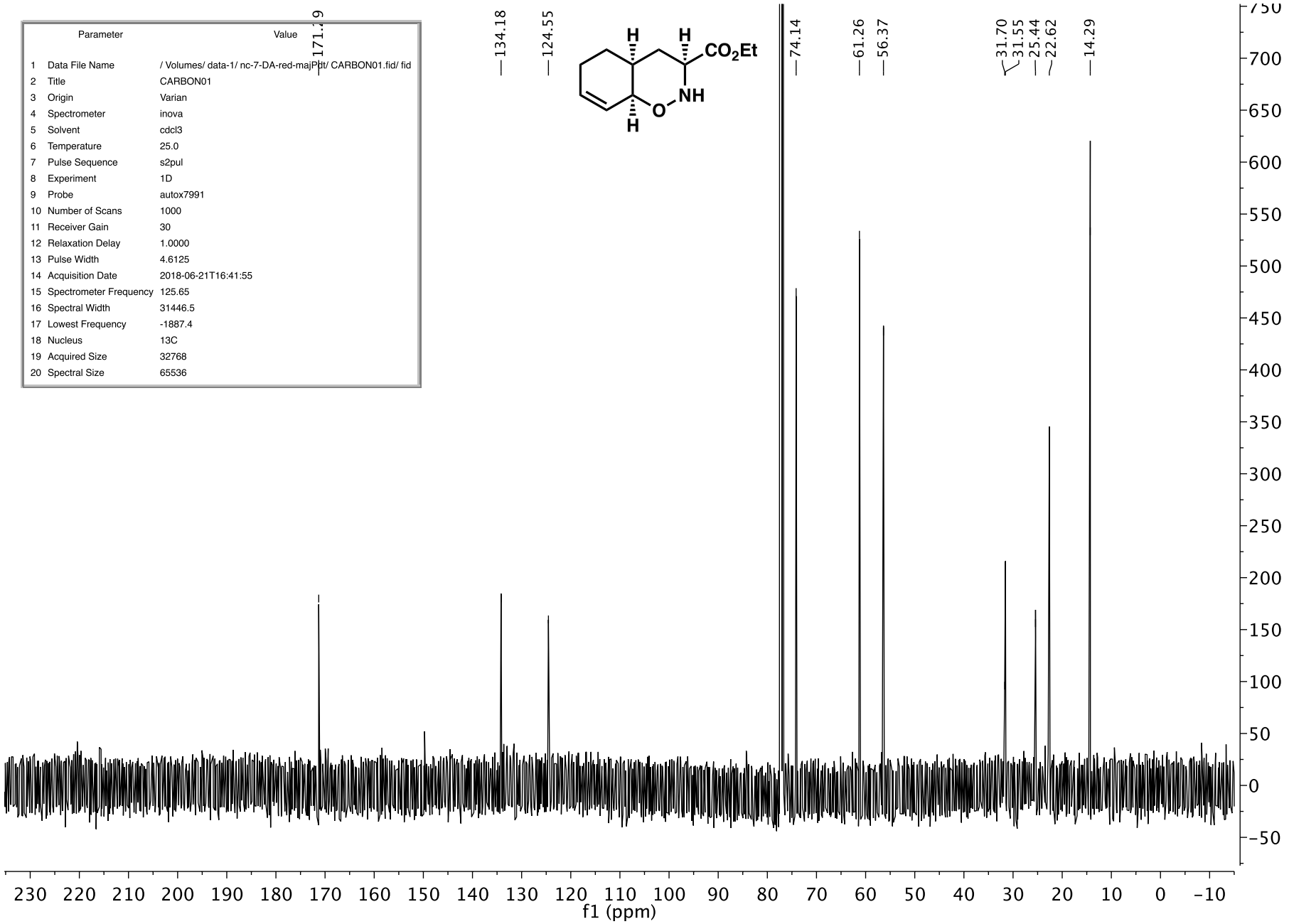

	Parameter	Value
1	Data File Name	/ Volumes/ nmrdata/ ncowper/ nmr/ nc-7-epox-DA/ 1/ fid
2	Title	nc-7-epox-DA.1.fid
3	Origin	Bruker BioSpin GmbH
4	Solvent	CDCl3
5	Temperature	295.2
6	Pulse Sequence	zg30
7	Probe	Z122623_0045 (CPP BBO 400S1 BB-H&F-D-05 Z)
8	Number of Scans	16
9	Receiver Gain	156.2
10	Relaxation Delay	1.0000
11	Pulse Width	11.7000
12	Acquisition Time	4.0894
13	Acquisition Date	2018-06-24T22:13:32
14	Spectrometer Frequency	400.13
15	Spectral Width	8012.8
16	Lowest Frequency	-1545.2
17	Nucleus	1H
18	Acquired Size	32768
19	Spectral Size	65536
20	Absolute Reference	

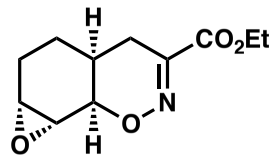

	Parameter	Value
1	Data File Name	/ Volumes/ nmrdata/ ncowper/ nmr/ nc-7-epox-DA/ 2/ ser
2	Title	nc-7-epox-DA.2.ser
3	Origin	Bruker BioSpin GmbH
4	Solvent	CDCl3
5	Temperature	295.1
6	Pulse Sequence	cosygpppqf
7	Probe	Z122623_0045 (CPP BBO 400S1 BB-H&F-D-05 Z)
8	Number of Scans	1
9	Receiver Gain	64.2
10	Relaxation Delay	2.0000
11	Pulse Width	11.7000
12	Acquisition Time	0.1970
13	Acquisition Date	2018-06-24T22:14:26
14	Spectrometer Frequency	(400.13, 400.13)
15	Spectral Width	(5197.5, 5197.5)
16	Lowest Frequency	(-198.0, -198.0)
17	Nucleus	(1H, 1H)
18	Acquired Size	(1024, 128)
19	Spectral Size	(1024, 1024)

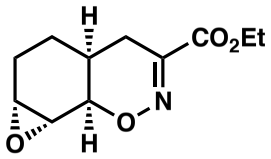

	Parameter	Value
1	Data File Name	/ Volumes/ nmrdata/ ncowper/ nmr/ nc-7-epox-DA/ 3/ fid
2	Title	nc-7-epox-DA.3.fid
3	Origin	Bruker BioSpin GmbH
4	Solvent	CDCl3
5	Temperature	295.1
6	Pulse Sequence	zgpg30
7	Probe	Z122623_0045 (CPP BBO 400S1 BB-H&F-D-05 Z)
8	Number of Scans	1024
9	Receiver Gain	78.7
10	Relaxation Delay	1.0000
11	Pulse Width	10.0000
12	Acquisition Time	1.3631
13	Acquisition Date	2018-06-24T23:01:20
14	Spectrometer Frequency	100.62
15	Spectral Width	24038.5
16	Lowest Frequency	-1946.0
17	Nucleus	13C
18	Acquired Size	32768
19	Spectral Size	65536
20	Absolute Reference	

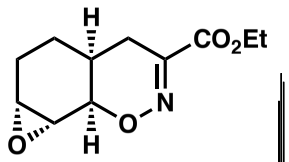

	Parameter	Value
1	Data File Name	/ Volumes/ nmr/ nc-si-propargyl triflate/ 1/ fid
2	Title	nc-si-propargyl triflate.1.fid
3	Origin	Bruker BioSpin GmbH
4	Solvent	CDCl3
5	Temperature	295.1
6	Pulse Sequence	zg30
7	Probe	Z122623_0045 (CPP BBO 400S1 BB-H&F-D-05 Z)
8	Number of Scans	16
9	Receiver Gain	78.7
10	Relaxation Delay	1.0000
11	Pulse Width	11.7000
12	Acquisition Time	4.0894
13	Acquisition Date	2018-07-01T09:15:34
14	Spectrometer Frequency	400.13
15	Spectral Width	8012.8
16	Lowest Frequency	-1545.2
17	Nucleus	1H
18	Acquired Size	32768
19	Spectral Size	65536
20	Absolute Reference	

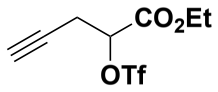

	Parameter	Value
1	Data File Name	/ Volumes/ nmr/ nc-si-propargyl triflate/ 2/ fid
2	Title	nc-si-propargyl triflate.2.fid
3	Origin	Bruker BioSpin GmbH
4	Solvent	CDCl3
5	Temperature	295.2
6	Pulse Sequence	zgpg30
7	Probe	Z122623_0045 (CPP BBO 400S1 BB-H&F-D-05 Z)
8	Number of Scans	512
9	Receiver Gain	55.5
10	Relaxation Delay	1.0000
11	Pulse Width	10.0000
12	Acquisition Time	1.3631
13	Acquisition Date	2018-07-01T09:36:48
14	Spectrometer Frequency	100.62
15	Spectral Width	24038.5
16	Lowest Frequency	-1944.9
17	Nucleus	13C
18	Acquired Size	32768
19	Spectral Size	65536
20	Absolute Reference	

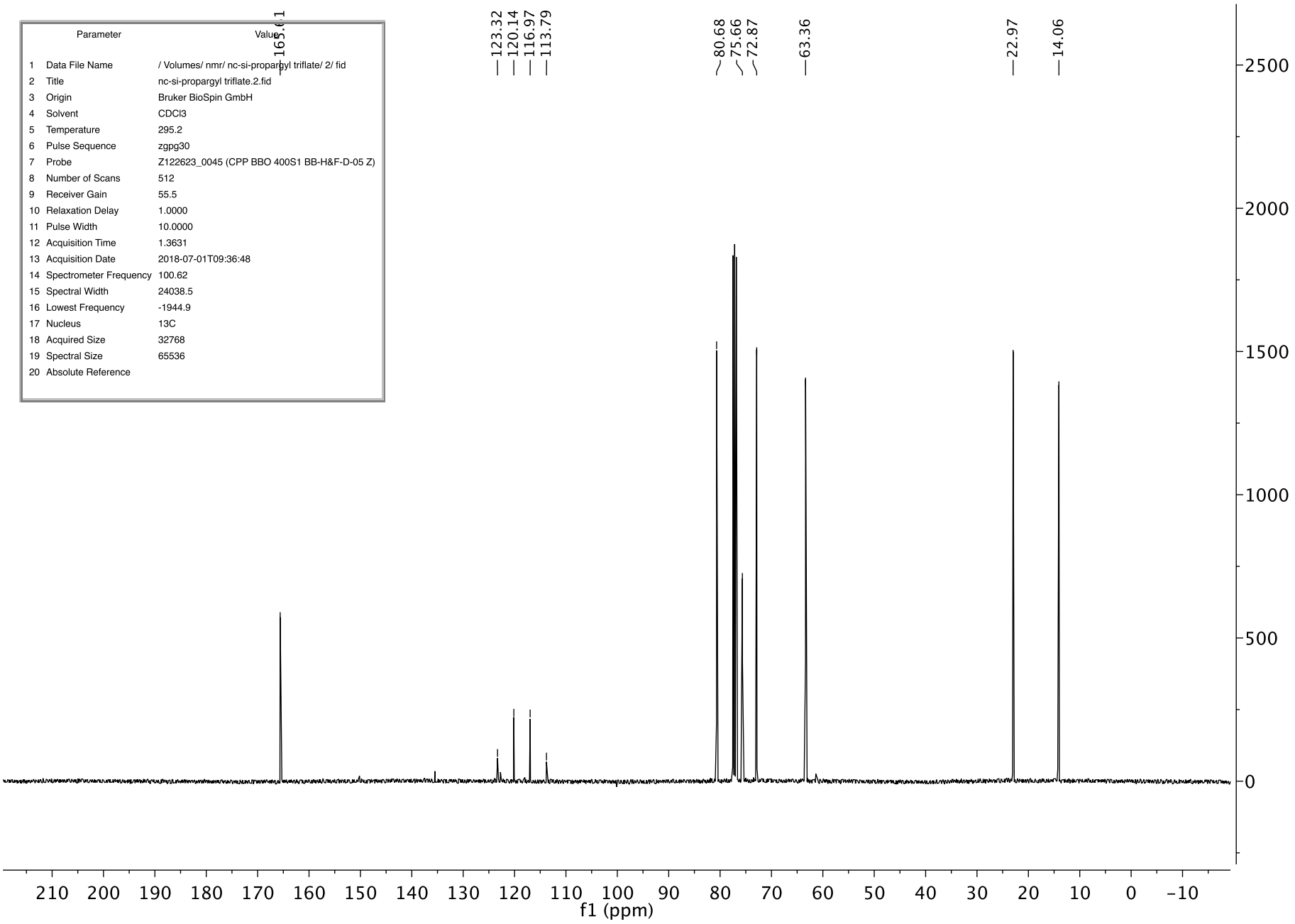

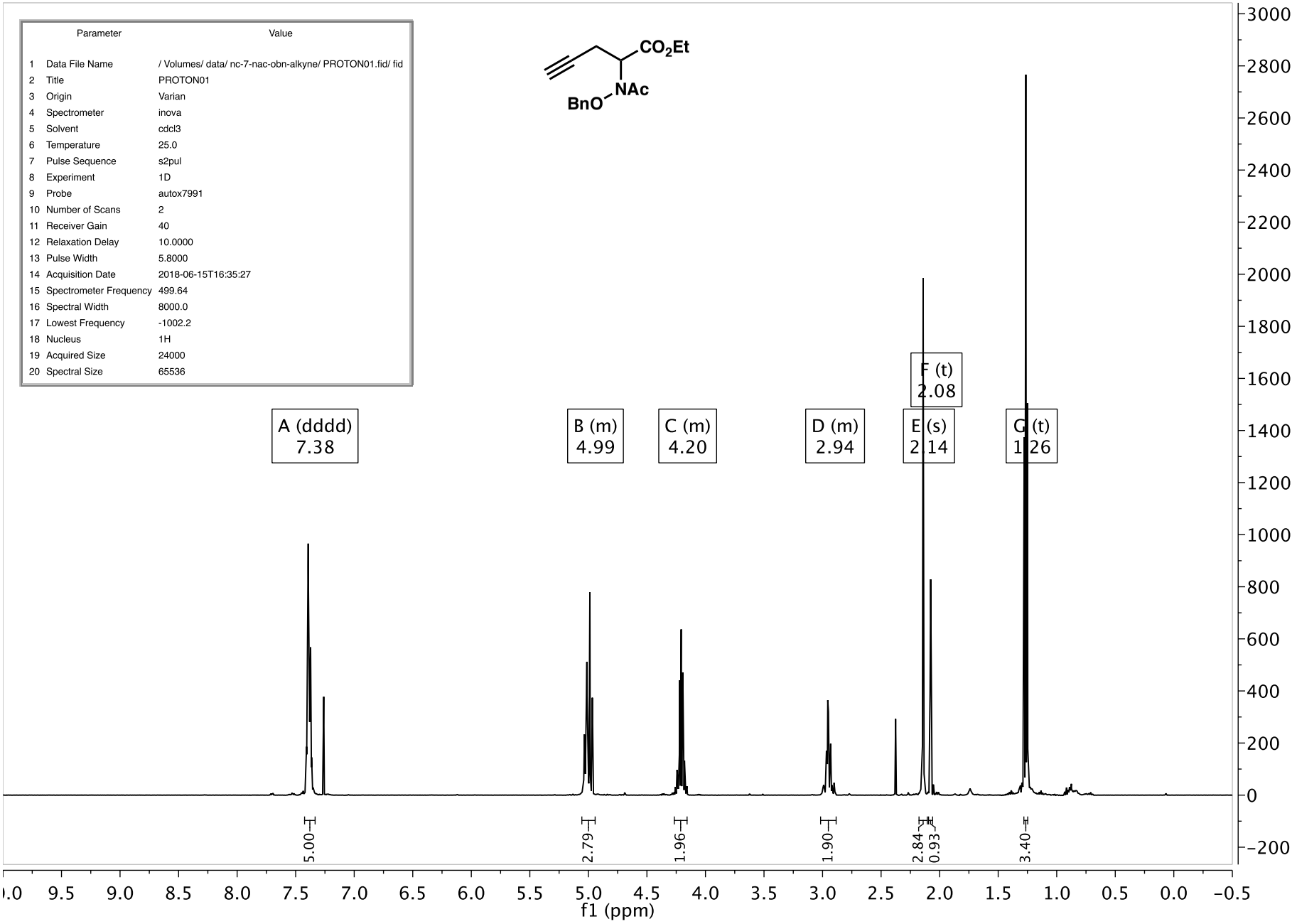
Parameter Value
1 Data File Name / Volumes/ data/ nc-7-nac-obn-alkyne/ PROTON01.fid/ fid
2 Title PROTON01
3 Origin Varian
4 Spectrometer inova
5 Solvent cdcl3
6 Temperature 25.0
7 Pulse Sequence s2pul
8 Experiment 1D
9 Probe autox7991
10 Number of Scans 2
11 Receiver Gain 40
12 Relaxation Delay 10.0000
13 Pulse Width 5.8000
14 Acquisition Date 2018-06-15T16:35:27
15 Spectrometer Frequency 499.64
16 Spectral Width 8000.0
17 Lowest Frequency -1002.2
18 Nucleus 1H
19 Acquired Size 24000
20 Spectral Size 65536
CO2Et
NAc
BnO
A (dddd) 7.38
B (m) 4.99
C (m) 4.20
D (m) 2.94
E (s) 2.14
F (t) 2.08
G (t) 1.26
5.00
2.79
1.96
1.90
2.84
0.93
3.40
f1 (ppm)

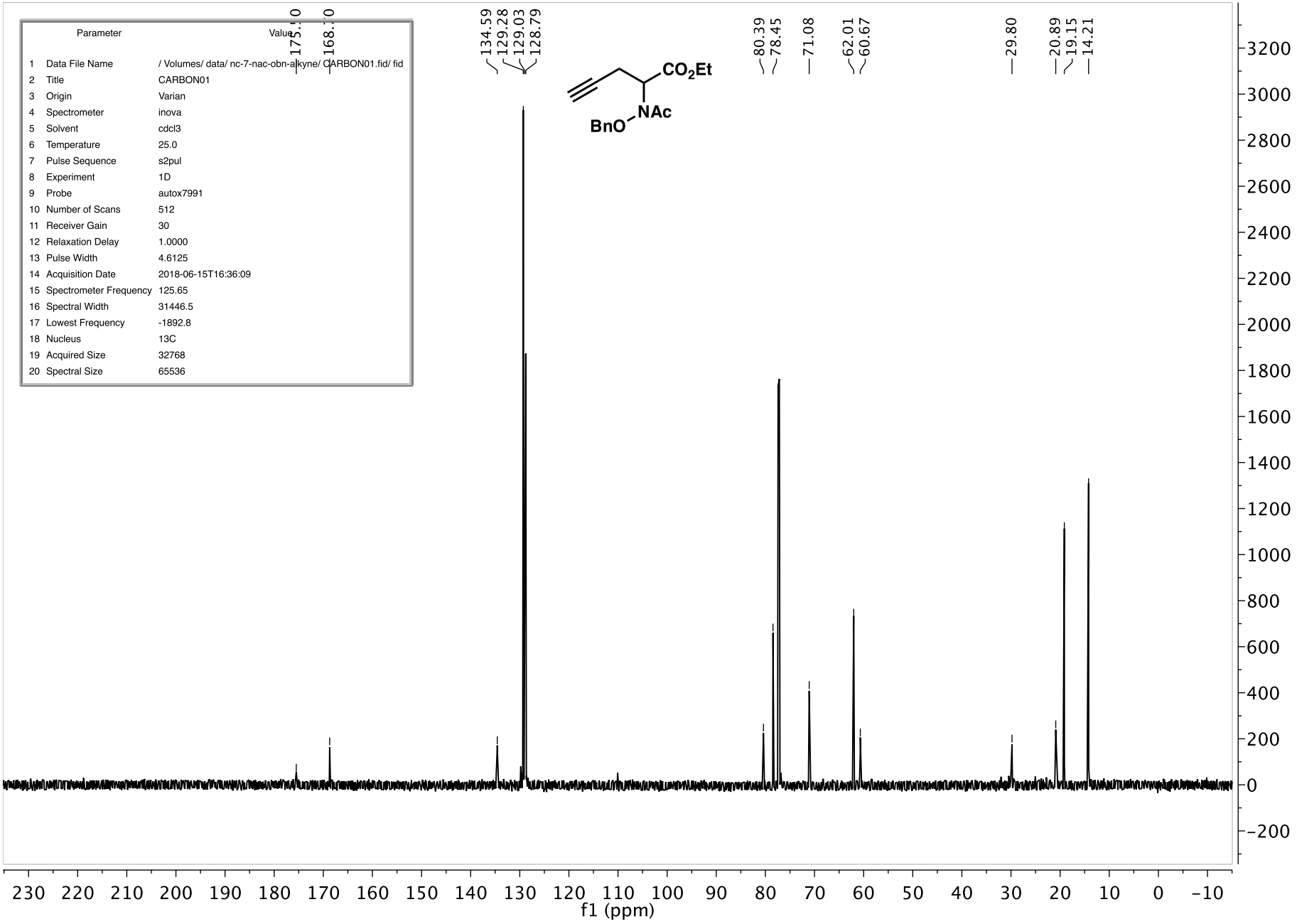
Parameter Value
1 Data File Name / Volumes/ data/ nc-7-nac-obn-alkyne/ CARBON01.fid/ fid
2 Title CARBON01
3 Origin Varian
4 Spectrometer inova
5 Solvent cdcl3
6 Temperature 25.0
7 Pulse Sequence s2pul
8 Experiment 1D
9 Probe autox7991
10 Number of Scans 512
11 Receiver Gain 30
12 Relaxation Delay 1.0000
13 Pulse Width 4.6125
14 Acquisition Date 2018-06-15T16:36:09
15 Spectrometer Frequency 125.65
16 Spectral Width 31446.5
17 Lowest Frequency -1892.8
18 Nucleus 13C
19 Acquired Size 32768
20 Spectral Size 65536
175.10
168.10
134.59
129.28
129.03
128.79
80.39
78.45
71.08
62.01
60.67
29.80
20.89
19.15
14.21
CO2Et
NAc
BnO
f1 (ppm)

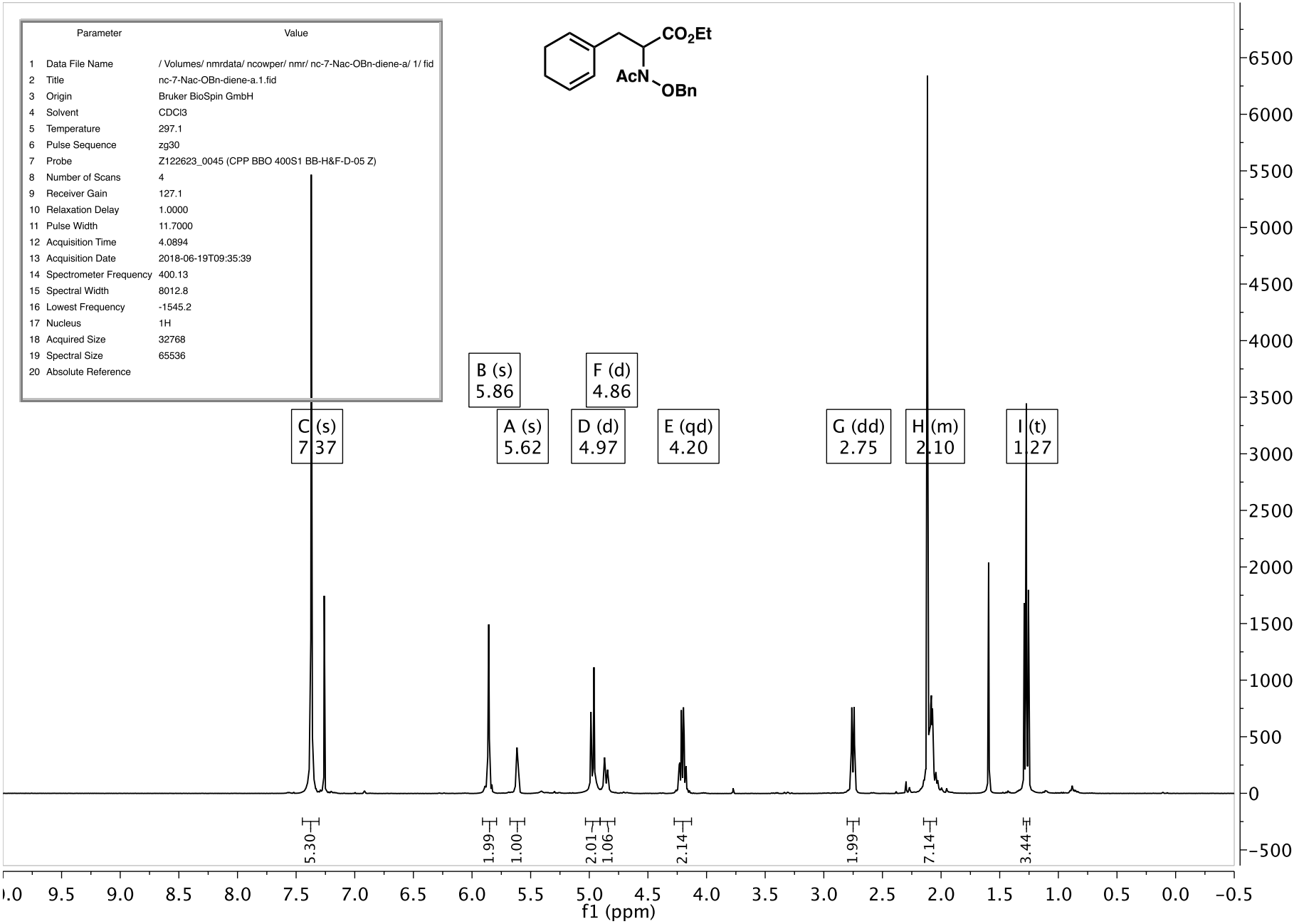
Parameter Value
1 Data File Name / Volumes/ nmrdata/ ncowper/ nmr/ nc-7-Nac-OBn-diene-a/ 1/ fid
2 Title nc-7-Nac-OBn-diene-a.1.fid
3 Origin Bruker BioSpin GmbH
4 Solvent CDCl3
5 Temperature 297.1
6 Pulse Sequence zg30
7 Probe Z122623_0045 (CPP BBO 400S1 BB-H&F-D-05 Z)
8 Number of Scans 4
9 Receiver Gain 127.1
10 Relaxation Delay 1.0000
11 Pulse Width 11.7000
12 Acquisition Time 4.0894
13 Acquisition Date 2018-06-19T09:35:39
14 Spectrometer Frequency 400.13
15 Spectral Width 8012.8
16 Lowest Frequency -1545.2
17 Nucleus 1H
18 Acquired Size 32768
19 Spectral Size 65536
20 Absolute Reference
CO2Et
AcN
OBn
C (s) 7.37
B (s) 5.86
A (s) 5.62
F (d) 4.86
D (d) 4.97
E (qd) 4.20
G (dd) 2.75
H (m) 2.10
I (t) 1.27
5.30
1.99
1.00
2.01
1.06
2.14
1.99
7.14
3.44
f1 (ppm)

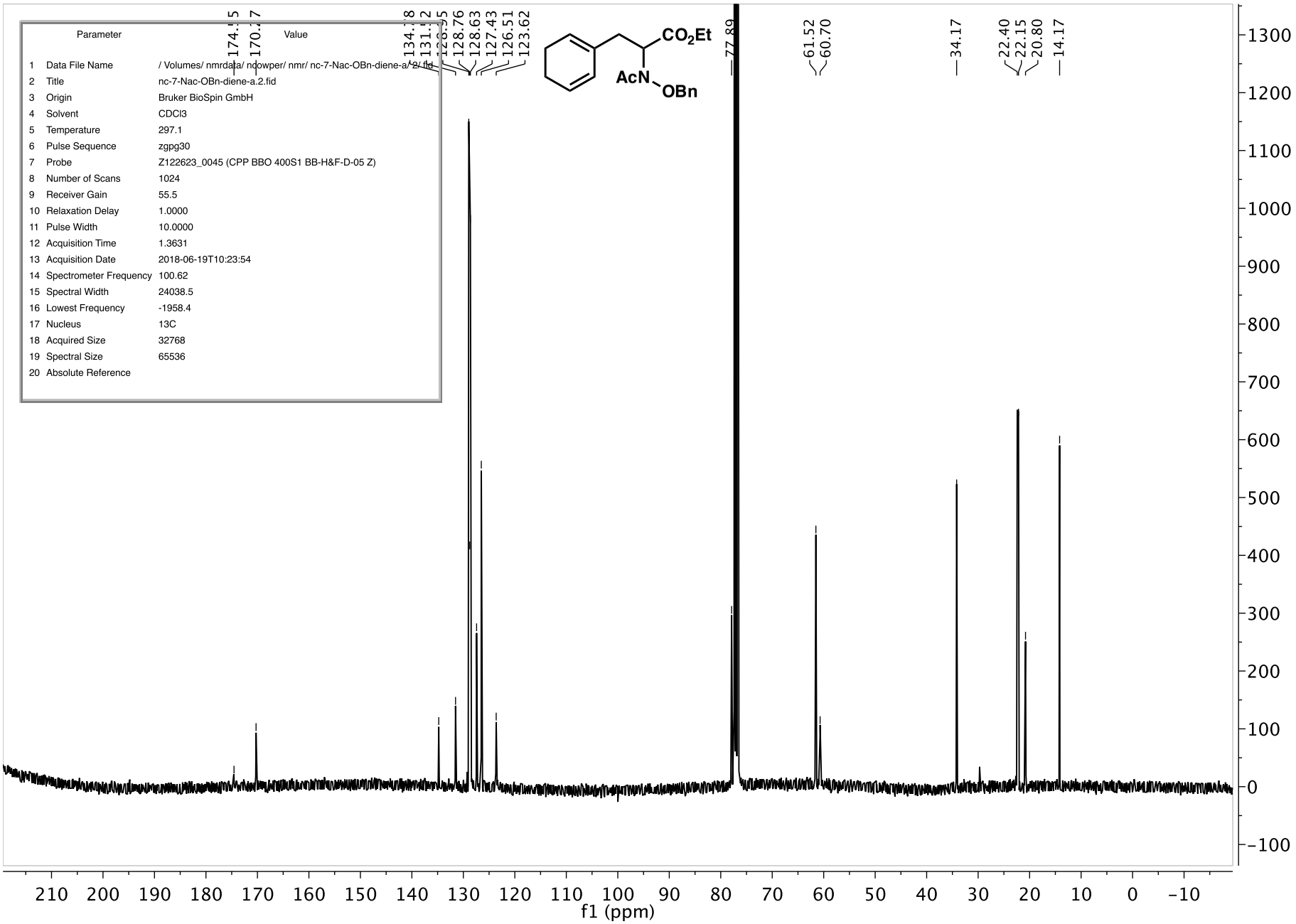
Parameter Value
1 Data File Name / Volumes/ nmrdata/ ndowper/ nmr/ nc-7-Nac-OBn-diene-a/2/fid
2 Title nc-7-Nac-OBn-diene-a.2.fid
3 Origin Bruker BioSpin GmbH
4 Solvent CDCl3
5 Temperature 297.1
6 Pulse Sequence zgpg30
7 Probe Z122623_0045 (CPP BBO 400S1 BB-H&F-D-05 Z)
8 Number of Scans 1024
9 Receiver Gain 55.5
10 Relaxation Delay 1.0000
11 Pulse Width 10.0000
12 Acquisition Time 1.3631
13 Acquisition Date 2018-06-19T10:23:54
14 Spectrometer Frequency 100.62
15 Spectral Width 24038.5
16 Lowest Frequency -1958.4
17 Nucleus 13C
18 Acquired Size 32768
19 Spectral Size 65536
20 Absolute Reference
174.15
170.27
134.18
131.12
128.76
128.63
127.43
126.51
123.62
77.89
61.52
60.70
34.17
22.40
22.15
20.80
14.17
CO2Et
AcN
OBn
f1 (ppm)

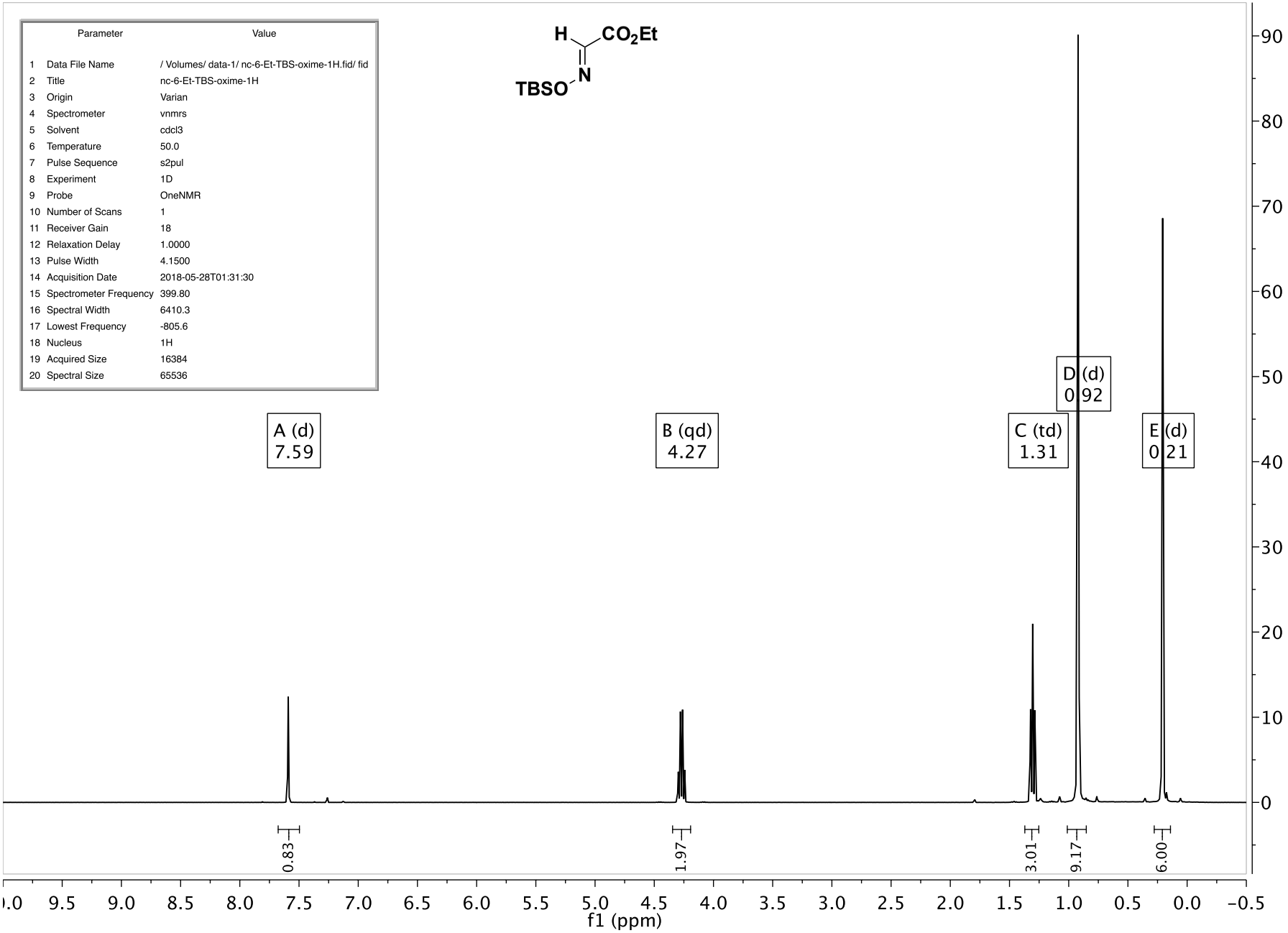
Parameter Value
1 Data File Name / Volumes/ data-1/ nc-6-Et-TBS-oxime-1H.fid/ fid
2 Title nc-6-Et-TBS-oxime-1H
3 Origin Varian
4 Spectrometer vnmrs
5 Solvent cdcl3
6 Temperature 50.0
7 Pulse Sequence s2pul
8 Experiment 1D
9 Probe OneNMR
10 Number of Scans 1
11 Receiver Gain 18
12 Relaxation Delay 1.0000
13 Pulse Width 4.1500
14 Acquisition Date 2018-05-28T01:31:30
15 Spectrometer Frequency 399.80
16 Spectral Width 6410.3
17 Lowest Frequency -805.6
18 Nucleus 1H
19 Acquired Size 16384
20 Spectral Size 65536
H
CO2Et
N
TBSO
A (d)
7.59
B (qd)
4.27
C (td)
1.31
D (d)
0.92
E (d)
0.21
0.83
1.97
3.01
9.17
6.00
f1 (ppm)

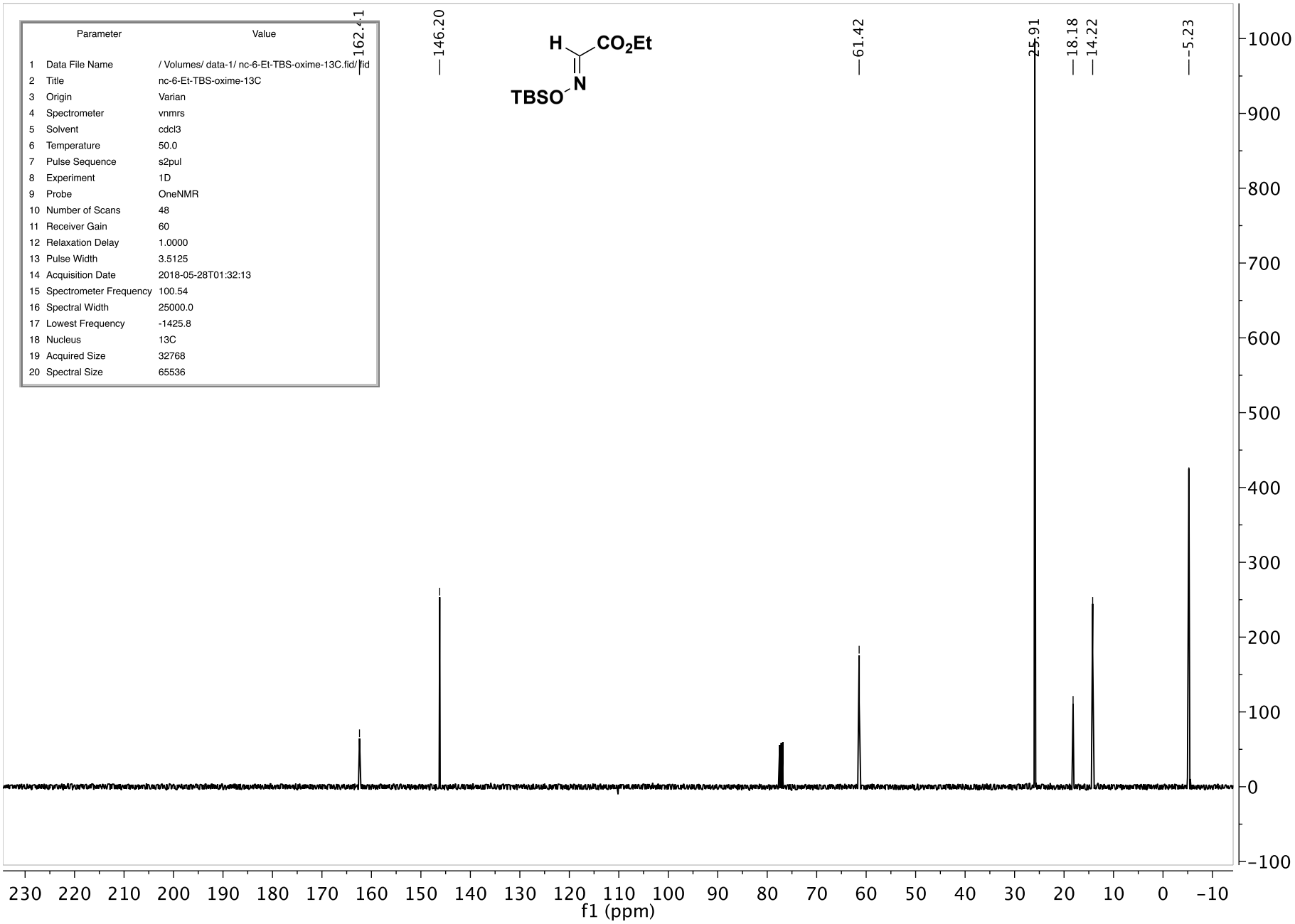
Parameter Value
1 Data File Name / Volumes/ data-1/ nc-6-Et-TBS-oxime-13C.fid/ fid
2 Title nc-6-Et-TBS-oxime-13C
3 Origin Varian
4 Spectrometer vnmrs
5 Solvent cdcl3
6 Temperature 50.0
7 Pulse Sequence s2pul
8 Experiment 1D
9 Probe OneNMR
10 Number of Scans 48
11 Receiver Gain 60
12 Relaxation Delay 1.0000
13 Pulse Width 3.5125
14 Acquisition Date 2018-05-28T01:32:13
15 Spectrometer Frequency 100.54
16 Spectral Width 25000.0
17 Lowest Frequency -1425.8
18 Nucleus 13C
19 Acquired Size 32768
20 Spectral Size 65536
162.41
146.20
61.42
25.91
18.18
14.22
-5.23
H
CO2Et
N
TBSO
1000
900
800
700
600
500
400
300
200
100
0
-100
230 220 210 200 190 180 170 160 150 140 130 120 110 100 90 80 70 60 50 40 30 20 10 0 -10
f1 (ppm)

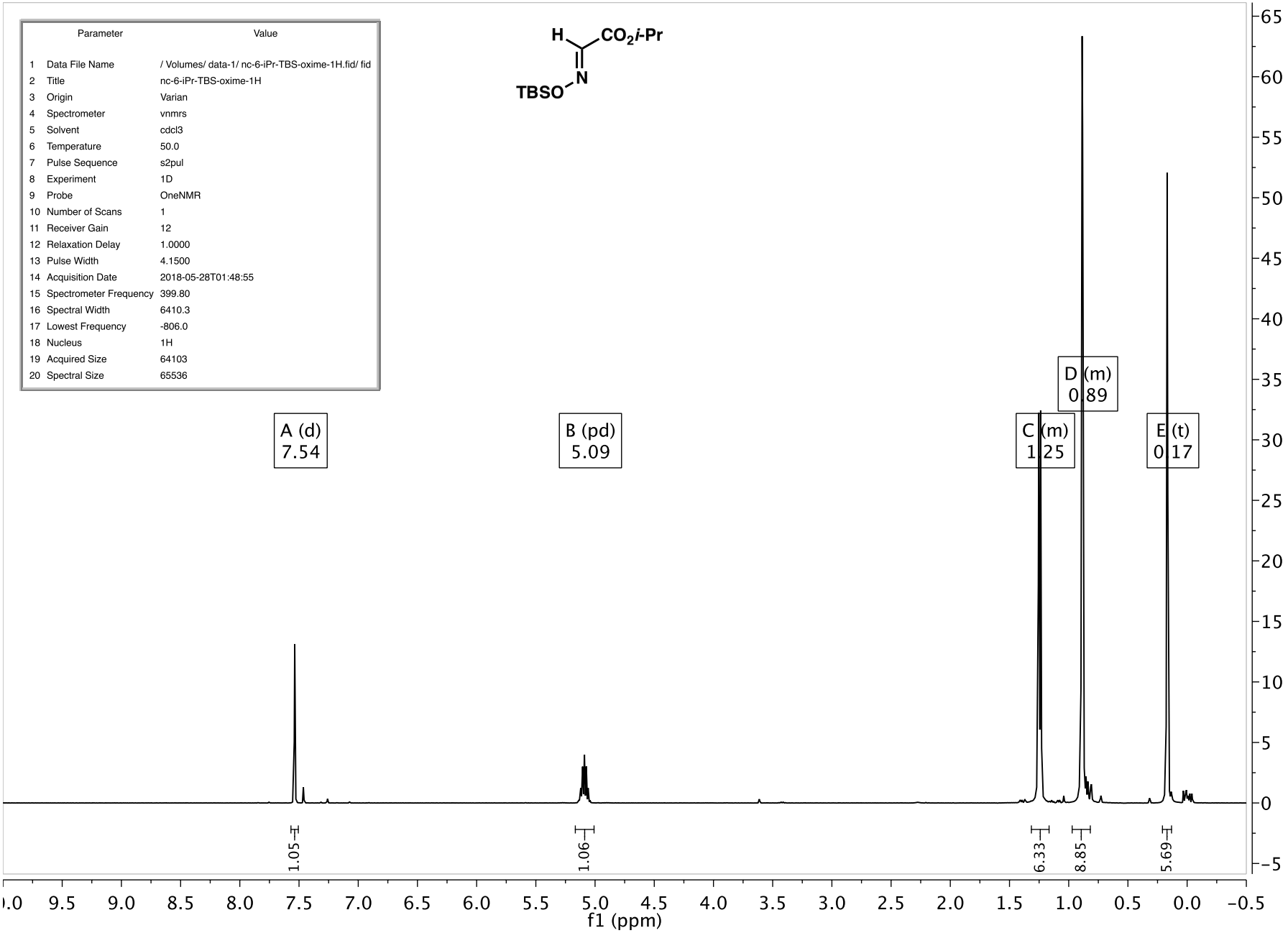
Parameter Value
1 Data File Name / Volumes/ data-1/ nc-6-iPr-TBS-oxime-1H.fid/ fid
2 Title nc-6-iPr-TBS-oxime-1H
3 Origin Varian
4 Spectrometer vnmrs
5 Solvent cdcl3
6 Temperature 50.0
7 Pulse Sequence s2pul
8 Experiment 1D
9 Probe OneNMR
10 Number of Scans 1
11 Receiver Gain 12
12 Relaxation Delay 1.0000
13 Pulse Width 4.1500
14 Acquisition Date 2018-05-28T01:48:55
15 Spectrometer Frequency 399.80
16 Spectral Width 6410.3
17 Lowest Frequency -806.0
18 Nucleus 1H
19 Acquired Size 64103
20 Spectral Size 65536
H
CO2i-Pr
N
TBSO
A (d) 7.54
B (pd) 5.09
C (m) 1.25
D (m) 0.89
E (t) 0.17
1.05
1.06
6.33
8.85
5.69
f1 (ppm)

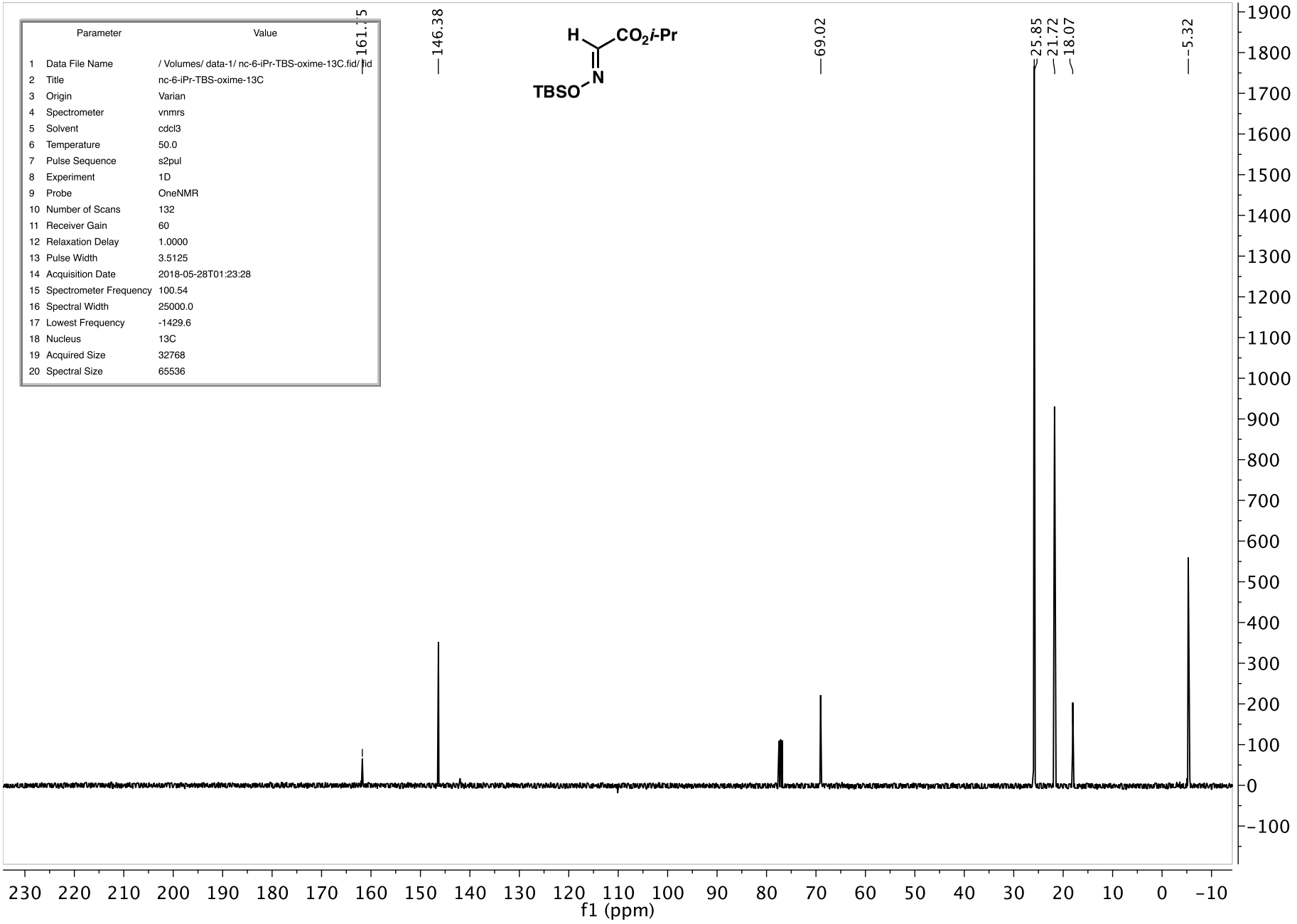
Parameter Value
1 Data File Name / Volumes/ data-1/ nc-6-iPr-TBS-oxime-13C.fid/ fid
2 Title nc-6-iPr-TBS-oxime-13C
3 Origin Varian
4 Spectrometer vnmrs
5 Solvent cdcl3
6 Temperature 50.0
7 Pulse Sequence s2pul
8 Experiment 1D
9 Probe OneNMR
10 Number of Scans 132
11 Receiver Gain 60
12 Relaxation Delay 1.0000
13 Pulse Width 3.5125
14 Acquisition Date 2018-05-28T01:23:28
15 Spectrometer Frequency 100.54
16 Spectral Width 25000.0
17 Lowest Frequency -1429.6
18 Nucleus 13C
19 Acquired Size 32768
20 Spectral Size 65536
161.15
146.38
69.02
25.85
21.72
18.07
-5.32
H
CO2i-Pr
N
TBSO
1900
1800
1700
1600
1500
1400
1300
1200
1100
1000
900
800
700
600
500
400
300
200
100
0
-100
230 220 210 200 190 180 170 160 150 140 130 120 110 100 90 80 70 60 50 40 30 20 10 0 -10
f1 (ppm)

	Parameter	Value
1	Data File Name	/ Volumes/ nmr/ nc-7-et-NH-alkyne/ 1/ fid
2	Title	nc-7-et-NH-alkyne.1.fid
3	Origin	Bruker BioSpin GmbH
4	Solvent	CDCl3
5	Temperature	297.2
6	Pulse Sequence	zg30
7	Probe	Z122623_0045 (CPP BBO 400S1 BB-H&F-D-05 Z)
8	Number of Scans	16
9	Receiver Gain	10.0
10	Relaxation Delay	1.0000
11	Pulse Width	11.7000
12	Acquisition Time	4.0894
13	Acquisition Date	2018-06-08T17:21:52
14	Spectrometer Frequency	400.13
15	Spectral Width	8012.8
16	Lowest Frequency	-1545.0
17	Nucleus	1H
18	Acquired Size	32768
19	Spectral Size	65536
20	Absolute Reference	

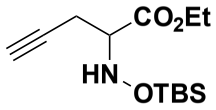

A (s) 5.58
B (q) 4.22
C (t) 3.60
D (dt) 2.55
E (t) 2.00
F (td) 1.27
G (d) 0.86
H (s) 0.08

1.00 2.03 1.00 2.02 0.96 3.15 9.33 6.10

f1 (ppm)

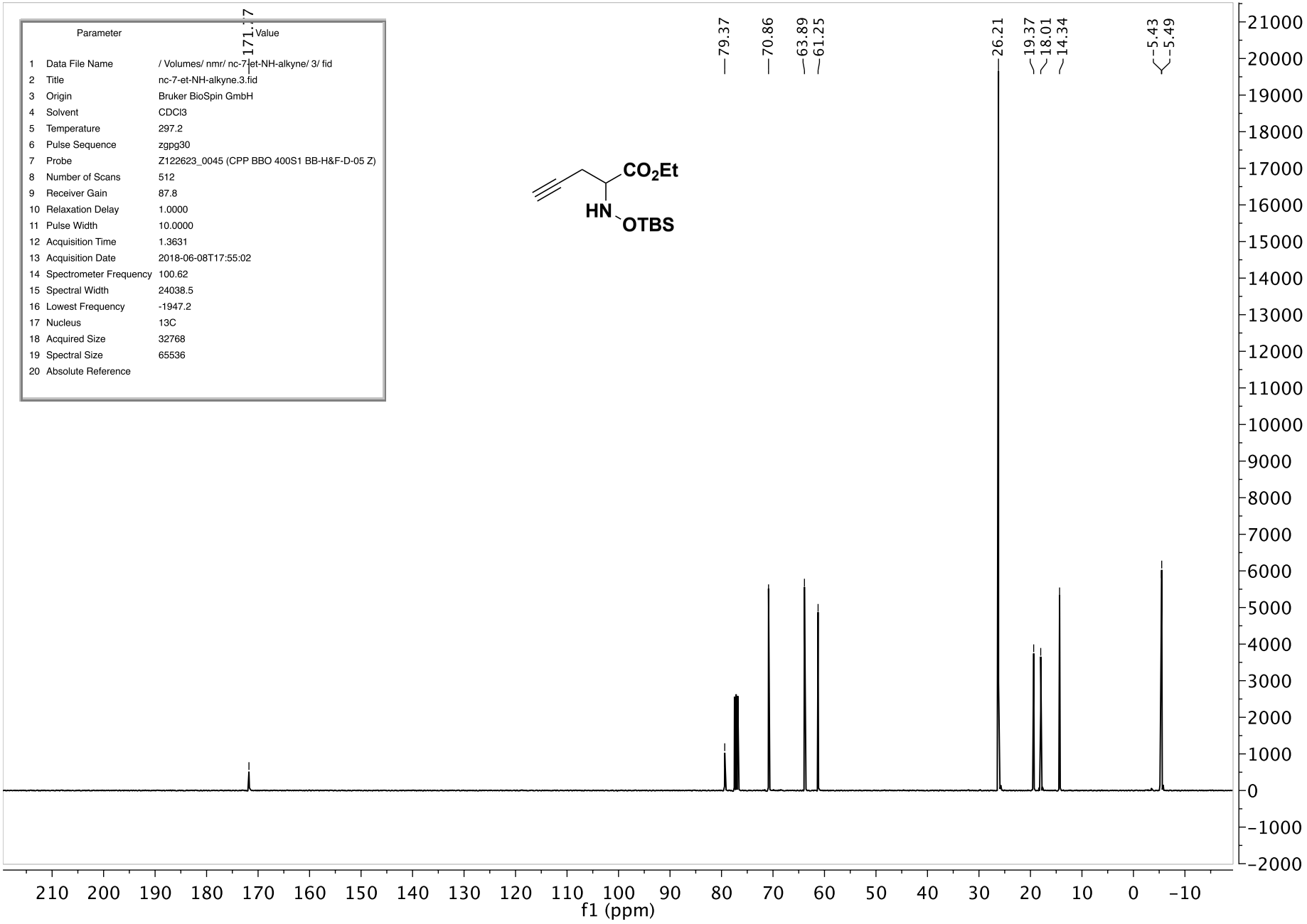

	Parameter	Value
1	Data File Name	/ Volumes/ nmr/ nc-7-et-NH-alkyne/ 3/ fid
2	Title	nc-7-et-NH-alkyne.3.fid
3	Origin	Bruker BioSpin GmbH
4	Solvent	CDCl3
5	Temperature	297.2
6	Pulse Sequence	zgpg30
7	Probe	Z122623_0045 (CPP BBO 400S1 BB-H&F-D-05 Z)
8	Number of Scans	512
9	Receiver Gain	87.8
10	Relaxation Delay	1.0000
11	Pulse Width	10.0000
12	Acquisition Time	1.3631
13	Acquisition Date	2018-06-08T17:55:02
14	Spectrometer Frequency	100.62
15	Spectral Width	24038.5
16	Lowest Frequency	-1947.2
17	Nucleus	13C
18	Acquired Size	32768
19	Spectral Size	65536
20	Absolute Reference	

	Parameter	Value
1	Data File Name	/ Volumes/ data/ nc-7-et-NH-allene.fid/ fid
2	Title	nc-7-et-NH-allene
3	Origin	Varian
4	Spectrometer	vnmrs
5	Solvent	cdcl3
6	Temperature	50.0
7	Pulse Sequence	s2pul
8	Experiment	1D
9	Probe	OneNMR
10	Number of Scans	1
11	Receiver Gain	14
12	Relaxation Delay	1.0000
13	Pulse Width	4.1500
14	Acquisition Date	2018-06-08T17:21:49
15	Spectrometer Frequency	399.80
16	Spectral Width	6410.3
17	Lowest Frequency	-702.8
18	Nucleus	1H
19	Acquired Size	64103
20	Spectral Size	65536

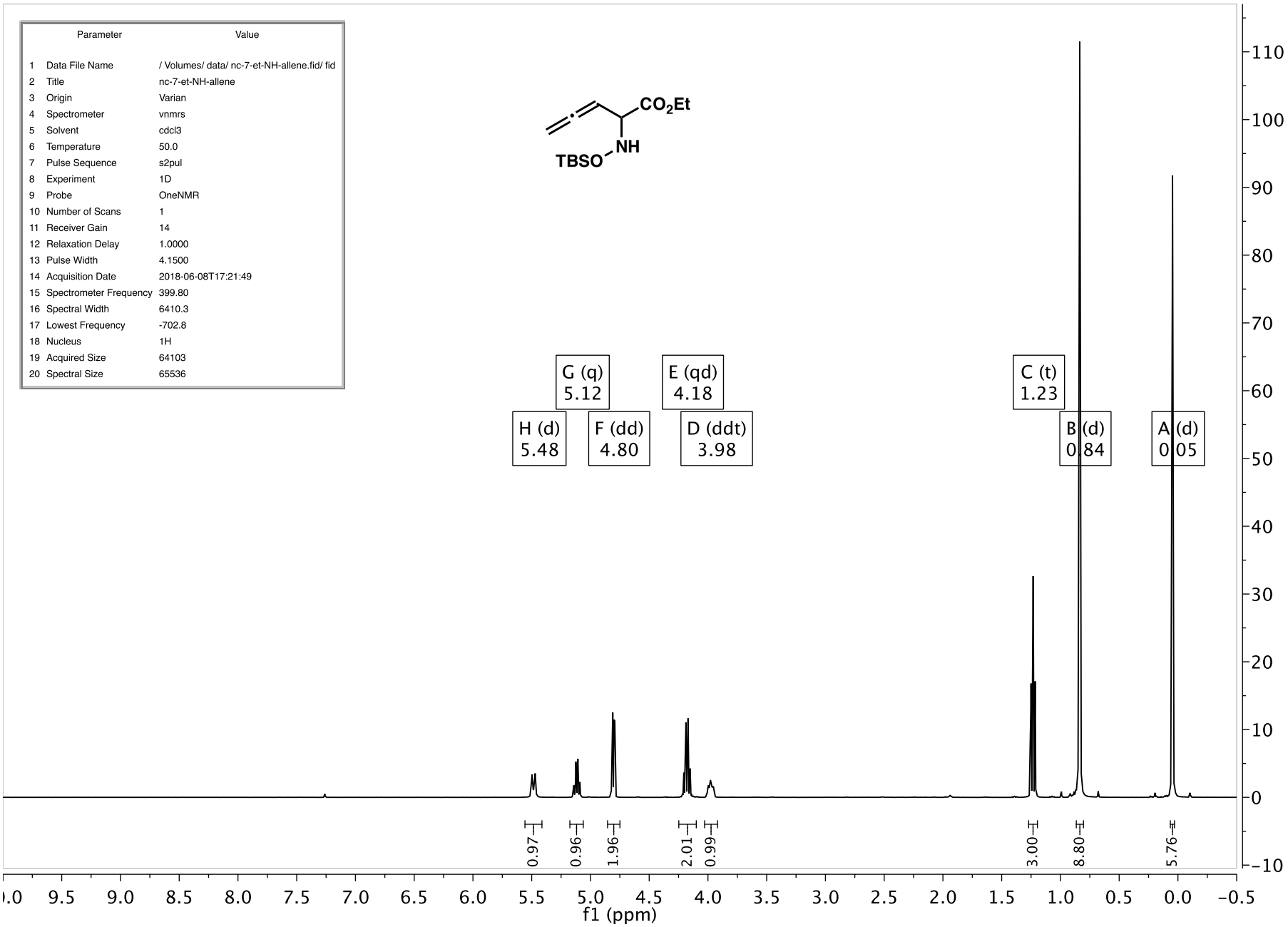

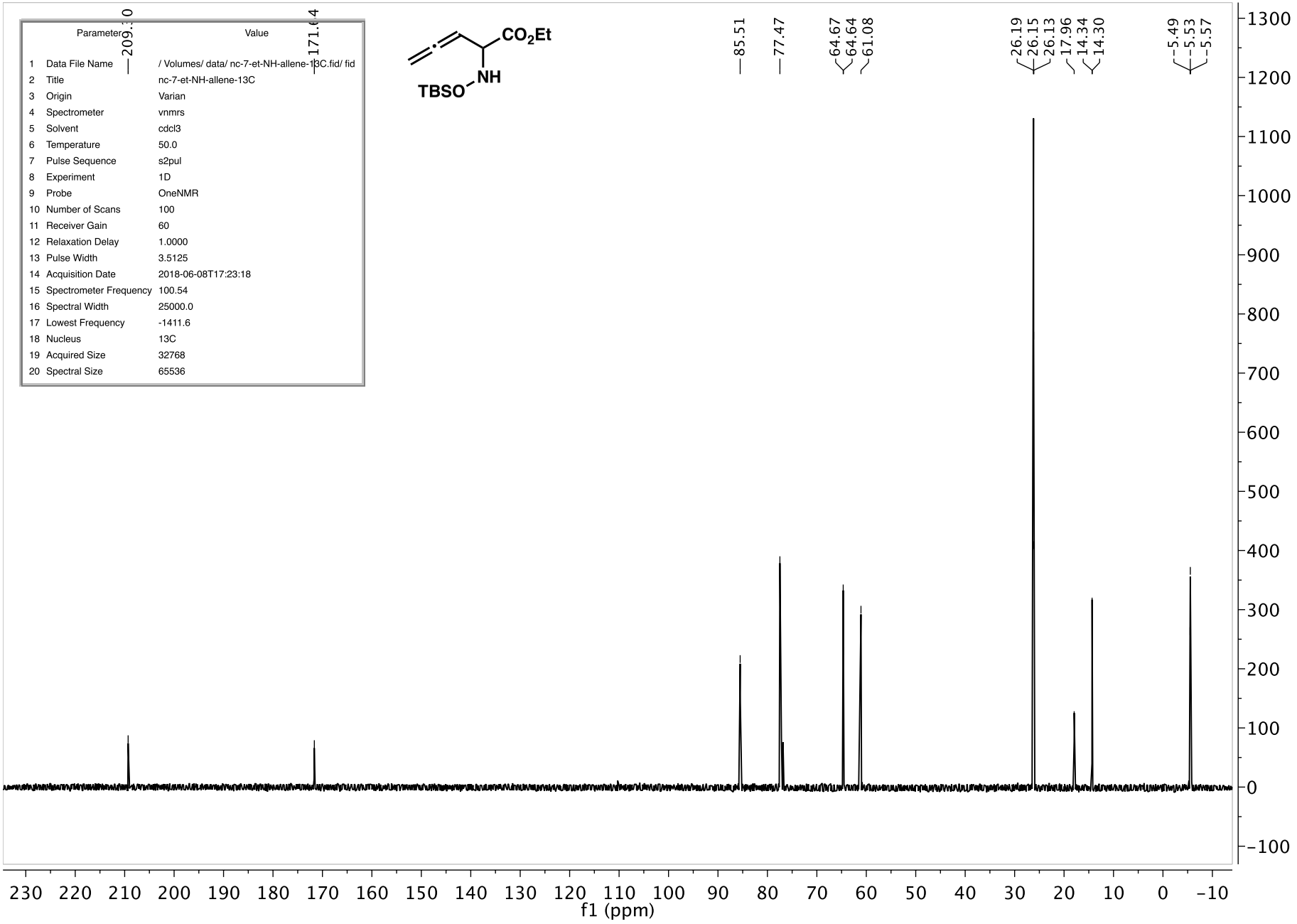

	Parameter	Value
1	Data File Name	/ Volumes/ data/ nc-7-et-NH-allene-13C.fid/ fid
2	Title	nc-7-et-NH-allene-13C
3	Origin	Varian
4	Spectrometer	vnmrs
5	Solvent	cdcl3
6	Temperature	50.0
7	Pulse Sequence	s2pul
8	Experiment	1D
9	Probe	OneNMR
10	Number of Scans	100
11	Receiver Gain	60
12	Relaxation Delay	1.0000
13	Pulse Width	3.5125
14	Acquisition Date	2018-06-08T17:23:18
15	Spectrometer Frequency	100.54
16	Spectral Width	25000.0
17	Lowest Frequency	-1411.6
18	Nucleus	13C
19	Acquired Size	32768
20	Spectral Size	65536

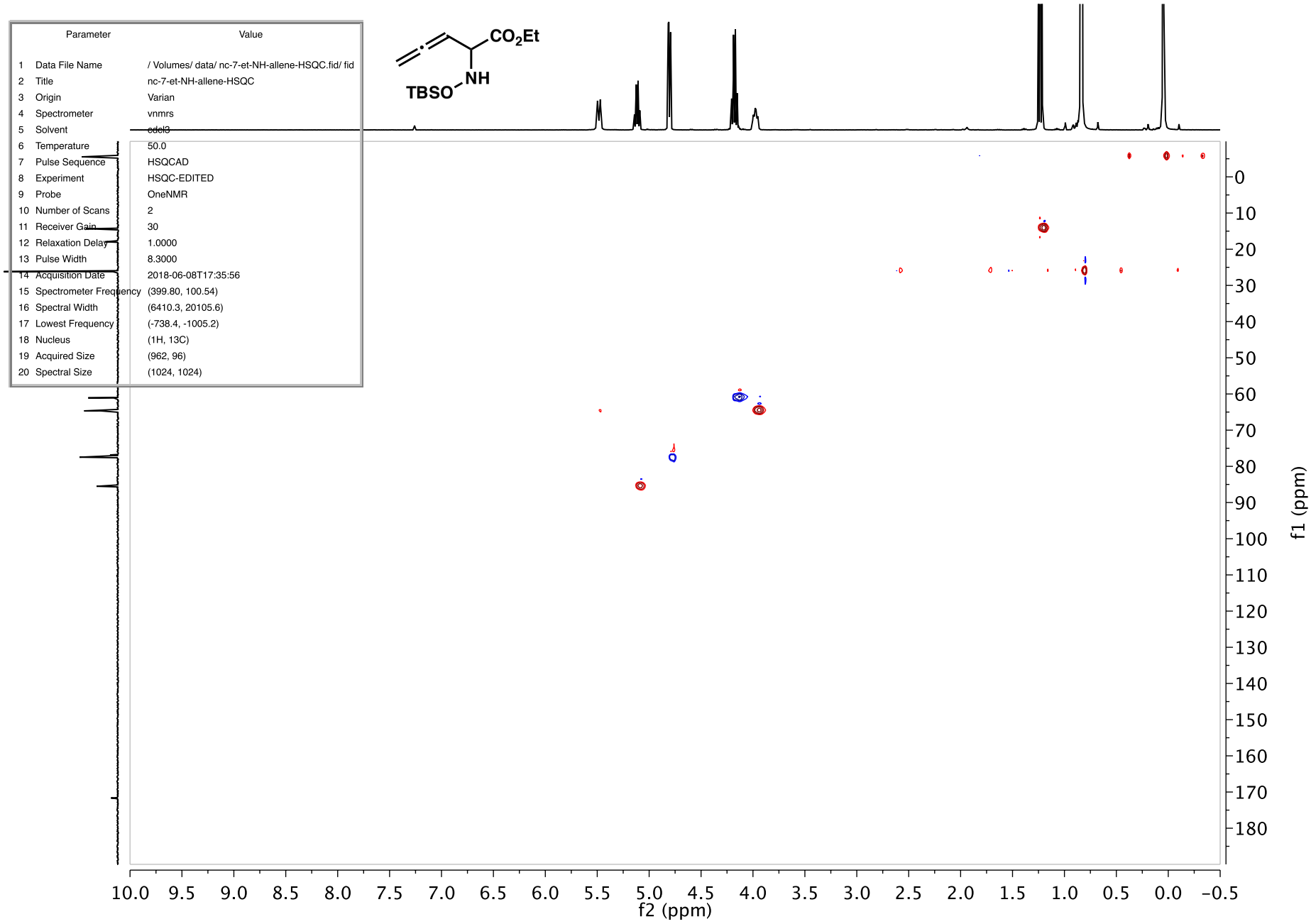
Parameter Value
1 Data File Name / Volumes/ data/ nc-7-et-NH-allene-HSQC.fid/ fid
2 Title nc-7-et-NH-allene-HSQC
3 Origin Varian
4 Spectrometer vnmrs
5 Solvent cdcl3
6 Temperature 50.0
7 Pulse Sequence HSQCAD
8 Experiment HSQC-EDITED
9 Probe OneNMR
10 Number of Scans 2
11 Receiver Gain 30
12 Relaxation Delay 1.0000
13 Pulse Width 8.3000
14 Acquisition Date 2018-06-08T17:35:56
15 Spectrometer Frequency (399.80, 100.54)
16 Spectral Width (6410.3, 20105.6)
17 Lowest Frequency (-738.4, -1005.2)
18 Nucleus (1H, 13C)
19 Acquired Size (962, 96)
20 Spectral Size (1024, 1024)
CO2Et
NH
TBSO
10.0 9.5 9.0 8.5 8.0 7.5 7.0 6.5 6.0 5.5 5.0 4.5 4.0 3.5 3.0 2.5 2.0 1.5 1.0 0.5 0.0 -0.5
f2 (ppm)
0 10 20 30 40 50 60 70 80 90 100 110 120 130 140 150 160 170 180
f1 (ppm)

	Parameter	Value
1	Data File Name	/ Volumes/ data-1/ nc-7-NH-ipR-alkyne/ PROTON01.fid/ fid
2	Title	PROTON01
3	Origin	Varian
4	Spectrometer	inova
5	Solvent	cdcl3
6	Temperature	25.0
7	Pulse Sequence	s2pul
8	Experiment	1D
9	Probe	autox7991
10	Number of Scans	2
11	Receiver Gain	44
12	Relaxation Delay	1.0000
13	Pulse Width	5.8000
14	Acquisition Date	2018-06-18T14:50:16
15	Spectrometer Frequency	499.64
16	Spectral Width	8000.0
17	Lowest Frequency	-1002.2
18	Nucleus	1H
19	Acquired Size	24000
20	Spectral Size	65536

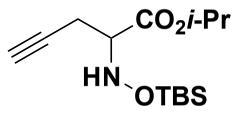

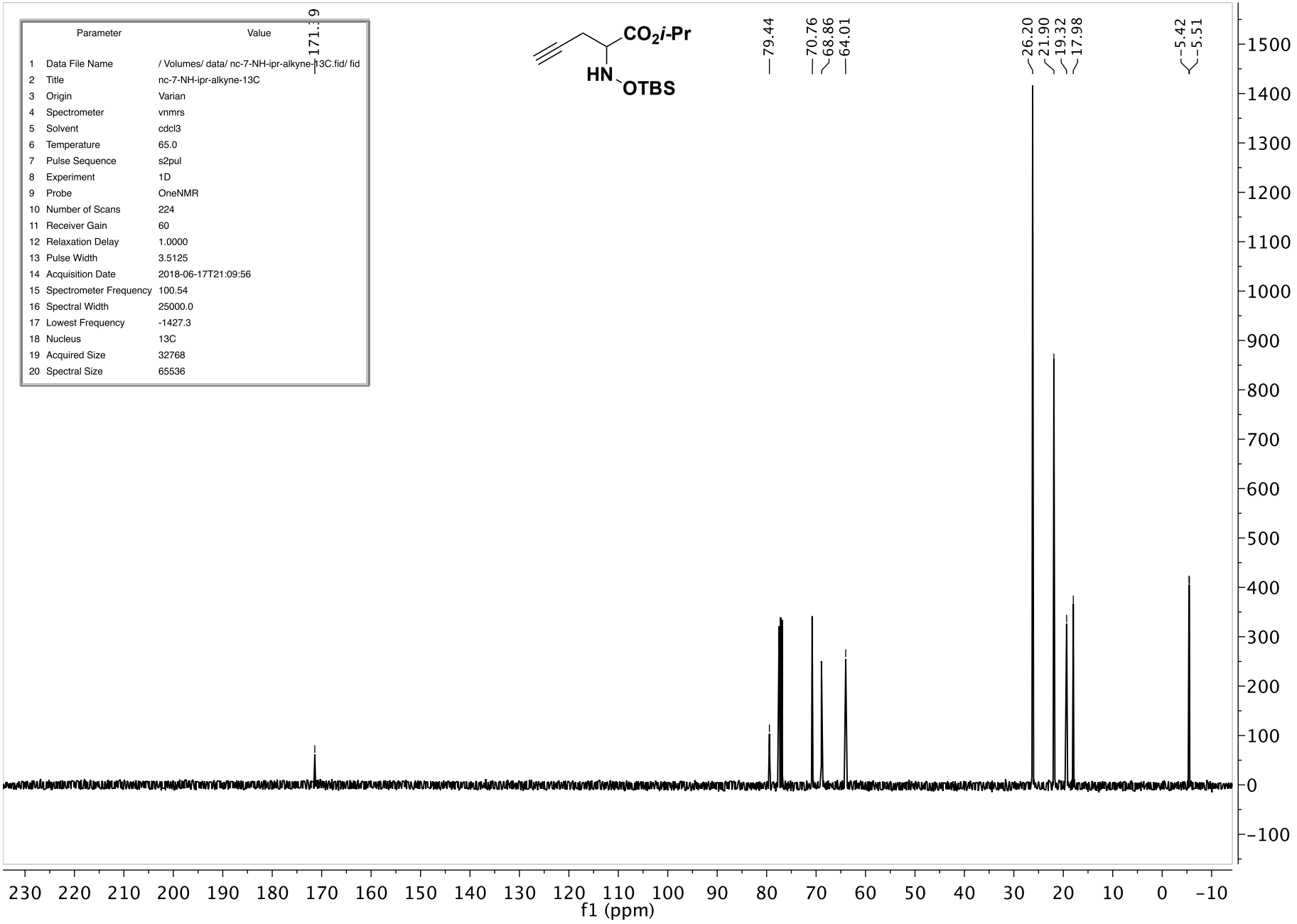
Parameter Value
1 Data File Name / Volumes/ data/ nc-7-NH-ipr-alkyne-13C.fid/ fid
2 Title nc-7-NH-ipr-alkyne-13C
3 Origin Varian
4 Spectrometer vnmrs
5 Solvent cdcl3
6 Temperature 65.0
7 Pulse Sequence s2pul
8 Experiment 1D
9 Probe OneNMR
10 Number of Scans 224
11 Receiver Gain 60
12 Relaxation Delay 1.0000
13 Pulse Width 3.5125
14 Acquisition Date 2018-06-17T21:09:56
15 Spectrometer Frequency 100.54
16 Spectral Width 25000.0
17 Lowest Frequency -1427.3
18 Nucleus 13C
19 Acquired Size 32768
20 Spectral Size 65536
171.39
CO2i-Pr
HN
OTBS
79.44
70.76
68.86
64.01
26.20
21.90
19.32
17.98
5.42
5.51
f1 (ppm)

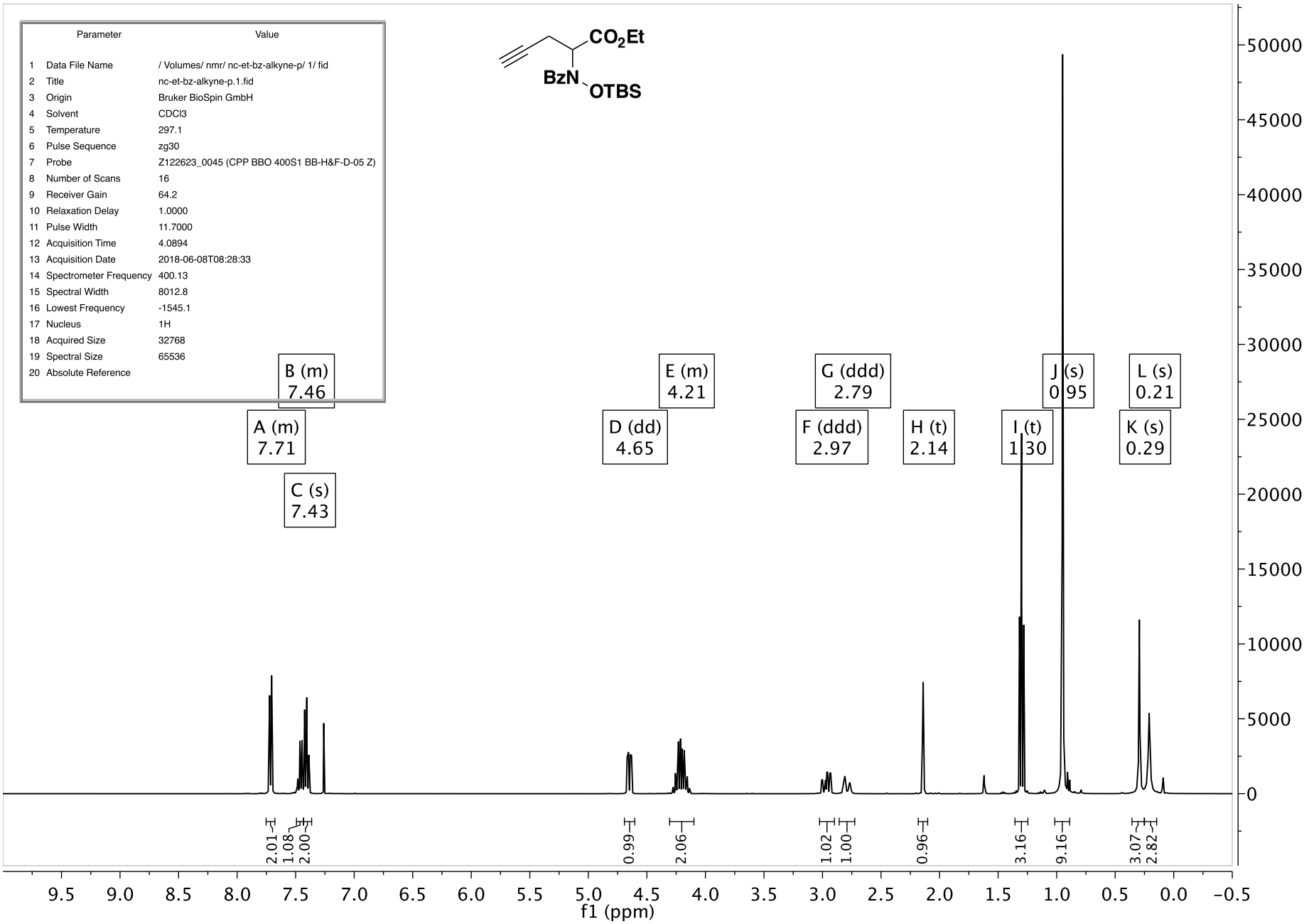
Parameter Value
1 Data File Name / Volumes/ nmr/ nc-et-bz-alkyne-p/ 1/ fid
2 Title nc-et-bz-alkyne-p.1.fid
3 Origin Bruker BioSpin GmbH
4 Solvent CDCl3
5 Temperature 297.1
6 Pulse Sequence zg30
7 Probe Z122623_0045 (CPP BBO 400S1 BB-H&F-D-05 Z)
8 Number of Scans 16
9 Receiver Gain 64.2
10 Relaxation Delay 1.0000
11 Pulse Width 11.7000
12 Acquisition Time 4.0894
13 Acquisition Date 2018-06-08T08:28:33
14 Spectrometer Frequency 400.13
15 Spectral Width 8012.8
16 Lowest Frequency -1545.1
17 Nucleus 1H
18 Acquired Size 32768
19 Spectral Size 65536
20 Absolute Reference
CO2Et
BzN
OTBS
B (m) 7.46
A (m) 7.71
C (s) 7.43
E (m) 4.21
D (dd) 4.65
G (ddd) 2.79
F (ddd) 2.97
H (t) 2.14
I (t) 1.30
J (s) 0.95
L (s) 0.21
K (s) 0.29
2.01
1.08
2.00
0.99
2.06
1.02
1.00
0.96
3.16
9.16
3.07
2.82
f1 (ppm)

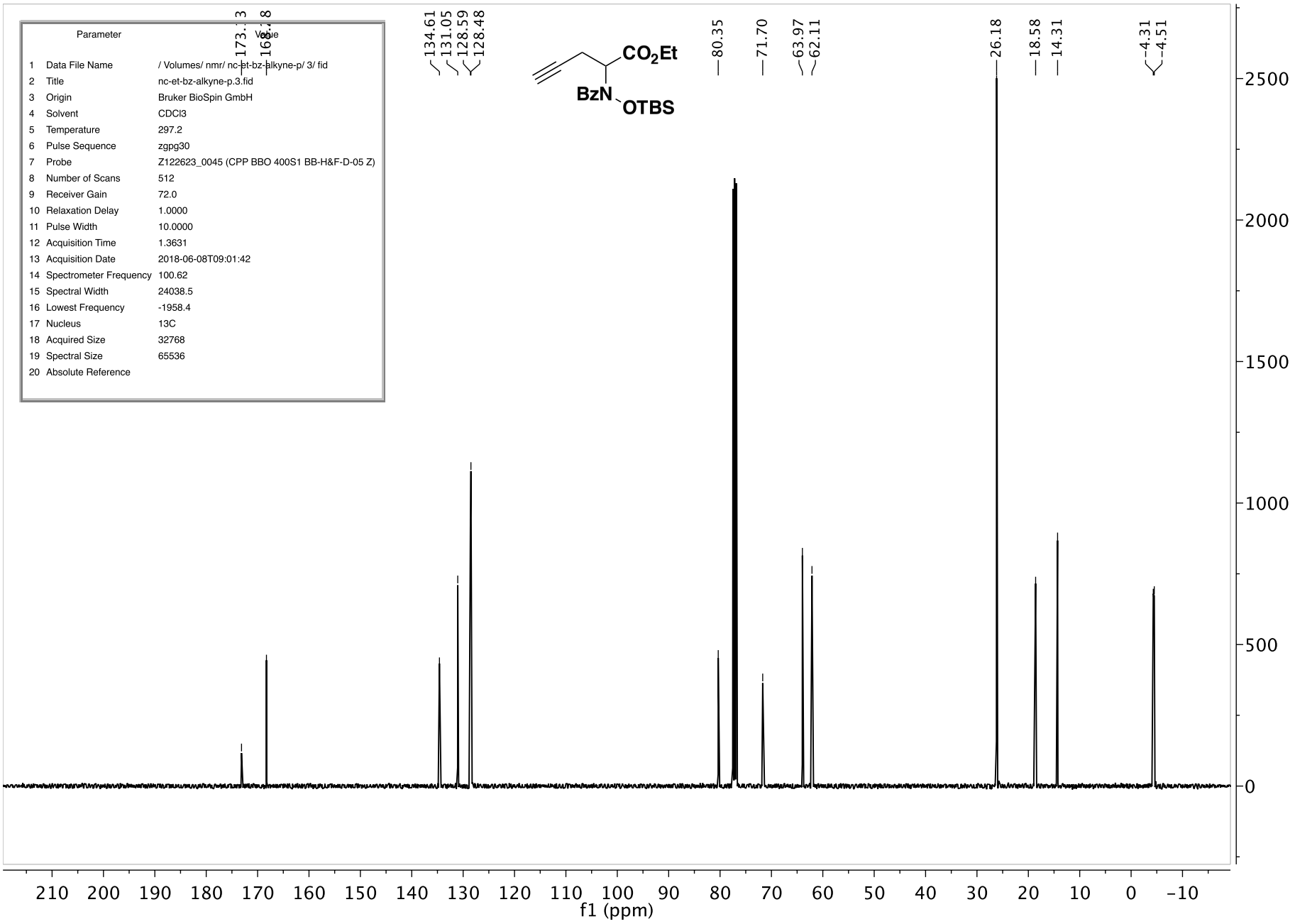
Parameter Value
1 Data File Name / Volumes/ nmr/ nc-et-bz-alkyne-p/ 3/ fid
2 Title nc-et-bz-alkyne-p.3.fid
3 Origin Bruker BioSpin GmbH
4 Solvent CDCl3
5 Temperature 297.2
6 Pulse Sequence zgpg30
7 Probe Z122623_0045 (CPP BBO 400S1 BB-H&F-D-05 Z)
8 Number of Scans 512
9 Receiver Gain 72.0
10 Relaxation Delay 1.0000
11 Pulse Width 10.0000
12 Acquisition Time 1.3631
13 Acquisition Date 2018-06-08T09:01:42
14 Spectrometer Frequency 100.62
15 Spectral Width 24038.5
16 Lowest Frequency -1958.4
17 Nucleus 13C
18 Acquired Size 32768
19 Spectral Size 65536
20 Absolute Reference
173.13
169.28
134.61
131.05
128.59
128.48
80.35
71.70
63.97
62.11
26.18
18.58
14.31
-4.31
-4.51
CO2Et
BzN
OTBS
2500
2000
1500
1000
500
0
210 200 190 180 170 160 150 140 130 120 110 100 90 80 70 60 50 40 30 20 10 0 -10
f1 (ppm)

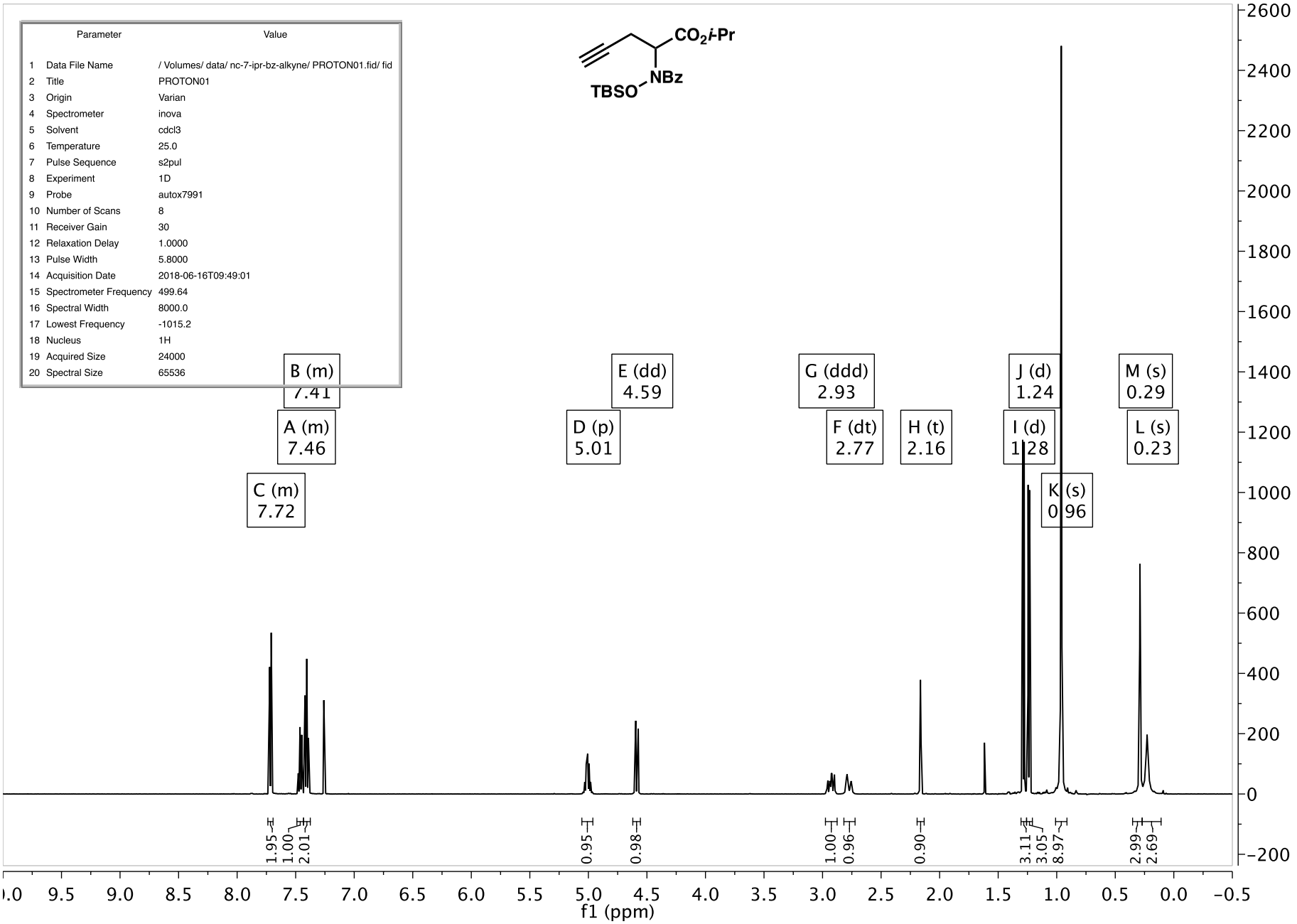
Parameter Value
1 Data File Name / Volumes/ data/ nc-7-ipr-bz-alkyne/ PROTON01.fid/ fid
2 Title PROTON01
3 Origin Varian
4 Spectrometer inova
5 Solvent cdcl3
6 Temperature 25.0
7 Pulse Sequence s2pul
8 Experiment 1D
9 Probe autox7991
10 Number of Scans 8
11 Receiver Gain 30
12 Relaxation Delay 1.0000
13 Pulse Width 5.8000
14 Acquisition Date 2018-06-16T09:49:01
15 Spectrometer Frequency 499.64
16 Spectral Width 8000.0
17 Lowest Frequency -1015.2
18 Nucleus 1H
19 Acquired Size 24000
20 Spectral Size 65536
CO2i-Pr
NBz
TBSO
B (m) 7.41
A (m) 7.46
C (m) 7.72
E (dd) 4.59
D (p) 5.01
G (ddd) 2.93
F (dt) 2.77
H (t) 2.16
J (d) 1.24
I (d) 1.28
K (s) 0.96
M (s) 0.29
L (s) 0.23
1.95
1.00
2.01
0.95
0.98
1.00
0.96
0.90
3.11
3.05
8.97
2.99
2.69
f1 (ppm)

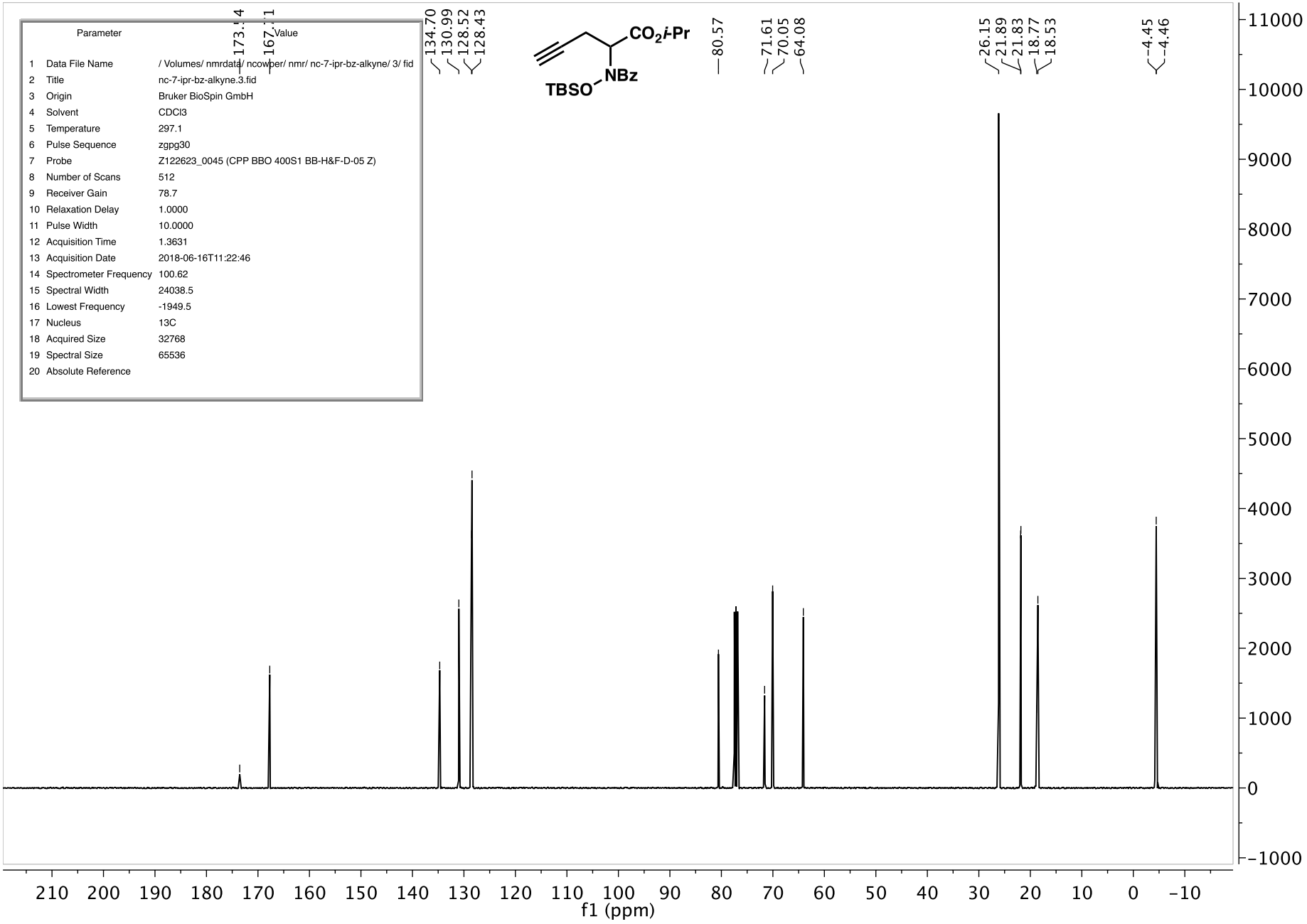
Parameter
Value
1 Data File Name / Volumes/ nmrdata/ ncowper/ nmr/ nc-7-ipr-bz-alkyne/ 3/ fid
2 Title nc-7-ipr-bz-alkyne.3.fid
3 Origin Bruker BioSpin GmbH
4 Solvent CDCl3
5 Temperature 297.1
6 Pulse Sequence zgpg30
7 Probe Z122623_0045 (CPP BBO 400S1 BB-H&F-D-05 Z)
8 Number of Scans 512
9 Receiver Gain 78.7
10 Relaxation Delay 1.0000
11 Pulse Width 10.0000
12 Acquisition Time 1.3631
13 Acquisition Date 2018-06-16T11:22:46
14 Spectrometer Frequency 100.62
15 Spectral Width 24038.5
16 Lowest Frequency -1949.5
17 Nucleus 13C
18 Acquired Size 32768
19 Spectral Size 65536
20 Absolute Reference
173.14
167.11
134.70
130.99
128.52
128.43
CO2i-Pr
NBz
TBSO
80.57
71.61
70.05
64.08
26.15
21.89
21.83
18.77
18.53
-4.45
-4.46
11000
10000
9000
8000
7000
6000
5000
4000
3000
2000
1000
0
-1000
210 200 190 180 170 160 150 140 130 120 110 100 90 80 70 60 50 40 30 20 10 0 -10
f1 (ppm)

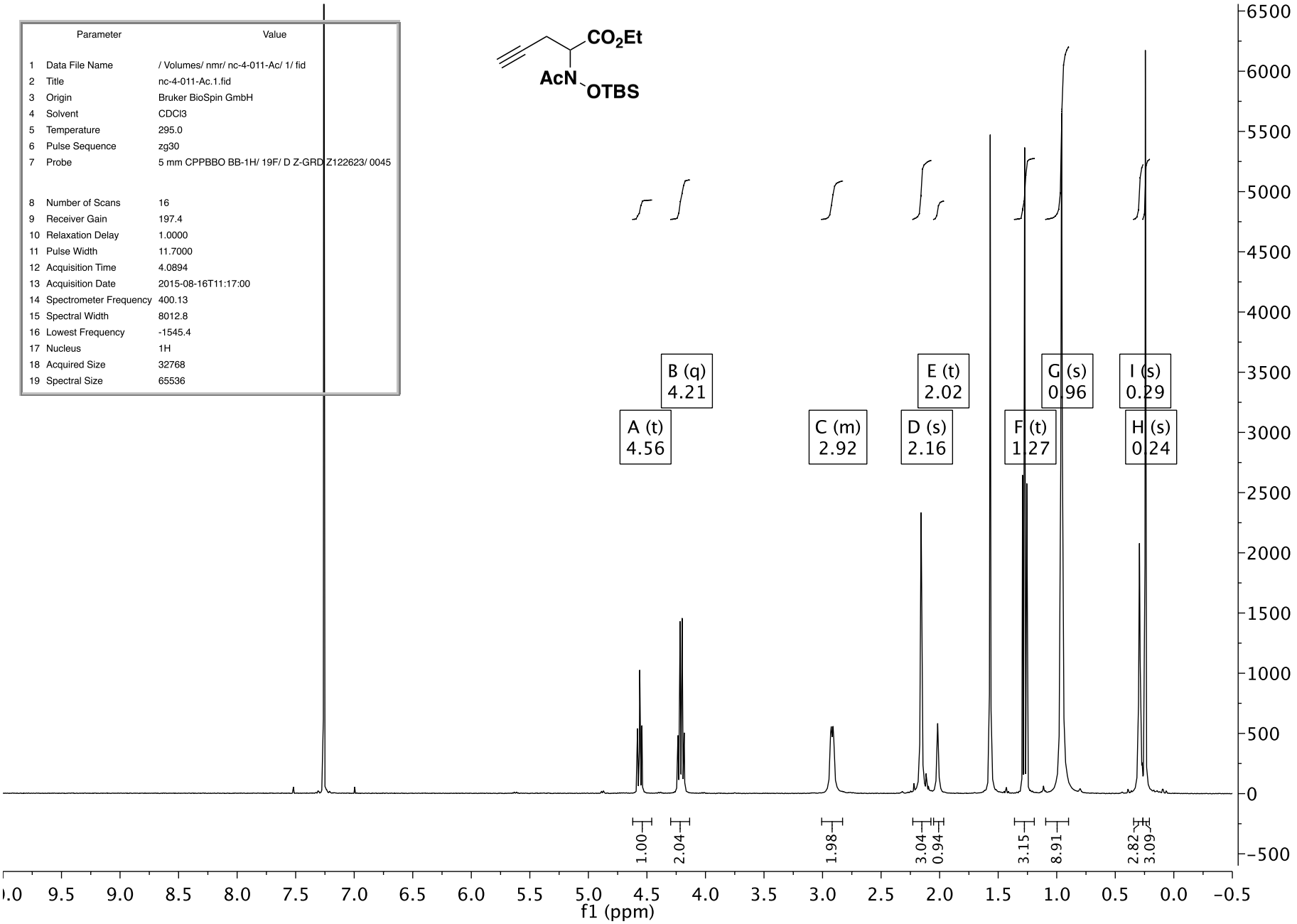
Parameter Value
1 Data File Name / Volumes/ nmr/ nc-4-011-Ac/ 1/ fid
2 Title nc-4-011-Ac.1.fid
3 Origin Bruker BioSpin GmbH
4 Solvent CDCl3
5 Temperature 295.0
6 Pulse Sequence zg30
7 Probe 5 mm CPPBBO BB-1H/ 19F/ D Z-GRD Z122623/ 0045
8 Number of Scans 16
9 Receiver Gain 197.4
10 Relaxation Delay 1.0000
11 Pulse Width 11.7000
12 Acquisition Time 4.0894
13 Acquisition Date 2015-08-16T11:17:00
14 Spectrometer Frequency 400.13
15 Spectral Width 8012.8
16 Lowest Frequency -1545.4
17 Nucleus 1H
18 Acquired Size 32768
19 Spectral Size 65536
CO2Et
AcN
OTBS
A (t) 4.56
B (q) 4.21
C (m) 2.92
D (s) 2.16
E (t) 2.02
F (t) 1.27
G (s) 0.96
H (s) 0.24
I (s) 0.29
1.00
2.04
1.98
3.04
0.94
3.15
8.91
2.82
3.09
f1 (ppm)

	Parameter	Value
1	Data File Name	/ Volumes/ data-1/ nc-7-NAc-OTBS-alkyne/ CARBON01.fid/ fid
2	Title	CARBON01
3	Origin	Varian
4	Spectrometer	inova
5	Solvent	cdcl3
6	Temperature	25.0
7	Pulse Sequence	s2pul
8	Experiment	1D
9	Probe	autox7991
10	Number of Scans	512
11	Receiver Gain	30
12	Relaxation Delay	1.0000
13	Pulse Width	4.6125
14	Acquisition Date	2018-06-20T23:39:25
15	Spectrometer Frequency	125.65
16	Spectral Width	31446.5
17	Lowest Frequency	-1903.7
18	Nucleus	13C
19	Acquired Size	32768
20	Spectral Size	65536

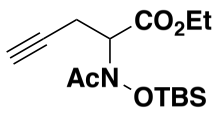

	Parameter	Value
1	Data File Name	/ Volumes/ nmr/ nc-7-Cl-Ac-alkyne/ 1/ fid
2	Title	nc-7-Cl-Ac-alkyne.1.fid
3	Origin	Bruker BioSpin GmbH
4	Solvent	CDCl3
5	Temperature	297.1
6	Pulse Sequence	zg30
7	Probe	Z122623_0045 (CPP BBO 400S1 BB-H&F-D-05 Z)
8	Number of Scans	16
9	Receiver Gain	30.3
10	Relaxation Delay	1.0000
11	Pulse Width	11.7000
12	Acquisition Time	4.0894
13	Acquisition Date	2018-06-15T16:41:18
14	Spectrometer Frequency	400.13
15	Spectral Width	8012.8
16	Lowest Frequency	-1592.1
17	Nucleus	1H
18	Acquired Size	32768
19	Spectral Size	65536
20	Absolute Reference	

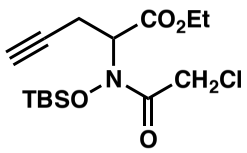

	Parameter	Value
1	Data File Name	/ Volumes/ nmr/ nc-7-Cl-Ac-alkyne/ 3/ fid
2	Title	nc-7-Cl-Ac-alkyne.3.fid
3	Origin	Bruker BioSpin GmbH
4	Solvent	CDCl3
5	Temperature	297.1
6	Pulse Sequence	zgpg30
7	Probe	Z122623_0045 (CPP BBO 400S1 BB-H&F-D-05 Z)
8	Number of Scans	512
9	Receiver Gain	87.8
10	Relaxation Delay	1.0000
11	Pulse Width	10.0000
12	Acquisition Time	1.3631
13	Acquisition Date	2018-06-15T17:14:25
14	Spectrometer Frequency	100.62
15	Spectral Width	24038.5
16	Lowest Frequency	-2048.4
17	Nucleus	13C
18	Acquired Size	32768
19	Spectral Size	65536
20	Absolute Reference	

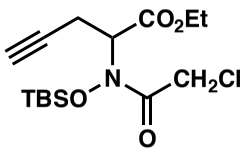

170.11
166.04
79.03
70.06
63.97
61.21
41.63
24.81
18.02
17.08
13.17
-5.42
-5.75

f1 (ppm)

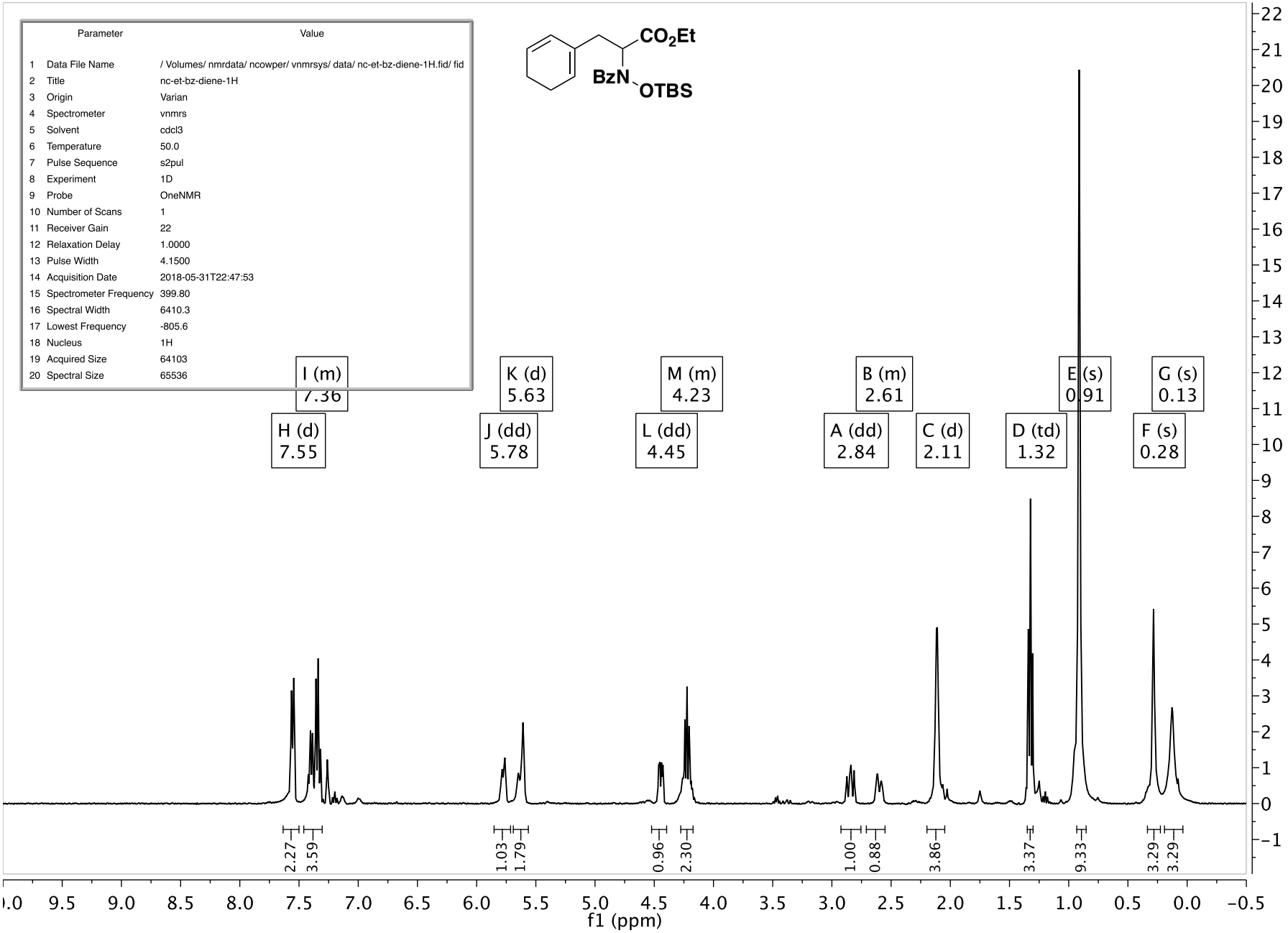
Parameter Value
1 Data File Name / Volumes/ nmrdata/ ncowper/ vnmrsys/ data/ nc-et-bz-diene-1H.fid/ fid
2 Title nc-et-bz-diene-1H
3 Origin Varian
4 Spectrometer vnmrs
5 Solvent cdcl3
6 Temperature 50.0
7 Pulse Sequence s2pul
8 Experiment 1D
9 Probe OneNMR
10 Number of Scans 1
11 Receiver Gain 22
12 Relaxation Delay 1.0000
13 Pulse Width 4.1500
14 Acquisition Date 2018-05-31T22:47:53
15 Spectrometer Frequency 399.80
16 Spectral Width 6410.3
17 Lowest Frequency -805.6
18 Nucleus 1H
19 Acquired Size 64103
20 Spectral Size 65536
CO2Et
BzN
OTBS
I (m) 7.36
H (d) 7.55
K (d) 5.63
J (dd) 5.78
M (m) 4.23
L (dd) 4.45
B (m) 2.61
A (dd) 2.84
C (d) 2.11
D (td) 1.32
E (s) 0.91
G (s) 0.13
F (s) 0.28
2.27
3.59
1.03
1.79
0.96
2.30
1.00
0.88
3.86
3.37
9.33
3.29
3.29
f1 (ppm)

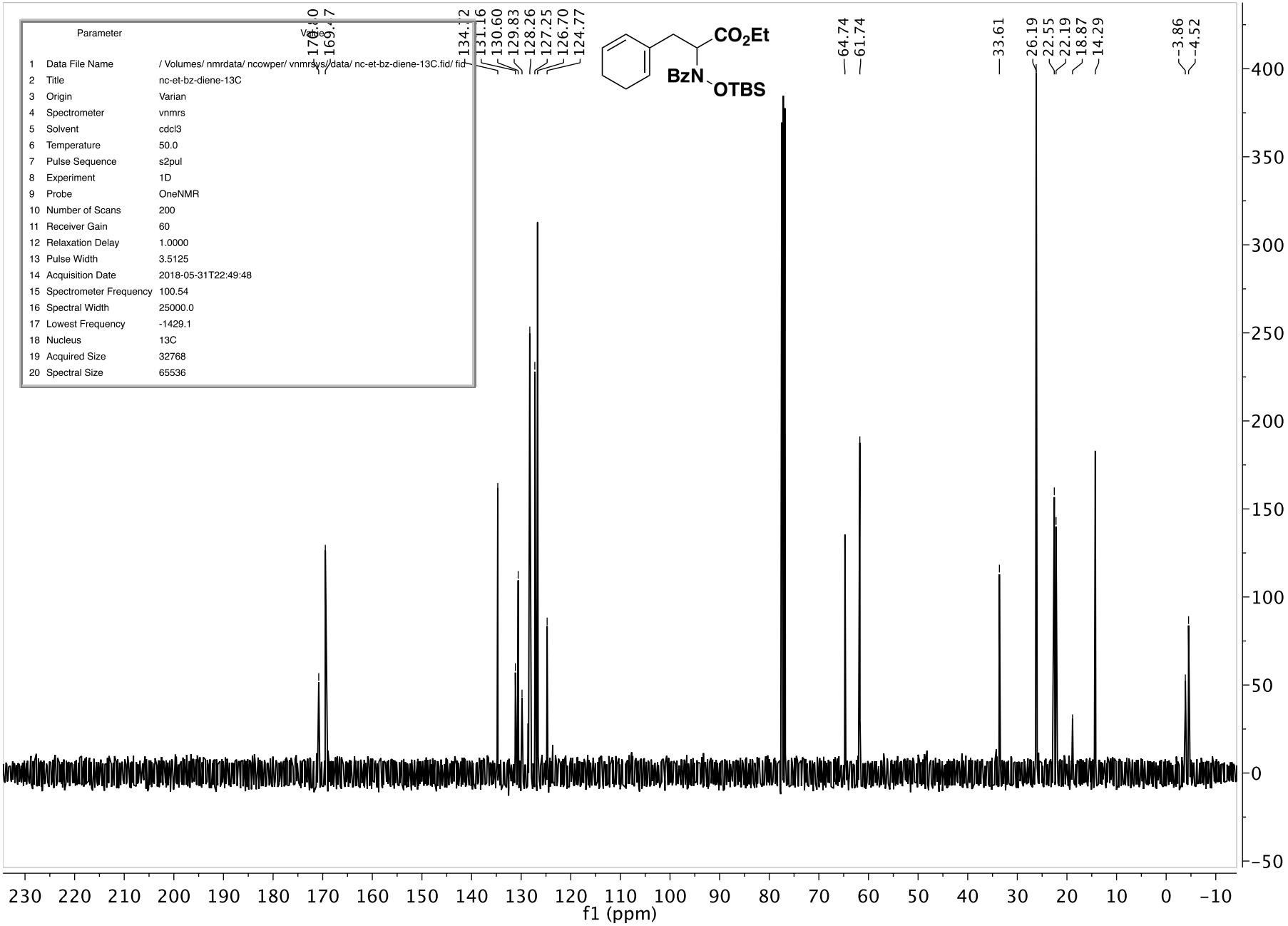
Parameter Value
1 Data File Name / Volumes/ nmrdata/ ncowper/ vnmrsys/data/ nc-et-bz-diene-13C.fid/ fid
2 Title nc-et-bz-diene-13C
3 Origin Varian
4 Spectrometer vnmrs
5 Solvent cdcl3
6 Temperature 50.0
7 Pulse Sequence s2pul
8 Experiment 1D
9 Probe OneNMR
10 Number of Scans 200
11 Receiver Gain 60
12 Relaxation Delay 1.0000
13 Pulse Width 3.5125
14 Acquisition Date 2018-05-31T22:49:48
15 Spectrometer Frequency 100.54
16 Spectral Width 25000.0
17 Lowest Frequency -1429.1
18 Nucleus 13C
19 Acquired Size 32768
20 Spectral Size 65536
169.7
134.12
131.16
130.60
129.83
128.26
127.25
126.70
124.77
64.74
61.74
33.61
26.19
22.55
22.19
18.87
14.29
-3.86
-4.52
CO2Et
BzN
OTBS
400
350
300
250
200
150
100
50
0
-50
230 220 210 200 190 180 170 160 150 140 130 120 110 100 90 80 70 60 50 40 30 20 10 0 -10
f1 (ppm)

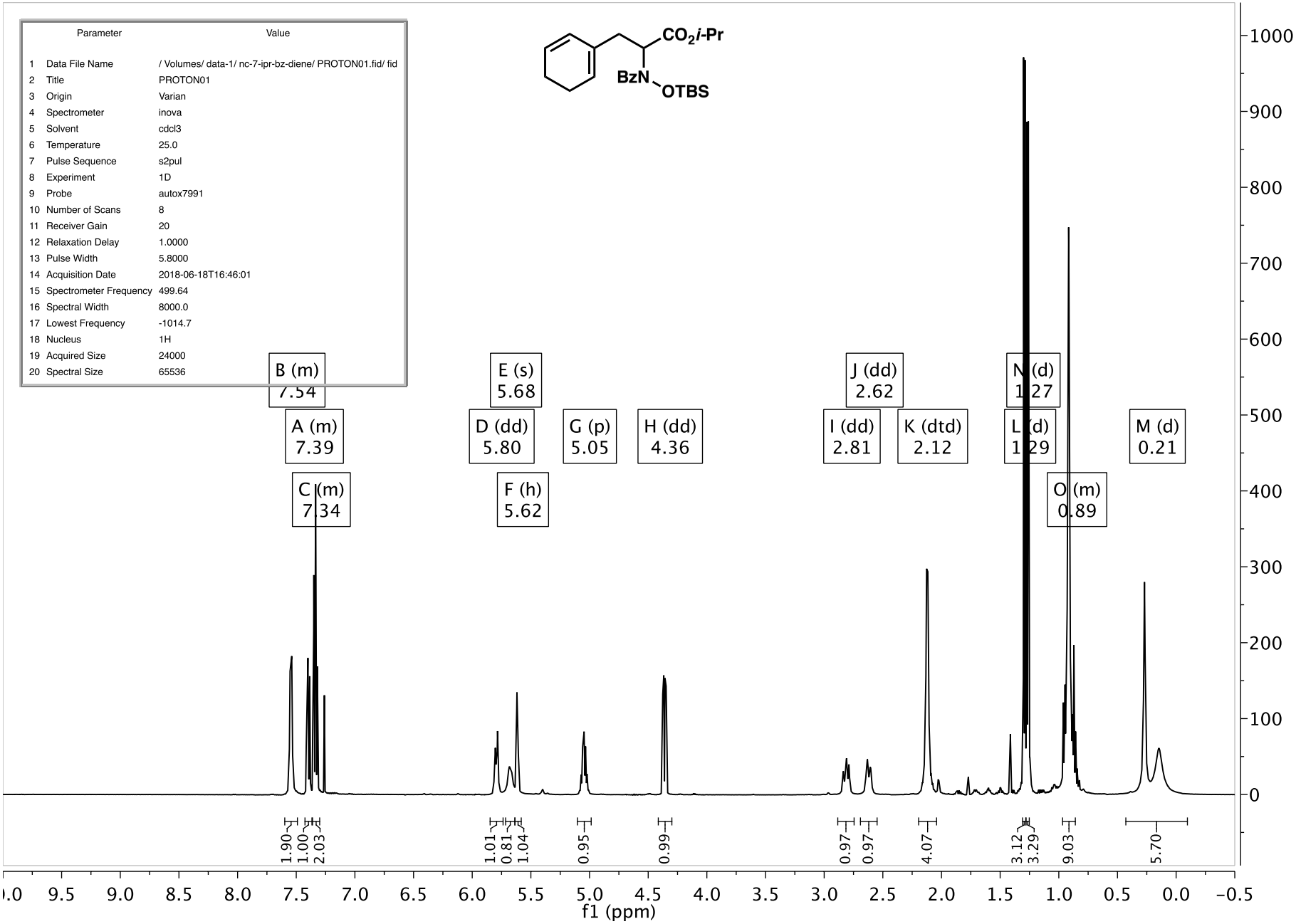
Parameter Value
1 Data File Name / Volumes/ data-1/ nc-7-ipr-bz-diene/ PROTON01.fid/ fid
2 Title PROTON01
3 Origin Varian
4 Spectrometer inova
5 Solvent cdcl3
6 Temperature 25.0
7 Pulse Sequence s2pul
8 Experiment 1D
9 Probe autox7991
10 Number of Scans 8
11 Receiver Gain 20
12 Relaxation Delay 1.0000
13 Pulse Width 5.8000
14 Acquisition Date 2018-06-18T16:46:01
15 Spectrometer Frequency 499.64
16 Spectral Width 8000.0
17 Lowest Frequency -1014.7
18 Nucleus 1H
19 Acquired Size 24000
20 Spectral Size 65536
CO2i-Pr
BzN
OTBS
B (m) 7.54
A (m) 7.39
C (m) 7.34
E (s) 5.68
D (dd) 5.80
F (h) 5.62
G (p) 5.05
H (dd) 4.36
J (dd) 2.62
I (dd) 2.81
K (dtd) 2.12
N (d) 1.27
L (d) 1.29
O (m) 0.89
M (d) 0.21
1.90
1.00
2.03
1.01
0.81
1.04
0.95
0.99
0.97
0.97
4.07
3.12
3.29
9.03
5.70
f1 (ppm)

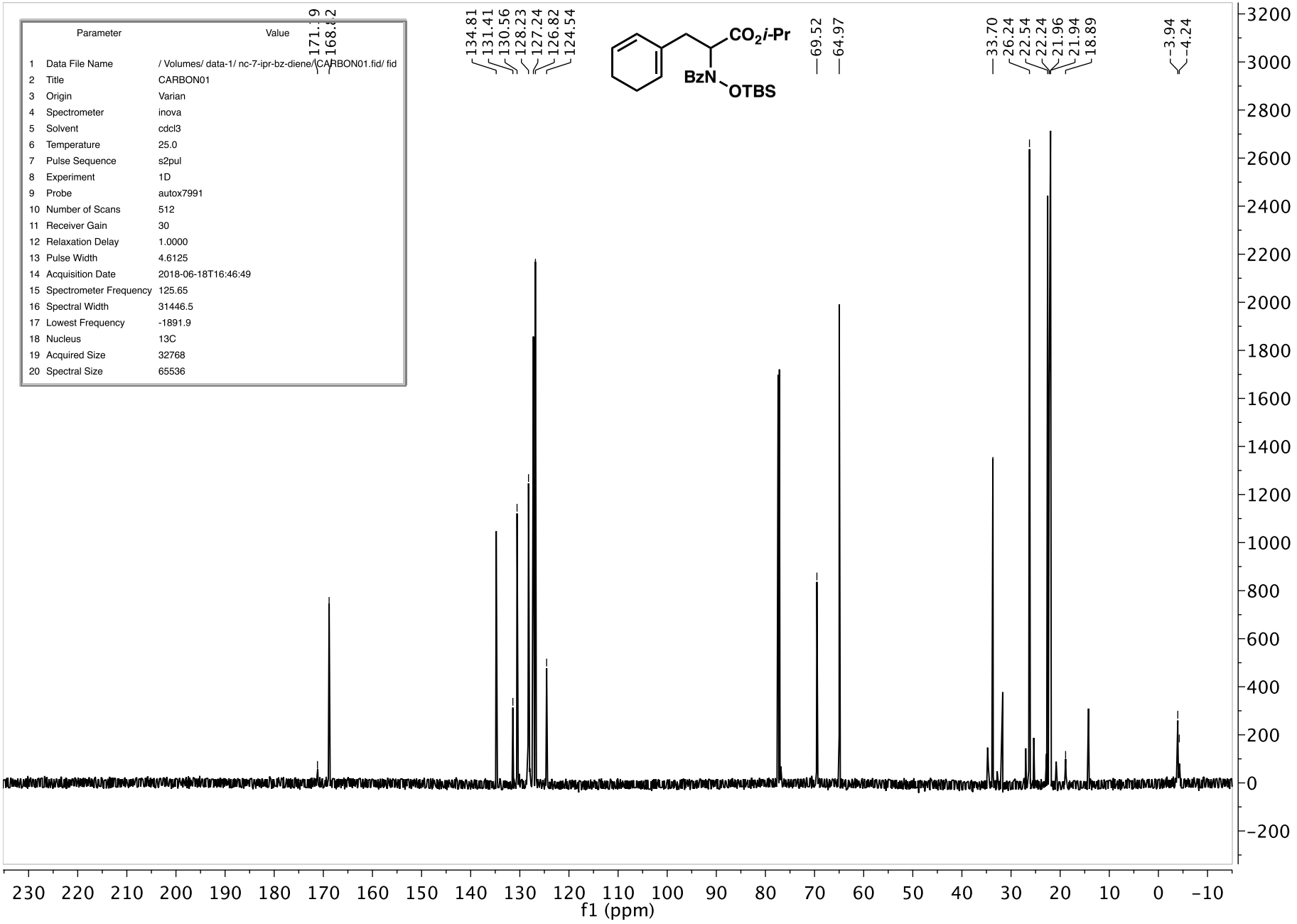
Parameter Value
1 Data File Name / Volumes/ data-1/ nc-7-ipr-bz-diene/CARBON01.fid/ fid
2 Title CARBON01
3 Origin Varian
4 Spectrometer inova
5 Solvent cdcl3
6 Temperature 25.0
7 Pulse Sequence s2pul
8 Experiment 1D
9 Probe autox7991
10 Number of Scans 512
11 Receiver Gain 30
12 Relaxation Delay 1.0000
13 Pulse Width 4.6125
14 Acquisition Date 2018-06-18T16:46:49
15 Spectrometer Frequency 125.65
16 Spectral Width 31446.5
17 Lowest Frequency -1891.9
18 Nucleus 13C
19 Acquired Size 32768
20 Spectral Size 65536
171.19
168.82
134.81
131.41
130.56
128.23
127.24
126.82
124.54
CO2i-Pr
BzN
OTBS
69.52
64.97
33.70
26.24
22.54
22.24
21.96
21.94
18.89
-3.94
-4.24
f1 (ppm)

	Parameter	Value
1	Data File Name	/ Volumes/ data/ nc-7-Ac-Et-Diene-cle/ PROTON01.fid/ fid
2	Title	PROTON01
3	Origin	Varian
4	Spectrometer	inova
5	Solvent	cdcl3
6	Temperature	25.0
7	Pulse Sequence	s2pul
8	Experiment	1D
9	Probe	autox7991
10	Number of Scans	8
11	Receiver Gain	32
12	Relaxation Delay	1.0000
13	Pulse Width	5.8000
14	Acquisition Date	2018-06-30T20:17:52
15	Spectrometer Frequency	499.64
16	Spectral Width	8000.0
17	Lowest Frequency	-1029.7
18	Nucleus	1H
19	Acquired Size	24000
20	Spectral Size	65536

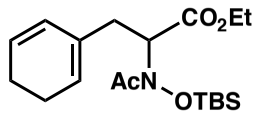

	Parameter	Value
1	Data File Name	/ Volumes/ nmrdata/ ncowper/ nmr/ nc-7-Ac-Et-Diene/ 3/ fid
2	Title	nc-7-Ac-Et-Diene.3.fid
3	Origin	Bruker BioSpin GmbH
4	Solvent	CDCl3
5	Temperature	295.2
6	Pulse Sequence	zgpg30
7	Probe	Z122623_0045 (CPP BBO 400S1 BB-H&F-D-05 Z)
8	Number of Scans	1500
9	Receiver Gain	64.2
10	Relaxation Delay	1.0000
11	Pulse Width	10.0000
12	Acquisition Time	1.3631
13	Acquisition Date	2018-07-01T06:41:38
14	Spectrometer Frequency	100.62
15	Spectral Width	24038.5
16	Lowest Frequency	-1948.2
17	Nucleus	13C
18	Acquired Size	32768
19	Spectral Size	65536
20	Absolute Reference	

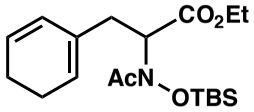

	Parameter	Value
1	Data File Name	/ Volumes/ data-1/ nc-7-Cl-diene/ PROTON01.fid/ fid
2	Title	PROTON01
3	Origin	Varian
4	Spectrometer	inova
5	Solvent	cdcl3
6	Temperature	25.0
7	Pulse Sequence	s2pul
8	Experiment	1D
9	Probe	autox7991
10	Number of Scans	8
11	Receiver Gain	22
12	Relaxation Delay	1.0000
13	Pulse Width	5.8000
14	Acquisition Date	2018-06-18T14:03:10
15	Spectrometer Frequency	499.64
16	Spectral Width	8000.0
17	Lowest Frequency	-1014.7
18	Nucleus	1H
19	Acquired Size	24000
20	Spectral Size	65536

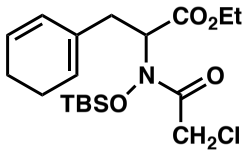

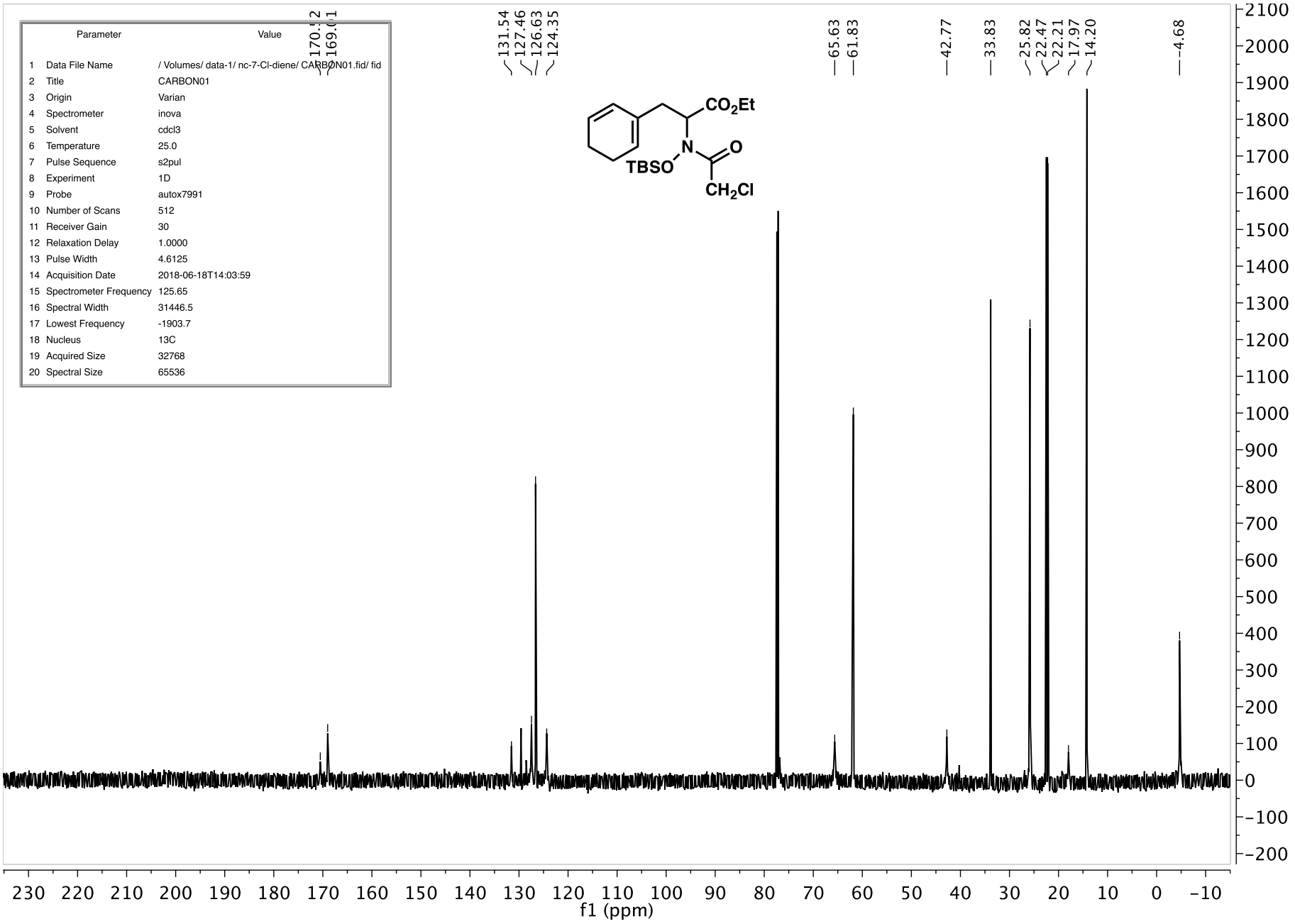
Parameter Value
1 Data File Name / Volumes/ data-1/ nc-7-Cl-diene/ CARBON01.fid/ fid
2 Title CARBON01
3 Origin Varian
4 Spectrometer inova
5 Solvent cdcl3
6 Temperature 25.0
7 Pulse Sequence s2pul
8 Experiment 1D
9 Probe autox7991
10 Number of Scans 512
11 Receiver Gain 30
12 Relaxation Delay 1.0000
13 Pulse Width 4.6125
14 Acquisition Date 2018-06-18T14:03:59
15 Spectrometer Frequency 125.65
16 Spectral Width 31446.5
17 Lowest Frequency -1903.7
18 Nucleus 13C
19 Acquired Size 32768
20 Spectral Size 65536
170.12
169.01
131.54
127.46
126.63
124.35
65.63
61.83
42.77
33.83
25.82
22.47
22.21
17.97
14.20
-4.68
CO2Et
N
O
TBSO
CH2Cl
f1 (ppm)

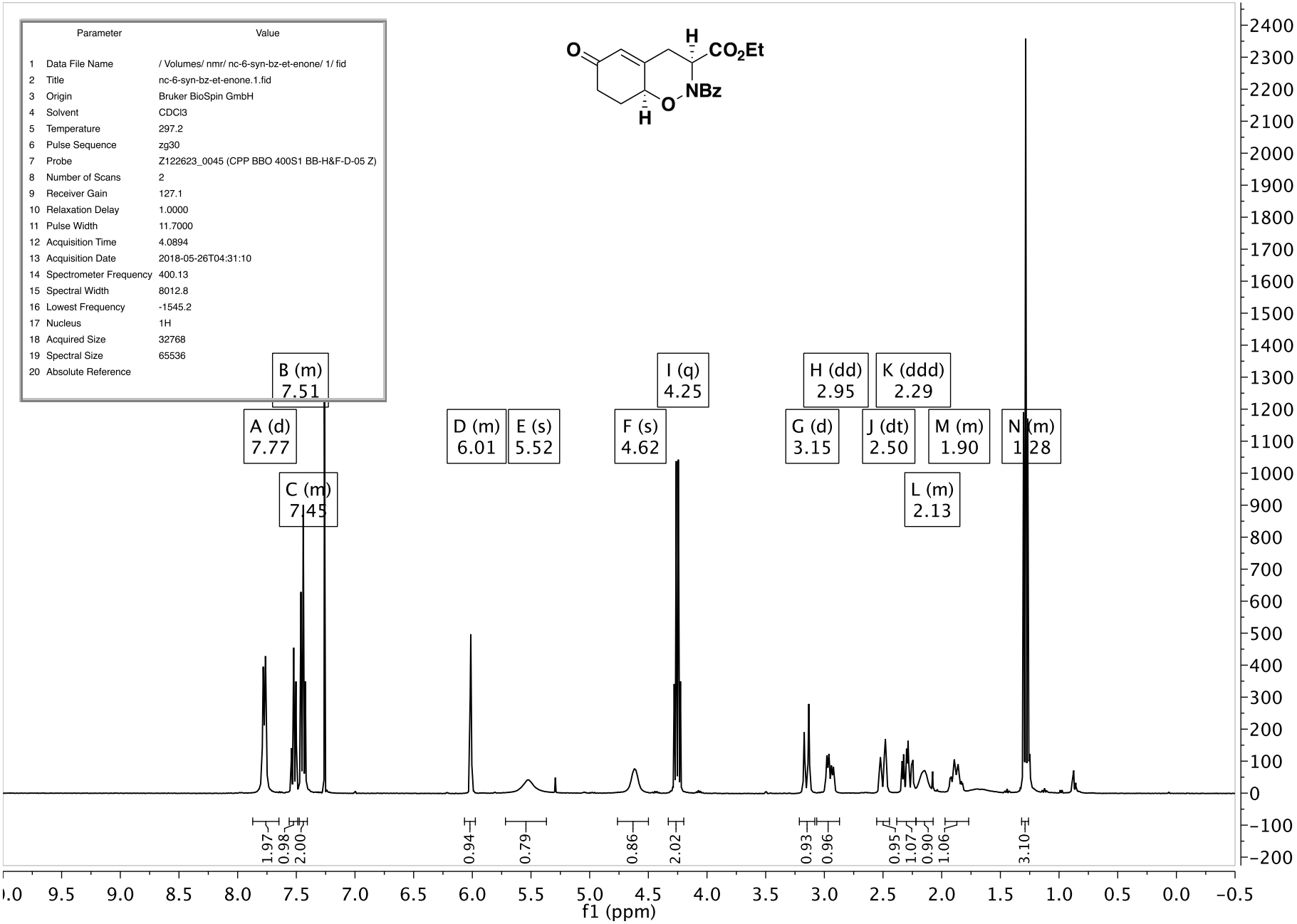
Parameter Value
1 Data File Name / Volumes/ nmr/ nc-6-syn-bz-et-enone/ 1/ fid
2 Title nc-6-syn-bz-et-enone.1.fid
3 Origin Bruker BioSpin GmbH
4 Solvent CDCl3
5 Temperature 297.2
6 Pulse Sequence zg30
7 Probe Z122623_0045 (CPP BBO 400S1 BB-H&F-D-05 Z)
8 Number of Scans 2
9 Receiver Gain 127.1
10 Relaxation Delay 1.0000
11 Pulse Width 11.7000
12 Acquisition Time 4.0894
13 Acquisition Date 2018-05-26T04:31:10
14 Spectrometer Frequency 400.13
15 Spectral Width 8012.8
16 Lowest Frequency -1545.2
17 Nucleus 1H
18 Acquired Size 32768
19 Spectral Size 65536
20 Absolute Reference
O
H
CO2Et
NBz
O
H
A (d) 7.77
B (m) 7.51
C (m) 7.45
D (m) 6.01
E (s) 5.52
F (s) 4.62
I (q) 4.25
G (d) 3.15
H (dd) 2.95
J (dt) 2.50
K (ddd) 2.29
L (m) 2.13
M (m) 1.90
N (m) 1.28
1.97
0.98
2.00
0.94
0.79
0.86
2.02
0.93
0.96
0.95
1.07
0.90
1.06
3.10
f1 (ppm)

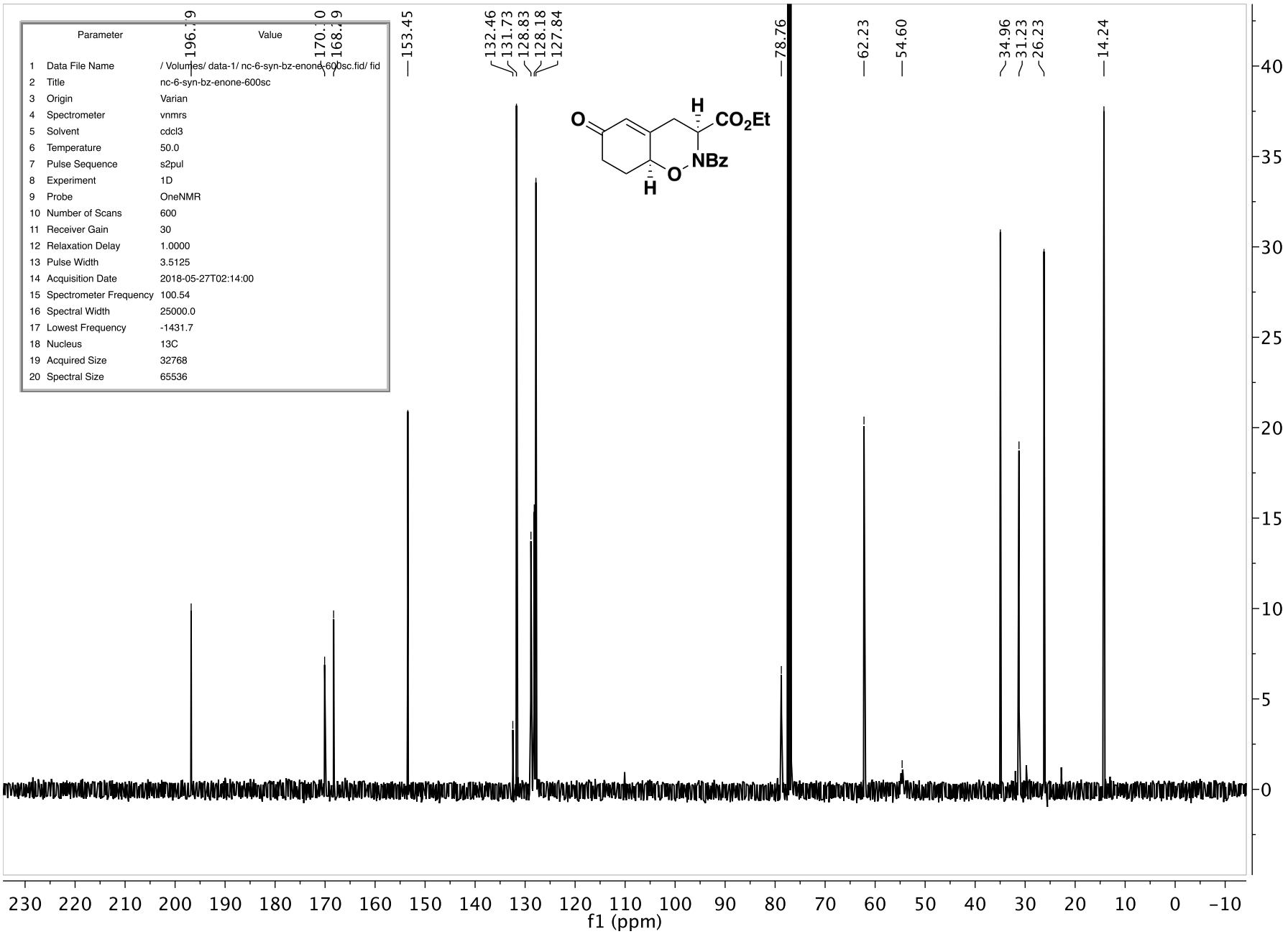

	Parameter	Value
1	Data File Name	/ Volumes/ data-1/ nc-6-syn-bz-enone-600sc.fid/ fid
2	Title	nc-6-syn-bz-enone-600sc
3	Origin	Varian
4	Spectrometer	vnmrs
5	Solvent	cdcl3
6	Temperature	50.0
7	Pulse Sequence	s2pul
8	Experiment	1D
9	Probe	OneNMR
10	Number of Scans	600
11	Receiver Gain	30
12	Relaxation Delay	1.0000
13	Pulse Width	3.5125
14	Acquisition Date	2018-05-27T02:14:00
15	Spectrometer Frequency	100.54
16	Spectral Width	25000.0
17	Lowest Frequency	-1431.7
18	Nucleus	13C
19	Acquired Size	32768
20	Spectral Size	65536

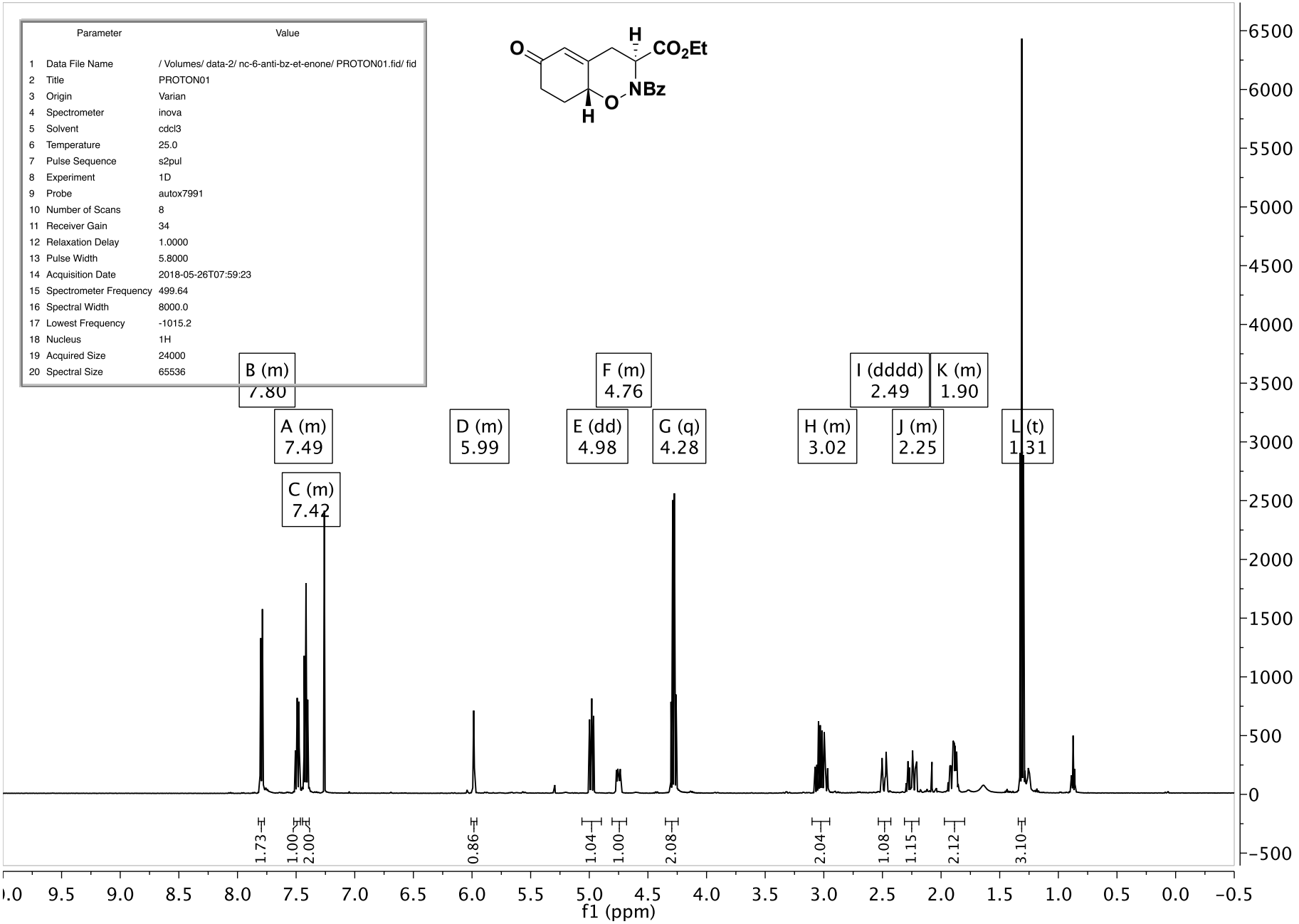
Parameter Value
1 Data File Name / Volumes/ data-2/ nc-6-anti-bz-et-enone/ PROTON01.fid/ fid
2 Title PROTON01
3 Origin Varian
4 Spectrometer inova
5 Solvent cdcl3
6 Temperature 25.0
7 Pulse Sequence s2pul
8 Experiment 1D
9 Probe autox7991
10 Number of Scans 8
11 Receiver Gain 34
12 Relaxation Delay 1.0000
13 Pulse Width 5.8000
14 Acquisition Date 2018-05-26T07:59:23
15 Spectrometer Frequency 499.64
16 Spectral Width 8000.0
17 Lowest Frequency -1015.2
18 Nucleus 1H
19 Acquired Size 24000
20 Spectral Size 65536
O
H
CO2Et
NBz
O
H
B (m) 7.80
A (m) 7.49
C (m) 7.42
D (m) 5.99
F (m) 4.76
E (dd) 4.98
G (q) 4.28
I (dddd) 2.49
K (m) 1.90
H (m) 3.02
J (m) 2.25
L (t) 1.31
1.73
1.00
2.00
0.86
1.04
1.00
2.08
2.04
1.08
1.15
2.12
3.10
f1 (ppm)

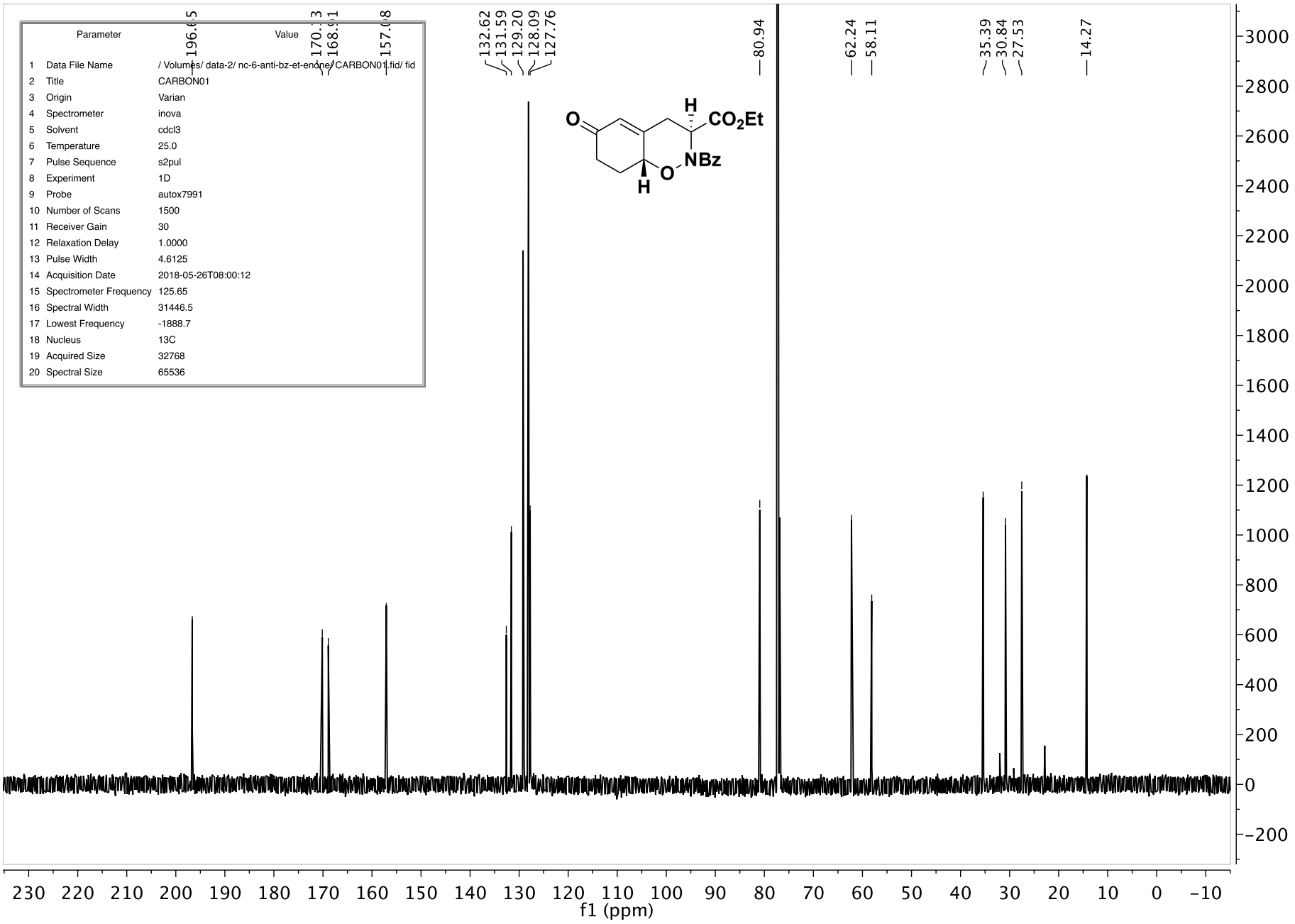
Parameter Value
1 Data File Name / Volumes/ data-2/ nc-6-anti-bz-et-enone/ CARBON01.fid/ fid
2 Title CARBON01
3 Origin Varian
4 Spectrometer inova
5 Solvent cdcl3
6 Temperature 25.0
7 Pulse Sequence s2pul
8 Experiment 1D
9 Probe autox7991
10 Number of Scans 1500
11 Receiver Gain 30
12 Relaxation Delay 1.0000
13 Pulse Width 4.6125
14 Acquisition Date 2018-05-26T08:00:12
15 Spectrometer Frequency 125.65
16 Spectral Width 31446.5
17 Lowest Frequency -1888.7
18 Nucleus 13C
19 Acquired Size 32768
20 Spectral Size 65536
196.05
170.13
168.91
157.08
132.62
131.59
129.20
128.09
127.76
80.94
62.24
58.11
35.39
30.84
27.53
14.27
O
H
CO2Et
NBz
O
H
3000
2800
2600
2400
2200
2000
1800
1600
1400
1200
1000
800
600
400
200
0
-200
230 220 210 200 190 180 170 160 150 140 130 120 110 100 90 80 70 60 50 40 30 20 10 0 -10
f1 (ppm)

	Parameter	Value
1	Data File Name	/ Volumes/ nmrdata/ ncowper/ nmr/ nc-7-ipr-bz-ox-cyc/ 1/ fid
2	Title	nc-7-ipr-bz-ox-cyc.1.fid
3	Origin	Bruker BioSpin GmbH
4	Solvent	CDCl3
5	Temperature	295.1
6	Pulse Sequence	zg30
7	Probe	Z122623_0045 (CPP BBO 400S1 BB-H&F-D-05 Z)
8	Number of Scans	16
9	Receiver Gain	72.0
10	Relaxation Delay	1.0000
11	Pulse Width	11.7000
12	Acquisition Time	4.0894
13	Acquisition Date	2018-07-01T02:31:01
14	Spectrometer Frequency	400.13
15	Spectral Width	8012.8
16	Lowest Frequency	-1569.0
17	Nucleus	1H
18	Acquired Size	32768
19	Spectral Size	65536
20	Absolute Reference	

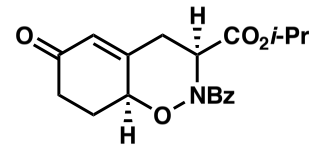

M (m) 7.50
L (d) 7.75
N (m) 7.43
A (m) 6.00
B (d) 5.52
C (h) 5.09
D (s) 4.61
F (dd) 2.93
H (ddd) 2.28
E (d) 3.13
G (dt) 2.49
J (m) 1.87
I (m) 2.13
K (d) 1.25

2.09 1.10 2.29 1.00 0.89 1.13 0.91 1.04 1.07 1.08 1.20 1.06 1.12 6.43

f1 (ppm)

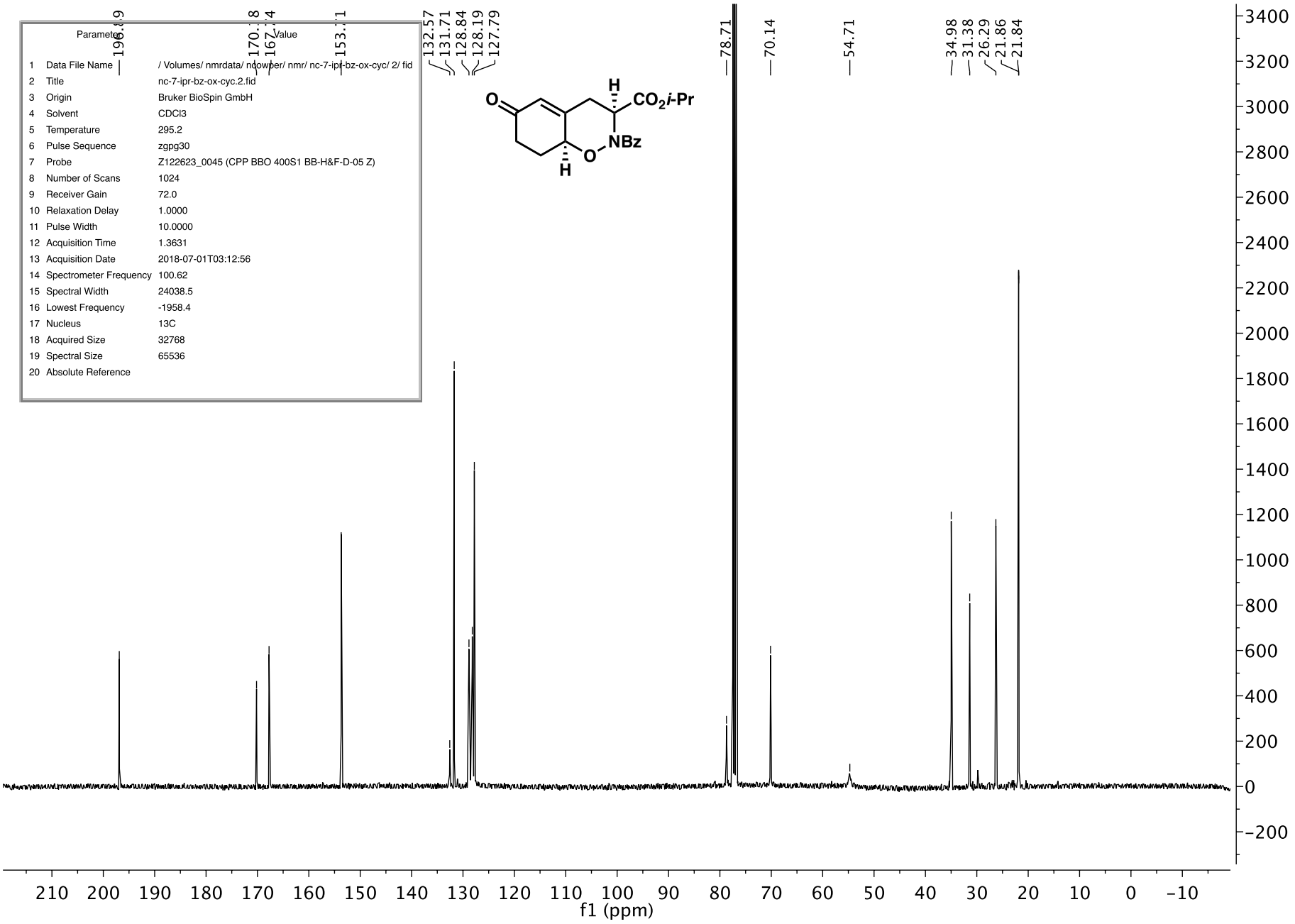
190.49
170.18
167.74
153.11
132.57
131.71
128.84
128.19
127.79
78.71
70.14
54.71
34.98
31.38
26.29
21.86
21.84
O
H
CO2i-Pr
NBz
O
H
Parameter
Value
1 Data File Name / Volumes/ nmrdata/ ndowper/ nmr/ nc-7-ipr-bz-ox-cyc/ 2/ fid
2 Title nc-7-ipr-bz-ox-cyc.2.fid
3 Origin Bruker BioSpin GmbH
4 Solvent CDCl3
5 Temperature 295.2
6 Pulse Sequence zgpg30
7 Probe Z122623_0045 (CPP BBO 400S1 BB-H&F-D-05 Z)
8 Number of Scans 1024
9 Receiver Gain 72.0
10 Relaxation Delay 1.0000
11 Pulse Width 10.0000
12 Acquisition Time 1.3631
13 Acquisition Date 2018-07-01T03:12:56
14 Spectrometer Frequency 100.62
15 Spectral Width 24038.5
16 Lowest Frequency -1958.4
17 Nucleus 13C
18 Acquired Size 32768
19 Spectral Size 65536
20 Absolute Reference
3400
3200
3000
2800
2600
2400
2200
2000
1800
1600
1400
1200
1000
800
600
400
200
0
-200
210 200 190 180 170 160 150 140 130 120 110 100 90 80 70 60 50 40 30 20 10 0 -10
f1 (ppm)

	Parameter	Value
1	Data File Name	/ Volumes/ data-1/ nc-7-ox-cyc-Ac/ PROTON01.fid/ fid
2	Title	PROTON01
3	Origin	Varian
4	Spectrometer	inova
5	Solvent	cdcl3
6	Temperature	25.0
7	Pulse Sequence	s2pul
8	Experiment	1D
9	Probe	autox7991
10	Number of Scans	8
11	Receiver Gain	30
12	Relaxation Delay	1.0000
13	Pulse Width	5.8000
14	Acquisition Date	2018-06-21T21:46:28
15	Spectrometer Frequency	499.64
16	Spectral Width	8000.0
17	Lowest Frequency	-1015.2
18	Nucleus	1H
19	Acquired Size	24000
20	Spectral Size	65536

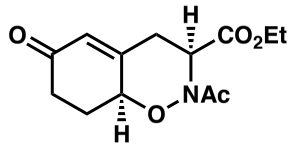

	Parameter	Value
1	Data File Name	/ Volumes/ data-1/ nc-7-ox-cyc-CH2Cl-syn-p/ PROTON01.fid/ fid
2	Title	PROTON01
3	Origin	Varian
4	Spectrometer	inova
5	Solvent	cdcl3
6	Temperature	25.0
7	Pulse Sequence	s2pul
8	Experiment	1D
9	Probe	autox7991
10	Number of Scans	4
11	Receiver Gain	42
12	Relaxation Delay	1.0000
13	Pulse Width	5.8000
14	Acquisition Date	2018-06-21T19:57:56
15	Spectrometer Frequency	499.64
16	Spectral Width	8000.0
17	Lowest Frequency	-1015.2
18	Nucleus	1H
19	Acquired Size	24000
20	Spectral Size	65536

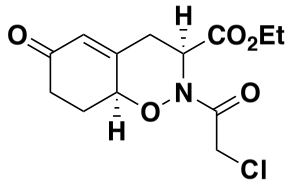

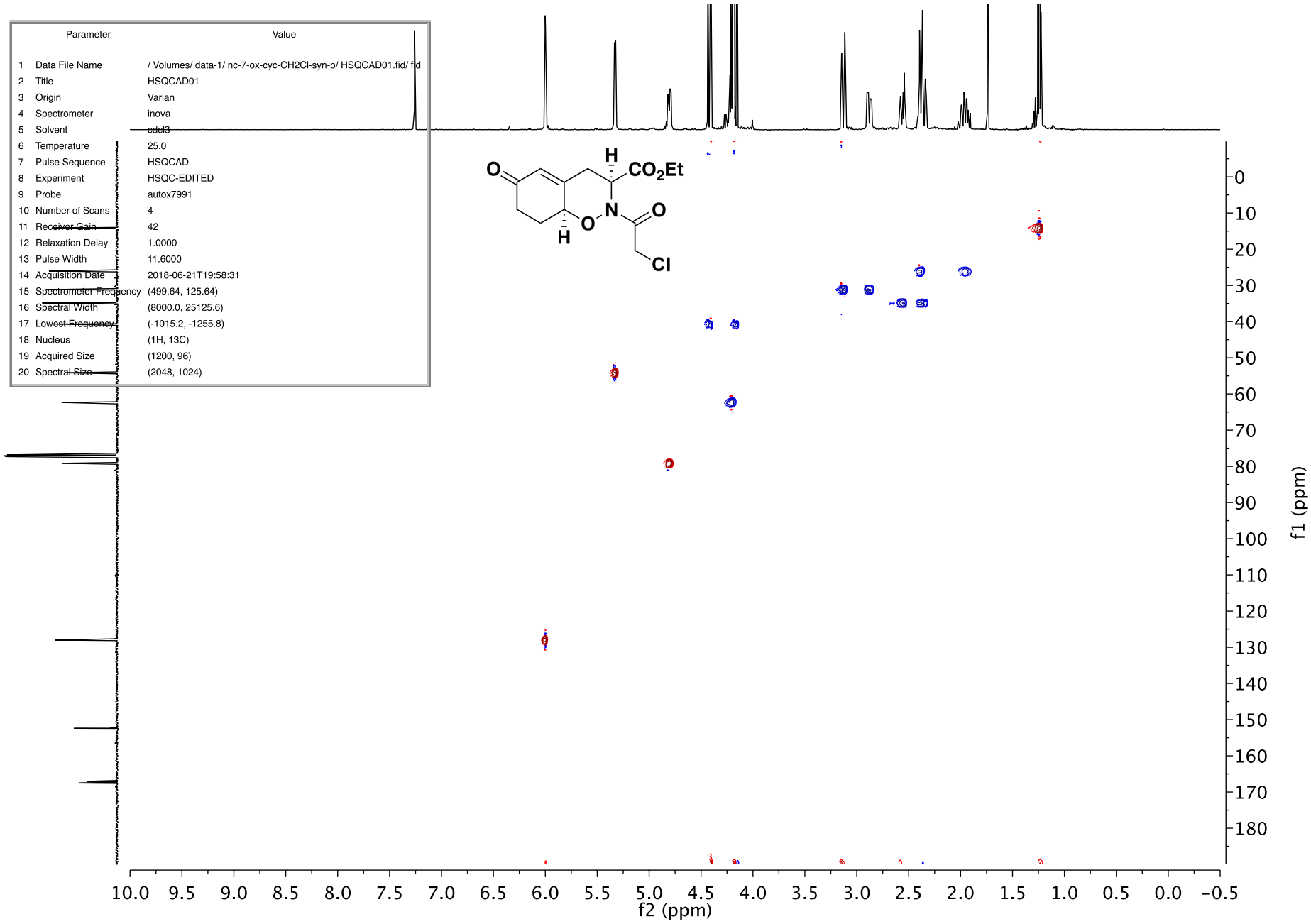
Parameter Value
1 Data File Name / Volumes/ data-1/ nc-7-ox-cyc-CH2Cl-syn-p/ HSQCAD01.fid/ fid
2 Title HSQCAD01
3 Origin Varian
4 Spectrometer inova
5 Solvent cdcl3
6 Temperature 25.0
7 Pulse Sequence HSQCAD
8 Experiment HSQC-EDITED
9 Probe autox7991
10 Number of Scans 4
11 Receiver Gain 42
12 Relaxation Delay 1.0000
13 Pulse Width 11.6000
14 Acquisition Date 2018-06-21T19:58:31
15 Spectrometer Frequency (499.64, 125.64)
16 Spectral Width (8000.0, 25125.6)
17 Lowest Frequency (-1015.2, -1255.8)
18 Nucleus (1H, 13C)
19 Acquired Size (1200, 96)
20 Spectral Size (2048, 1024)
O
H
CO2Et
N
O
O
H
Cl
10.0 9.5 9.0 8.5 8.0 7.5 7.0 6.5 6.0 5.5 5.0 4.5 4.0 3.5 3.0 2.5 2.0 1.5 1.0 0.5 0.0 -0.5
f2 (ppm)
0 10 20 30 40 50 60 70 80 90 100 110 120 130 140 150 160 170 180
f1 (ppm)

	Parameter	Value
1	Data File Name	/ Volumes/ data-1/ nc-7-ox-cyc-CH2Cl-syn-p/ CARBON01.fid/ fid
2	Title	CARBON01
3	Origin	Varian
4	Spectrometer	inova
5	Solvent	cdcl3
6	Temperature	25.0
7	Pulse Sequence	s2pul
8	Experiment	1D
9	Probe	autox7991
10	Number of Scans	1000
11	Receiver Gain	30
12	Relaxation Delay	1.0000
13	Pulse Width	4.6125
14	Acquisition Date	2018-06-21T20:14:42
15	Spectrometer Frequency	125.65
16	Spectral Width	31446.5
17	Lowest Frequency	-1903.7
18	Nucleus	13C
19	Acquired Size	32768
20	Spectral Size	65536

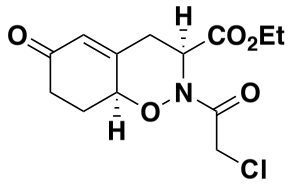

	Parameter	Value
1	Data File Name	/ Volumes/ data-1/ nc-7-free-NH-solvent-contaminated.fid/ fid
2	Title	nc-7-free-NH-solvent-contaminated
3	Origin	Varian
4	Spectrometer	vnmrs
5	Solvent	cdcl3
6	Temperature	65.0
7	Pulse Sequence	s2pul
8	Experiment	1D
9	Probe	OneNMR
10	Number of Scans	15
11	Receiver Gain	48
12	Relaxation Delay	1.0000
13	Pulse Width	4.1500
14	Acquisition Date	2018-07-01T23:28:23
15	Spectrometer Frequency	399.80
16	Spectral Width	6410.3
17	Lowest Frequency	-807.2
18	Nucleus	1H
19	Acquired Size	12821
20	Spectral Size	65536

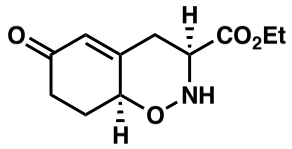

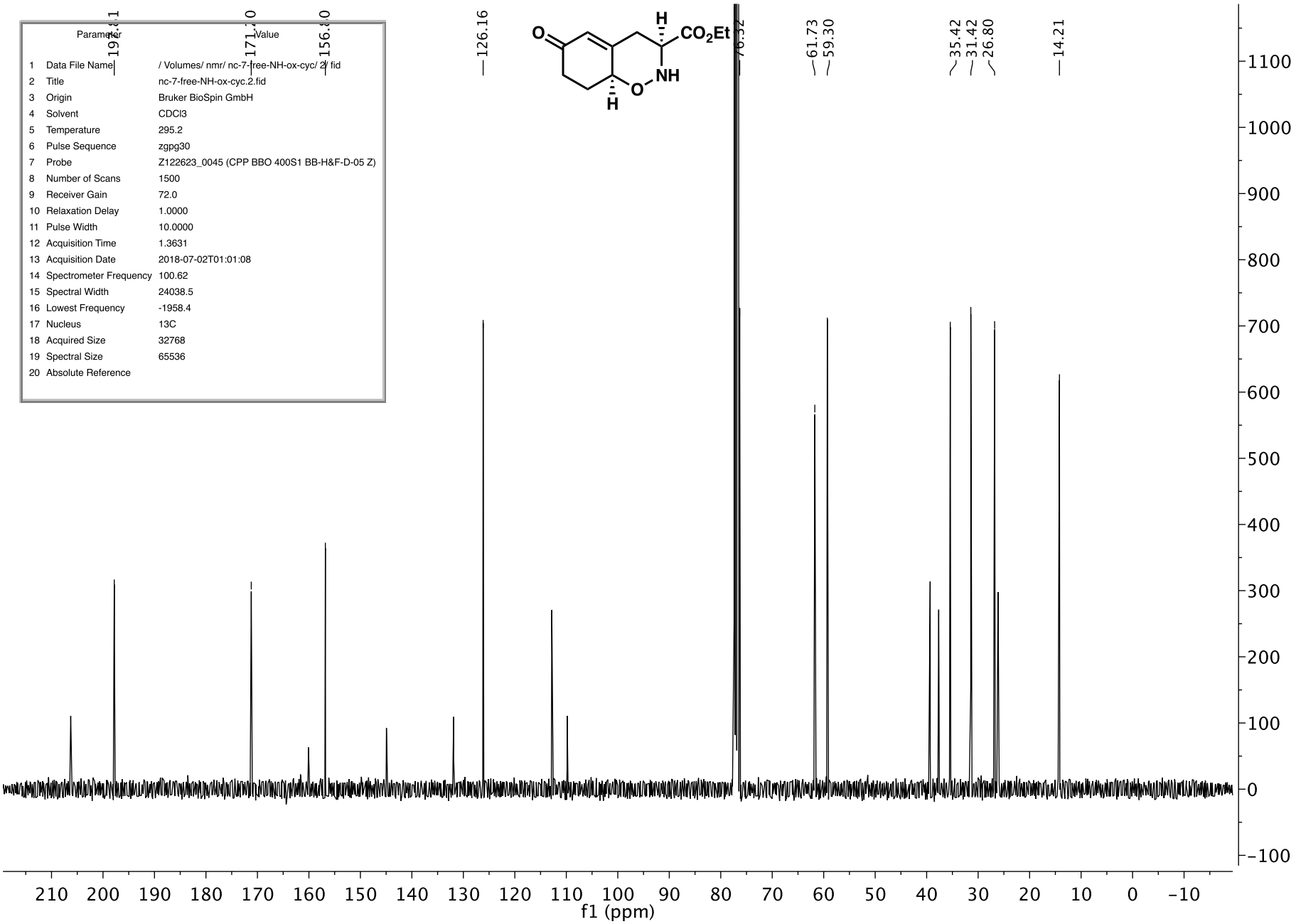
Parameter Value
1 Data File Name / Volumes/ nmr/ nc-7-free-NH-ox-cyc/ 2/ fid
2 Title nc-7-free-NH-ox-cyc.2.fid
3 Origin Bruker BioSpin GmbH
4 Solvent CDCl3
5 Temperature 295.2
6 Pulse Sequence zgpg30
7 Probe Z122623_0045 (CPP BBO 400S1 BB-H&F-D-05 Z)
8 Number of Scans 1500
9 Receiver Gain 72.0
10 Relaxation Delay 1.0000
11 Pulse Width 10.0000
12 Acquisition Time 1.3631
13 Acquisition Date 2018-07-02T01:01:08
14 Spectrometer Frequency 100.62
15 Spectral Width 24038.5
16 Lowest Frequency -1958.4
17 Nucleus 13C
18 Acquired Size 32768
19 Spectral Size 65536
20 Absolute Reference
126.16
61.73
59.30
35.42
31.42
26.80
14.21
O
H
CO2Et
NH
O
H
f1 (ppm)

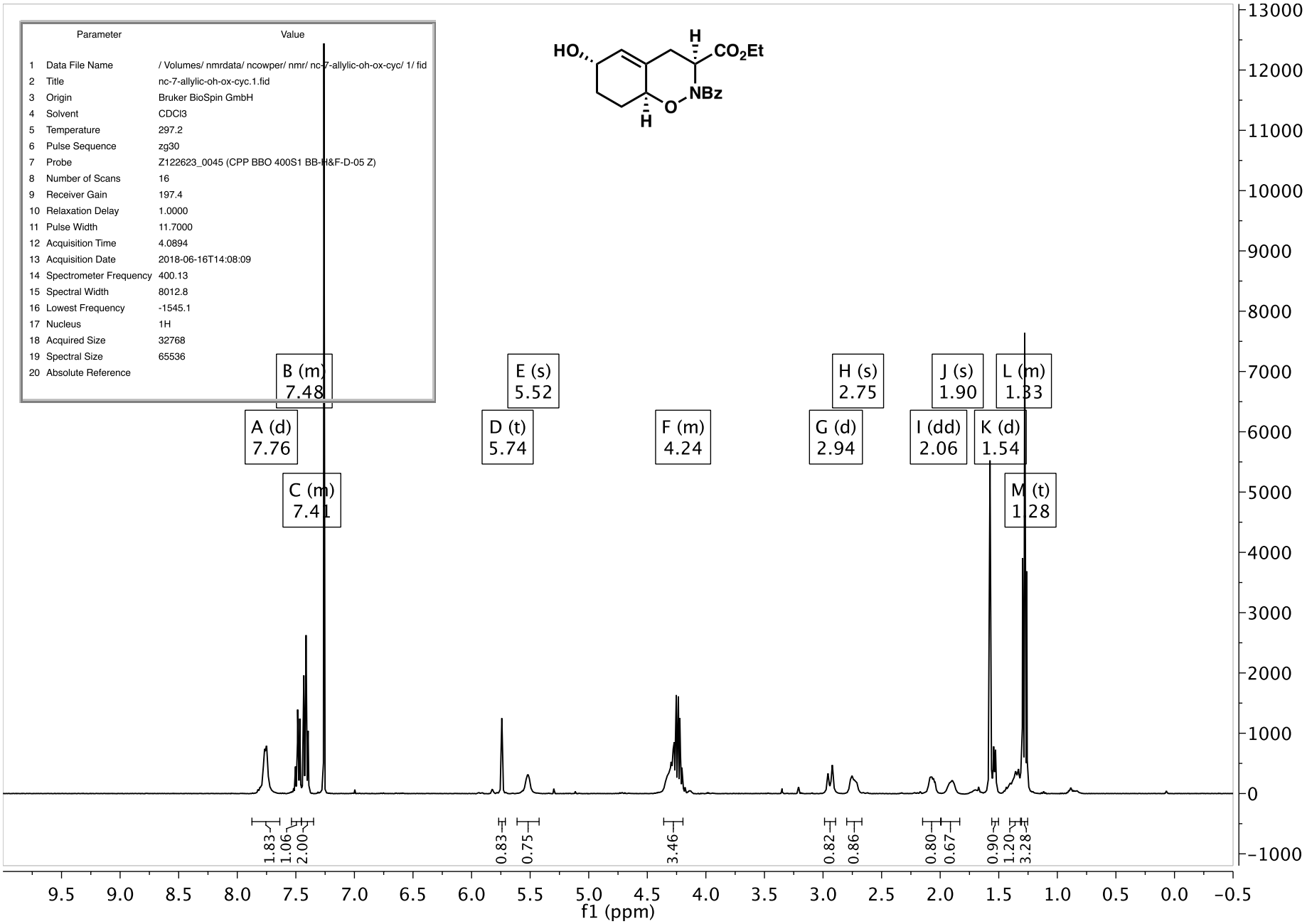
Parameter Value
1 Data File Name / Volumes/ nmrdata/ ncowper/ nmr/ nc-7-allylic-oh-ox-cyc/ 1/ fid
2 Title nc-7-allylic-oh-ox-cyc.1.fid
3 Origin Bruker BioSpin GmbH
4 Solvent CDCl3
5 Temperature 297.2
6 Pulse Sequence zg30
7 Probe Z122623_0045 (CPP BBO 400S1 BB-H&F-D-05 Z)
8 Number of Scans 16
9 Receiver Gain 197.4
10 Relaxation Delay 1.0000
11 Pulse Width 11.7000
12 Acquisition Time 4.0894
13 Acquisition Date 2018-06-16T14:08:09
14 Spectrometer Frequency 400.13
15 Spectral Width 8012.8
16 Lowest Frequency -1545.1
17 Nucleus 1H
18 Acquired Size 32768
19 Spectral Size 65536
20 Absolute Reference
HO
H
CO2Et
NBz
O
H
B (m) 7.48
A (d) 7.76
C (m) 7.41
E (s) 5.52
D (t) 5.74
F (m) 4.24
H (s) 2.75
G (d) 2.94
J (s) 1.90
I (dd) 2.06
L (m) 1.33
K (d) 1.54
M (t) 1.28
1.83
1.06
2.00
0.83
0.75
3.46
0.82
0.86
0.80
0.67
0.90
1.20
3.28
f1 (ppm)

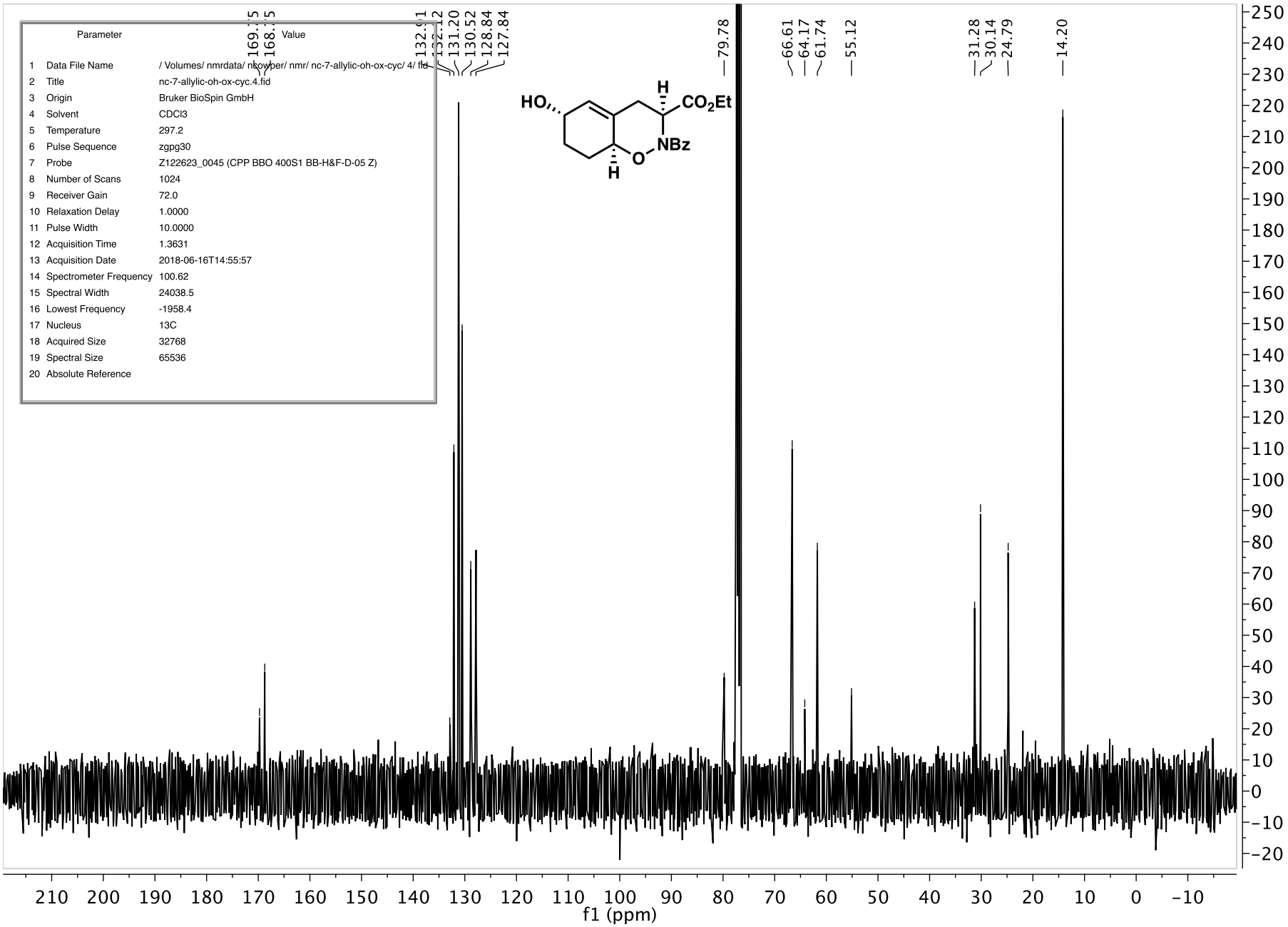
Parameter Value
1 Data File Name / Volumes/ nmrdata/ nbowber/ nmr/ nc-7-allylic-oh-ox-cyc/ 4/ fid
2 Title nc-7-allylic-oh-ox-cyc.4.fid
3 Origin Bruker BioSpin GmbH
4 Solvent CDCl3
5 Temperature 297.2
6 Pulse Sequence zgpg30
7 Probe Z122623_0045 (CPP BBO 400S1 BB-H&F-D-05 Z)
8 Number of Scans 1024
9 Receiver Gain 72.0
10 Relaxation Delay 1.0000
11 Pulse Width 10.0000
12 Acquisition Time 1.3631
13 Acquisition Date 2018-06-16T14:55:57
14 Spectrometer Frequency 100.62
15 Spectral Width 24038.5
16 Lowest Frequency -1958.4
17 Nucleus 13C
18 Acquired Size 32768
19 Spectral Size 65536
20 Absolute Reference
169.15
168.15
132.61
132.12
131.20
130.52
128.84
127.84
79.78
66.61
64.17
61.74
55.12
31.28
30.14
24.79
14.20
HO
H
CO2Et
NBz
O
H
f1 (ppm)

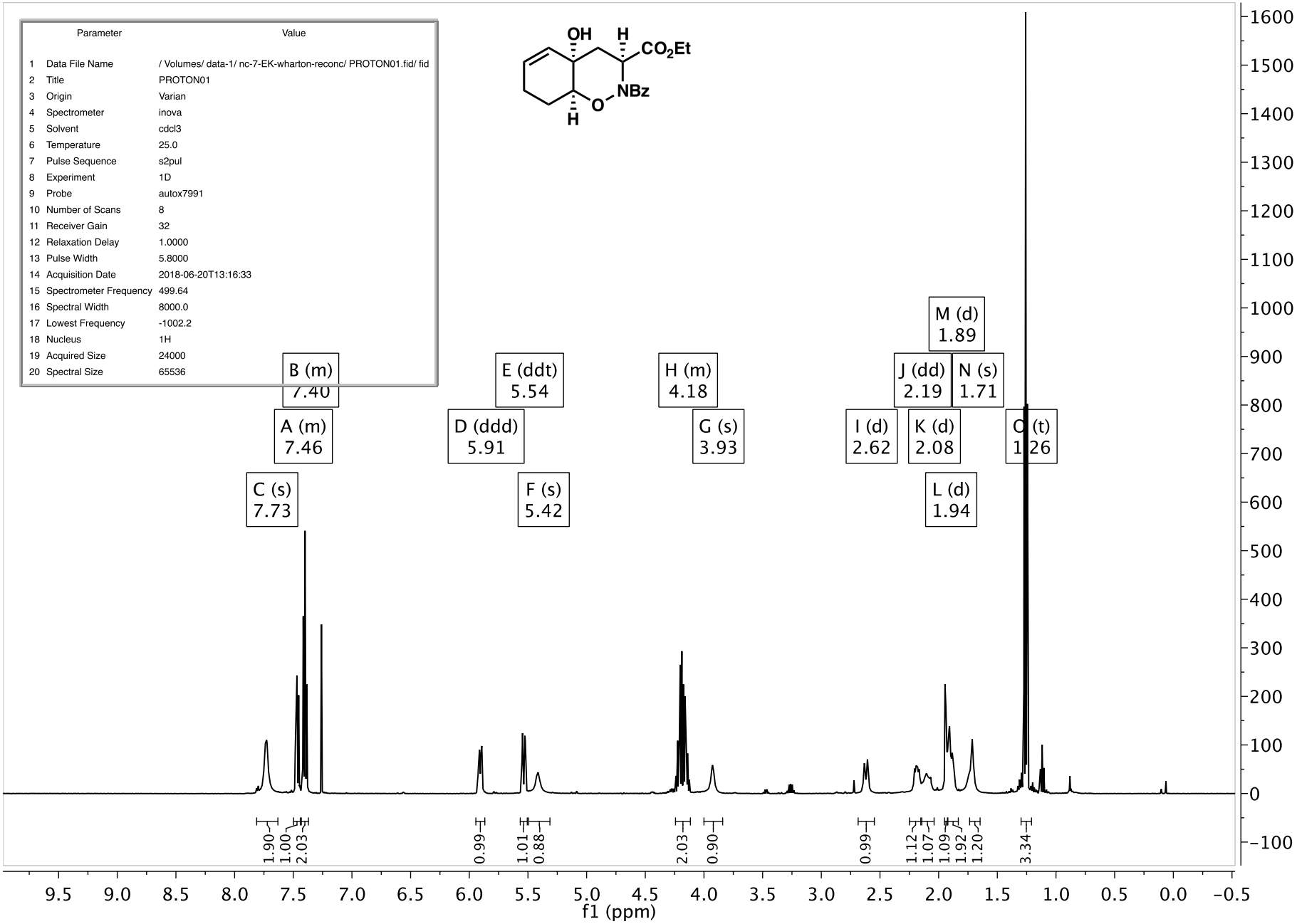
Parameter Value
1 Data File Name / Volumes/ data-1/ nc-7-EK-wharton-reconc/ PROTON01.fid/ fid
2 Title PROTON01
3 Origin Varian
4 Spectrometer inova
5 Solvent cdcl3
6 Temperature 25.0
7 Pulse Sequence s2pul
8 Experiment 1D
9 Probe autox7991
10 Number of Scans 8
11 Receiver Gain 32
12 Relaxation Delay 1.0000
13 Pulse Width 5.8000
14 Acquisition Date 2018-06-20T13:16:33
15 Spectrometer Frequency 499.64
16 Spectral Width 8000.0
17 Lowest Frequency -1002.2
18 Nucleus 1H
19 Acquired Size 24000
20 Spectral Size 65536
OH
H
CO2Et
NBz
O
H
B (m)
7.40
A (m)
7.46
C (s)
7.73
E (ddt)
5.54
D (ddd)
5.91
F (s)
5.42
H (m)
4.18
G (s)
3.93
M (d)
1.89
J (dd)
2.19
N (s)
1.71
I (d)
2.62
K (d)
2.08
L (d)
1.94
O (t)
1.26
1.90
1.00
2.03
0.99
1.01
0.88
2.03
0.90
0.99
1.12
1.07
1.09
1.92
1.20
3.34
f1 (ppm)

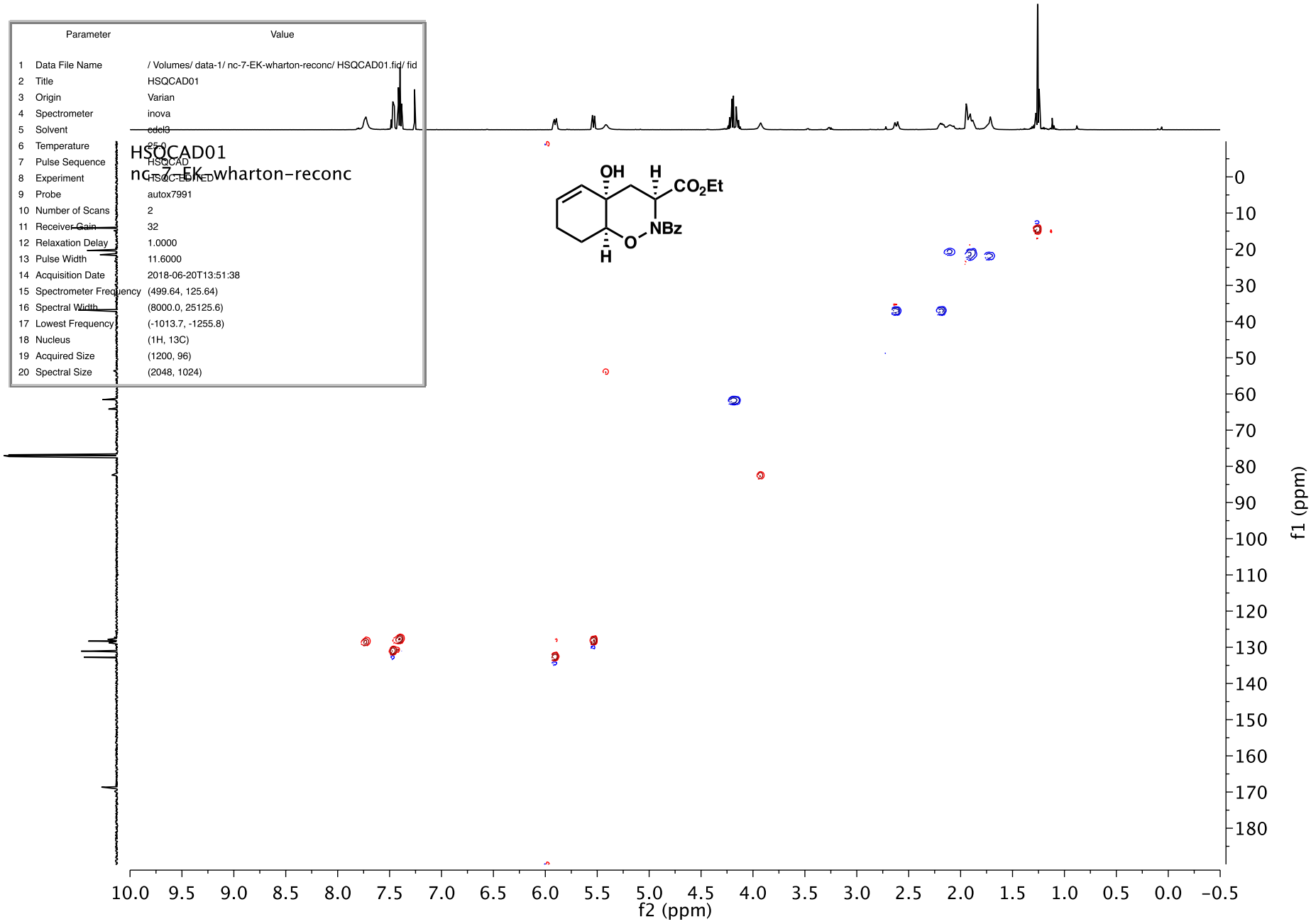
Parameter Value
1 Data File Name / Volumes/ data-1/ nc-7-EK-wharton-reconc/ HSQCAD01.fid/ fid
2 Title HSQCAD01
3 Origin Varian
4 Spectrometer inova
5 Solvent cdcl3
6 Temperature 25.0
7 Pulse Sequence HSQCAD
8 Experiment HSQC-EDITED
9 Probe autox7991
10 Number of Scans 2
11 Receiver Gain 32
12 Relaxation Delay 1.0000
13 Pulse Width 11.6000
14 Acquisition Date 2018-06-20T13:51:38
15 Spectrometer Frequency (499.64, 125.64)
16 Spectral Width (8000.0, 25125.6)
17 Lowest Frequency (-1013.7, -1255.8)
18 Nucleus (1H, 13C)
19 Acquired Size (1200, 96)
20 Spectral Size (2048, 1024)
HSQCAD01
nc-7-EK-wharton-reconc
OH
H
CO2Et
NBz
O
H
10.0 9.5 9.0 8.5 8.0 7.5 7.0 6.5 6.0 5.5 5.0 4.5 4.0 3.5 3.0 2.5 2.0 1.5 1.0 0.5 0.0 -0.5
f2 (ppm)
0 10 20 30 40 50 60 70 80 90 100 110 120 130 140 150 160 170 180
f1 (ppm)

CARBON01

nc-7-EK-wharton-reconc

	Parameter	Value
1	Data File Name	/ Volumes/ data-1/ nc-7-EK-wharton-reconc/ CARBON01.fid/ fid
2	Title	CARBON01
3	Origin	Varian
4	Spectrometer	inova
5	Solvent	cdcl3
6	Temperature	25.0
7	Pulse Sequence	s2pul
8	Experiment	1D
9	Probe	autox7991
10	Number of Scans	1000
11	Receiver Gain	30
12	Relaxation Delay	1.0000
13	Pulse Width	4.6125
14	Acquisition Date	2018-06-20T13:17:22
15	Spectrometer Frequency	125.65
16	Spectral Width	31446.5
17	Lowest Frequency	-1903.7
18	Nucleus	13C
19	Acquired Size	32768
20	Spectral Size	65536

169.49
168.76
133.17
132.90
131.18
128.86
128.40
127.91
82.54
64.29
61.68
53.74
36.88
21.64
20.46
14.26

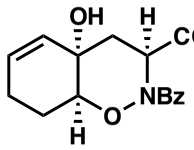

2400
2200
2000
1800
1600
1400
1200
1000
800
600
400
200
0
-200

230 220 210 200 190 180 170 160 150 140 130 120 110 100 90 80 70 60 50 40 30 20 10 0 -10

f1 (ppm)

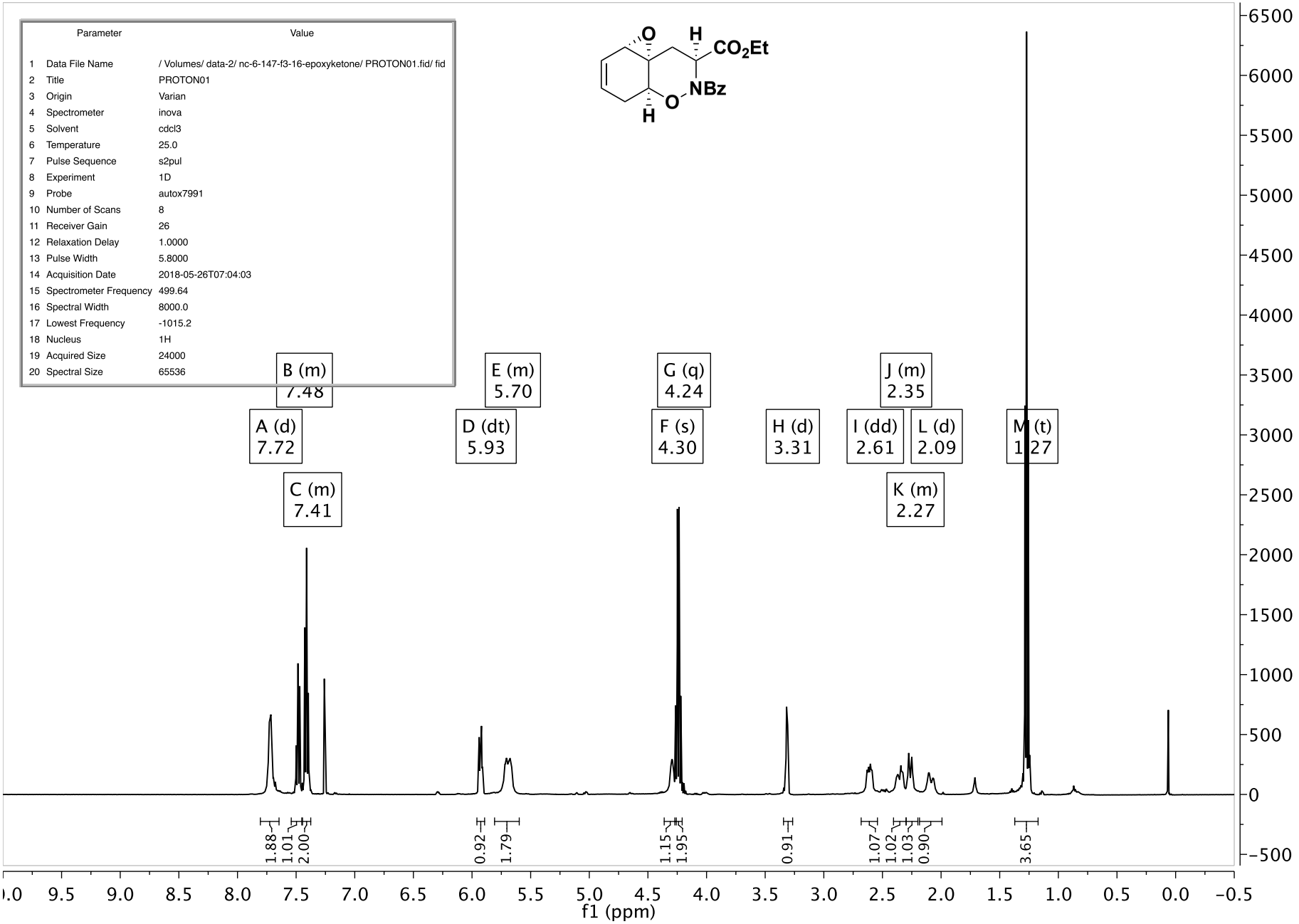
Parameter Value
1 Data File Name / Volumes/ data-2/ nc-6-147-f3-16-epoxyketone/ PROTON01.fid/ fid
2 Title PROTON01
3 Origin Varian
4 Spectrometer inova
5 Solvent cdcl3
6 Temperature 25.0
7 Pulse Sequence s2pul
8 Experiment 1D
9 Probe autox7991
10 Number of Scans 8
11 Receiver Gain 26
12 Relaxation Delay 1.0000
13 Pulse Width 5.8000
14 Acquisition Date 2018-05-26T07:04:03
15 Spectrometer Frequency 499.64
16 Spectral Width 8000.0
17 Lowest Frequency -1015.2
18 Nucleus 1H
19 Acquired Size 24000
20 Spectral Size 65536
O
H
CO2Et
NBz
O
H
A (d) 7.72
B (m) 7.48
C (m) 7.41
D (dt) 5.93
E (m) 5.70
F (s) 4.30
G (q) 4.24
H (d) 3.31
I (dd) 2.61
J (m) 2.35
K (m) 2.27
L (d) 2.09
M (t) 1.27
1.88
1.01
2.00
0.92
1.79
1.15
1.95
0.91
1.07
1.02
1.03
0.90
3.65
6500
6000
5500
5000
4500
4000
3500
3000
2500
2000
1500
1000
500
0
-500
9.5
9.0
8.5
8.0
7.5
7.0
6.5
6.0
5.5
5.0
4.5
4.0
3.5
3.0
2.5
2.0
1.5
1.0
0.5
0.0
-0.5
f1 (ppm)

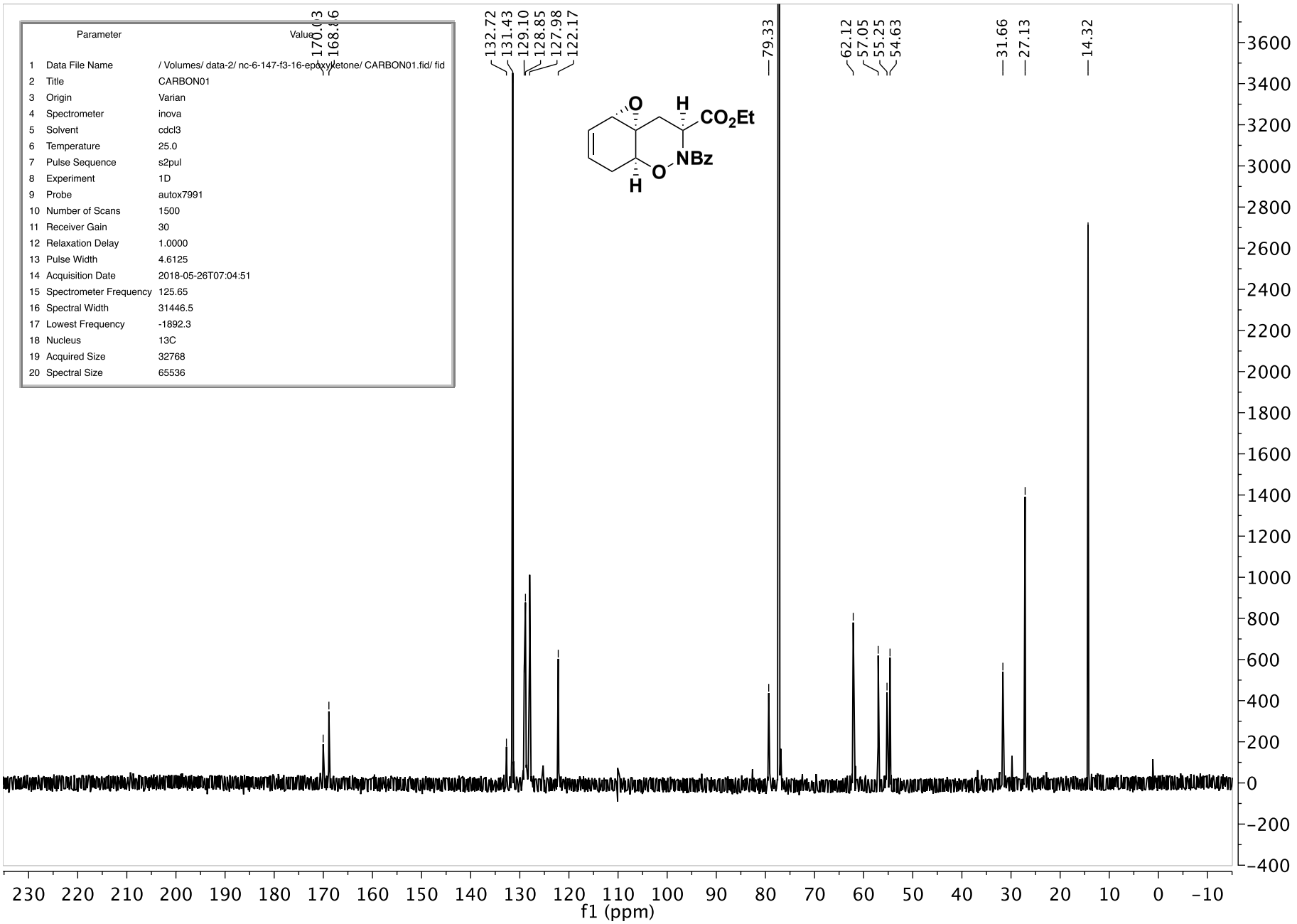
Parameter Value
1 Data File Name / Volumes/ data-2/ nc-6-147-f3-16-epoxyketone/ CARBON01.fid/ fid
2 Title CARBON01
3 Origin Varian
4 Spectrometer inova
5 Solvent cdcl3
6 Temperature 25.0
7 Pulse Sequence s2pul
8 Experiment 1D
9 Probe autox7991
10 Number of Scans 1500
11 Receiver Gain 30
12 Relaxation Delay 1.0000
13 Pulse Width 4.6125
14 Acquisition Date 2018-05-26T07:04:51
15 Spectrometer Frequency 125.65
16 Spectral Width 31446.5
17 Lowest Frequency -1892.3
18 Nucleus 13C
19 Acquired Size 32768
20 Spectral Size 65536
170.03
168.26
132.72
131.43
129.10
128.85
127.98
122.17
79.33
62.12
57.05
55.25
54.63
31.66
27.13
14.32
O
H
CO2Et
NBz
O
H
3600
3400
3200
3000
2800
2600
2400
2200
2000
1800
1600
1400
1200
1000
800
600
400
200
0
-200
-400
230 220 210 200 190 180 170 160 150 140 130 120 110 100 90 80 70 60 50 40 30 20 10 0 -10
f1 (ppm)

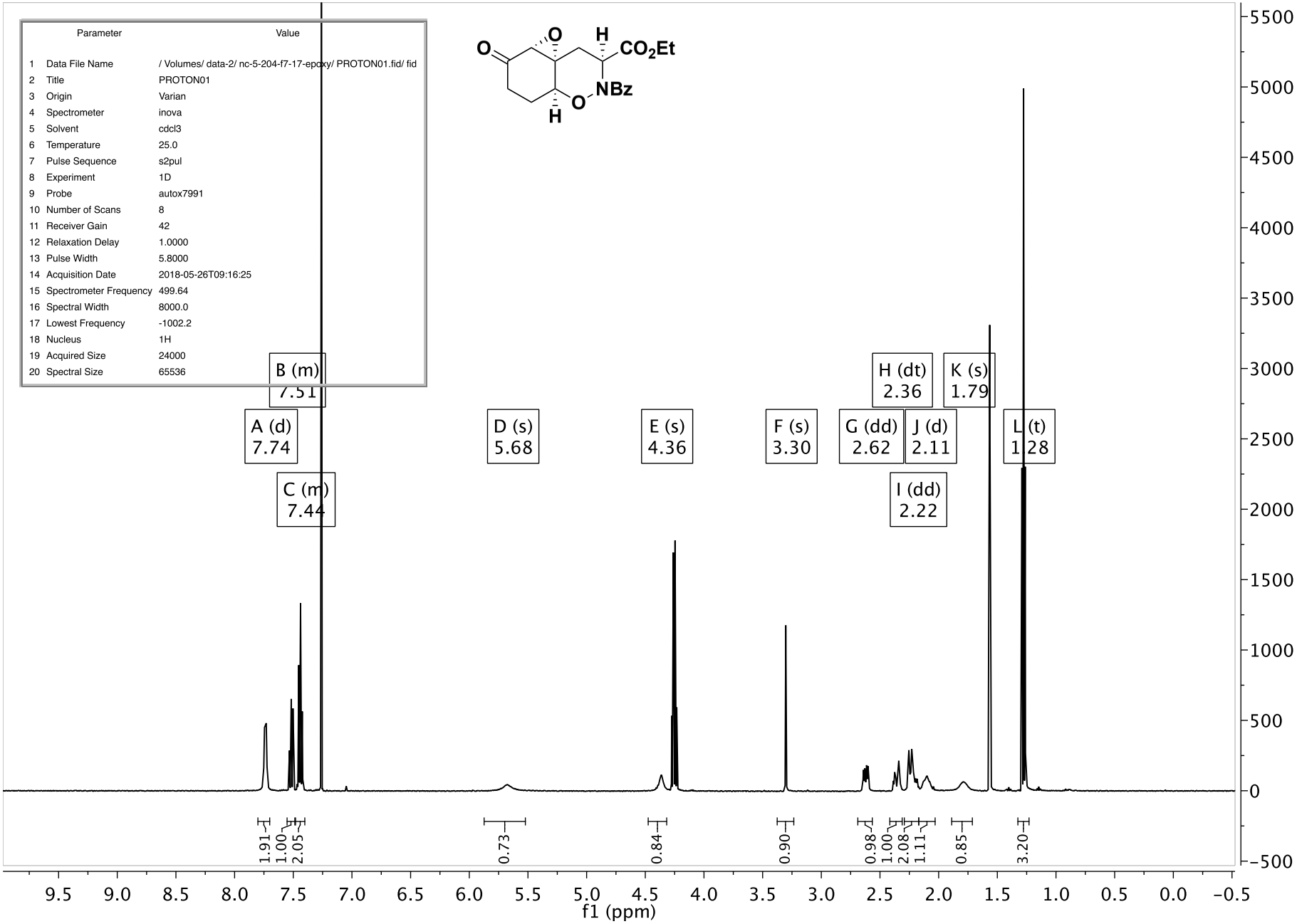
Parameter Value
1 Data File Name / Volumes/ data-2/ nc-5-204-f7-17-epoxy/ PROTON01.fid/ fid
2 Title PROTON01
3 Origin Varian
4 Spectrometer inova
5 Solvent cdcl3
6 Temperature 25.0
7 Pulse Sequence s2pul
8 Experiment 1D
9 Probe autox7991
10 Number of Scans 8
11 Receiver Gain 42
12 Relaxation Delay 1.0000
13 Pulse Width 5.8000
14 Acquisition Date 2018-05-26T09:16:25
15 Spectrometer Frequency 499.64
16 Spectral Width 8000.0
17 Lowest Frequency -1002.2
18 Nucleus 1H
19 Acquired Size 24000
20 Spectral Size 65536
O
O
H
CO2Et
NBz
O
H
B (m)
7.51
A (d)
7.74
C (m)
7.44
D (s)
5.68
E (s)
4.36
F (s)
3.30
G (dd)
2.62
H (dt)
2.36
I (dd)
2.22
J (d)
2.11
K (s)
1.79
L (t)
1.28
1.91
1.00
2.05
0.73
0.84
0.90
0.98
1.00
2.08
1.11
0.85
3.20
f1 (ppm)

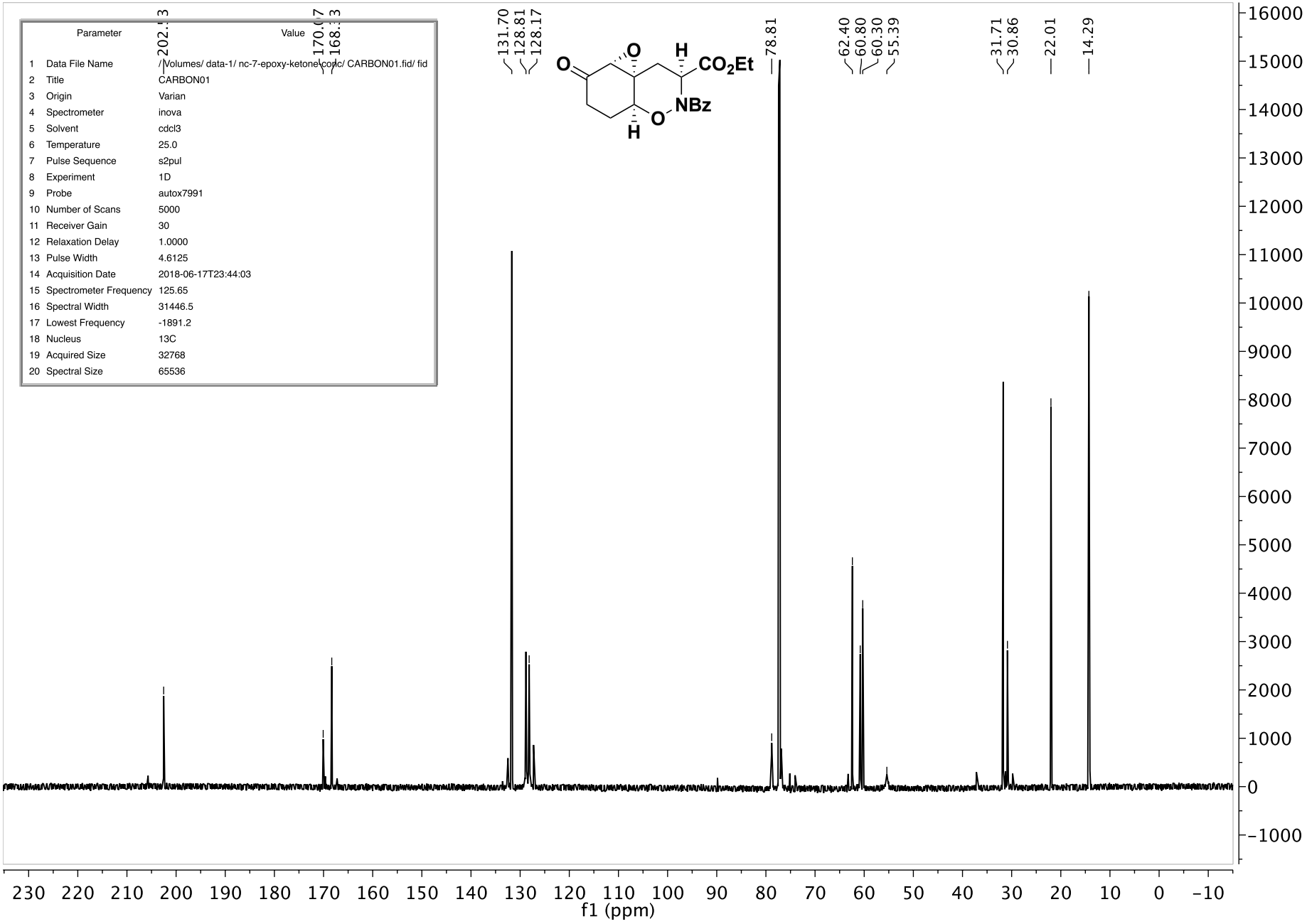
Parameter Value
1 Data File Name /Volumes/ data-1/ nc-7-epoxy-ketone.com/c/ CARBON01.fid/ fid
2 Title CARBON01
3 Origin Varian
4 Spectrometer inova
5 Solvent cdcl3
6 Temperature 25.0
7 Pulse Sequence s2pul
8 Experiment 1D
9 Probe autox7991
10 Number of Scans 5000
11 Receiver Gain 30
12 Relaxation Delay 1.0000
13 Pulse Width 4.6125
14 Acquisition Date 2018-06-17T23:44:03
15 Spectrometer Frequency 125.65
16 Spectral Width 31446.5
17 Lowest Frequency -1891.2
18 Nucleus 13C
19 Acquired Size 32768
20 Spectral Size 65536
202.13
170.07
168.33
131.70
128.81
128.17
78.81
62.40
60.80
60.30
55.39
31.71
30.86
22.01
14.29
O
O
H
CO2Et
NBz
O
H
16000
15000
14000
13000
12000
11000
10000
9000
8000
7000
6000
5000
4000
3000
2000
1000
0
-1000
230 220 210 200 190 180 170 160 150 140 130 120 110 100 90 80 70 60 50 40 30 20 10 0 -10
f1 (ppm)

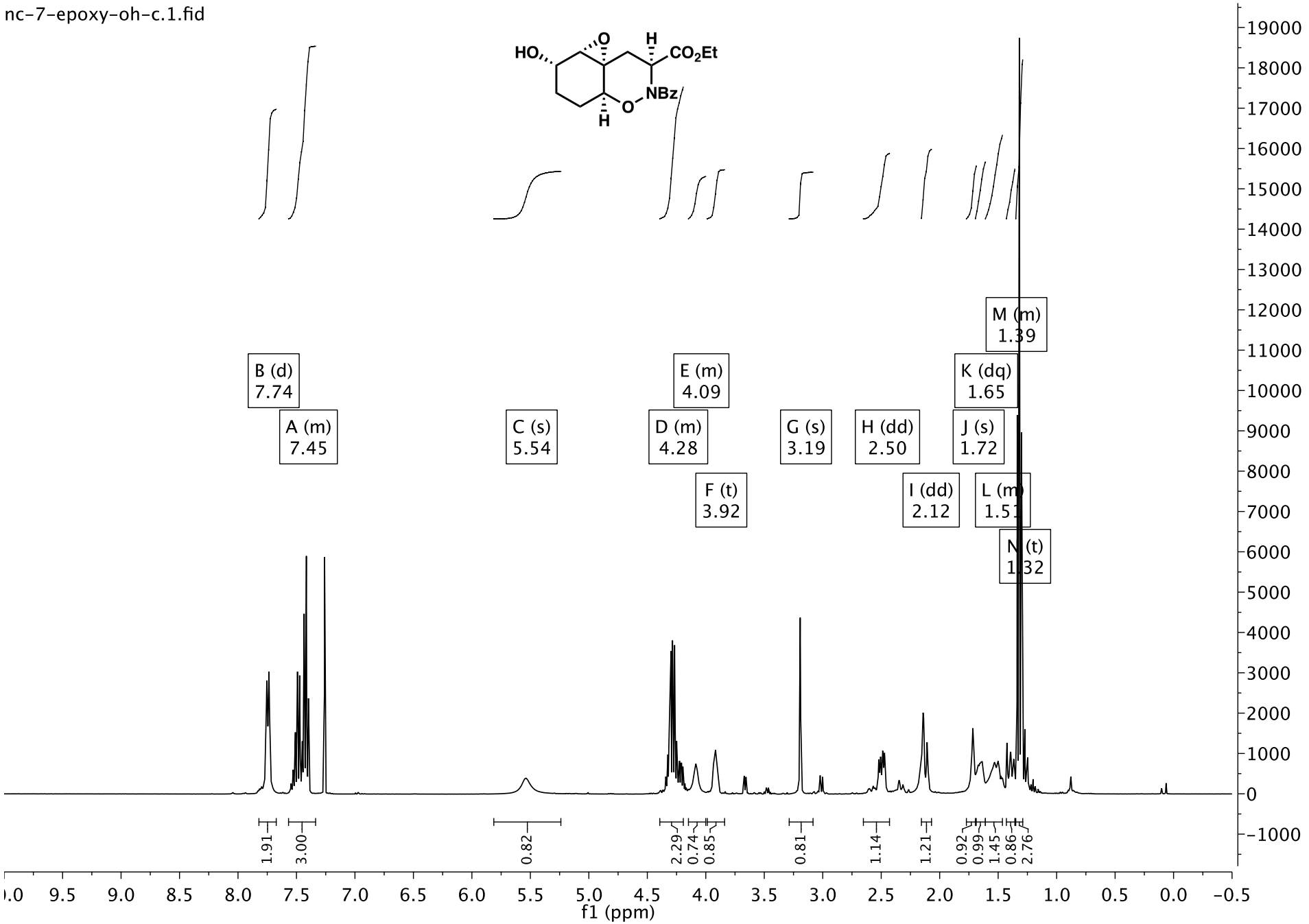
nc-7-epoxy-oh-c.1.fid
HO
O
H
CO2Et
NBz
O
H
B (d)
7.74
A (m)
7.45
C (s)
5.54
E (m)
4.09
D (m)
4.28
F (t)
3.92
G (s)
3.19
H (dd)
2.50
I (dd)
2.12
K (dq)
1.65
J (s)
1.72
M (m)
1.39
L (m)
1.51
N (t)
1.32
1.91
3.00
0.82
2.29
0.74
0.85
0.81
1.14
1.21
0.92
0.99
1.45
0.86
2.76
f1 (ppm)

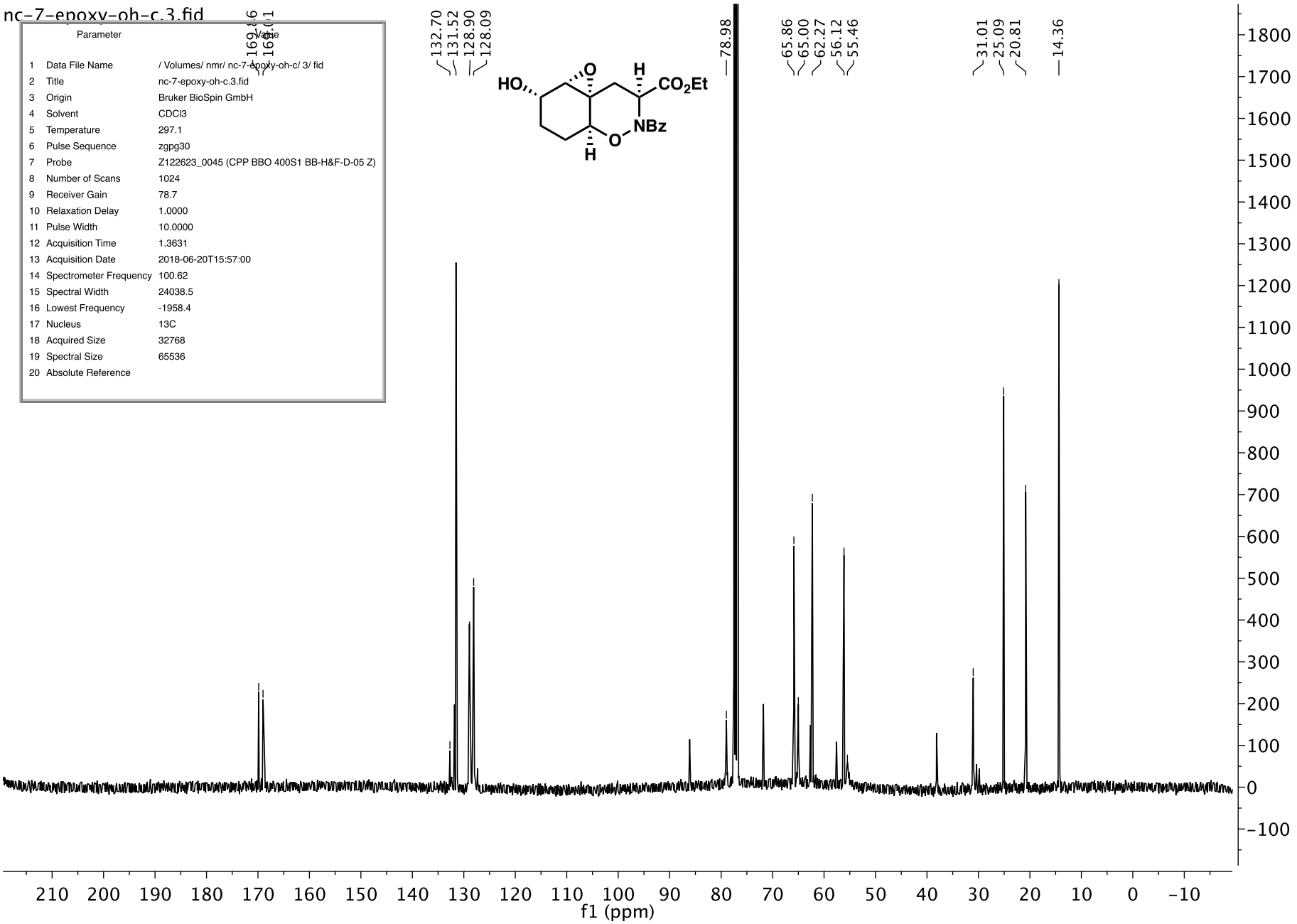
nc-7-epoxy-oh-c.3.fid
Parameter
Value
1 Data File Name / Volumes/ nmr/ nc-7-epoxy-oh-c/ 3/ fid
2 Title nc-7-epoxy-oh-c.3.fid
3 Origin Bruker BioSpin GmbH
4 Solvent CDCl3
5 Temperature 297.1
6 Pulse Sequence zgpg30
7 Probe Z122623_0045 (CPP BBO 400S1 BB-H&F-D-05 Z)
8 Number of Scans 1024
9 Receiver Gain 78.7
10 Relaxation Delay 1.0000
11 Pulse Width 10.0000
12 Acquisition Time 1.3631
13 Acquisition Date 2018-06-20T15:57:00
14 Spectrometer Frequency 100.62
15 Spectral Width 24038.5
16 Lowest Frequency -1958.4
17 Nucleus 13C
18 Acquired Size 32768
19 Spectral Size 65536
20 Absolute Reference
169.86
166.01
132.70
131.52
128.90
128.09
78.98
65.86
65.00
62.27
56.12
55.46
31.01
25.09
20.81
14.36
HO
O
H
CO2Et
NBz
O
H
f1 (ppm)

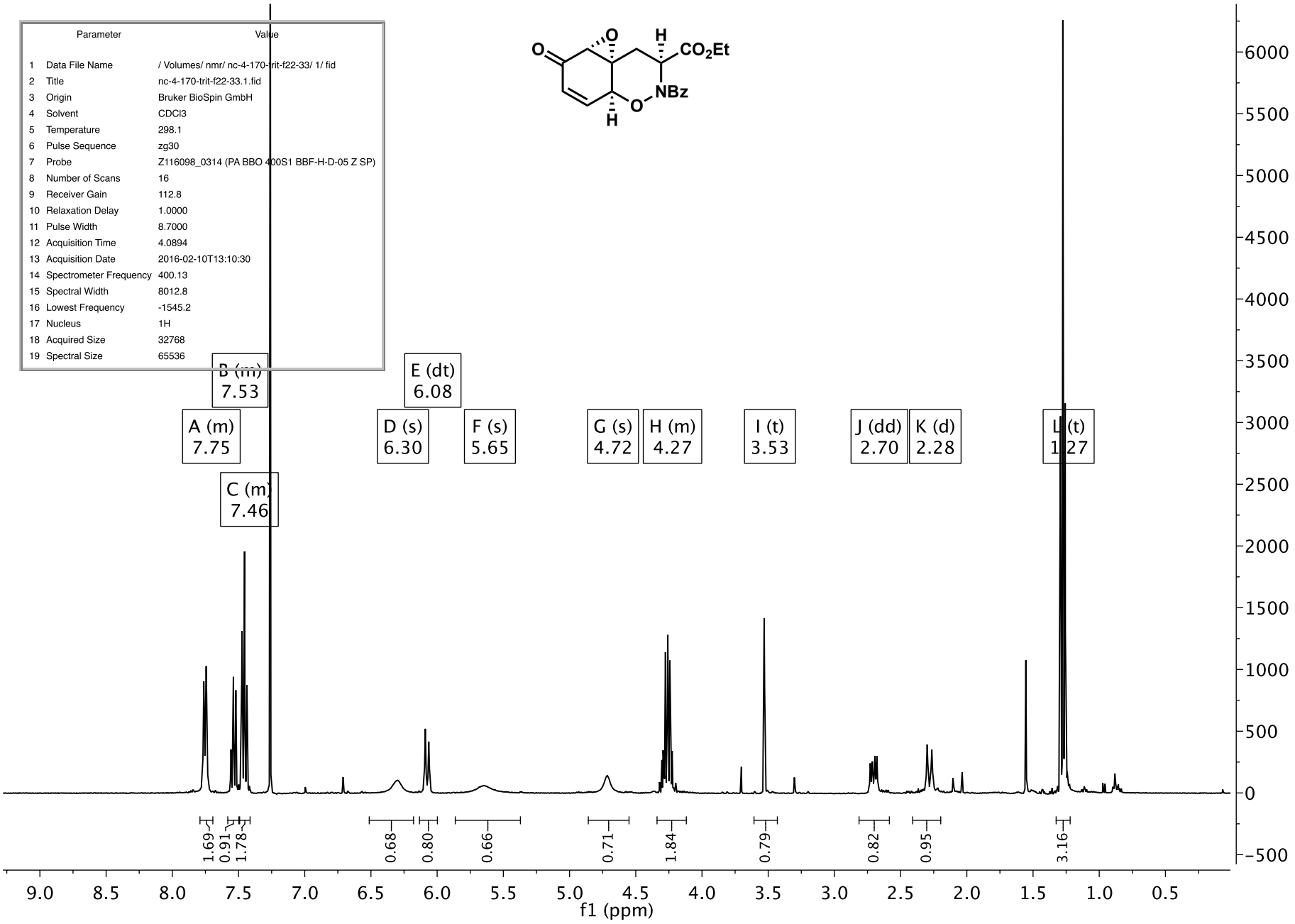
Parameter Value
1 Data File Name / Volumes/ nmr/ nc-4-170-rit-f22-33/ 1/ fid
2 Title nc-4-170-trit-f22-33.1.fid
3 Origin Bruker BioSpin GmbH
4 Solvent CDCl3
5 Temperature 298.1
6 Pulse Sequence zg30
7 Probe Z116098_0314 (PA BBO 400S1 BBF-H-D-05 Z SP)
8 Number of Scans 16
9 Receiver Gain 112.8
10 Relaxation Delay 1.0000
11 Pulse Width 8.7000
12 Acquisition Time 4.0894
13 Acquisition Date 2016-02-10T13:10:30
14 Spectrometer Frequency 400.13
15 Spectral Width 8012.8
16 Lowest Frequency -1545.2
17 Nucleus 1H
18 Acquired Size 32768
19 Spectral Size 65536
O
O
H
CO2Et
NBz
O
H
B (m) 7.53
E (dt) 6.08
A (m) 7.75
D (s) 6.30
F (s) 5.65
G (s) 4.72
H (m) 4.27
I (t) 3.53
J (dd) 2.70
K (d) 2.28
L (t) 1.27
C (m) 7.46
1.69
0.91
1.78
0.68
0.80
0.66
0.71
1.84
0.79
0.82
0.95
3.16
6000
5500
5000
4500
4000
3500
3000
2500
2000
1500
1000
500
0
-500
9.0
8.5
8.0
7.5
7.0
6.5
6.0
5.5
5.0
4.5
4.0
3.5
3.0
2.5
2.0
1.5
1.0
0.5
f1 (ppm)

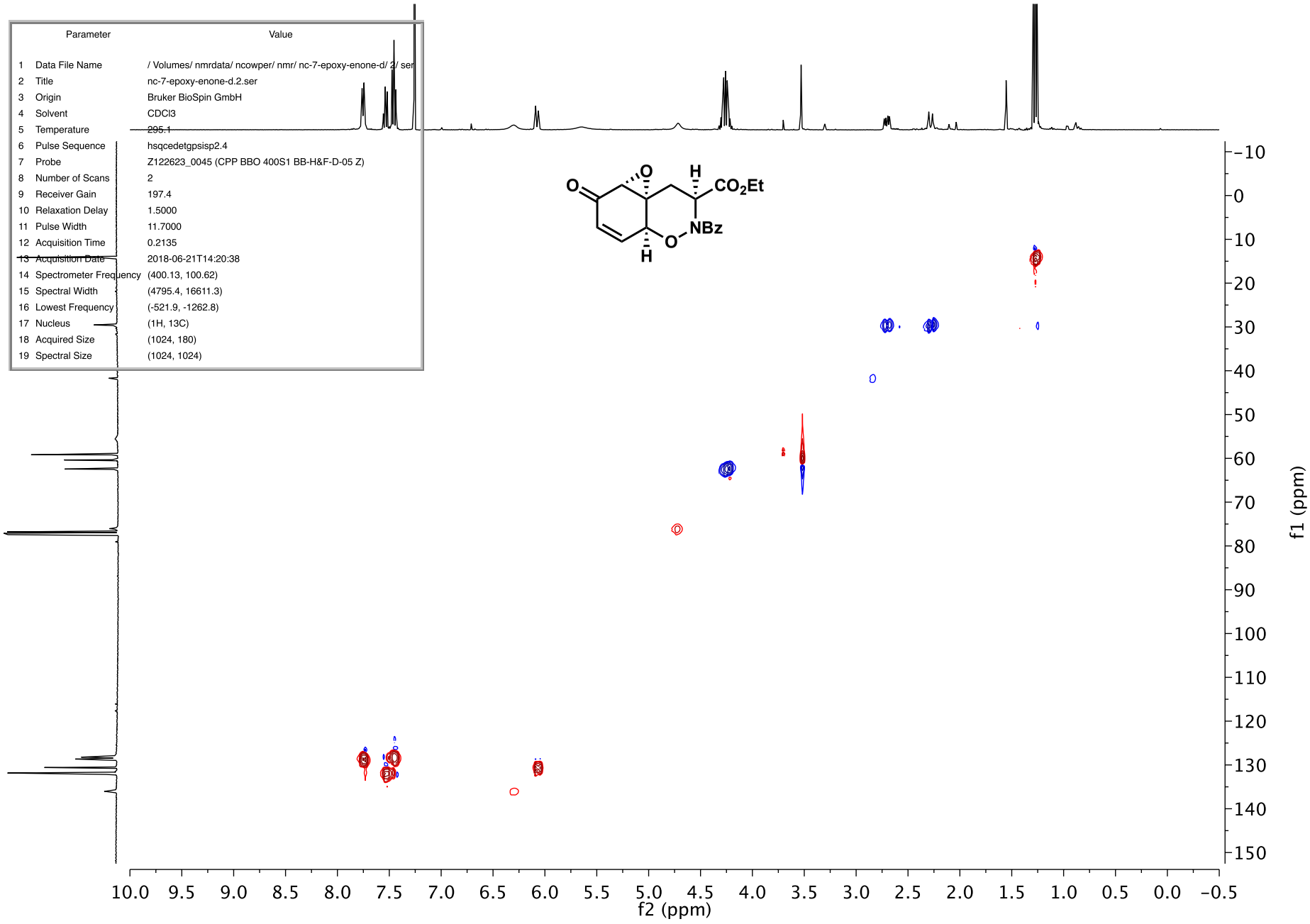
Parameter Value
1 Data File Name / Volumes/ nmrdata/ ncowper/ nmr/ nc-7-epoxy-enone-d/ 2/ ser
2 Title nc-7-epoxy-enone-d.2.ser
3 Origin Bruker BioSpin GmbH
4 Solvent CDCl3
5 Temperature 295.1
6 Pulse Sequence hsqcedetgpsisp2.4
7 Probe Z122623_0045 (CPP BBO 400S1 BB-H&F-D-05 Z)
8 Number of Scans 2
9 Receiver Gain 197.4
10 Relaxation Delay 1.5000
11 Pulse Width 11.7000
12 Acquisition Time 0.2135
13 Acquisition Date 2018-06-21T14:20:38
14 Spectrometer Frequency (400.13, 100.62)
15 Spectral Width (4795.4, 16611.3)
16 Lowest Frequency (-521.9, -1262.8)
17 Nucleus (1H, 13C)
18 Acquired Size (1024, 180)
19 Spectral Size (1024, 1024)
O
O
H
CO2Et
NBz
O
H
10.0 9.5 9.0 8.5 8.0 7.5 7.0 6.5 6.0 5.5 5.0 4.5 4.0 3.5 3.0 2.5 2.0 1.5 1.0 0.5 0.0 -0.5
f2 (ppm)
-10 0 10 20 30 40 50 60 70 80 90 100 110 120 130 140 150
f1 (ppm)

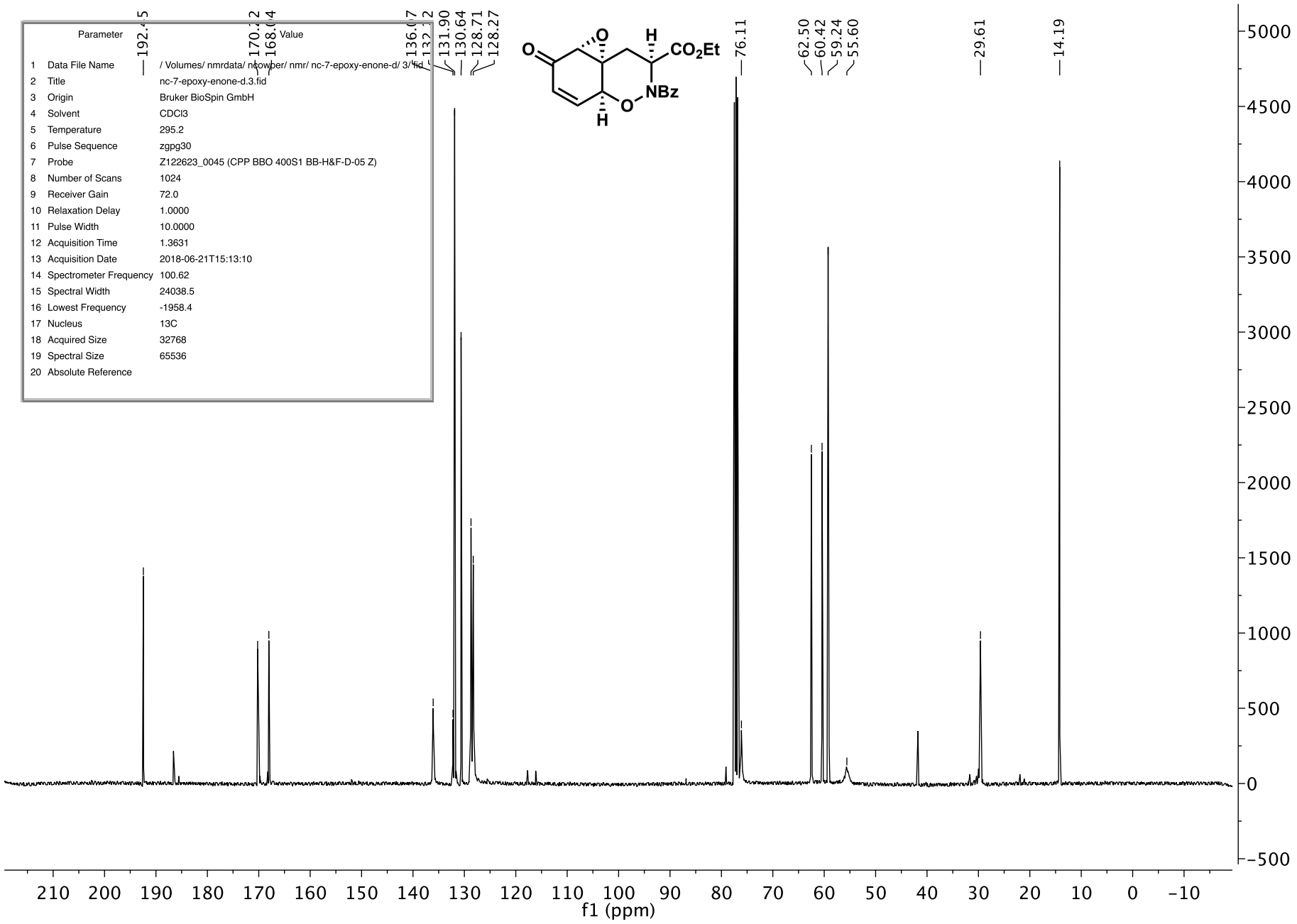
192.45
170.12
168.04
136.07
132.12
131.90
130.64
128.71
128.27
76.11
62.50
60.42
59.24
55.60
29.61
14.19
O
H
CO2Et
NBz
O
H
Parameter Value
1 Data File Name / Volumes/ nmrdata/ ntowber/ nmr/ nc-7-epoxy-enone-d/ 3/fid
2 Title nc-7-epoxy-enone-d.3.fid
3 Origin Bruker BioSpin GmbH
4 Solvent CDCl3
5 Temperature 295.2
6 Pulse Sequence zgpg30
7 Probe Z122623_0045 (CPP BBO 400S1 BB-H&F-D-05 Z)
8 Number of Scans 1024
9 Receiver Gain 72.0
10 Relaxation Delay 1.0000
11 Pulse Width 10.0000
12 Acquisition Time 1.3631
13 Acquisition Date 2018-06-21T15:13:10
14 Spectrometer Frequency 100.62
15 Spectral Width 24038.5
16 Lowest Frequency -1958.4
17 Nucleus 13C
18 Acquired Size 32768
19 Spectral Size 65536
20 Absolute Reference
5000
4500
4000
3500
3000
2500
2000
1500
1000
500
0
-500
210 200 190 180 170 160 150 140 130 120 110 100 90 80 70 60 50 40 30 20 10 0 -10
f1 (ppm)

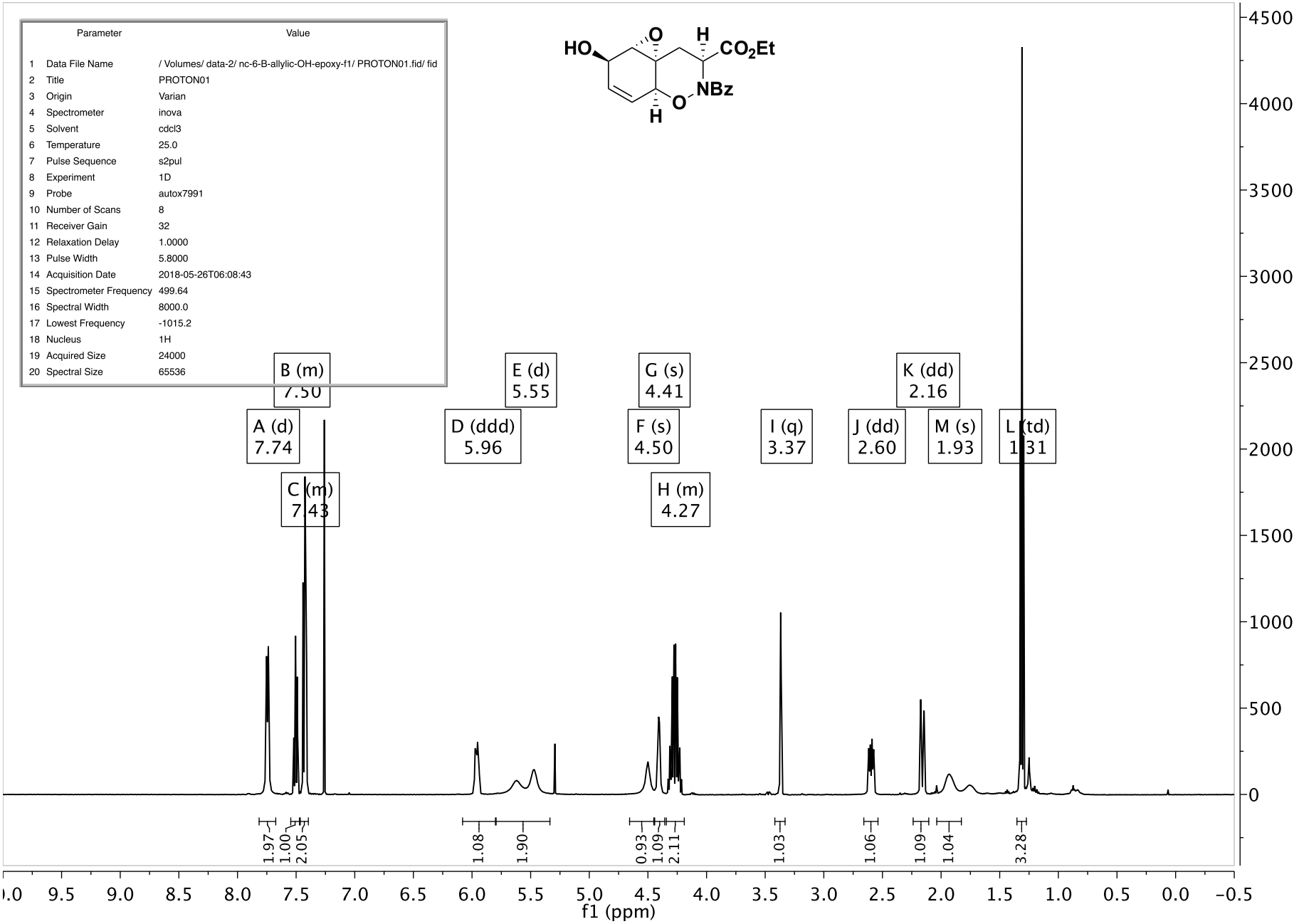
Parameter Value
1 Data File Name / Volumes/ data-2/ nc-6-B-allylic-OH-epoxy-f1/ PROTON01.fid/ fid
2 Title PROTON01
3 Origin Varian
4 Spectrometer inova
5 Solvent cdcl3
6 Temperature 25.0
7 Pulse Sequence s2pul
8 Experiment 1D
9 Probe autox7991
10 Number of Scans 8
11 Receiver Gain 32
12 Relaxation Delay 1.0000
13 Pulse Width 5.8000
14 Acquisition Date 2018-05-26T06:08:43
15 Spectrometer Frequency 499.64
16 Spectral Width 8000.0
17 Lowest Frequency -1015.2
18 Nucleus 1H
19 Acquired Size 24000
20 Spectral Size 65536
HO
O
H
CO2Et
NBz
O
H
A (d) 7.74
B (m) 7.50
C (m) 7.43
D (ddd) 5.96
E (d) 5.55
F (s) 4.50
G (s) 4.41
H (m) 4.27
I (q) 3.37
J (dd) 2.60
K (dd) 2.16
M (s) 1.93
L (td) 1.31
1.97
1.00
2.05
1.08
1.90
0.93
1.09
2.11
1.03
1.06
1.09
1.04
3.28
f1 (ppm)

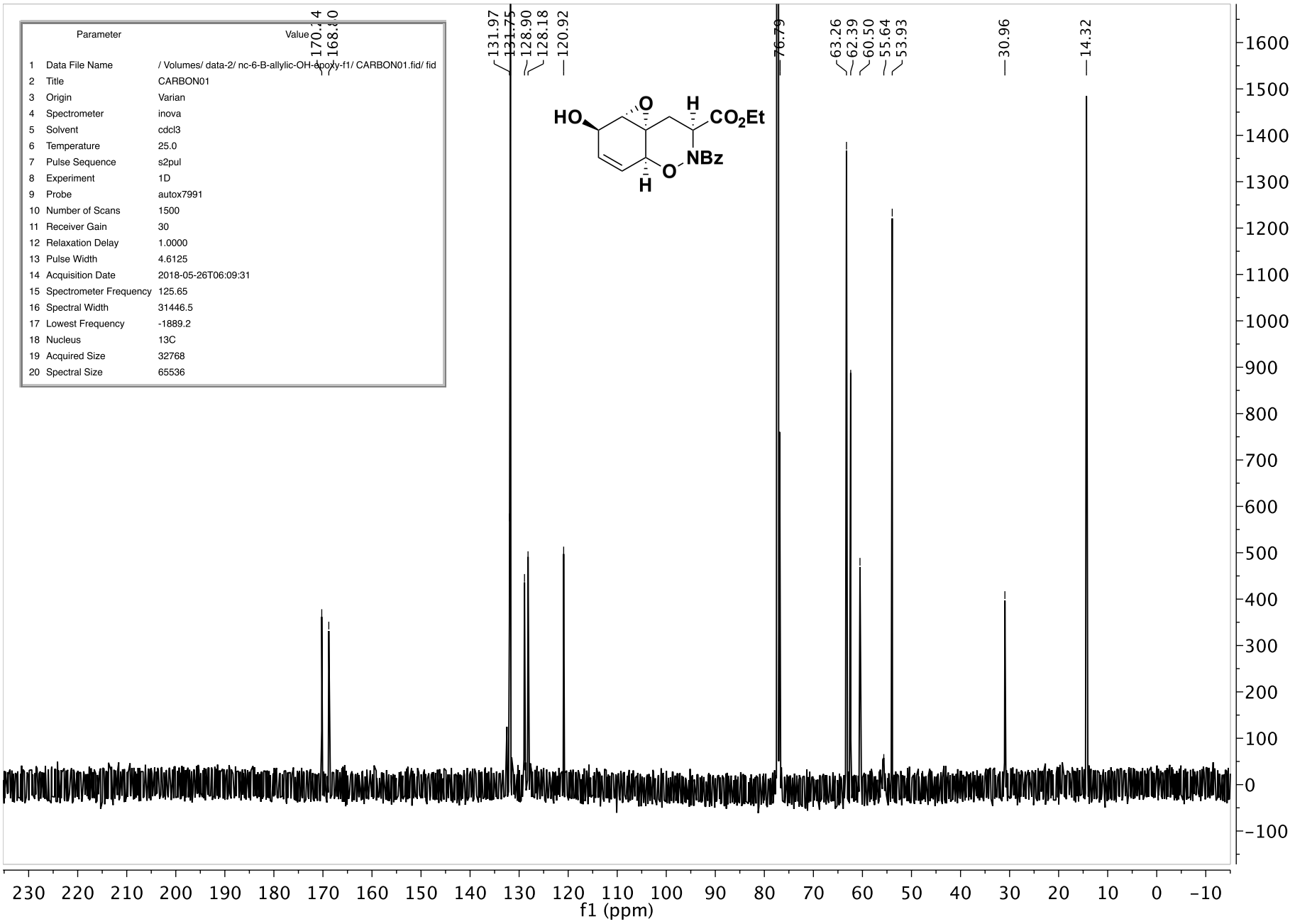
Parameter Value
1 Data File Name / Volumes/ data-2/ nc-6-B-allylic-OH-epoxy-f1/ CARBON01.fid/ fid
2 Title CARBON01
3 Origin Varian
4 Spectrometer inova
5 Solvent cdcl3
6 Temperature 25.0
7 Pulse Sequence s2pul
8 Experiment 1D
9 Probe autox7991
10 Number of Scans 1500
11 Receiver Gain 30
12 Relaxation Delay 1.0000
13 Pulse Width 4.6125
14 Acquisition Date 2018-05-26T06:09:31
15 Spectrometer Frequency 125.65
16 Spectral Width 31446.5
17 Lowest Frequency -1889.2
18 Nucleus 13C
19 Acquired Size 32768
20 Spectral Size 65536
170.14
168.80
131.97
131.75
128.90
128.18
120.92
76.79
63.26
62.39
60.50
55.64
53.93
30.96
14.32
HO
O
H
CO2Et
NBz
O
H
1600
1500
1400
1300
1200
1100
1000
900
800
700
600
500
400
300
200
100
0
-100
230 220 210 200 190 180 170 160 150 140 130 120 110 100 90 80 70 60 50 40 30 20 10 0 -10
f1 (ppm)

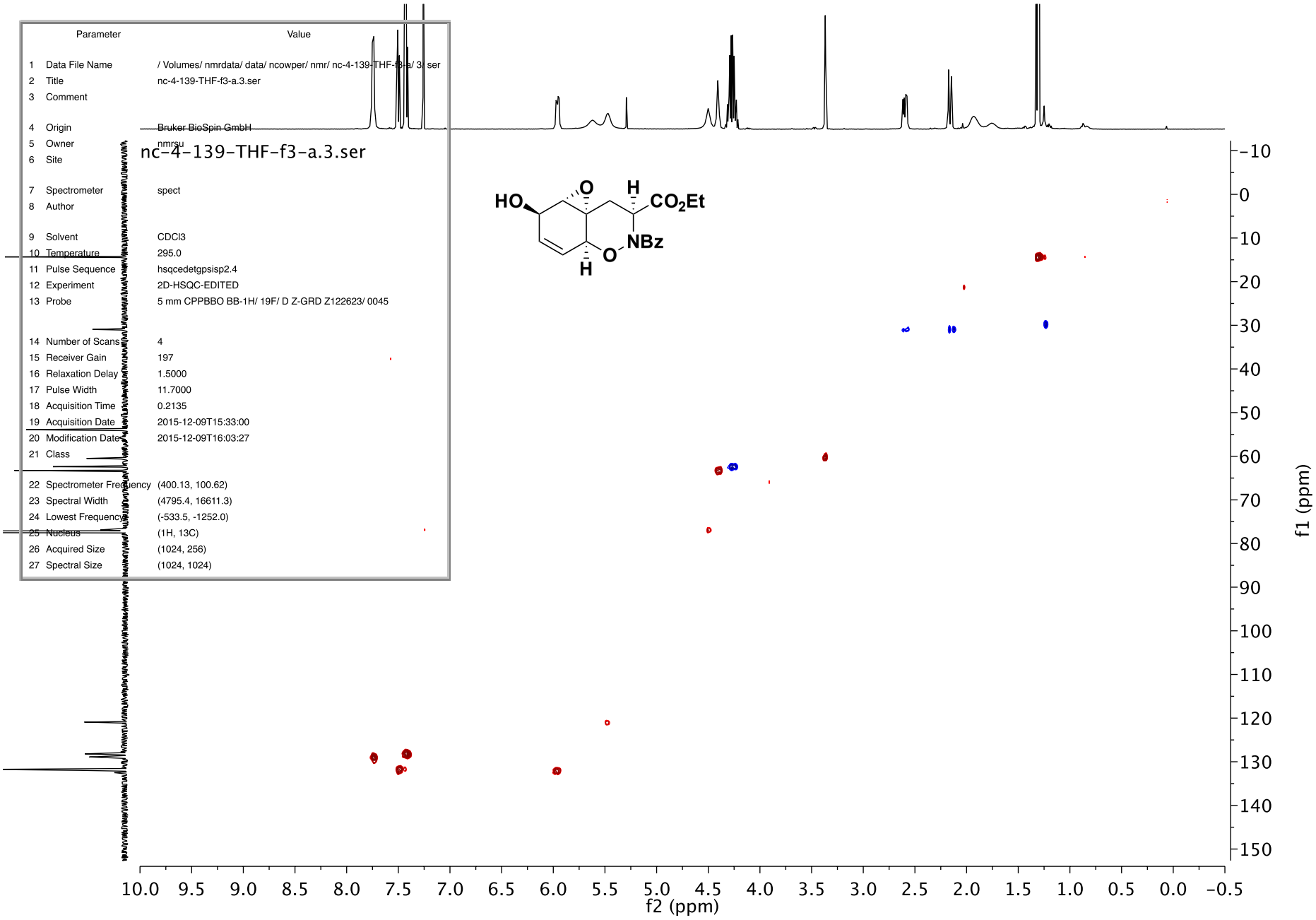

	Parameter	Value
1	Data File Name	/ Volumes/ nmrdata/ data/ ncowper/ nmr/ nc-4-139-THF-f3-a/ 3/ ser
2	Title	nc-4-139-THF-f3-a.3.ser
3	Comment	
4	Origin	Bruker BioSpin GmbH
5	Owner	nmrsu
6	Site	
7	Spectrometer	spect
8	Author	
9	Solvent	CDCl3
10	Temperature	295.0
11	Pulse Sequence	hsqcedetgpsisp2.4
12	Experiment	2D-HSQC-EDITED
13	Probe	5 mm CPPBBO BB-1H/ 19F/ D Z-GRD Z122623/ 0045
14	Number of Scans	4
15	Receiver Gain	197
16	Relaxation Delay	1.5000
17	Pulse Width	11.7000
18	Acquisition Time	0.2135
19	Acquisition Date	2015-12-09T15:33:00
20	Modification Date	2015-12-09T16:03:27
21	Class	
22	Spectrometer Frequency	(400.13, 100.62)
23	Spectral Width	(4795.4, 16611.3)
24	Lowest Frequency	(-533.5, -1252.0)
25	Nucleus	(1H, 13C)
26	Acquired Size	(1024, 256)
27	Spectral Size	(1024, 1024)

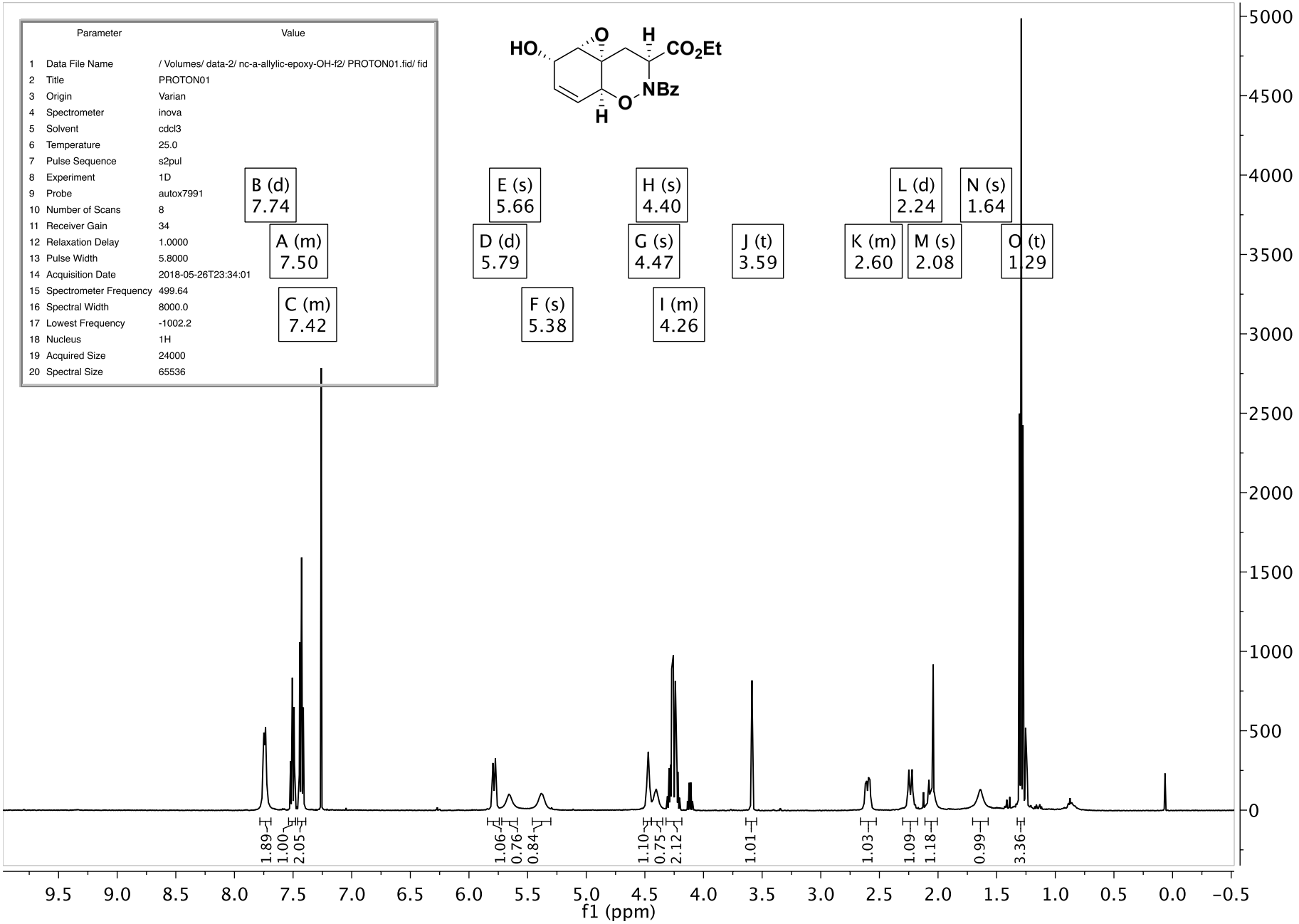
Parameter Value
1 Data File Name / Volumes/ data-2/ nc-a-allylic-epoxy-OH-f2/ PROTON01.fid/ fid
2 Title PROTON01
3 Origin Varian
4 Spectrometer inova
5 Solvent cdcl3
6 Temperature 25.0
7 Pulse Sequence s2pul
8 Experiment 1D
9 Probe autox7991
10 Number of Scans 8
11 Receiver Gain 34
12 Relaxation Delay 1.0000
13 Pulse Width 5.8000
14 Acquisition Date 2018-05-26T23:34:01
15 Spectrometer Frequency 499.64
16 Spectral Width 8000.0
17 Lowest Frequency -1002.2
18 Nucleus 1H
19 Acquired Size 24000
20 Spectral Size 65536
HO
O
H
CO2Et
NBz
O
H
B (d) 7.74
A (m) 7.50
C (m) 7.42
E (s) 5.66
D (d) 5.79
F (s) 5.38
H (s) 4.40
G (s) 4.47
I (m) 4.26
J (t) 3.59
L (d) 2.24
K (m) 2.60
M (s) 2.08
N (s) 1.64
O (t) 1.29
1.89
1.00
2.05
1.06
0.76
0.84
1.10
0.75
2.12
1.01
1.03
1.09
1.18
0.99
3.36
5000
4500
4000
3500
3000
2500
2000
1500
1000
500
0
9.5
9.0
8.5
8.0
7.5
7.0
6.5
6.0
5.5
5.0
4.5
4.0
3.5
3.0
2.5
2.0
1.5
1.0
0.5
0.0
-0.5
f1 (ppm)

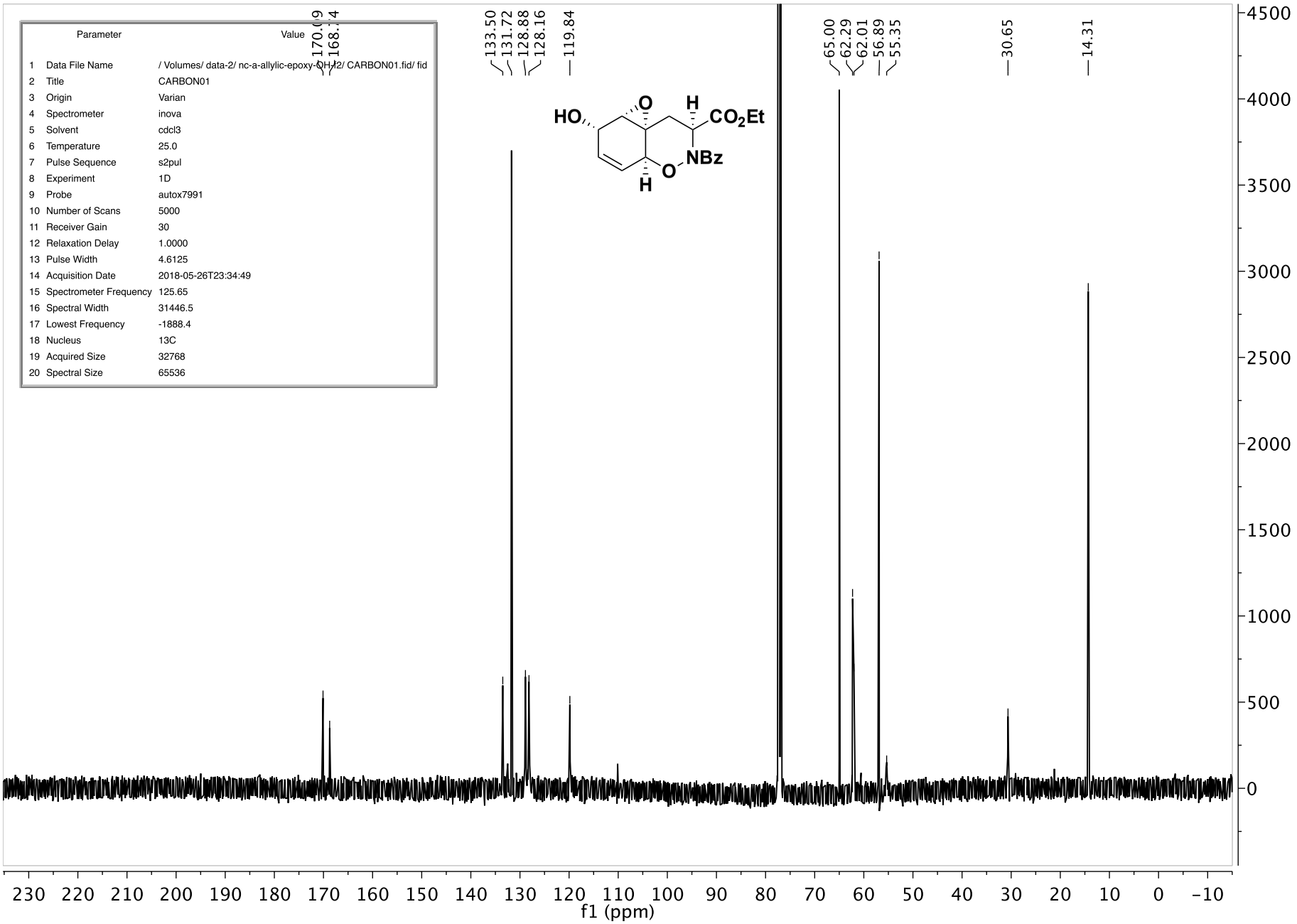
Parameter Value
1 Data File Name / Volumes/ data-2/ nc-a-allylic-epoxy-OH-2/ CARBON01.fid/ fid
2 Title CARBON01
3 Origin Varian
4 Spectrometer inova
5 Solvent cdcl3
6 Temperature 25.0
7 Pulse Sequence s2pul
8 Experiment 1D
9 Probe autox7991
10 Number of Scans 5000
11 Receiver Gain 30
12 Relaxation Delay 1.0000
13 Pulse Width 4.6125
14 Acquisition Date 2018-05-26T23:34:49
15 Spectrometer Frequency 125.65
16 Spectral Width 31446.5
17 Lowest Frequency -1888.4
18 Nucleus 13C
19 Acquired Size 32768
20 Spectral Size 65536
170.09
168.14
133.50
131.72
128.88
128.16
119.84
65.00
62.29
62.01
56.89
55.35
30.65
14.31
HO
O
H
CO2Et
NBz
O
H
4500
4000
3500
3000
2500
2000
1500
1000
500
0
230 220 210 200 190 180 170 160 150 140 130 120 110 100 90 80 70 60 50 40 30 20 10 0 -10
f1 (ppm)

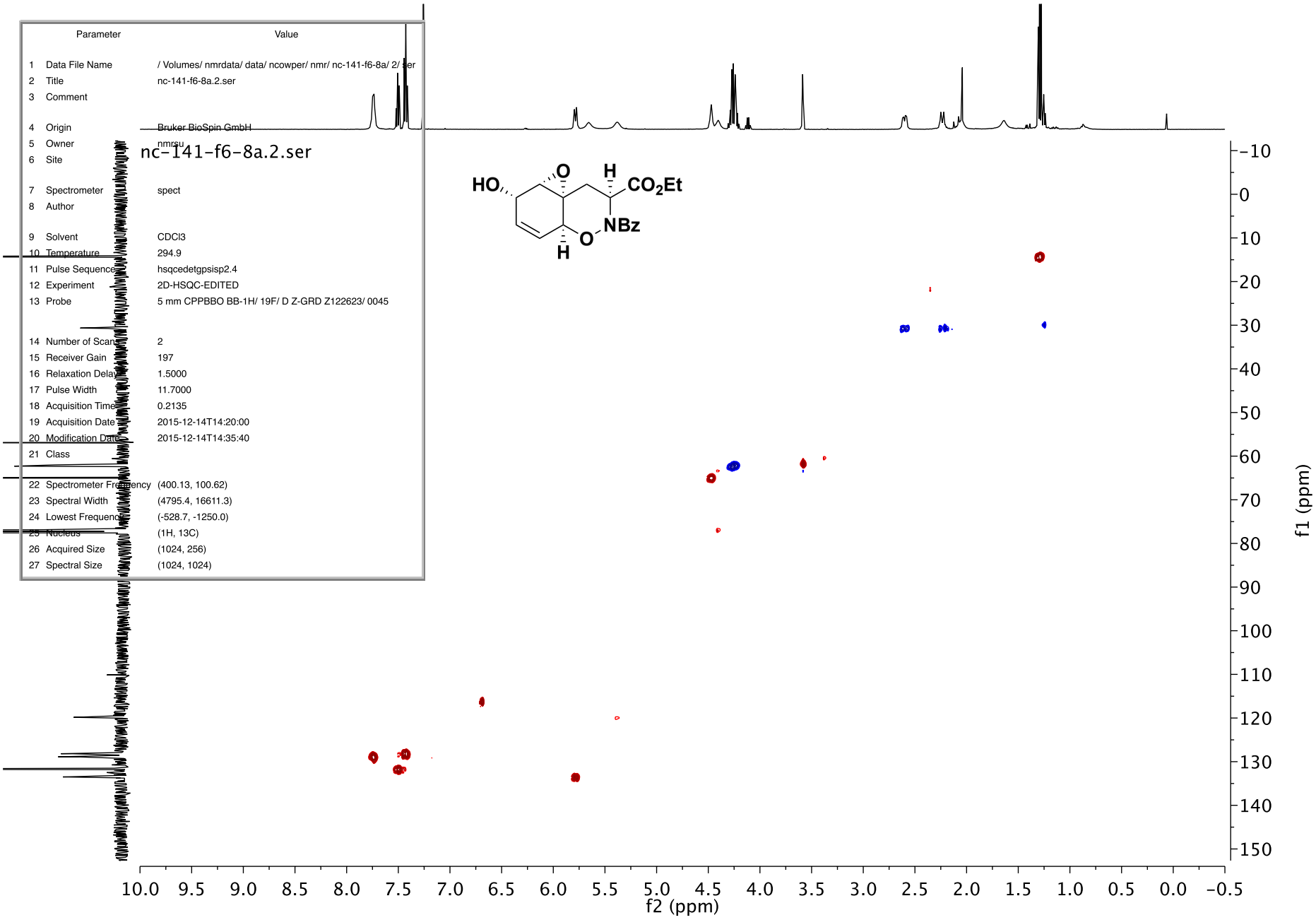

	Parameter	Value
1	Data File Name	/ Volumes/ nmrdata/ data/ ncowper/ nmr/ nc-141-f6-8a/ 2/ ser
2	Title	nc-141-f6-8a.2.ser
3	Comment	
4	Origin	Bruker BioSpin GmbH
5	Owner	nmrsu
6	Site	
7	Spectrometer	spect
8	Author	
9	Solvent	CDCl3
10	Temperature	294.9
11	Pulse Sequence	hsqcedetgpsisp2.4
12	Experiment	2D-HSQC-EDITED
13	Probe	5 mm CPPBBO BB-1H/ 19F/ D Z-GRD Z122623/ 0045
14	Number of Scans	2
15	Receiver Gain	197
16	Relaxation Delay	1.5000
17	Pulse Width	11.7000
18	Acquisition Time	0.2135
19	Acquisition Date	2015-12-14T14:20:00
20	Modification Date	2015-12-14T14:35:40
21	Class	
22	Spectrometer Frequency	(400.13, 100.62)
23	Spectral Width	(4795.4, 16611.3)
24	Lowest Frequency	(-528.7, -1250.0)
25	Nucleus	(1H, 13C)
26	Acquired Size	(1024, 256)
27	Spectral Size	(1024, 1024)

	Parameter	Value
1	Data File Name	/ Volumes/ data/ nc-4-196-20C-1sc.fid/ fid
2	Title	nc-4-196-20C-1sc
3	Origin	Varian
4	Spectrometer	vnmrs
5	Solvent	cdcl3
6	Temperature	75.0
7	Pulse Sequence	s2pul
8	Experiment	1D
9	Probe	OneNMR
10	Number of Scans	1
11	Receiver Gain	16
12	Relaxation Delay	1.0000
13	Pulse Width	4.1500
14	Acquisition Date	2016-03-02T17:11:28
15	Spectrometer Frequency	399.80
16	Spectral Width	6410.3
17	Lowest Frequency	-806.4
18	Nucleus	1H
19	Acquired Size	12821
20	Spectral Size	65536

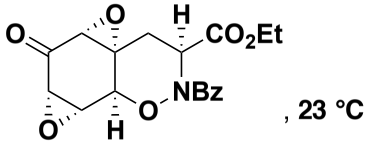

, 23 °C

	Parameter	Value
1	Data File Name	/ Volumes/ data/ nc-4-196-46C-shimmed-1sc-10s-at.fid/ fid
2	Title	nc-4-196-46C-shimmed-1sc-10s-at
3	Origin	Varian
4	Spectrometer	vnmrs
5	Solvent	cdcl3
6	Temperature	46.0
7	Pulse Sequence	s2pul
8	Experiment	1D
9	Probe	OneNMR
10	Number of Scans	1
11	Receiver Gain	48
12	Relaxation Delay	1.0000
13	Pulse Width	4.1500
14	Acquisition Date	2016-03-02T17:38:56
15	Spectrometer Frequency	399.80
16	Spectral Width	6410.3
17	Lowest Frequency	-806.4
18	Nucleus	1H
19	Acquired Size	64103
20	Spectral Size	131072

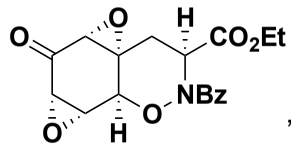

, 46 °C

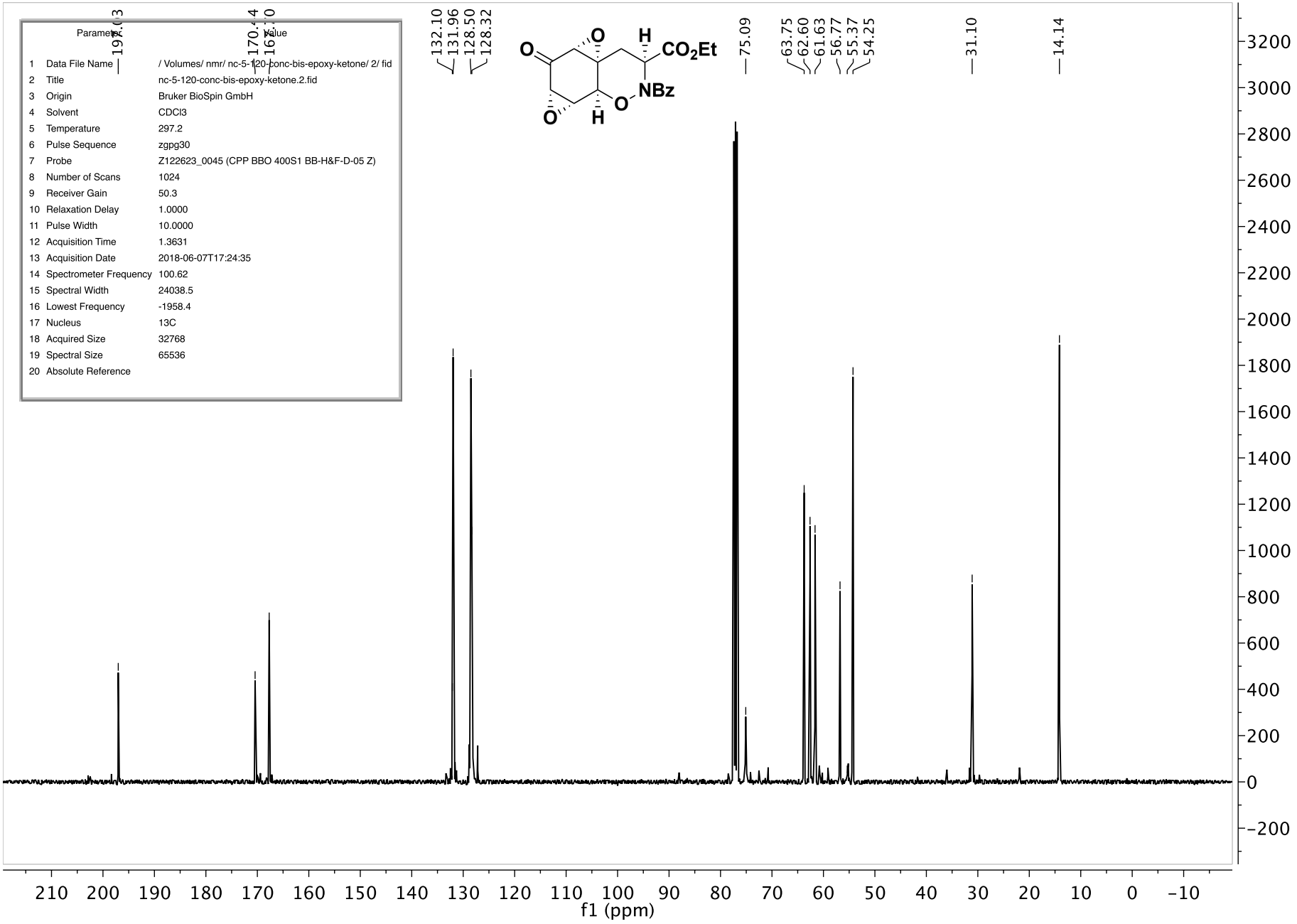
197.03
170.44
169.10
132.10
131.96
128.50
128.32
75.09
63.75
62.60
61.63
56.77
55.37
54.25
31.10
14.14
O
H
CO2Et
NBz
O
O
H
Parameter
Value
1 Data File Name / Volumes/ nmr/ nc-5-120-conc-bis-epoxy-ketone/ 2/ fid
2 Title nc-5-120-conc-bis-epoxy-ketone.2.fid
3 Origin Bruker BioSpin GmbH
4 Solvent CDCl3
5 Temperature 297.2
6 Pulse Sequence zgpg30
7 Probe Z122623_0045 (CPP BBO 400S1 BB-H&F-D-05 Z)
8 Number of Scans 1024
9 Receiver Gain 50.3
10 Relaxation Delay 1.0000
11 Pulse Width 10.0000
12 Acquisition Time 1.3631
13 Acquisition Date 2018-06-07T17:24:35
14 Spectrometer Frequency 100.62
15 Spectral Width 24038.5
16 Lowest Frequency -1958.4
17 Nucleus 13C
18 Acquired Size 32768
19 Spectral Size 65536
20 Absolute Reference
3200
3000
2800
2600
2400
2200
2000
1800
1600
1400
1200
1000
800
600
400
200
0
-200
210 200 190 180 170 160 150 140 130 120 110 100 90 80 70 60 50 40 30 20 10 0 -10
f1 (ppm)

	Parameter	Value
1	Data File Name	/ Volumes/ data-1/ nc-7-epoxy-keto-diol/ PROTON01.fid/ fid
2	Title	PROTON01
3	Origin	Varian
4	Spectrometer	inova
5	Solvent	cdcl3
6	Temperature	25.0
7	Pulse Sequence	s2pul
8	Experiment	1D
9	Probe	autox7991
10	Number of Scans	8
11	Receiver Gain	30
12	Relaxation Delay	1.0000
13	Pulse Width	5.8000
14	Acquisition Date	2018-06-22T17:06:43
15	Spectrometer Frequency	499.64
16	Spectral Width	8000.0
17	Lowest Frequency	-1002.2
18	Nucleus	1H
19	Acquired Size	24000
20	Spectral Size	65536

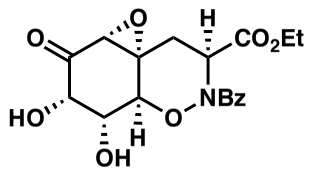

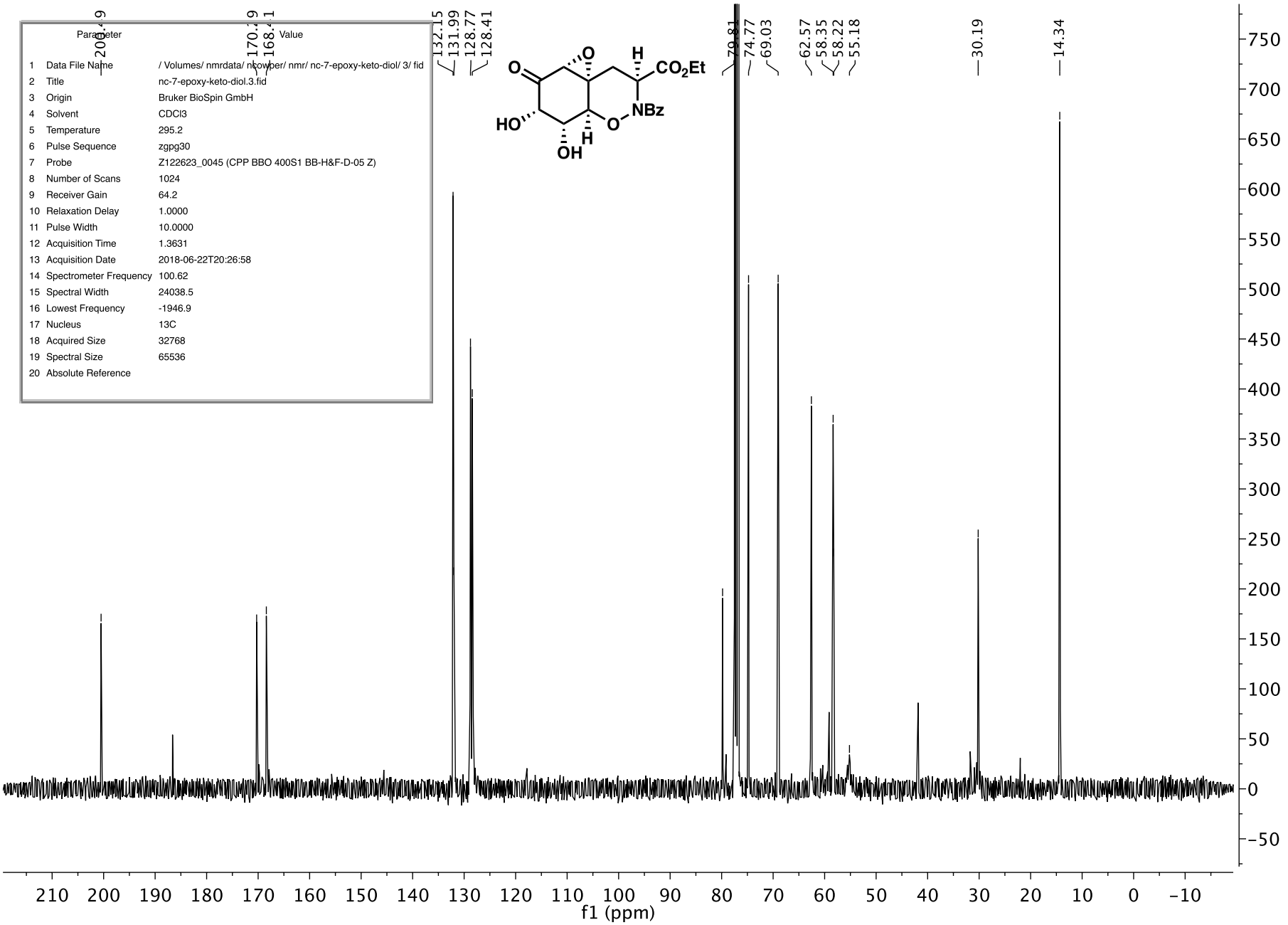

	Parameter	Value
1	Data File Name	/ Volumes/ nmrdata/ ncowper/ nmr/ nc-7-epoxy-keto-diol/ 3/ fid
2	Title	nc-7-epoxy-keto-diol.3.fid
3	Origin	Bruker BioSpin GmbH
4	Solvent	CDCl3
5	Temperature	295.2
6	Pulse Sequence	zgpg30
7	Probe	Z122623_0045 (CPP BBO 400S1 BB-H&F-D-05 Z)
8	Number of Scans	1024
9	Receiver Gain	64.2
10	Relaxation Delay	1.0000
11	Pulse Width	10.0000
12	Acquisition Time	1.3631
13	Acquisition Date	2018-06-22T20:26:58
14	Spectrometer Frequency	100.62
15	Spectral Width	24038.5
16	Lowest Frequency	-1946.9
17	Nucleus	13C
18	Acquired Size	32768
19	Spectral Size	65536
20	Absolute Reference	

	Parameter	Value
1	Data File Name	/ Volumes/ nmrdata/ ncowper/ nmr/ nc-7-wharton-15-19/ 1/ fid
2	Title	nc-7-wharton-15-19.1.fid
3	Origin	Bruker BioSpin GmbH
4	Solvent	CDCl3
5	Temperature	295.1
6	Pulse Sequence	zg30
7	Probe	Z122623_0045 (CPP BBO 400S1 BB-H&F-D-05 Z)
8	Number of Scans	16
9	Receiver Gain	197.4
10	Relaxation Delay	1.0000
11	Pulse Width	11.7000
12	Acquisition Time	4.0894
13	Acquisition Date	2018-06-28T19:35:08
14	Spectrometer Frequency	400.13
15	Spectral Width	8012.8
16	Lowest Frequency	-1545.5
17	Nucleus	1H
18	Acquired Size	32768
19	Spectral Size	65536
20	Absolute Reference	

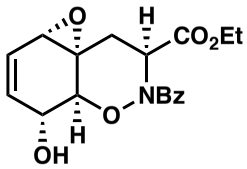

D (d) 7.72
C (m) 7.50
E (m) 7.43
G (m) 6.08
F (dd) 6.19
H (s) 5.66
I (s) 4.30
J (q) 4.24
A (s) 3.92
B (dt) 3.41
K (dd) 2.69
L (m) 2.31
M (m) 1.67
N (t) 1.27

2.00 1.08 2.18 0.94 0.81 0.68 0.82 1.93 0.86 0.93 0.99 0.85 0.90 3.45

f1 (ppm)

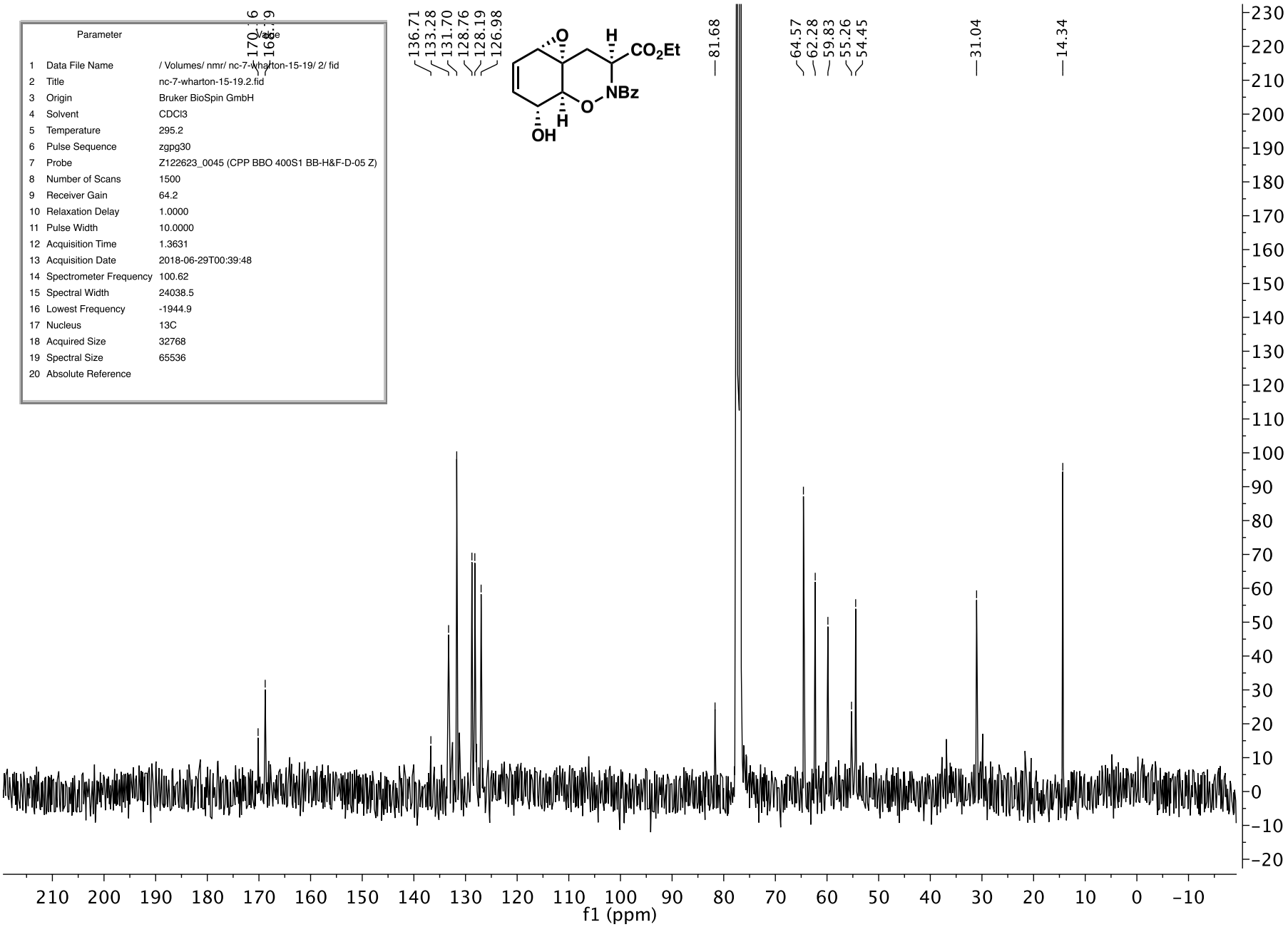
Parameter Value
1 Data File Name / Volumes/ nmr/ nc-7-wharton-15-19/ 2/ fid
2 Title nc-7-wharton-15-19.2.fid
3 Origin Bruker BioSpin GmbH
4 Solvent CDCl3
5 Temperature 295.2
6 Pulse Sequence zgpg30
7 Probe Z122623_0045 (CPP BBO 400S1 BB-H&F-D-05 Z)
8 Number of Scans 1500
9 Receiver Gain 64.2
10 Relaxation Delay 1.0000
11 Pulse Width 10.0000
12 Acquisition Time 1.3631
13 Acquisition Date 2018-06-29T00:39:48
14 Spectrometer Frequency 100.62
15 Spectral Width 24038.5
16 Lowest Frequency -1944.9
17 Nucleus 13C
18 Acquired Size 32768
19 Spectral Size 65536
20 Absolute Reference
170.16
166.19
136.71
133.28
131.70
128.76
128.19
126.98
81.68
64.57
62.28
59.83
55.26
54.45
31.04
14.34
O
H
CO2Et
NBz
O
OH
H
f1 (ppm)

	Parameter	Value
1	Data File Name	/ Volumes/ nmrdata/ ncowper/ nmr/ nc-7-allylic-triol-c/ 1/ fid
2	Title	nc-7-allylic-triol-c.1.fid
3	Origin	Bruker BioSpin GmbH
4	Solvent	CDCl3
5	Temperature	295.1
6	Pulse Sequence	zg30
7	Probe	Z122623_0045 (CPP BBO 400S1 BB-H&F-D-05 Z)
8	Number of Scans	16
9	Receiver Gain	197.4
10	Relaxation Delay	1.0000
11	Pulse Width	11.7000
12	Acquisition Time	4.0894
13	Acquisition Date	2018-06-29T19:15:32
14	Spectrometer Frequency	400.13
15	Spectral Width	8012.8
16	Lowest Frequency	-1545.5
17	Nucleus	1H
18	Acquired Size	32768
19	Spectral Size	65536
20	Absolute Reference	

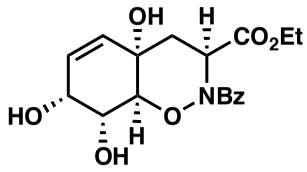

B (ddt) 7.42
A (m) 7.49
C (s) 7.68
D (s) 5.64
E (d) 5.33
G (s) 4.27
H (qd) 4.19
F (s) 4.02
I (s) 3.56
J (d) 3.24
K (s) 2.59
O (dd) 2.24
M (t) 1.27

1.78 1.00 1.86 1.84 0.77 1.26 2.18 0.90 0.93 0.79 0.96 1.05 3.24

f1 (ppm)

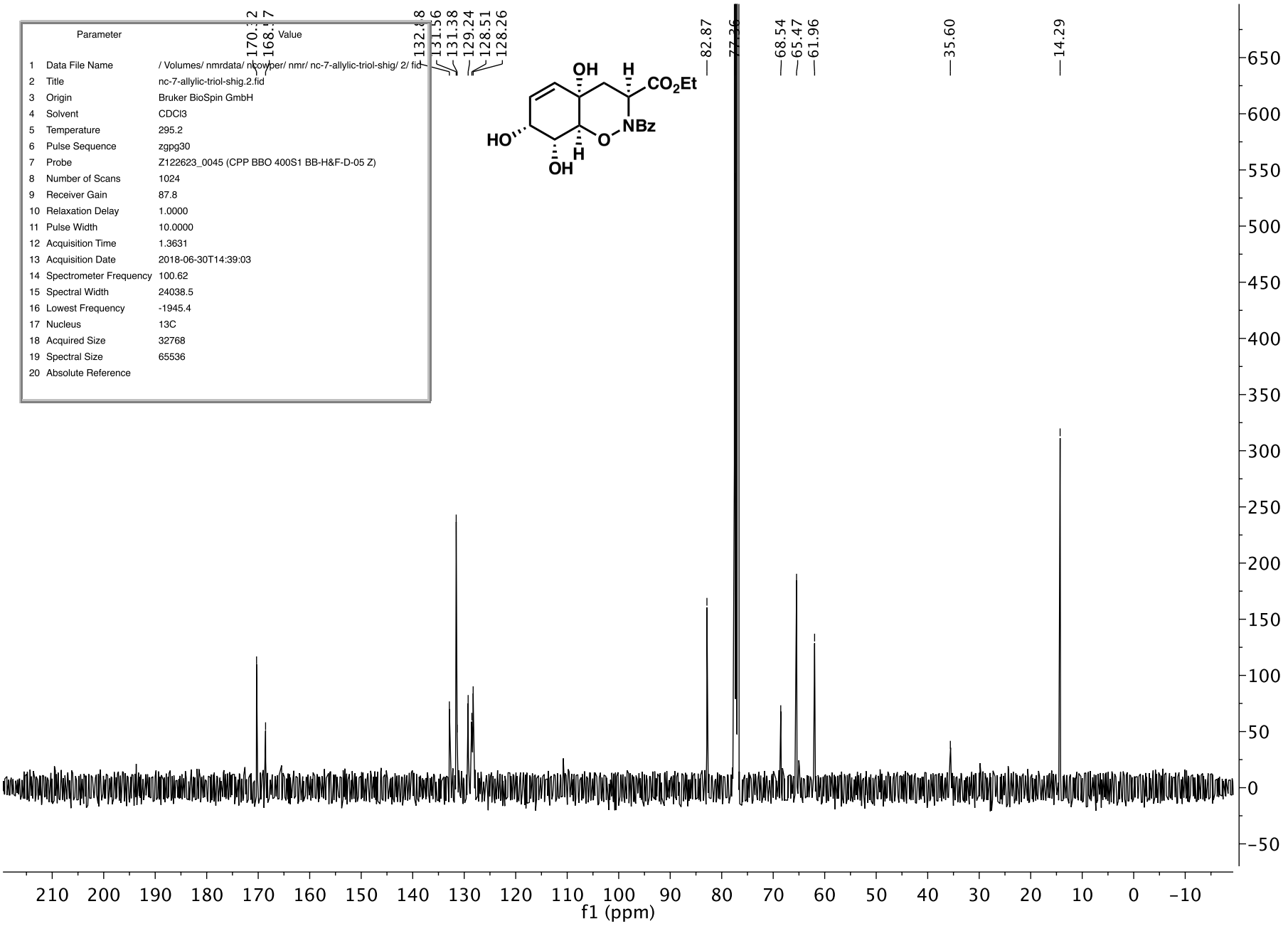
Parameter Value
1 Data File Name / Volumes/ nmrdata/ ncowper/ nmr/ nc-7-allylic-triol-shig/ 2/ fid
2 Title nc-7-allylic-triol-shig.2.fid
3 Origin Bruker BioSpin GmbH
4 Solvent CDCl3
5 Temperature 295.2
6 Pulse Sequence zgpg30
7 Probe Z122623_0045 (CPP BBO 400S1 BB-H&F-D-05 Z)
8 Number of Scans 1024
9 Receiver Gain 87.8
10 Relaxation Delay 1.0000
11 Pulse Width 10.0000
12 Acquisition Time 1.3631
13 Acquisition Date 2018-06-30T14:39:03
14 Spectrometer Frequency 100.62
15 Spectral Width 24038.5
16 Lowest Frequency -1945.4
17 Nucleus 13C
18 Acquired Size 32768
19 Spectral Size 65536
20 Absolute Reference
170.12
168.17
132.48
131.56
131.38
129.24
128.51
128.26
82.87
77.36
68.54
65.47
61.96
35.60
14.29
OH
H
CO2Et
HO
NBz
O
H
OH
650
600
550
500
450
400
350
300
250
200
150
100
50
0
-50
210 200 190 180 170 160 150 140 130 120 110 100 90 80 70 60 50 40 30 20 10 0 -10
f1 (ppm)

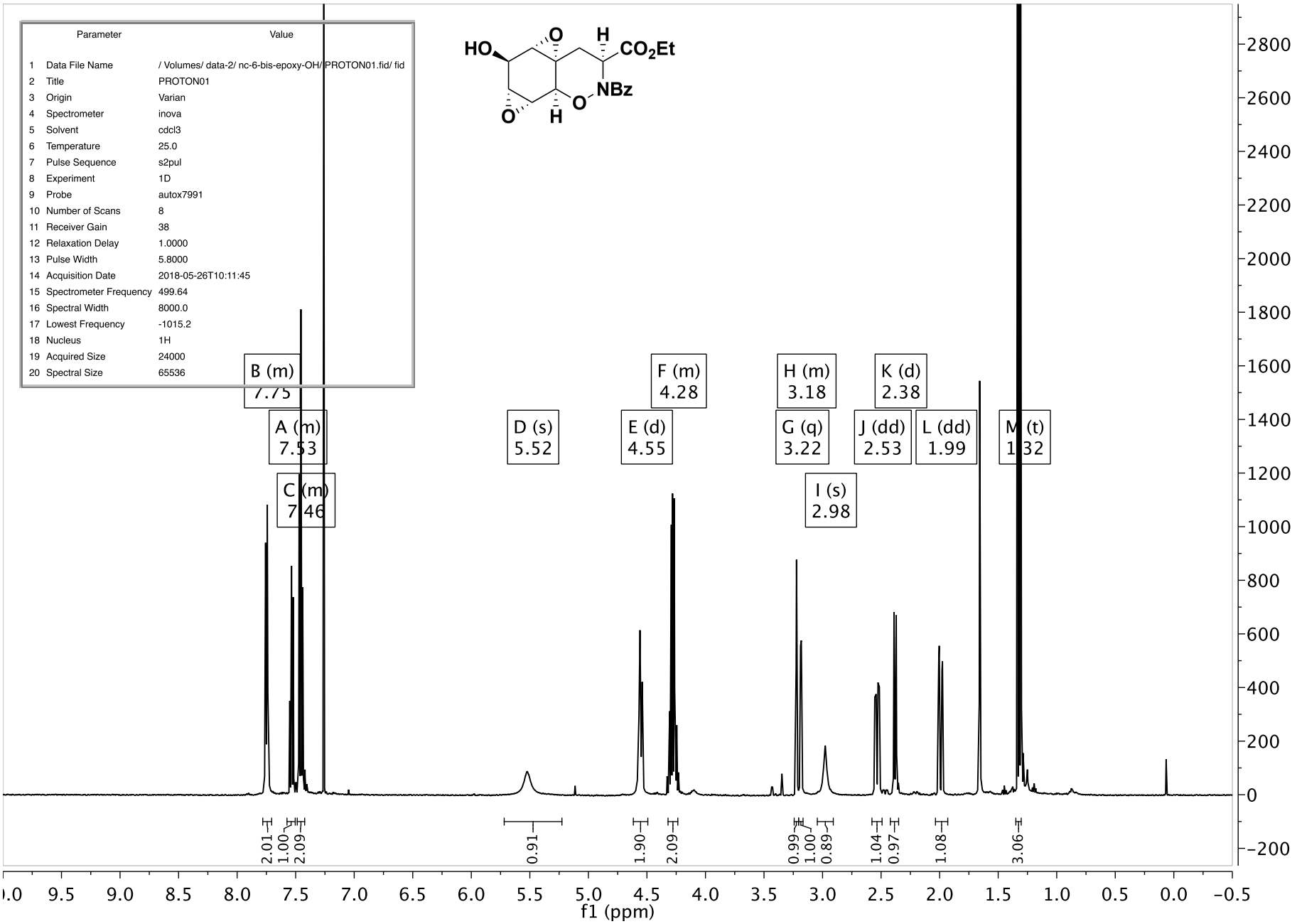
Parameter Value
1 Data File Name / Volumes/ data-2/ nc-6-bis-epoxy-OH/ PROTON01.fid/ fid
2 Title PROTON01
3 Origin Varian
4 Spectrometer inova
5 Solvent cdcl3
6 Temperature 25.0
7 Pulse Sequence s2pul
8 Experiment 1D
9 Probe autox7991
10 Number of Scans 8
11 Receiver Gain 38
12 Relaxation Delay 1.0000
13 Pulse Width 5.8000
14 Acquisition Date 2018-05-26T10:11:45
15 Spectrometer Frequency 499.64
16 Spectral Width 8000.0
17 Lowest Frequency -1015.2
18 Nucleus 1H
19 Acquired Size 24000
20 Spectral Size 65536
HO
O
H
CO2Et
NBz
O
O
H
B (m)
7.75
A (m)
7.53
C (m)
7.46
D (s)
5.52
F (m)
4.28
E (d)
4.55
H (m)
3.18
G (q)
3.22
I (s)
2.98
K (d)
2.38
J (dd)
2.53
L (dd)
1.99
M (t)
1.32
2.01
1.00
2.09
0.91
1.90
2.09
0.99
1.00
0.89
1.04
0.97
1.08
3.06
f1 (ppm)

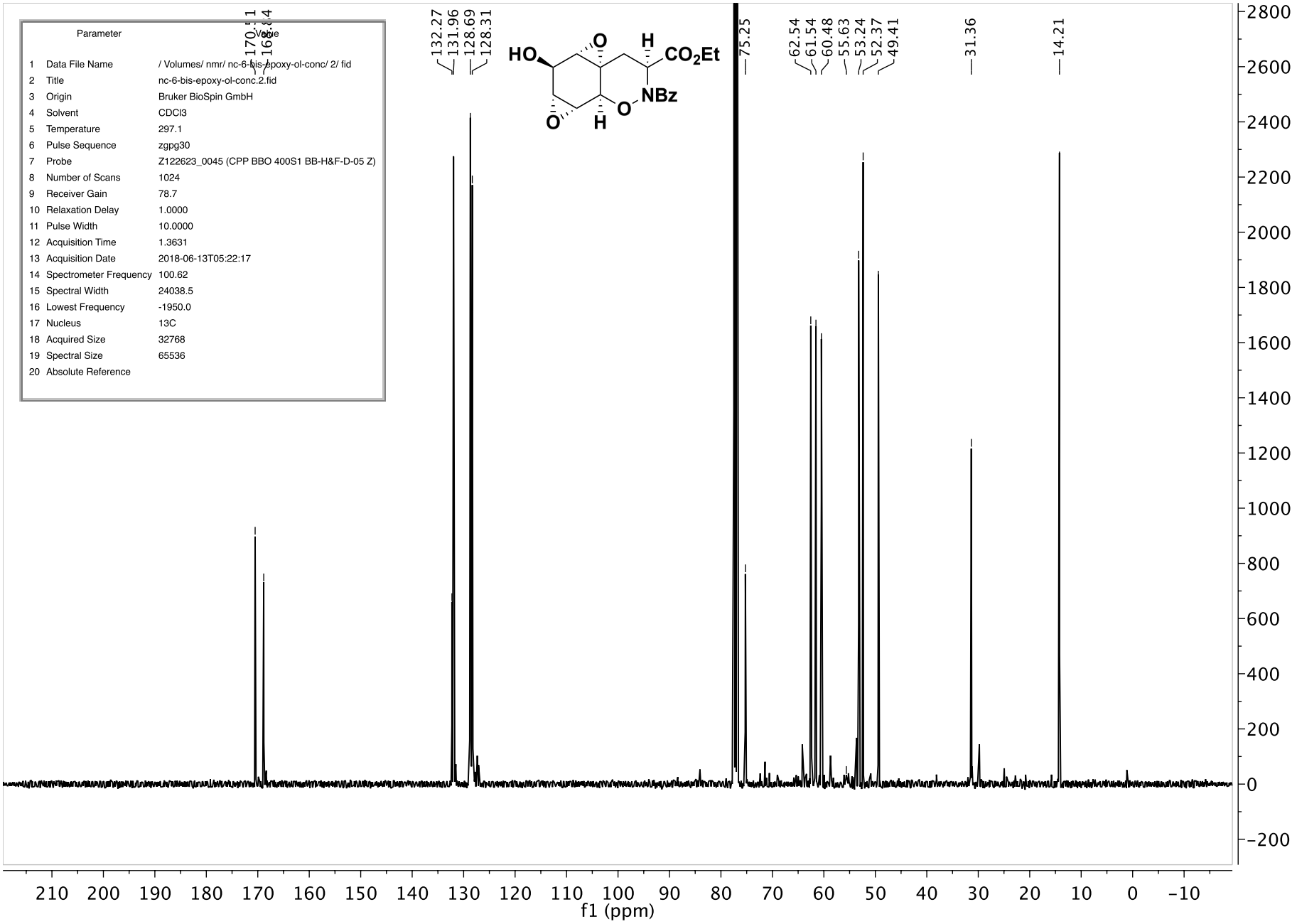
Parameter Value
1 Data File Name / Volumes/ nmr/ nc-6-bis-epoxy-ol-conc/ 2/ fid
2 Title nc-6-bis-epoxy-ol-conc.2.fid
3 Origin Bruker BioSpin GmbH
4 Solvent CDCl3
5 Temperature 297.1
6 Pulse Sequence zgpg30
7 Probe Z122623_0045 (CPP BBO 400S1 BB-H&F-D-05 Z)
8 Number of Scans 1024
9 Receiver Gain 78.7
10 Relaxation Delay 1.0000
11 Pulse Width 10.0000
12 Acquisition Time 1.3631
13 Acquisition Date 2018-06-13T05:22:17
14 Spectrometer Frequency 100.62
15 Spectral Width 24038.5
16 Lowest Frequency -1950.0
17 Nucleus 13C
18 Acquired Size 32768
19 Spectral Size 65536
20 Absolute Reference
170.11
166.84
132.27
131.96
128.69
128.31
75.25
62.54
61.54
60.48
55.63
53.24
52.37
49.41
31.36
14.21
HO
O
H
CO2Et
NBz
O
O
H
f1 (ppm)

	Parameter	Value
1	Data File Name	/ Volumes/ nmr/ nc-6-192-f5-11/ 1/ fid
2	Title	nc-6-192-f5-11.1.fid
3	Origin	Bruker BioSpin GmbH
4	Solvent	CDCl3
5	Temperature	294.9
6	Pulse Sequence	zg30
7	Probe	Z122623_0045 (CPP BBO 400S1 BB-H&F-D-05 Z)
8	Number of Scans	16
9	Receiver Gain	197.4
10	Relaxation Delay	1.0000
11	Pulse Width	11.7000
12	Acquisition Time	4.0894
13	Acquisition Date	2017-07-31T16:59:43
14	Spectrometer Frequency	400.13
15	Spectral Width	8012.8
16	Lowest Frequency	-1545.6
17	Nucleus	1H
18	Acquired Size	32768
19	Spectral Size	65536

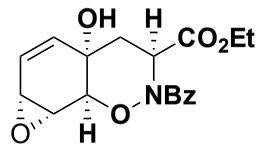

	Parameter	Value
1	Data File Name	/ Volumes/ nmr/ nc-5-197-f17-35-h/ 1/ fid
2	Title	nc-5-197-f17-35-h.1.fid
3	Origin	Bruker BioSpin GmbH
4	Solvent	CDCl3
5	Temperature	294.9
6	Pulse Sequence	zg30
7	Probe	Z122623_0045 (CPP BBO 400S1 BB-H&F-D-05 Z)
8	Number of Scans	16
9	Receiver Gain	176.8
10	Relaxation Delay	1.0000
11	Pulse Width	11.7000
12	Acquisition Time	4.0894
13	Acquisition Date	2016-12-16T17:11:45
14	Spectrometer Frequency	400.13
15	Spectral Width	8012.8
16	Lowest Frequency	-1579.4
17	Nucleus	1H
18	Acquired Size	32768
19	Spectral Size	65536
20	Absolute Reference	

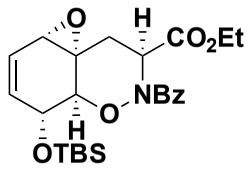

	Parameter	Value
1	Data File Name	/ Volumes/ nmr/ nc-5-197-f17-35/ 1/ fid
2	Title	nc-5-197-f17-35.1.fid
3	Origin	Bruker BioSpin GmbH
4	Solvent	CDCl3
5	Temperature	294.9
6	Pulse Sequence	zgpg30
7	Probe	Z122623_0045 (CPP BBO 400S1 BB-H&F-D-05 Z)
8	Number of Scans	1024
9	Receiver Gain	72.0
10	Relaxation Delay	2.0000
11	Pulse Width	10.0000
12	Acquisition Time	1.3631
13	Acquisition Date	2016-12-15T16:36:28
14	Spectrometer Frequency	100.62
15	Spectral Width	24038.5
16	Lowest Frequency	-1932.3
17	Nucleus	13C
18	Acquired Size	32768
19	Spectral Size	65536
20	Absolute Reference	

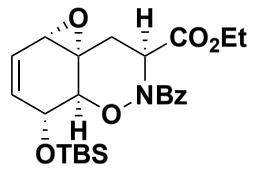

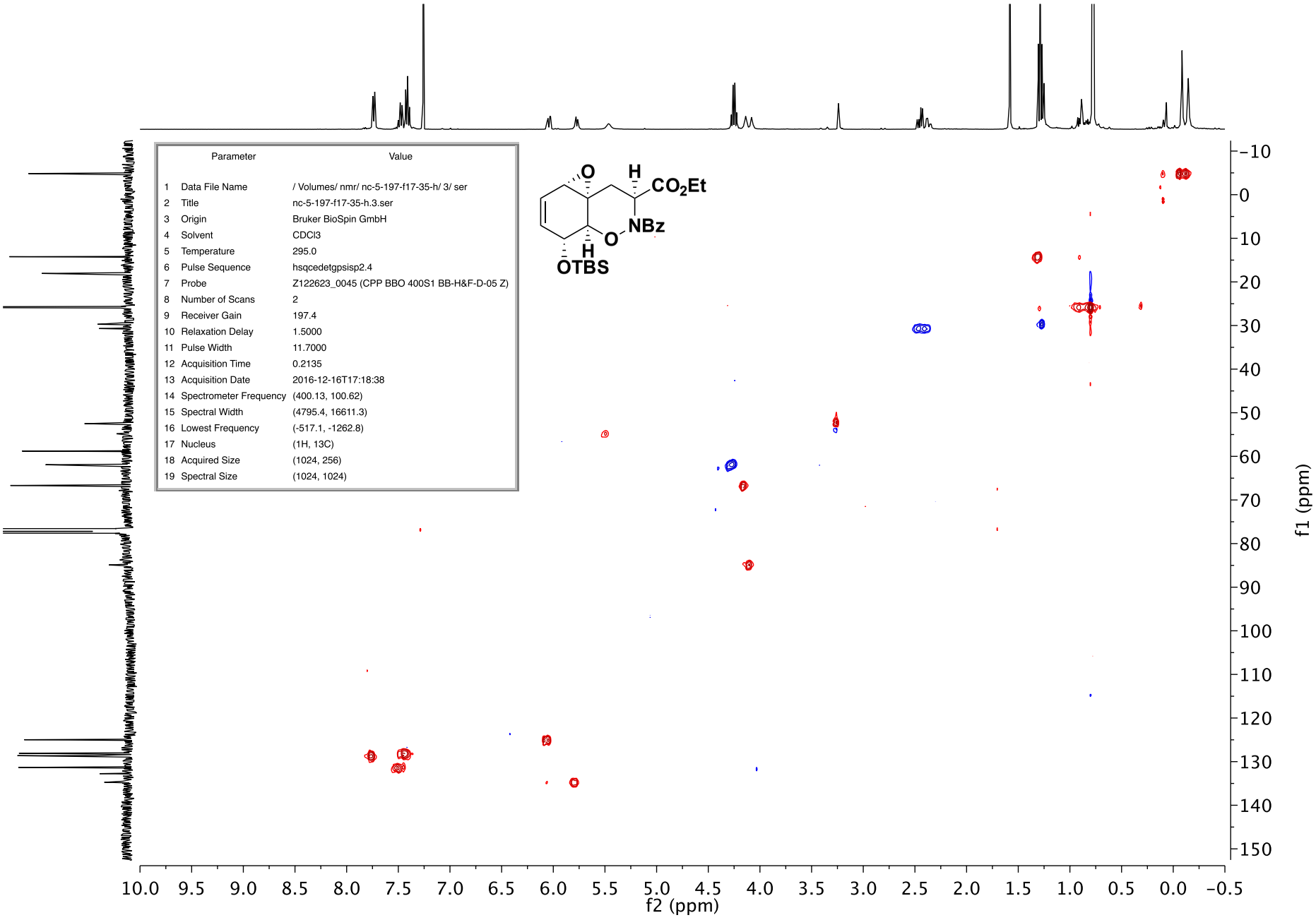
Parameter Value
1 Data File Name / Volumes/ nmr/ nc-5-197-f17-35-h/ 3/ ser
2 Title nc-5-197-f17-35-h.3.ser
3 Origin Bruker BioSpin GmbH
4 Solvent CDCl3
5 Temperature 295.0
6 Pulse Sequence hsqcedetgpsisp2.4
7 Probe Z122623_0045 (CPP BBO 400S1 BB-H&F-D-05 Z)
8 Number of Scans 2
9 Receiver Gain 197.4
10 Relaxation Delay 1.5000
11 Pulse Width 11.7000
12 Acquisition Time 0.2135
13 Acquisition Date 2016-12-16T17:18:38
14 Spectrometer Frequency (400.13, 100.62)
15 Spectral Width (4795.4, 16611.3)
16 Lowest Frequency (-517.1, -1262.8)
17 Nucleus (1H, 13C)
18 Acquired Size (1024, 256)
19 Spectral Size (1024, 1024)
O
H
CO2Et
NBz
O
H
OTBS
10.0 9.5 9.0 8.5 8.0 7.5 7.0 6.5 6.0 5.5 5.0 4.5 4.0 3.5 3.0 2.5 2.0 1.5 1.0 0.5 0.0 -0.5
f2 (ppm)
-10 0 10 20 30 40 50 60 70 80 90 100 110 120 130 140 150
f1 (ppm)

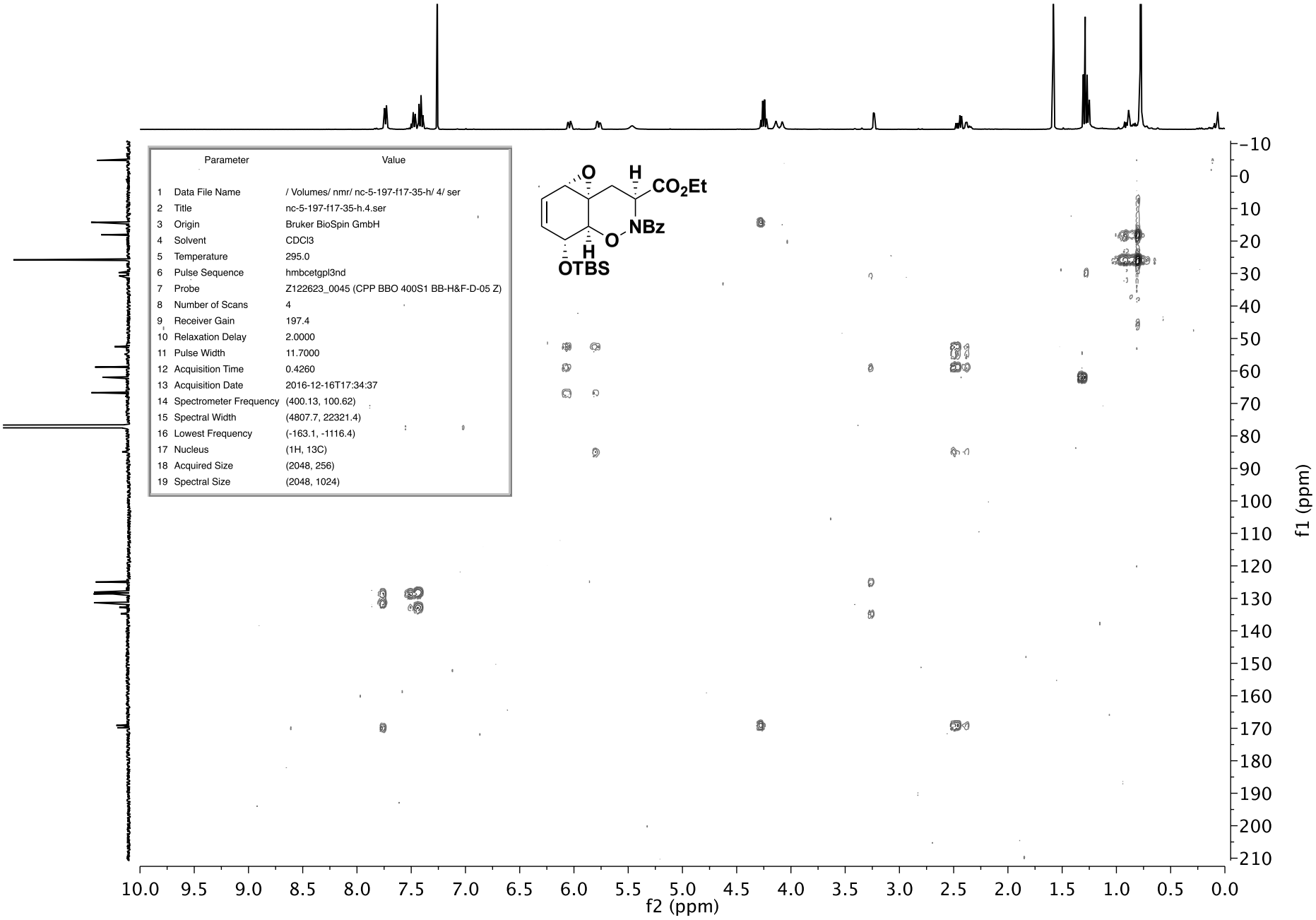
Parameter Value
1 Data File Name / Volumes/ nmr/ nc-5-197-f17-35-h/ 4/ ser
2 Title nc-5-197-f17-35-h.4.ser
3 Origin Bruker BioSpin GmbH
4 Solvent CDCl3
5 Temperature 295.0
6 Pulse Sequence hmbcetgpl3nd
7 Probe Z122623_0045 (CPP BBO 400S1 BB-H&F-D-05 Z)
8 Number of Scans 4
9 Receiver Gain 197.4
10 Relaxation Delay 2.0000
11 Pulse Width 11.7000
12 Acquisition Time 0.4260
13 Acquisition Date 2016-12-16T17:34:37
14 Spectrometer Frequency (400.13, 100.62)
15 Spectral Width (4807.7, 22321.4)
16 Lowest Frequency (-163.1, -1116.4)
17 Nucleus (1H, 13C)
18 Acquired Size (2048, 256)
19 Spectral Size (2048, 1024)
O
H
CO2Et
NBz
O
H
OTBS
10.0 9.5 9.0 8.5 8.0 7.5 7.0 6.5 6.0 5.5 5.0 4.5 4.0 3.5 3.0 2.5 2.0 1.5 1.0 0.5 0.0
f2 (ppm)
-10 0 10 20 30 40 50 60 70 80 90 100 110 120 130 140 150 160 170 180 190 200 210
f1 (ppm)

	Parameter	Value
1	Data File Name	/ Volumes/ nmrdata/ ncowper/ nmr/ nc-5-198-f9-14-h/ 1/ fid
2	Title	nc-5-198-f9-14-h.1.fid
3	Origin	Bruker BioSpin GmbH
4	Solvent	CDCl3
5	Temperature	294.9
6	Pulse Sequence	zg30
7	Probe	Z122623_0045 (CPP BBO 400S1 BB-H&F-D-05 Z)
8	Number of Scans	16
9	Receiver Gain	197.4
10	Relaxation Delay	1.0000
11	Pulse Width	11.7000
12	Acquisition Time	4.0894
13	Acquisition Date	2016-12-19T02:26:37
14	Spectrometer Frequency	400.13
15	Spectral Width	8012.8
16	Lowest Frequency	-1545.3
17	Nucleus	1H
18	Acquired Size	32768
19	Spectral Size	65536
20	Absolute Reference	

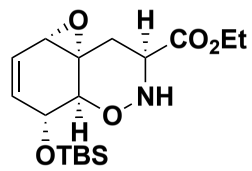

Parameter		Value
1	Data File Name	/ Volumes/ nmrdata/ ncowper/ nmr/ nc-5-198-f9-14-h/ 2/ ser
2	Title	nc-5-198-f9-14-h.2.ser
3	Origin	Bruker BioSpin GmbH
4	Solvent	CDCl3
5	Temperature	294.9
6	Pulse Sequence	hsqcedetgpsisp2.4
7	Probe	Z122623_0045 (CPP BBO 400S1 BB-H&F-D-05 Z)
8	Number of Scans	2
9	Receiver Gain	197.4
10	Relaxation Delay	1.5000
11	Pulse Width	11.7000
12	Acquisition Time	0.2135
13	Acquisition Date	2016-12-19T02:28:29
14	Spectrometer Frequency	(400.13, 100.62)
15	Spectral Width	(4795.4, 16611.3)
16	Lowest Frequency	(-530.7, -1262.8)
17	Nucleus	(1H, 13C)
18	Acquired Size	(1024, 256)
19	Spectral Size	(1024, 1024)

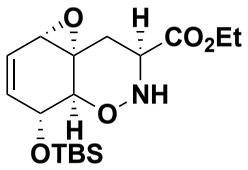

	Parameter	Value
1	Data File Name	/ Volumes/ data/ nc-7-western-fragment/ CARBON01.fid/ fid
2	Title	CARBON01
3	Origin	Varian
4	Spectrometer	inova
5	Solvent	cdcl3
6	Temperature	25.0
7	Pulse Sequence	s2pul
8	Experiment	1D
9	Probe	autox7991
10	Number of Scans	4288
11	Receiver Gain	30
12	Relaxation Delay	1.0000
13	Pulse Width	4.6125
14	Acquisition Date	2018-07-03T06:35:39
15	Spectrometer Frequency	125.65
16	Spectral Width	31446.5
17	Lowest Frequency	-1886.2
18	Nucleus	13C
19	Acquired Size	32768
20	Spectral Size	65536

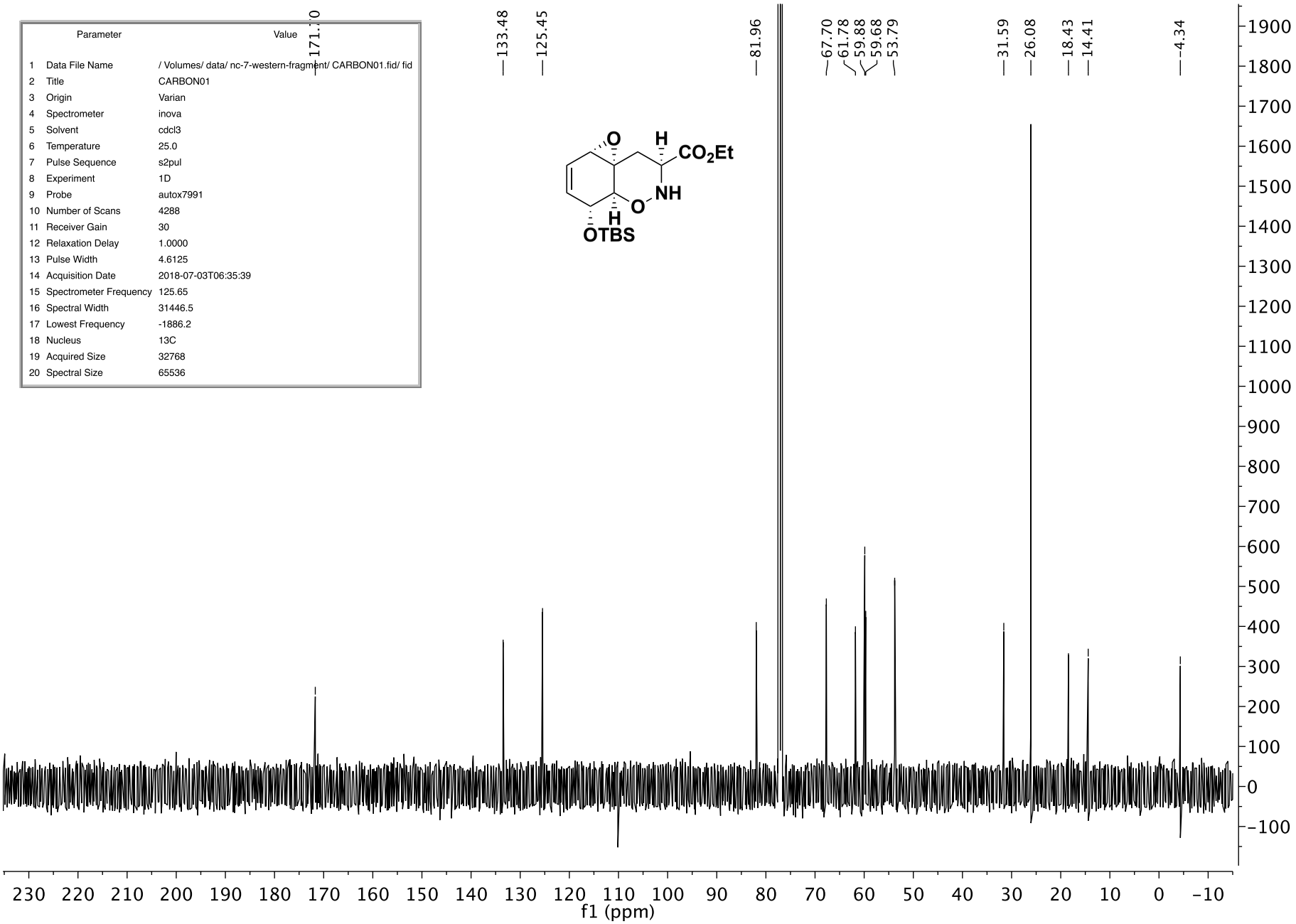

	Parameter	Value
1	Data File Name	/ Volumes/ nmr/ nc-7-triMeO-aa-Boc-OMe/ 1/ fid
2	Title	nc-7-triMeO-aa-Boc-OMe.1.fid
3	Origin	Bruker BioSpin GmbH
4	Solvent	CDCl3
5	Temperature	295.1
6	Pulse Sequence	zg30
7	Probe	Z122623_0045 (CPP BBO 400S1 BB-H&F-D-05 Z)
8	Number of Scans	16
9	Receiver Gain	30.3
10	Relaxation Delay	1.0000
11	Pulse Width	11.7000
12	Acquisition Time	4.0894
13	Acquisition Date	2018-06-24T10:43:32
14	Spectrometer Frequency	400.13
15	Spectral Width	8012.8
16	Lowest Frequency	-1564.9
17	Nucleus	1H
18	Acquired Size	32768
19	Spectral Size	65536
20	Absolute Reference	

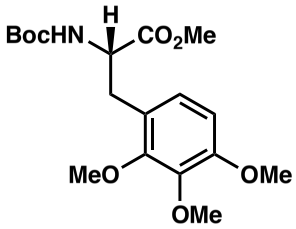

	Parameter	Value
1	Data File Name	/ Volumes/ data-1/ nc-SI-Boc-triMeO-Phe-OMe-13C.fid/ fid
2	Title	nc-SI-Boc-triMeO-Phe-OMe-13C
3	Origin	Varian
4	Spectrometer	vnmrs
5	Solvent	cdcl3
6	Temperature	65.0
7	Pulse Sequence	s2pul
8	Experiment	1D
9	Probe	OneNMR
10	Number of Scans	128
11	Receiver Gain	60
12	Relaxation Delay	1.0000
13	Pulse Width	3.5125
14	Acquisition Date	2018-06-23T22:00:28
15	Spectrometer Frequency	100.54
16	Spectral Width	25000.0
17	Lowest Frequency	-1441.9
18	Nucleus	13C
19	Acquired Size	32768
20	Spectral Size	65536

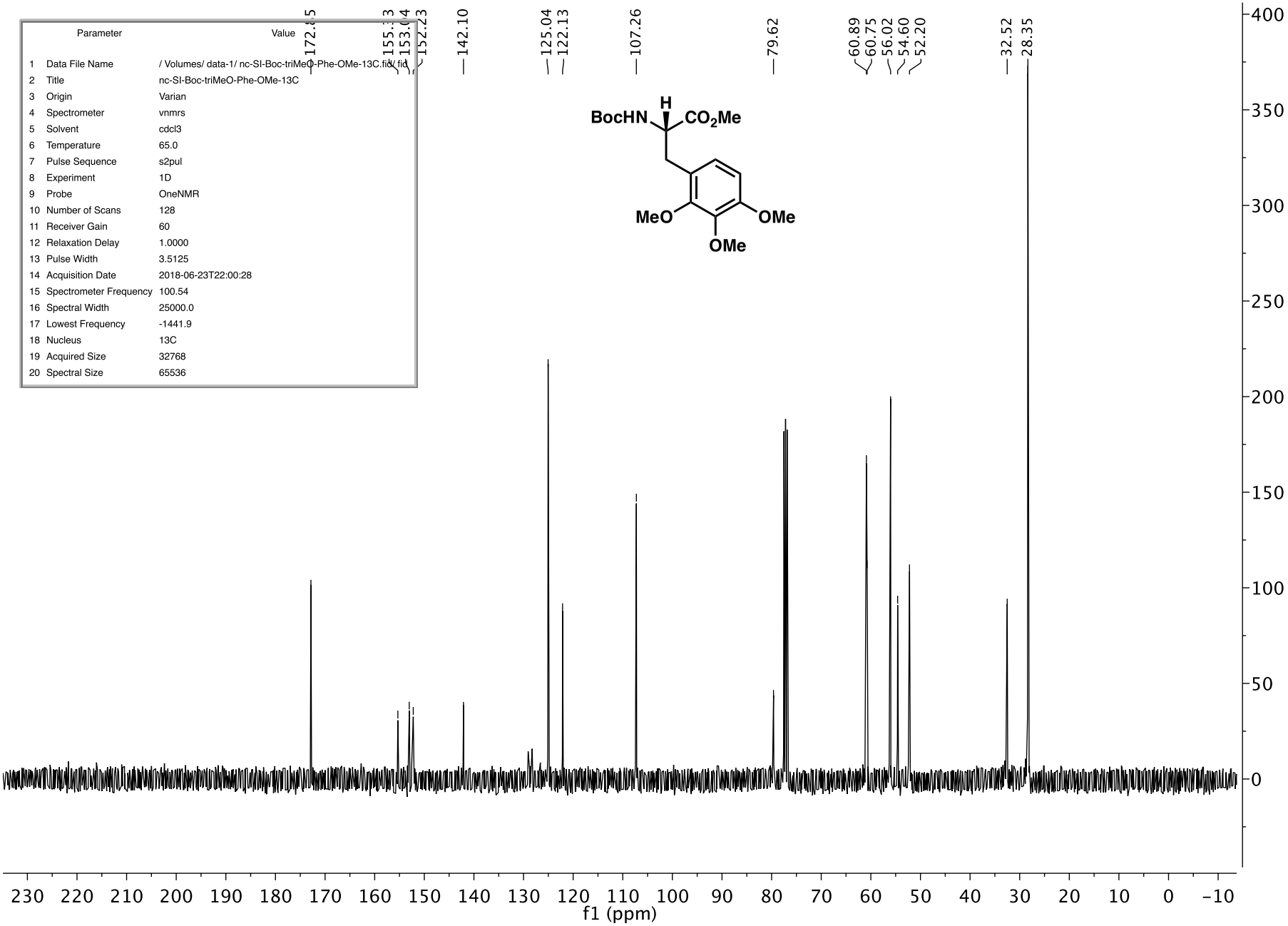

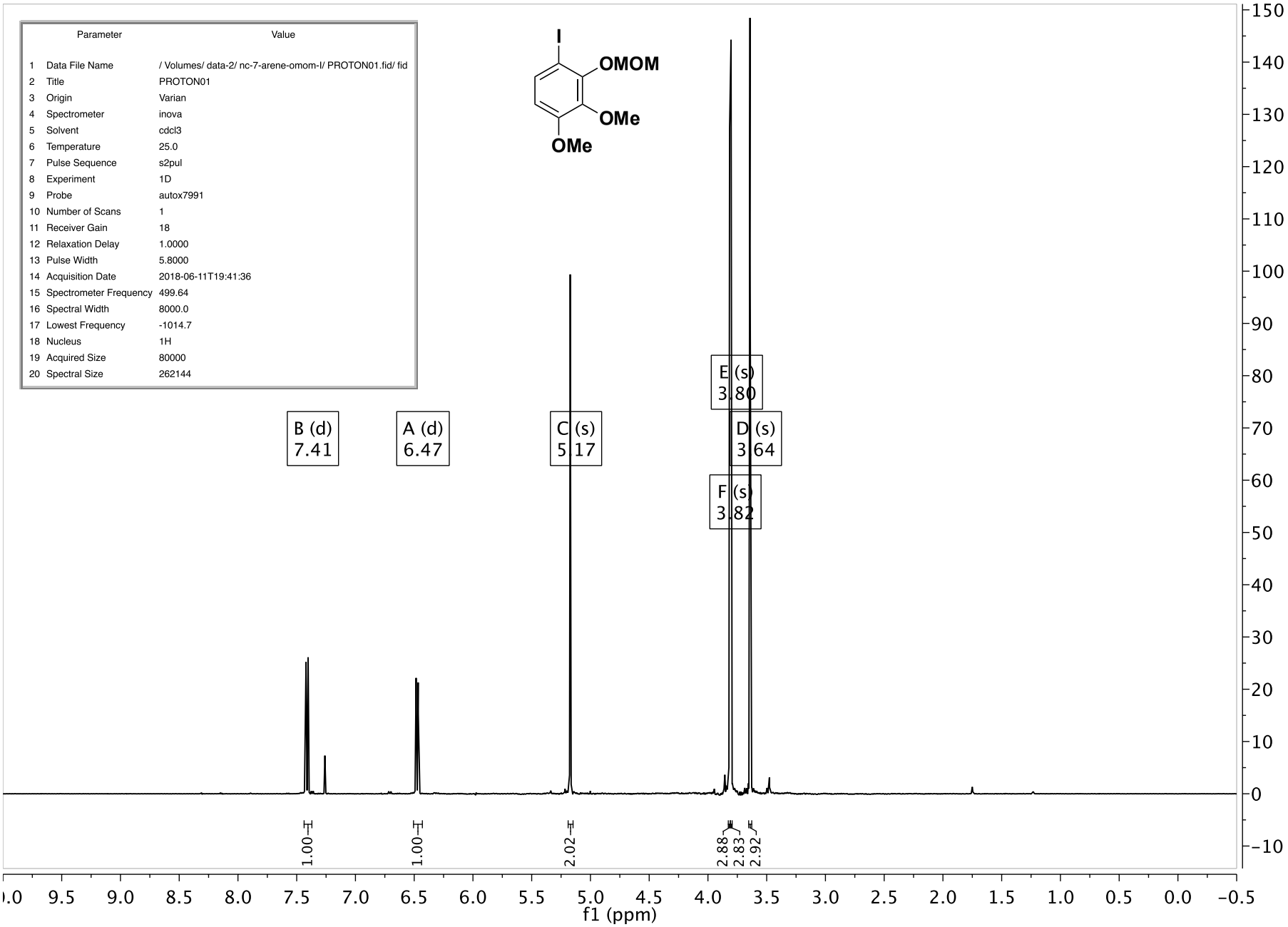
Parameter Value
1 Data File Name / Volumes/ data-2/ nc-7-arene-omom-I/ PROTON01.fid/ fid
2 Title PROTON01
3 Origin Varian
4 Spectrometer inova
5 Solvent cdcl3
6 Temperature 25.0
7 Pulse Sequence s2pul
8 Experiment 1D
9 Probe autox7991
10 Number of Scans 1
11 Receiver Gain 18
12 Relaxation Delay 1.0000
13 Pulse Width 5.8000
14 Acquisition Date 2018-06-11T19:41:36
15 Spectrometer Frequency 499.64
16 Spectral Width 8000.0
17 Lowest Frequency -1014.7
18 Nucleus 1H
19 Acquired Size 80000
20 Spectral Size 262144
I
OMOM
OMe
OMe
B (d) 7.41
A (d) 6.47
C (s) 5.17
E (s) 3.80
D (s) 3.64
F (s) 3.82
1.00
1.00
2.02
2.88
2.83
2.92
f1 (ppm)

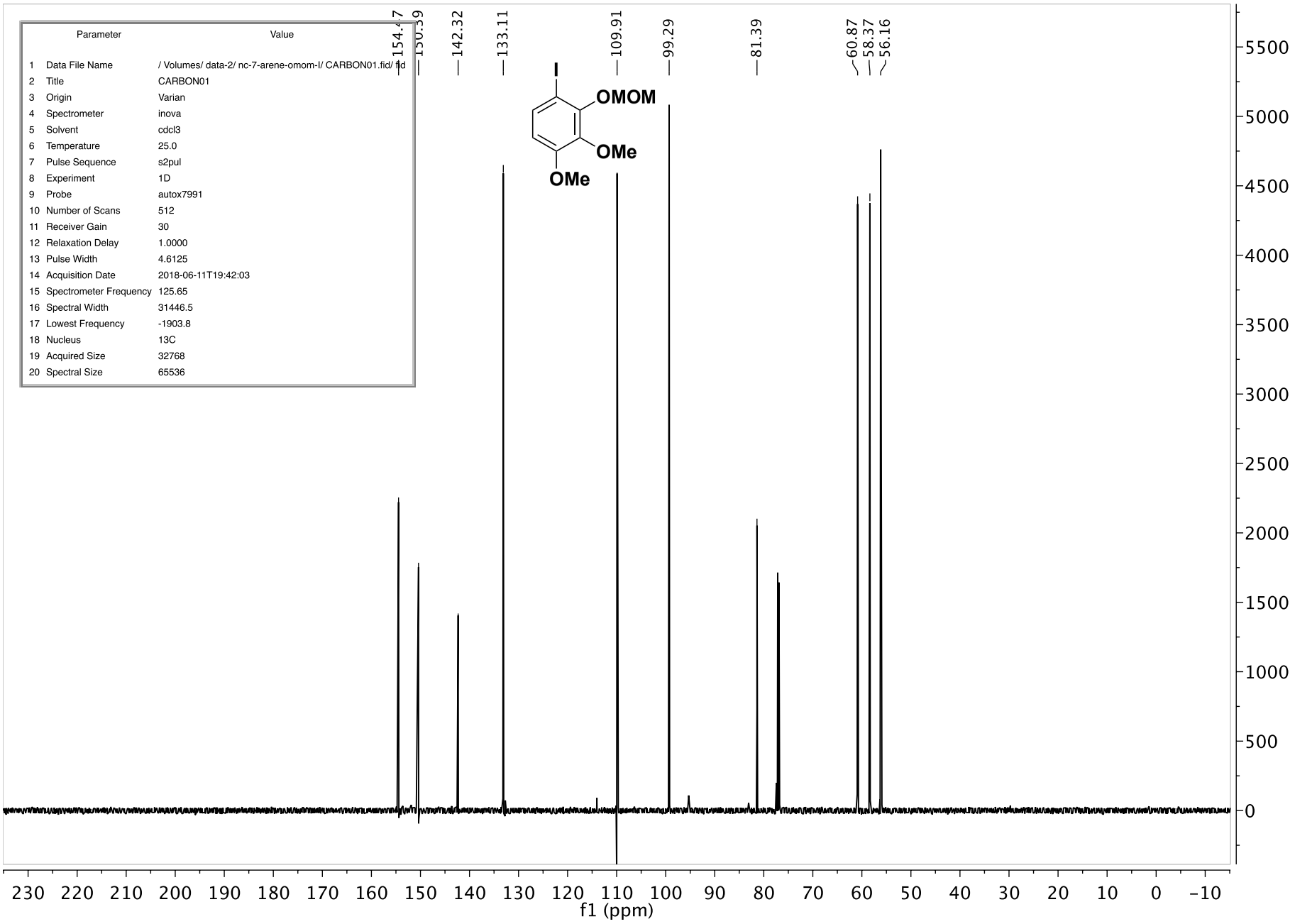
Parameter Value
1 Data File Name / Volumes/ data-2/ nc-7-arene-omom-I/ CARBON01.fid/ fid
2 Title CARBON01
3 Origin Varian
4 Spectrometer inova
5 Solvent cdcl3
6 Temperature 25.0
7 Pulse Sequence s2pul
8 Experiment 1D
9 Probe autox7991
10 Number of Scans 512
11 Receiver Gain 30
12 Relaxation Delay 1.0000
13 Pulse Width 4.6125
14 Acquisition Date 2018-06-11T19:42:03
15 Spectrometer Frequency 125.65
16 Spectral Width 31446.5
17 Lowest Frequency -1903.8
18 Nucleus 13C
19 Acquired Size 32768
20 Spectral Size 65536
154.47
150.39
142.32
133.11
109.91
99.29
81.39
60.87
58.37
56.16
OMOM
OMe
OMe
5500
5000
4500
4000
3500
3000
2500
2000
1500
1000
500
0
230 220 210 200 190 180 170 160 150 140 130 120 110 100 90 80 70 60 50 40 30 20 10 0 -10
f1 (ppm)

	Parameter	Value
1	Data File Name	/ Volumes/ nmr/ nc-7-mom-boc-ome-a/ 1/ fid
2	Title	nc-7-mom-boc-ome-a.1.fid
3	Origin	Bruker BioSpin GmbH
4	Solvent	CDCl3
5	Temperature	295.1
6	Pulse Sequence	zg30
7	Probe	Z122623_0045 (CPP BBO 400S1 BB-H&F-D-05 Z)
8	Number of Scans	16
9	Receiver Gain	10.0
10	Relaxation Delay	1.0000
11	Pulse Width	11.7000
12	Acquisition Time	4.0894
13	Acquisition Date	2018-06-27T06:00:48
14	Spectrometer Frequency	400.13
15	Spectral Width	8012.8
16	Lowest Frequency	-1544.8
17	Nucleus	1H
18	Acquired Size	32768
19	Spectral Size	65536
20	Absolute Reference	

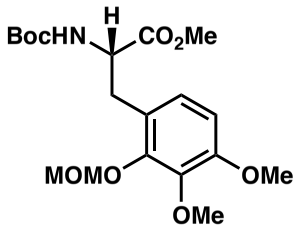

	Parameter	Value
1	Data File Name	/ Volumes/ data/ nc-7-boc-mom-13C.fid/ fid
2	Title	nc-7-boc-mom-13C
3	Origin	Varian
4	Spectrometer	vnmrs
5	Solvent	cdcl3
6	Temperature	65.0
7	Pulse Sequence	s2pul
8	Experiment	1D
9	Probe	OneNMR
10	Number of Scans	140
11	Receiver Gain	60
12	Relaxation Delay	1.0000
13	Pulse Width	3.5125
14	Acquisition Date	2018-06-26T10:20:51
15	Spectrometer Frequency	100.54
16	Spectral Width	25000.0
17	Lowest Frequency	-1431.1
18	Nucleus	13C
19	Acquired Size	32768
20	Spectral Size	65536

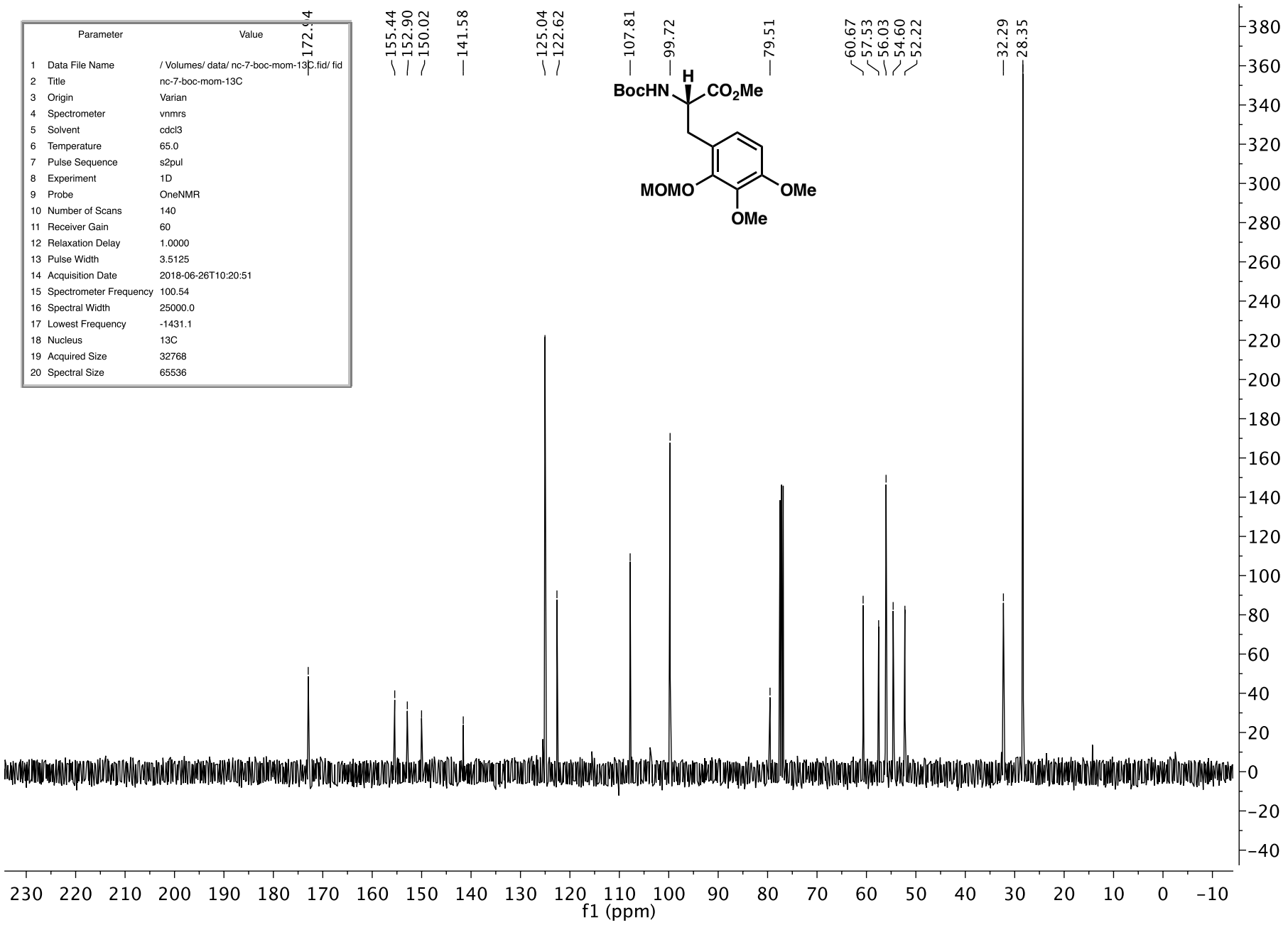

	Parameter	Value
1	Data File Name	/ Volumes/ nmrdata/ ncowper/ nmr/ nc-3-109-trimethoxy-Co2H/ 1/ fid
2	Title	nc-3-109-trimethoxy-Co2H.1.fid
3	Origin	Bruker BioSpin GmbH
4	Solvent	CDCl3
5	Temperature	295.1
6	Pulse Sequence	zg30
7	Probe	Z122623_0045 (CPP BBO 400S1 BB-H&F-D-05 Z)
8	Number of Scans	16
9	Receiver Gain	142.8
10	Relaxation Delay	1.0000
11	Pulse Width	11.7000
12	Acquisition Time	4.0894
13	Acquisition Date	2018-07-02T13:50:51
14	Spectrometer Frequency	400.13
15	Spectral Width	8012.8
16	Lowest Frequency	-1545.5
17	Nucleus	1H
18	Acquired Size	32768
19	Spectral Size	65536
20	Absolute Reference	

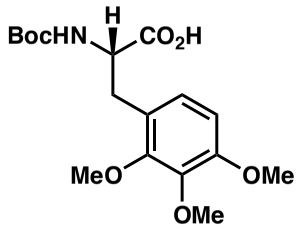

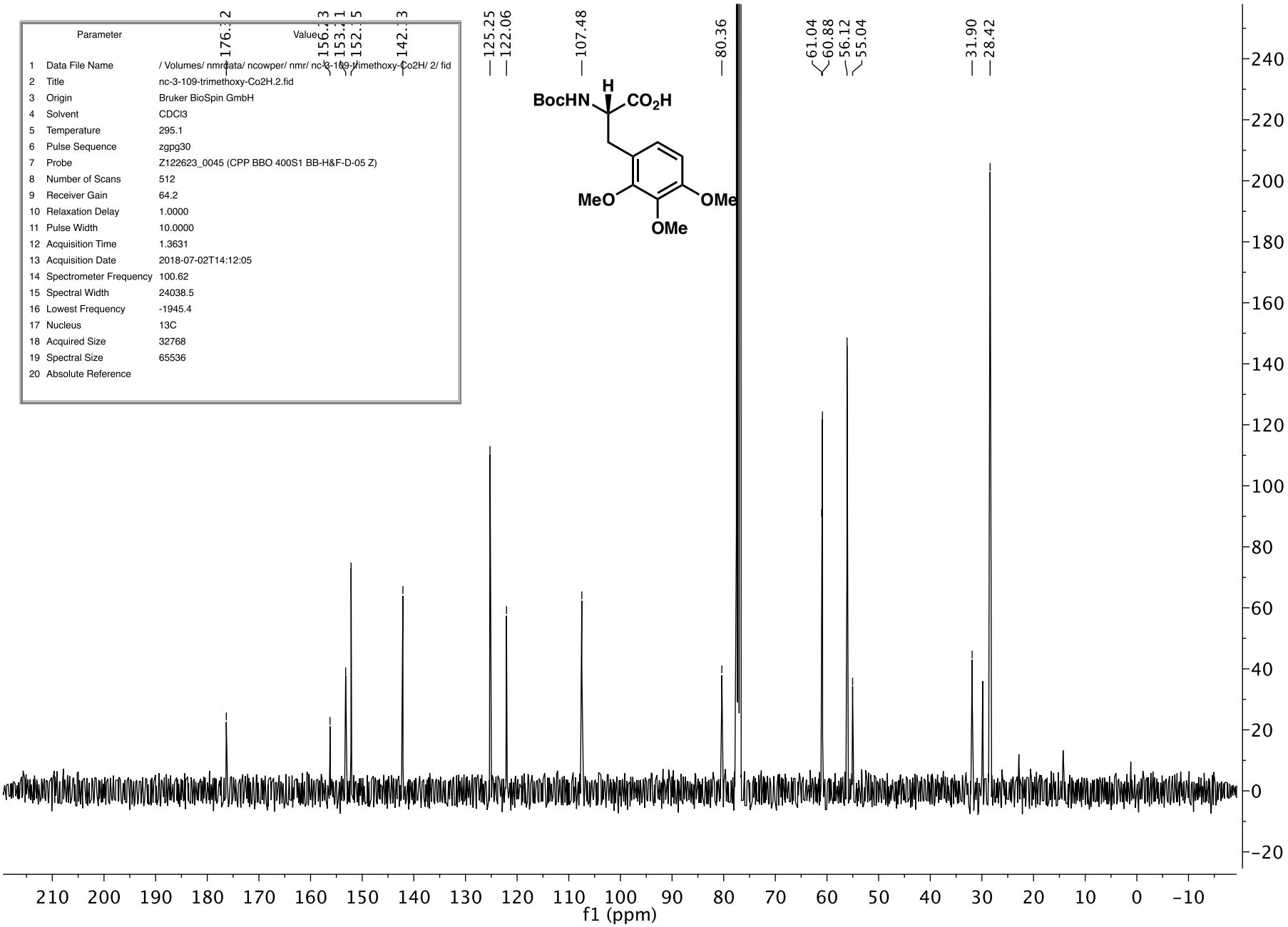

	Parameter	Value
1	Data File Name	/ Volumes/ nmrdata/ ncowper/ nmr/ nc-3-109-trimethoxy-Co2H/ 2/ fid
2	Title	nc-3-109-trimethoxy-Co2H.2.fid
3	Origin	Bruker BioSpin GmbH
4	Solvent	CDCl3
5	Temperature	295.1
6	Pulse Sequence	zgpg30
7	Probe	Z122623_0045 (CPP BBO 400S1 BB-H&F-D-05 Z)
8	Number of Scans	512
9	Receiver Gain	64.2
10	Relaxation Delay	1.0000
11	Pulse Width	10.0000
12	Acquisition Time	1.3631
13	Acquisition Date	2018-07-02T14:12:05
14	Spectrometer Frequency	100.62
15	Spectral Width	24038.5
16	Lowest Frequency	-1945.4
17	Nucleus	13C
18	Acquired Size	32768
19	Spectral Size	65536
20	Absolute Reference	

	Parameter	Value
1	Data File Name	/ Volumes/ nmr/ nc-7-boc-MOM-CO2H-pure/ 1/ fid
2	Title	nc-7-boc-MOM-CO2H-pure.1.fid
3	Origin	Bruker BioSpin GmbH
4	Solvent	CDCl3
5	Temperature	295.2
6	Pulse Sequence	zg30
7	Probe	Z122623_0045 (CPP BBO 400S1 BB-H&F-D-05 Z)
8	Number of Scans	16
9	Receiver Gain	98.9
10	Relaxation Delay	1.0000
11	Pulse Width	11.7000
12	Acquisition Time	4.0894
13	Acquisition Date	2018-07-02T18:43:24
14	Spectrometer Frequency	400.13
15	Spectral Width	8012.8
16	Lowest Frequency	-1545.3
17	Nucleus	1H
18	Acquired Size	32768
19	Spectral Size	65536
20	Absolute Reference	

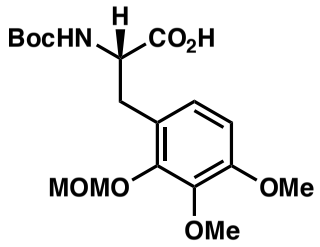

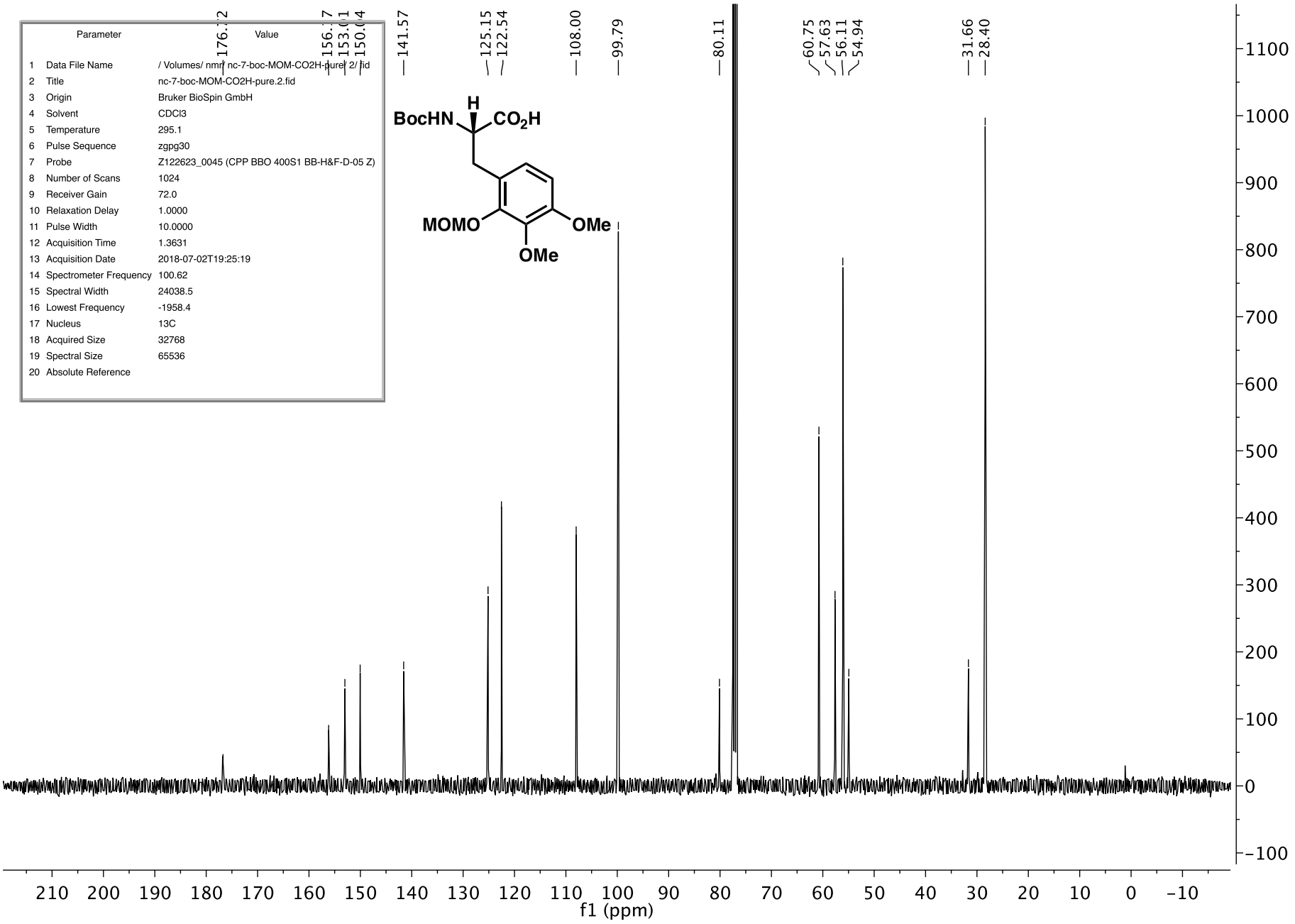
Parameter Value
1 Data File Name / Volumes/ nmr/ nc-7-boc-MOM-CO2H-pure/ 2/ fid
2 Title nc-7-boc-MOM-CO2H-pure.2.fid
3 Origin Bruker BioSpin GmbH
4 Solvent CDCl3
5 Temperature 295.1
6 Pulse Sequence zgpg30
7 Probe Z122623_0045 (CPP BBO 400S1 BB-H&F-D-05 Z)
8 Number of Scans 1024
9 Receiver Gain 72.0
10 Relaxation Delay 1.0000
11 Pulse Width 10.0000
12 Acquisition Time 1.3631
13 Acquisition Date 2018-07-02T19:25:19
14 Spectrometer Frequency 100.62
15 Spectral Width 24038.5
16 Lowest Frequency -1958.4
17 Nucleus 13C
18 Acquired Size 32768
19 Spectral Size 65536
20 Absolute Reference
176.12
156.17
153.01
150.04
141.57
125.15
122.54
108.00
99.79
80.11
60.75
57.63
56.11
54.94
31.66
28.40
BocHN
H
CO2H
MOMO
OMe
OMe
f1 (ppm)

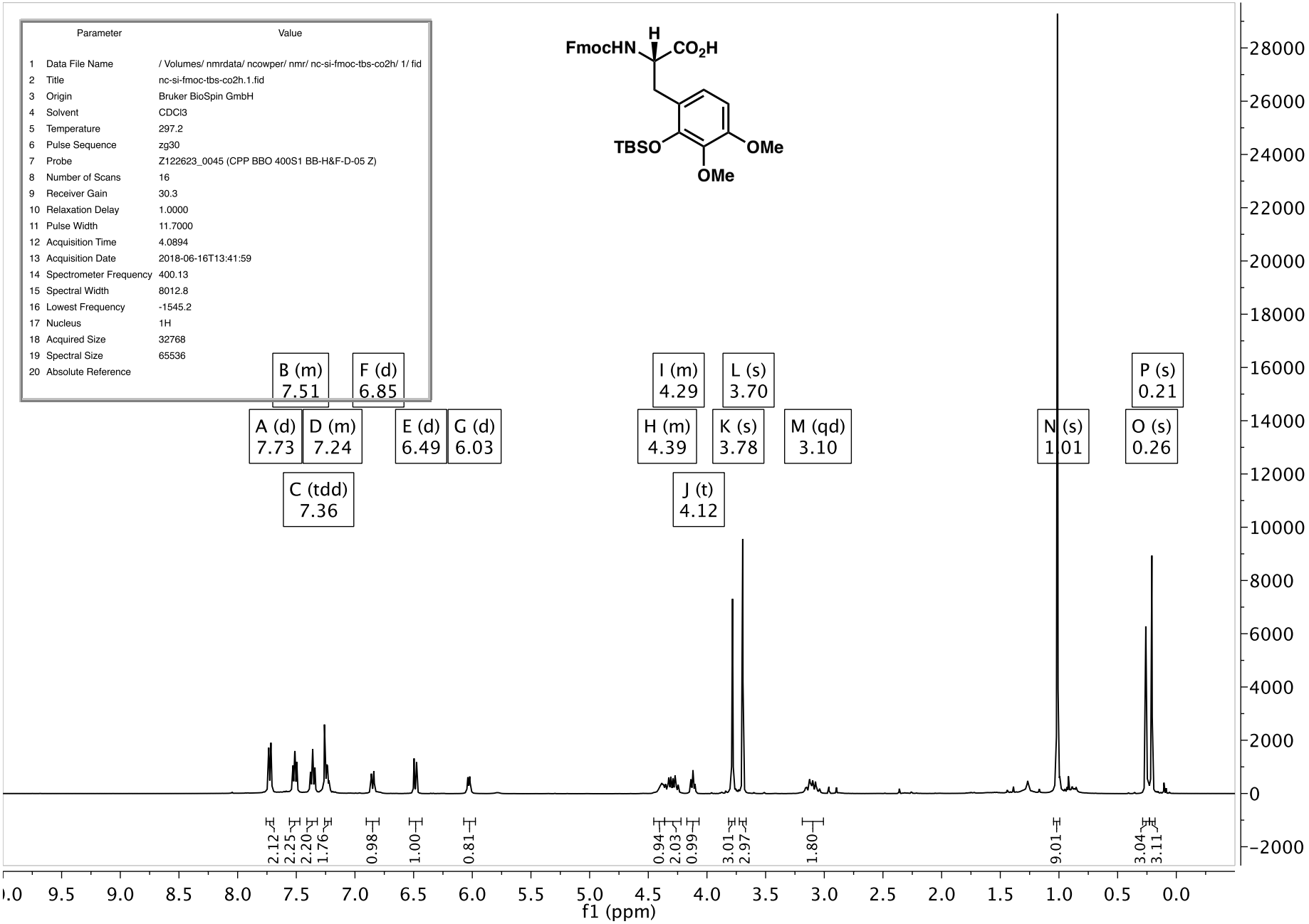
Parameter Value
1 Data File Name / Volumes/ nmrdata/ ncowper/ nmr/ nc-si-fmoc-tbs-co2h/ 1/ fid
2 Title nc-si-fmoc-tbs-co2h.1.fid
3 Origin Bruker BioSpin GmbH
4 Solvent CDCl3
5 Temperature 297.2
6 Pulse Sequence zg30
7 Probe Z122623_0045 (CPP BBO 400S1 BB-H&F-D-05 Z)
8 Number of Scans 16
9 Receiver Gain 30.3
10 Relaxation Delay 1.0000
11 Pulse Width 11.7000
12 Acquisition Time 4.0894
13 Acquisition Date 2018-06-16T13:41:59
14 Spectrometer Frequency 400.13
15 Spectral Width 8012.8
16 Lowest Frequency -1545.2
17 Nucleus 1H
18 Acquired Size 32768
19 Spectral Size 65536
20 Absolute Reference
FmocHN
H
CO2H
TBSO
OMe
OMe
A (d) 7.73
B (m) 7.51
C (tdd) 7.36
D (m) 7.24
E (d) 6.49
F (d) 6.85
G (d) 6.03
H (m) 4.39
I (m) 4.29
J (t) 4.12
K (s) 3.78
L (s) 3.70
M (qd) 3.10
N (s) 1.01
O (s) 0.26
P (s) 0.21
2.12
2.25
2.20
1.76
0.98
1.00
0.81
0.94
2.03
0.99
3.01
2.97
1.80
9.01
3.04
3.11
f1 (ppm)

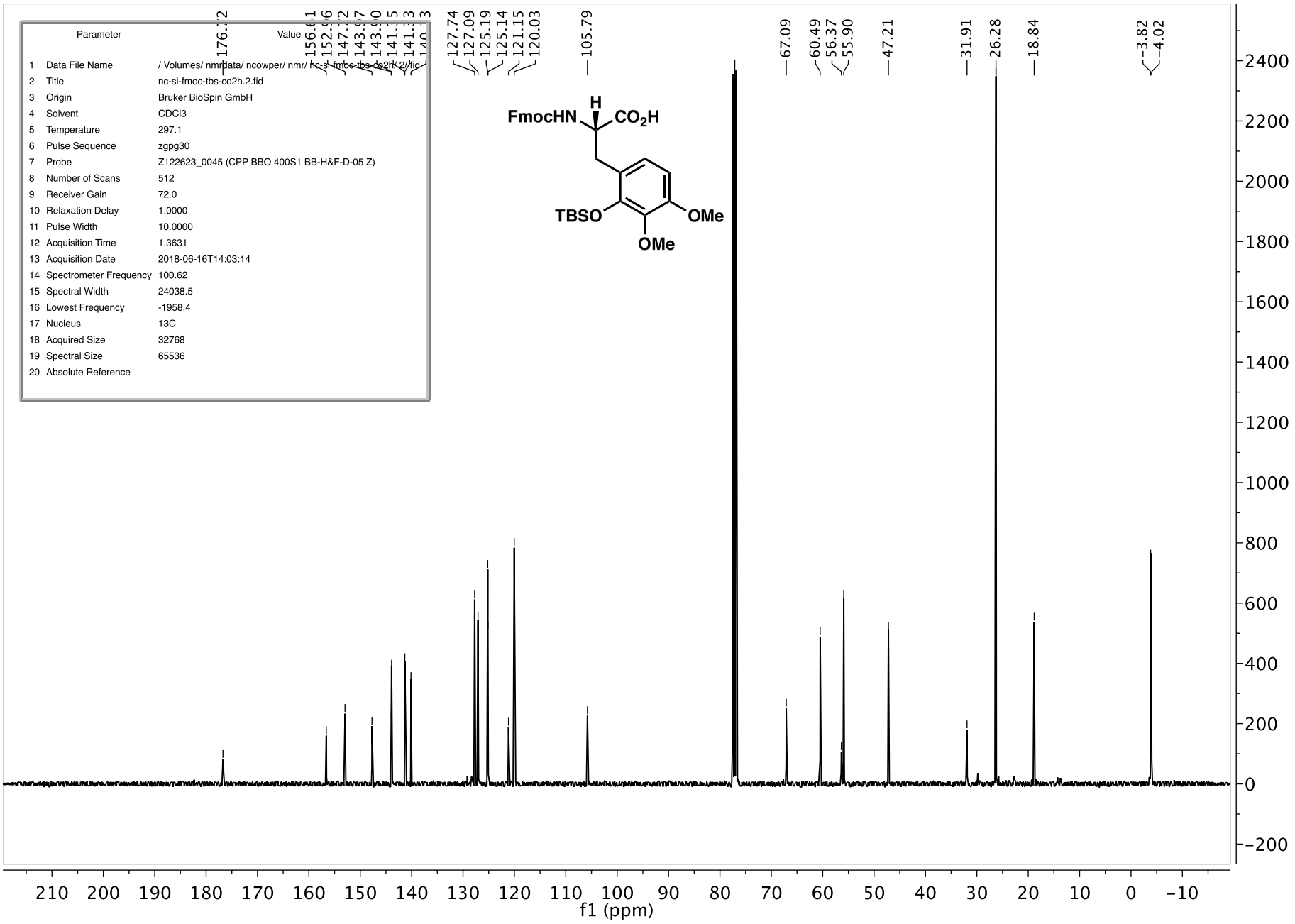
Parameter Value
1 Data File Name / Volumes/ nmrdata/ ncowper/ nmr/ nc-si-fmoc-tbs-co2h/2/fid
2 Title nc-si-fmoc-tbs-co2h.2.fid
3 Origin Bruker BioSpin GmbH
4 Solvent CDCl3
5 Temperature 297.1
6 Pulse Sequence zgpg30
7 Probe Z122623_0045 (CPP BBO 400S1 BB-H&F-D-05 Z)
8 Number of Scans 512
9 Receiver Gain 72.0
10 Relaxation Delay 1.0000
11 Pulse Width 10.0000
12 Acquisition Time 1.3631
13 Acquisition Date 2018-06-16T14:03:14
14 Spectrometer Frequency 100.62
15 Spectral Width 24038.5
16 Lowest Frequency -1958.4
17 Nucleus 13C
18 Acquired Size 32768
19 Spectral Size 65536
20 Absolute Reference
176.12
156.61
152.06
147.12
143.67
143.00
141.35
141.13
140.13
127.74
127.09
125.19
125.14
121.15
120.03
105.79
67.09
60.49
56.37
55.90
47.21
31.91
26.28
18.84
3.82
-4.02
FmocHN
H
CO2H
TBSO
OMe
OMe
2400
2200
2000
1800
1600
1400
1200
1000
800
600
400
200
0
-200
210 200 190 180 170 160 150 140 130 120 110 100 90 80 70 60 50 40 30 20 10 0 -10
f1 (ppm)

	Parameter	Value
1	Data File Name	/ Volumes/ nmr/ nc-7-dihydro-oxazine-epox/ 1/ fid
2	Title	nc-7-dihydro-oxazine-epox.1.fid
3	Origin	Bruker BioSpin GmbH
4	Solvent	CDCl3
5	Temperature	295.1
6	Pulse Sequence	zg30
7	Probe	Z122623_0045 (CPP BBO 400S1 BB-H&F-D-05 Z)
8	Number of Scans	16
9	Receiver Gain	197.4
10	Relaxation Delay	1.0000
11	Pulse Width	11.7000
12	Acquisition Time	4.0894
13	Acquisition Date	2018-07-03T15:24:51
14	Spectrometer Frequency	400.13
15	Spectral Width	8012.8
16	Lowest Frequency	-1545.6
17	Nucleus	1H
18	Acquired Size	32768
19	Spectral Size	65536
20	Absolute Reference	

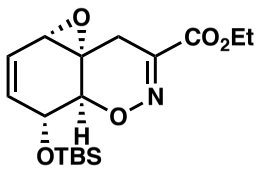

B (ddd) 5.92
A (m) 6.08
C (s) 5.30
E (q) 4.36
D (ddd) 4.46
F (d) 4.04
H (d) 3.00
G (dd) 3.29
I (d) 2.59
K (t) 1.37
L (d) 0.90
J (d) 0.12

0.75 0.78 0.50 0.72 1.55 0.73 0.74 0.66 0.71 3.18 8.85 6.00

f1 (ppm)

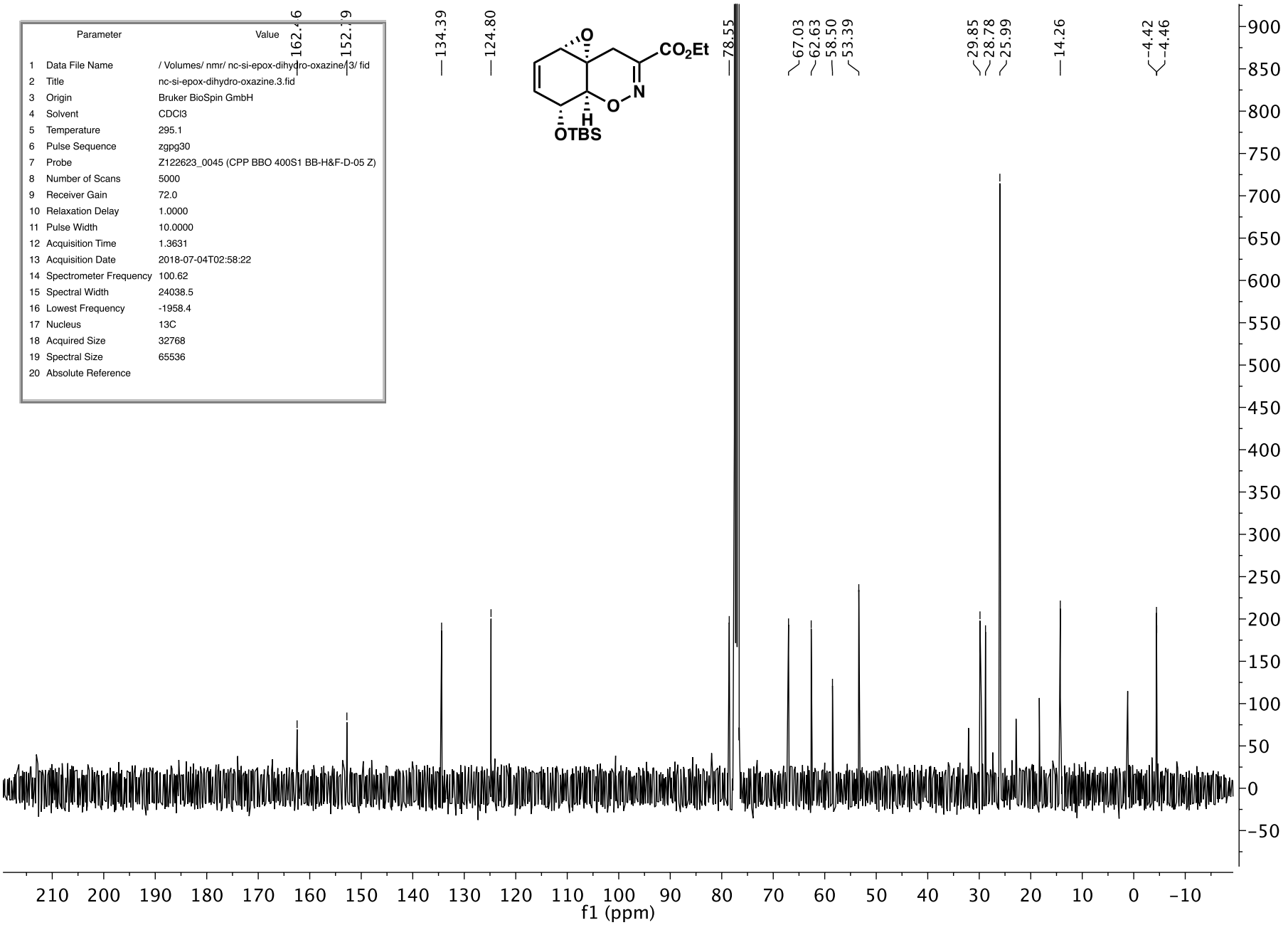
Parameter Value
1 Data File Name / Volumes/ nmr/ nc-si-epox-dihydro-oxazine/3/ fid
2 Title nc-si-epox-dihydro-oxazine.3.fid
3 Origin Bruker BioSpin GmbH
4 Solvent CDCl3
5 Temperature 295.1
6 Pulse Sequence zgpg30
7 Probe Z122623_0045 (CPP BBO 400S1 BB-H&F-D-05 Z)
8 Number of Scans 5000
9 Receiver Gain 72.0
10 Relaxation Delay 1.0000
11 Pulse Width 10.0000
12 Acquisition Time 1.3631
13 Acquisition Date 2018-07-04T02:58:22
14 Spectrometer Frequency 100.62
15 Spectral Width 24038.5
16 Lowest Frequency -1958.4
17 Nucleus 13C
18 Acquired Size 32768
19 Spectral Size 65536
20 Absolute Reference
162.46
152.19
134.39
124.80
78.55
67.03
62.63
58.50
53.39
29.85
28.78
25.99
14.26
-4.42
-4.46
O
CO2Et
N
O
H
OTBS
f1 (ppm)

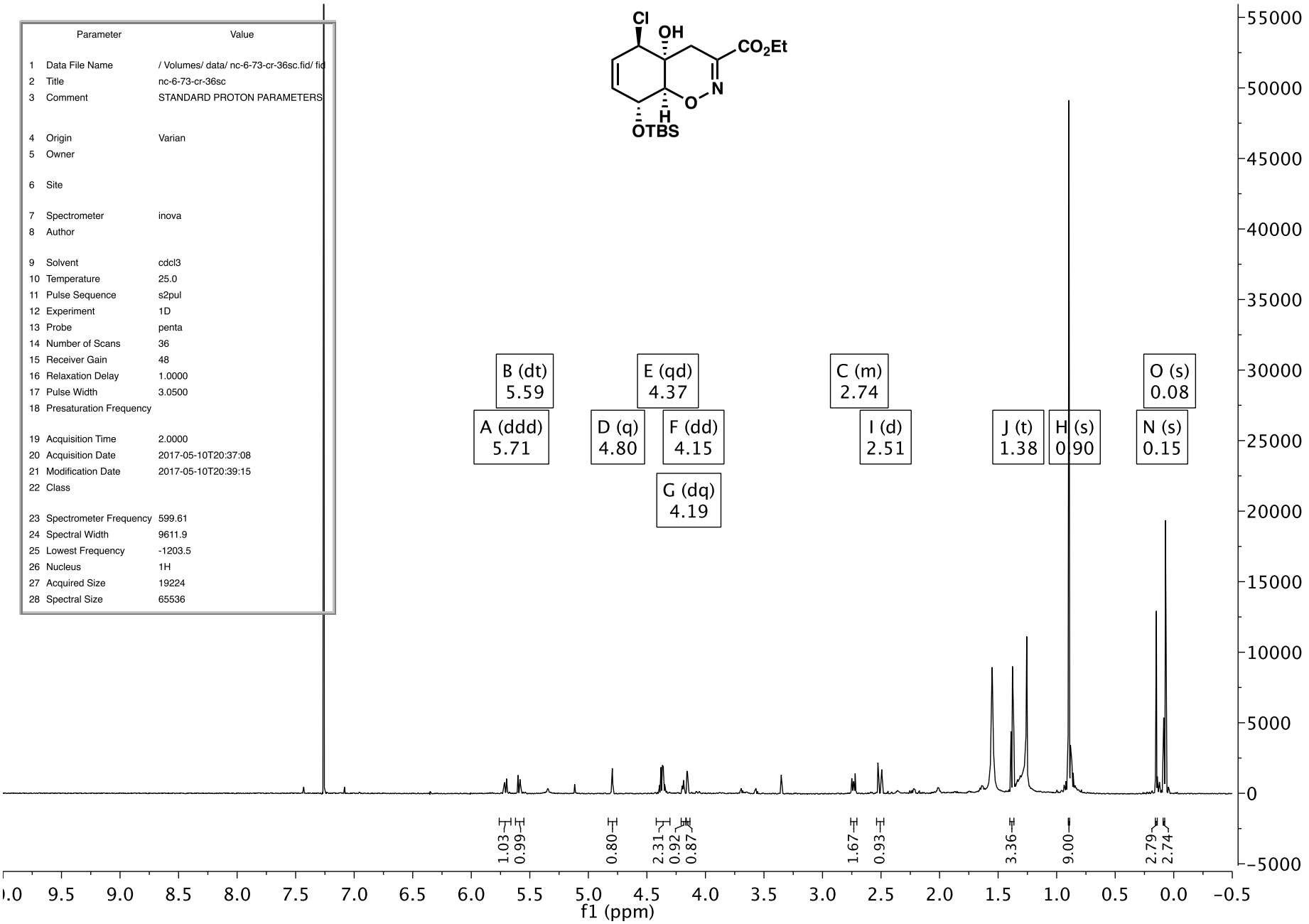

	Parameter	Value
1	Data File Name	/ Volumes/ data/ nc-6-73-cr-36sc.fid/ fid
2	Title	nc-6-73-cr-36sc
3	Comment	STANDARD PROTON PARAMETERS
4	Origin	Varian
5	Owner	
6	Site	
7	Spectrometer	inova
8	Author	
9	Solvent	cdcl3
10	Temperature	25.0
11	Pulse Sequence	s2pul
12	Experiment	1D
13	Probe	penta
14	Number of Scans	36
15	Receiver Gain	48
16	Relaxation Delay	1.0000
17	Pulse Width	3.0500
18	Presaturation Frequency	
19	Acquisition Time	2.0000
20	Acquisition Date	2017-05-10T20:37:08
21	Modification Date	2017-05-10T20:39:15
22	Class	
23	Spectrometer Frequency	599.61
24	Spectral Width	9611.9
25	Lowest Frequency	-1203.5
26	Nucleus	1H
27	Acquired Size	19224
28	Spectral Size	65536

	Parameter	Value
1	Data File Name	/ Volumes/ nmr-1/ nc-7-cl-open/ 2/ fid
2	Title	nc-7-cl-open.2.fid
3	Origin	Bruker BioSpin GmbH
4	Solvent	CDCl3
5	Temperature	295.1
6	Pulse Sequence	zgpg30
7	Probe	Z122623_0045 (CPP BBO 400S1 BB-H&F-D-05 Z)
8	Number of Scans	9000
9	Receiver Gain	78.7
10	Relaxation Delay	1.0000
11	Pulse Width	10.0000
12	Acquisition Time	1.3631
13	Acquisition Date	2018-07-05T04:19:41
14	Spectrometer Frequency	100.62
15	Spectral Width	24038.5
16	Lowest Frequency	-1958.4
17	Nucleus	13C
18	Acquired Size	32768
19	Spectral Size	65536
20	Absolute Reference	

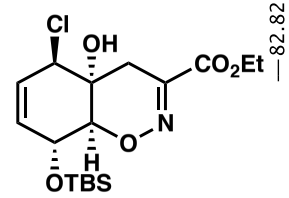

160.18
129.35
127.32
82.82
68.01
67.17
63.02
62.54
29.85
28.64
25.82
14.30
-4.58
-5.00

f1 (ppm)

Chapter 3

Development of the First Catalytic Asymmetric Alkylation of an Oxime and its Application to the Synthesis of Enantioenriched Amines

3.1 INTRODUCTION

Amino acids and chiral amines are of great utility in the synthetic chemistry. They find application in many areas including building blocks for fine synthesis, as catalysts, ligands for transition metals, or as chemical probes in biological systems.[1–3] Prominent examples of chiral amines in catalysis are the cinchona alkaloids and proline; however, these enantioenriched nitrogenous compounds are isolated from the chiral pool. Despite their great utility, nature favors the generation of a single enantiomer of these compounds; therefore, if the unnatural enantiomer is required it must be derived through synthetic means.[4]

Chiral amines can be generated synthetically through a variety of tactics: chiral auxiliaries bound at nitrogen or otherwise appended to the substrate can undergo highly diastereoselective addition of organometallic nucleophiles (Scheme 3.1ab). In a similar vein, the use of stoichiometric chiral nucleophiles can generate similarly enantioenriched products with the added advantage that auxiliary no

Scheme 3.1. *Examples of Strategies for the asymmetric synthesis of chiral amines*

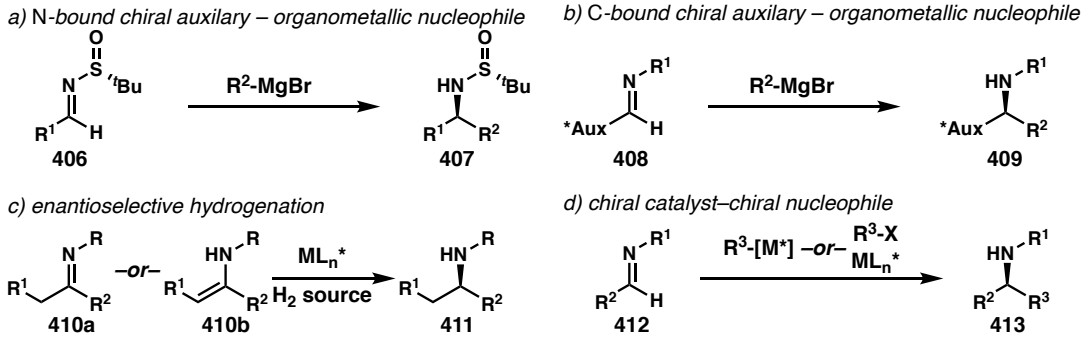

longer needs to be cleaved. Alternatively, chiral amines can be generated through enantioselective catalysis of the imine, or tautomeric enamine, through hydrogenation (Scheme 3.1c).[5] An enticing approach to the synthesis of non-canonical amino acids and other chiral amines is an asymmetric 1,2-addition to an imine with a chiral catalyst or nucleophile.[6] In the case of metal-based catalysis, it is critical to prevent irreversible coordination of the metal center and concurrent catalyst poisoning due to the highly Lewis basic products. The variety of applications for unnatural amino acids in organic chemistry have led to a focus upon their synthesis commonly achieved through a multi-step Strecker synthesis.[7,8] Another common approach for their production is alkylation of benzophenone–derived Schiff bases in conjugation with a chiral phase transfer catalysts or chiral glycine–derived Schiff bases.[9,10] Asymmetric addition to imines to form enantioenriched amines has been successfully realized with several nucleophiles.[11–13] Despite this work examples of asymmetric homopropargylation of imine electrophiles has been limited.

The first example of an asymmetric homopropargylation of an imine was achieved through copper catalysis with a single example XX (Scheme3.2a); *N*-tosyl imines were later revisited as electrophiles in conjunction with silver catalysis establishing improved substrate scope and enantioselectivities (Scheme 3.2d).[14,15] The use of a stoichiometric chiral moiety has been found to be effective either through the attack of a chiral allenyl borane on a protected imine (Scheme 3.2b);[16] or the 1,2–addition of propargylic nucleophiles to a chiral *tert*-butyl sulfinyl imine (Scheme 3.2c).[17–21] Alkylation of a glycine–derived Schiff base, as previously alluded to can provide propargyl glycine derivatives either through the stiochiometric generation of a chiral complex or through the use of a chiral phase transfer catalyst.[22]

Scheme 3.2. *Known examples of the asymmetric homopropargylation of imines*

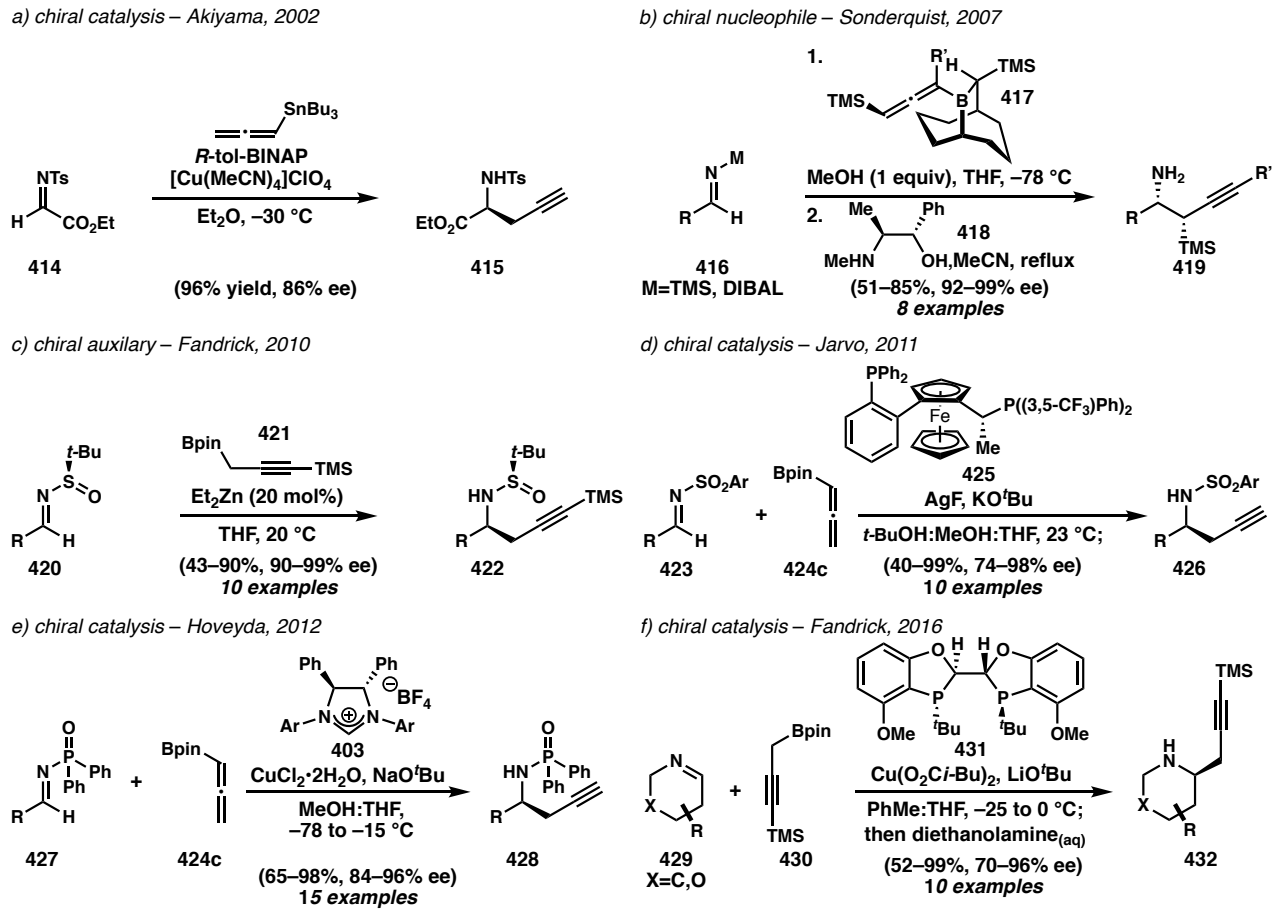

Copper catalysis has been effectively engaged in the catalytic asymmetric homopropargylation of *N*-phosphinoyl imines[23] as well as cyclic aldimines (Scheme 3.2ef).[24] Most examples of asymmetric alkylation of imines demonstrate limited substrate scope with variable yields and rely on *N*-deprotection conditions that are strongly acidic or reducing. These restrictions limit their application to more sensitive substrates and lead to poor recovery of the desired free amine.

Providing new catalytic systems to deliver alkynylated derivatives are of particular interest as they are highly derivatizable.[25] Furthermore, amino acid derivatives such as propargyl glycine can be incorporated into proteins to later undergo click chemistry to either enrich a synthesized protein or tag it with a labelling reagent.[26] Alkynylation has several challenges, over the related allylations and crotylations, as a well-defined cyclic transition state is less favored and allenylation is competitive.[27]

3.2 PREVIOUS WORK IN OXIME ALKYLATION

Oximes are an intriguing substrate for an analogous asymmetric 1,2-addition. Not only could chiral amines be accessed from the alkylated products through the cleavage of the weak N-O bond (~35 kcal•mol^{-1})[28] but an α-hydroxylamine ester product could be used directly in α-ketoacid–hydroxylamine (KAHA) peptide coupling, pioneered by Bode and coworkers.[29]

Previous examples of 1,2-additions to oximes are limited in both the racemic and asymmetric sense. Addition via alkyl radical[30,31], boronate allylation[32,33] and organometallic addition[34] have been observed. To date, however, a stoichiometric amount of chiral information integrated into the nucleophile (Scheme 3.3a) or as an auxiliary appended to the substrate (Scheme 3.3b-e) are required in synthesis of enantioenriched hydroxylamines through alkylation. To the best of our knowledge, there are no current examples of asymmetric catalysis to generate an enantioenriched hydroxylamine. This challenging reactivity is not unanticipated as the mixing of the oxygen lone pair with π* of the C-N double bond lowers the electrophilicity of the substrate. Furthermore, once the product is formed, due to the alpha effect, the nitrogen lone pair can form a strong interaction with Lewis acids leading to catalyst poisoning or decomposition.[35]

Scheme 3.3. *Known methods to generate enantioenriched hydroxylamines*

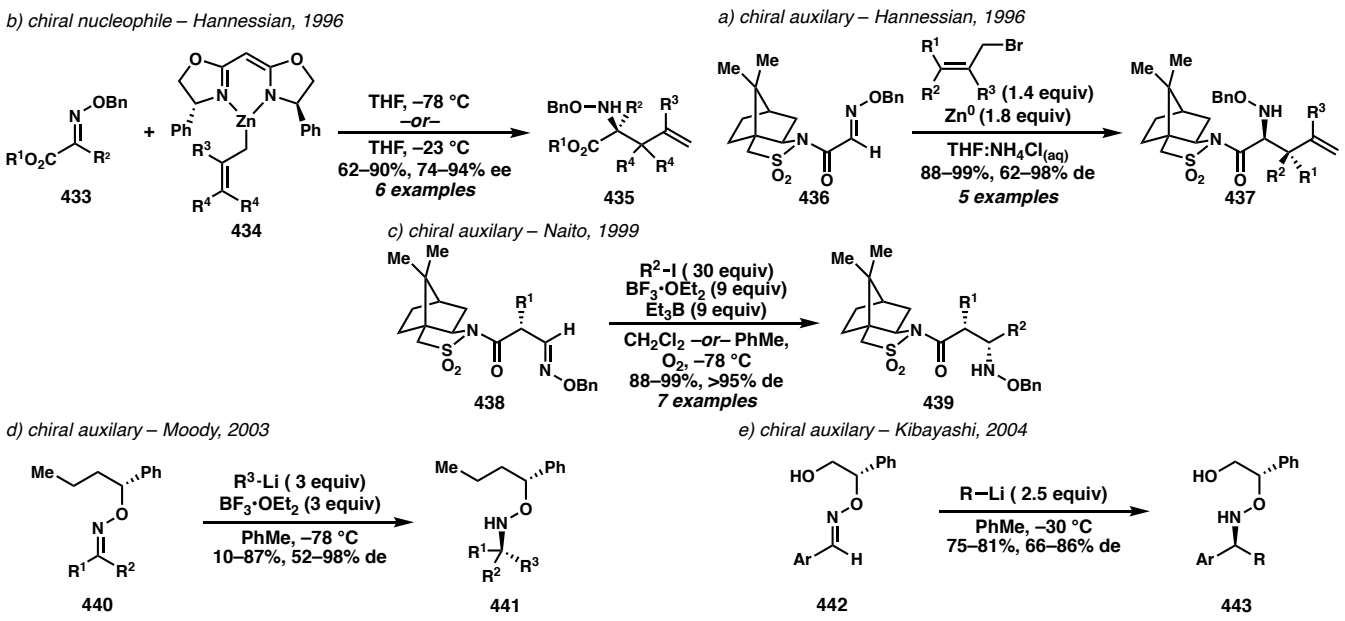

3.3 THE DEVELOPMENT AN ENANTIOSELECTIVE PROPARGYLATION OF AN OXIME

The racemic propargylation of oxime ester proceed with the use of an allenyl zinc nucleophile as has been previously observed by in additions to *N*-alkyl imines (See Chaper 2.3).[36] To develop the first example of a catalytic asymmetric addition to an oxime electrophile both Lewis acidic and transmetallative reaction manifolds were explored. A high–throughput screening procedure was devised using a phenethyl glyoxalate-derived oxime, filtration work-up, quantitative NMR to provide expedient analysis of enantioselectivity and yield. Initial studies using of chiral Lewis acids to activate the electrophile in conjunction with allenyl organometallic nucleophiles, such as stannanes and organozincs, can gave no appreciable enantioinduction. Transiently generating a chiral nucleophile through boronate ligand exchange, on the other hand, product **445a** with appreciable enantioinduction albeit in trace yield (Table 3.1, entry 1).[37] Further screens of chiral diols and additives were unable to improve reactivity but reflection upon the more extensively explored asymmetric addition of carbonyl-containing compounds suggested that copper catalysis could provide the turnover desired.[24,38,39]

Table 3.1. Selected entries in the optimization of reaction conditions

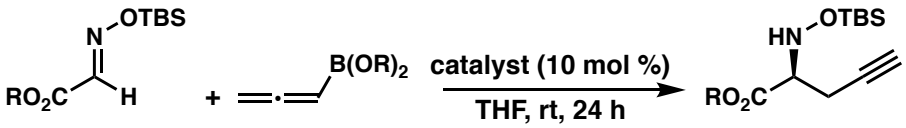

444a (1.0 equiv) | 424 (2.0 equiv) | R=CH_2CH_2Ph | 445a

entry	$B(OR)_2$	catalyst	yield (%)	ee (%)
1	424a, B_{gly}	3,3'-Br-BINOL	3	66
2	424a	$Cu(CO_2i\text{-}Pr)_2$; BINAP[a]	2	63
3	424a	$Cu(MeCN)_4BF_4$; T-BINAP[a]	7	72
4	424a	$Cu(MeCN)_4BF_4$; TADDOL-P-NMe_2[a]	70	30
5	424a	$Cu(MeCN)_4BF_4$; DifluorPhos[a]	11	80
6	424a	$Cu(MeCN)_4BF_4$; BTFM-GarPhos[a]	24	82
7	424a	$Cu(MeCN)_4BF_4$; BTFM-GarPhos	30	95
8	424a	Cu(BTFM-Garphos)$(MeCN)_2BF_4$	50	92
9	424b, B_{pin}	Cu(BTFM-Garphos)$(MeCN)_2BF_4$	6	62
10	424c, B_{neo}	Cu(BTFM-Garphos)$(MeCN)_2BF_4$	85	96

[a] Li(OtBu) (9.5 mol%) added

Encouragingly, a screen of copper–phosphine complexes with an allenyl boronate gave moderate enantioduction, albeit in trace yield (Table 3.1, entry 2). An extensive ligand screening effort identified two families of ligands with contrasting reactivity: *bis*-phosphines (entry 3), which gave no turnover but higher enantioinduction, and phosphoramidates (entry 4), which gave higher turnover but low ee.

Postulating that greater π-acidity of phosphoramidates imparted greater reactivity, electron-poor bisphosphines were screened.[40] Gratifyingly, both commercially available electron-poor phosphines Difluorphos (entry 5) and BTFM-Garphos (entry 6) generated product with elevated ee. Significantly, BTFM-Garphos was the first bisphosphine ligand to achieve a turnover. In contrast to conventional metal-catalyzed, boronate-mediated alkylations a series of control experiments demonstrated that catalytic base was not required to activate the boronate for transmetallation to the copper center. Indeed, upon exclusion of catalytic base both a slight improvement to yield was observed as well as strong enantioinduction (Table 3.1, entry 7).

Figure 3.1. *Catalyst decomplexation after ligand-metal prestir by ^{31}P NMR, t=0, 2h, 4h, then 4h intervals*

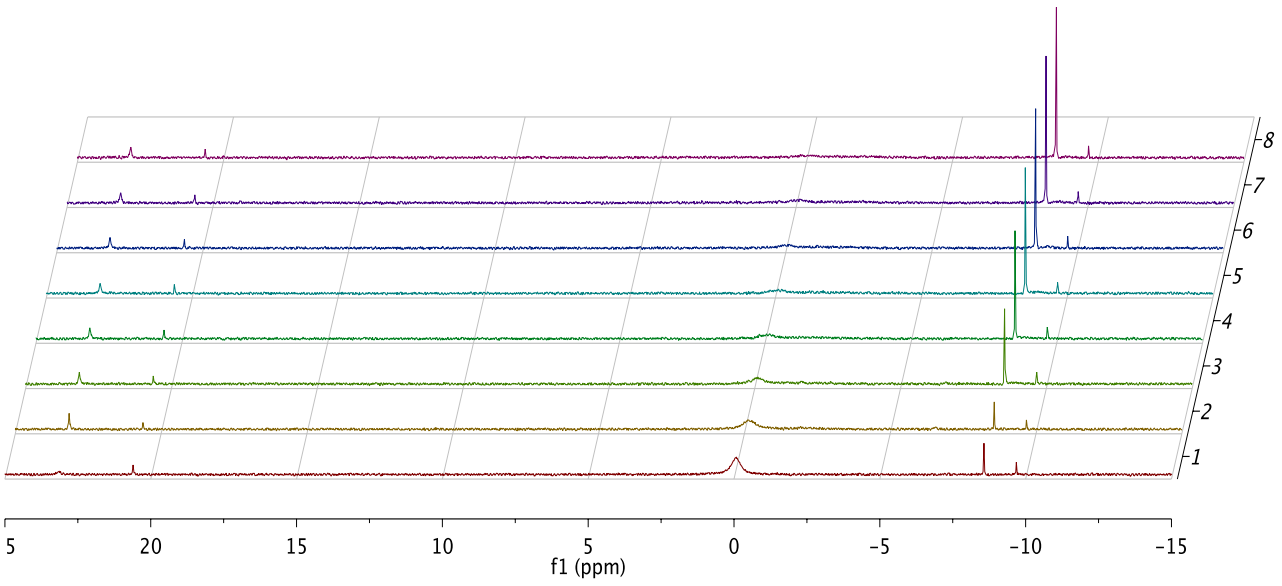

At this point, the transformation was highly enantioselective but turnover remained low and efforts to further improve the yield through additive and ligand screening were stymied. In an effort to gain

greater insight into the alkylation it was monitored by NMR. The pre–catalyst is generated by pre–stirring the ligand and metal source for 10 minutes prior to the addition of the oxime electrophile and the boronate. When monitored by ^{31}P NMR observed rapid decomplexation of the ligand from copper with 50% dissociation observed after eight hours and only trace catalyst present after 24 hours (Figure 3.1). Correspondent to this, ^{1}H NMR showed a small induction time followed by a period of rapid product formation which slowed in rate as time progressed and active catalyst decreased in concentration. To improve the yield and eliminate the observed induction time, an isolated pre-complexed catalyst was used in place of a ligand–metal pre–stir and improved yield was observed with negligible erosion of ee (Table 3.1, entry 8).

Figure 3.2. Monitoring oxime alkylation by ^{1}H NMR varying boronate linker with pre-complexed catalyst

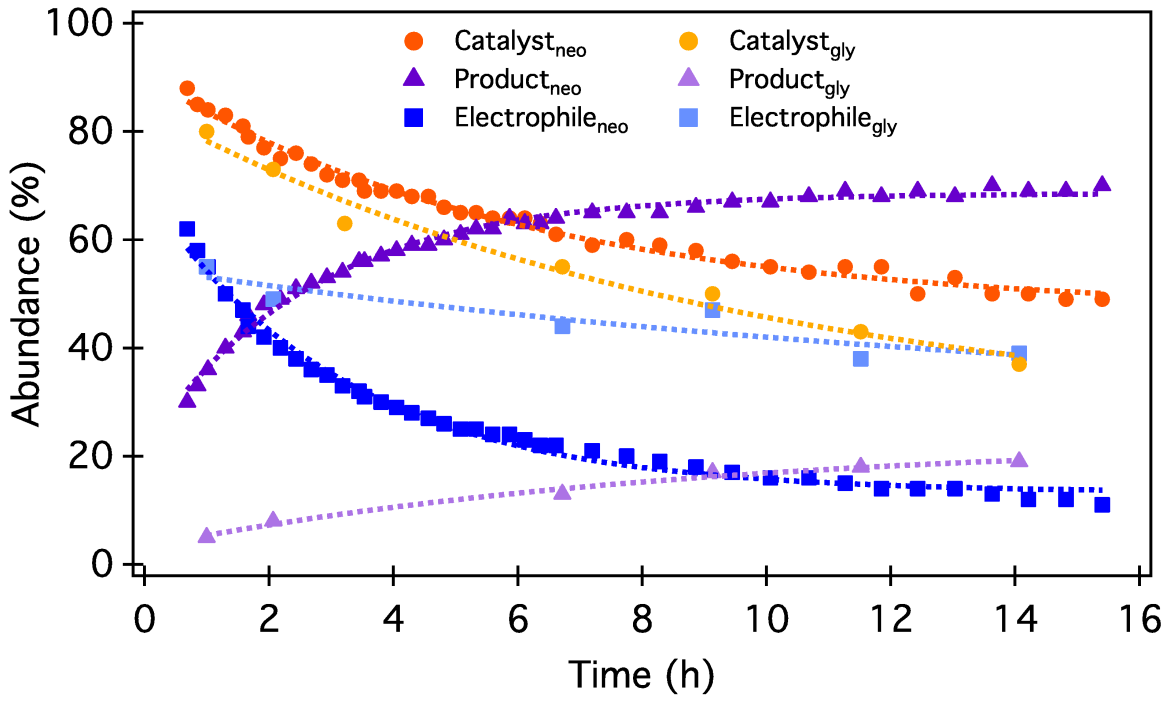

Finally, attention turned to the optimization of the boronate ester. The allenyl boronate was not completely consumed during the reaction; however, an excess of boronate provided improved robustness. The bulk of the boronate ester could affect both the rate of transmetallation as well as the rate of catalyst poisoning by limiting coordination of the Lewis basic hydroxylamine nitrogen to the copper center. To

probe this hypothesis, bulkier boronate esters were employed: while the pinacol ester demonstrated diminished reactivity and enantioinduction (entry 9, Table 3.1); gratifyingly, the neopentyl ester not only dramatically improved turnover but also provided a highly enantioenriched product (entry 10, Table 3.1). A comparison of the allenyl dioxaboralane and dioxaborinanes showed that the neopentyl ester improves both the initial rate of the reaction (Pgly, Pneo, Figure 3.2) as well as limiting off-pathway decomposition of the starting material (Sgly, Sneo). The half-life of active catalyst also lengthened from eight hours to 14 hours when the neopentyl ester was employed (Cneo).

The nature of this excellent reactivity was quite sensitive to the nature of the ester on the substrate, while linear alkyl esters gave excellent results, even moderate perturbations to more hindered esters, including benzyl, gave substantially poorer yields and selectivities. Subjection of amide substrates to the optimized conditions similarly led to depressed reactivity. Despite these limitations, the simplicity of the conditions employed in the homopropargylation of oxime ester **444a** lend to easy scalability; the alkylation of **444b** was scaled up to gram scale, retaining the desired reactivity and 88% of the electron poor phosphine ligand was recovered cleanly.

Table 3.2. *Selected substrates for asymmetric propargylation of oximes and Boc-imines*

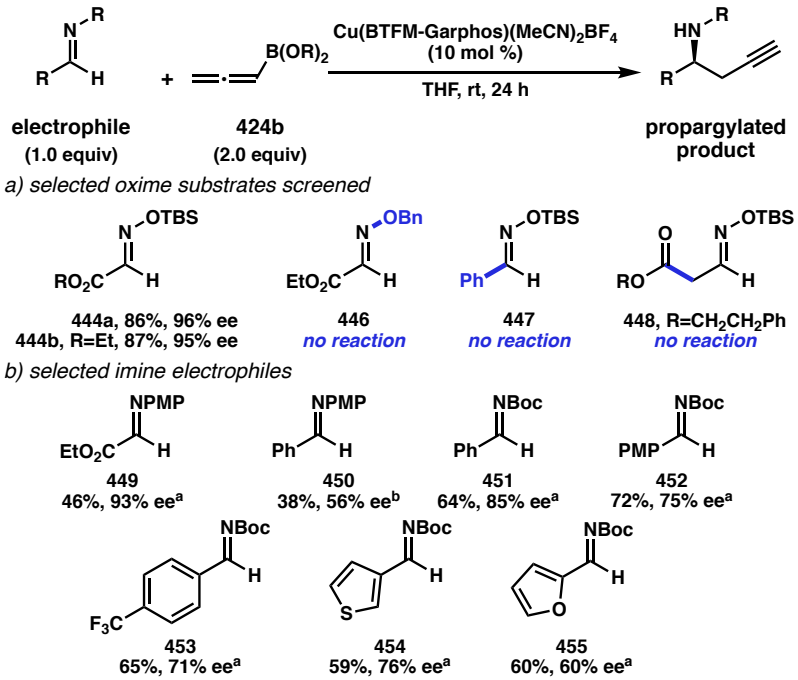

Seeking to gain an understanding of the limitations of the system we found that the glyoxalate derived oxime **444** is a special substrate. The presence and proximity of a carbonyl in the oxime electrophile was critical to good reactivity. Both benzaldoxime **447** and 3-oximinopropanoate **448** (Table 3.2) were completely unreactive to the optimized conditions. Furthermore, the addition of catalytic base to encourage the transfer of the allenyl fragment onto the copper center were ineffective at rescuing reactivity. Other glyoxalate–derived electrophiles were reactive as replacing the oxime moiety with an *N*-aryl imine which reacted with good efficiency but a depressed enantioselectivity at room temperature (**449**, Table 3.2). Cooling the homopropargylation of imine **449** restored enantioselectivity comparable to the successful oxime electrophiles. Under the optimized conditions, substrates which lacked a Lewis basic moiety, such as *N*-aryl benzaldimine **450**, showed non-trivial reactivity in contrast to less electrophilic benzaldoxime **447** yet with far lower enantioselectivity. To further establish the importance of further justified pre-coordination of the substrate was required for good reactivity. To this end we surveyed *N*-boc imines as a possible alternative substrate class for propargylation as complementary method Hoveyda's allenylation.[41] While reactivity was restored for these substrates the enantioselectivities observed were not exceptional, however a solvent swap to toluene did provide a small improvement in that respect with little detriment to yield.

During these studies, $Cu(PPh_3)_2(acac)$ proved an effective catalyst for the racemic homopropargylation of these electrophiles. This achiral catalyst also reacted well when an allyl boronate **456** was used in place of the allenyl boronate **424b** to form **457** in high yield (entry 1, Scheme 3.4a). Unfortunately, this reactivity was not reflected when the newly developed asymmetric catalyst was used. Both dioxaborolane and dioxaborinane generated a low yield of the allylated product; however, in line with the homopropargylation, the neopentyl ester rescued reactivity to a degree albeit with negligible enantioselectivity (entry 3, Scheme 3.4a). This massive erosion in selectivity between the propargylation and allylation is likely due to differences bond angles in a transition states.

When a substituted allenyl boronate **458** was engaged under the optimized reaction conditions both the allene and propargylated products were observed in low yield, both with non-trivial enantioinduction (Condition B, Scheme3.4b). It is notable that the ratio of between alkyne and allene appears tied to the nature of the ligand. While triphenylphosphine favors formation of the alkyne **459a** the electron–poor bisphosphine BTFM-Garphos favors formation of the allene **459b**. This shift in product distribution is suggestive that an isomerization event generating these two products is dependent on the nature of the copper center.

Scheme 3.4. *Attempts to use other boronate esters in copper-catalyzed alkylations*

a) Alkylation of an oxime with allyl boronates

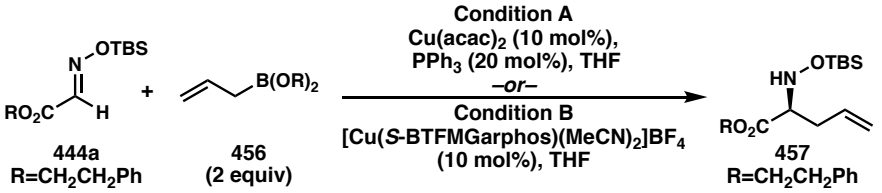

entry	conditions	$B(OR)_2$	yield (%)	ee (%)
1	PPh_3	Bgly	92%	—
2	BTFM-GarPhos	Bgly	5%	ND
3	BTFM-GarPhos	Bneo	34%	14%

b) Alkylation of an oxime with a substituted allenyl boronate

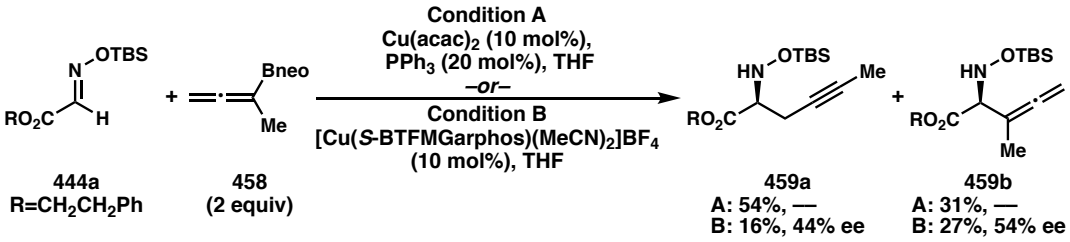

The patterns of reactivity along with combined with the NMR studies, informed a mechanistic hypothesis of this transformation. Initial loss of a labile nitrile ligand from the precatalyst **460** (Scheme 3.5) would provide a site for transmetallation. NMR monitoring of the reaction suggests the formation of a reactive boron-ate complex, control experiments demonstrated that this was not a result of phosphine coordination to boron. Therefore, the Lewis basic oxime nitrogen is proposed to activate the boronate ester to form an activated complex **462** to facilitate transmetallation of the allenyl fragment onto the copper center **461** in an S_N2' fashion. The resulting propargylated organocuprate **463** can then equilibrate

with the allenyl isomer **465**. Given the necessity of a Lewis basic moiety in close proximity the electrophilic carbon, it is therefore thought that exchange of the ancillary nitrile ligand with the carbonyl of the ester of the electrophile not only brings the allenyl fragment into close proximity with electrophilic carbon in a pre-organized fashion but also would inductive activates the substrate for alkylation. It is proposed, therefore, that the delivery of the nucleophilic fragment proceeds through a cyclic transition state to yield a propargylated B-N adduct that is hydrolyzed readily upon work-up.

Scheme 3.5. *Mechanistic hypothesis of the copper-catalyzed alkylation of an oxime*

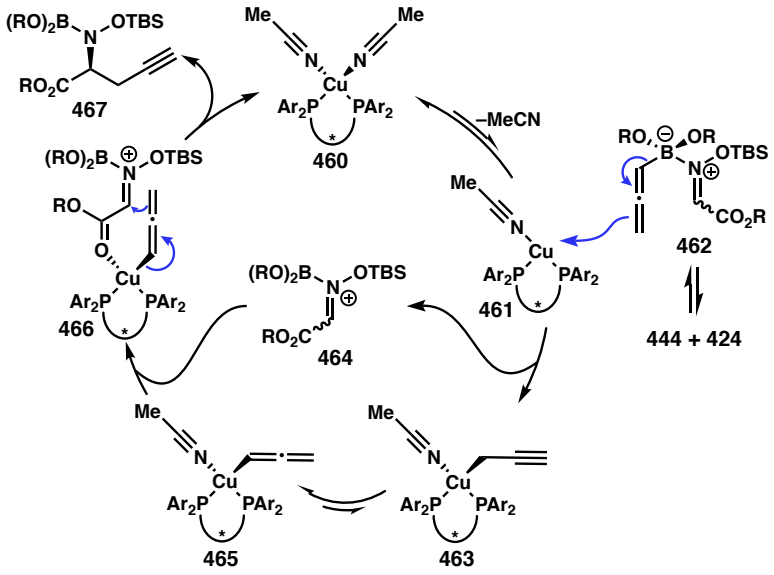

3.4 ELABORATION OF ENANTIOENRICH *N*-SILOXY AMINO ESTERS

While glyoxylate–derived oximes appear uniquely reactive to the conditions disclosed herein, enantioenriched hydroxylamines are useful intermediates for chemical synthesis. Particularly as a means to access enantioencriched propargyl glycine. Heterogeneous methods to cleave N-O bonds including as Raney-Ni, palladium or activated zinc lead to competitive alkyne reduction. Thankfully, acylation of the nitrogen followed by reduction with SmI_2 did provide the desired protected amino ester **469** in low yield; however, simply exposing of **445b** to pyruvic acid in wet DMSO formed the enantioenriched *N*-acetyl propargylglycine in a single step (Scheme 3.5a). Given the importance of propargyl glycine as a

biological studies to tag proteins we were delighted to find that **470** was formed in high yield under typical Cu-catalyzed "click" reaction conditions. To further improves access other unnatural *N*-hydroxyamino ester we also found that **445b** could undergo high-yielding Sonagashira couplings after *N*-acylation.

Scheme 3.5. *Elaboration of hydroxyamino esters*

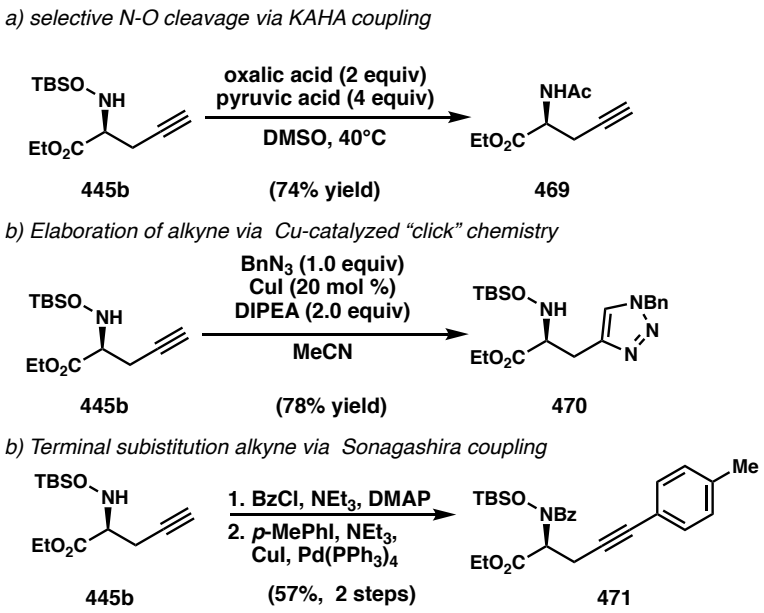

3.5 CONCLUSIONS AND OUTLOOK

In conclusion, the use of an electron–poor chiral bisphosphine resulted in the development of the first catalytic asymmetric alkylation of an oxime. While this reactivity was highly specialized to glyoxalate–derived oximes these simple conditions could also be applied to the homopropagylation of imines electrophiles with moderate enantioinduction. Furthermore, it is established that the propargylated products of the reactions can be elaborated both at the alkyne and at the nitrogen orthogonally.

While other boronates were not amenable to the reaction conditions they demonstrated good reactivity when an achiral catalyst was used. This suggests that Cu-bisphosphine catalysis could be a general solution the asymmetric alkylation of oximes however further ligand development is needed.

3.6 EXPERIMENTAL SECTION

3.6.1 MATERIALS AND METHODS

Unless otherwise stated, reactions were performed under a nitrogen atmosphere using freshly dried solvents. Tetrahydrofuran (THF), methylene chloride CH_2Cl_2), acetonitrile (MeCN), dimethylformamide (DMF), benzene (PhH), diethyl ether (Et_2O) and toluene (PhMe) were dried by passing through activated alumina columns. Unless otherwise stated, chemicals and reagents were used as received. Triethylamine (Et_3N) was distilled over calcium hydride prior to use. All reactions were monitored by thin-layer chromatography using EMD/Merck silica gel 60 F254 pre-coated plates (0.25 mm) and were visualized by UV, *p*-anisaldehyde, vanillian, CAM or $KMnO_4$ staining. Flash column chromatography was performed either as described by Still et al.[31] using silica gel (partical size 0.032-0.063) purchased from Silicycle. Optical rotations were measured on a Jasco P-2000 polarimeter using a 100 mm path-length cell at 589 nm. ^1H and ^{13}C NMR spectra were recorded on a Varian 400 MR (at 400 MHz and 101 MHz, respectively), or a Varian Inova 500 (at 500 MHz and 126 MHz, respectively), and are reported relative to internal $CHCl_3$ (^1H, δ = 7.26), or DMSO (^1H, δ = 2.50), and $CDCl_3$ (^{13}C, δ = 77.0), or DMSO (^{13}C, δ =40.0). Data for ^1H NMR spectra are reported as follows: chemical shift (δ ppm) (multiplicity, coupling constant (Hz), integration). Multiplicity and qualifier abbreviations are as follows: s =singlet, d = doublet, t = triplet, q = quartet, m = multiplet, br = broad, app = apparent. IR spectra were recorded on a Perkin Elmer Paragon 1000 spectrometer and are reported in frequency of absorption ($cm.^{-1}$). HRMS were acquired using an Agilent 6200 Series TOF with an Agilent G1978A Multimode source in electrospray ionization (ESI), atmospheric pressure chemical ionization (APCI), or mixed (MM) ionization mode. Analytical chiral HPLC was performed with an Agilent 1100 Series HPLC utilizing Chiralpak AD or Chiralcel OD-H columns (4.6 mm x 25 S7 cm) obtained from Daicel

Chemical Industries, Ltd with visualization at 254 nm.

3.4.2 PREPERATIVE PROCEDURES AND SPECTROSCOPIC DATA

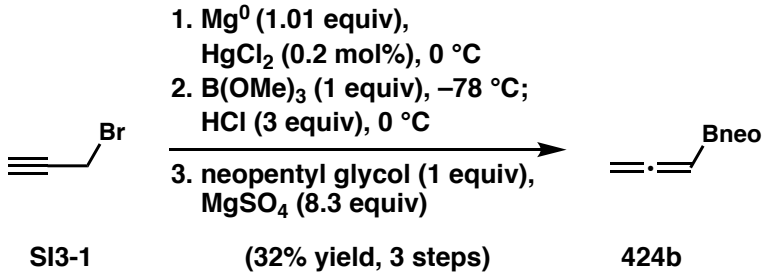

Adapted from: OL, 2011, p.4020; Org Syn. 1981, 60,41.

To freshly activated Mg^0 (6.11g, 251.3mmol, 1.01 equiv), add $HgCl_2$ (115mg, 0.425 mmol, 0.2 mol%) and suspend in Et_2O (50 mL). Propargyl bromide(29.79g, 250 mmol, 1.0 equiv) in PhMe (80 wt%, 27.8mL) was further diluted with additional Et_2O (170 mL). A small amount of the propargyl bromide solution (10 mL) was added to the suspension of Mg^0. Initiation was achieved through gentle heating of the resulting mixture. Cool in a salt/ice bath and add the remaining propargyl bromide solution as a slow, steady stream. After addition is complete, stir at ambient temperature for 1h. Cannulate the resulting Grignard solution, over 45 minute period, into a solution of freshly distilled trimethyl borate (26.0g, 27.9mL, 250 mmol, 1.0 equiv) in Et_2O (250 mL) cooled to –78 °C. After completion of Grignard addition, allow mixture to warm to ambient temperature. Cool the suspension once more to 0 °C and cannulate 3M $HCl_{(aq)}$ (250 mL, 3 equiv) dropwise into over 3h. Stir mixture until solids disappear, approximately 1h, and a further 20 minutes at ambient temperature. Separate the organic layer and wash the aqueous layer with Et_2O (3×150 mL); dry the combined organics over $MgSO_4$. Decant dried organics into a 2L round bottom flask and wash the remaining solids with dry Et_2O (100 mL). Concentrate solution under reduced pressure until the 500mL remain and backfill with argon. Add anhydrous $MgSO_4$ (250g,

2.08 mol, 8.31 equiv) and neopentyl glycol (26.04g, 250 mmol, 1.0 equiv). Rinse down solids with Et_2O (50 mL) and stir under argon with an overhead stirrer for 40h. Filter off solids using a large swivel frit. Take the caked solids and rinse with Et_2O (4×100 mL) through a packed sand filter. Recombine organic and remove solvent through a vacuum transfer. Add pentanes (400mL) to the remaining residue and cool to 0 °C. Filter off precipitated solids with a large swivel frit and remove pentane through a vacuum transfer. The remaining yellow oil is purified by kugelrohr distillation (90 °C/ 5.0 Torr → 110 °C/1.0 Torr) to yield a clear oil (12.61g, 83.0 mmol, 32% yield)

^{1}H NMR (400 MHz, $CDCl_3$) δ 4.82 (t, *J* = 7.0 Hz, 1H), 4.61 (d, *J* = 7.0 Hz, 2H), 3.66 (s, 4H), 0.98 (s, 6H).

^{13}C NMR (126 MHz, $CDCl_3$) δ 217.90, 72.47, 69.77, 31.84, 21.82.

^{11}B NMR (128 MHz, $CDCl_3$) δ 26.48.

FTIR (AT-IR) 2961.46, 2886.72, 1934.21, 1477.56, 1414.40, 1377.85, 1327.80, 1256.69, 1224.66, 1181.98, 1129.78, 812.31, 681.34, 667.05 cm^{-1}

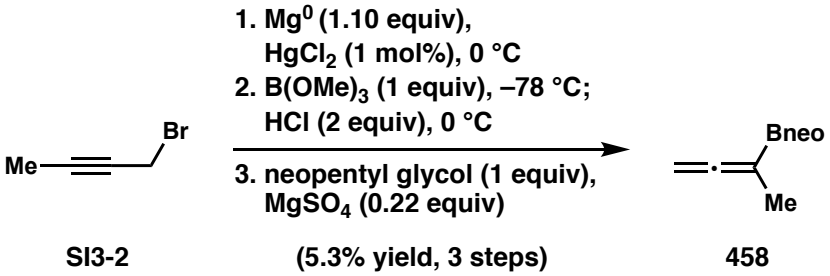

Flame dry freshly activated Mg^0 (802mg, 33.0 mmol, 1.10 equiv) and $HgCl_2$ (81.4 mg, 0.30 mmol, 1.0 mol %) under argon. Cool to 0 °C and add Et_2O (3 mL) and stir 5 minutes. Add 1-bromo-2-butyne (665mg, 0.44 mL, 5.0 mmol, 0.16 equiv) dropwise maintaining an internal temperature at 5 °C. Stir vigorously to initiate Grignard formation. Cannulate the remainder of 1-bromo-2-butyne (3.33 g, 2.19 mL, 25.0 mmol, 0.84 equiv) dropwise as a solution in Et_2O (20 mL) into the reaction. Remove cooling bath after addition of bromide is complete and stir mixture at ambient temperature

for 4h30m. Cool mixture to –78 °C and add $B(OMe)_3$ (3.12g, 3.35 mL, 30.0 mmol, 1.00 equiv). Stirred solution for 1h at –78 °C then raise the temperature to 0 °C for an additional 1h. Add 2M HCl (30 mL, 2.0 equiv) stir for 30 minutes. Separate organic layer and extract aqueous layer three times with Et_2O (3×20 mL). Wash combined organic layer with brine and dry over Na_2SO_4. Concentrate crude mixture to ~30 mL under argon. Add anhydrous $MgSO_4$ (800 mg, 6.6 mol, 0.22 equiv) and neopentyl glycol (3.13 g, 30.0 mmol, 1.0 equiv) as a solution in Et_2O (20 mL). Stir mixture at ambient temperature for 24h. Filter off solids and concentrate *in vacuo* to yield crude product. Purify by flash chromatography (silica, 5→50% Et_2O/Hexanes) to yield a XX (265mg, 1.60 mmol, 5.3 % yield) as a clear oil.

^{1}H NMR (500 MHz, $CDCl_3$) δ 4.55 (d, *J* = 3.2 Hz, 2H), 3.66 (d, *J* = 0.7 Hz, 4H), 1.67 (t, *J* = 3.2 Hz, 3H), 0.97 (d, *J* = 0.7 Hz, 6H).

^{13}C NMR (126 MHz, $CDCl_3$) δ 214.88, 72.65, 69.94, 31.87, 21.95, 15.20.

^{11}B NMR (128 MHz, $CDCl_3$) δ 26.97.

FTIR (AT-IR) 2961.08, 2888.58, 1932.18, 1476.92, 1414.06, 1377.28, 1368.34, 1339.46, 1304.51, 1252.74, 1221.90, 1204.31, 1130.36, 812.52, 703.27, 681.75, 624.42 cm^{-1}

3.4.3. Synthesis of Electrophile Substrates

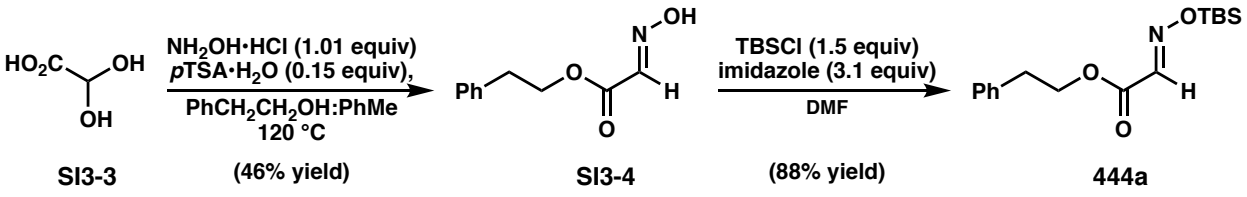

Combine glyoxylic acid monohydrate (3.00g, 32.59mmol, 1.0 equiv), hydroxylamine•HCl (2.29g, 32.92, 1.01 equiv), *p*-toluenesulfonic acid monohydrate(930.2mg, 4.89mmol 0.15 equiv) and phenethyl alcohol (11.7mL, 11.9g, 3.0 equiv) in toluene (10 mL). Heat mixture with a Dean-Stark

trap to 50 °C and ramp to 120 °C over 80 min. Reflux overnight. Cool to ambient temperature, add EtOAc (100 mL). Wash organics layers with $NaHCO_{3(aq)}$ (100mL), then NH_4Cl (20 mL), then pH=7 buffer (20 mL) and finally brine (40mL). Dry organics over Na_2SO_4. Purify by flash chromatography (silica, 300 g, 20→40% EtOAc/Hexanes) to yield S**1** (2.92g, 15.1 mmol, 46% yield) as a pale liquid.

^{1}H NMR (400 MHz, $CDCl_3$) δ 10.88 (s, 1H), 7.55 (d, *J* = 1.7 Hz, 1H), 7.35 – 7.27 (m, 2H), 7.27 – 7.17 (m, 3H), 4.45 (td, *J* = 7.2, 1.6 Hz, 2H), 3.06 – 2.94 (m, 2H).

^{13}C NMR (101 MHz, $CDCl_3$) δ 162.44, 141.47, 137.10, 128.87, 128.59, 126.75, 66.15, 34.77.

FTIR (AT-IR) 3322.11, 3028.17, 2359.63, 1721.19, 1622.35, 1497.30, 1453.99, 1306.73, 1257.07, 1193.59, 1009.49, 917.54, 744.20, 697.56, 667.93 cm^{-1}

HRMS (TOF, ES+) calc'd for $C_{10}H_{11}NO_3$ $[M+H]^+$ 194.0812, found 194.0819(ppm=-3.76)

Take up S**1** (566.5 mg, 2.93 mmol, 1.0 equiv) in DMF (5 mL). Add imidazole (618.2 mg, 9.08 mmol, 1.5 equiv) and TBSCl (663.2 mg, 4.40 mmol, 3.1 equiv) and stir at ambient temperature for 24h. Dilute in 6:1 DI H_2O:brine (26 mL) and extract with Et_2O (19 mL). Wash organic layer with brine (3.5 mL). Dry over Na_2SO_4, filter, and concentrate to yield the crude product. Purify by flash chromatography (silica, 3→5% EtOAc/Hexanes) to yield pure **1a** (795.1 mg, 2.59 mmol, 88% yield)

^{1}H NMR (400 MHz, $CDCl_3$) δ 7.60 (d, *J* = 1.2 Hz, 1H), 7.33 – 7.26 (m, 2H), 7.26 – 7.19 (m, 3H), 4.42 (td, *J* = 6.9, 1.3 Hz, 2H), 2.98 (t, *J* = 6.9 Hz, 2H), 0.97 (d, *J* = 1.7 Hz, 9H), 0.25 (d, *J* = 1.7 Hz, 6H).

^{13}C NMR (101 MHz, $CDCl_3$) δ 162.24, 145.88, 137.57, 129.05, 128.52, 126.67, 65.78, 35.01, 25.89, 18.14, -5.28.

FTIR (AT-IR) 2930.10, 2857.88, 1746.89, 1724.23, 1595.23, 1471.85, 1314.23, 1252.38, 1182.26, 1012.32, 974.59, 834.85, 784.87, 748.45, 697.31 cm^{-1}

HRMS (TOF, ES+) calc'd for $C_{16}H_{25}NO_3Si$ $[M+H]^+$ 308.1676, found 308.1676 (ppm=0.15)

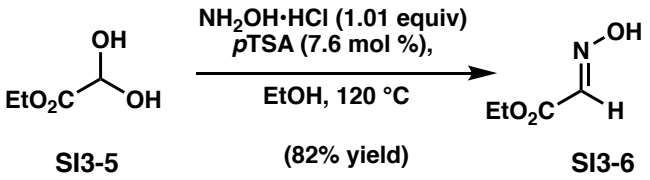

Charge a round bottom flask with glyoxylic acid monohydrate (20.0 g, 217 mmol 1.00 equiv), hydroxylamine hydrochloride (15.3 g, 220 mmol, 1.01 equiv), *p*TSA•H_2O (3.12 g, 16 mmol, 7.6 mol%) and ethanol (260 mL). Fit with a Socklett extractor charged with activated 4Å molecular sieves and a reflux condenser. Heat the mixture at 120°C for 9 hours. Cool reaction to room temperature. Concentrate in vacuo then dilute oil in Et_2O (400 mL) and $NaHCO_{3(sat)}$ (240 mL). Separate organic layer and wash organics with $NH_4Cl_{(sat)}$ (100mL) followed by pH=7 buffer (100 mL). Test aqueous layer for product and re-extract with Et_2O(150 mL), if necessary. Wash combined organics with brine(100 mL). Dry over Na_2SO_4, filter, and concentrate *in vacuo* to give clean **S2** (20.9 g, 174 mmol, 82% yield) as a pale yellow oil. Physical and spectral properties were consistent with literature values.[42]

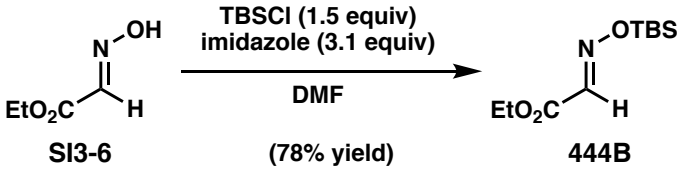

Combine **S2** (31.18g, 266 mmol), imidazole(55.76g, 819 mmol) and TBSCl (61.80g, 410 mmol) in DMF (210 mL). Stir at ambient temperature for 72h. Pour mixture into 6:1 DI:brine (2.1 L). Extract with Et_2O (1.5L). Wash organic layer with brine(300 mL). Dry over Na_2SO_4, filter and

concentrate in vacuo to yield crude product. Purify by flash chromatography (silica, 3.5-4.5% Et_2O/Hexanes) to provide **1b** (47.8 g, 207 mmol, 78% yield) as a clear oil.

^{1}H NMR (400 MHz, $CDCl_3$) δ 7.59 (d, *J* = 1.5 Hz, 1H), 4.27 (qd, *J* = 7.1, 1.4 Hz, 2H), 1.31 (td, *J* = 7.1, 1.5 Hz, 3H), 0.92 (d, *J* = 1.9 Hz, 9H), 0.21 (d, *J* = 1.7 Hz, 6H).

^{13}C NMR (101 MHz, $CDCl_3$) δ 162.41, 146.20, 61.42, 25.91, 18.18, 14.22, -5.23.

FTIR (AT-IR) 2930.90, 2858.64, 2359.72, 1748.16, 1724.8, 1596.93, 1472.39, 1370.20, 1315.32, 1253.03, 1190.11, 1035.38, 968.41, 835.09, 785.05, 690.07, 667.95 cm^{-1}

HRMS (TOF, ES+) calc'd for $C_{20}H_{21}NO_3Si$ $[M+H]^+$ 232.1363, found 232.1365 (ppm=-0.66)

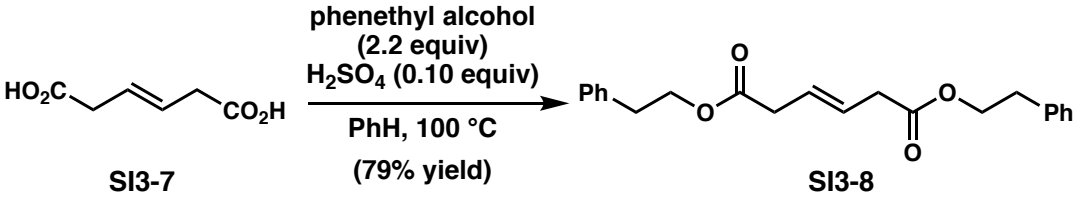

SI3-7 SI3-8

Combine trans-β-hydromuconic acid (1.39g, 9.92 mmol, 1.0 equiv), phenethyl alcohol (2.65g, 2.60 mL, 21.71 mmol, 2.2 equiv) and sulfuric acid (50 μL, 92mg, 0.94 mmol, 0.10 equiv) in benzene (50 mL). Heat to 100 °C with a Dean–Stark trap for 16h. Cool to ambient temperature and dilute with Et_2O and wash with $NaHCO_{3(aq)}$, and then brine. Dry organics over $MgSO_4$, filter, and concentrate *in vacuo* to yield diphenethyl (*E*)-hex-3-enedioate with trace impurities (2.75g, mmol, 79% yield) as a beige solid which was used in the next reaction without any further purification. An analytically pure sample could be obtained by solvation of **S2** in minimal CH_2Cl_2 to partially remove a color impurity. Partial concentration followed by trituration with pentanes provides a white solid.

^{1}H NMR (500 MHz, $CDCl_3$) δ 7.33 – 7.28 (m, 4H), 7.26 – 7.19 (m, 6H), 5.69 – 5.59 (m, 2H), 4.30 (t, *J* = 7.1 Hz, 4H), 3.12 – 3.02 (m, 4H), 2.94 (t, *J* = 7.1 Hz, 4H)

^{13}C NMR (126 MHz, $CDCl_3$) δ 171.56, 137.82, 129.05, 128.62, 126.72, 126.03, 65.30, 37.99, 35.19.

FTIR (AT-IR) 3028.47, 1784.57, 1728.66, 1603.24, 1496.92, 1453.99, 1398.83, 1358.33, 1154.71, 1086.89, 1030.78, 967.39, 921.34, 810.32, 749.84, 698.56 cm^{-1}

HRMS (TOF, ES+) calc'd for $C_{22}H_{24}O_4$ $[M+H]^+$ 353.1747, found 353.1739 (ppm=2.37)

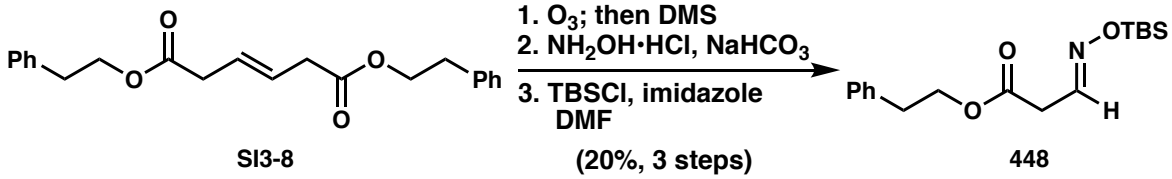

SI3-8 448

Sparge a solution of **S2** (500mg, 1.42 mmol, 0.50 equiv) with O_2 for five minutes. Cool to –78 °C. Sparge with O_3, stirring at –78 °C for five minutes until a persisitent blue color is observed. Sparge with O_2 for 10 minutes until the solution is colorless. Add dimethyl sulfide (1.00 mL, 0.84 g, 13.5 mmol, 4.8 equiv) and sparge with argon for five minutes. Concentrate in vacuo to yield the crude aldehyde as a yellow oil (487 mg) which was immediately take up in CH_2Cl_2 (2 mL) before adding DI H_2O (12 mL) followed by hydroxylamine hydrochloride (193.2mg, 2.78 mmol, 0.98 equiv) and $NaHCO_3$ (276 mg, 3.29, 1.15 equiv). Stir vigorously at ambient temperature 24h. Separate organic layer and wash aqueous with additional CH_2Cl_2 (5 mL). Wash combined organics with $NaHCO_{3(sat)}$ (2 mL) followed by brine (5 mL). Dry organics over Na_2SO_4, filter and concentrate *in vacuo* to yield crude oxime (386 mg) as a mixture of E/Z isomers. Dissolve the crude oxime in DMF (2.5 mL). Add imidazole (393 mg, 5.77 mmol, 2.0 equiv) and TBSCl (420 mg, 2.79 mmol, 0.98 equiv). Stir at ambient temperature 16h. Add Et_2O (40 mL) and 6:1 DI H_2O/brine (30 mL) and separate organics. Extract aqueous layer with Et_2O (5 mL). Wash combine organics with brine. Dry organics over Na_2SO_4, filter and concentrate *in vacuo* to yield crude

siloxime (496 mg) as a mixture of E/Z isomers. Purify by flash chromatography (4-10% Et_2O/Hexanes) to yield **1d** (180 mg, 0.560 mmol, 20% yield over three steps).

^{1}H NMR (500 MHz, $CDCl_3$; major isomer designated by *, minor isomer designated by §) δ 7.58 (t, *J* = 6.2 Hz, 1H§), 7.35 – 7.28 (m, 2H*, 2H§), 7.25 – 7.19 (m, 3H*, 3H§), 7.14 (t, *J* = 4.8 Hz, 1H*), 4.34 (td, *J* = 7.1, 4.1 Hz, 2H*, 2H§), 3.42 (d, *J* = 4.8 Hz, 2H*), 3.25 (d, *J* = 6.2 Hz, 2H§), 2.96 (td, *J* = 7.0, 2.6 Hz, 2H*, 2H§), 0.94 (s, 9H§), 0.93 (s, 9H*), 0.18 (s, 6H*), 0.17 (s, 9H§).

^{13}C NMR (126 MHz, $CDCl_3$) δ 169.51, 169.40, 148.56, 147.84, 137.61, 137.59, 128.98, 128.67, 126.78, 65.71, 65.62, 35.42, 35.12, 31.46, 26.14, 26.06, 18.19, -5.18, -5.20.

FTIR (AT-IR) 677.62, 698.10, 748.18, 782.57, 834.98, 916.93, 1165.67, 1250.38, 1340.16, 1389.87, 1471.86, 1738.81, 2856.77, 2928.98 cm^{-1}

HRMS (TOF, ES+) calc'd for $C_{17}H_{27}NO_3Si$ $[M+H]^+$ 322.1833, found 322.1839 (ppm=1.87)

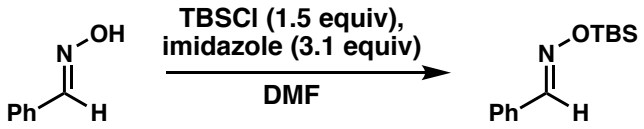

SI3-10 **(19% yield)** **447**

Dissolve phenyl aldoxime[43] (1.21g, 10.00 mmol, 1.00 equiv), imidazole (2.11g, 31.00 mmol, 3.10 equiv), and TBSCl (2.26g, 15.00 mmol, 1.50 equiv) and in DMF (10 mL) . Stir at ambient temperature for 16h. Dilute with Et_2O, wash with organics with DI H_2O:brine (6:1). Dry over Na_2SO_4, filter and concentrate *in vacuo* to yield crude product. Purification by flash chromatography (silica, 0→100% Et_2O/Hexanes) to yield pure **1e** (438 mg, 19% yield) as a clear oil. Physical and spectral properties were consistent with literature values.[44]

Note: Synthesis of **1c** and known imines electrophiles (**12c-f**) were made by literature procedures and their physical and spectral properties were consistent with literature values.[45,46,41]

3.4.4. Copper Catalyzed Reactions and Product Characterization

General procedure A for the racemic copper–catalyzed alkylation of oxime ester

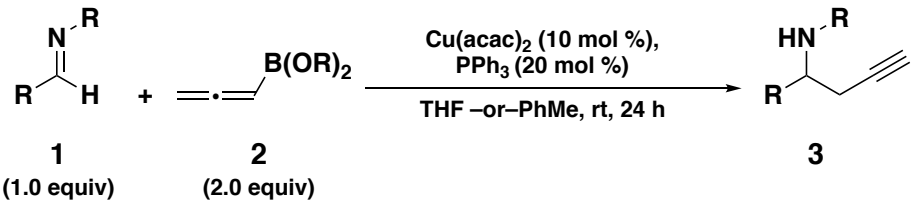

Stir $Cu(acac)_2$ (5.7mg, 0.216 mmol, 0.10 equiv) and PPh_3 (0.12 equiv) in THF or PhMe (1.08 mL, 0.2 M) for 10 minutes at ambient temperature. Add **2c** (65.7 mg, 0.432mmol, 2.0 equiv) followed by electrophile (0.22 mmol, 1.0 equiv). Seal under N_2 and continue to stir at ambient temperature for 24h. Dilute with EtOAc (1 mL) and diethanolamine (0.2 mL) and stir 15 minutes. Dilute with DI H_2O and extract with EtOAc (3x2 mL). Dry organic layer over Na_2SO_4, filter, and concentrate to yield crude product. Purify crude mixture by flash chromatography.

General Procedure B for the asymmetric copper–catalyzed alkylation

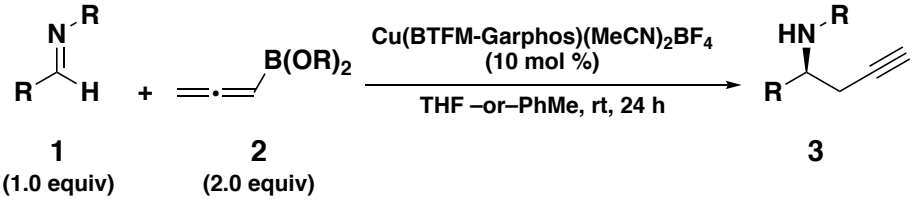

In a N_2-filled glovebox, dilute Cu(*S*-BTFMGarphos)$(MeCN)_2BF_4$ (28 mg, 0.020 mmol, 0.10 equiv) with THF –or– PhMe (0.5 mL). Add electrophile (0.20 mmol) followed by **2c** (60.8 mg, 0.40 mmol, 2.0 equiv, 2 equiv) directly to the solution. Seal solution under N_2 and stir at ambient temperature for 16h. Dilute with EtOAc (2 mL) and diethanolamine (80 μL) and stir 15 minutes. Dilute with DI H_2O (3.0 mL) and extract with EtOAc (3×4.0 mL). Dry organics over

Na_2SO_4, filter and concentrate *in vacuo* to yield crude product. ^{1}H NMR yields with dimethyl terephthalate (10 mol%) as a standard. Purification by flash chromatography.

Separatory Conditions and Characterization of Products

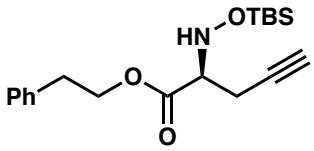

445b: Prepared from **444a** (61.5 mg, 0.200 mmol) using General Procedure **B** in THF**.** Yield by ^{1}H NMR with internal standard (10 mol% dimethyl terephalate) Purification by flash chromatography (silica, 2.5%Et_2O/ 10%CH_2Cl_2/10%PhMe/Hexanes) to yield **444a** (40.9 mg, 0.118 mmol, 59% yield) as a clear oil. The enantiomeric excess was determined to be 96% by chiral SFC analysis (AD, 2.5 mL/min, 1% IPA in CO_2, λ = 254 nm): t_R(minor) = 6.148 min, t_R(major) =5.116 min.

^{1}H NMR (400 MHz, $CDCl_3$): δ 7.33 – 7.28 (m, 2H), 7.24 (ddt, *J* = 7.6, 1.2, 0.6 Hz, 4H), 4.47 – 4.30 (m, 3H), 3.63 (t, *J* = 6.4 Hz, 1H), 2.98 (t, *J* = 7.1 Hz, 3H), 2.53 (tdd, *J* = 16.8, 6.4, 2.6 Hz, 2H), 2.04 – 1.93 (m, 1H), 0.89 (d, *J* = 0.5 Hz, 11H), 0.11 (d, *J* = 3.2 Hz, 6H).

^{13}C NMR (101 MHz, $CDCl_3$) δ 171.71, 137.73, 129.01, 128.64, 126.73, 79.34, 70.98, 65.68, 63.94, 35.19, 26.28, 19.41, 18.07, -5.38, -5.43.

FTIR (AT-IR) 3309.43, 2928.68, 2856.23, 1739.08, 1497.68, 1471.5, 1389, 1345.74, 1279.25, 1248.5, 1178.39, 1055.21, 974.31, 900.14, 833.73, 780.66, 747.8, 698.5, 644.51 cm^{-1}

HRMS (TOF, ES+) calc'd for $C_{19}H_{29}NO_3Si$ $[M+H]^+$ 348.1989, found 348.1998 (ppm=-2.45)

$[\alpha]_D^{23}$ –16.3 (*c* = 1.0, $CHCl_3$).

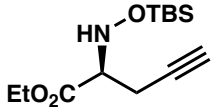

445b: Prepared from **444b** (1.00 g, 4.322 mmol, 1.0 equiv), **424b** (295 mg, 1.944 mmol, 2.0 equiv) and freshly prepared Cu(*S*-BTFMGarphos)$(MeCN)_2BF_4$ (0.432 mmol, 0.10 equiv) Note: Stir $Cu(MeCN)_4BF_4$ (135.9 mg,

0.432 mmol, 0.10 equiv) and *S*-BTFMGarphos (512.6 mg, 0.432 mmol, 0.10 equiv) in MeCN for 10 minutes before concentrating *in vacuo* to a yield a white powder. Using an appropriately scaled General Procedure **2** in THF (21.6 mL)**.** Purification by flash chromatography (silica, 2.5%Et_2O/10%CH_2Cl_2/10%PhMe/Hexanes) provided both product (1.01 g, 3.76 mmol, 87% yield) and recovered ligand (450 mg, 88% recovery) Note: Any product fractions contaminated with ligand were concentrated and triturated with cold pentanes, before an azeotrope with PhMe. The enantiomeric excess was determined after benzoylation to be 95% by chiral SFC analysis.

^{1}H NMR (400 MHz, $CDCl_3$) δ 5.58 (s, 1H), 4.22 (q, *J* = 7.1 Hz, 2H), 3.60 (t, *J* = 6.4 Hz, 1H), 2.55 (dt, *J* = 6.4, 3.0 Hz, 2H), 2.00 (t, *J* = 2.7 Hz, 1H), 1.27 (td, *J* = 7.1, 0.7 Hz, 3H), 0.86 (d, *J* = 1.0 Hz, 9H), 0.08 (s, 6H).

^{13}C NMR (101 MHz, $CDCl_3$) δ 171.77, 79.37, 70.86, 63.89, 61.25, 26.21, 19.37, 18.01, 14.34, -5.43, -5.49.

FTIR (AT-IR) 3313.49, 2929.08, 2856.83, 2361.12, 2340.34, 1738.61, 1472.12, 1370.05, 1342.99, 1248.41, 1215.41, 1186.14, 1054.34, 904.00, 834.61, 780.54, 667.96 cm^{-1}

HRMS (TOF, ES+) calc'd for $C_{13}H_{25}NO_3Si$ $[M+H]^+$ 272.1676, found 272.1674 (ppm=0.91)

$[\alpha]_D^{23}$ –18.0° (*c* = 1.0, $CHCl_3$).

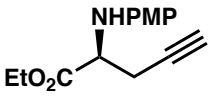

SI3-9: Prepared from **449** (20.2 mg, 0.100 mmol) using a modified General Procedure **2** in THF at –78 °C for 36h using a 5mL Schlenk tube. Purification by flash chromatography (silica, 15%Et_2O/10%CH_2Cl_2 /10%PhMe/Hexanes) to yield **SI3-9** (11.3 mg, 0.046 mmol, 46% yield) as a clear oil. The enantiomeric excess was determined to be 93% by chiral SFC analysis (AD-H, 2.5 mL/min, 8% IPA in CO_2, λ = 254 nm): t_R(minor) = 7.850 min, t_R(major) = 7.138 min.

^{1}H NMR (500 MHz, $CDCl_3$) δ 6.82 – 6.70 (m, 2H), 6.71 – 6.56 (m, 2H), 4.28 – 4.18 (m, 2H), 4.16 (t, J = 5.5 Hz, 1H), 3.74 (s, 3H), 2.75 (dd, J = 5.4, 2.7 Hz, 2H), 2.08 (t, J = 2.6 Hz, 1H), 1.27 (t, J = 7.1 Hz, 3H).

^{13}C NMR (126 MHz, $CDCl_3$) δ 172.26, 153.20, 140.21, 115.85, 115.00, 78.99, 71.73, 61.64, 56.46, 55.82, 23.07, 14.38.

FTIR (AT-IR) 2878.46, 2359.83, 1734.61, 1512.59, 1214.47, 1035.14, 750.2, 667.76 cm^{-1}

HRMS (TOF, ES+) calc'd for $C_{14}H_{17}NO_3$ $[M+H]^+$ 248.1281, found 248.1280 (ppm=0.48)

$[\alpha]_D^{23}$ +18.7° (*c* = 1.0, $CHCl_3$).

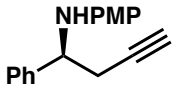

SI3-10: Prepared from **450** (21.2 mg, 0.100 mmol) using General Procedure **2** in THF**.** Yield determined to be 38% by NMR (10 mol% dimethyl terephthalate). Physical and spectral properties were consistent with literature values.[47] The enantiomeric excess was determined to be 56% by chiral SFC analysis (AS-H, 2.5 mL/min, 4% IPA in CO_2, λ = 210 nm): t_R(minor) = 7.777 min, t_R(major) = 8.391 min.

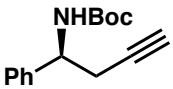

SI3-11: Prepared from **450** (41.0 mg, 0.200 mmol) using General Procedure **2** in PhMe**.** Purification by flash chromatography (silica, 10%Et_2O/10%CH_2Cl_2/ 10%PhMe/ Hexanes) to yield **SI3-11** (31.2 mg, 0.127 mmol, 64% yield) as a white solid. The enantiomeric excess was determined to be 85% by chiral SFC analysis (IC, 2.5 mL/min, 3% IPA in CO_2, λ = 210 nm): t_R(minor) = 8.278 min, t_R(major) = 6.991 min.

^{1}H NMR (400 MHz, $CDCl_3$) δ 7.39 – 7.23 (m, 5H), 5.16 (s, 1H), 5.00 – 4.50 (m, 1H), 2.85 – 2.55 (m, 2H), 2.00 (t, *J* = 2.6 Hz, 1H), 1.43 (s, 9H).

^{13}C NMR (101 MHz, $CDCl_3$) δ 155.18, 141.10, 128.62, 127.69, 126.44, 80.07, 79.89, 71.50, 52.65, 28.47, 26.53.

FTIR (AT-IR): 3298.44, 2977.06, 1693.35, 1495.09, 1454.71, 1391.08, 1365.46, 1246.52, 1162.62, 1078.25, 1050.37, 1017.56, 951.85, 859.79, 753.00, 698.10, 632.69 cm^{-1}

HRMS (TOF, ES+) calc'd for $C_{15}H_{19}NO_2$ $[M+H]^+$ 246.1489, found 246.1486 (ppm=1.04)

$[\alpha]_D^{23}$ –33.4° (*c* = 1.0, $CHCl_3$)

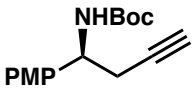

SI3-12: Prepared from **12c** (47.1 mg, 0.200 mmol) using General Procedure **2** in PhMe**.** Purification by flash chromatography (silica, 7→15%Et_2O/10% CH_2Cl_2/10%PhMe/ Hexanes) to yield **13c** (39.5 mg, 0.143 mmol, 72% yield) as a white solid. The enantiomeric excess was determined to be 73% by chiral SFC analysis (AD-H, 2.5 mL/min, 2% IPA in CO_2, λ = 210 nm): t_R(minor) = 7.440 min, t_R(major) = 7.012 min.

^{1}H NMR (400 MHz, $CDCl_3$) δ 7.32 – 7.20 (m, 2H), 6.94 – 6.82 (m, 2H), 5.11 (s, 1H), 4.83 (s, 1H), 3.79 (s, 3H), 2.70 (pd, *J* = 14.7, 13.2, 8.6 Hz, 2H), 2.00 (t, *J* = 2.6 Hz, 1H), 1.43 (s, 9H).

^{13}C NMR (101 MHz, $CDCl_3$) δ 159.05, 155.15, 133.27, 127.60, 113.96, 80.29, 79.80, 71.38, 55.34, 52.15, 28.46, 26.50.

FTIR (AT-IR) 3294.27, 2976.11, 2930.51, 1695.09, 1613.30, 1512.19, 1391.26, 1365.93, 1296.78, 1244.83, 1163.94, 1110.88, 1033.71, 862.18, 831.44, 779.23, 640.34 cm^{-1}

HRMS (TOF, ES+) calc'd for $C_{16}H_{21}NO_3$ $[M+H]^+$ 276.1594, found 276.1592 (ppm=0.80)

$[\alpha]_D^{23}$ –37.7 (*c* = 1.0, $CHCl_3$).

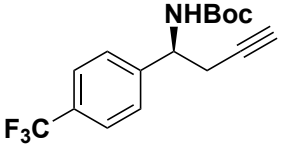

SI3-13: Prepared from **12X** (54.6mg, 0.200 mmol) using General Procedure **2** in PhMe**.** Purification by flash chromatography (silica,

10%Et_2O/ 10%CH_2Cl_2/10%PhMe/ Hexanes) to yield **13X** (41.0mg mg, 0.130 mmol, 65% yield) as a white solid. The enantiomeric excess was determined by chiral SFC analysis to be 71% (AD-H, 2.5 mL/min, 2% IPA in CO_2, λ = 210 nm): t_R(minor) = 5.322 min, t_R(major) = 6.650 min.

^{1}H NMR (400 MHz, $CDCl_3$) δ 7.60 (d, J = 8.1 Hz, 2H), 7.46 (d, J = 8.1 Hz, 2H), 5.40 – 5.09 (m, 1H), 5.08 – 4.79 (m, 1H), 2.86 – 2.53 (m, 2H), 2.04 (t, J = 2.6 Hz, 1H), 1.43 (s, 9H).

^{13}C NMR (101 MHz, $CDCl_3$) δ 155.08, 145.26, 129.94 (q, *J* = 32.4 Hz), 126.81, 125.62 (q, *J* = 3.7 Hz), 122.87, 80.32, 79.24, 72.21, 52.29, 28.45, 26.45.

FTIR (AT-IR) 3312.68, 2979.57, 1694.52, 1620.25, 1498.22, 1422.19, 1367.11, 1323.46, 1279.78, 1248.84, 1160.67, 1122.33, 1067.87, 1017.04, 840.57, 643.93 cm^{-1}

HRMS (TOF, ES+) calc'd for $C_{16}H_{18}F_3NO_2$ $[M+H]^+$ 314.1362, found 314.1370 (ppm=–2.42)

$[\alpha]_D^{23}$ –20.5° (*c* = 1.0, $CHCl_3$).

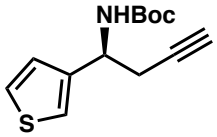

SI3-14: Prepared from **12e** (42.3 mg, 0.200 mmol) using General Procedure **2** in PhMe**.** Purification by flash chromatography (silica, 10%Et_2O/10%CH_2Cl_2/ 10%PhMe/ Hexanes) to yield **13e** (29.8mg mg, 0.119 mmol, 59% yield) as a white solid. The enantiomeric excess was determined by chiral SFC analysis to be 76% (OD-H, 2.5 mL/min, 1% IPA in CO_2, λ = 210 nm): t_R(minor) = 11.423 min, t_R(major) = 10.681 min.

^{1}H NMR (400 MHz, $CDCl_3$) δ 7.33 (dd, *J* = 5.0, 3.0 Hz, 1H), 7.27 (dd, *J* = 2.8, 1.2 Hz, 1H), 7.12 (dd, *J* = 5.0, 1.4 Hz, 1H), 5.11 (s, 1H), 5.03 (s, 1H), 2.78 (qdd, *J* = 16.8, 5.5, 2.7 Hz, 2H), 2.06 (t, *J* = 2.6 Hz, 1H), 1.49 (s, 9H).

^{13}C NMR (101 MHz, $CDCl_3$) δ 155.14, 142.19, 126.42, 126.20, 121.46, 80.28, 79.94, 71.50, 48.76, 28.49, 25.92.

FTIR (AT-IR) 3299.32, 2977.13, 2360.00, 1694.07, 1496.67, 1391.64, 1365.96, 1328.22, 1246.99, 1162.16, 1051.38, 1019.27, 849.62, 781.82, 636.53 cm^{-1}

HRMS (TOF, ES+) calc'd for $C_{13}H_{17}NO_2S$ $[M+H]^+$ 252.1053, found 252.1045 (ppm=3.08)

$[\alpha]_D^{23}$ –32.0 (*c* = 1.0, $CHCl_3$).

S3C2-3

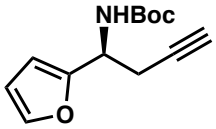

SI3-15: Prepared from **12f** (39.0 mg, 0.200 mmol) using General Procedure **2** in THF. Purification by flash chromatography (silica, 5% Et_2O/10% CH_2Cl_2/10% PhMe/Hexanes) to yield **13f** (28.4 mg, 60% yield) as a clear oil. The enantiomeric excess was determined to be 60% by chiral SFC analysis (AD-H, 2.5 mL/min, 2% IPA in CO_2, λ = 210 nm): t_R(minor) = 5.895 min, t_R(major) = 6.192 min

^{1}H NMR (400 MHz, $CDCl_3$) δ 7.36 (dd, *J* = 1.8, 0.9 Hz, 1H), 6.32 (dd, *J* = 3.3, 1.8 Hz, 1H), 6.27 (dt, *J* = 3.3, 0.9 Hz, 1H), 5.07 (s, 1H), 4.98 (s, 1H), 2.75 (dt, *J* = 5.5, 1.8 Hz, 2H), 1.99 (t, *J* = 2.6 Hz, 1H), 1.46 (s, 9H).

^{13}C NMR (101 MHz, $CDCl_3$) δ 155.05, 153.40, 142.17, 110.36, 106.64, 80.12, 79.81, 71.14, 47.42, 28.48, 24.44.

FTIR (AT-IR) 3299.51, 2977.82, 2930.12, 1698.08, 1498.78, 1456.01, 1428.43, 1391.91, 1366.51, 1336.32, 1247.83, 1162.69, 1076.41, 1050.52, 1009.24, 941.43, 910.82, 884.51, 865.88, 811.90, 736.07, 642.95, 597.65 cm^{-1}

HRMS (TOF, ES+) calc'd for $C_{13}H_{17}NO_3$ $[M+H]^+$ 236.1281, found 236.1276 (ppm=-2.20)

$[\alpha]_D^{23}$ –22.6° (*c* = 1.0, $CHCl_3$).

Racemic Copper catalyzed allylation of oxime ether

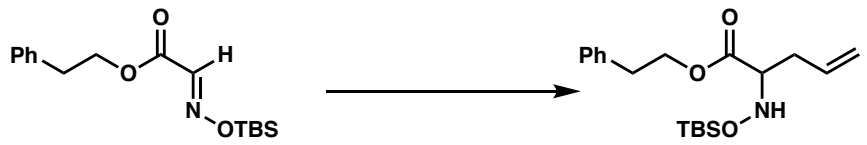

To a solution of **444a** (15.4mg, 0.20 mmol, 1.0 equiv) in THF (0.15 mL) add **2a** (16.3, 0.100 mmol, 2.0 equiv) followed by [Cu(*S*-BTFMGarphos)$(MeCN)_2$]BF_4 (7.1mg, 0.0050 mmol, 0.10 equiv) or with Cu $(acac)_2$ (0.0050 mmol, 0.10 equiv)and PPh_3 (0.20 equiv). Rinse down catalyst with additional THF (0.10 mL). Stir racemic alkylation for 5h, asymmetric alkylation for 12h, at ambient temperature. Add diethanolamine (20 μL) as a solution in EtOAc (0.5 mL). Stir 10 minutes at ambient temperature. Add DI H_2O (1.0 mL). Extract with crude mixture with EtOAc four times. Dry over Na_2SO_4, filter and concentrate *in vacuo* to yield crude product. Purify by flash chromatography (silica, 2.5%Et_2O/10%CH_2Cl_2/10%PhMe/Hexanes) to yield **457** as a clear oil (60.6 mg, 0.186 mmol, 87% yield). Enantiomers were separated by chiral SFC analysis (AD-H, 2.5 mL/min, 2% IPA in CO2, λ = 210 nm): t_R(minor) = 2.724 min, t_R(major) = 4.528 min

^{1}H NMR (500 MHz, $CDCl_3$) δ 7.34 – 7.29 (m, 2H), 7.26 – 7.21 (m, 3H), 5.70 (ddt, J = 17.1, 10.1, 7.1 Hz, 1H), 5.47 (d, J = 8.1 Hz, 1H), 5.09 – 5.00 (m, 2H), 4.38 (t, J = 7.0 Hz, 2H), 3.53 (q, J = 7.6 Hz, 1H), 2.97 (t, J = 7.0 Hz, 2H), 2.32 – 2.22 (m, 2H), 0.90 (s, 9H), 0.10 (d, J = 4.3 Hz, 6H).

^{13}C NMR (126 MHz, $CDCl_3$) δ 173.64, 137.82, 133.16, 129.02, 128.60, 126.69, 118.01, 65.61, 65.31, 35.25, 33.97, 26.35, 18.10, -5.34, -5.39.

FTIR (AT-IR) 2955.32. 2928.25, 2855.86, 1738.49, 1641.92, 1497.53, 1471.50, 1462.13, 1388.74, 1344.25, 1246.95, 1181.89, 1051.22, 992.86, 917.49, 833.26, 779.87, 747.64, 698.04, 667.31 cm^{-1}

HRMS (TOF, ES+) calc'd for $C_{19}H_{31}NO_3Si$ $[M+H]^+$ 349.2146, found 349. 2147 (ppm=-0.29)

Copper catalyzed asymmetric alkylation with a substituted allene

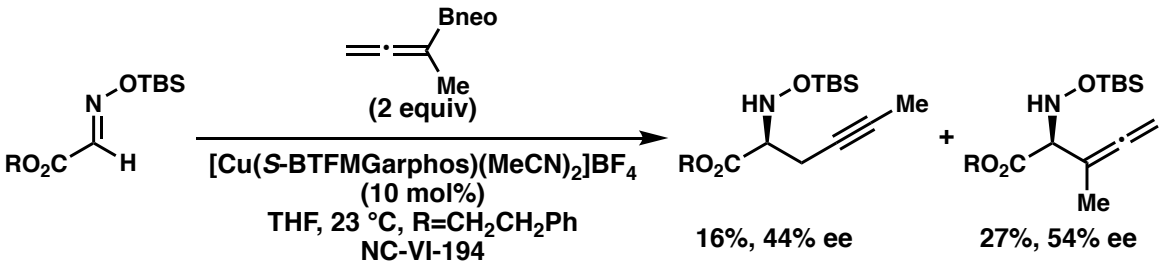

Follow general Procedure A with substituted **458** on a 0.100 mmol scale. To a solution of XX (15.4mg, 0.050 mmol, 1.0 equiv) in THF (0.15 mL) add boronateXX (16.3, 0.100 mmol, 2.0 equiv) followed by [Cu(*S*-BTFMGarphos)(MeCN)$_2$]BF$_4$ (7.1mg, 0.0050 mmol, 0.10 equiv) or with Cu (acac)$_2$ and PPh$_3$. Rinse down catalyst with an additional THF (0.10 mL). Stir racemic alkylation 5h, asymmetric 12h. Dilute with 20 μL diethanolamine in 0.5 mL EtOAc. Stir 10 minutes at ambient temperature. Add 1 mL H_2O. Extract with EtOAc four times. Dry over Na_2SO_4, filter and concentrate *in vacuo* to yield crude product. Yields by ^{1}H NMR with an internal standard (dimethyl terephthalate, 10 mol %): *S*-BTFM-Garphos: 16% **7a**, 27% **7b**; PPh$_3$: 54% **7a**, 31% **7b**

Purification by flash chromatography gave **7a** and **7b** as a mixture of isomers (12.2mg, 34% yield total). Preparatory TLC (7.5% Et$_2$O/Hexanes) provides clean samples of **7a** and **7b** for characterization.

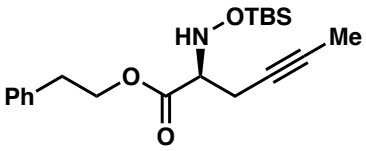

459a: The enantiomeric excess was determined to be 44% by chiral SFC analysis (AD-H (Column 2, 2.5 mL/min, 1% IPA in CO_2, λ = 254 nm): t_R(minor) = 6.780 min, t_R(major) = 5.451 min.

^{1}H NMR (400 MHz, $CDCl_3$) δ 7.34 – 7.28 (m, 2H), 7.25 – 7.20 (m, 3H), 5.57 (d, J = 9.7 Hz, 1H), 4.39 (td, J = 7.1, 2.1 Hz, 2H), 3.58 (q, J = 7.8, 7.3 Hz, 1H), 2.97 (t, J = 7.1 Hz, 2H), 2.54 – 2.38 (m, 2H), 1.74 (t, J = 2.6 Hz, 3H), 0.89 (s, 9H), 0.10 (s, 6H).

^{13}C NMR (101 MHz, $CDCl_3$) δ 172.28, 137.83, 129.03, 128.65, 126.73, 78.52, 73.86, 65.54, 64.50, 35.27, 26.33, 19.85, 18.12, 3.66, -5.34, -5.41.

FTIR (AT-IR) 2954.61, 2926.83, 2855.19, 2359.46, 2340.28, 1739.39, 1471.67, 1455.85, 1387.70, 1360.88, 1275.45, 1248.56, 1176.62, 1052.00, 1008.32, 936.64, 835.23, 780.98, 764.44, 749.28, 698.52, 667.93 cm^{-1}

HRMS (TOF, ES+) calc'd for $C_{20}H_{31}NO_3Si$ $[M+H]^+$ 362.2146, found 362.2147 (ppm=-0.28)

$[\alpha]_D^{23}$: –3.82° (*c* = 0.10, $CHCl_3$).

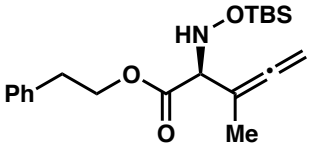

459b: The enantiomeric excess was determined to be 44% by chiral SFC analysis (AD-H(C2), 2.5 mL/min, 1% IPA in CO_2, λ = 254 nm): t_R(minor) = 4.884 min, t_R(major) = 3.733 min.

^{1}H NMR (400 MHz, $CDCl_3$) δ 7.33 – 7.27 (m, 2H), 7.25 – 7.20 (m, 3H), 5.56 (d, J = 12.0 Hz, 1H), 4.77 – 4.62 (m, 2H), 4.38 (td, J = 7.1, 3.3 Hz, 2H), 3.87 (dt, J = 11.9, 2.3 Hz, 1H), 2.97 (td, J = 7.0, 2.0 Hz, 2H), 1.73 (td, J = 3.2, 0.4 Hz, 3H), 0.89 (s, 9H), 0.10 (d, J = 7.1 Hz, 6H).

^{13}C NMR (101 MHz, CDCl3) δ 206.62, 171.80, 137.88, 129.06, 128.62, 126.70, 94.32, 68.39, 65.60, 35.27, 26.39, 18.16, 17.08, -5.32, -5.33.

FTIR (AT-IR) 2954.34, 2927.61, 2855.65, 2359.52, 2340.26, 1957.65, 1742.48, 1497.43, 1471.54, 1461.90, 1361.23, 1329.87, 1275.49, 1247.46, 1189.46, 1047.01, 999.42, 832.06, 780.37, 764.60, 749.17, 698.20, 667.89 cm^{-1}

HRMS (TOF, ES+) calc'd for $C_{20}H_{31}NO_3Si$ $[M+H]^+$ 362.2146, found 362.2146 (ppm=-0.01)

$[\alpha]_D^{23}$: +1.345° (*c* = 0.11, $CHCl_3$).

4. Synthesis of enantioenriched derivatives

Formation of N-acetylpropargyl glycine by decarboxylative coupling

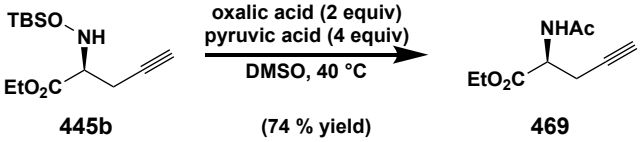

445b (74 % yield) **469**

To a solution of 3a (27.1 mg, 0.100 mmol, 1.0 equiv) in wet DMSO (1.0 mL) add oxalic acid (mg, 2.0 equiv) and pyruvic acid (mg, 4.0 equiv). Seal mixture under air and stir at 40 °C for 18 hours. Cool to ambient temperature and dilute in pH=7 buffer (10 mL). Extract crude mixture with three times with EtOAc and twice with 10% i-PrOH/CH_2Cl_2. Dry organic layer over Na_2SO_4, filter and concentrate to yield crude product. Purification by flash chromatography (silica, 20→50% EtOAc/Hexanes) yields 9 (13.6mg, 0.741 mmol, 74% yield) as colorless crystals.

^{1}H NMR (400 MHz, $CDCl_3$) δ 6.34 (d, *J* = 7.6 Hz, 1H), 4.72 (dt, *J* = 7.8, 4.6 Hz, 1H), 4.34 – 4.17 (m, 2H), 2.83 – 2.71 (m, 2H), 2.06 (s, 3H), 2.02 (t, *J* = 2.6 Hz, 1H), 1.29 (t, *J* = 7.1 Hz, 3H).

^{13}C NMR (101 MHz, $CDCl_3$) δ 170.51, 169.97, 78.60, 71.65, 62.13, 50.73, 23.29, 22.63, 14.28.

FTIR (AT-IR) 3309.21, 3286.98, 1727.34, 1645.05, 1544.92, 1422.68, 1369.94, 1345.49, 1278.11, 1228.63, 1192.86, 1133.72, 1055.73, 1026.11, 943.06, 911.25, 857.89, 703.64, 655.55, 598.75 cm^{-1}

HRMS (TOF, ES+) calc'd for $C_9H_{13}NO_3$ $[M+H]^+$ 184.0968, found 184.0966 (ppm=-1.09)

$[\alpha]_D^{23}$ +97.5° (*c* = 1.0, $CHCl_3$).

Copper-catalyzed "Click" chemistry with *N*-siloxy amine

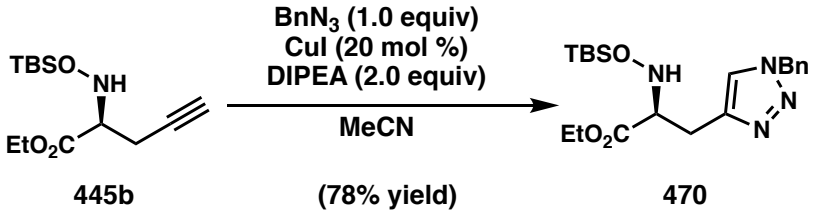

Stir CuI (38.1 mg, 0.020 mmol, 0.20 equiv) and DIPEA (0.300 mmol, 3.0 equiv) in MeCN (1.0 mL) for five minutes. Add 1b (27.1 mg, 0.100 mmol, 1.0 equiv) followed by benzyl azide (13.8 mg, 14.5 mL, 0.100 mmol, 1.0 equiv). Stir at ambient temperature for 2h30m. Dilute in pH=7 buffer (3.5 mL) and extract crude mixture four times EtOAc (4×5mL) taking care to allow time for the emulsion to clear. Dry combined organic over Na_2SO_4, filter through celite and concentrate to yield the crude product. Purification by flash chromatography (30→40% EtOAc/Hexanes) provides 11 (31.8 mg, 0.078 mmol, 78% yield) as a pale-yellow oil.

^{1}H NMR (400 MHz, $CDCl_3$) δ 7.37 – 7.29 (m, 3H), 7.25 – 7.18 (m, 2H), 5.57 (s, 1H), 5.45 (d, *J* = 2.9 Hz, 2H), 4.19 – 4.01 (m, 2H), 3.72 (d, *J* = 7.1 Hz, 1H), 3.01 (dd, *J* = 15.0, 6.2 Hz, 1H), 2.88 (dd, *J* = 15.0, 7.8 Hz, 1H), 1.15 (t, *J* = 7.1 Hz, 3H), 0.80 (s, 9H), -0.06 (d, *J* = 6.5 Hz, 6H).

^{13}C NMR (101 MHz, $CDCl_3$) δ 173.28, 144.06, 134.81, 129.21, 128.83, 128.20, 122.12, 65.26, 61.06, 54.22, 26.21, 26.08, 18.00, 14.28, -5.41, -5.46.

FTIR (AT-IR) 2928.52, 2855.45, 1734.08, 1461.97, 1361.75, 1335.81, 1247.76, 1216.08, 1184.28, 1122.52, 1047.32, 939.38, 901.01, 833.97, 780.04, 721.51, 697.84, 666.92 cm^{-1}

HRMS (TOF, ES+) calc'd for $C_{20}H_{32}N_4O_3Si$ $[M+H]^+$ 405.2316, found 405.2318 (ppm=-0.39)

$[\alpha]_D^{23}$ –12.5° (*c* = 1.0, $CHCl_3$).

Acylation of enantioenriched alkyne

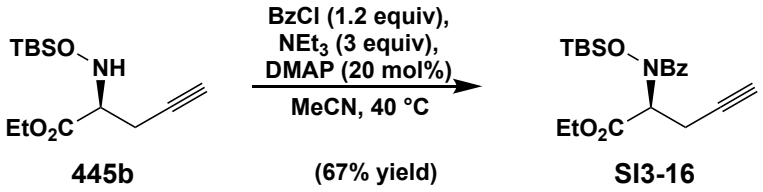

To a solution of **445b** (534 mg, 1.97 mmol, 1.0 equiv) in MeCN (2.0 mL) add DIPEA (0.68 mL, 508 mg, 3.93 mmol, 2 equiv) and benzoyl chloride (0.40 mL, 484mg, 3.44 mmol, 1.75 equiv) at ambient temperature. Heat mixture to 40 °C stirring vigorously 3h. Dilute in Et_2O (25 mL) and wash organics with 2x with pH=7 phosphate buffer (20 mL), then brine (20 mL). Dry organic layer with Na_2SO_4. Filter and concentrate. Take up residue with in pentanes and cool solution to –20 °C and filter rapidly through celite. Concentrate crude material and purify on florisil (20% Et_2O/Hexanes) to yield **SI3-16** (492 mg, 1.31 mmol, 67% yield) as a colorless crystallizing oil.

SFC analysis (IC, 5% *i*-PrOH in CO_2) t_R(major): 6.748 min; t_R(minor): 8.324 min; 94% ee

^{1}H NMR (400 MHz, $CDCl_3$) δ 7.76 – 7.65 (m, 2H), 7.53 – 7.35 (m, 3H), 4.65 (dd, *J* = 10.5, 4.5 Hz, 1H), 4.21 (qdd, *J* = 10.7, 7.0, 3.6 Hz, 2H), 2.97 (ddd, *J* = 17.4, 10.6, 2.7 Hz, 1H), 2.89 – 2.70 (m, 1H), 2.14 (t, *J* = 2.7 Hz, 1H), 1.30 (t, *J* = 7.1 Hz, 3H), 0.95 (s, 9H), 0.30 (s, 3H), 0.21 (s, 3H).

^{13}C NMR (101 MHz, $CDCl_3$) δ 173.13, 168.28, 134.61, 131.05, 128.59, 128.48, 80.35, 71.70, 63.97, 62.11, 26.18, 18.58, 14.31, -4.31, -4.51.

FTIR (AT-IR) 3310.03, 2929.56, 2857.22, 2359.18, 1744.02, 1694.62, 1472.02, 1446.93, 1390.26, 1362.25, 1289.85, 1250.00, 1226.16, 1186.10, 1072.43, 1017.66, 964.62, 920.36, 831.69, 809.32, 783.13, 748.13, 703.47, 674.24, 654.39 cm^{-1}

HRMS (TOF, ES+) calc'd for $C_{20}H_{30}NO_4Si$ $[M+H]^+$ 376.1939, found 376.1934

$[\alpha]_D^{23}$ –89.9° (*c*=1.0, $CHCl_3$)

Sonagashira coupling of benzoylated alkyne

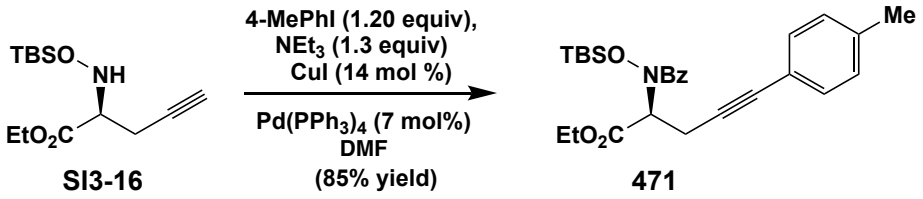

Add 4-iodotoluene (26.2 mg, 0.120 mmol, 1.20 equiv) to 3b (37.5 mg, 0.100 mmol, 1.00 equiv) in DMF (0.84 mL) followed by triethylamine (13 mg, 18 µL, 0.130 mmol, 1.30 equiv) and $Pd(PPh_3)_4$ (8.1 mg, 0.007 mmol, 0.07 equiv). Finally add CuI (2.6 mg, 0.014 mmol, 0.14 equiv). Seal and stir at ambient temperature 48h. Dilute with pH=7 buffer (8.5 mL) and filter off solids. Extract this mixture with EtOAc four times. Dry over Na_2SO_4, filter and concentrate *in vacuo* to yield crude 10. Purification by flash chromatography (silica, 10% EtOAc/Hexanes) yields 9 (39.4mg, 0.085 mmol, 85% yield) as a pale yellow oil.

^{1}H NMR (400 MHz, $CDCl_3$) δ 7.77 – 7.68 (m, 2H), 7.47 – 7.40 (m, 1H), 7.39 – 7.31 (m, 4H), 7.17 – 7.11 (m, 2H), 4.71 (dd, *J* = 11.0, 4.1 Hz, 1H), 4.34 – 4.11 (m, 2H), 3.19 (dd, *J* = 17.5, 11.1 Hz, 1H), 2.96 (dd, *J* = 17.5, 4.1 Hz, 1H), 2.36 (s, 3H), 1.31 (t, *J* = 7.1 Hz, 3H), 0.98 (s, 8H), 0.34 (s, 3H), 0.25 (s, 3H).

^{13}C NMR (101 MHz, $CDCl_3$) δ 173.23, 168.49, 138.33, 134.77, 131.53, 130.97, 129.29, 128.58, 128.41, 120.32, 85.31, 83.72, 64.42, 62.05, 26.22, 21.61, 19.50, 18.88, 14.35, -4.31, -4.39.

FTIR (AT-IR) 2928.59, 2856.73, 1744.86, 1694.26, 1510.29, 1471.57, 1446.59, 1362.89, 1250.43, 1183.24, 1021.70, 968.05, 919.34, 832.59, 814.99, 782.88, 749.82, 698.18, 677.26 cm^{-1}

HRMS (TOF, ES+) calc'd for $C_{27}H_{35}NO_4Si$ $[M+H]^+$ 466.2408, found 466.2415 (ppm=-1.48)

$[\alpha]_D^{23}$ +20.4°(*c* = 1.0, $CHCl_3$).

3.6.4. SFC traces for racemic and enantioenriched products

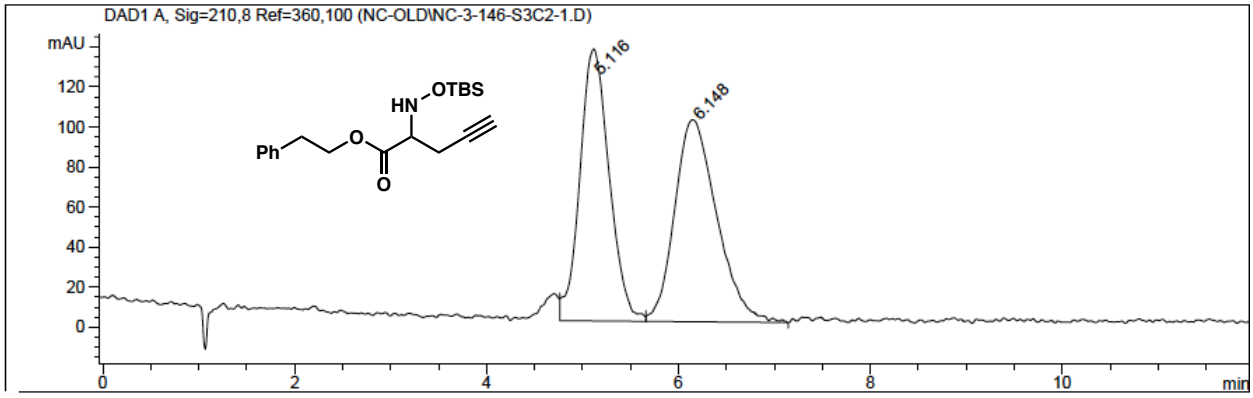

Peak #	RetTime [min]	Type	Width [min]	Area [mAU*s]	Height [mAU]	Area %
1	5.116	VV	0.3203	2889.85913	135.78705	48.4120
2	6.148	VV	0.4361	3079.43994	100.88213	51.5880

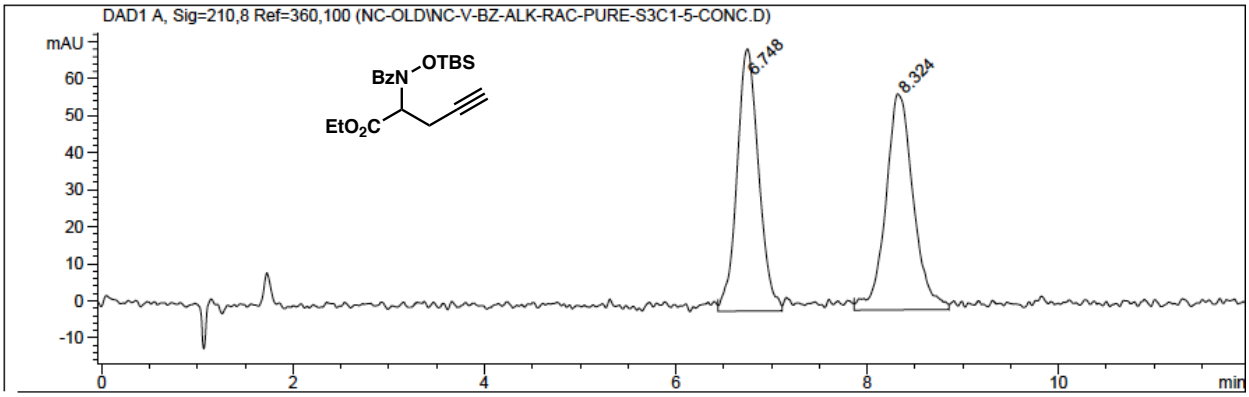

Peak #	RetTime [min]	Type	Width [min]	Area [mAU*s]	Height [mAU]	Area %
1	6.748	VV	0.2318	1116.34790	70.85162	48.8551
2	8.324	VV	0.2857	1168.67224	58.33414	51.1449

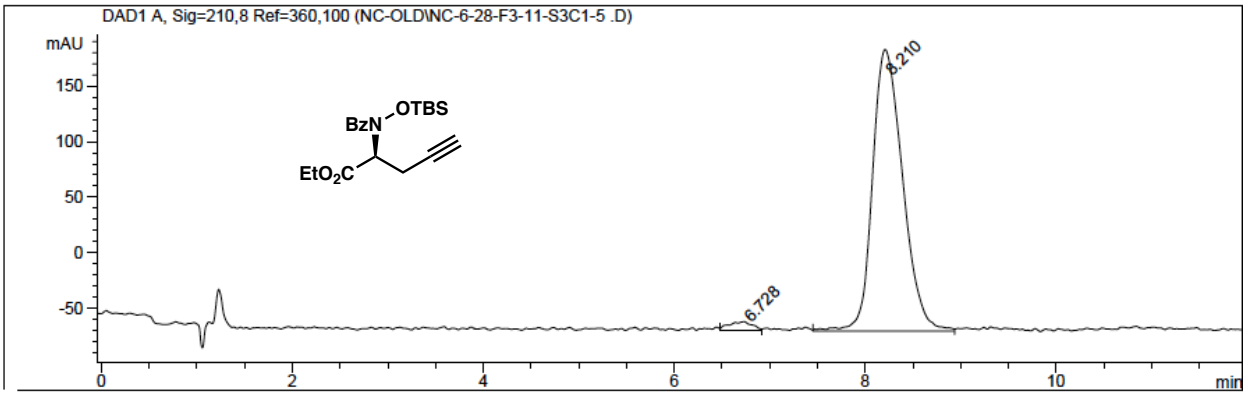

Peak #	RetTime [min]	Type	Width [min]	Area [mAU*s]	Height [mAU]	Area %
1	6.728	VV	0.2246	147.39131	8.40454	2.5675
2	8.210	VV	0.3533	5593.31201	253.61139	97.4325

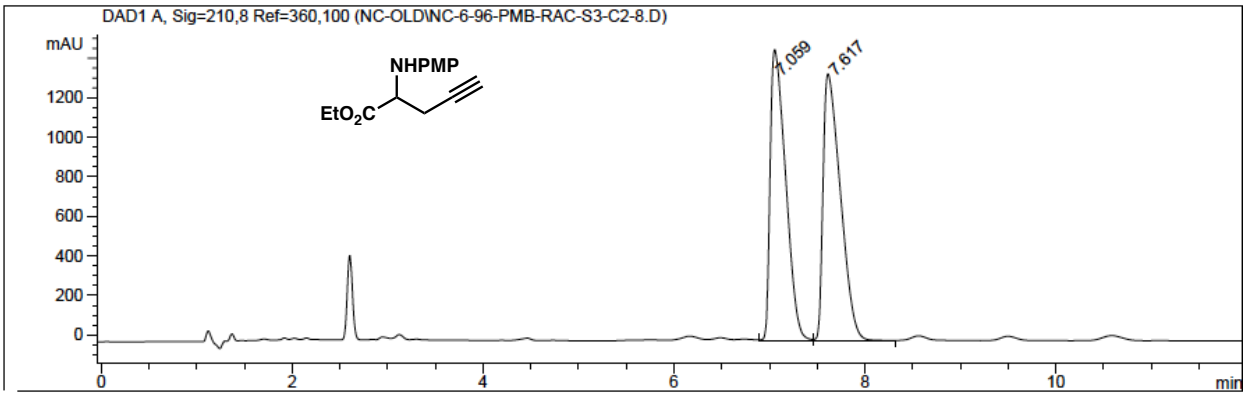

Peak #	RetTime [min]	Type	Width [min]	Area [mAU*s]	Height [mAU]	Area %
1	7.059	VV	0.1840	1.66779e4	1473.56030	49.3552
2	7.617	VB	0.2040	1.71137e4	1348.96606	50.6448

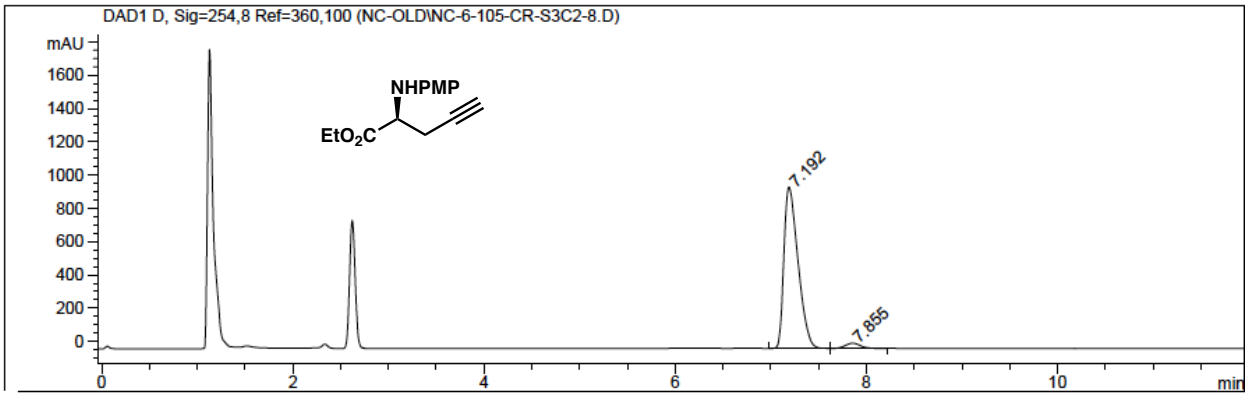

Peak #	RetTime [min]	Type	Width [min]	Area [mAU*s]	Height [mAU]	Area %
1	7.192	VV	0.1559	9936.06641	967.10529	96.5754
2	7.855	VB	0.1670	352.33801	32.37125	3.4246

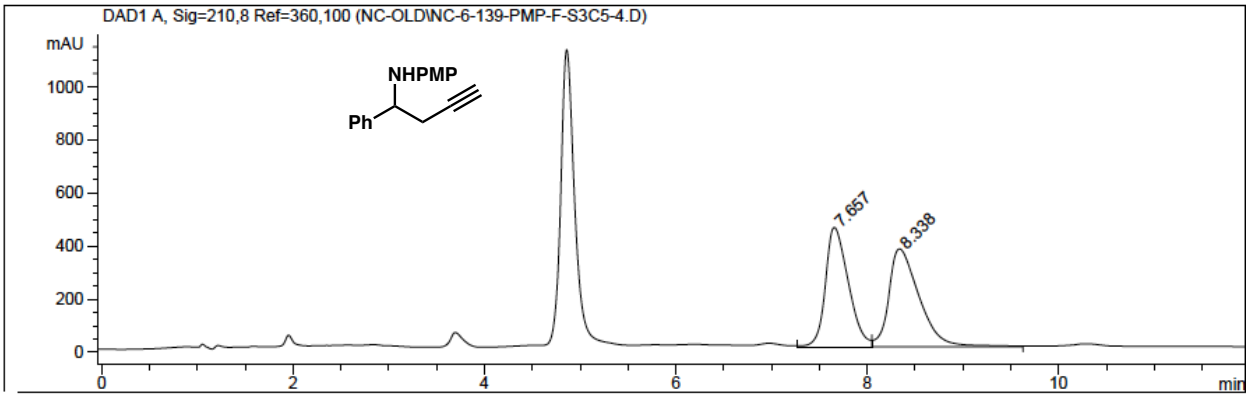

Peak #	RetTime [min]	Type	Width [min]	Area [mAU*s]	Height [mAU]	Area %
1	7.657	VV	0.2584	7492.73389	449.74838	47.8226
2	8.338	VB	0.3306	8175.02490	368.81750	52.1774

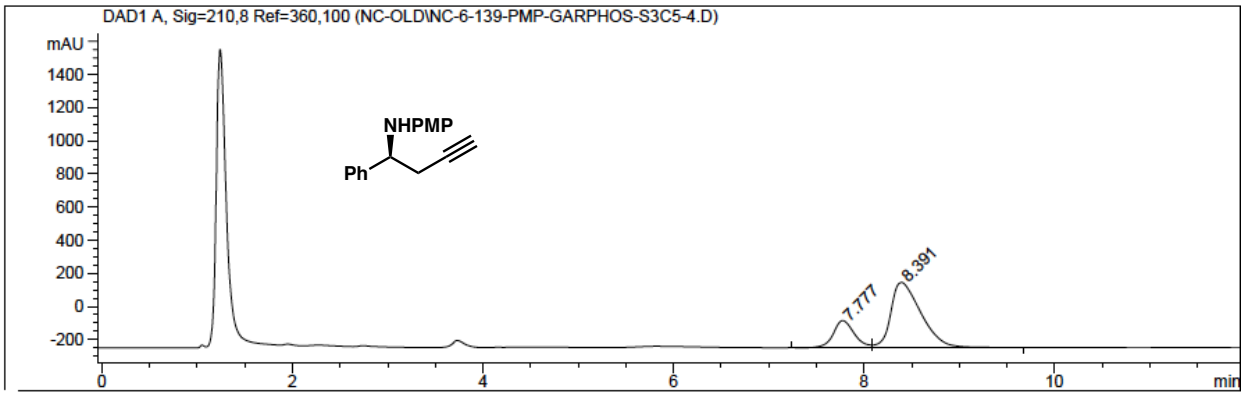

Peak #	RetTime [min]	Type	Width [min]	Area [mAU*s]	Height [mAU]	Area %
1	7.777	VV	0.2344	2506.78564	163.96179	22.2847
2	8.391	VB	0.3382	8742.10645	395.01102	77.7153

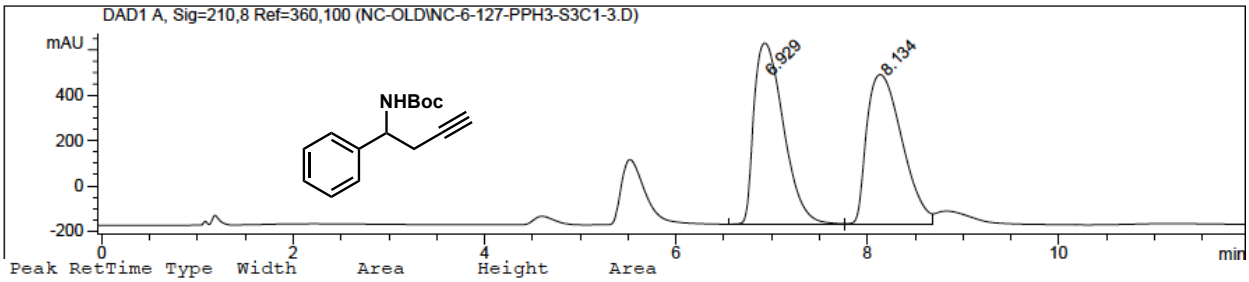

Peak #	RetTime [min]	Type	Width [min]	Area [mAU*s]	Height [mAU]	Area %
1	6.929	BV	0.3451	1.74015e4	802.00781	50.4168
2	8.134	VV	0.4132	1.71138e4	662.97357	49.5832

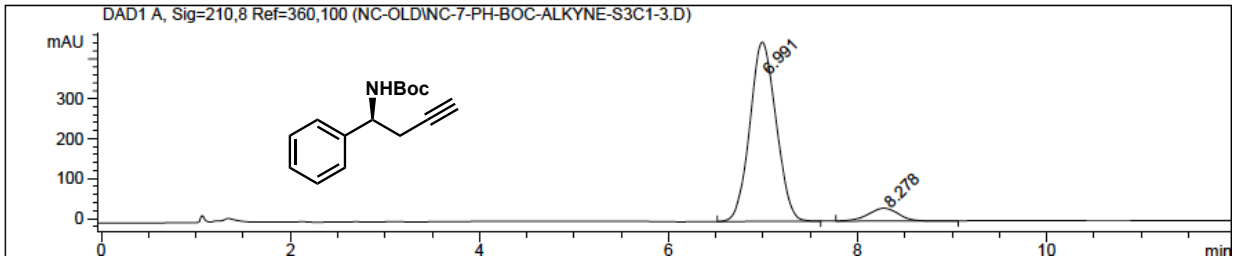

Peak #	RetTime [min]	Type	Width [min]	Area [mAU*s]	Height [mAU]	Area %
1	6.991	BB	0.2977	8682.42676	448.75708	92.3885
2	8.278	BB	0.3470	715.30627	32.21863	7.6115

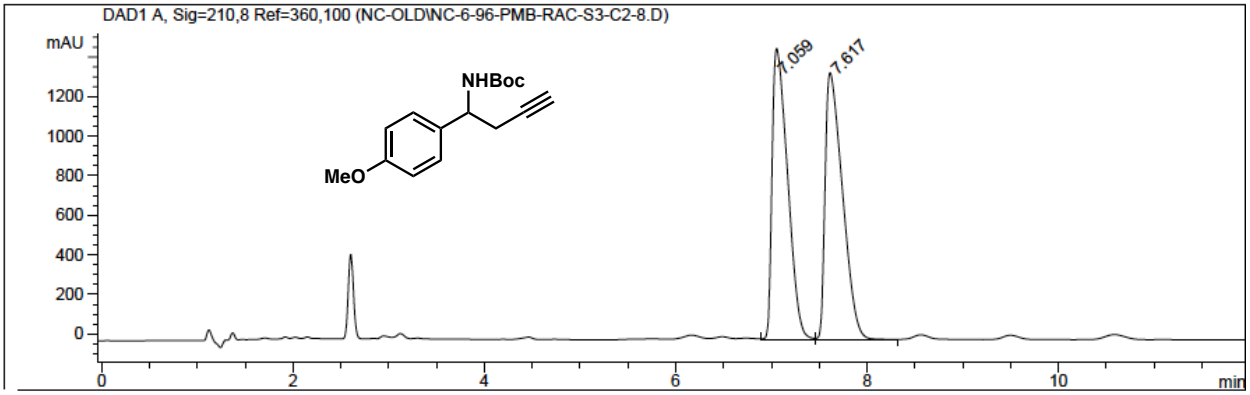

Peak #	RetTime [min]	Type	Width [min]	Area [mAU*s]	Height [mAU]	Area %
1	7.059	VV	0.1840	1.66779e4	1473.56030	49.3552
2	7.617	VB	0.2040	1.71137e4	1348.96606	50.6448

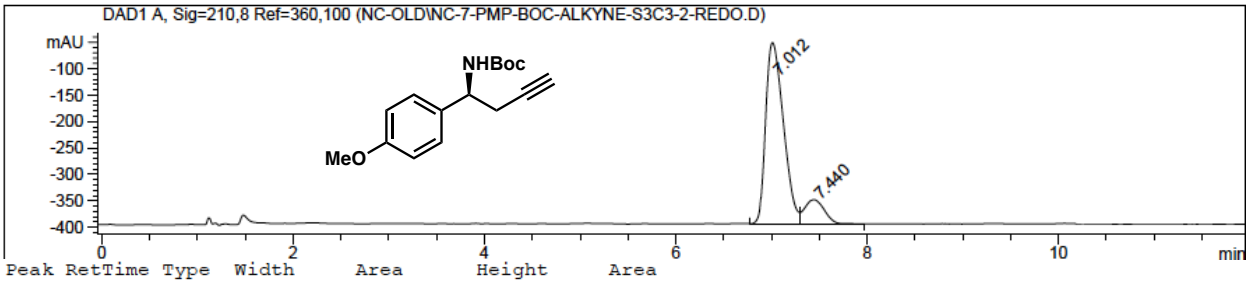

Peak #	RetTime [min]	Type	Width [min]	Area [mAU*s]	Height [mAU]	Area %
1	7.012	VV	0.2031	4444.66406	343.12326	86.5817
2	7.440	VB	0.2319	688.82776	46.75987	13.4183

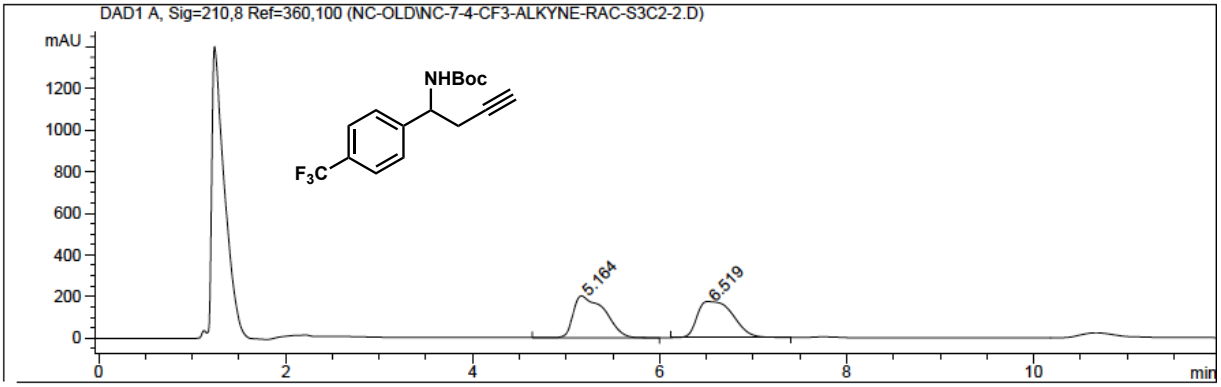

Peak #	RetTime [min]	Type	Width [min]	Area [mAU*s]	Height [mAU]	Area %
1	5.164	VB	0.3106	4669.19482	201.27870	49.8833
2	6.519	BV	0.3615	4691.05029	174.58394	50.1167

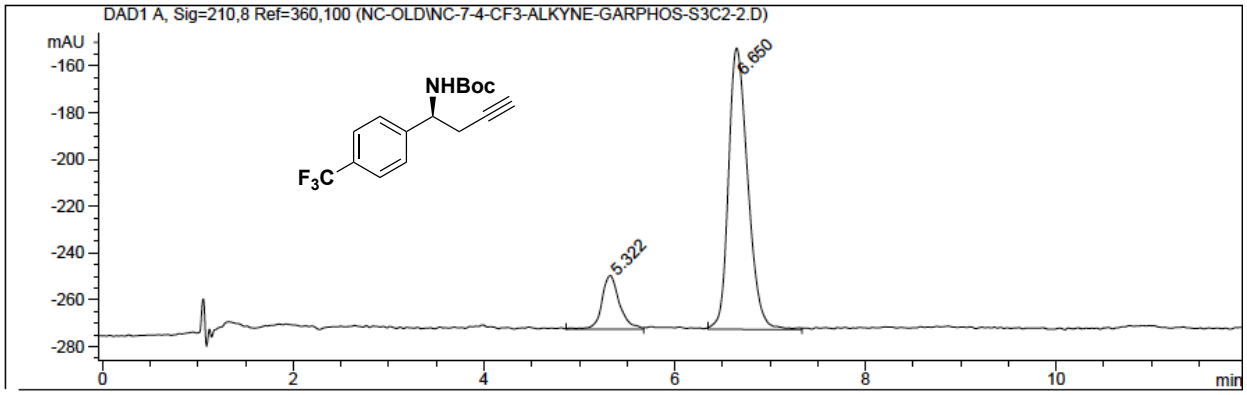

Peak #	RetTime [min]	Type	Width [min]	Area [mAU*s]	Height [mAU]	Area %
1	5.322	VV	0.1987	296.25833	22.93293	14.8763
2	6.650	BB	0.2167	1695.21912	120.06935	85.1237

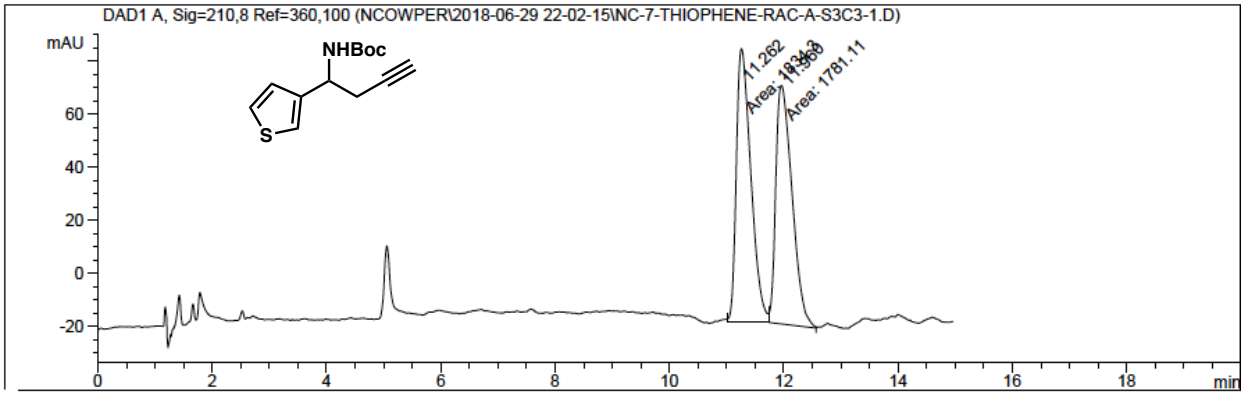

Peak #	RetTime [min]	Type	Width [min]	Area [mAU*s]	Height [mAU]	Area %
1	11.262	MM	0.2955	1834.29541	103.45673	50.7355
2	11.960	MM	0.3292	1781.11438	90.16128	49.2645

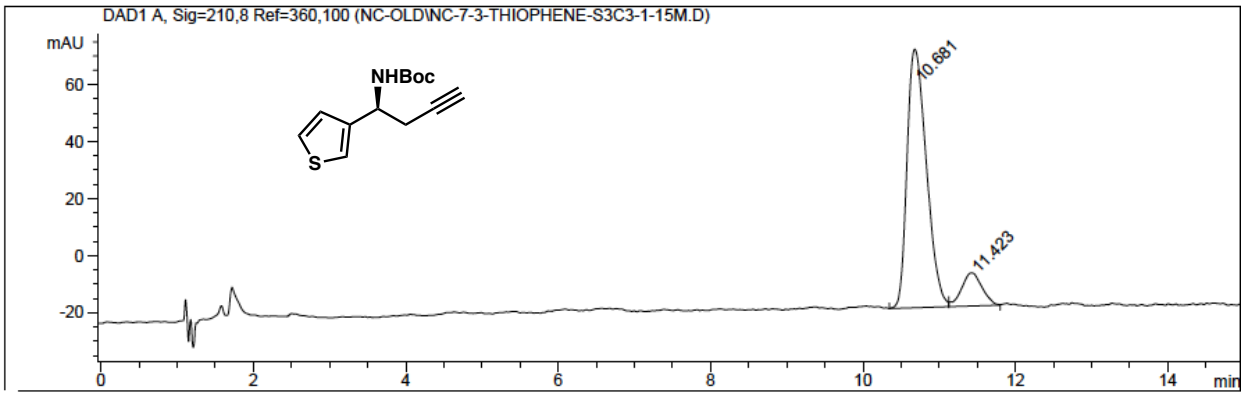

Peak #	RetTime [min]	Type	Width [min]	Area [mAU*s]	Height [mAU]	Area %
1	10.681	VV	0.2821	1601.03503	90.65076	88.0523
2	11.423	VBA	0.2710	217.24181	11.57412	11.9477

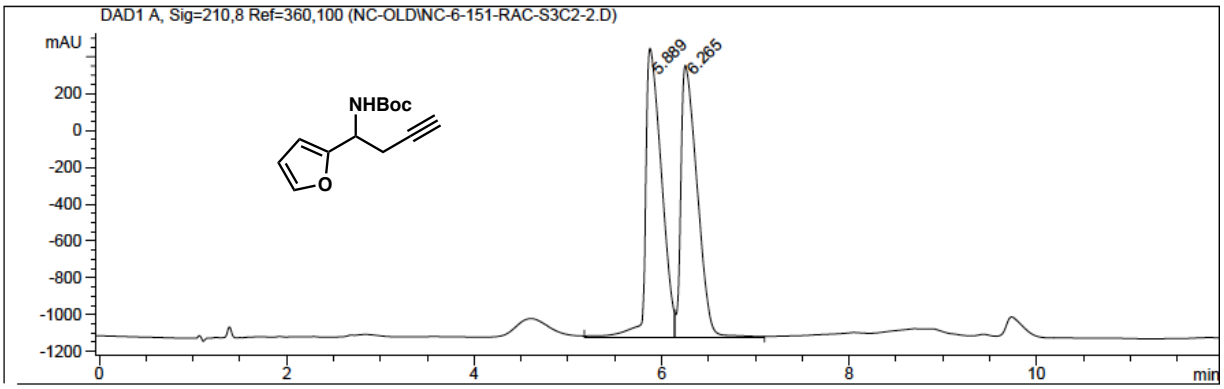

Peak #	RetTime [min]	Type	Width [min]	Area [mAU*s]	Height [mAU]	Area %
1	5.889	VV	0.1927	1.85401e4	1537.33643	50.8321
2	6.265	VV	0.1955	1.79331e4	1457.98987	49.1679

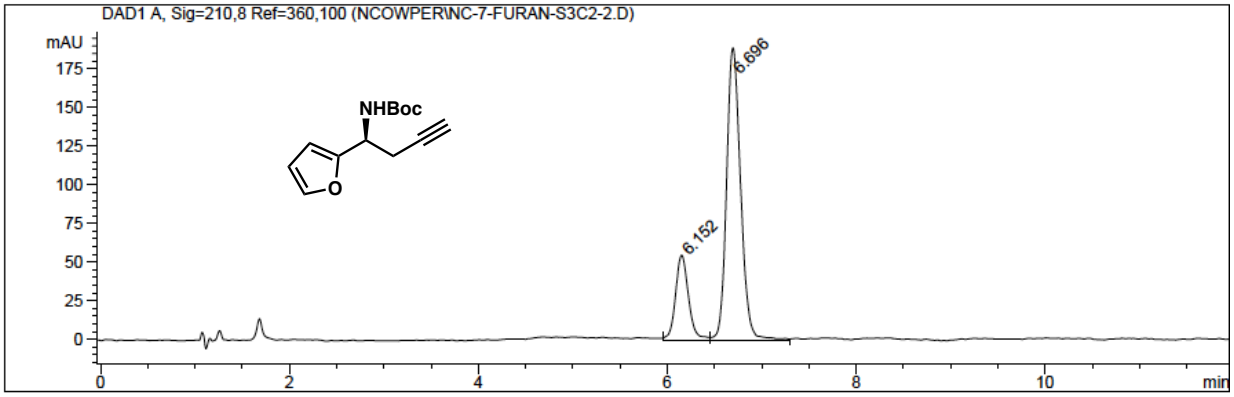

Peak #	RetTime [min]	Type	Width [min]	Area [mAU*s]	Height [mAU]	Area %
1	6.152	BV	0.1496	538.44879	55.28022	21.3945
2	6.696	VB	0.1618	1978.31079	189.51505	78.6055

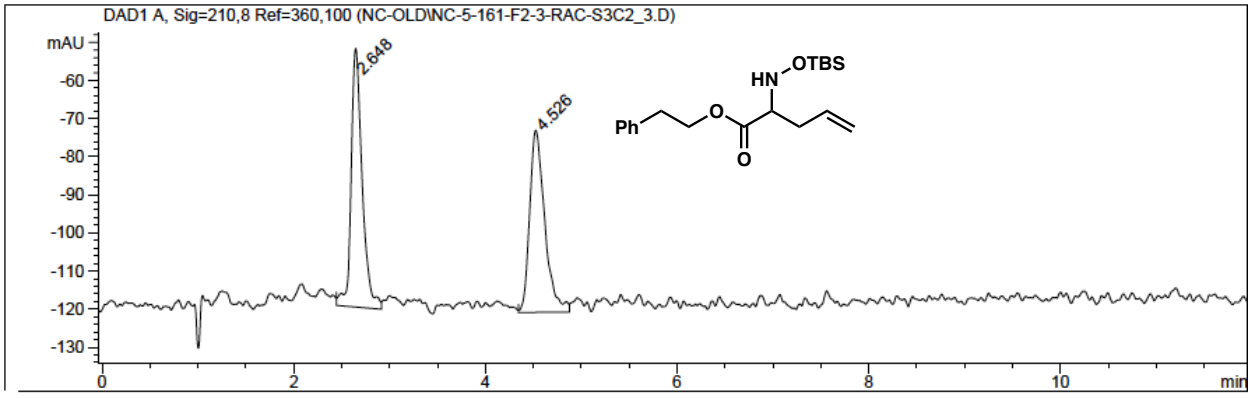

Peak #	RetTime [min]	Type	Width [min]	Area [mAU*s]	Height [mAU]	Area %
1	2.648	VV	0.1220	544.44684	67.56007	50.9520
2	4.526	VV	0.1641	524.10187	47.72316	49.0480

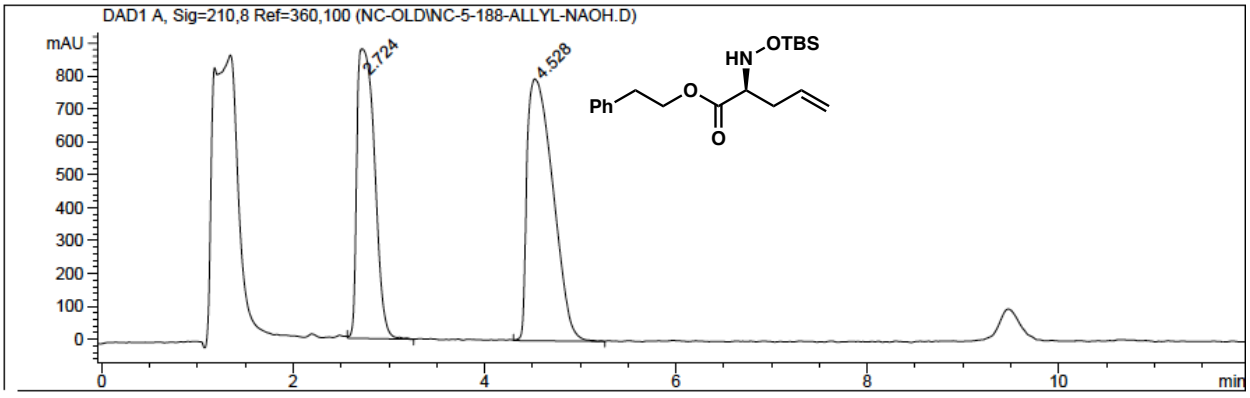

Peak #	RetTime [min]	Type	Width [min]	Area [mAU*s]	Height [mAU]	Area %
1	2.724	VV	0.2101	1.13312e4	880.60944	43.1650
2	4.528	VV	0.3150	1.49197e4	794.89777	56.8350

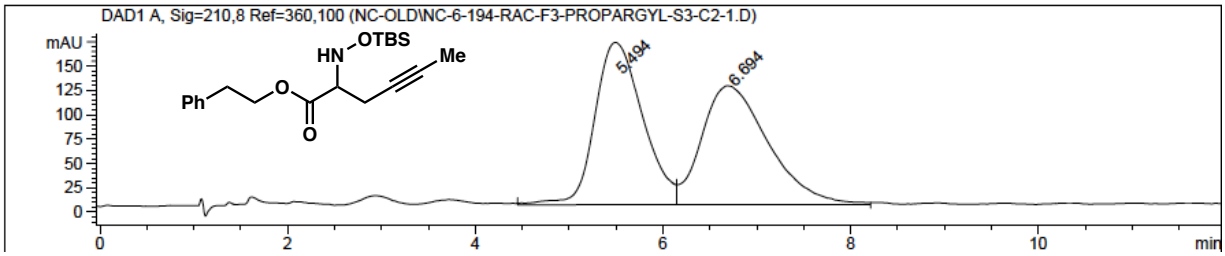

Peak #	RetTime [min]	Type	Width [min]	Area [mAU*s]	Height [mAU]	Area %
1	5.494	BV	0.5462	5913.11963	166.56648	49.6272
2	6.694	VB	0.7418	6001.95117	122.03557	50.3728

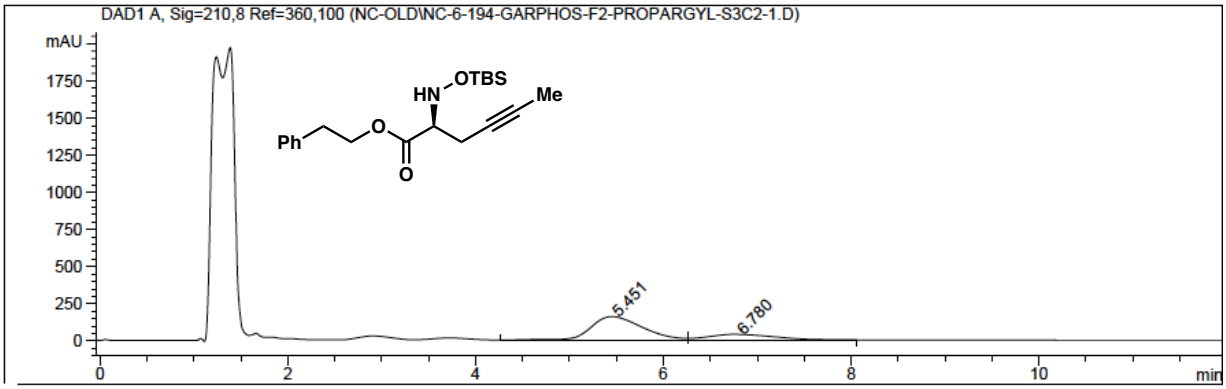

Peak #	RetTime [min]	Type	Width [min]	Area [mAU*s]	Height [mAU]	Area %
1	5.451	VV	0.5655	6026.38477	157.83055	75.9028
2	6.780	VB	0.7182	1913.22034	38.60706	24.0972

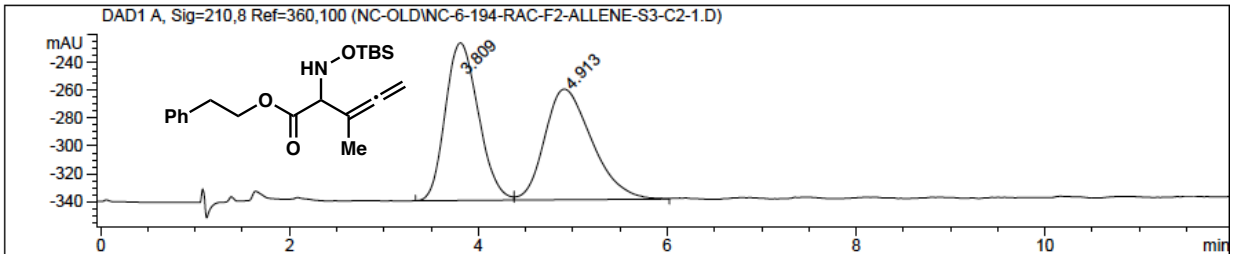

Peak #	RetTime [min]	Type	Width [min]	Area [mAU*s]	Height [mAU]	Area %
1	3.809	BV	0.3801	2756.37012	113.20204	49.9358
2	4.913	VB	0.5340	2763.45605	79.41681	50.0642

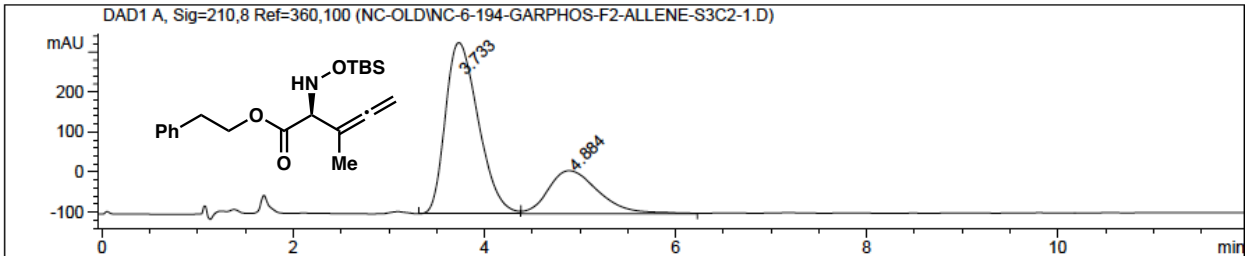

Peak #	RetTime [min]	Type	Width [min]	Area [mAU*s]	Height [mAU]	Area %
1	3.733	VV	0.3800	1.02720e4	427.98087	72.0986
2	4.884	VB	0.5698	3975.18066	107.89998	27.9014

3.6.5. X-ray crystallographic data of desilylated hydroxylamine (p16469_b)

Crystal was obtained in analogy to 3b-Bz with 2-Br-benzoyl chloride. Recrystallized from $CHCl_3$/Hexanes. Layer diffusion between 1:1 $CHCl_3$/Hexanes and Hexanes yielded X-ray quality crystals of the desilylated hydroxylamine.

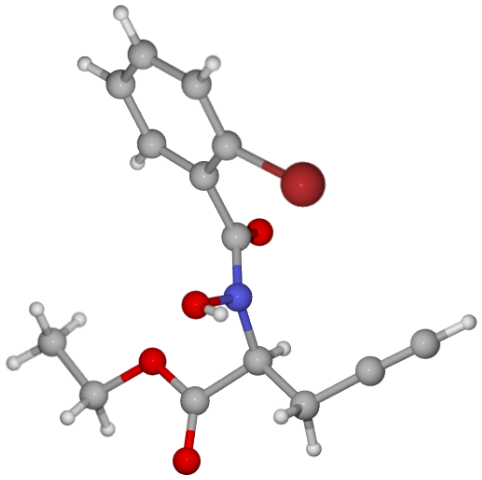

Table 1. Crystal data and structure refinement for final p16469_b.

Identification code	p16469_b
Empirical formula	C14 H14 Br N O4
Formula weight	340.17
Temperature	100(2) K
Wavelength	0.71073 Å

Crystal system	Monoclinic	
Space group	$P12_11$	
Unit cell dimensions	a = 8.6346(7) Å	α = 90°.
	b = 5.6380(5) Å	β = 103.728(3)°
	c = 15.6510(13) Å	γ = 90°
Volume	740.15(11) $Å^3$	
Z	2	
Density (calculated)	1.410 Mg/m^3	
Absorption coefficient 0	2.788 mm^{-1}	
F(000)	344	
Crystal size	0.23 × 0.15 × 0.07 mm^3	
Theta range for data collection	2.428 to 45.369°	
Index ranges	-16<=h<=17, -11<=k<=11, -31<=l<=31	
Reflections collected	68030	
Independent reflections	12256 [R(int) = 0.0378]	
Completeness to theta = 25.000°	99.7 %	
Absorption correction	Semi-empirical from equivalents	
Max. and min. transmission	0.747 and 0.716	
Refinement method	Full-matrix least-squares on F2	
Data / restraints / parameters	12256/1/183	
Goodness-of-fit on F2	0.989	
Final R indices [I>2sigma(I)]	R1 = 0.0241, wR2 = 0.0526	
R indices (all data)	R1 = 0.0305, wR2 = 0.0541	
Extinction coefficient	n/a	
Largest diff. peak and hole	0.526 and -0.838 e.$Å^{-3}$	

Table 2. Atomic coordinates ($\times 10^4$) and equivalent isotropic displacement parameters (Å 2×10^3) for final p16469_b. U(eq) is defined as one third of the trace of the orthogonalized U^{ij} tensor.

	x	**y**	**z**	**U_{eq}**
Br1	0.15673(2)	0.20544(3)	0.66433(2)	0.02070(3)
O1	0.86808(9)	0.26712(16)	0.92479(6)	0.01991(14)
O2	0.80569(9)	0.56641(15)	0.82777(6)	0.01865(13)
O3	0.54192(7)	0.19604(14)	0.73103(4)	0.01256(9)
O4	0.492	0.0738	0.7396	0.019
N1	0.43360(9)	0.76829(12)	0.77810(5)	0.01514(11)
C1	0.50418(9)	0.38290(13)	0.78093(5)	0.00968(10)
C2	0.77148(10)	0.39468(16)	0.87841(6)	0.01261(12)
C3	0.59223(10)	0.38553(15)	0.87231(5)	0.00991(11)
C4	0.5623	0.5331	0.9	0.012
C5	0.55204(9)	0.17365(15)	0.92407(5)	0.01207(13)
C6	0.5754	0.025	0.8959	0.014
C7	0.6205	0.1778	0.9845	0.014
C8	0.38480(10)	0.17397(16)	0.92825(6)	0.01385(14)
C9	0.24845(11)	0.1758(2)	0.93395(7)	0.01919(18)
C10	0.1407	0.1773	0.9384	0.023
C11	0.43888(10)	0.58063(14)	0.73832(5)	0.00977(11)
C12	0.37367(10)	0.56879(15)	0.64074(5)	0.01081(11)
C13	0.25012(11)	0.42021(17)	0.59858(6)	0.01398(13)
C14	0.18903(13)	0.4296(2)	0.50811(7)	0.01944(17)

Table 3. Bond lengths [Å] and angles [°] for final p16469_b

Br1–C8	1.8892(9)
O1–C1	1.2052(12)
O2–C1	1.3282(11)
O2–C13	1.4559(13)
O3–H3	0.8400
O3–N1	1.3953(10)
O4–C6	1.2340(11)
N1–C2	1.4518(11)
N1–C6	1.3517(11)
C1–C2	1.5288(12)
C2–H2	1.0000
C2–C3	1.5287(11)
C3–H3A	0.9900
C3–H3B	0.9900
C3–C4	1.4610(11)
C4–C5	1.2017(12)
C5–H5	0.9500
C6–C7	1.4986(11)
C7–C8	1.3932(13)
C7–C12	1.3987(12)
C8–C9	1.3899(14)
C9–H9	0.9500
C9–C10	1.3905(15)
C10–H10	0.9500
C10–C11	1.3858(16)
C11–H11	0.9500
C11–C12	1.3931(13)
C12–H12	0.9500
C13–H13A	0.9900
C13–H13B	0.9900
C13–C14	1.5054(17)
C14–H14A	0.9800
C14–H14B	0.9800
C14–H14C	0.9800

C1–O2–C13	115.36(8)
N1–O3–H3	109.5
O3–N1–C2	114.95(6)
C6–N1–O3	118.17(7)
C6–N1–C2	122.50(7)
O1–C1–O2	125.05(9)
O1–C1–C2	124.28(8)
O2–C1–C2	110.65(8)
N1–C2–C1	110.34(7)
N1–C2–H2	107.8
N1–C2–C3	112.48(7)
C1–C2–H2	107.8
C3–C2–C1	110.31(7)
C3–C2–H2	107.8
C2–C3–H3A	109.2
C2–C3–H3B	109.2
H3A–C3–H3B	107.9
C4–C3–C2	111.95(7)

C4–C3–H3A	109.2
C4–C3–H3B	109.2
C5–C4–C3	178.30(10)
C4–C5–H5	180.0
O4–C6–N1	121.28(8)
O4–C6–C7	120.17(8)
N1–C6–C7	118.55(7)
C8–C7–C6	124.73(7)
C8–C7–C12	118.27(8)
C12–C7–C6	116.78(8)
C7–C8–Br1	120.35(6)
C9–C8–Br1	118.14(7)
C9–C8–C7	121.49(9)
C8–C9–H9	120.4
C8–C9–C10	119.29(10)
C10–C9–H9	120.4
C9–C10–H10	119.8
C11–C10–C9	120.33(9)
C11–C10–H10	119.8
C10–C11–H11	120.1
C10–C11–C12	119.88(9)
C12–C11–H11	120.1
C7–C12–H12	119.6
C11–C12–C7	120.70(9)
C11–C12–H12	119.6
O2–C13–H13A	110.3
O2–C13–H13B	110.3
O2–C13–C14	107.04(9)
H13A–C13–H13B	108.6
C14–C13–H13A	110.3
C14–C13–H13B	110.3
C13–C14–H14A	109.5
C13–C14–H14B	109.5
C13–C14–H14C	109.5
H14A–C14–H14B	109.5
H14A–C14–H14C	109.5

Symmetry transformations used to generate equivalent atoms:

Table 4. Anisotropic displacement parameters ($Å^2$) for final p16469_b. The anisotropic displacement factor exponent takes the form: $-2p^2[h^2 a^{*2}U^{11} + ... + 2 h k a^* b^* U^{12}]$

	U^{11}	U^{22}	U^{33}	U^{23}	U^{13}	U^{12}
Br1	0.01666(4)	0.02574(5)	0.01784(4)	0.00477(4)	0.00036(3)	-0.01092(4)
O1	0.0128(2)	0.0248(4)	0.0218(3)	0.0102(3)	0.0035(2)	0.0027(2)
O2	0.0128(2)	0.0203(3)	0.0226(3)	0.0095(3)	0.0035(2)	-0.0029(2)
O3	0.0179(2)	0.0080(2)	0.0122(2)	-0.0020(2)	0.00421(17)	0.0012(2)
O4	0.0234(3)	0.0083(2)	0.0131(2)	-0.00124(19)	0.0030(2)	0.0014(2)
N1	0.0128(2)	0.0076(2)	0.0080(2)	-0.00085(18)	0.00111(19)	0.00054(19)
C1	0.0118(3)	0.0137(3)	0.0119(3)	0.0014(2)	0.0019(2)	-0.0021(2)
C2	0.0109(3)	0.0099(3)	0.0084(3)	0.0002(2)	0.0013(2)	-0.0013(2)
C3	0.0123(3)	0.0127(4)	0.0108(3)	0.0025(2)	0.0019(2)	-0.0012(2)
C4	0.0139(3)	0.0153(4)	0.0119(3)	0.0031(2)	0.0024(2)	-0.0019(2)
C5	0.0148(3)	0.0245(5)	0.0180(3)	0.0066(3)	0.0035(3)	-0.0002(3)
C6	0.0115(3)	0.0083(3)	0.0095(3)	0.0004(2)	0.0023(2)	0.0000(2)
C7	0.0129(3)	0.0101(3)	0.0092(3)	0.0010(2)	0.0023(2)	-0.0001(2)

C8	0.0126(3)	0.0166(3)	0.0114(3)	0.0020(3)	0.0003(2)	-0.0022(3)
C9	0.0164(4)	0.0268(5)	0.0123(3)	0.0014(3)	-0.0022(3)	-0.0031(3)
C10	0.0211(4)	0.0267(5)	0.0104(3)	0.0041(3)	0.0004(3)	0.0014(3)
C11	0.0262(4)	0.0187(5)	0.0120(3)	0.0044(3)	0.0058(3)	-0.0009(3)
C12	0.0216(3)	0.0122(4)	0.0122(3)	0.0016(2)	0.0048(2)	-0.0025(3)
C13	0.0139(4)	0.0264(5)	0.0263(5)	0.0092(4)	0.0048(3)	-0.0038(3)
C14	0.0238(5)	0.0323(6)	0.0394(7)	0.0178(5)	0.0113(5)	-0.0040(4)

3.6 REFERENCES

(1) Caputo, C. A.; Jones, N. Developments in Asymmetric Catalysis by Metal Complexes of Chiral Chelating Nitrogen -Donor Ligands. *Dalton Trans.* **2007**, No. 41, 4627–4640.

(2) Paolo, M.; Mauro, M.; Armando, C.; Giuseppe, B. Asymmetric Aminocatalysis—Gold Rush in Organic Chemistry. *Angew. Chem. Int. Ed.* **2008**, *47* (33), 6138–6171.

(3) Ruiz-Castillo, P.; Buchwald, S. L. Applications of Palladium-Catalyzed C–N Cross-Coupling Reactions. *Chem. Rev.* **2016**, *116* (19), 12564–12649.

(4) Finefield, J.; Sherman, D. H.; Kreitman, M.; Williams, R. M. Enantiomeric Natural Products: Occurrence and Biogenesis. *Angew. Chem. Int. Ed.* **2012**, *51* (20), 4802–4836.

(5) Xie, J.-H.; Zhu, S.-F.; Zhou, Q.-L. Transition Metal-Catalyzed Enantioselective Hydrogenation of Enamines and Imines. *Chem. Rev.* **2011**, *111* (3), 1713–1760.

(6) Kobayashi, S.; Ishitani, H. Catalytic Enantioselective Addition to Imines. *Chem. Rev.* **1999**, *99* (5), 1069–1094.

(7) Wang, J.; Liu, X.; Feng, X. Asymmetric Strecker Reactions. *Chem. Rev.* **2011**, *111* (11), 6947–6983.

(8) Yan, H.; Oh, J. S.; Lee, J.-W.; Song, C. E. Scalable Organocatalytic Asymmetric Strecker Reactions Catalysed by a Chiral Cyanide Generator. *Nat. Commun.* **2012**, *3*, 1212.

(9) Li, L.; Zhang, Z.; Zhu, X.; Popa, A.; Wang, S. Asymmetric Alkylation of a Tert-Butyl Benzophenone Schiff Base Derivative in Water. *Synlett* **2005**, *2005* (12), 1873–1876.

(10) Wang, Z.; Huang, D.; Xu, P.; Dong, X.; Wang, X.; Dai, Z. The Asymmetric Alkylation Reaction of Glycine Derivatives Catalyzed by the Novel Chiral Phase Transfer Catalysts. *Tetrahedron Lett.* **2015**, *56* (9), 1067–1071.

(11) Enders, D.; Reinhold, U. Asymmetric Synthesis of Amines by Nucleophilic 1,2-Addition of Organometallic Reagents to the CN-Double Bond. *Tetrahedron Asymmetry* **1997**, *8* (12), 1895–1946.

(12) Bloch, R. Additions of Organometallic Reagents to CN Bonds: Reactivity and Selectivity. *Chem. Rev.* **1998**, *98* (4), 1407–1438.

(13) Friestad, G. K.; Mathies, A. K. Recent Developments in Asymmetric Catalytic Addition to CN Bonds. *Tetrahedron* **2007**, *63* (12), 2541–2569.

(14) Kagoshima, H.; Uzawa, T.; Akiyama, T. Catalytic, Enantioselective Propargyl- and Allenylation Reactions of α-Imino Ester. *Chem. Lett.* **2002**, *31* (3), 298–299.

(15) M. Wisniewska, H.; R. Jarvo, E. Enantioselective Silver-Catalyzed Propargylation of Imines. *Chem. Sci.* **2011**, *2* (4), 807–810.

(16) Gonzalez, A. Z.; Soderquist, J. A. β-Silylated Homopropargylic Amines via the Asymmetric Allenylboration of Aldimines. *Org. Lett.* **2007**, *9* (6), 1081–1084.

(17) Fandrick, D. R.; Johnson, C. S.; Fandrick, K. R.; Reeves, J. T.; Tan, Z.; Lee, H.; Song, J. J.; Yee, N. K.; Senanayake, C. H. Highly Diastereoselective Zinc-Catalyzed Propargylation of Tert-Butanesulfinyl Imines. *Org. Lett.* **2010**, *12* (4), 748–751.
(18) Cyklinsky, M.; Botuha, C.; Chemla, F.; Ferreira, F.; Pérez-Luna, A. Diastereoselective Synthesis of Enantiopure Homopropargylic N-Tert-Butylsulfinylamines. *Synlett* **2011**, *2011* (18), 2681–2684.
(19) Louvel, J.; Chemla, F.; Demont, E.; Ferreira, F.; Pérez-Luna, A.; Voituriez, A. Stereoselective Synthesis of Syn-β-Amino Propargylic Ethers: Application to the Asymmetric Syntheses of (+)-β-Conhydrine and (−)-Balanol. *Adv. Synth. Catal.* **2011**, *353* (11–12), 2137–2151.
(20) Guo, T.; Song, R.; Yuan, B.-H.; Chen, X.-Y.; Sun, X.-W.; Lin, G.-Q. Highly Efficient Asymmetric Construction of Quaternary Carbon-Containing Homoallylic and Homopropargylic Amines. *Chem. Commun.* **2013**, *49* (47), 5402–5404.
(21) García-Muñoz, M. J.; Zacconi, F.; Foubelo, F.; Yus, M. Indium-Promoted Diastereo- and Regioselective Propargylation of Chiral Sulfinylimines. *Eur. J. Org. Chem.* **2013**, *2013* (7), 1287–1295.
(22) Sun, G.; Wei, M.; Luo, Z.; Liu, Y.; Chen, Z.; Wang, Z. An Alternative Scalable Process for the Synthesis of the Key Intermediate of Omarigliptin. *Org. Process Res. Dev.* **2016**, *20* (12), 2074–2079.
(23) Vieira, E. M.; Haeffner, F.; Snapper, M. L.; Hoveyda, A. H. A Robust, Efficient, and Highly Enantioselective Method for Synthesis of Homopropargyl Amines. *Angew. Chem. Int. Ed.* **2012**, *51* (27), 6618–6621.
(24) Fandrick, D. R.; Hart, C. A.; Okafor, I. S.; Mercadante, M. A.; Sanyal, S.; Masters, J. T.; Sarvestani, M.; Fandrick, K. R.; Stockdill, J. L.; Grinberg, N.; et al. Copper-Catalyzed Asymmetric Propargylation of Cyclic Aldimines. *Org. Lett.* **2016**, *18* (23), 6192–6195.
(25) Trost, B. M.; Tracy, J. S. Organic Synthesis. Use of Alkynes as a Key to Innovation in Designing Structure for Function. *Isr. J. Chem.* **2018**, *58* (1–2), 18–27.
(26) Lang, K.; Chin, J. W. Cellular Incorporation of Unnatural Amino Acids and Bioorthogonal Labeling of Proteins. *Chem. Rev.* **2014**, *114* (9), 4764–4806.
(27) Fandrick, K. R.; Ogikubo, J.; Fandrick, D. R.; Patel, N. D.; Saha, J.; Lee, H.; Ma, S.; Grinberg, N.; Busacca, C. A.; Senanayake, C. H. Copper-Catalyst-Controlled Site-Selective Allenylation of Ketones and Aldehydes with Propargyl Boronates. *Org. Lett.* **2013**, *15* (6), 1214–1217.
(28) Blake, J. A.; Pratt, D. A.; Lin, S.; Walton, J. C.; Mulder, P.; Ingold, K. U. Thermolyses of O-Phenyl Oxime Ethers. A New Source of Iminyl Radicals and a New Source of Aryloxyl Radicals. *J. Org. Chem.* **2004**, *69* (9), 3112–3120.
(29) Bode, J. W.; Fox, R. M.; Baucom, K. D. Chemoselective Amide Ligations by Decarboxylative Condensations of N-Alkylhydroxylamines and α-Ketoacids. *Angew. Chem. Int. Ed.* **2006**, *45* (8), 1248–1252.
(30) Miyabe, H.; Ushiro, C.; Ueda, M.; Yamakawa, K.; Naito, T. Asymmetric Synthesis of α-Amino Acids Based on Carbon Radical Addition to Glyoxylic Oxime Ether. *J. Org. Chem.* **2000**, *65* (1), 176–185.
(31) Halland, N.; Jørgensen, K. A. Intermolecular Addition of Alkyl Radicals to Imines in the Absence and in the Presence of a Lewis Acid. *J. Chem. Soc. [Perkin 1]* **2001**, *0* (11), 1290–1295.

(32) Hoffmann, R. W.; Eichler, G.; Endesfelder, A. Addition von Allylboronsäureestern an Schiffsche Basen Und Oxime. *Liebigs Ann. Chem.* **1983**, *1983* (11), 2000–2007.
(33) Hoffmann, R. W.; Endesfelder, A. Diastereoselective Addition of Crotylboronates to Oximes. *Liebigs Ann. Chem.* **1987**, *1987* (3), 215–219.
(34) Hanessian, S.; Yang, R.-Y. Enantioselective Allylation of α-Ketoester Oximes with an External Chiral Ligand: Asymmetric Synthesis of Allylglycines and Allylalanine. *Tetrahedron Lett.* **1996**, *37* (50), 8997–9000.
(35) Hughes, M. N.; Shrimanker, K. Metal Complexes of Hydroxylamine. *Inorganica Chim. Acta* **1976**, *18*, 69–76.
(36) Courtois, G.; Miginiac, L. Etude de La Régiosélectivité de l'action Des Organozinciques Sur Les α-Iminoesters: Synthèse d'α-Aminoesters C-Substitués Par Un Groupe α-Insaturé Ou α-Fonctionnel. *J. Organomet. Chem.* **1989**, *376* (2), 235–243.
(37) Barnett, D. S.; Schaus, S. E. Asymmetric Propargylation of Ketones Using Allenylboronates Catalyzed by Chiral Biphenols. *Org. Lett.* **2011**, *13* (15), 4020–4023.
(38) Fandrick, D. R.; Fandrick, K. R.; Reeves, J. T.; Tan, Z.; Tang, W.; Capacci, A. G.; Rodriguez, S.; Song, J. J.; Lee, H.; Yee, N. K.; et al. Copper Catalyzed Asymmetric Propargylation of Aldehydes. *J. Am. Chem. Soc.* **2010**, *132* (22), 7600–7601.
(39) Fandrick, K. R.; Fandrick, D. R.; Reeves, J. T.; Gao, J.; Ma, S.; Li, W.; Lee, H.; Grinberg, N.; Lu, B.; Senanayake, C. H. A General Copper–BINAP-Catalyzed Asymmetric Propargylation of Ketones with Propargyl Boronates. *J. Am. Chem. Soc.* **2011**, *133* (27), 10332–10335.
(40) Korenaga, T.; Osaki, K.; Maenishi, R.; Sakai, T. Electron-Poor Chiral Diphosphine Ligands: High Performance for Rh-Catalyzed Asymmetric 1,4-Addition of Arylboronic Acids at Room Temperature. *Org. Lett.* **2009**, *11* (11), 2325–2328.
(41) Wu, H.; Haeffner, F.; Hoveyda, A. H. An Efficient, Practical, and Enantioselective Method for Synthesis of Homoallenylamides Catalyzed by an Aminoalcohol-Derived, Boron-Based Catalyst. *J. Am. Chem. Soc.* **2014**, *136* (10), 3780–3783.
(42) Mower, M. P.; Blackmond, D. G. Mechanistic Rationalization of Unusual Sigmoidal Kinetic Profiles in the Machetti–De Sarlo Cycloaddition Reaction. *J. Am. Chem. Soc.* **2015**, *137* (6), 2386–2391.
(43) Schwarz, L.; Girreser, U.; Clement, B. Synthesis and Characterization of Para-Substituted N,N′-Dihydroxybenzamidines and Their Derivatives as Model Compounds for a Class of Prodrugs. *Eur. J. Org. Chem.* **2014**, *2014* (9), 1961–1975.
(44) Hoffman, R. V.; Buntain, G. A. A New Synthesis of Oxime Derivatives from Carbonyl Compounds and N,O-Bis(Trimethylsilyl)Hydroxylamine. *Synthesis* **1987**, *1987* (9), 831–833.
(45) Godineau, E.; Landais, Y. Multicomponent Radical Processes: Synthesis of Substituted Piperidinones. *J. Am. Chem. Soc.* **2007**, *129* (42), 12662–12663.
(46) Trost, B. M.; Silverman, S. M. Enantioselective Construction of Pyrrolidines by Palladium-Catalyzed Asymmetric [3 + 2] Cycloaddition of Trimethylenemethane with Imines. *J. Am. Chem. Soc.* **2012**, *134* (10), 4941–4954.
(47) Tong, S.; Piemontesi, C.; Wang, Q.; Wang, M.-X.; Zhu, J. Silver-Catalyzed Three-Component 1,1-Aminoacylation of Homopropargylamines: α-Additions for Both Terminal Alkynes and Isocyanides. *Angew. Chem. Int. Ed.* **2017**, *56* (27), 7958–7962.
(1) Caputo, C. A.; Jones, N. Developments in Asymmetric Catalysis by Metal Complexes of Chiral Chelating Nitrogen -Donor Ligands. *Dalton Trans.* **2007**, No. 41, 4627–4640.

(2) Paolo, M.; Mauro, M.; Armando, C.; Giuseppe, B. Asymmetric Aminocatalysis—Gold Rush in Organic Chemistry. *Angew. Chem. Int. Ed.* **2008**, *47* (33), 6138–6171.
(3) Ruiz-Castillo, P.; Buchwald, S. L. Applications of Palladium-Catalyzed C–N Cross-Coupling Reactions. *Chem. Rev.* **2016**, *116* (19), 12564–12649.
(4) Finefield, J.; Sherman, D. H.; Kreitman, M.; Williams, R. M. Enantiomeric Natural Products: Occurrence and Biogenesis. *Angew. Chem. Int. Ed.* **2012**, *51* (20), 4802–4836.
(5) Xie, J.-H.; Zhu, S.-F.; Zhou, Q.-L. Transition Metal-Catalyzed Enantioselective Hydrogenation of Enamines and Imines. *Chem. Rev.* **2011**, *111* (3), 1713–1760.
(6) Kobayashi, S.; Ishitani, H. Catalytic Enantioselective Addition to Imines. *Chem. Rev.* **1999**, *99* (5), 1069–1094.
(7) Wang, J.; Liu, X.; Feng, X. Asymmetric Strecker Reactions. *Chem. Rev.* **2011**, *111* (11), 6947–6983.
(8) Yan, H.; Oh, J. S.; Lee, J.-W.; Song, C. E. Scalable Organocatalytic Asymmetric Strecker Reactions Catalysed by a Chiral Cyanide Generator. *Nat. Commun.* **2012**, *3*, 1212.
(9) Li, L.; Zhang, Z.; Zhu, X.; Popa, A.; Wang, S. Asymmetric Alkylation of a Tert-Butyl Benzophenone Schiff Base Derivative in Water. *Synlett* **2005**, *2005* (12), 1873–1876.
(10) Wang, Z.; Huang, D.; Xu, P.; Dong, X.; Wang, X.; Dai, Z. The Asymmetric Alkylation Reaction of Glycine Derivatives Catalyzed by the Novel Chiral Phase Transfer Catalysts. *Tetrahedron Lett.* **2015**, *56* (9), 1067–1071.
(11) Enders, D.; Reinhold, U. Asymmetric Synthesis of Amines by Nucleophilic 1,2-Addition of Organometallic Reagents to the CN-Double Bond. *Tetrahedron Asymmetry* **1997**, *8* (12), 1895–1946.
(12) Bloch, R. Additions of Organometallic Reagents to CN Bonds: Reactivity and Selectivity. *Chem. Rev.* **1998**, *98* (4), 1407–1438.
(13) Friestad, G. K.; Mathies, A. K. Recent Developments in Asymmetric Catalytic Addition to CN Bonds. *Tetrahedron* **2007**, *63* (12), 2541–2569.
(14) Kagoshima, H.; Uzawa, T.; Akiyama, T. Catalytic, Enantioselective Propargyl- and Allenylation Reactions of α-Imino Ester. *Chem. Lett.* **2002**, *31* (3), 298–299.
(15) M. Wisniewska, H.; R. Jarvo, E. Enantioselective Silver-Catalyzed Propargylation of Imines. *Chem. Sci.* **2011**, *2* (4), 807–810.
(16) Gonzalez, A. Z.; Soderquist, J. A. β-Silylated Homopropargylic Amines via the Asymmetric Allenylboration of Aldimines. *Org. Lett.* **2007**, *9* (6), 1081–1084.
(17) Fandrick, D. R.; Johnson, C. S.; Fandrick, K. R.; Reeves, J. T.; Tan, Z.; Lee, H.; Song, J. J.; Yee, N. K.; Senanayake, C. H. Highly Diastereoselective Zinc-Catalyzed Propargylation of Tert-Butanesulfinyl Imines. *Org. Lett.* **2010**, *12* (4), 748–751.
(18) Cyklinsky, M.; Botuha, C.; Chemla, F.; Ferreira, F.; Pérez-Luna, A. Diastereoselective Synthesis of Enantiopure Homopropargylic N-Tert-Butylsulfinylamines. *Synlett* **2011**, *2011* (18), 2681–2684.
(19) Louvel, J.; Chemla, F.; Demont, E.; Ferreira, F.; Pérez-Luna, A.; Voituriez, A. Stereoselective Synthesis of Syn-β-Amino Propargylic Ethers: Application to the Asymmetric Syntheses of (+)-β-Conhydrine and (−)-Balanol. *Adv. Synth. Catal.* **2011**, *353* (11–12), 2137–2151.
(20) Guo, T.; Song, R.; Yuan, B.-H.; Chen, X.-Y.; Sun, X.-W.; Lin, G.-Q. Highly Efficient Asymmetric Construction of Quaternary Carbon-Containing Homoallylic and Homopropargylic Amines. *Chem. Commun.* **2013**, *49* (47), 5402–5404.

(21) García-Muñoz, M. J.; Zacconi, F.; Foubelo, F.; Yus, M. Indium-Promoted Diastereo- and Regioselective Propargylation of Chiral Sulfinylimines. *Eur. J. Org. Chem.* **2013**, *2013* (7), 1287–1295.
(22) Sun, G.; Wei, M.; Luo, Z.; Liu, Y.; Chen, Z.; Wang, Z. An Alternative Scalable Process for the Synthesis of the Key Intermediate of Omarigliptin. *Org. Process Res. Dev.* **2016**, *20* (12), 2074–2079.
(23) Vieira, E. M.; Haeffner, F.; Snapper, M. L.; Hoveyda, A. H. A Robust, Efficient, and Highly Enantioselective Method for Synthesis of Homopropargyl Amines. *Angew. Chem. Int. Ed.* **2012**, *51* (27), 6618–6621.
(24) Fandrick, D. R.; Hart, C. A.; Okafor, I. S.; Mercadante, M. A.; Sanyal, S.; Masters, J. T.; Sarvestani, M.; Fandrick, K. R.; Stockdill, J. L.; Grinberg, N.; et al. Copper-Catalyzed Asymmetric Propargylation of Cyclic Aldimines. *Org. Lett.* **2016**, *18* (23), 6192–6195.
(25) Trost, B. M.; Tracy, J. S. Organic Synthesis. Use of Alkynes as a Key to Innovation in Designing Structure for Function. *Isr. J. Chem.* **2018**, *58* (1–2), 18–27.
(26) Lang, K.; Chin, J. W. Cellular Incorporation of Unnatural Amino Acids and Bioorthogonal Labeling of Proteins. *Chem. Rev.* **2014**, *114* (9), 4764–4806.
(27) Fandrick, K. R.; Ogikubo, J.; Fandrick, D. R.; Patel, N. D.; Saha, J.; Lee, H.; Ma, S.; Grinberg, N.; Busacca, C. A.; Senanayake, C. H. Copper-Catalyst-Controlled Site-Selective Allenylation of Ketones and Aldehydes with Propargyl Boronates. *Org. Lett.* **2013**, *15* (6), 1214–1217.
(28) Blake, J. A.; Pratt, D. A.; Lin, S.; Walton, J. C.; Mulder, P.; Ingold, K. U. Thermolyses of O-Phenyl Oxime Ethers. A New Source of Iminyl Radicals and a New Source of Aryloxyl Radicals. *J. Org. Chem.* **2004**, *69* (9), 3112–3120.
(29) Bode, J. W.; Fox, R. M.; Baucom, K. D. Chemoselective Amide Ligations by Decarboxylative Condensations of N-Alkylhydroxylamines and α-Ketoacids. *Angew. Chem. Int. Ed.* **2006**, *45* (8), 1248–1252.
(30) Miyabe, H.; Ushiro, C.; Ueda, M.; Yamakawa, K.; Naito, T. Asymmetric Synthesis of α-Amino Acids Based on Carbon Radical Addition to Glyoxylic Oxime Ether. *J. Org. Chem.* **2000**, *65* (1), 176–185.
(31) Halland, N.; Jørgensen, K. A. Intermolecular Addition of Alkyl Radicals to Imines in the Absence and in the Presence of a Lewis Acid. *J. Chem. Soc. [Perkin 1]* **2001**, *0* (11), 1290–1295.
(32) Hoffmann, R. W.; Eichler, G.; Endesfelder, A. Addition von Allylboronsäureestern an Schiffsche Basen Und Oxime. *Liebigs Ann. Chem.* **1983**, *1983* (11), 2000–2007.
(33) Hoffmann, R. W.; Endesfelder, A. Diastereoselective Addition of Crotylboronates to Oximes. *Liebigs Ann. Chem.* **1987**, *1987* (3), 215–219.
(34) Hanessian, S.; Yang, R.-Y. Enantioselective Allylation of α-Ketoester Oximes with an External Chiral Ligand: Asymmetric Synthesis of Allylglycines and Allylalanine. *Tetrahedron Lett.* **1996**, *37* (50), 8997–9000.
(35) Hughes, M. N.; Shrimanker, K. Metal Complexes of Hydroxylamine. *Inorganica Chim. Acta* **1976**, *18*, 69–76.
(36) Courtois, G.; Miginiac, L. Etude de La Régiosélectivité de l'action Des Organozinciques Sur Les α-Iminoesters: Synthèse d'α-Aminoesters C-Substitués Par Un Groupe α-Insaturé Ou α-Fonctionnel. *J. Organomet. Chem.* **1989**, *376* (2), 235–243.
(37) Barnett, D. S.; Schaus, S. E. Asymmetric Propargylation of Ketones Using Allenylboronates Catalyzed by Chiral Biphenols. *Org. Lett.* **2011**, *13* (15), 4020–4023.

(38) Fandrick, D. R.; Fandrick, K. R.; Reeves, J. T.; Tan, Z.; Tang, W.; Capacci, A. G.; Rodriguez, S.; Song, J. J.; Lee, H.; Yee, N. K.; et al. Copper Catalyzed Asymmetric Propargylation of Aldehydes. *J. Am. Chem. Soc.* **2010**, *132* (22), 7600–7601.
(39) Fandrick, K. R.; Fandrick, D. R.; Reeves, J. T.; Gao, J.; Ma, S.; Li, W.; Lee, H.; Grinberg, N.; Lu, B.; Senanayake, C. H. A General Copper–BINAP-Catalyzed Asymmetric Propargylation of Ketones with Propargyl Boronates. *J. Am. Chem. Soc.* **2011**, *133* (27), 10332–10335.
(40) Korenaga, T.; Osaki, K.; Maenishi, R.; Sakai, T. Electron-Poor Chiral Diphosphine Ligands: High Performance for Rh-Catalyzed Asymmetric 1,4-Addition of Arylboronic Acids at Room Temperature. *Org. Lett.* **2009**, *11* (11), 2325–2328.
(41) Wu, H.; Haeffner, F.; Hoveyda, A. H. An Efficient, Practical, and Enantioselective Method for Synthesis of Homoallenylamides Catalyzed by an Aminoalcohol-Derived, Boron-Based Catalyst. *J. Am. Chem. Soc.* **2014**, *136* (10), 3780–3783.
(42) Mower, M. P.; Blackmond, D. G. Mechanistic Rationalization of Unusual Sigmoidal Kinetic Profiles in the Machetti–De Sarlo Cycloaddition Reaction. *J. Am. Chem. Soc.* **2015**, *137* (6), 2386–2391.
(43) Schwarz, L.; Girreser, U.; Clement, B. Synthesis and Characterization of Para-Substituted N,N′-Dihydroxybenzamidines and Their Derivatives as Model Compounds for a Class of Prodrugs. *Eur. J. Org. Chem.* **2014**, *2014* (9), 1961–1975.
(44) Hoffman, R. V.; Buntain, G. A. A New Synthesis of Oxime Derivatives from Carbonyl Compounds and N,O-Bis(Trimethylsilyl)Hydroxylamine. *Synthesis* **1987**, *1987* (9), 831–833.
(45) Godineau, E.; Landais, Y. Multicomponent Radical Processes: Synthesis of Substituted Piperidinones. *J. Am. Chem. Soc.* **2007**, *129* (42), 12662–12663.
(46) Trost, B. M.; Silverman, S. M. Enantioselective Construction of Pyrrolidines by Palladium-Catalyzed Asymmetric [3 + 2] Cycloaddition of Trimethylenemethane with Imines. *J. Am. Chem. Soc.* **2012**, *134* (10), 4941–4954.
(47) Tong, S.; Piemontesi, C.; Wang, Q.; Wang, M.-X.; Zhu, J. Silver-Catalyzed Three-Component 1,1-Aminoacylation of Homopropargylamines: α-Additions for Both Terminal Alkynes and Isocyanides. *Angew. Chem. Int. Ed.* **2017**, *56* (27), 7958–7962.

Appendix 2

Spectra Relevant to Chapter 3:

Development of the First Catalytic Asymmetric Alkylation of an Oxime and its Application to the Synthesis of Enantioenriched Amines

	Parameter	Value
1	Data File Name	/ Volumes/ data-1/ nc-5-58-distilled-1H.fid/ fid
2	Title	nc-5-58-distilled-1H
3	Origin	Varian
4	Spectrometer	vnmrs
5	Solvent	cdcl3
6	Temperature	25.0
7	Pulse Sequence	s2pul
8	Experiment	1D
9	Probe	OneNMR
10	Number of Scans	14
11	Receiver Gain	32
12	Relaxation Delay	1.0000
13	Pulse Width	4.1500
14	Acquisition Date	2016-08-08T02:56:02
15	Spectrometer Frequency	399.80
16	Spectral Width	6410.3
17	Lowest Frequency	-806.4
18	Nucleus	1H
19	Acquired Size	16384
20	Spectral Size	65536

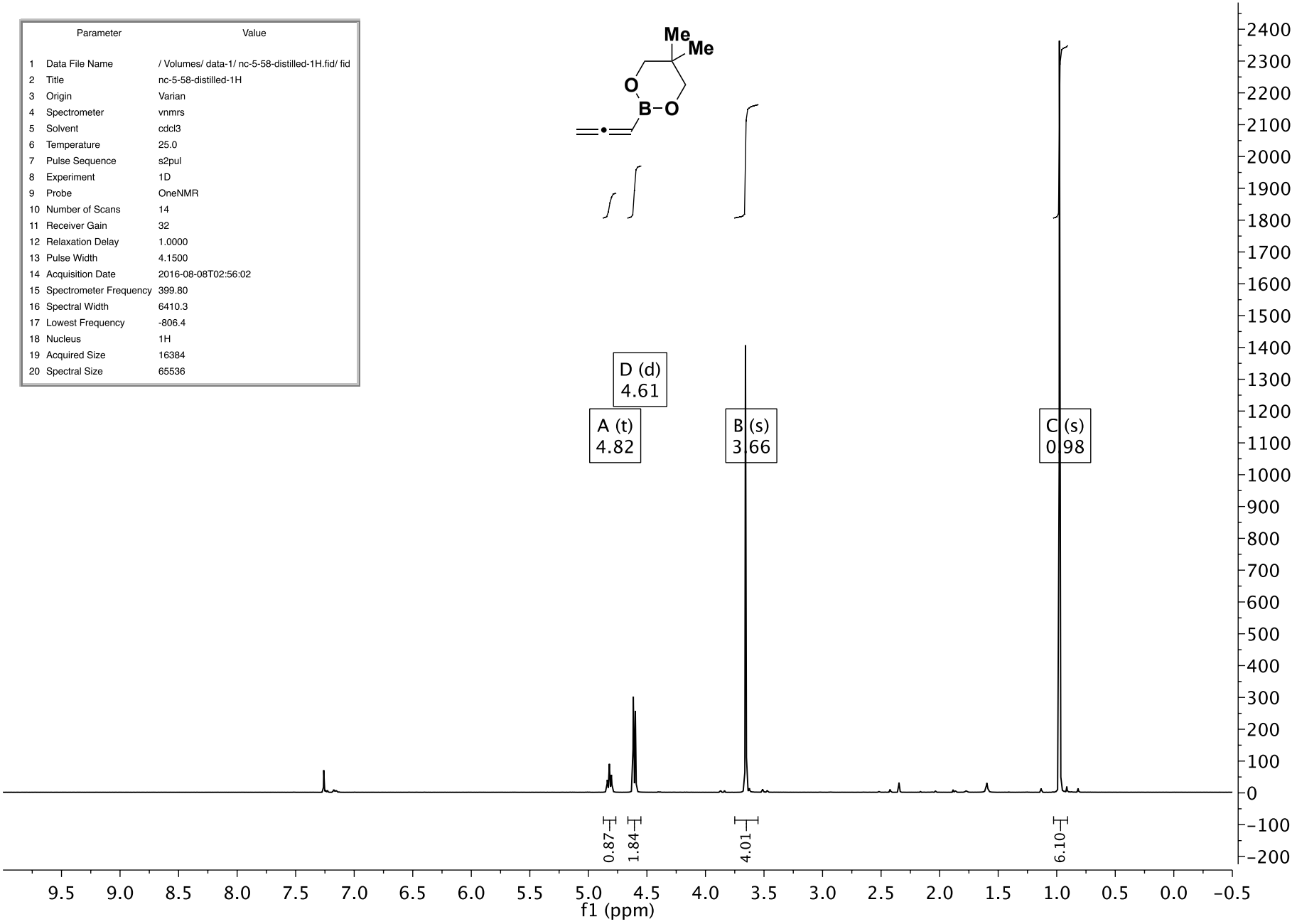

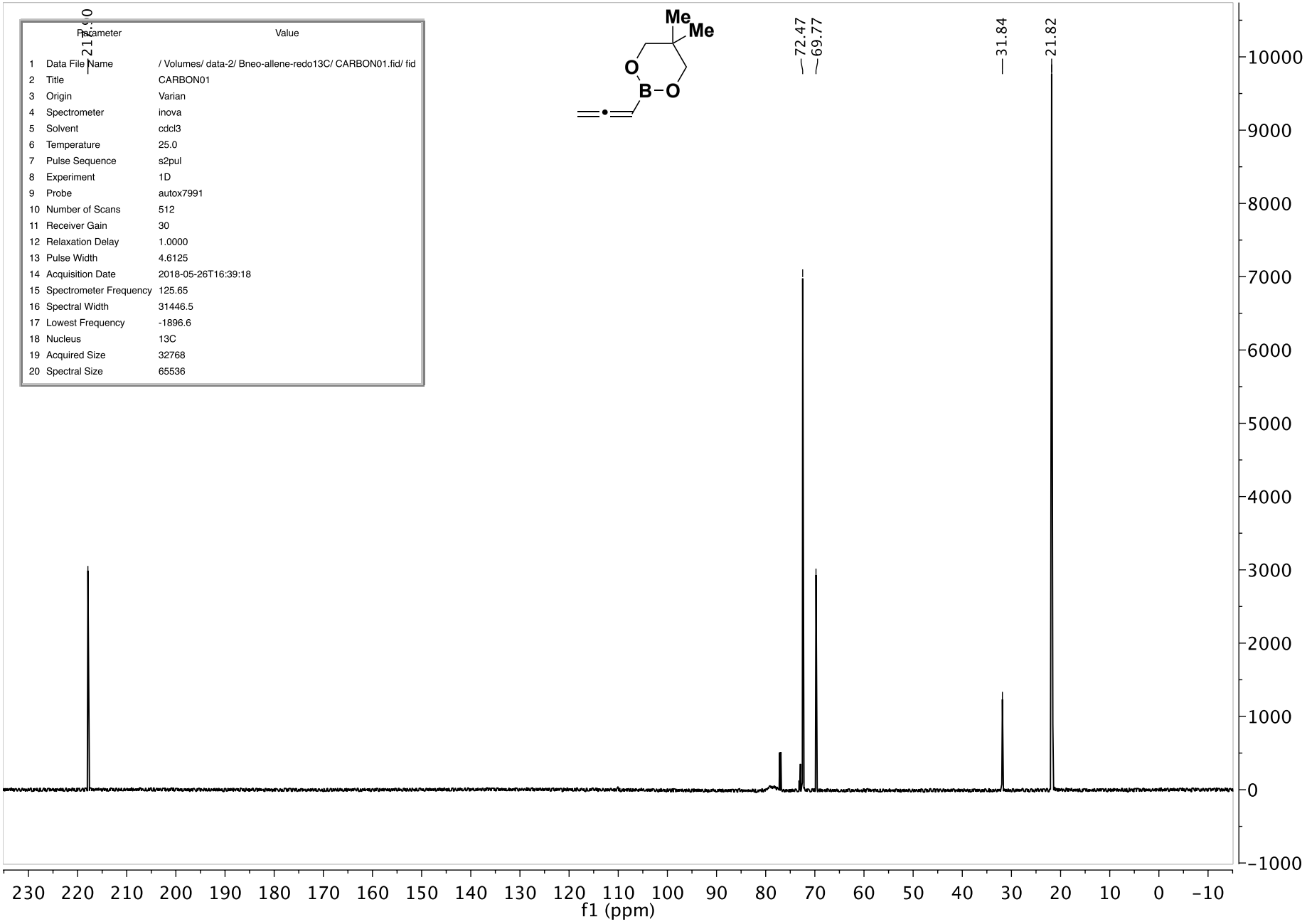

	Parameter	Value
1	Data File Name	/ Volumes/ data-2/ Bneo-allene-redo13C/ CARBON01.fid/ fid
2	Title	CARBON01
3	Origin	Varian
4	Spectrometer	inova
5	Solvent	cdcl3
6	Temperature	25.0
7	Pulse Sequence	s2pul
8	Experiment	1D
9	Probe	autox7991
10	Number of Scans	512
11	Receiver Gain	30
12	Relaxation Delay	1.0000
13	Pulse Width	4.6125
14	Acquisition Date	2018-05-26T16:39:18
15	Spectrometer Frequency	125.65
16	Spectral Width	31446.5
17	Lowest Frequency	-1896.6
18	Nucleus	13C
19	Acquired Size	32768
20	Spectral Size	65536

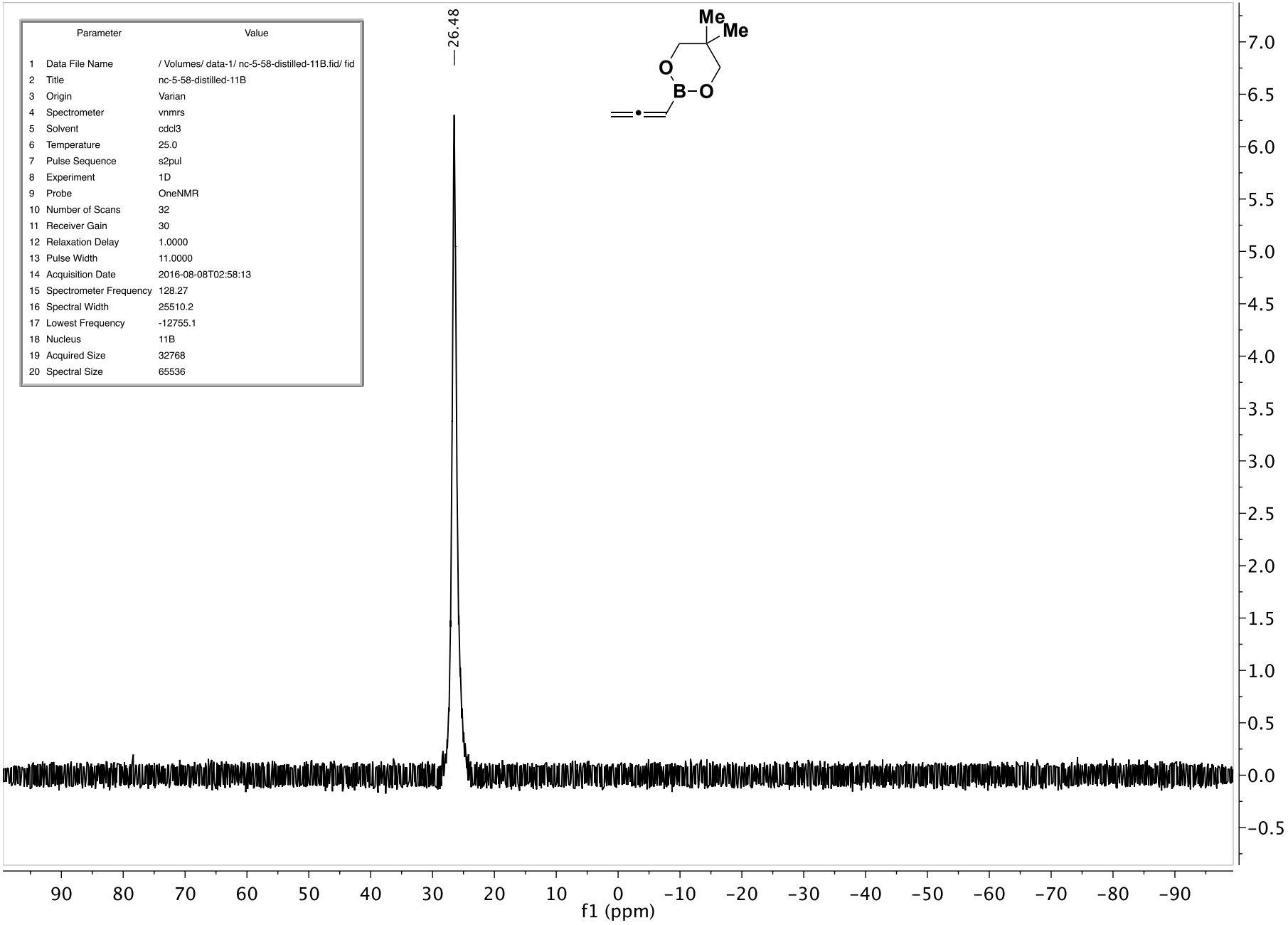
Parameter Value
1 Data File Name / Volumes/ data-1/ nc-5-58-distilled-11B.fid/ fid
2 Title nc-5-58-distilled-11B
3 Origin Varian
4 Spectrometer vnmrs
5 Solvent cdcl3
6 Temperature 25.0
7 Pulse Sequence s2pul
8 Experiment 1D
9 Probe OneNMR
10 Number of Scans 32
11 Receiver Gain 30
12 Relaxation Delay 1.0000
13 Pulse Width 11.0000
14 Acquisition Date 2016-08-08T02:58:13
15 Spectrometer Frequency 128.27
16 Spectral Width 25510.2
17 Lowest Frequency -12755.1
18 Nucleus 11B
19 Acquired Size 32768
20 Spectral Size 65536
26.48
Me
Me
O
B–O
7.0
6.5
6.0
5.5
5.0
4.5
4.0
3.5
3.0
2.5
2.0
1.5
1.0
0.5
0.0
-0.5
90 80 70 60 50 40 30 20 10 0 -10 -20 -30 -40 -50 -60 -70 -80 -90
f1 (ppm)

	Parameter	Value
1	Data File Name	/ Volumes/ data/ nc-Me-allene-Bneo/ PROTON01.fid/ fid
2	Title	PROTON01
3	Origin	Varian
4	Spectrometer	inova
5	Solvent	cdcl3
6	Temperature	25.0
7	Pulse Sequence	s2pul
8	Experiment	1D
9	Probe	autox7991
10	Number of Scans	8
11	Receiver Gain	28
12	Relaxation Delay	1.0000
13	Pulse Width	5.8000
14	Acquisition Date	2018-05-27T05:22:47
15	Spectrometer Frequency	499.64
16	Spectral Width	8000.0
17	Lowest Frequency	-1015.2
18	Nucleus	1H
19	Acquired Size	24000
20	Spectral Size	65536

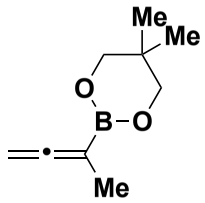

	Parameter	Value
1	Data File Name	/ Volumes/ data/ nc-Me-allene-Bneo/ CARBON01.fid/ fid
2	Title	CARBON01
3	Origin	Varian
4	Spectrometer	inova
5	Solvent	cdcl3
6	Temperature	25.0
7	Pulse Sequence	s2pul
8	Experiment	1D
9	Probe	autox7991
10	Number of Scans	2500
11	Receiver Gain	30
12	Relaxation Delay	1.0000
13	Pulse Width	4.6125
14	Acquisition Date	2018-05-27T05:23:38
15	Spectrometer Frequency	125.65
16	Spectral Width	31446.5
17	Lowest Frequency	-1888.2
18	Nucleus	13C
19	Acquired Size	32768
20	Spectral Size	65536

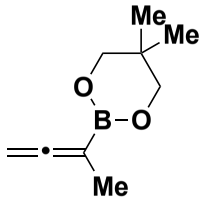

72.65
69.94
31.87
21.95
15.20

f1 (ppm)

	Parameter	Value
1	Data File Name	/ Volumes/ data-1/ nc-sub-allene-bneo.fid/ fid
2	Title	nc-sub-allene-bneo
3	Origin	Varian
4	Spectrometer	vnmrs
5	Solvent	cdcl3
6	Temperature	50.0
7	Pulse Sequence	s2pul
8	Experiment	1D
9	Probe	OneNMR
10	Number of Scans	20
11	Receiver Gain	30
12	Relaxation Delay	1.0000
13	Pulse Width	11.0000
14	Acquisition Date	2018-05-27T17:22:02
15	Spectrometer Frequency	128.27
16	Spectral Width	25510.2
17	Lowest Frequency	-12755.1
18	Nucleus	11B
19	Acquired Size	32768
20	Spectral Size	65536

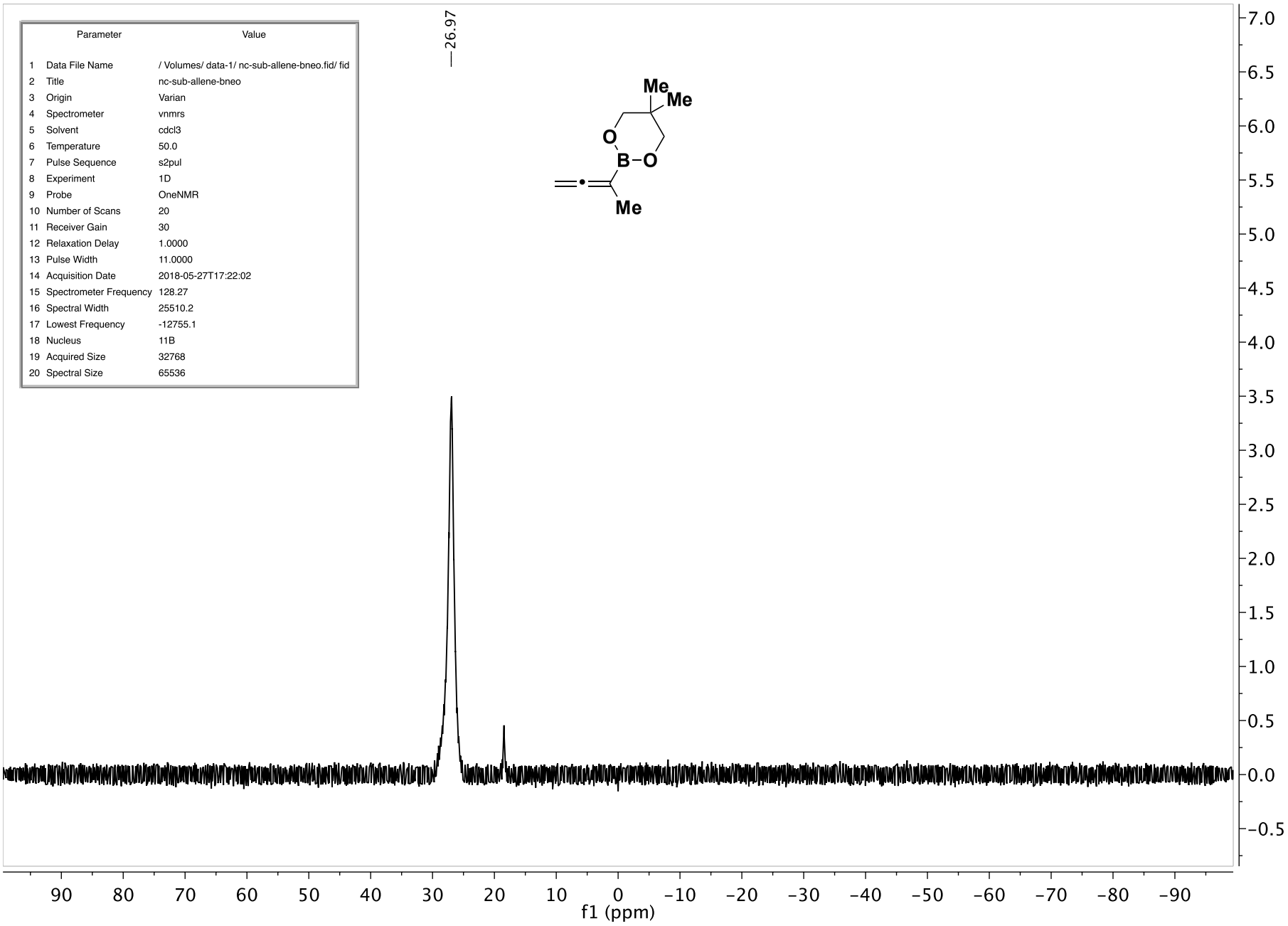

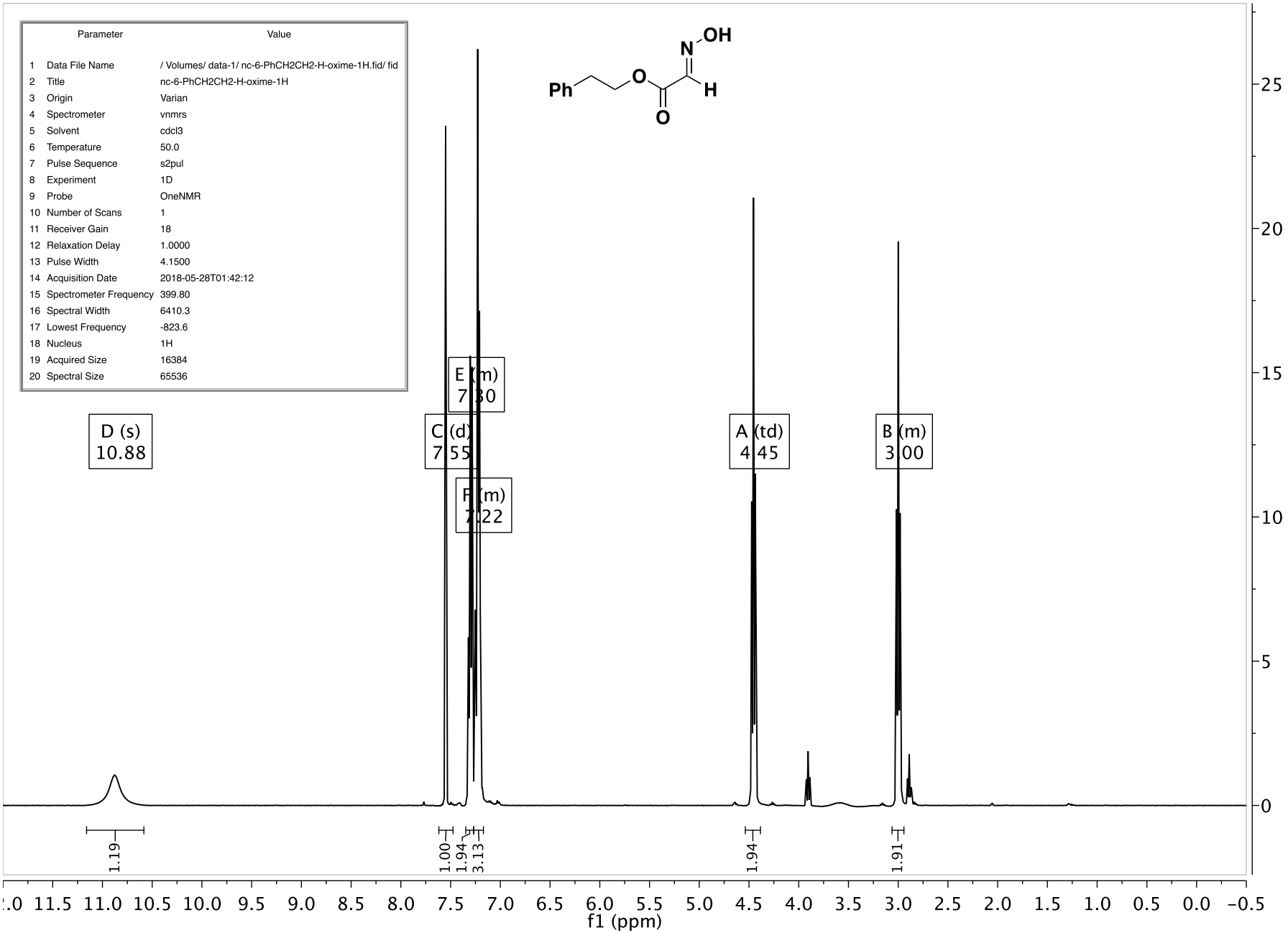
Parameter Value
1 Data File Name / Volumes/ data-1/ nc-6-PhCH2CH2-H-oxime-1H.fid/ fid
2 Title nc-6-PhCH2CH2-H-oxime-1H
3 Origin Varian
4 Spectrometer vnmrs
5 Solvent cdcl3
6 Temperature 50.0
7 Pulse Sequence s2pul
8 Experiment 1D
9 Probe OneNMR
10 Number of Scans 1
11 Receiver Gain 18
12 Relaxation Delay 1.0000
13 Pulse Width 4.1500
14 Acquisition Date 2018-05-28T01:42:12
15 Spectrometer Frequency 399.80
16 Spectral Width 6410.3
17 Lowest Frequency -823.6
18 Nucleus 1H
19 Acquired Size 16384
20 Spectral Size 65536
OH
N
Ph
O
H
O
D (s)
10.88
C (d)
7.55
E (m)
7.30
F (m)
7.22
A (td)
4.45
B (m)
3.00
1.19
1.00
1.94
3.13
1.94
1.91
25
20
15
10
5
0
11.5 11.0 10.5 10.0 9.5 9.0 8.5 8.0 7.5 7.0 6.5 6.0 5.5 5.0 4.5 4.0 3.5 3.0 2.5 2.0 1.5 1.0 0.5 0.0 -0.5
f1 (ppm)

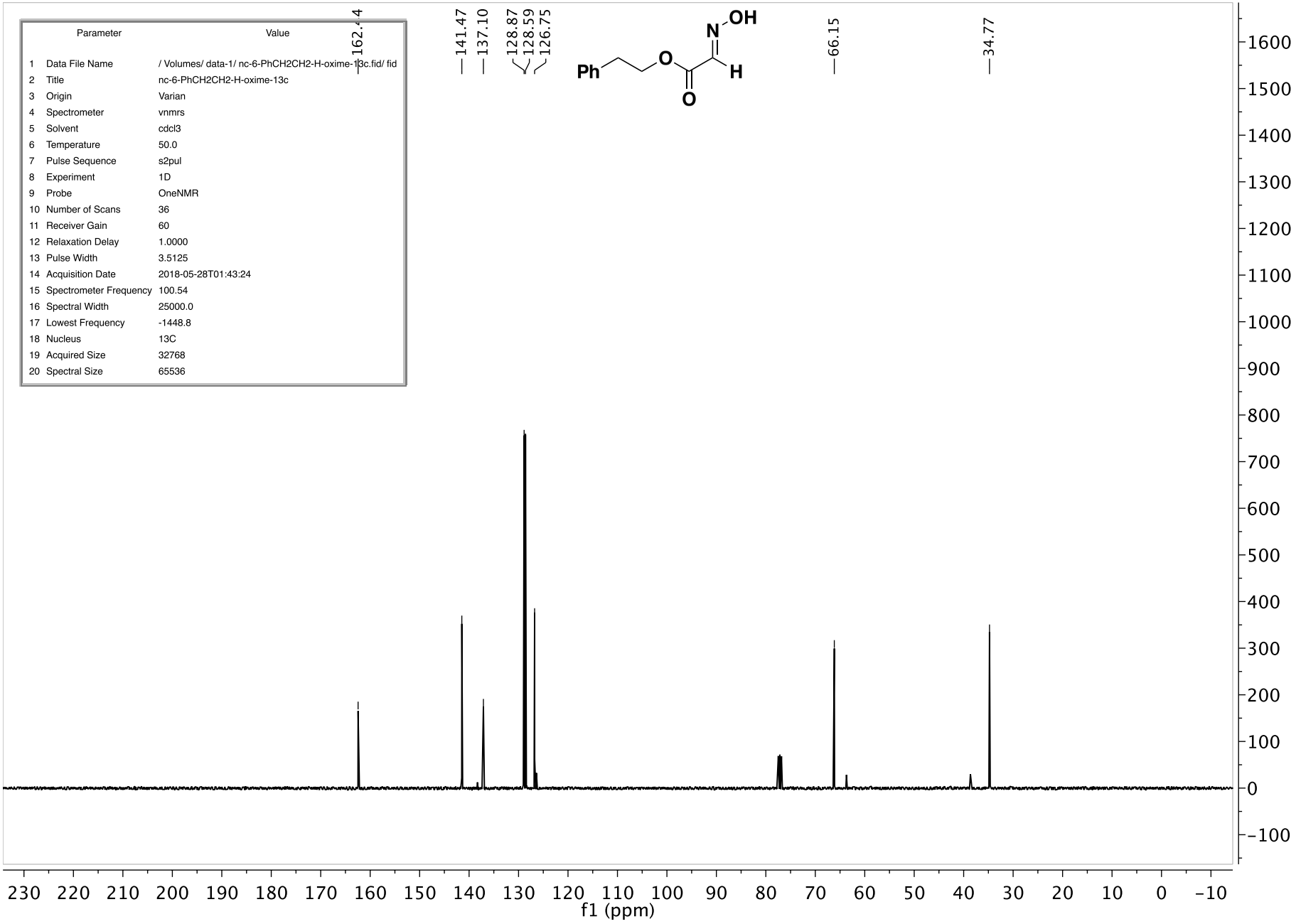
Parameter Value
1 Data File Name / Volumes/ data-1/ nc-6-PhCH2CH2-H-oxime-13c.fid/ fid
2 Title nc-6-PhCH2CH2-H-oxime-13c
3 Origin Varian
4 Spectrometer vnmrs
5 Solvent cdcl3
6 Temperature 50.0
7 Pulse Sequence s2pul
8 Experiment 1D
9 Probe OneNMR
10 Number of Scans 36
11 Receiver Gain 60
12 Relaxation Delay 1.0000
13 Pulse Width 3.5125
14 Acquisition Date 2018-05-28T01:43:24
15 Spectrometer Frequency 100.54
16 Spectral Width 25000.0
17 Lowest Frequency -1448.8
18 Nucleus 13C
19 Acquired Size 32768
20 Spectral Size 65536
162.44
141.47
137.10
128.87
128.59
126.75
66.15
34.77
Ph
O
N
OH
H
O
1600
1500
1400
1300
1200
1100
1000
900
800
700
600
500
400
300
200
100
0
-100
230 220 210 200 190 180 170 160 150 140 130 120 110 100 90 80 70 60 50 40 30 20 10 0 -10
f1 (ppm)

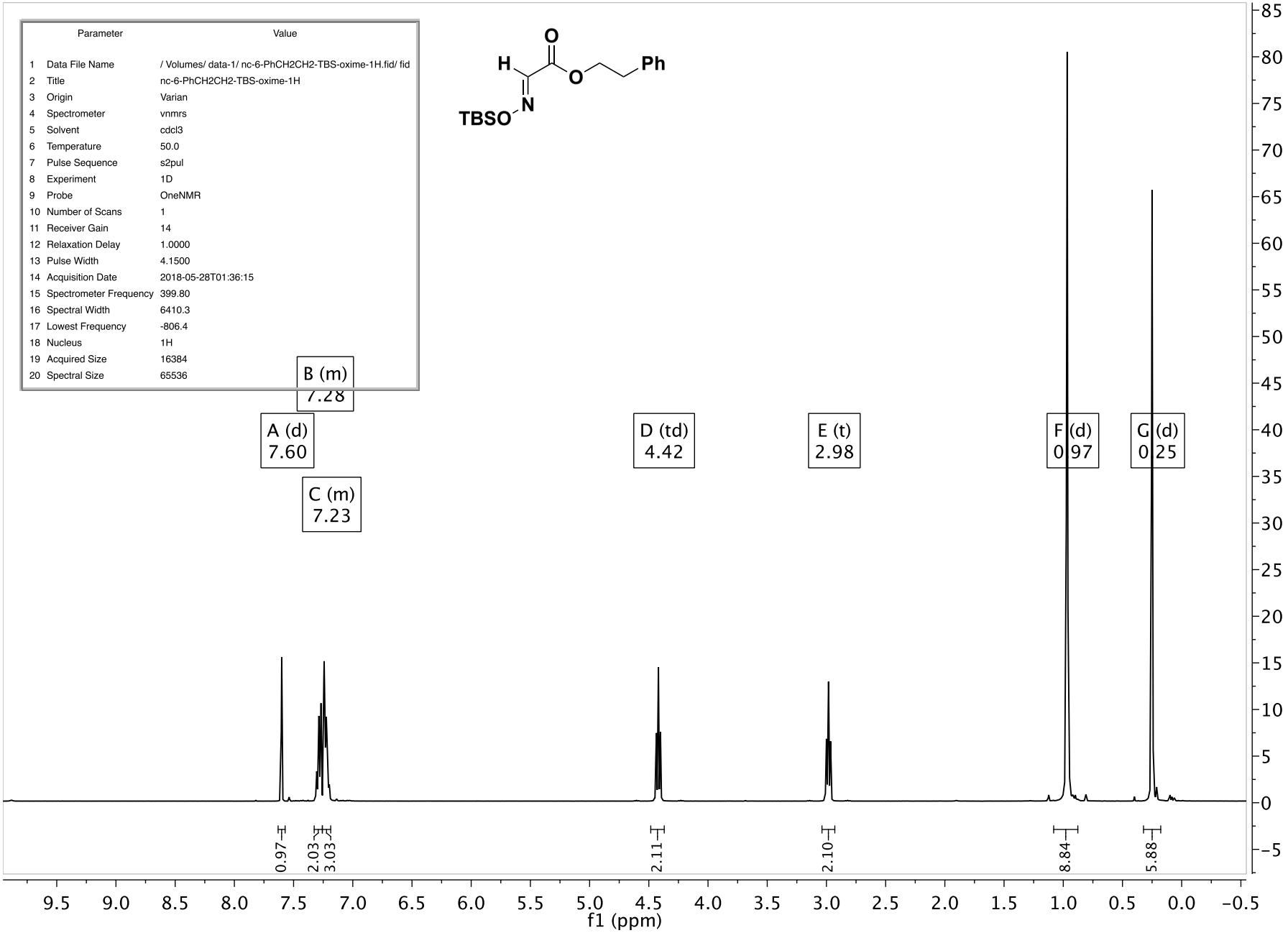
Parameter Value
1 Data File Name / Volumes/ data-1/ nc-6-PhCH2CH2-TBS-oxime-1H.fid/ fid
2 Title nc-6-PhCH2CH2-TBS-oxime-1H
3 Origin Varian
4 Spectrometer vnmrs
5 Solvent cdcl3
6 Temperature 50.0
7 Pulse Sequence s2pul
8 Experiment 1D
9 Probe OneNMR
10 Number of Scans 1
11 Receiver Gain 14
12 Relaxation Delay 1.0000
13 Pulse Width 4.1500
14 Acquisition Date 2018-05-28T01:36:15
15 Spectrometer Frequency 399.80
16 Spectral Width 6410.3
17 Lowest Frequency -806.4
18 Nucleus 1H
19 Acquired Size 16384
20 Spectral Size 65536
O
H
O
Ph
N
TBSO
B (m)
7.28
A (d)
7.60
C (m)
7.23
D (td)
4.42
E (t)
2.98
F (d)
0.97
G (d)
0.25
0.97
2.03
3.03
2.11
2.10
8.84
5.88
9.5 9.0 8.5 8.0 7.5 7.0 6.5 6.0 5.5 5.0 4.5 4.0 3.5 3.0 2.5 2.0 1.5 1.0 0.5 0.0 -0.5
f1 (ppm)
85 80 75 70 65 60 55 50 45 40 35 30 25 20 15 10 5 0 -5

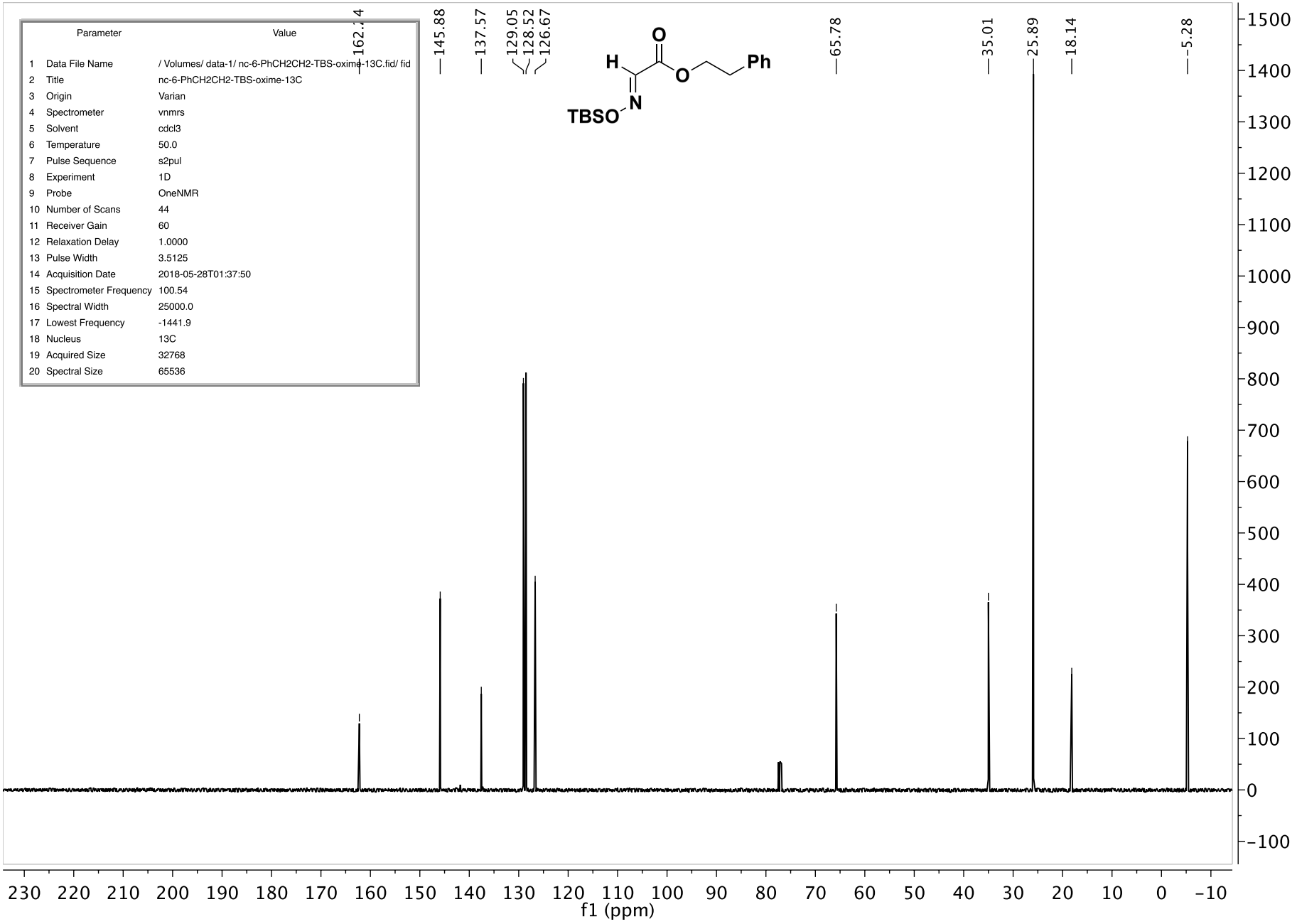
Parameter Value
1 Data File Name / Volumes/ data-1/ nc-6-PhCH2CH2-TBS-oxime-13C.fid/ fid
2 Title nc-6-PhCH2CH2-TBS-oxime-13C
3 Origin Varian
4 Spectrometer vnmrs
5 Solvent cdcl3
6 Temperature 50.0
7 Pulse Sequence s2pul
8 Experiment 1D
9 Probe OneNMR
10 Number of Scans 44
11 Receiver Gain 60
12 Relaxation Delay 1.0000
13 Pulse Width 3.5125
14 Acquisition Date 2018-05-28T01:37:50
15 Spectrometer Frequency 100.54
16 Spectral Width 25000.0
17 Lowest Frequency -1441.9
18 Nucleus 13C
19 Acquired Size 32768
20 Spectral Size 65536
162.24
145.88
137.57
129.05
128.52
126.67
65.78
35.01
25.89
18.14
-5.28
O
H
O
Ph
N
TBSO
1500
1400
1300
1200
1100
1000
900
800
700
600
500
400
300
200
100
0
-100
230 220 210 200 190 180 170 160 150 140 130 120 110 100 90 80 70 60 50 40 30 20 10 0 -10
f1 (ppm)

	Parameter	Value
1	Data File Name	/ Volumes/ nmr/ nc-5-141-repure/ 1/ fid
2	Title	nc-5-141-repure.1.fid
3	Origin	Bruker BioSpin GmbH
4	Solvent	CDCl3
5	Temperature	295.0
6	Pulse Sequence	zg30
7	Probe	Z122623_0045 (CPP BBO 400S1 BB-H&F-D-05 Z)
8	Number of Scans	16
9	Receiver Gain	142.8
10	Relaxation Delay	1.0000
11	Pulse Width	11.7000
12	Acquisition Time	4.0894
13	Acquisition Date	2016-11-07T17:25:49
14	Spectrometer Frequency	400.13
15	Spectral Width	8012.8
16	Lowest Frequency	-1545.6
17	Nucleus	1H
18	Acquired Size	32768
19	Spectral Size	65536

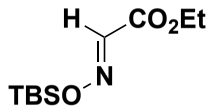

	Parameter	Value
1	Data File Name	/ Volumes/ data/ diphenethyl-ester-recrys/ PROTON01.fid/ fid
2	Title	PROTON01
3	Origin	Varian
4	Spectrometer	inova
5	Solvent	cdcl3
6	Temperature	25.0
7	Pulse Sequence	s2pul
8	Experiment	1D
9	Probe	autox7991
10	Number of Scans	8
11	Receiver Gain	32
12	Relaxation Delay	1.0000
13	Pulse Width	5.8000
14	Acquisition Date	2018-06-01T07:05:57
15	Spectrometer Frequency	499.64
16	Spectral Width	8000.0
17	Lowest Frequency	-1016.2
18	Nucleus	1H
19	Acquired Size	24000
20	Spectral Size	65536

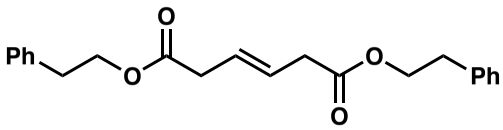

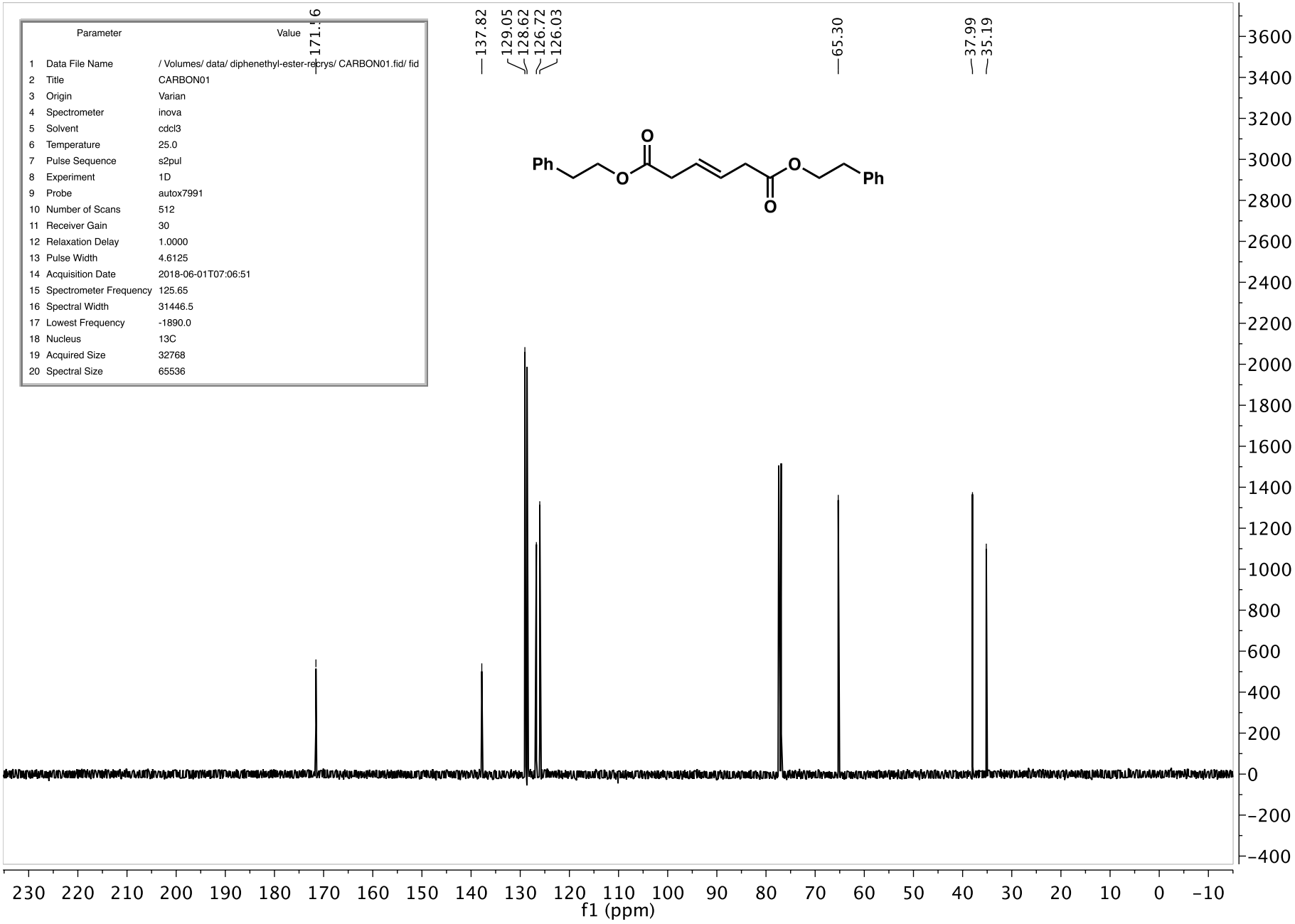
Parameter Value
1 Data File Name / Volumes/ data/ diphenethyl-ester-recrys/ CARBON01.fid/ fid
2 Title CARBON01
3 Origin Varian
4 Spectrometer inova
5 Solvent cdcl3
6 Temperature 25.0
7 Pulse Sequence s2pul
8 Experiment 1D
9 Probe autox7991
10 Number of Scans 512
11 Receiver Gain 30
12 Relaxation Delay 1.0000
13 Pulse Width 4.6125
14 Acquisition Date 2018-06-01T07:06:51
15 Spectrometer Frequency 125.65
16 Spectral Width 31446.5
17 Lowest Frequency -1890.0
18 Nucleus 13C
19 Acquired Size 32768
20 Spectral Size 65536
171.16
137.82
129.05
128.62
126.72
126.03
65.30
37.99
35.19
Ph
O
O
O
O
O
Ph
3600
3400
3200
3000
2800
2600
2400
2200
2000
1800
1600
1400
1200
1000
800
600
400
200
0
-200
-400
230 220 210 200 190 180 170 160 150 140 130 120 110 100 90 80 70 60 50 40 30 20 10 0 -10
f1 (ppm)

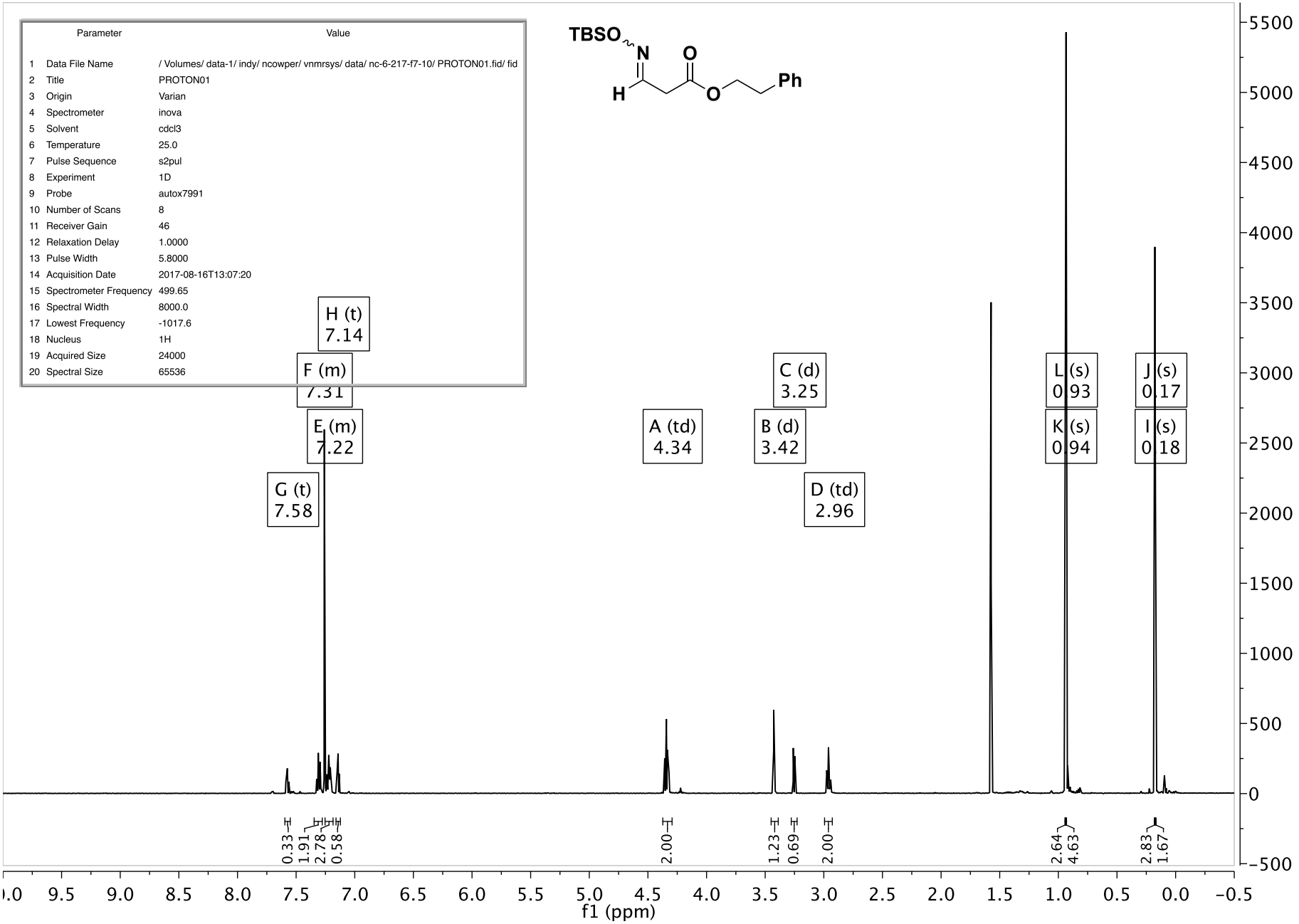
Parameter Value
1 Data File Name / Volumes/ data-1/ indy/ ncowper/ vnmrsys/ data/ nc-6-217-f7-10/ PROTON01.fid/ fid
2 Title PROTON01
3 Origin Varian
4 Spectrometer inova
5 Solvent cdcl3
6 Temperature 25.0
7 Pulse Sequence s2pul
8 Experiment 1D
9 Probe autox7991
10 Number of Scans 8
11 Receiver Gain 46
12 Relaxation Delay 1.0000
13 Pulse Width 5.8000
14 Acquisition Date 2017-08-16T13:07:20
15 Spectrometer Frequency 499.65
16 Spectral Width 8000.0
17 Lowest Frequency -1017.6
18 Nucleus 1H
19 Acquired Size 24000
20 Spectral Size 65536
TBSO
N
O
H
O
Ph
H (t) 7.14
F (m) 7.31
E (m) 7.22
G (t) 7.58
A (td) 4.34
C (d) 3.25
B (d) 3.42
D (td) 2.96
L (s) 0.93
K (s) 0.94
J (s) 0.17
I (s) 0.18
0.33
1.91
2.78
0.58
2.00
1.23
0.69
2.00
2.64
4.63
2.83
1.67
f1 (ppm)

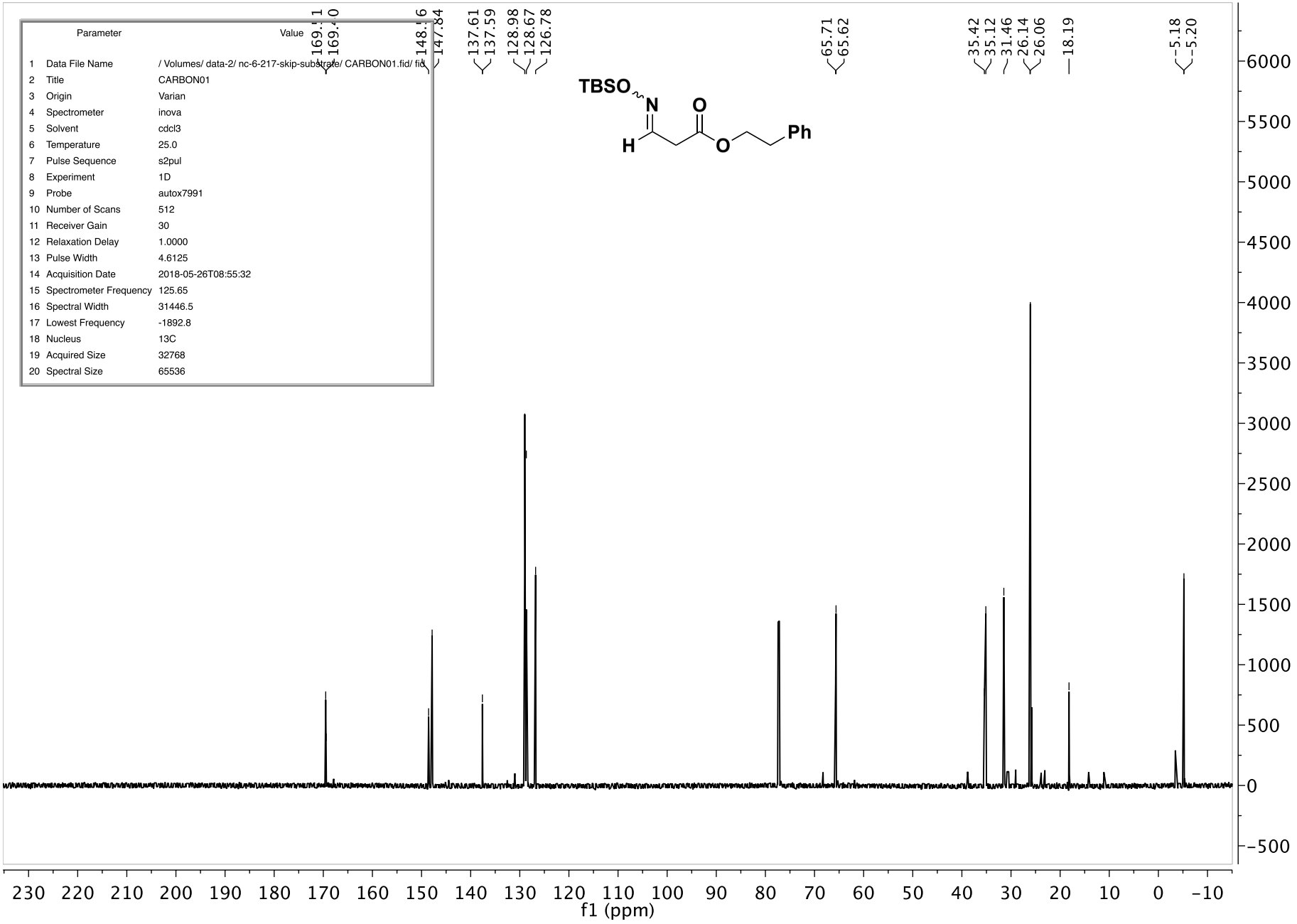
Parameter Value
1 Data File Name / Volumes/ data-2/ nc-6-217-skip-substrate/ CARBON01.fid/ fid
2 Title CARBON01
3 Origin Varian
4 Spectrometer inova
5 Solvent cdcl3
6 Temperature 25.0
7 Pulse Sequence s2pul
8 Experiment 1D
9 Probe autox7991
10 Number of Scans 512
11 Receiver Gain 30
12 Relaxation Delay 1.0000
13 Pulse Width 4.6125
14 Acquisition Date 2018-05-26T08:55:32
15 Spectrometer Frequency 125.65
16 Spectral Width 31446.5
17 Lowest Frequency -1892.8
18 Nucleus 13C
19 Acquired Size 32768
20 Spectral Size 65536
169.11
169.40
148.16
147.84
137.61
137.59
128.98
128.67
126.78
65.71
65.62
35.42
35.12
31.46
26.14
26.06
18.19
5.18
5.20
TBSO
N
O
H
O
Ph
6000
5500
5000
4500
4000
3500
3000
2500
2000
1500
1000
500
0
-500
230 220 210 200 190 180 170 160 150 140 130 120 110 100 90 80 70 60 50 40 30 20 10 0 -10
f1 (ppm)

	Parameter	Value
1	Data File Name	/ Volumes/ nmr/ nc-4-130-c2-f14-25/ 1/ fid
2	Title	nc-4-130-c2-f14-25.1.fid
3	Origin	Bruker BioSpin GmbH
4	Solvent	CDCl3
5	Temperature	295.0
6	Pulse Sequence	zg30
7	Probe	Z122623_0045 (CPP BBO 400S1 BB-H&F-D-05 Z)
8	Number of Scans	16
9	Receiver Gain	142.8
10	Relaxation Delay	1.0000
11	Pulse Width	11.7000
12	Acquisition Time	4.0894
13	Acquisition Date	2016-04-29T15:36:28
14	Spectrometer Frequency	400.13
15	Spectral Width	8012.8
16	Lowest Frequency	-1545.6
17	Nucleus	1H
18	Acquired Size	32768
19	Spectral Size	65536

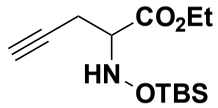

	Parameter	Value
1	Data File Name	/ Volumes/ nmr/ phenethyl-oxime-alkyne/ 1/ fid
2	Title	phenethyl-oxime-alkyne.1.fid
3	Origin	Bruker BioSpin GmbH
4	Solvent	CDCl3
5	Temperature	297.1
6	Pulse Sequence	zg30
7	Probe	Z122623_0045 (CPP BBO 400S1 BB-H&F-D-05 Z)
8	Number of Scans	16
9	Receiver Gain	30.3
10	Relaxation Delay	1.0000
11	Pulse Width	11.7000
12	Acquisition Time	4.0894
13	Acquisition Date	2018-06-02T06:54:36
14	Spectrometer Frequency	400.13
15	Spectral Width	8012.8
16	Lowest Frequency	-1552.3
17	Nucleus	1H
18	Acquired Size	32768
19	Spectral Size	65536
20	Absolute Reference	

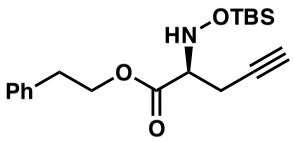

C (m) 7.22
B (m) 7.29
A (d) 5.58
D (td) 4.39
E (dt) 3.62
F (t) 2.97
G (m) 2.52
H (t) 1.97
I (s) 0.88
J (d) 0.10

2.00
3.06
1.00
2.04
1.01
2.04
1.99
0.92
9.18
6.01

f1 (ppm)

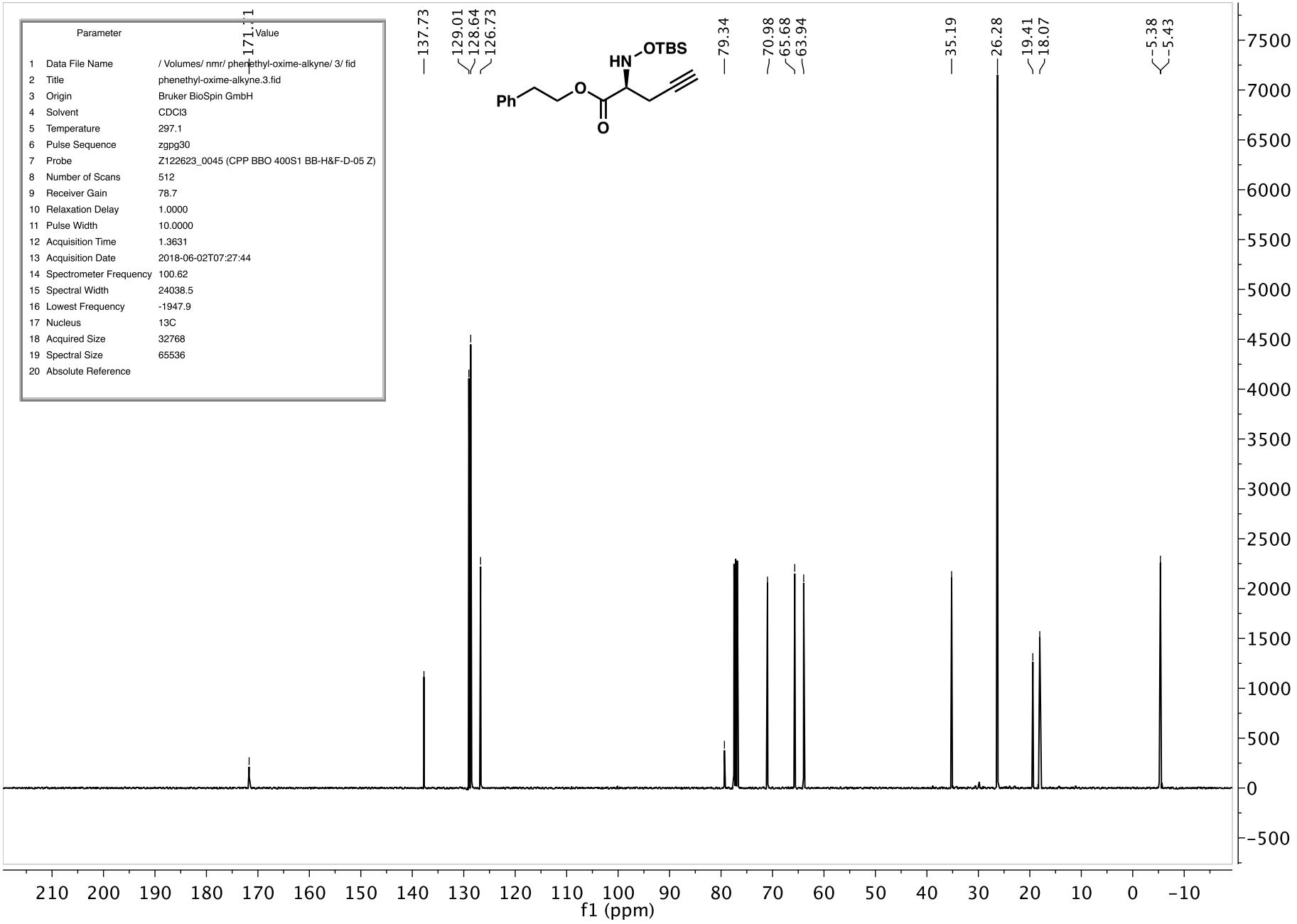
Parameter Value
1 Data File Name / Volumes/ nmr/ phenethyl-oxime-alkyne/ 3/ fid
2 Title phenethyl-oxime-alkyne.3.fid
3 Origin Bruker BioSpin GmbH
4 Solvent CDCl3
5 Temperature 297.1
6 Pulse Sequence zgpg30
7 Probe Z122623_0045 (CPP BBO 400S1 BB-H&F-D-05 Z)
8 Number of Scans 512
9 Receiver Gain 78.7
10 Relaxation Delay 1.0000
11 Pulse Width 10.0000
12 Acquisition Time 1.3631
13 Acquisition Date 2018-06-02T07:27:44
14 Spectrometer Frequency 100.62
15 Spectral Width 24038.5
16 Lowest Frequency -1947.9
17 Nucleus 13C
18 Acquired Size 32768
19 Spectral Size 65536
20 Absolute Reference
171.11
137.73
129.01
128.64
126.73
79.34
70.98
65.68
63.94
35.19
26.28
19.41
18.07
-5.38
-5.43
HN
OTBS
Ph
O
O
f1 (ppm)

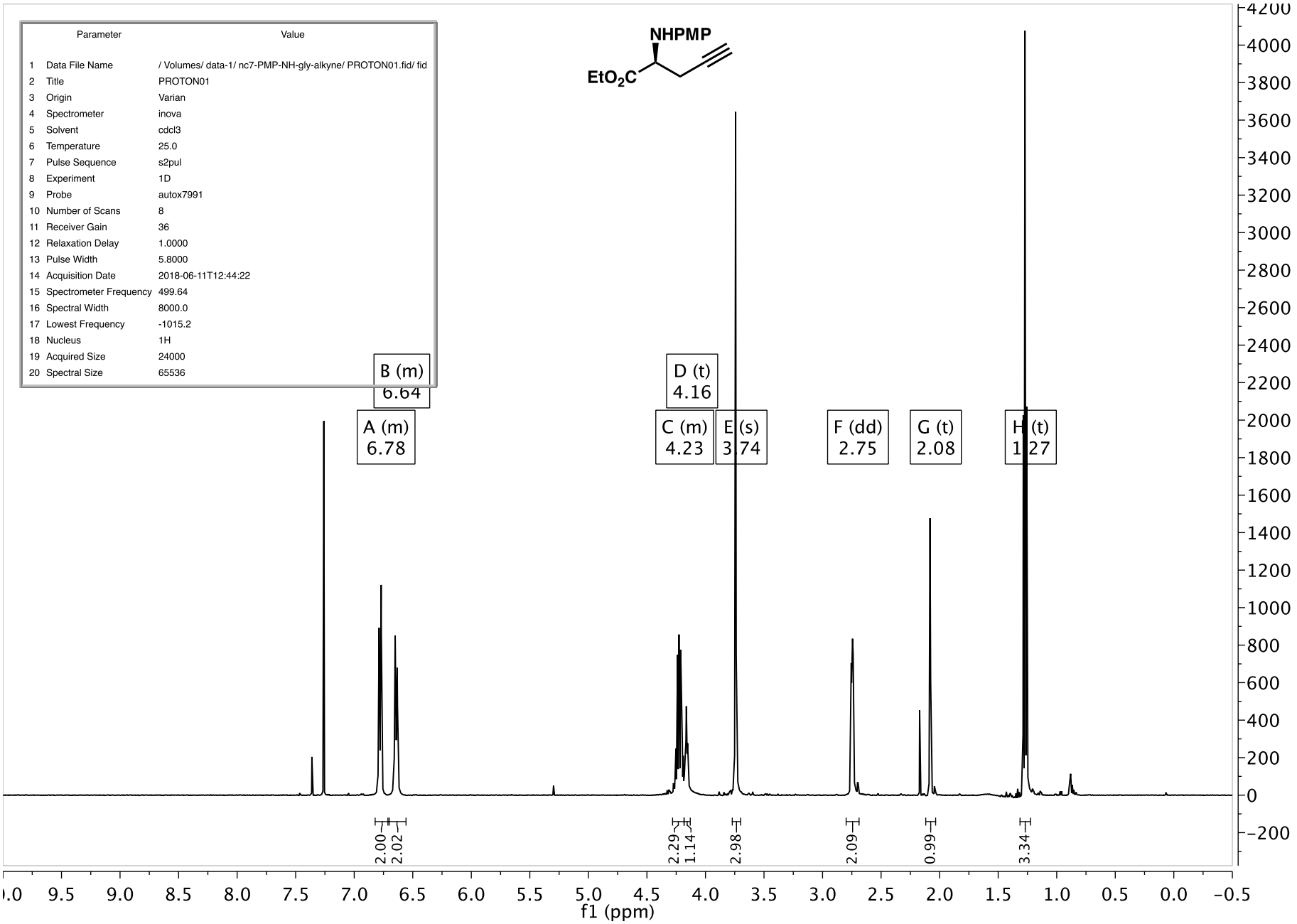
Parameter Value
1 Data File Name / Volumes/ data-1/ nc7-PMP-NH-gly-alkyne/ PROTON01.fid/ fid
2 Title PROTON01
3 Origin Varian
4 Spectrometer inova
5 Solvent cdcl3
6 Temperature 25.0
7 Pulse Sequence s2pul
8 Experiment 1D
9 Probe autox7991
10 Number of Scans 8
11 Receiver Gain 36
12 Relaxation Delay 1.0000
13 Pulse Width 5.8000
14 Acquisition Date 2018-06-11T12:44:22
15 Spectrometer Frequency 499.64
16 Spectral Width 8000.0
17 Lowest Frequency -1015.2
18 Nucleus 1H
19 Acquired Size 24000
20 Spectral Size 65536
NHPMP
EtO2C
B (m) 6.64
A (m) 6.78
D (t) 4.16
C (m) 4.23
E (s) 3.74
F (dd) 2.75
G (t) 2.08
H (t) 1.27
2.00
2.02
2.29
1.14
2.98
2.09
0.99
3.34
f1 (ppm)

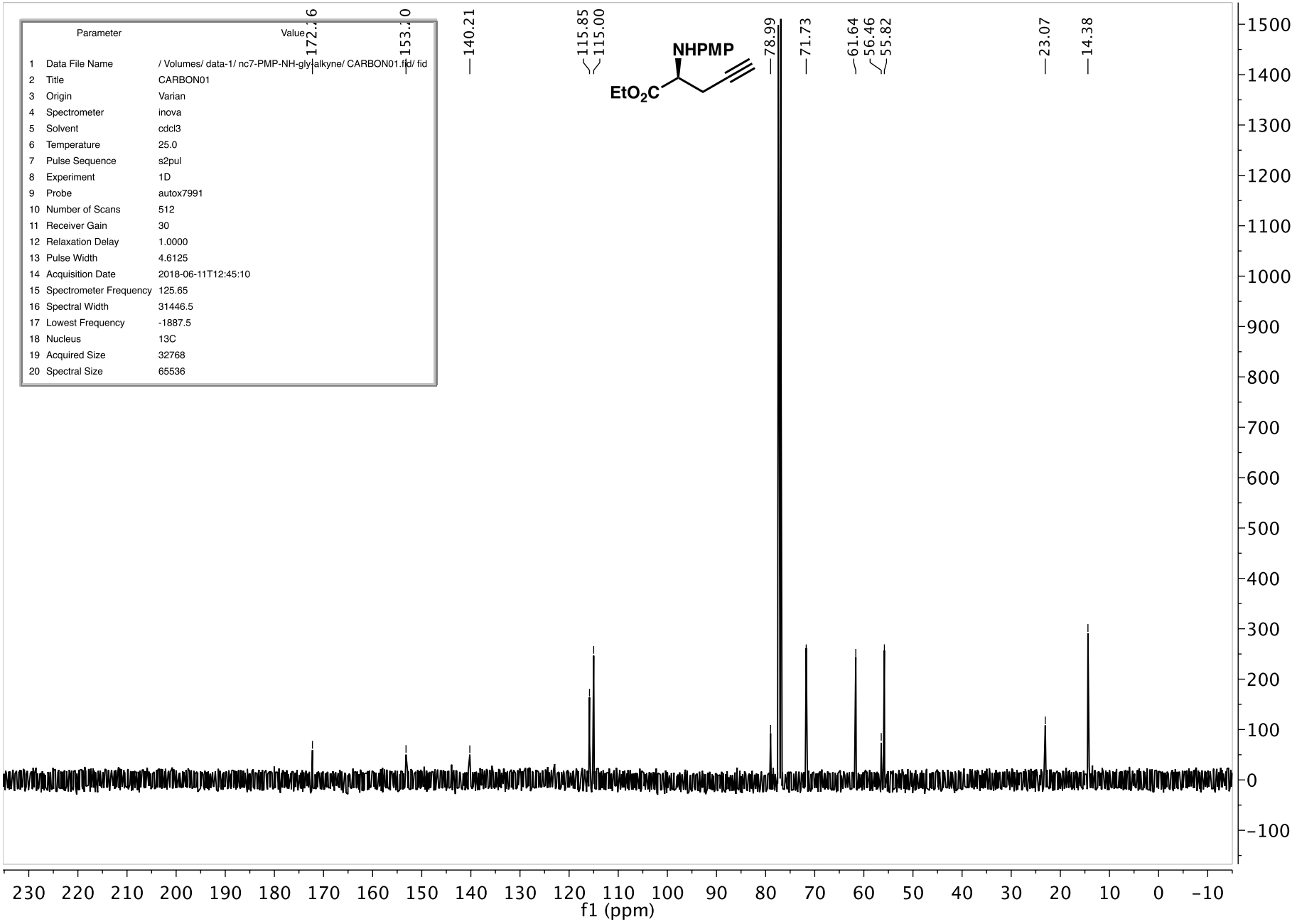
Parameter Value
1 Data File Name / Volumes/ data-1/ nc7-PMP-NH-gly-alkyne/ CARBON01.fid/ fid
2 Title CARBON01
3 Origin Varian
4 Spectrometer inova
5 Solvent cdcl3
6 Temperature 25.0
7 Pulse Sequence s2pul
8 Experiment 1D
9 Probe autox7991
10 Number of Scans 512
11 Receiver Gain 30
12 Relaxation Delay 1.0000
13 Pulse Width 4.6125
14 Acquisition Date 2018-06-11T12:45:10
15 Spectrometer Frequency 125.65
16 Spectral Width 31446.5
17 Lowest Frequency -1887.5
18 Nucleus 13C
19 Acquired Size 32768
20 Spectral Size 65536
172.26
153.10
140.21
115.85
115.00
NHPMP
EtO2C
78.99
71.73
61.64
56.46
55.82
23.07
14.38
f1 (ppm)

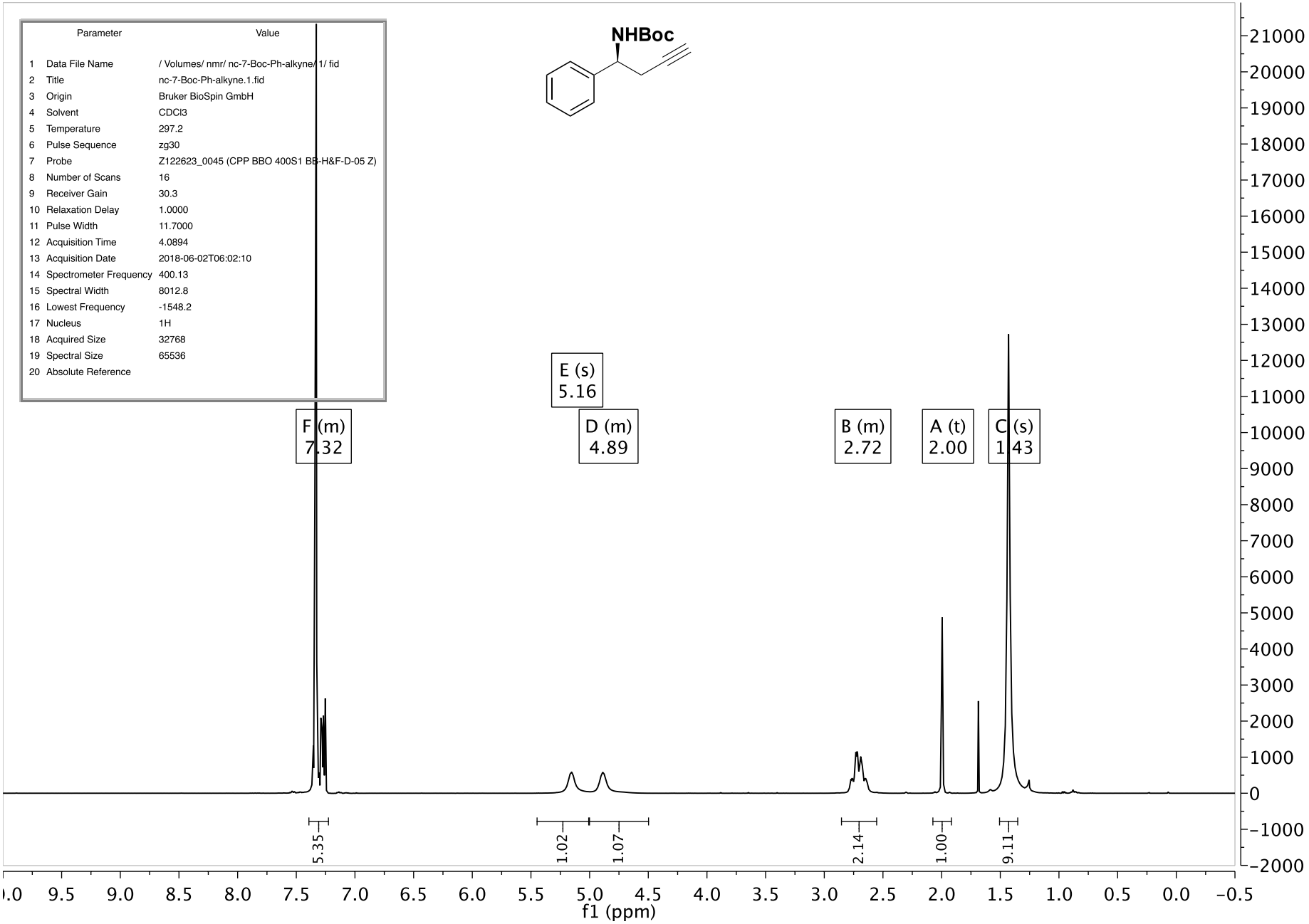

	Parameter	Value
1	Data File Name	/ Volumes/ nmr/ nc-7-Boc-Ph-alkyne/1/ fid
2	Title	nc-7-Boc-Ph-alkyne.1.fid
3	Origin	Bruker BioSpin GmbH
4	Solvent	CDCl3
5	Temperature	297.2
6	Pulse Sequence	zg30
7	Probe	Z122623_0045 (CPP BBO 400S1 BB-H&F-D-05 Z)
8	Number of Scans	16
9	Receiver Gain	30.3
10	Relaxation Delay	1.0000
11	Pulse Width	11.7000
12	Acquisition Time	4.0894
13	Acquisition Date	2018-06-02T06:02:10
14	Spectrometer Frequency	400.13
15	Spectral Width	8012.8
16	Lowest Frequency	-1548.2
17	Nucleus	1H
18	Acquired Size	32768
19	Spectral Size	65536
20	Absolute Reference	

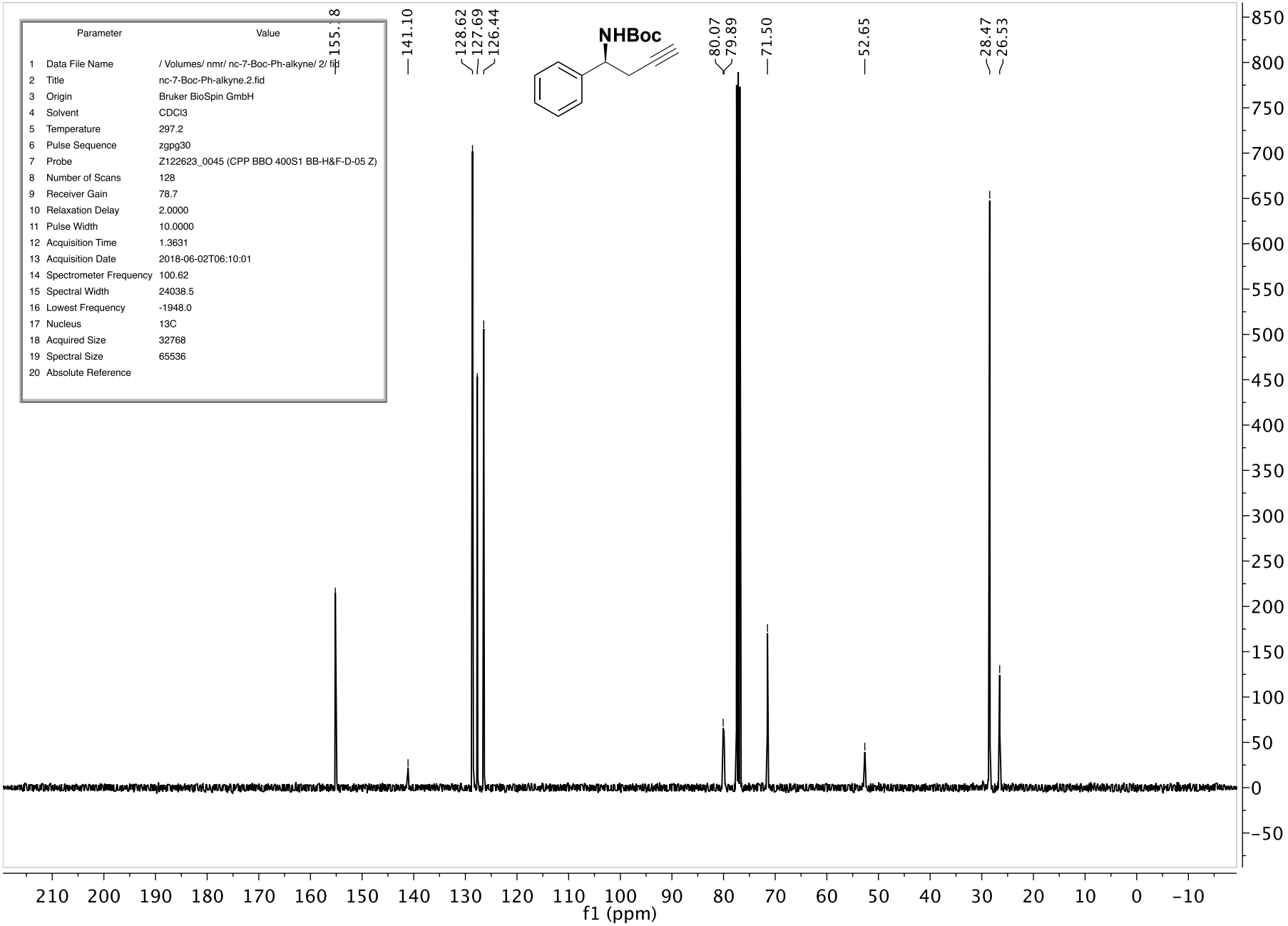
Parameter Value
1 Data File Name / Volumes/ nmr/ nc-7-Boc-Ph-alkyne/ 2/ fid
2 Title nc-7-Boc-Ph-alkyne.2.fid
3 Origin Bruker BioSpin GmbH
4 Solvent CDCl3
5 Temperature 297.2
6 Pulse Sequence zgpg30
7 Probe Z122623_0045 (CPP BBO 400S1 BB-H&F-D-05 Z)
8 Number of Scans 128
9 Receiver Gain 78.7
10 Relaxation Delay 2.0000
11 Pulse Width 10.0000
12 Acquisition Time 1.3631
13 Acquisition Date 2018-06-02T06:10:01
14 Spectrometer Frequency 100.62
15 Spectral Width 24038.5
16 Lowest Frequency -1948.0
17 Nucleus 13C
18 Acquired Size 32768
19 Spectral Size 65536
20 Absolute Reference
155.18
141.10
128.62
127.69
126.44
NHBoc
80.07
79.89
71.50
52.65
28.47
26.53
f1 (ppm)

	Parameter	Value
1	Data File Name	/ Volumes/ nmr/ nc-7-Boc-PMP-alkyne/ 3/ fid
2	Title	nc-7-Boc-PMP-alkyne.3.fid
3	Origin	Bruker BioSpin GmbH
4	Solvent	CDCl3
5	Temperature	297.1
6	Pulse Sequence	zg30
7	Probe	Z122623_0045 (CPP BBO 400S1 BB-H&F-D-05 Z)
8	Number of Scans	16
9	Receiver Gain	30.3
10	Relaxation Delay	1.0000
11	Pulse Width	11.7000
12	Acquisition Time	4.0894
13	Acquisition Date	2018-06-02T05:49:57
14	Spectrometer Frequency	400.13
15	Spectral Width	8012.8
16	Lowest Frequency	-1574.0
17	Nucleus	1H
18	Acquired Size	32768
19	Spectral Size	65536
20	Absolute Reference	

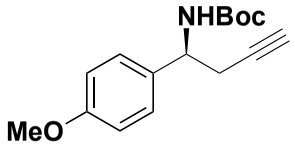

A (m) 7.26
B (m) 6.87
D (s) 5.11
E (s) 4.83
F (s) 3.79
G (pd) 2.70
H (t) 2.00
C (s) 1.43

2.00 1.92 0.89 0.92 2.92 1.92 0.90 8.71

40000 35000 30000 25000 20000 15000 10000 5000 0

9.5 9.0 8.5 8.0 7.5 7.0 6.5 6.0 5.5 5.0 4.5 4.0 3.5 3.0 2.5 2.0 1.5 1.0 0.5 0.0 -0.5

f1 (ppm)

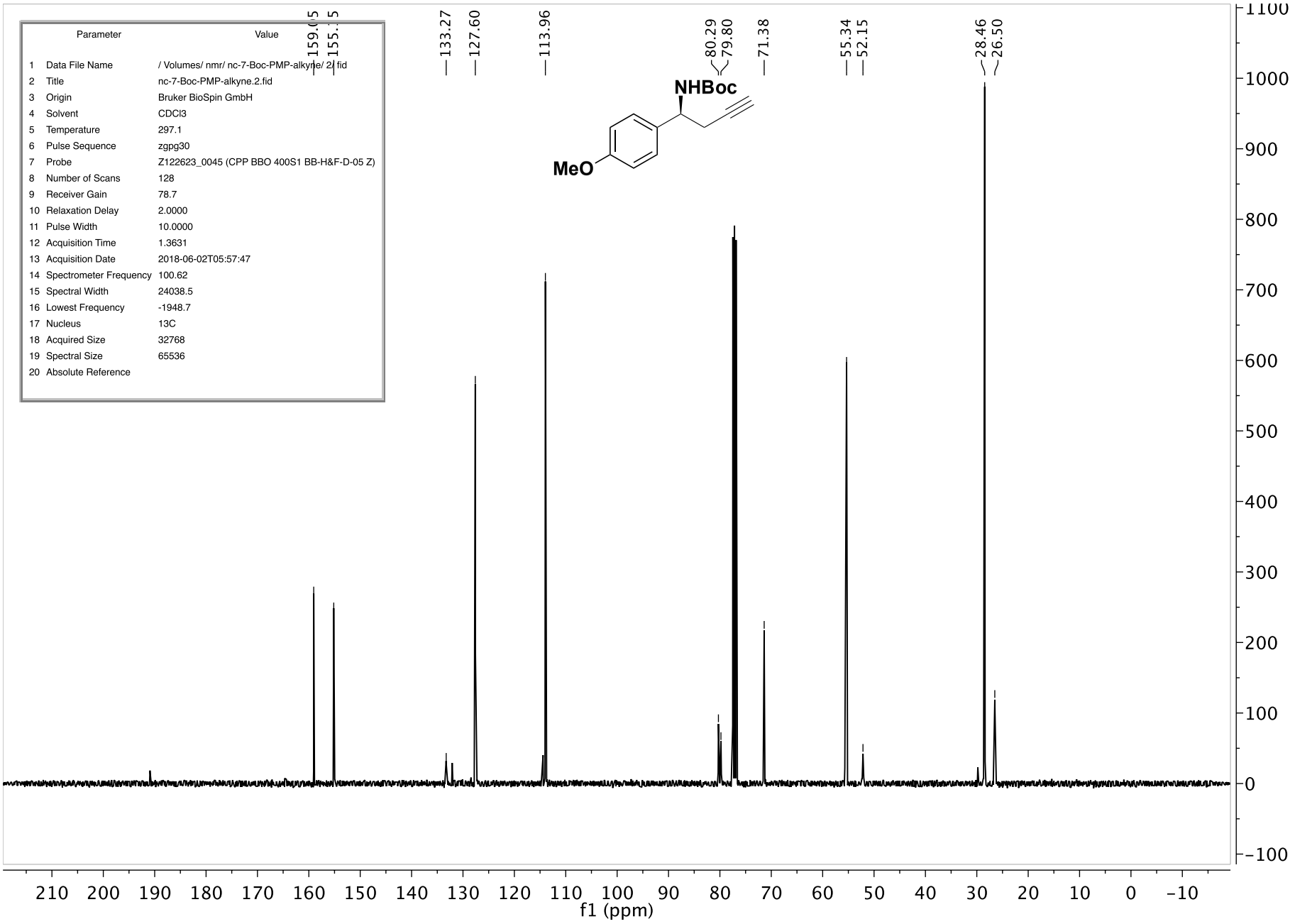
Parameter Value
1 Data File Name / Volumes/ nmr/ nc-7-Boc-PMP-alkyne/ 2/ fid
2 Title nc-7-Boc-PMP-alkyne.2.fid
3 Origin Bruker BioSpin GmbH
4 Solvent CDCl3
5 Temperature 297.1
6 Pulse Sequence zgpg30
7 Probe Z122623_0045 (CPP BBO 400S1 BB-H&F-D-05 Z)
8 Number of Scans 128
9 Receiver Gain 78.7
10 Relaxation Delay 2.0000
11 Pulse Width 10.0000
12 Acquisition Time 1.3631
13 Acquisition Date 2018-06-02T05:57:47
14 Spectrometer Frequency 100.62
15 Spectral Width 24038.5
16 Lowest Frequency -1948.7
17 Nucleus 13C
18 Acquired Size 32768
19 Spectral Size 65536
20 Absolute Reference
159.05
155.15
133.27
127.60
113.96
80.29
79.80
71.38
55.34
52.15
28.46
26.50
NHBoc
MeO
f1 (ppm)

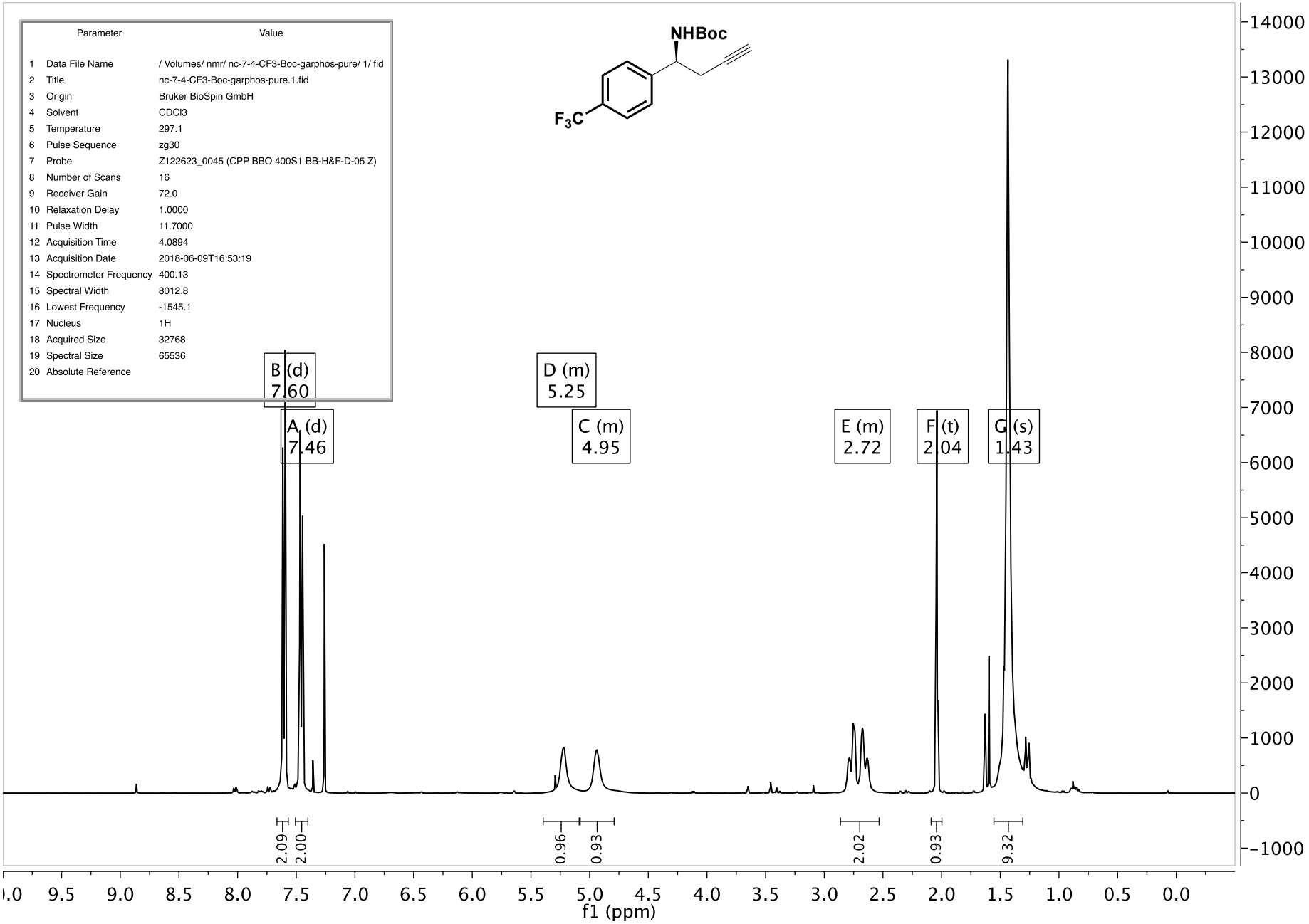
Parameter Value
1 Data File Name / Volumes/ nmr/ nc-7-4-CF3-Boc-garphos-pure/ 1/ fid
2 Title nc-7-4-CF3-Boc-garphos-pure.1.fid
3 Origin Bruker BioSpin GmbH
4 Solvent CDCl3
5 Temperature 297.1
6 Pulse Sequence zg30
7 Probe Z122623_0045 (CPP BBO 400S1 BB-H&F-D-05 Z)
8 Number of Scans 16
9 Receiver Gain 72.0
10 Relaxation Delay 1.0000
11 Pulse Width 11.7000
12 Acquisition Time 4.0894
13 Acquisition Date 2018-06-09T16:53:19
14 Spectrometer Frequency 400.13
15 Spectral Width 8012.8
16 Lowest Frequency -1545.1
17 Nucleus 1H
18 Acquired Size 32768
19 Spectral Size 65536
20 Absolute Reference
NHBoc
F3C
B (d) 7.60
A (d) 7.46
D (m) 5.25
C (m) 4.95
E (m) 2.72
F (t) 2.04
G (s) 1.43
2.09
2.00
0.96
0.93
2.02
0.93
9.32
f1 (ppm)

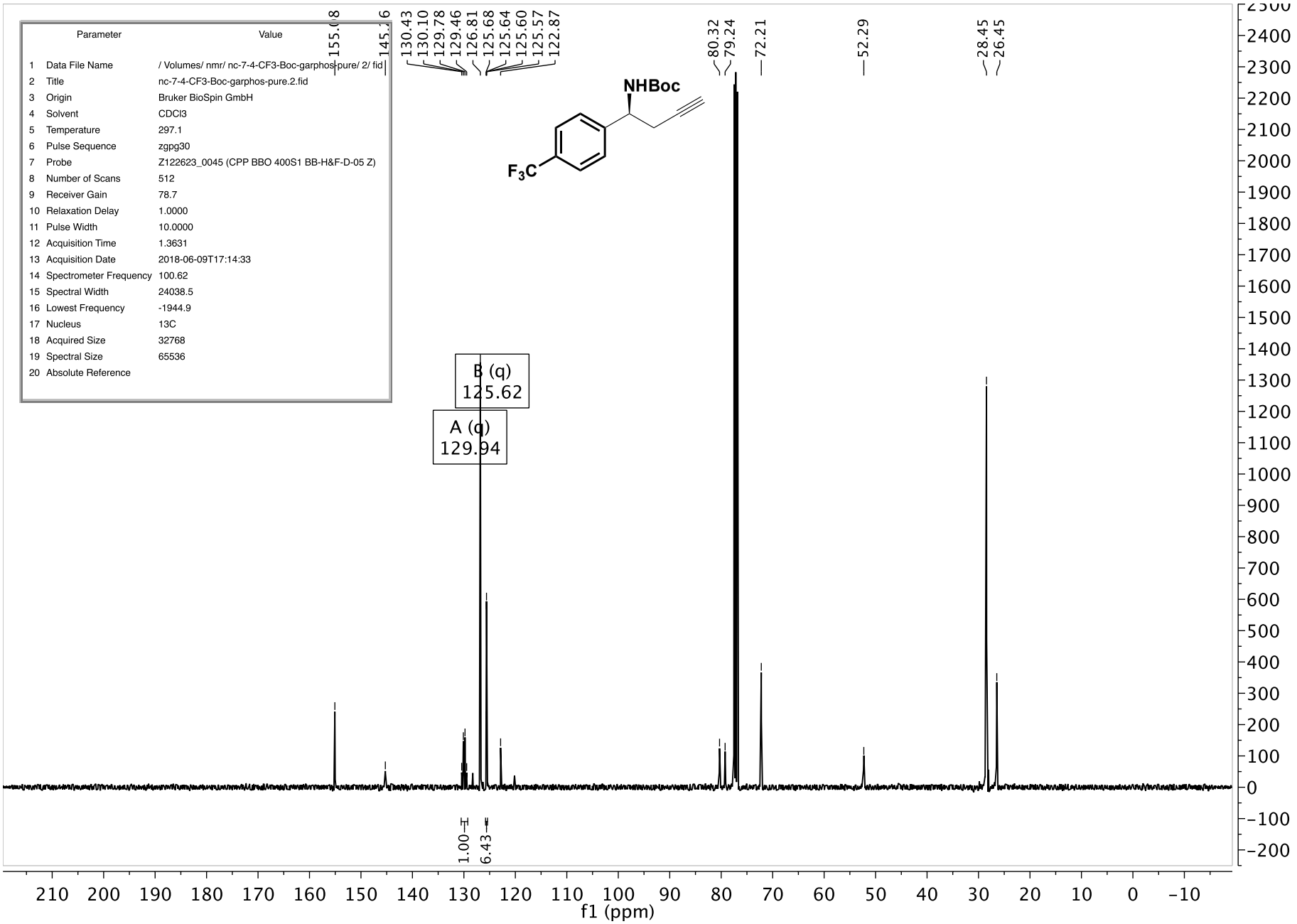
Parameter Value
1 Data File Name / Volumes/ nmr/ nc-7-4-CF3-Boc-garphos-pure/ 2/ fid
2 Title nc-7-4-CF3-Boc-garphos-pure.2.fid
3 Origin Bruker BioSpin GmbH
4 Solvent CDCl3
5 Temperature 297.1
6 Pulse Sequence zgpg30
7 Probe Z122623_0045 (CPP BBO 400S1 BB-H&F-D-05 Z)
8 Number of Scans 512
9 Receiver Gain 78.7
10 Relaxation Delay 1.0000
11 Pulse Width 10.0000
12 Acquisition Time 1.3631
13 Acquisition Date 2018-06-09T17:14:33
14 Spectrometer Frequency 100.62
15 Spectral Width 24038.5
16 Lowest Frequency -1944.9
17 Nucleus 13C
18 Acquired Size 32768
19 Spectral Size 65536
20 Absolute Reference
155.08
145.26
130.43
130.10
129.78
129.46
126.81
125.68
125.64
125.60
125.57
122.87
80.32
79.24
72.21
52.29
28.45
26.45
NHBoc
F3C
B (q)
125.62
A (q)
129.94
1.00
6.43
f1 (ppm)

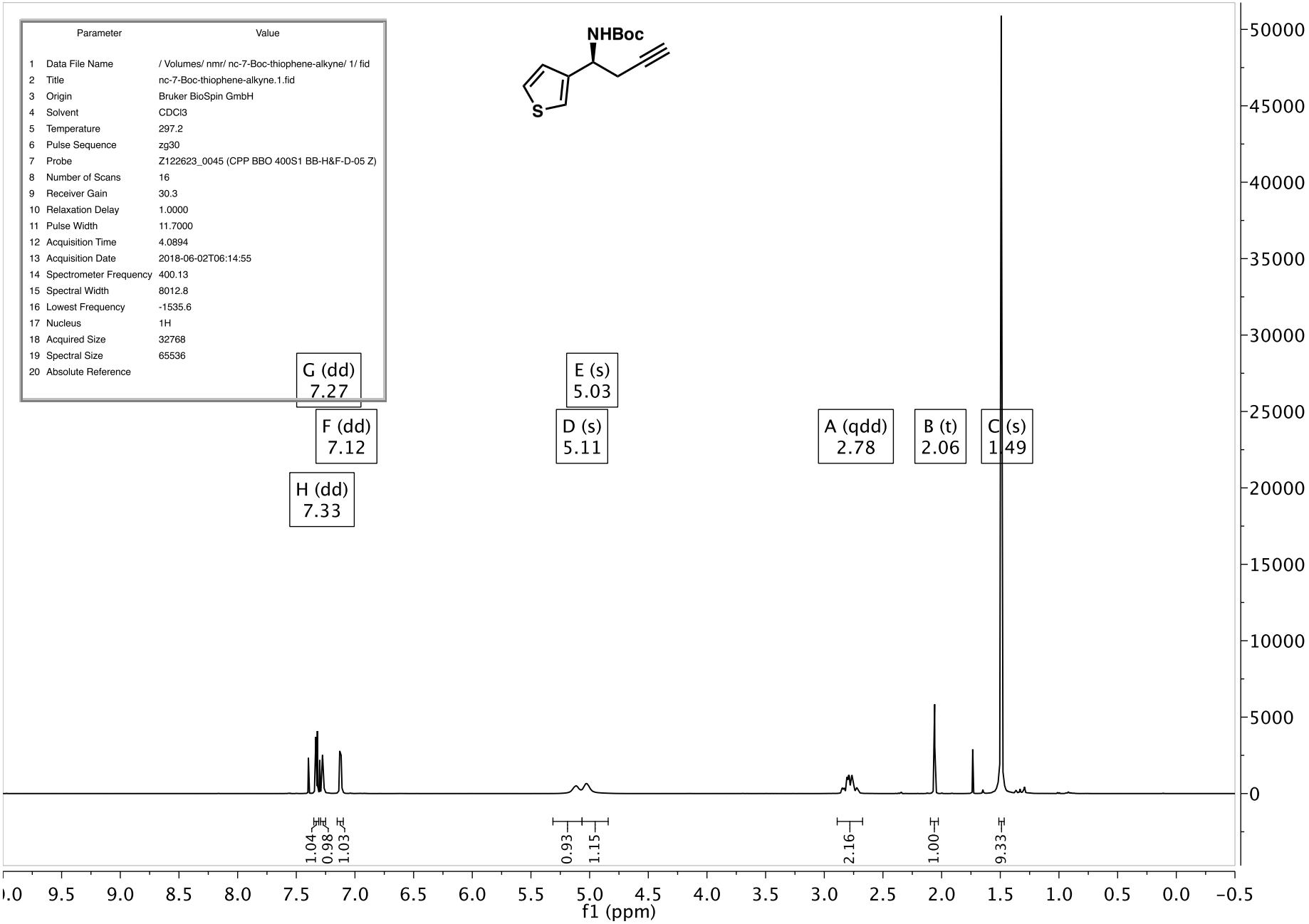
Parameter Value
1 Data File Name / Volumes/ nmr/ nc-7-Boc-thiophene-alkyne/ 1/ fid
2 Title nc-7-Boc-thiophene-alkyne.1.fid
3 Origin Bruker BioSpin GmbH
4 Solvent CDCl3
5 Temperature 297.2
6 Pulse Sequence zg30
7 Probe Z122623_0045 (CPP BBO 400S1 BB-H&F-D-05 Z)
8 Number of Scans 16
9 Receiver Gain 30.3
10 Relaxation Delay 1.0000
11 Pulse Width 11.7000
12 Acquisition Time 4.0894
13 Acquisition Date 2018-06-02T06:14:55
14 Spectrometer Frequency 400.13
15 Spectral Width 8012.8
16 Lowest Frequency -1535.6
17 Nucleus 1H
18 Acquired Size 32768
19 Spectral Size 65536
20 Absolute Reference
NHBoc
S
G (dd) 7.27
F (dd) 7.12
H (dd) 7.33
E (s) 5.03
D (s) 5.11
A (qdd) 2.78
B (t) 2.06
C (s) 1.49
1.04
0.98
1.03
0.93
1.15
2.16
1.00
9.33
f1 (ppm)

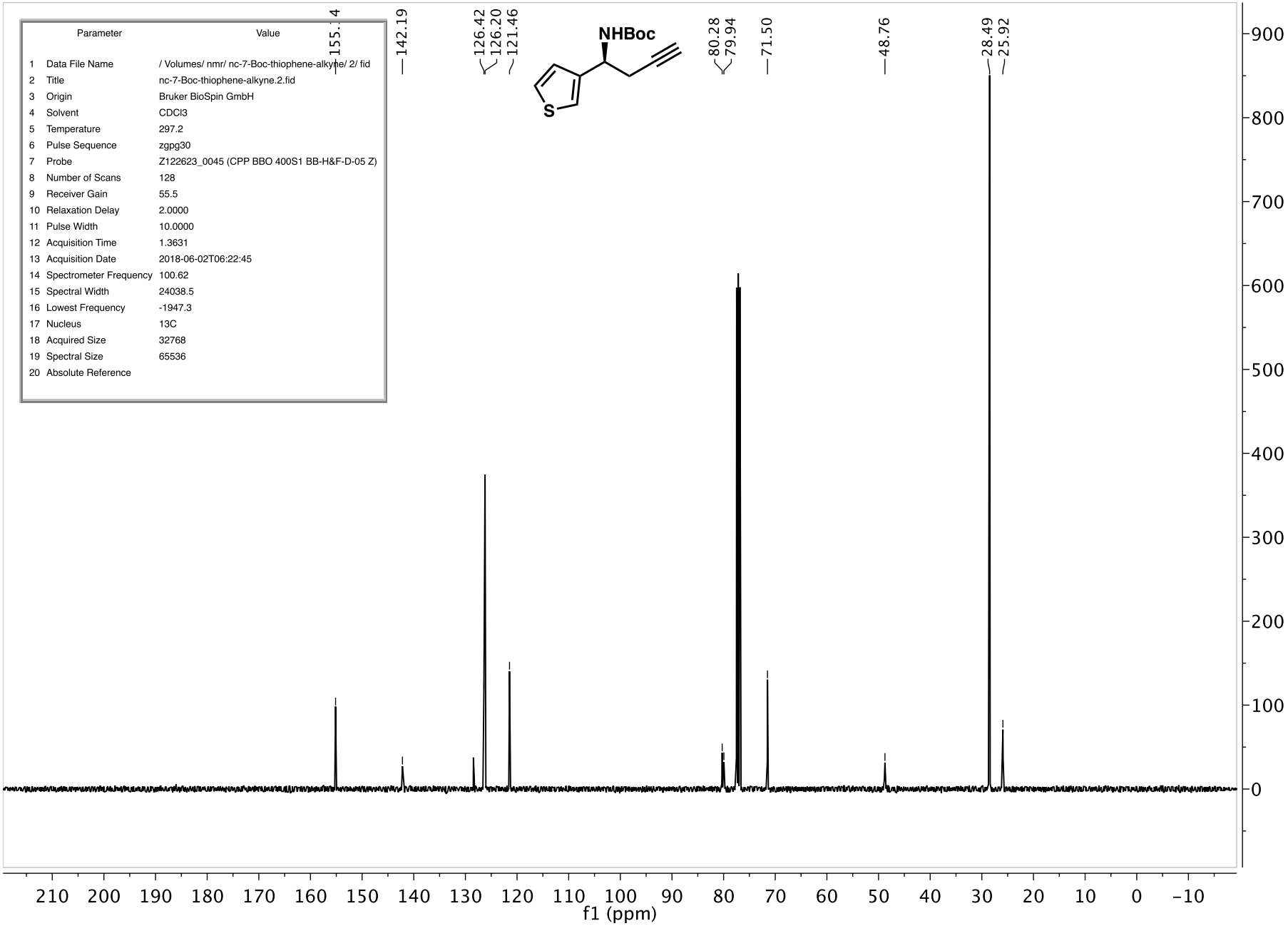
Parameter Value
1 Data File Name / Volumes/ nmr/ nc-7-Boc-thiophene-alkyne/ 2/ fid
2 Title nc-7-Boc-thiophene-alkyne.2.fid
3 Origin Bruker BioSpin GmbH
4 Solvent CDCl3
5 Temperature 297.2
6 Pulse Sequence zgpg30
7 Probe Z122623_0045 (CPP BBO 400S1 BB-H&F-D-05 Z)
8 Number of Scans 128
9 Receiver Gain 55.5
10 Relaxation Delay 2.0000
11 Pulse Width 10.0000
12 Acquisition Time 1.3631
13 Acquisition Date 2018-06-02T06:22:45
14 Spectrometer Frequency 100.62
15 Spectral Width 24038.5
16 Lowest Frequency -1947.3
17 Nucleus 13C
18 Acquired Size 32768
19 Spectral Size 65536
20 Absolute Reference
155.4
142.19
126.42
126.20
121.46
NHBoc
S
80.28
79.94
71.50
48.76
28.49
25.92
900
800
700
600
500
400
300
200
100
0
210 200 190 180 170 160 150 140 130 120 110 100 90 80 70 60 50 40 30 20 10 0 -10
f1 (ppm)

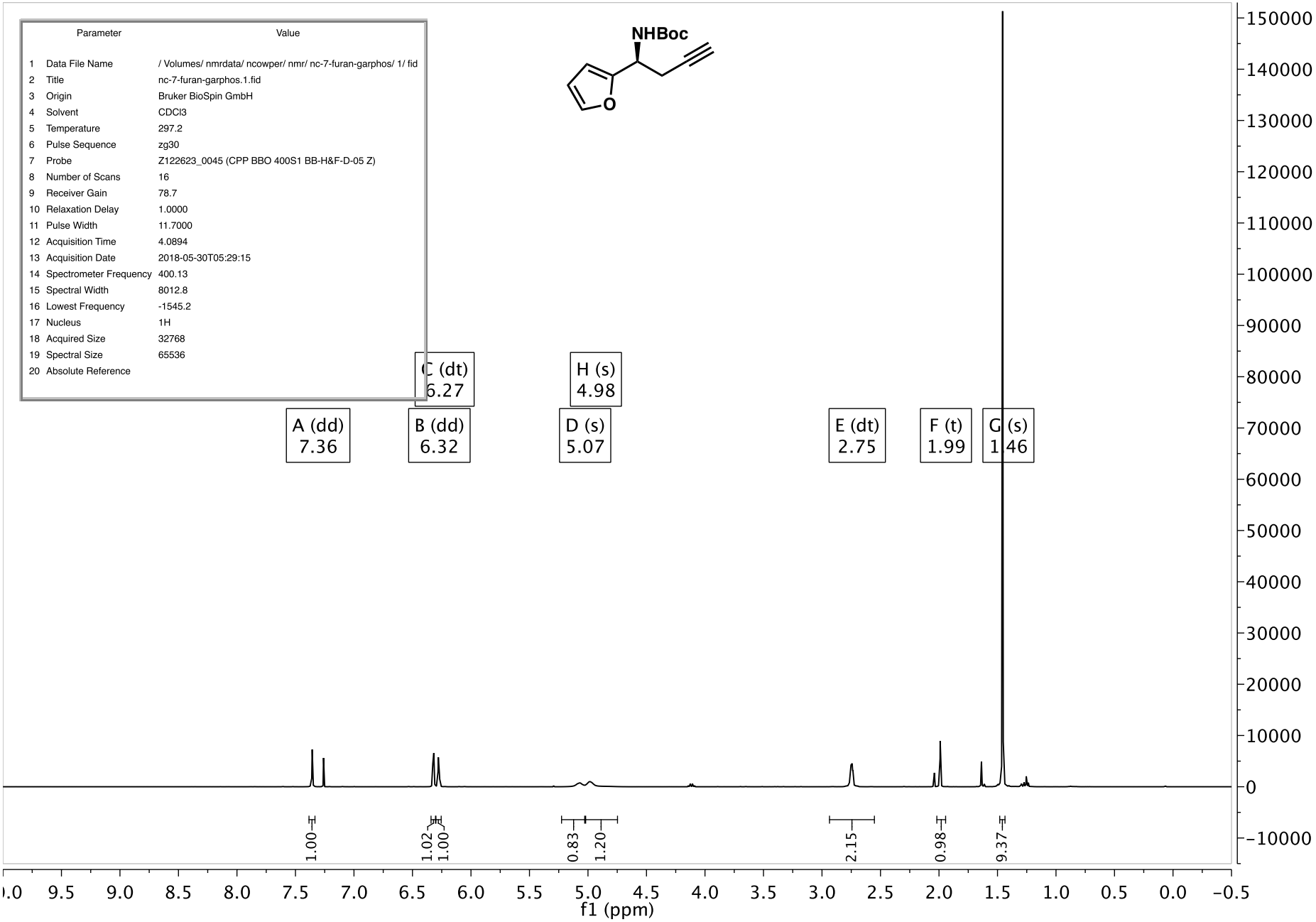
Parameter Value
1 Data File Name / Volumes/ nmrdata/ ncowper/ nmr/ nc-7-furan-garphos/ 1/ fid
2 Title nc-7-furan-garphos.1.fid
3 Origin Bruker BioSpin GmbH
4 Solvent CDCl3
5 Temperature 297.2
6 Pulse Sequence zg30
7 Probe Z122623_0045 (CPP BBO 400S1 BB-H&F-D-05 Z)
8 Number of Scans 16
9 Receiver Gain 78.7
10 Relaxation Delay 1.0000
11 Pulse Width 11.7000
12 Acquisition Time 4.0894
13 Acquisition Date 2018-05-30T05:29:15
14 Spectrometer Frequency 400.13
15 Spectral Width 8012.8
16 Lowest Frequency -1545.2
17 Nucleus 1H
18 Acquired Size 32768
19 Spectral Size 65536
20 Absolute Reference
NHBoc
O
A (dd) 7.36
B (dd) 6.32
C (dt) 6.27
D (s) 5.07
H (s) 4.98
E (dt) 2.75
F (t) 1.99
G (s) 1.46
1.00
1.02
1.00
0.83
1.20
2.15
0.98
9.37
f1 (ppm)

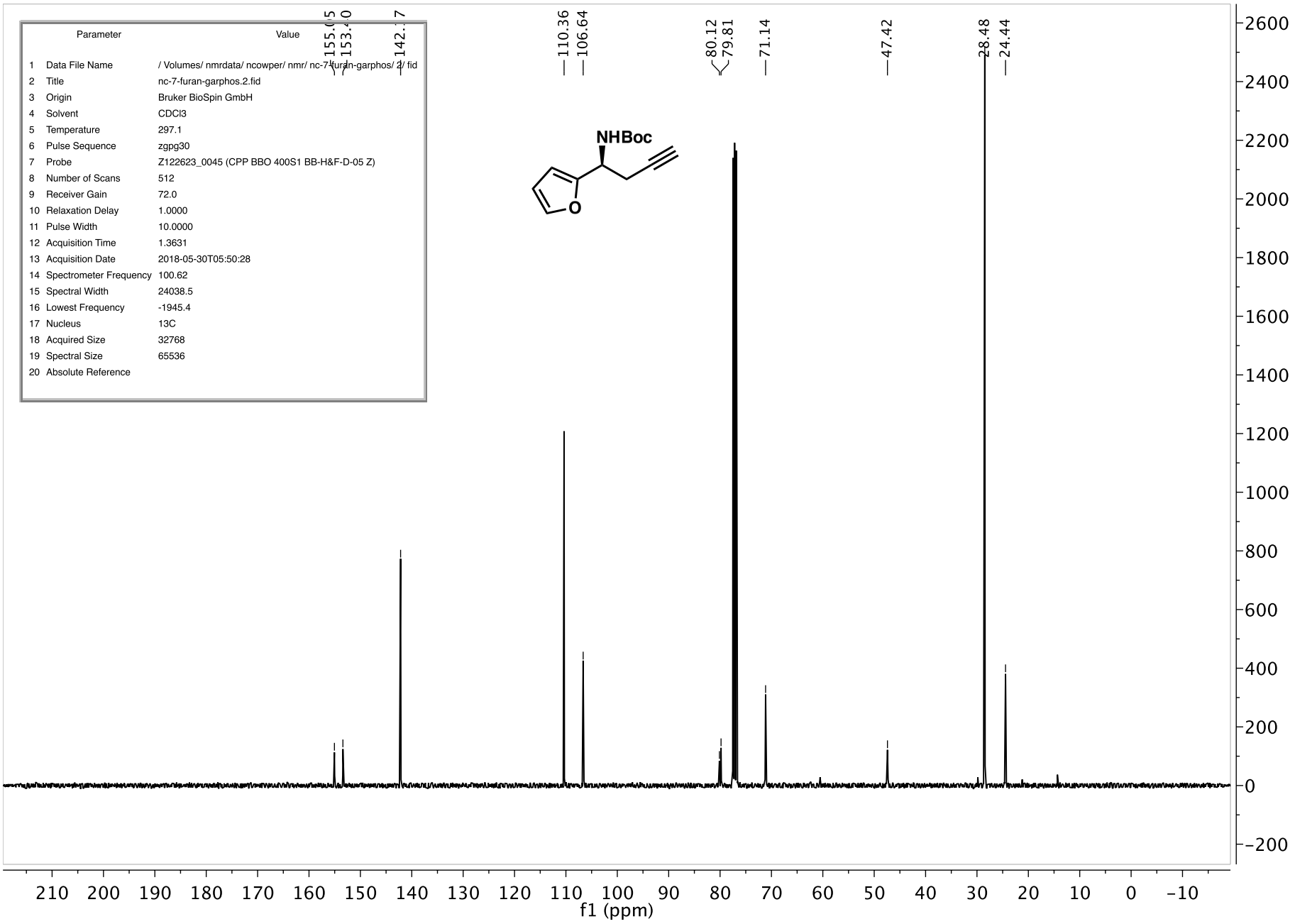
Parameter Value
1 Data File Name / Volumes/ nmrdata/ ncowper/ nmr/ nc-7-furan-garphos/ 2/ fid
2 Title nc-7-furan-garphos.2.fid
3 Origin Bruker BioSpin GmbH
4 Solvent CDCl3
5 Temperature 297.1
6 Pulse Sequence zgpg30
7 Probe Z122623_0045 (CPP BBO 400S1 BB-H&F-D-05 Z)
8 Number of Scans 512
9 Receiver Gain 72.0
10 Relaxation Delay 1.0000
11 Pulse Width 10.0000
12 Acquisition Time 1.3631
13 Acquisition Date 2018-05-30T05:50:28
14 Spectrometer Frequency 100.62
15 Spectral Width 24038.5
16 Lowest Frequency -1945.4
17 Nucleus 13C
18 Acquired Size 32768
19 Spectral Size 65536
20 Absolute Reference
155.05
153.20
142.17
110.36
106.64
80.12
79.81
71.14
47.42
28.48
24.44
NHBoc
O
2600
2400
2200
2000
1800
1600
1400
1200
1000
800
600
400
200
0
−200
210 200 190 180 170 160 150 140 130 120 110 100 90 80 70 60 50 40 30 20 10 0 −10
f1 (ppm)

	Parameter	Value
1	Data File Name	/ Volumes/ nmrdata/ ncowper/ nmr/ nc-7-subme-prop-shig/ 1/ fid
2	Title	nc-7-subme-prop-shig.1.fid
3	Origin	Bruker BioSpin GmbH
4	Solvent	CDCl3
5	Temperature	295.1
6	Pulse Sequence	zg30
7	Probe	Z122623_0045 (CPP BBO 400S1 BB-H&F-D-05 Z)
8	Number of Scans	16
9	Receiver Gain	197.4
10	Relaxation Delay	1.0000
11	Pulse Width	11.7000
12	Acquisition Time	4.0894
13	Acquisition Date	2018-07-01T03:18:16
14	Spectrometer Frequency	400.13
15	Spectral Width	8012.8
16	Lowest Frequency	-1545.4
17	Nucleus	1H
18	Acquired Size	32768
19	Spectral Size	65536
20	Absolute Reference	

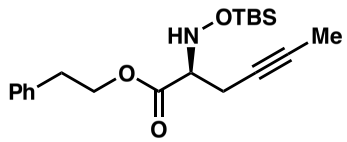

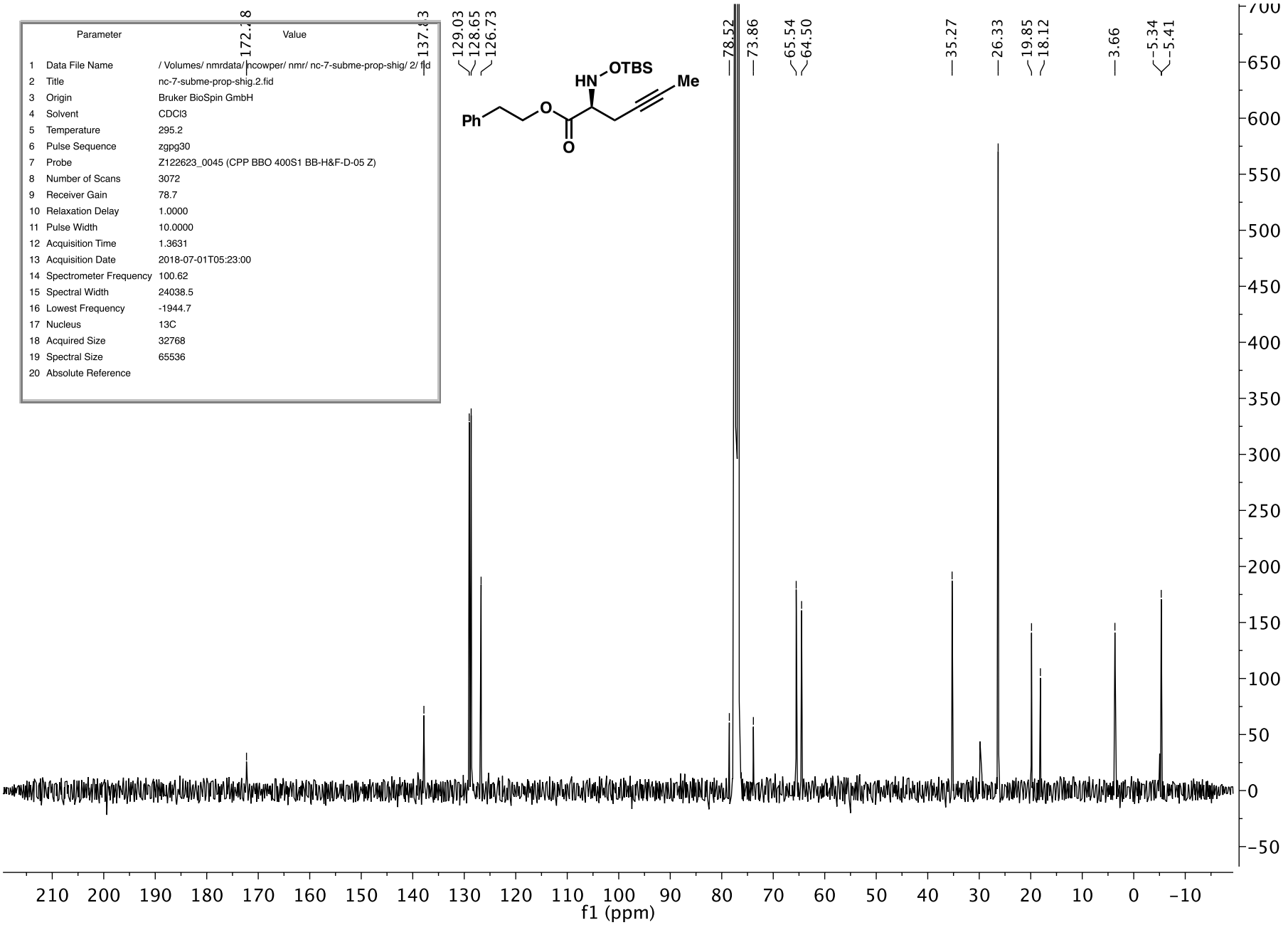
Parameter Value
1 Data File Name / Volumes/ nmrdata/ ncowper/ nmr/ nc-7-subme-prop-shig/ 2/ fid
2 Title nc-7-subme-prop-shig.2.fid
3 Origin Bruker BioSpin GmbH
4 Solvent CDCl3
5 Temperature 295.2
6 Pulse Sequence zgpg30
7 Probe Z122623_0045 (CPP BBO 400S1 BB-H&F-D-05 Z)
8 Number of Scans 3072
9 Receiver Gain 78.7
10 Relaxation Delay 1.0000
11 Pulse Width 10.0000
12 Acquisition Time 1.3631
13 Acquisition Date 2018-07-01T05:23:00
14 Spectrometer Frequency 100.62
15 Spectral Width 24038.5
16 Lowest Frequency -1944.7
17 Nucleus 13C
18 Acquired Size 32768
19 Spectral Size 65536
20 Absolute Reference
172.18
137.03
129.03
128.65
126.73
78.52
73.86
65.54
64.50
35.27
26.33
19.85
18.12
3.66
-5.34
-5.41
HN
OTBS
Me
Ph
O
O
f1 (ppm)

	Parameter	Value
1	Data File Name	/ Volumes/ nmrdata/ ncowper/ nmr/ nc-7-sub-ee-f1/ 1/ fid
2	Title	nc-7-sub-ee-f1.1.fid
3	Origin	Bruker BioSpin GmbH
4	Solvent	CDCl3
5	Temperature	295.1
6	Pulse Sequence	zg30
7	Probe	Z122623_0045 (CPP BBO 400S1 BB-H&F-D-05 Z)
8	Number of Scans	16
9	Receiver Gain	197.4
10	Relaxation Delay	1.0000
11	Pulse Width	11.7000
12	Acquisition Time	4.0894
13	Acquisition Date	2018-06-28T14:17:55
14	Spectrometer Frequency	400.13
15	Spectral Width	8012.8
16	Lowest Frequency	-1545.6
17	Nucleus	1H
18	Acquired Size	32768
19	Spectral Size	65536
20	Absolute Reference	

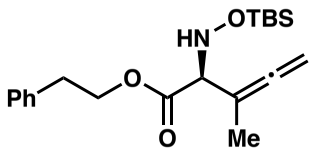

J (m) 7.23
I (m) 7.30
H (d) 5.56
G (m) 4.69
F (td) 4.38
E (dt) 3.87
C (td) 2.97
D (td) 1.73
B (s) 0.89
A (d) 0.10

2.06 2.96 0.94 1.95 2.00 0.96 1.99 2.98 9.26 6.00

f1 (ppm)

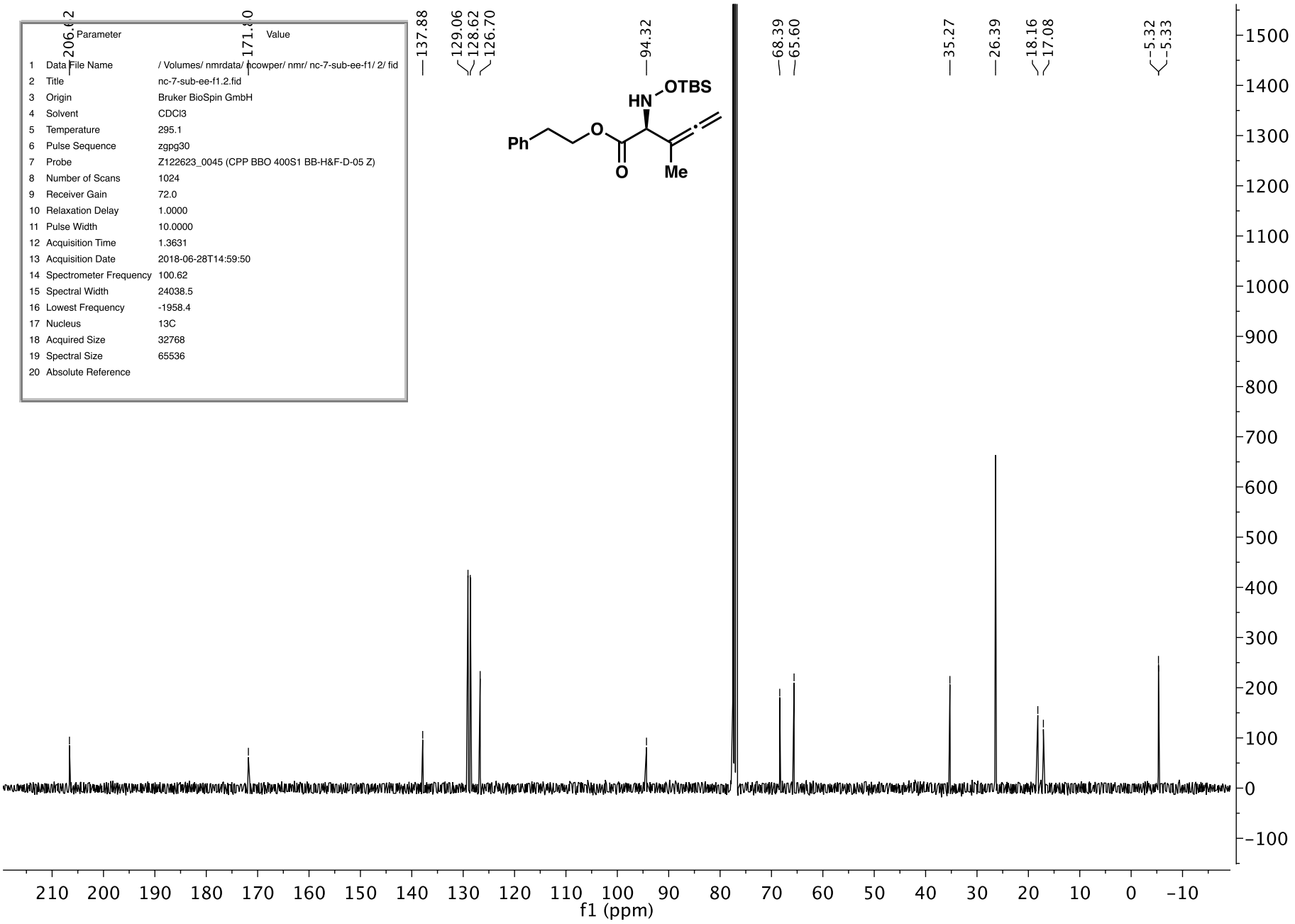

	Parameter	Value
1	Data File Name	/ Volumes/ nmrdata/ ncowper/ nmr/ nc-7-sub-ee-f1/ 2/ fid
2	Title	nc-7-sub-ee-f1.2.fid
3	Origin	Bruker BioSpin GmbH
4	Solvent	CDCl3
5	Temperature	295.1
6	Pulse Sequence	zgpg30
7	Probe	Z122623_0045 (CPP BBO 400S1 BB-H&F-D-05 Z)
8	Number of Scans	1024
9	Receiver Gain	72.0
10	Relaxation Delay	1.0000
11	Pulse Width	10.0000
12	Acquisition Time	1.3631
13	Acquisition Date	2018-06-28T14:59:50
14	Spectrometer Frequency	100.62
15	Spectral Width	24038.5
16	Lowest Frequency	-1958.4
17	Nucleus	13C
18	Acquired Size	32768
19	Spectral Size	65536
20	Absolute Reference	

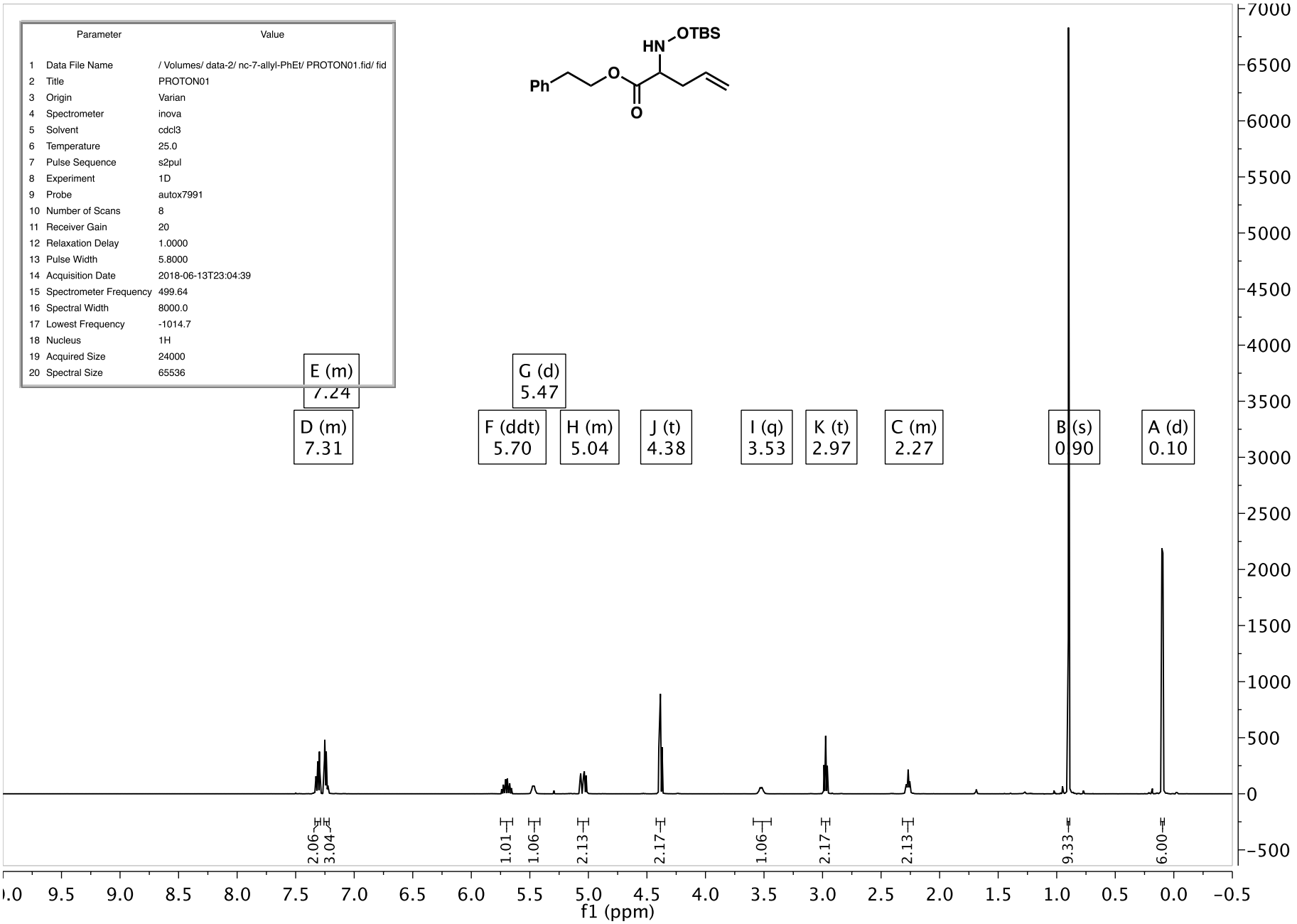
Parameter Value
1 Data File Name / Volumes/ data-2/ nc-7-allyl-PhEt/ PROTON01.fid/ fid
2 Title PROTON01
3 Origin Varian
4 Spectrometer inova
5 Solvent cdcl3
6 Temperature 25.0
7 Pulse Sequence s2pul
8 Experiment 1D
9 Probe autox7991
10 Number of Scans 8
11 Receiver Gain 20
12 Relaxation Delay 1.0000
13 Pulse Width 5.8000
14 Acquisition Date 2018-06-13T23:04:39
15 Spectrometer Frequency 499.64
16 Spectral Width 8000.0
17 Lowest Frequency -1014.7
18 Nucleus 1H
19 Acquired Size 24000
20 Spectral Size 65536
HN
OTBS
Ph
O
O
E (m) 7.24
G (d) 5.47
D (m) 7.31
F (ddt) 5.70
H (m) 5.04
J (t) 4.38
I (q) 3.53
K (t) 2.97
C (m) 2.27
B (s) 0.90
A (d) 0.10
2.06
3.04
1.01
1.06
2.13
2.17
1.06
2.17
2.13
9.33
6.00
f1 (ppm)

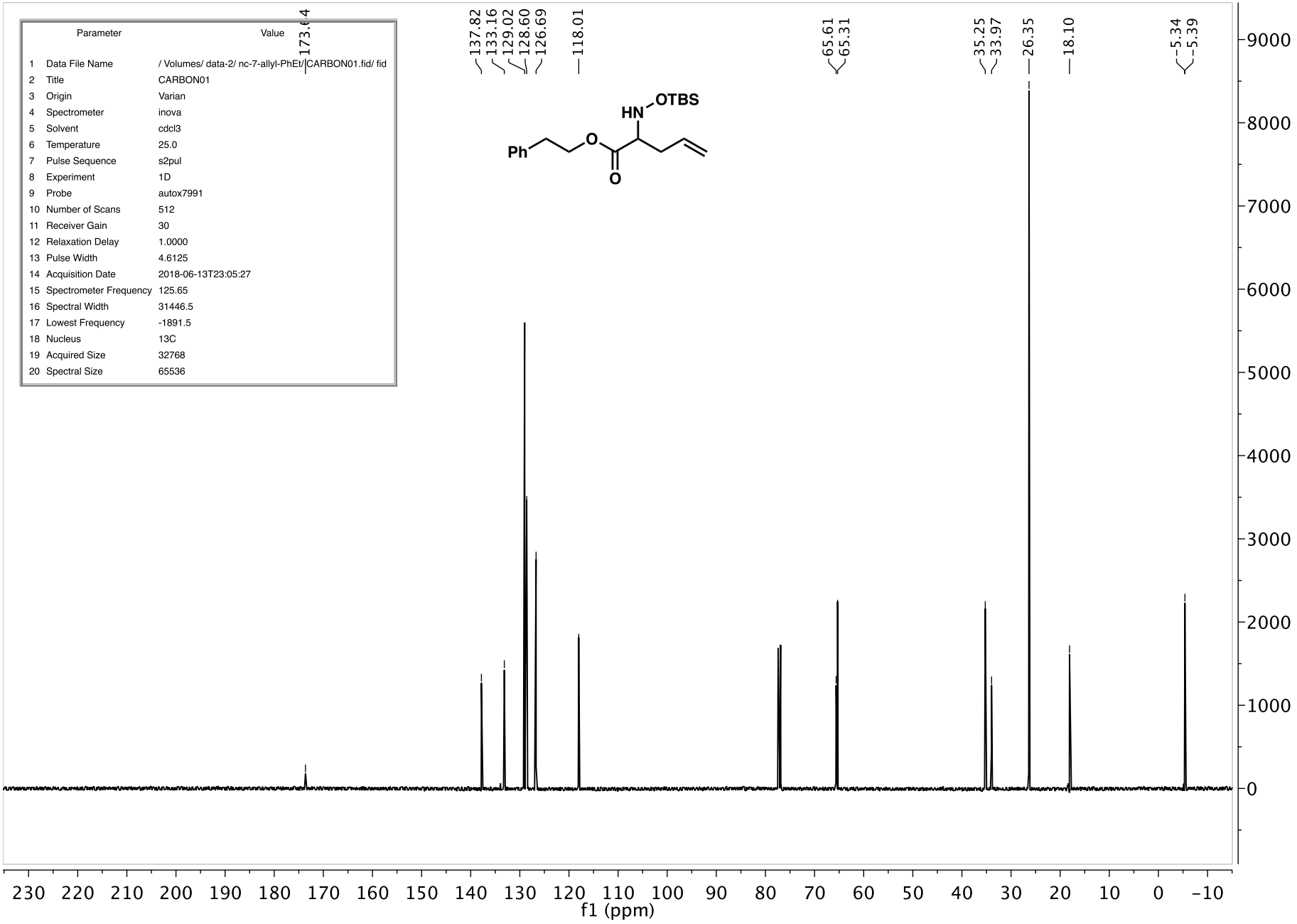
Parameter Value
1 Data File Name / Volumes/ data-2/ nc-7-allyl-PhEt/CARBON01.fid/ fid
2 Title CARBON01
3 Origin Varian
4 Spectrometer inova
5 Solvent cdcl3
6 Temperature 25.0
7 Pulse Sequence s2pul
8 Experiment 1D
9 Probe autox7991
10 Number of Scans 512
11 Receiver Gain 30
12 Relaxation Delay 1.0000
13 Pulse Width 4.6125
14 Acquisition Date 2018-06-13T23:05:27
15 Spectrometer Frequency 125.65
16 Spectral Width 31446.5
17 Lowest Frequency -1891.5
18 Nucleus 13C
19 Acquired Size 32768
20 Spectral Size 65536
173.64
137.82
133.16
129.02
128.60
126.69
118.01
65.61
65.31
35.25
33.97
26.35
18.10
5.34
5.39
HN
OTBS
Ph
O
O
9000
8000
7000
6000
5000
4000
3000
2000
1000
0
230 220 210 200 190 180 170 160 150 140 130 120 110 100 90 80 70 60 50 40 30 20 10 0 -10
f1 (ppm)

	Parameter	Value
1	Data File Name	/ Volumes/ nmr/ nc-7-et-ac-propargyl-glycine/ 1/ fid
2	Title	nc-7-et-ac-propargyl-glycine.1.fid
3	Origin	Bruker BioSpin GmbH
4	Solvent	CDCl3
5	Temperature	297.1
6	Pulse Sequence	zg30
7	Probe	Z122623_0045 (CPP BBO 400S1 BB-H&F-D-05 Z)
8	Number of Scans	16
9	Receiver Gain	98.9
10	Relaxation Delay	1.0000
11	Pulse Width	11.7000
12	Acquisition Time	4.0894
13	Acquisition Date	2018-06-04T11:38:20
14	Spectrometer Frequency	400.13
15	Spectral Width	8012.8
16	Lowest Frequency	-1545.4
17	Nucleus	1H
18	Acquired Size	32768
19	Spectral Size	65536
20	Absolute Reference	

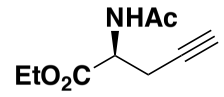

A (d) 6.34
B (dt) 4.72
C (m) 4.24
D (m) 2.76
E (t) 2.02
F (s) 2.06
G (t) 1.29

1.00 1.03 2.12 2.19 3.13 1.00 3.24

f1 (ppm)

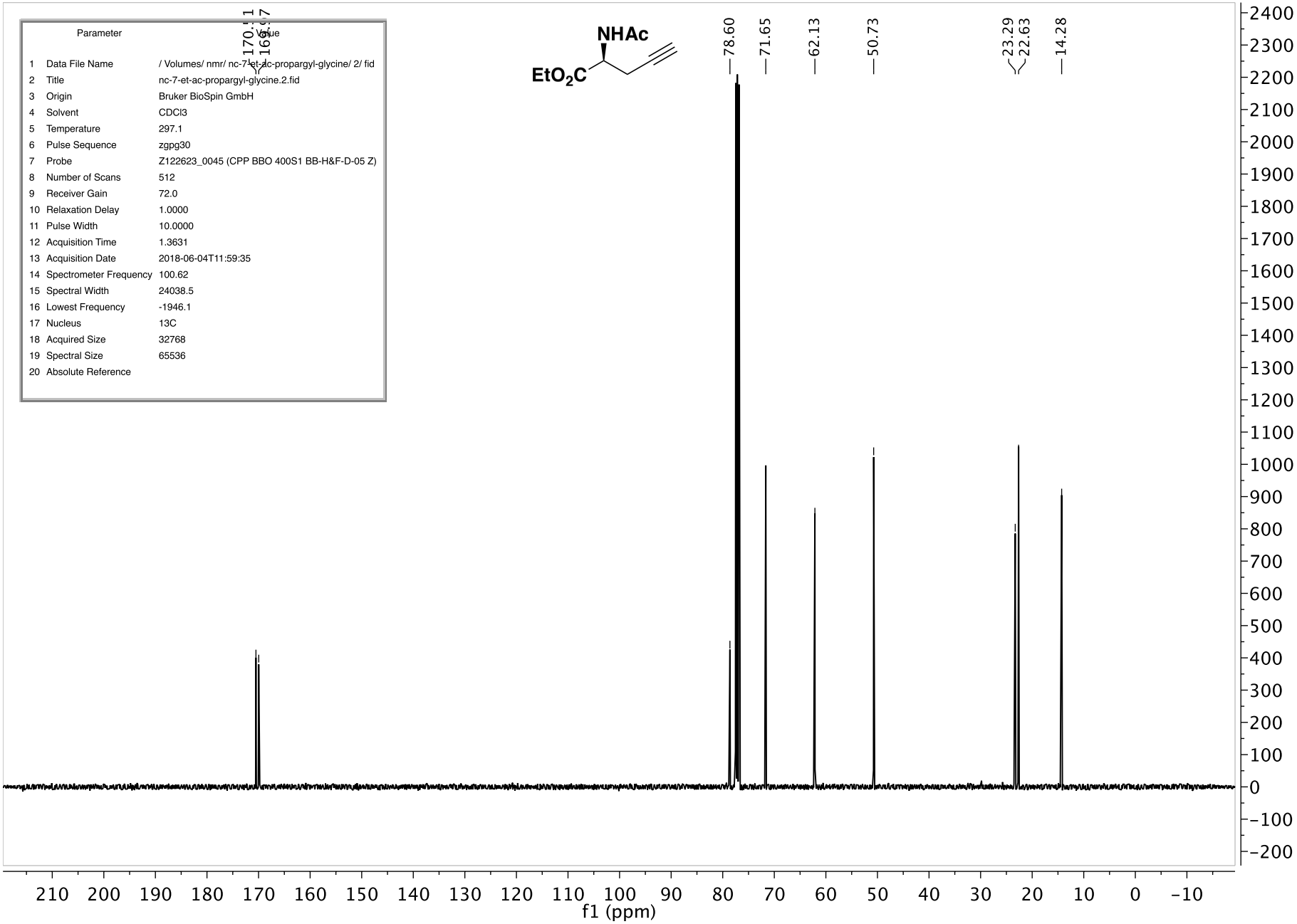
Parameter Value
1 Data File Name / Volumes/ nmr/ nc-7-et-ac-propargyl-glycine/ 2/ fid
2 Title nc-7-et-ac-propargyl-glycine.2.fid
3 Origin Bruker BioSpin GmbH
4 Solvent CDCl3
5 Temperature 297.1
6 Pulse Sequence zgpg30
7 Probe Z122623_0045 (CPP BBO 400S1 BB-H&F-D-05 Z)
8 Number of Scans 512
9 Receiver Gain 72.0
10 Relaxation Delay 1.0000
11 Pulse Width 10.0000
12 Acquisition Time 1.3631
13 Acquisition Date 2018-06-04T11:59:35
14 Spectrometer Frequency 100.62
15 Spectral Width 24038.5
16 Lowest Frequency -1946.1
17 Nucleus 13C
18 Acquired Size 32768
19 Spectral Size 65536
20 Absolute Reference
NHAc
EtO2C
170.11
169.67
78.60
71.65
62.13
50.73
23.29
22.63
14.28
f1 (ppm)

	Parameter	Value
1	Data File Name	/ Volumes/ nmr/ nc-et-bz-alkyne-p/ 1/ fid
2	Title	nc-et-bz-alkyne-p.1.fid
3	Origin	Bruker BioSpin GmbH
4	Solvent	CDCl3
5	Temperature	297.1
6	Pulse Sequence	zg30
7	Probe	Z122623_0045 (CPP BBO 400S1 BB-H&F-D-05 Z)
8	Number of Scans	16
9	Receiver Gain	64.2
10	Relaxation Delay	1.0000
11	Pulse Width	11.7000
12	Acquisition Time	4.0894
13	Acquisition Date	2018-06-08T08:28:33
14	Spectrometer Frequency	400.13
15	Spectral Width	8012.8
16	Lowest Frequency	-1545.1
17	Nucleus	1H
18	Acquired Size	32768
19	Spectral Size	65536
20	Absolute Reference	

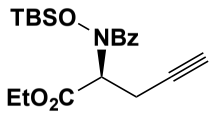

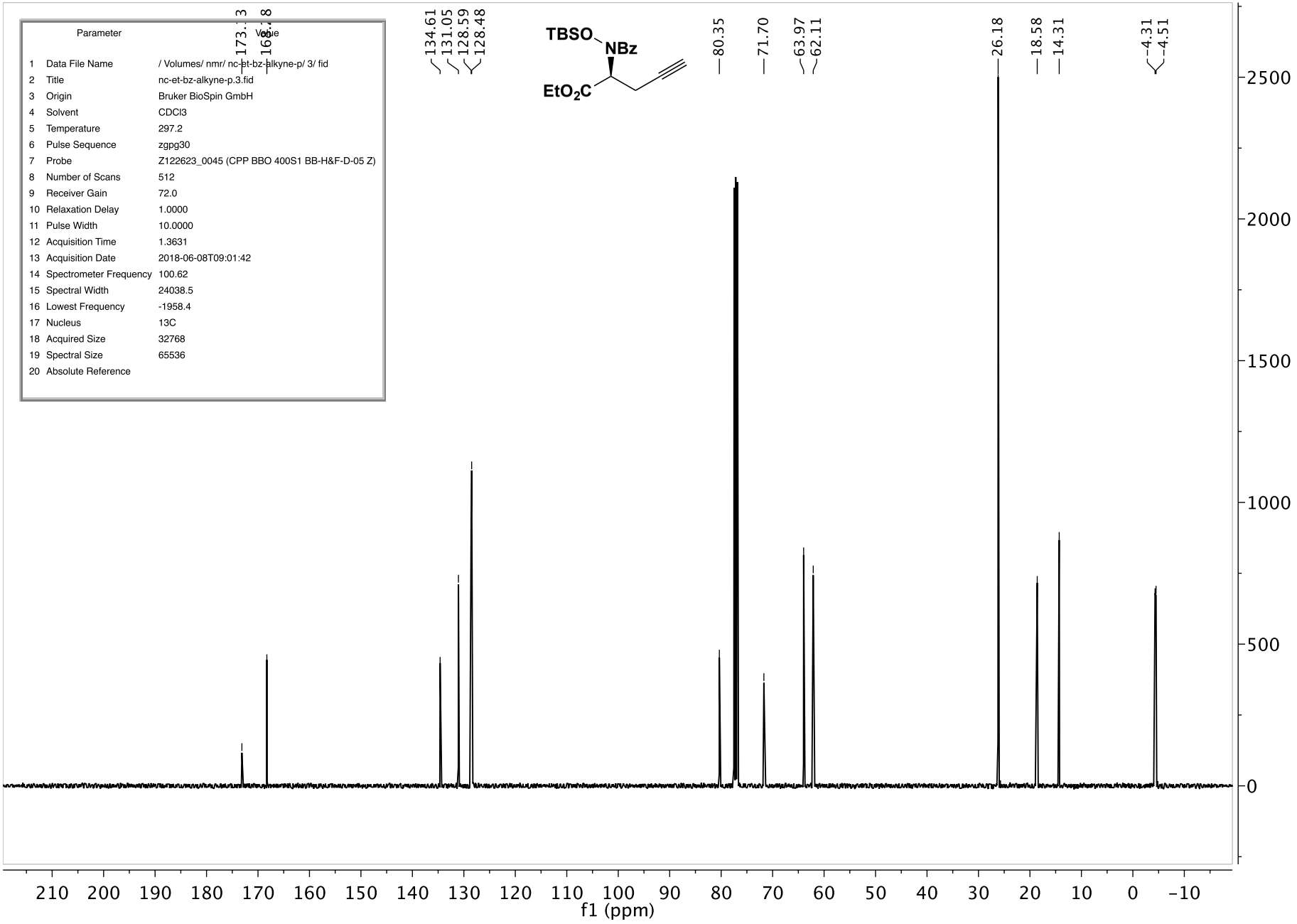
173.3
168.8
134.61
131.05
128.59
128.48
TBSO
NBz
EtO2C
80.35
71.70
63.97
62.11
26.18
18.58
14.31
-4.31
-4.51
Parameter
Value
1 Data File Name / Volumes/ nmr/ nc-et-bz-alkyne-p/ 3/ fid
2 Title nc-et-bz-alkyne-p.3.fid
3 Origin Bruker BioSpin GmbH
4 Solvent CDCl3
5 Temperature 297.2
6 Pulse Sequence zgpg30
7 Probe Z122623_0045 (CPP BBO 400S1 BB-H&F-D-05 Z)
8 Number of Scans 512
9 Receiver Gain 72.0
10 Relaxation Delay 1.0000
11 Pulse Width 10.0000
12 Acquisition Time 1.3631
13 Acquisition Date 2018-06-08T09:01:42
14 Spectrometer Frequency 100.62
15 Spectral Width 24038.5
16 Lowest Frequency -1958.4
17 Nucleus 13C
18 Acquired Size 32768
19 Spectral Size 65536
20 Absolute Reference
2500
2000
1500
1000
500
0
210 200 190 180 170 160 150 140 130 120 110 100 90 80 70 60 50 40 30 20 10 0 -10
f1 (ppm)

	Parameter	Value
1	Data File Name	/ Volumes/ nmr/ sonagashira-pdt/ 1/ fid
2	Title	sonagashira-pdt.1.fid
3	Origin	Bruker BioSpin GmbH
4	Solvent	CDCl3
5	Temperature	297.2
6	Pulse Sequence	zg30
7	Probe	Z122623_0045 (CPP BBO 400S1 BB-H&F-D-05 Z)
8	Number of Scans	16
9	Receiver Gain	64.2
10	Relaxation Delay	1.0000
11	Pulse Width	11.7000
12	Acquisition Time	4.0894
13	Acquisition Date	2018-06-02T06:27:22
14	Spectrometer Frequency	400.13
15	Spectral Width	8012.8
16	Lowest Frequency	-1545.1
17	Nucleus	1H
18	Acquired Size	32768
19	Spectral Size	65536
20	Absolute Reference	

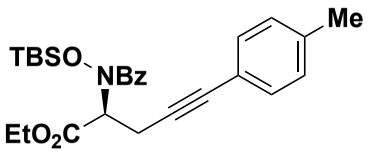

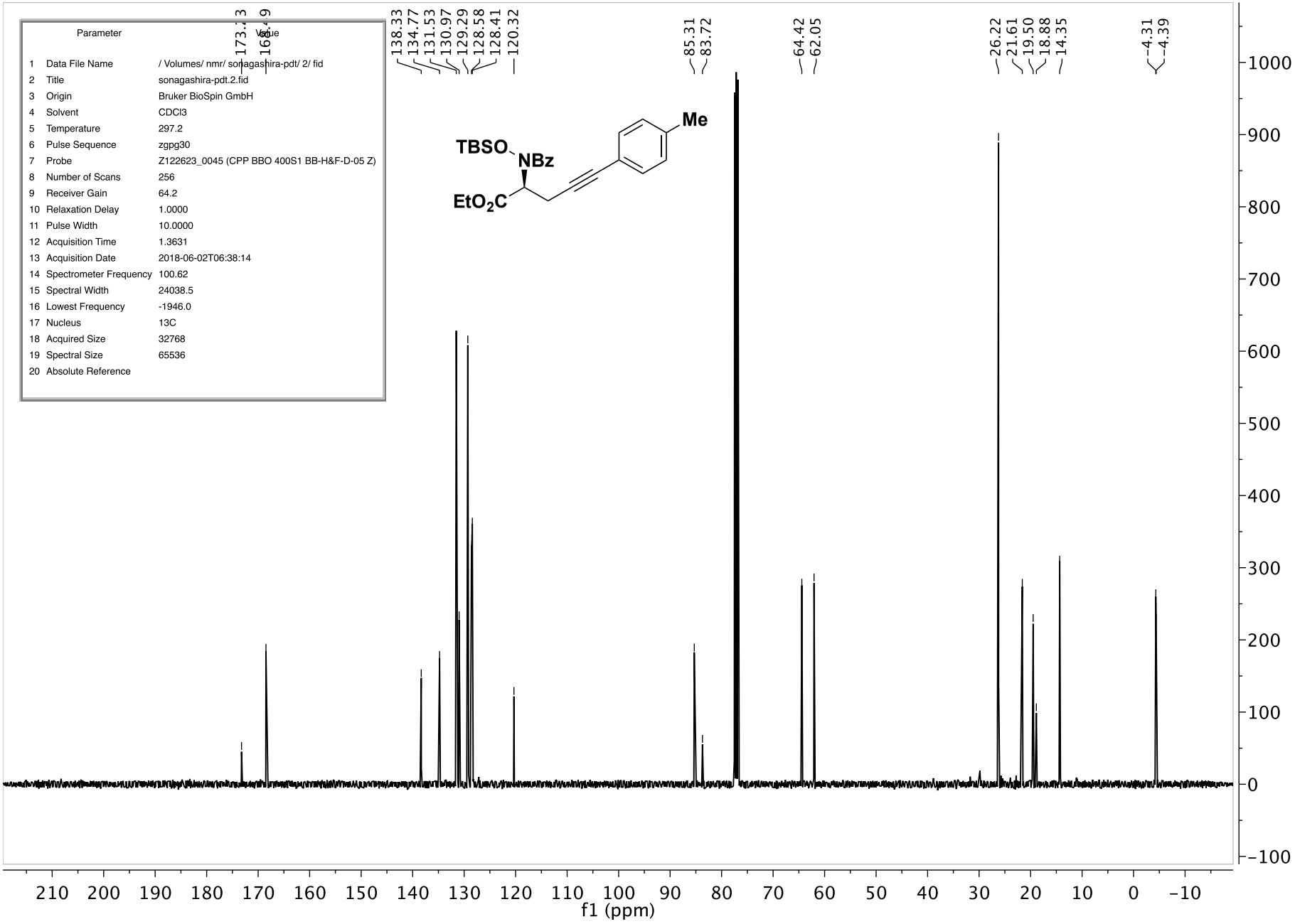
Parameter Value
1 Data File Name / Volumes/ nmr/ sonagashira-pdt/ 2/ fid
2 Title sonagashira-pdt.2.fid
3 Origin Bruker BioSpin GmbH
4 Solvent CDCl3
5 Temperature 297.2
6 Pulse Sequence zgpg30
7 Probe Z122623_0045 (CPP BBO 400S1 BB-H&F-D-05 Z)
8 Number of Scans 256
9 Receiver Gain 64.2
10 Relaxation Delay 1.0000
11 Pulse Width 10.0000
12 Acquisition Time 1.3631
13 Acquisition Date 2018-06-02T06:38:14
14 Spectrometer Frequency 100.62
15 Spectral Width 24038.5
16 Lowest Frequency -1946.0
17 Nucleus 13C
18 Acquired Size 32768
19 Spectral Size 65536
20 Absolute Reference
173.23
169.49
138.33
134.77
131.53
130.97
129.29
128.58
128.41
120.32
85.31
83.72
64.42
62.05
26.22
21.61
19.50
18.88
14.35
-4.31
-4.39
TBSO
NBz
EtO2C
Me
f1 (ppm)

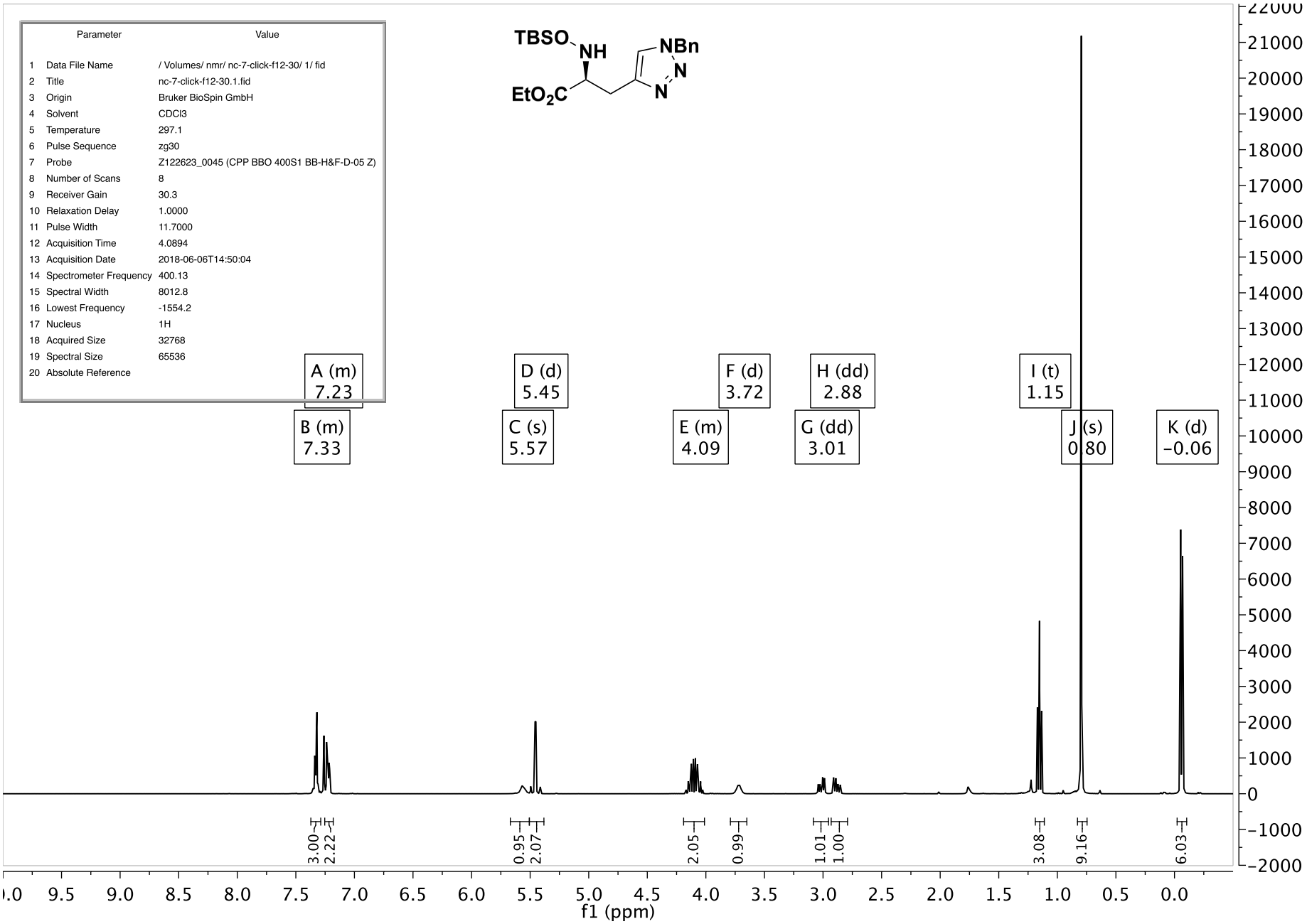
Parameter Value
1 Data File Name / Volumes/ nmr/ nc-7-click-f12-30/ 1/ fid
2 Title nc-7-click-f12-30.1.fid
3 Origin Bruker BioSpin GmbH
4 Solvent CDCl3
5 Temperature 297.1
6 Pulse Sequence zg30
7 Probe Z122623_0045 (CPP BBO 400S1 BB-H&F-D-05 Z)
8 Number of Scans 8
9 Receiver Gain 30.3
10 Relaxation Delay 1.0000
11 Pulse Width 11.7000
12 Acquisition Time 4.0894
13 Acquisition Date 2018-06-06T14:50:04
14 Spectrometer Frequency 400.13
15 Spectral Width 8012.8
16 Lowest Frequency -1554.2
17 Nucleus 1H
18 Acquired Size 32768
19 Spectral Size 65536
20 Absolute Reference
TBSO
NH
NBn
N
N
EtO2C
A (m) 7.23
B (m) 7.33
D (d) 5.45
C (s) 5.57
F (d) 3.72
E (m) 4.09
H (dd) 2.88
G (dd) 3.01
I (t) 1.15
J (s) 0.80
K (d) -0.06
3.00
2.22
0.95
2.07
2.05
0.99
1.01
1.00
3.08
9.16
6.03
f1 (ppm)

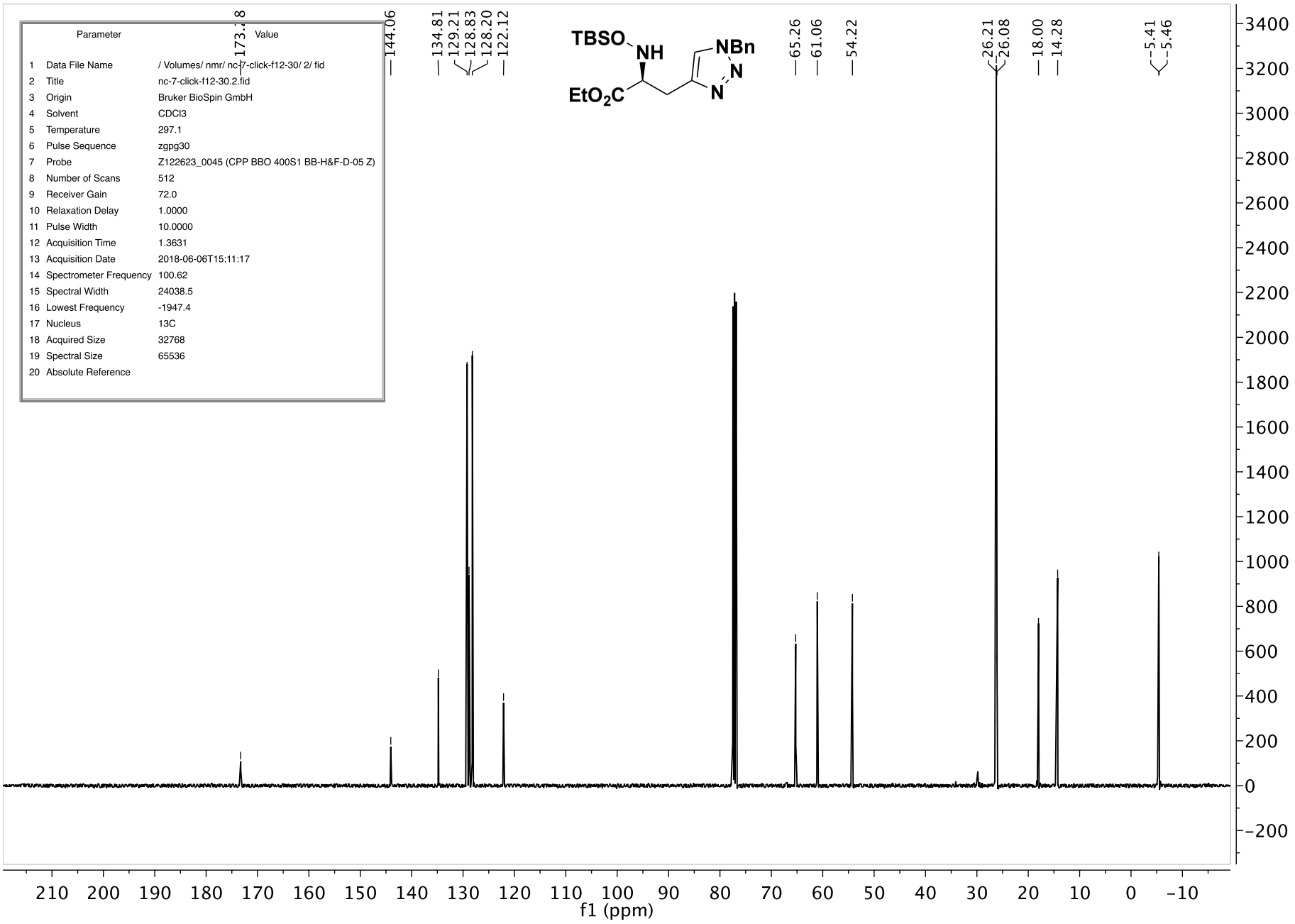
Parameter Value
1 Data File Name / Volumes/ nmr/ nc-7-click-f12-30/ 2/ fid
2 Title nc-7-click-f12-30.2.fid
3 Origin Bruker BioSpin GmbH
4 Solvent CDCl3
5 Temperature 297.1
6 Pulse Sequence zgpg30
7 Probe Z122623_0045 (CPP BBO 400S1 BB-H&F-D-05 Z)
8 Number of Scans 512
9 Receiver Gain 72.0
10 Relaxation Delay 1.0000
11 Pulse Width 10.0000
12 Acquisition Time 1.3631
13 Acquisition Date 2018-06-06T15:11:17
14 Spectrometer Frequency 100.62
15 Spectral Width 24038.5
16 Lowest Frequency -1947.4
17 Nucleus 13C
18 Acquired Size 32768
19 Spectral Size 65536
20 Absolute Reference
173.28
144.06
134.81
129.21
128.83
128.20
122.12
TBSO
NH
NBn
N
N
EtO2C
65.26
61.06
54.22
26.21
26.08
18.00
14.28
-5.41
-5.46
f1 (ppm)